DEVELOPMENTS IN ENVIRONMENTAL SCIENCE 8

Series Editor: S.V. Krupa

WILDLAND FIRES AND AIR POLLUTION

Edited by

ANDRZEJ BYTNEROWICZ,
MICHAEL ARBAUGH, ALLEN RIEBAU
AND CHRISTIAN ANDERSEN

Wildland Fires and Air Pollution

Previous Volumes in this Series

AIR POLLUTION SCIENCE FOR THE 21ST CENTURY, I
Edited by Jill Austin, Peter Brimblecombe and William Sturges

OZONE AIR POLLUTION IN THE SIERRA NEVADA – DISTRIBUTION AND EFFECTS ON FORESTS, II
Edited by A. Bytnerowicz, M.J. Arbaugh and R. Alonso

AIR POLLUTION, GLOBAL CHANGE AND FORESTS IN THE NEW MILLENNIUM, III
Edited by D.F. Karnosky, K.E. Percy, A.H. Chappelka, C. Simpson and J. Pikkarainen

CROSS-BORDER RESOURCE MANAGEMENT: THEORY AND PRACTICE, IV
Edited by R. Guo

CONCEPTS AND APPLICATIONS IN ENVIRONMENTAL GEOCHEMISTRY, V
Edited by Dibyendu Sarkar, Rupali Datta and Robyn Hannigan

AIR POLLUTION MODELING AND ITS APPLICATION XVIII, VI
Edited by Carlos Borrego and Eberhard Renner

PERSISTENT ORGANIC POLLUTANTS IN ASIA: SOURCES, DISTRIBUTIONS, TRANSPORT AND FATE, VII
Edited by An Li, Shinsuke Tanabe, Guibin Jiang, John P. Giesy and Paul K.S. Lam

WILDLAND FIRES AND AIR POLLUTION, VIII
Edited by Andrzej Bytnerowicz, Michael Arbaugh, Allen R. Riebau and Christian Andersen

Wildland Fires and Air Pollution

Edited by

Andrzej Bytnerowicz
USDA Forest Service, Riverside, CA

Michael J. Arbaugh
USDA Forest Service, Riverside, CA

Allen R. Riebau
USDA Forest Service, Washington, D.C.

Christian Andersen
U.S. Environmental Protection Agency, Corvallis, OR

ELSEVIER

Amsterdam – Boston – Heidelberg – London – New York – Oxford
Paris – San Diego – San Francisco – Singapore – Sydney – Tokyo

Elsevier
Radarweg 29, PO Box 211, 1000 AE Amsterdam, The Netherlands
The Boulevard, Langford Lane, Kidlington, Oxford OX5 1GB, UK

First edition 2009

British Library Cataloguing in Publication Data
A catalogue record for this book is available from the British Library

Library of Congress Cataloging-in-Publication Data
A catalog record for this book is available from the Library of Congress

ISBN: 978-0-08-055609-3
ISSN: 1474-8177

For information on all Elsevier publications
visit our website at books.elsevier.com

Printed and bound in Hungary

09 10 11 12 13 10 9 8 7 6 5 4 3 2 1

Dedication to Dr. Sue A. Ferguson

Picture caption: Sue sailing on Lake Washington, September 2005.

This book is dedicated to Dr. Sue A. Ferguson, atmospheric scientist, friend and colleague, visionary, and enthusiastic participant in life. We lost Sue to breast cancer on December 18, 2005, on a beautiful, crisp, blue-sky Seattle day. Her memory and inspiration continue to live on, however, in the legacy she founded in the atmospheric science community: first in her 13-year career in Avalanche Forecasting, then in her 13-year career as a Research Meteorologist with the USDA Forest Service.

Sue thought big, never hesitating to tackle difficult problems or situations. She saw the potential of what could be accomplished by bringing together brilliant and dedicated people to push the boundaries of science and the imagination. As an Avalanche Forecaster, she started the

Avalanche Review, now a premier publication in the field. As a Research Meteorologist with the Forest Service she was a member of the Fire and Environmental Research Applications (FERA) Team and then went on to found the Atmosphere and Fire Interactions Research and Engineering (AirFIRE) Team. Her vision led to the development of the BlueSky Smoke Prediction System—a system on the forefront of technology and innovation that provides real-time predictions of smoke concentrations from prescribed fires, wildfires, and agricultural fires. Sue helped form the Northwest Regional Modeling Center (NWRMC) that provides daily scientific products for the fire weather, meteorological, and air quality communities and serves as a template for other regional modeling consortiums nationally. In addition to all these accomplishments, Sue still loved to encourage and participate in hands-on science, leading field campaigns (with a tethersonde affectionately known as "Wally") to measure smoke and meteorological parameters during fires and mentoring young high school future-scientists-of-the-world. Sue touched many lives, and we are all the better for knowing her and her pioneering spirit.

Contents

List of Contributors xi

Biographies xxi

Acknowledgements xli

Preface xliii

Introduction xlv

Section I: General Information and Emissions

1. Impacts of Vegetation Fire Emissions on the Environment, Human Health, and Security: A Global Perspective 3
2. Climatic and Weather Factors Affecting Fire Occurrence and Behavior 37
3. Characterizing Sources of Emissions from Wildland Fires 61
4. Chemical Composition of Wildland Fire Emissions 79
5. Effects of Wildland Fire on Regional and Global Carbon Stocks in a Changing Environment 109
6. Airborne Remote Sensing of Wildland Fires 139

Section II: Ambient Air Quality, Visibility and Human Health—Regional Perspectives

7. Effects of Forest Fires on Visibility and Air Quality 171
8. Assessment of Forest Fire Impacts and Emissions in the European Union Based on the European Forest Fire Information System 197

9. Forest Fires and Air Quality Issues in Southern Europe 209

10. Spatial and Temporal Trends in Distribution of Forest Fires in Central and Eastern Europe 233

11. A Mega-Fire Event in Central Russia: Fire Weather, Radiative, and Optical Properties of the Atmosphere, and Consequences for Subboreal Forest Plants 247

12. Vegetation Fires, Smoke Emissions, and Dispersion of Radionuclides in the Chernobyl Exclusion Zone 265

13. Remote Sensing Applications of Wildland Fire and Air Quality in China 277

14. Smoke from Wildfires and Prescribed Burning in Australia: Effects on Human Health and Ecosystems 289

Section III: Ecological Impacts of Forest Fires and Air Pollution

15. Global Warming and Stress Complexes in Forests of Western North America 319

16. A Probabilistic View of Chaparral and Forest Fire Regimes in Southern California and Northern Baja California 339

17. Air Pollution Increases Forest Susceptibility to Wildfires: A Case Study in the San Bernardino Mountains in Southern California 365

18. Fire Effects on Carbon and Nitrogen Cycling in Forests of The Sierra Nevada 405

19. Management Options for Mitigating Nitrogen (N) Losses from N-Saturated Mixed-Conifer Forests in California 425

20. Interactive Effects of Climate and Wildland Fires on Forests and other Ecosystems—Section III Synthesis 457

Section IV: Management Issues

21. Fire Danger and Fire Behavior Modeling Systems in Australia, Europe, and North America 471

22. Regional Real-Time Smoke Prediction Systems 499

23. Managing Smoke from Wildfires and Prescribed Burning in Southern Australia 535

24. A Statistical Model for Forecasting Hourly Ozone Levels During Fire Season 551

25. Managing Air Pollution Impacted Forests of California 567

Section V: Concluding Section

26. Integrating Research on Wildland Fires and Air Quality: Needs and Recommendations 585

Author Index 603

Subject Index 629

This page intentionally left blank

List of Contributors

Mark Adams — Laboratory for Ecosystem Science and Sustainability, School of Biological, Earth and Environmental Sciences, University of New South Wales, Sydney 2052, New South Wales, Australia; E-mail: m.adams@unsw.edu.au

Christian Andersen — US Environmental Protection Agency, National Health and Environmental Effects Research Laboratory, 200 SW 35th St., Corvallis, OR 97333, USA; E-mail: Andersen.Christian@epamail.epa.gov

Meinrat O. Andreae — Biogeochemistry Department, Max Planck Institute for Chemistry, P.O. Box 3060, D 55020 Mainz, Germany; E-mail: andreae@mpch-mainz.mpg.de

Michael J. Arbaugh — USDA Forest Service, Pacific Southwest Research Station, 4955 Canyon Crest Drive, Riverside, CA 92507, USA; E-mail: marbaugh@fs.fed.us

Stephen Baker — USDA Forest Service, Rocky Mountain Research Station, Fire Sciences Laboratory, 5775 US Highway 10 West, Missoula, MT 59808, USA; E-mail: sbaker03@fs.fed.us

Paulo Barbosa — European Commission Joint Research Centre, Institute for Environment and Sustainability, Land Management and Natural Hazards Unit, TP 261, 21027 Ispra (VA), Italy; E-mail: Paulo.BARBOSA@ec.europa.eu

Tina Bell — School of Forest and Ecosystem Science, The University of Melbourne, 1 Water Street, Creswick 3363, Victoria, Australia; E-mail: tlbell@unimelb.edu.au

Randall P. Benson	South Dakota School of Mines & Technology, Department of Atmospheric Sciences, 501 E. Saint Joseph Street, Rapid City, SD 57701, USA; E-mail: randall.benson@sdsmt.edu
Oleg O. Bondarenko	State Specialized Scientific and Industrial Enterprise, Chernobyl Radioecological Centre, Chernobyl, Kiev Region, Ukraine; E-mail: boa@ecocentre.mns.gov.ua
Timothy Brown	Desert Research Institute, 2215 Raggio Parkway, Reno, NV 89512, USA; E-mail: tim.brown@dri.edu
Andrzej Bytnerowicz	USDA Forest Service, Pacific Southwest Research Station, 4955 Canyon Crest Drive, Riverside, CA 92507, USA; E-mail: abytnerowicz@fs.fed.us
Andrea Camia	European Commission Joint Research Centre, Institute for Environment and Sustainability, Land Management and Natural Hazards Unit, TP 261, 21027 Ispra (VA), Italy; E-mail: Andrea.CAMIA@jrc.it
Deborah J. Chavez	USDA Forest Service, Pacific Southwest Research Station, 4955 Canyon crest Drive, Riverside, CA 92507, USA; E-mail: dchavez@fs.fed.us
Nataly Y. Chubarova	Moscow State University, Faculty of Geography, Leninskie Gory, GSP-1, 119991 Moscow, Russia; E-mail: chubarova2006@rambler.ru
Susan G. Conard	USDA Forest Service, Research and Development, Rosslyn Plaza-C, 4th Floor, 1601 North Kent Street, Arlington, VA 22209, USA; E-mail: sconard@fs.fed.us
Roland R. Draxler	NOAA Air Resources Laboratory, R/ARL-SSMC3, 1315 East West Hwy, Silver Spring, MD 20910, USA; E-mail: Roland.Draxler@noaa.gov
Alexander Dunn	Environmental Coordinator, Beaverhead-Deerlodge National Forest, 420 Barrett Street, Dillon, MT 59725, USA; E-mail: adunn@fs.fed.us

Annie Esperanza Sequoia and Kings Canyon National Parks, Three Rivers, CA 93271, USA;
E-mail: annie_esperanza@nps.gov

Mark E. Fenn USDA Forest Service, Pacific Southwest Research Station, 4955 Canyon Crest Drive, Riverside, CA 92507, USA;
E-mail: mfenn@fs.fed.us

Sue A. Ferguson USDA Forest Service, Pacific Northwest Research Center, Pacific Wildland Fire Sciences Laboratory, 34th Street, Suite 201, Seattle, WA 98103, USA

Marco Ferretti TerraData environmetrics, Dipartimento di Scienze Ambientali 'G. Sarfatti', Università degli Studi di Siena, Via P.A. Mattioli 4, 53100 Siena, Italy;
E-mail: ferretti@terradata.it

Douglas G. Fox Cooperative Institute for Research in the Atmosphere, Colorado State University, 1375 Campus Delivery, Fort Collins, CO 80524, USA;
E-Mail: Fox@cira.colostate.edu

Ernesto Franco-Vizcaíno Departamento de Ecologia, Centro de Investigacion n Cientifica y de Educacion n Superior de Ensenada (CICESE), Ensenada, Baja California, Mexico;
E-mail: franco@cicese.mx

Francis M. Fujioka USDA Forest Service, Pacific Southwest Research Station, 4955 Canyon Crest Drive, Riverside, CA 92507, USA;
E-mail: ffujioka@fs.fed.us

A. Malcolm Gill CSIRO Plant Industry, GPO Box 1600, Canberra, ACT 2601, Australia;
E-mail: Malcolm.Gill@csiro.au

Benjamín S. Gimeno Ecotoxicology of Air Pollution, CIEMAT (Ed. 70), Avda. Comlutense 22, 28040 Madrid, Spain;
E-mail: benjamin.gimeno@ciemat.es

Johann G. Goldammer	The Global Fire Monitoring Center (GFMC), Max Planck Institute for Chemistry, c/o Freiburg University/United Nations University, Georges-Koehler-Allee 75, D-79110 Freiburg, Germany; E-mail: johann.goldammer@fire.uni-freiburg.de
Nancy E. Grulke	USDA Forest Service, Pacific Southwest Research Station, 4955 Canyon Crest Drive, Riverside, CA 92507, USA; E-mail: ngrulke@fs.fed.us
Wei Min Hao	USDA Forest Service, Rocky Mountain Research Station, Fire Sciences Laboratory, 5775 US Highway 10 West, Missoula, MT 59808, USA; E-mail: whao@fs.fed.us
Xianjun Hao	EastFIRE Lab, College of Science, George Mason University, 4400 University Blvd., Fairfax, VA 22030, USA; E-mail: xhao1@gmu.edu
Jeanne Hoadley	USDA Forest Service, 1474 Rodeo Rd., Santa Fe, NM 87505, USA; E-mail: jhoadlay@fs.fed.us
Carolyn F. Hunsaker	USDA Forest Service, Pacific Southwest Research Station, Forestry Sciences Laboratory, 2081 E. Sierra Avenue, Fresno, CA 93710-4639, USA; E-mail: chunsaker@fs.fed.us
Diane Hutton	USDA Forest Service, Beaverhead-Deerlodge National Forest, Wisdom, MT, 59761, USA; E-mail: dhutton@fs.fed.us
Dale W. Johnson	Natural Resources and Environmental Science, Fleischmann Ag Bldg, MS 370, University of Nevada, Reno, NV 89557, USA; E-mail: dwj@cabnr.unr.edu
Julide Kahyaoglu-Koracin	Division of Atmospheric Sciences, Desert Research Institute, 2215 Raggio Parkway, Reno, NV 89512, USA; E-mail: Julide.Koracin@dri.edu

Jan Kucera — European Commission Joint Research Centre, Institute for Environment and Sustainability, Land Management and Natural Hazards Unit, TP 261, 21027 Ispra (VA), Italy; E-mail: Jan.KUCERA@jrc.it

Narasimhan (Sim) K. Larkin — Pacific Wildland Fire Sciences Laboratory, 400 N 34th St, Suite 201, Seattle, WA 98103, USA; E-mail: larkin@fs.fed.us

Giorgio Libertà — European Commission Joint Research Centre, Institute for Environment and Sustainability, Land Management and Natural Hazards Unit, TP 261, 21027 Ispra (VA), Italy; E-mail: giorgio.liberta@irc.it

Jeremy J. Littell — College of Forest Resources, University of Washington, Box 352100, Seattle 98195-2100, USA; E-mail: jlittell@u.washington.edu

Yongqiang Liu — Forestry Sciences Laboratory, USDA Forest Service, 320 Green St., Athens, GA 30602, USA; E-mail: yliu@fs.fed.us

Enrico Marchi — Dipartimento di Scienze e Tecnologie Ambientali Forestali, Università di Firenze, Via S. Bonaventura, 13, 50145 Firenze, Italy; E-mail: emarchi@unifi.it

Lachlan McCaw — Bushfire Cooperative Research Center, Department of Environment and Conservation, Locked Bag 2, Manjimup, WA 6258, Australia; E-mail: Lachie.Mccaw@dec.wa.gov.au

Donald McKenzie — USDA Forest Service, Pacific Northwest Research Station, Pacific Wildland Fire Sciences Lab, 400 N 34th St, Suite 201, Seattle, WA 98103, USA; E-mail: donaldmckenzie@fs.fed.us

Thomas Meixner — Department of Hydrology and Water Resources, University of Arizona, Tucson, AZ 85721, USA; E-mail: tmeixner@hwr.arizona.edu

Millán M. Millán	FUNDACION CEAM, Parque Tecnológico, c/o Charles R. Darwin, 14, E-46980 Paterna (Valencia), Spain; E-mail: pilarz@ceam.es
Watkins W. Miller	Natural Resources and Environmental Science, 1000 Valley Road, University of Nevada, Reno, NV 89512, USA; E-mail: wilymalr@cabnr.unr.edu
Graham Mills	Bureau of Meteorology Research Centre, GPO Box 1289, Melbourne, Victoria 3001, Australia; E-mail: g.mills@bom.gov.au
Richard A. Minnich	Geology Department, University of California, Riverside, CA 92521, USA; E-mail: richard.minnich@ucr.edu
Ana Isabel Miranda	GEMAC-Grupo de Emissões, Modelação e Alterações Climáticas, Dep. Ambiente e Ordenamento, Universidade de Aveiro, 3810-193 Aveiro, Portugal; E-mail: miranda@ua.pt
Susan M. O'Neill	USDA Natural Resources Conservation Service, 1201 NE Lloyd Blvd., Suite 1000, Portland, OR 97232-1202, USA; E-mail: susan.oneill@por.usda.gov
Roger D. Ottmar	USDA Forest Service, Pacific Northwest Research Station, 400 North 34th Street, Suite 201, Seattle, WA 98103, USA; E-mail: rottmar@fs.fed.us
Timothy D. Paine	Department of Entomology, University of California, Riverside, CA 92521, USA; E-mail: timothy.paine@ucr.edu
Ilaria Palumbo	European Commission Joint Research Centre, Institute for Environment and Sustainability, Land Management and Natural Hazards Unit, TP 261, 21027 Ispra (VA), Italy; E-mail: Ilaria.PALUMBO@gmail.com

David L. Peterson	USDA Forest Service, Pacific Northwest Research Station, Pacific Wildland Fire Sciences Lab, 400 N 34th St, Suite 201, Seattle, WA 98103, USA; E-mail: dpeterson@fs.fed.us
Haiganoush K. Preisler	USDA Forest Service, Pacific Southwest Research Station, Albany, CA 94710, USA; E-mail: hpreisler@fs.fed.us
Nickolay G. Prilepsky	Faculty of Biology, Geobotany Department, Lomonosov Moscow State University, Leninskie Gory, GSP-1, 119991, Moscow, Russia
Trent Procter	US Forest Service, Region 5, 900 W. Grand, Porterville, CA 93527, USA; E-mail: tprocter@fs.fed.us
Xianlin Qin	Research Institute of Forest Resources Information Techniques, Chinese Academy of Forestry, Beijing, P. R. China; E-mail: noaags@forestry.ac.cn
John J. Qu	EastFIRE Lab, College of Science, George Mason University, 4400 University Blvd., Fairfax, VA 22030, USA; E-mail: jqu@gmu.edu
Allen R. Riebau	USDA Forest Service, Research and Development, Rosslyn Plaza-C, 4th Floor, 1601 North Kent Street, Arlington, VA 22209, USA; E-mail: ariebau@msn.com
Philip J. Riggan	USDA Forest Service, Pacific Southwest Research Station, 4955 Canyon Crest Drive, Riverside, CA 92507, USA; E-mail: priggan@fs.fed.us
John O. Roads	Scripps Institution of Oceanography, UCSD, 9500 Gilman Dr., Mail Code 0024 La Jolla, CA 92093-0224, USA; E-mail: jroads@ucsd.edu
Glenn Rolph	NOAA Air Resources Laboratory, R/ARL-SSMC3, 1315 East West Hwy, Silver Spring, MD 20910, USA; E-mail: Glenn.Rolph@noaa.gov

Alexei N. Rublev — Russian Research Center, Kurchatov Institute, Kurchatov Square, 123182 Moscow, Russia; E-mail: rublev@imp.kiae.ru

Mark Ruminski — NOAA/NESDIS Satellite Analysis Branch, 5200 Auth Rd., Rm 401 E/SP23, Camp Springs, MD 20746, USA; E-mail: Mark.Ruminski@noaa.gov

Jesus San-Miguel-Ayanz — European Commission Joint Research Centre, Institute for Environment and Sustainability, Land Management and Natural Hazards Unit, TP 261, 21027 Ispra (VA), Italy; E-mail: Jesus.SAN-MIGUEL@jrc.it

David V. Sandberg — 24768 Llewellyn Road, Corvallis, OR 97333, USA; E-mail: sandbergd@peak.org

Guido Schmuck — European Commission Joint Research Centre, Institute for Environment and Sustainability, Land Management and Natural Hazards Unit, TP 261, 21027 Ispra (VA), Italy; E-mail: Guido.SCHMUCK@jrc.it

Steve J. Seybold — USDA Forest Service, Pacific Southwest Research Station, 720 Olive Drive, Suite D, Davis, CA 95616, USA; E-mail: sseybold@fs.fed.us

Allen M. Solomon — USDA Forest Service, Research and Development, Rosslyn Plaza-C, 4th Floor, 1601 North Kent Street, Arlington, VA 22209, USA; E-mail: allensolomon@fs.fed.us

Milt Statheropoulos — Laboratory of Inorganic and Analytical Chemistry, School of Chemical Engineering, National Technical University of Athens, Iroon Polytechniou 9 st, 15773 Athens, Greece; E-mail: stathero@chemeng.ntua.gr

Ryszard Szczygieł — Forest Protection Department, Forest Research Institute, ul. Braci Lesnej 3, 05-090 Sekocin Stary, Poland; E-mail: r.szczygiel@ibles.waw.pl

Robert G. Tissell	USDA Forest Service, Pacific Southwest Research Station, 4955 Canyon Crest Drive, Riverside, CA 92507, USA; E-mail: rtissell@fs.fed.us
Barbara Ubysz	Forest Protection Department, Forest Research Institute, ul. Braci Lesnej 3, 05-090 Sekocin Stary, Poland; E-mail: b.ubysz@ibles.waw.pl
Shawn P. Urbanski	USDA Forest Service, RMRS Fire Sciences Laboratory, 5775 US Highway 10 West, Missoula, MT 59808, USA; E-mail: surbanski@fe.fed.us
Joseph K. Vaughan	Laboratory for Atmospheric Research, Department of Civil and Environmental Engineering, Washington State University, Pullman, WA 99164-2910, USA; E-mail: jvaughan@wsu.edu
Domingos X. Viegas	Departamento de Engenharia Mecânica, Universidade de Coimbra-Polo II, Rua Luís Reis dos Santos, 3030-788 Coimbra, Portugal; E-mail: xavier.viegas@dem.uc.pt
Alan Wain	Bushfire Cooperative Research Centre, Bureau of Meteorology Research Centre, GPO Box 1289, Melbourne, Victoria 3001, Australia; E-mail: a.wain@bom.gov.au
David R. Weise	USDA Forest Service, Pacific Southwest Research Station, 4955 Canyon Crest Drive, Riverside, CA 92507, USA; E-mail: dweise@fs.fed.us
B. Mike Wotton	Great Lakes Forestry Centre, Canadian Forest Service, Natural Resources Canada, 1219 Queen Street East, Sault Ste. Marie, Ontario, P6A 2E5, Canada; E-mail: mwotton@NRCan.gc.ca
Haoruo Yi	Research Institute of Forest Resources Information Techniques, Chinese Academy of Forestry, Beijing, China; E-mail: yihr@forestry.ac.cn

Fengming Yuan — Department of Hydrology and Water Resources, University of Arizona, Tucson, AZ 85721, USA; E-mail: fmyuan@hwr.arizona.edu

Tomasz Zawiła-Niedźwiecki — University of Applied Sciences, Faculty of Forestry, Alfred-Möller-Str.1, 16225 Eberswalde, Germany; E-mail: tzawila@fh-eberswalde.de

Shiyuan (Sharon) Zhong — Department of Geography, Center for Global Climate Change and Earth Observation, Michigan State University, East Lansing, MI 48824, USA; E-mail: zhongs@msu.edu

Sergiy Zibtsev — Institute of Forestry and Landscape Architecture, National Agricultural University, Kiev, Ukraine; E-mail: sergiy.zibtsev@nauu.kiev.ua

Biographies

Mark Adams, Ph.D., is a Professor of Ecology and Ecosystem Science at the University of New South Wales and Adjunct Professor at the University of Western Australia. He was a member of the Board of Trustees for the World Agroforestry Centre in Nairobi, Kenya for six years. Mark holds editorial responsibilities for several journals and publishes widely in forest, fire, and range ecology. Mark has been a QEII Fellow and has received other prestigious fellowships and awards from the Australian Academy of Science, the University of Canterbury, the Alexander von Humboldt Foundation, the French National Research Institute, and the British Council.

Christian Andersen, Ph.D., is a plant physiologist with the Environmental Protection Agency in Corvallis, Oregon, and he is a member of the Graduate Faculty at Oregon State University. He has studied the effects of air pollution on plants for over 20 years, and has worked with the Office of Air and Radiation in assessing the risk of forests to ozone in the United States. His research has addressed the effects of stress on root physiology, including the role of ozone stress in altering below-ground processes. His current research interests include the role of air quality in altering ecosystem services such as carbon sequestration and water quality.

Meinrat O. Andreae is a director of the Biogeochemistry Department and Scientific Member at the Max Planck Institute for Chemistry, Biogeochemistry Department, Mainz, Germany. He has studied earth sciences at the universities of Karlsruhe and Göttingen. He holds Ph.D. in Oceanography from the Scripps Institution of Oceanography, University of California, San Diego. Before moving back to Germany, he has worked as an Assistant Professor, an Associate Professor, and Professor at the Florida State University, Tallahassee.

Michael J. Arbaugh earned a B.S. degree in Biology from the University of California, Riverside in1980; an M.S. degree in Statistics from the University of California, Riverside in 1984; and a Ph.D. in Forest Ecology from Colorado State University, Ft. Collins in 1995. His research interests include understanding the multiple air pollutant effects on ecosystems, long-term changes in forest composition, and passive air pollution monitor development and application to Class I areas.

Stephen Baker is a chemist at the US Forest Service Fire Sciences Laboratory Missoula, Montana, where he specializes in sampling techniques and gas chromatography analysis of fire emissions. He has done fire emissions sampling and research in Alaska, Mexico, Chile, and the southeastern and western United States. He is currently involved in fire emissions and soil respiration research in Siberia, as part of FIREBEAR, a cooperative fire research project between the US Forest Service and Russia. He has a B.S. in Chemistry from Northern Arizona University and an M.S. in Forestry from the University of Montana.

Paulo Barbosa has a Ph.D. in Forest Engineering from the Technical University of Lisbon (2000), an M.Sc. in Rural Planning in Relation to the Environment from the International Centre for Advanced Mediterranean Agronomic Studies (1993), and a degree in Forest Engineering from the Technical University of Lisbon (1990). He has worked as a researcher on GIS and Remote Sensing applications at the Agronomic Research Institute, Zaragoza, Spain (1991–1993) at the Space Applications Institute of the EC Joint Research Centre (1994–1999) and at the National Centre for Geographic Information (CNIG) Lisbon, Portugal (1999–2000). He has been responsible for the development and implementation of the European Forest Fire Information System (EFFIS). He is currently at the Institute for Prospective Technological Studies of the EC Joint Research Centre.

Tina Bell, Ph.D., is a Senior Research Fellow in the School of Forest and Ecosystem Science at the University of Melbourne. Prior to this Tina completed a Research and Teaching Fellowship at the University of Western Australia and a Post Doctoral Fellowship at the University of Cape Town in South Africa. Her research is in the broad area of ecology and physiology of plants with particular interest in plants from fire-prone ecosystems. Her current project leadership has taken her into the fields of emissions in smoke from wildfires and the effects of smoke on human health and the environment.

Randall P. Benson received his B.F.A. from Texas Christian University, majoring in Communications Graphics. He did graduate work in the Meteorology Department at the University of Utah, earning an M.S. in 1996. He completed his Ph.D. from the Atmospheric and Environmental Sciences program at South Dakota School of Mines & Technology in 2006 by developing a statistical model to predict wildfire occurrence. In addition to serving as the State Fire Meteorologist, he also teaches atmospheric science and fire science. Dr. Benson has worked previously in private industry as a research climatologist and a forecasting meteorologist.

Oleg O. Bondarenko, Ph.D., is currently the Director of the Chernobyl Radioecological Centre, State Specialized Scientific and Industrial Enterprise in Chernobyl, Kiev Region, Ukraine.

Timothy Brown, Ph.D., is the founder and director of the Program for Climate, Ecosystem and Fire Applications (CEFA) at the Desert Research Institute (DRI), and Associate Research Professor at DRI in Reno. His primary academic interests include applied research in climatology and meteorology in relation to wildland fire; the application of scientific information for decision-making, strategic planning and policy; statistical data analysis; and scientific visualization. Dr. Brown actively serves in a liaison role between scientific and decision-maker/stakeholder communities as a key mission of CEFA.

Andrzej Bytnerowicz is a Senior Scientist with the US Forest Service, Pacific Southwest Research Station in Riverside, CA. He is also a Visiting Professor at the Department of Environmental Sciences, University of California in Riverside. He earned M.Sc. in Food Chemistry from the Warsaw Agricultural University, Poland, in 1972, and Ph.D. in Natural Sciences from the Silesian University in Katowice, Poland. His main research interests are atmospheric deposition to natural ecosystems and effects of air pollution and climatic change on forest ecosystems. He is a Deputy Coordinator of Research Group 7.01 "Impacts of Air Pollution and Climate Change on Forest Ecosystems" of the International Union of Forest Research Organizations (IUFRO).

Andrea Camia holds Ph.D. in Forestry and is a Research Scientist at the Institute of Environment and Sustainability of the European Commission Joint Research Centre since 2004. He has been actively involved in the international wildland fire research arena for the last 20 years. His main interests in the wildland fire domain are focused on meteorological fire danger assessment methods, fire risk assessment and mapping, fuel modelling and mapping, historical fire data management and analysis. He is currently responsible for the operation of the European Forest Fire Information System (EFFIS) of the European Commission.

Deborah J. Chavez received a B.Sc. in Sociology from the University of California at Riverside in 1980, and a Ph.D. in Sociology from University of California at Riverside in 1986. She is currently a research social scientist at the Pacific Southwest Research Station, USDA Forest Service, in Riverside, CA. She specializes in outdoor recreation research and research on law enforcement.

Nataly Y. Chubarova, Ph.D., is a leading scientist at the Lomonosov Moscow State University (MSU). Since 1985 she has worked at the Meteorological Observatory, Faculty of Geography of MSU. Her scientific interests are in the field of atmospheric physics and mainly are devoted to the analysis of ultraviolet irradiance at the Earth's surface. She is responsible of UVB monitoring program and aerosol program (within the AERONET network) at the MSU.

Susan G. Conard is a National Program Leader for Fire Ecology Research and a Wildland Fire Research and Development Strategic Program Area Lead person in Washington Office of the US Forest Service. She got her Ph.D. and M.S. in Plant Ecology from the University of California, Davis, and B.A. in Environmental Studies from the Antioch College, Yellow Springs, OH. She is a Deputy Coordinator of Division 8 of the International Union of Forest Research Organizations. She is a member of the Steering Group of the International Boreal Forest Research Association and on the Editorial Advisory Committee for the International Journal of Wildland Fire.

Roland R. Draxler has been a research meteorologist with NOAA's Air Resources Laboratory (ARL) since 1975. Currently he leads the headquarter division's ''Transport Modeling and Assessment Group''. His research interests are focused on long-range transport modeling, designing response systems for atmospheric emergencies, and air quality forecasting. Most of his recent development efforts have been related to improving the HYSPLIT atmospheric transport and dispersion model. Prior to working at ARL, Mr. Draxler received an M.Sc. at the Pennsylvania State University (1975), worked as a Research Associate at TRC of New England (1972–1973), and received a B.S. from the State University of New York Maritime College (1972).

Alexander Dunn received a B.S. in Environmental Studies from the University of Oregon in 1998, and an M.Sc. in Environmental Studies from the University of Montana in 2004. He is currently Program Manager for the Western Forestry Leadership Coalition, US Forest Service, Rocky Mountain Region, State and Private Forestry in Lakewood, CO. He specializes in landscape scale policy, planning, and implementation with an emphasis on wildfire management and sustainable forestry.

Annie Esperanza is an air resources specialist with the National Park Service, based in Sequoia and Kings Canyon National Parks in

California. A graduate of Humboldt State University, she has worked on air-related research and monitoring efforts in the Sierra Nevada for over 25 years. Other professional pursuits involve educational outreach as it relates to air quality and global climate change.

Mark E. Fenn is a Research Plant Pathologist with the US Forest Service, Pacific Southwest Research Station in Riverside, CA. He earned a B.S. degree in plant pathology from the University of Arizona in 1981 and a Ph.D. in plant pathology from the University of California, Riverside in 1986. His main research interests include the development of methods for measuring nitrogen deposition in remote sites with the aim of determining atmospheric input thresholds at which ecosystem components are impacted, using empirical and ecosystem modeling approaches. He is also a member of the Mexican Academy of Sciences.

Sue A. Ferguson was a meteorologist and scientist whose career spanned both avalanche forecasting and fire weather and smoke research. As a mountain weather forecaster at the National Weather Service, she founded the now-preeminent Avalanche Review journal, and helped advance the science of avalanche forecasting. As a meteorologist with the US Forest Service, she was the creator and leader of the AirFire Team, which focused on weather, climate, and air quality issues surrounding wildland fire, and was a founding member of the Northwest Regional Modeling Center (NWRMC), which provides daily scientific products for the fire weather, meteorological, air quality, energy, and other communities. The success of the NWRMC led to the development of the national Fire Consortia for the Advanced Modeling of Meteorology and Smoke (FCAMMS), and to the development of the BlueSky Smoke Modeling Framework. Sue received her B.S. in Physics in 1976 from the University of Massachusetts and her Ph.D. in Geophysics/Atmospheric Science in 1984 from the University of Washington.

Marco Ferretti studied Forest Sciences at the University of Florence (Italy) and obtained his Ph.D. from the University of Siena (Italy). Since 1987 his interest is monitoring environmental (air pollution) effects on forests. In particular, his interest is to ensure that monitoring design and implementation are scientifically sound and quality assured. He has served at the International Union of Forest Research Organizations as a coordinator of a Working Group on Detection Monitoring and Evaluation and as a chairman of the UN/ECE ICP-Forests Quality Assurance Committee. He is lecturer at the University of Siena and co-ordinator of the Italian Task Force on Integrated Evaluation of Forest Monitoring.

Douglas G. Fox, Ph.D., QEP is a senior research scientist, emeritus at the Cooperative Institute for Research in the Atmosphere (CIRA) at Colorado State University in Fort Collins. Prior to joining CIRA he was director of the Terrestrial Ecosystems Regional Research and Analysis (TERRA) Laboratory, and scientist and program manager for global change research at the Rocky Mountain Research Station. He currently resides on the Isle of Man.

Ernesto Franco-Vizcaíno obtained the Ph.D. in Soil Science in 1986 at the University of California, Riverside. Since then he has worked on coastal, desert, and mountain ecosystems in Baja California. He is currently adjunct faculty at both the Centro de Investigación Cientïfica y de Educación Superior de Ensenada (CICESE) and California State University, Monterey Bay (CSUMB). His research interests include soil ecology, water relations of native plants, and management and conservation of ecosystems. Ernesto's activities have been focused on improving public understanding of Baja California's natural beauty and promoting the conservation of its wildlands.

Francis M. Fujioka is a research meteorologist for the US Forest Service, Pacific Southwest Research Station in Riverside, CA. He earned a B.S. in Geoscience and M.S. in Meteorology from the University of Hawaii, an M.A. in Statistics from the University of California, Berkeley, and a Ph.D. in Earth Science from the University of California, Riverside. He currently leads the Fire Management Research Unit at the Riverside Fire Lab in California.

A. Malcolm Gill, Ph.D., has been a full-time research fire ecologist since 1971. During most of this time he has been employed by CSIRO Plant Industry in Canberra, Australia. His interests include the effects of fire on organisms, water quality and the urban interface, fire behaviour, and fire weather. Currently he is an Honorary Research Fellow at CSIRO Plant Industry and a Visiting Fellow at the Australian National University in Canberra; he is also a contributor to Australia's Bushfire Cooperative Research Centre based in Melbourne.

Benjamin S. Gimeno is a Research Ecologist with the Ecotoxicology of Air Pollution laboratory of the Centro de Investigaciones Energéticas Medioambientales y Tecnológicas (CIEMAT) in Madrid, Spain. He earned his degree in Biology in 1984 and his Ph.D. in Biology in 1997 from the Madrid Complutense University. His main research interest is the determination of critical loads and levels of air pollutants. He is a specialist in tropospheric ozone phytotoxicity and more recently he has been involved in research related with the adverse effects of nitrogen deposition in Mediterranean ecosystems. He is the coordinator of the Spanish activities related with the United Nations—Economic Commission for Europe International Cooperative (UN-ECE) Working Group on Effects of the Convention on Long-Range Transboundary Air Pollution (CLRTAP). He is a also a member of the steering committees of the UN-ECE Panel on Effects of Air Pollution on Natural Vegetation and Crops (ICP-Vegetation) and the European Science Foundation Programme, Nitrogen in Europe (NinE).

Johann G. Goldammer, Ph.D., is a head of the Fire Ecology and Biomass Burning Research Group, Max Planck Institute for Chemistry, and Director of the Global Fire Monitoring Center (GFMC), Germany, an Associate Institute of the United Nations University (UNU) and Freiburg University, where he is serving as professor for fire ecology. He is coordinator the UNISDR Wildland Fire Advisory Group and the UNISDR Global Wildland Fire Network and co-authored and co-edited the Health Guidelines for Vegetation Fire Events on behalf of the UN.

Nancy E. Grulke received a B.Sc. in Botany from Duke University in 1978, and a Ph.D. in Botany from University of Washington in 1983. She is currently a research plant physiologist at the Pacific Southwest Research Station, US Forest Service, in Riverside, CA. She specializes in whole tree responses to atmospheric pollution (O_3, CO_2, N deposition) and drought stress in mixed conifer forests of California.

Wei Min Hao, Ph.D., is a senior scientist and team leader for fire chemistry research in the Fire, Fuel, and Smoke Science Program at the US Forest Service's Rocky Mountain Research Station. Dr. Hao leads an interdisciplinary team to study the impacts of fires on air quality, atmospheric chemistry, and climate at regional and global scales. He received a B.S. degree in chemistry from Fu Jen Catholic University in Taiwan in 1976, two M.S. degrees in geochemistry and toxicology from Massachusetts Institute of Technology in 1979 and 1981, and a Ph.D. degree in atmospheric chemistry from Harvard University in 1986.

Xianjun Hao, Ph.D., is a research scientist at EastFIRE Lab, College of Science, George Mason University. His major research areas are satellite remote sensing, geosciences, fire sciences, and high performance computing.

Jeanne Hoadley is an Air and Water Quality Specialist with the US Forest Service serving the five national forests in New Mexico. Previously, she served as a Meteorologist on the Atmosphere and Fire Interaction Research and Engineering (AirFIRE) team doing technology transfer and applied studies related to the BlueSky modeling framework. She also completed research related to applications of the MM5 mesoscale meteorological model to Fire Weather forecasting. Jeanne has 18 years experience with the National Weather Service working as an Incident Meteorologist, Fire Weather Forecaster, Fire Weather Program Manager, and Senior Forecaster. She holds B.S. and M.A. degrees in Geography.

Carolyn F. Hunsaker, Ph.D., is a research ecologist with the US Forest Service's Sierra Nevada Research Center, Fresno, CA. Prior to joining the Forest Service in 1998, Carolyn was a scientist at Oak Ridge National Laboratory in Tennessee for 16 years. Dr. Hunsaker is the lead scientist for the Kings River Experimental Watershed, which she started in 2000. Her research interests are understanding stream ecosystems and their associated watersheds, landscape ecology, remote sensing of forest structure, and environmental monitoring and assessment. She is an adjunct faculty member at California State University Fresno.

Diane Hutton is the Fire Management Officer at Wisdom and Wise River Ranger Districts of the Beaverhead-Deerlodge National Forest, US Forest Service in Wisdom, Montana. She coordinates and directs the fire management activities for two ranger districts. The responsibility includes fire suppression, prevention, detection, and prescribed fire on approximately 400,000 ha. She received a B.S. degree in Forestry from Washington State University in 1978 and an M.S. degree in silviculture and forest ecology from University of Montana in 1984. She is also currently serving as the Incident Commander for the Northern Rockies Fire Use Management Team.

Dale W. Johnson is a Professor of Soils in the Department of Environmental and Resource Sciences, College of Agriculture, University of Nevada, Reno (UNR). He received his Ph.D. in forest soils from the University of Washington in 1975, and held positions at Oak Ridge National Laboratory from 1977 to 1989 and jointly at the Desert Research Institute and UNR between 1989 and 2001 before becoming full-time professor at UNR in 2001. His research interests are in soil chemistry and nutrient cycling and include studies on acid deposition, fertilization, harvesting, CO_2 enrichment, nitrogen fixation, and fire.

Julide Kahyaoglu-Koracin is an atmospheric modeler in the Bay Area Air Quality Management District. She earned her Ph.D. in Atmospheric Sciences in 2004 from the University of Nevada, Reno, and her M.S. in Physics in 2000 from the University of Marmara, Istanbul, Turkey. Her research interests include numerical simulations and transport and dispersion studies of atmospheric pollutants, emissions inventory development and emissions modeling of air pollutants, numerical weather predictions, data assimilation and forecasting, climate change, and its interactions with air quality.

Jan Kucera works as a junior researcher at Joint Research Centre (JRC) of European Commission on the field of forest fires and natural disaster monitoring. He received his Ph.D. on Remote Sensing and GIS from the University of Tokyo (2002) and M.Eng. from the Czech Technical University on Land Surveying and Geodesy (1999). He worked as a researcher (2002–2003) at the University of Tokyo. He joined Institute of Environment and Sustainability of the European Union Joint Research Center in 2004.

Narasimhan (Sim) K. Larkin is a Research Physical Climatologist with the US Forest Service's (USFS) Atmosphere and Fire Interaction Research and Engineering (AirFIRE) Team in Seattle, Washington. He works on climate change and air quality issues connected with wildland fire, as well as issues of climate variability. He is the co-author of the first papers to detail the statistically significant patterns and impacts of El Niño and La Nina. Currently he leads the USFS BlueSky smoke modeling project. Sim received a B.A. from the University of California, Berkeley studying physics and Ph.D. from the University of Washington, Seattle studying climate diagnostics.

Giorgio Libertà works as a GIS expert at the Institute of Environment and Sustainability – Land Management & Natural Hazards Unit of the EC Joint Research Centre since the end of 1997. For about 20 years he has been developing GIS applications related to data acquisition tools, mapping production, agricultural statistics, geological and environment monitoring systems, forest fire simulation, forest fire risks index, planning and management of metro area transport system, remote sensing data, Web GIS applications, GIS analysis with integration of vector and raster data.

Jeremy J. Littell is a research scientist at the JISAO CSES Climate Impacts Group, University of Washington. His research focuses on the relationships between climate and forest ecosystems, including fire, tree growth, species distributions, and adaptation to climate change. His field work spans montane and treeline forests in a dozen national forests and five National Parks. He holds a Ph.D. from the College of Forest Resources at the University of Washington, and an M.S. in Land Resources and Environmental Science from Montana State University.

Yongqiang Liu, Ph.D., is a research meteorologist at the Center for Forest Disturbance Science, US Forest Service. He received his Ph.D. degree in atmospheric dynamics from the Institute of Atmospheric Physics, Chinese Academy of Sciences, Beijing, China in 1990. His current research interests include wildland fire and their environmental effects, land–atmosphere interactions, regional climate modeling, and climate change.

Enrico Marchi works at the Department of Environmental Science and Technology in Forestry, University of Florence, Italy. He is an Associate Professor of Wood Technology & Forest Operations at the University of Florence (Italy), Faculty of Agriculture. He holds Ph.D. in Wood Sciences from the University of Florence.

His research interests are forest fire prevention and suppression, forest operations planning and management (thinning and final harvesting), cable-extraction systems, multi-functional forest roads planning, ergonomy, health and safety in firefighting, and forest operations. He is also interested in technical–professional information and training activities for firefighters and forest operators.

Lachlan McCaw, Ph.D., is a Principal Research Scientist with the Department of Environment and Conservation Western Australia and is an active participant in the Bushfire Cooperative Research Centre. Since 1981 he has investigated the behaviour and ecological effects of fires in forests, woodlands, and shrublands of south-western Australia. Current research interests include fire behaviour prediction, fuel moisture modeling, combustion of coarse woody fuels in eucalypt forest fires, and fire history. He devotes substantial time to knowledge transfer with fire practitioners.

Donald McKenzie, Ph.D., is a research ecologist with the US Forest Service, Pacific Wildland Fire Sciences Laboratory. His current research interests include the landscape ecology of fire, particularly in mountain ecosystems, the effects of wildfire on regional air quality and the global carbon cycle, the effects of global warming on forest species distributions, and modeling of the spatial patterns of historical fires.

Thomas Meixner is an associate Professor of Hydrochemistry in the Department of Hydrology and Water Resources at the University of Arizona in Tucson, Arizona. He received a B.S. in Soil and Water Conservation and BA in the History of Science from the University of Maryland in 1992 and a Ph.D. in Hydrology in 1999 from the University of Arizona. From 1999–2005 he was an Assistant Professor at the University of California, Riverside. His research interests focus on how hydrologic processes such as hydrologic flowpath, hydrologic residence time and precipitation intermittency and seasonality influence and control biogeochemical fluxes from the plot to landscape scale.

Millán M. Millán, M.Sc., Ph.D., designed the COSPEC for the remote sensing of SO_2. He joined Environment Canada in 1972 to study dispersion from tall stacks and developed methodologies that have been used in more than 40 countries. He returned to Spain in 1981 and has participated in more than 19 European Commission projects on air pollution, meteorology, and climate in the Mediterranean Basin.

Watkins W. Miller, Ph.D., is currently Associate Director of Research for the University of Nevada, Reno, Academy for the Environment, and a Professor of Soils & Hydrology in the Department of Natural Resources & Environmental Science, College of Agriculture, Biotechnology, & Natural Resources. His current research considers the effects of wildfire and various biomass management strategies in the Lake Tahoe Basin and eastern Sierras on ecosystem response and discharge water quality. Of specific interest are the effects of fire suppression, controlled burning, and mechanical harvest on changes in soil compaction, water repellency, preferential flow, overland/litter interflow, plot condition, and vegetative cover.

Graham Mills has undergraduate science degrees from the University of Adelaide, and postgraduate degrees from Flinders University of South Australia and Monash University. He has worked for the Australian Bureau of Meteorology for more than 40 years, and in its research branches since 1975. Initial priorities were the development of operational limited area NWP systems, with particular emphasis on data assimilation. These have evolved to the application of mesoscale NWP to high-impact weather events, including intense subtropical and extratropical cyclones, severe convective weather, and fire weather. He manages the Bushfire Cooperative Research Centre fire weather research projects.

Richard A. Minnich received a B.A. in Geography in 1968, an M.A. in Geography in 1970, both from University of California, Riverside, and Ph.D. in Geography in 1978 from the University of California, Los Angeles. He is a Professor in the Department of Earth Sciences, University of California, Riverside. His research focuses on the fire ecology of Mediterranean ecosystems of California and northern Baja California. Studies operate at the landscape-scale to establish fire regime properties of ecosystems, including fire size, frequency and return intervals, denudation of vegetation, post-fire successions, and how fire disturbances exert selection in the distribution of plant communities. Documentation and quantification of these properties requires the use of remote sensing and geographic information systems, complimented by field sampling. Studies compare fire regimes under different management systems in southern California and Mexico, emphasizing Californian chaparral and conifer forest.

Ana Isabel Miranda is an Environmental Engineer, graduated by the University of Aveiro in 1989. Since then, she is doing research at the Department of Environment and Planning from this University. Her Ph.D. thesis focused on the effects of forest fire on air quality. She collaborated in several European and national research projects related to forest fires, namely MINERVE I and II, INFLAME, ACRE, SPREAD, ERAS, and EUFIRELAB. Her research interests include air quality, forest fires, and climate change. Currently she is an Associate Professor at the University of Aveiro and she coordinates the research group ‘‘Emissions, Modelling and Climate Change’’.

Susan M. O'Neill is an Air Quality Scientist with the USDA Natural Resources Conservation Service (NRCS) Air Quality and Atmospheric Change (AQAC) Team, focusing on particulate matter and ozone formation issues as they relate to agriculture. Previously, Susan was a Research Air Quality Engineer with the USDA Forest Service, Atmosphere and Fire Interaction Research and Engineering (AirFIRE) Team. With the AirFIRE Team she was the Development Team Leader for the BlueSkyRAINS Smoke Prediction System, a system designed to forecast PM2.5 concentrations from prescribed fires and wildfires. Susan has a B.S in Mechanical Engineering, an M.S. in Environmental Engineering, and a Ph.D. in Civil Engineering.

Roger D. Ottmar is a Research Forester with the Fire and Environmental Research Applications Team, Pacific Northwest Research Station, US Forest Service in Seattle, Washington. He has been involved with fuels, fire, and smoke-related research for over 30 years and is leading efforts to continue the development of (1) a natural fuels photo series; (2) fuel consumption and emission production models by combustion phase and fuelbed layer for forested and non-forested fuel types across North America; and (3) a system to characterize and classify fuelbeds.

Timothy D. Paine received a B.S. in Entomology and a B.A. in History from the University of California, Davis in 1973 and a Ph.D. in Entomology from UC Davis in 1981. He is currently a professor and entomologist in the Entomology Department at the University of California, Riverside. His research is focused on the impact of environmental stress on insect/plant/microorganism interactions in managed and unmanaged forests, chemical ecology, and biological control.

Ilaria Palumbo has studied Environmental Science at the University of Milano. In 2007 she got her Ph.D. in Forest Ecology at the University of

Tuscia (Viterbo). Since 2002 she analyzed the ecological impacts of fires in the African and Mediterranean ecosystems. During her Ph.D. work she improved a RS-based method for the quantification of fire emissions in the Mediterranean ecosystem. She is currently employed as a research associate at the University of Leicester and her work contributes to the CARBOAFRICA Project. Her current research focuses on the burned areas mapping methods and the estimation of savannas fire emissions.

David L. Peterson, Ph.D., is a Research Biologist with the US Forest Service Pacific Northwest Research Station in Seattle and Professor in the College of Forest Resources, University of Washington. He has conducted research on fire ecology and climate change in mountain ecosystems throughout the western United States. He is a principal investigator for the Western Mountain Initiative and a contributing author for Intergovernmental Panel on Climate Change reports. He currently works on hazardous fuel treatment issues in the West and on adaptation options for managing natural resources in a warmer climate.

Haiganoush K. Preisler is a research statistician with US Forest Service, Pacific Southwest Research Station. She earned her Ph.D. in Statistics in 1977 from the University of California, Berkeley and her M.Sc. in 1972 from the American University of Beirut, Lebanon. Her current work focuses on statistical modeling and analysis of environmental data in particular as it relates to forecasting forest threats.

Nickolay G. Prilepsky, Ph.D., is an Assistant Professor at the Geobotany Department of Biological Faculty, Lomonosov Moscow State University. After postgraduate studies since 1990 he works at Geobotany Department, Biological Faculty, Moscow State University. Area of current expertise: phenology and ecology of plants, floristics.

Trent Procter is currently the Air Quality Program Manager for the Pacific Southwest Region of the US Forest Service. He provides program and technical guidance to the Region's 18 national forests. He has 30 years of experience with the Forest Service and has served in his present position since 2004. He holds a B.S. in Natural Resource Management from Cal Poly, San Luis Obispo. His experience includes tracking the status and change of forest resource values that can be impacted by air pollution as well as air quality regulatory consultation and policy development.

Xianlin Qin, Ph.D., is an associate professor of the Institute of Forest Resources Information Techniques, Chinese Academy of Forestry (CAF), Beijing, China. He has pursued the research on forest fire remote sensing since 1996. He has worked on several projects relative to forest fire research by using Remote Sensing and GIS Techniques such as ''National Forecast System of Forest Fire Danger'', ''Satellite Remote Sensing Monitoring Technique and its Demonstration on Vegetation Change and Vegetation Combustion'', ''Forest Fire Monitoring Demonstration by Satellite Remote Sensing in China'', and ''Tropical Forest Fire Monitoring and Management System Based on Satellite Remote Sensing Data in China'', etc. More than 10 papers about forest fire have been published in recent years.

John J. Qu, Ph.D., is an associate professor at Department of Earth Systems and Geoinformation Sciences, College of Science, and is Co-Director and founder of EastFIRE Lab at George Mason University. His major research areas are satellite remote sensing, Earth systems sciences, fire sciences, and GIS applications.

Allen R. Riebau, is currently working as a principal air quality scientist and consultant in Western Australia. He worked for the United States government for 32 years in various capacities with his last assignment, in which he severed for almost 10 years as Chief Atmospheric Scientist for US Forest Service Research and Development in Washington, D.C. He holds AAS, B.S., M.S. degrees in environmental sciences, ecology, and biology and a Ph.D. in Earth Resources Management (air quality and ecosystems focus area) from Colorado State University. His areas of expertise include minerals management and air quality, wildland fire and wildland fire smoke, air quality impacts to ecosystems, and climate variability.

Philip J. Riggan is an ecologist with the US Forest Service, Pacific Southwest Research Station, stationed at the Riverside Fire Laboratory, Riverside, California. He holds Ph.D. from the College of Forest Resources at the University of Washington (1979) and B.Sc. in chemistry from San Diego State University. Dr. Riggan has conducted research on remote measurement of wildfire properties; the ecology and effects of fire in Mediterranean-type ecosystems of California; and the global consequences of wildland fire in tropical ecosystems. He has been Principal Investigator and leader of the Forest Service/IBAMA *Working Group on Fire and Environmental Change in Tropical Ecosystems* and led eight airborne campaigns in Brazil that made the first high-resolution, synoptic, and quantitative remote sensing measurements of large wildland fires. He is currently Principal Investigator on projects developing and applying thermal-imaging technology for wildfire measurement in the western United States.

John O. Roads is a Director of the Climate Research Division at the Scripps Institution of Oceanography and a Professor at the University of

California in San Diego. He received his Ph.D. in Meteorology in 1977 from the Massachusetts Institute of Technology, Cambridge, M.A. and B.A. in Physics 1972 from the University of Colorado, Boulder, CO.

Glenn Rolph is a research meteorologist with the National Oceanic and Atmospheric Administration's Air Resources Laboratory in Silver Spring, Maryland. His work is primarily focused on transport and dispersion modeling with an emphasis on building better model user interfaces. He has published several papers on the use of the HYSPLIT transport and dispersion model for acid rain deposition and developed a web-based system of tools that enable researchers to run the HYSPLIT model and explore the meteorological data used by the model. Recently, he has been working with a team at NOAA to implement the Smoke Forecast Tool into operations at the National Weather Service.

Alexei N. Rublev received his Ph.D. in 1985 and M.S. at the Dzerzhinsky Military Academy, Moscow, 1976. He has been a senior Research Scientist at the Institute of Molecular Physics since 1992. His area of expertise are optical radiative transfer in random media, mathematical models for interpretation of satellite and ground-based radiometric measurements.

Mark Ruminski received his B.S. and M.S. degrees in Meteorology from St Louis University. He has worked in NOAA for the past 23 years, mainly in an operational capacity analyzing and forecasting weather, land, and atmospheric hazards such as tropical storms, volcanic eruptions and flash floods. Since 1999 he has been the fire program team leader in the NOAA/NESDIS Satellite Analysis Branch (SAB) and worked with the team that developed the Hazard Mapping System that is used to generate NOAA's satellite-based daily fire and smoke analysis for North America. Mark has recently been involved with transferring the HMS technology to Mexico, Thailand, and Panama.

Jesús San-Miguel-Ayanz is a Senior Researcher at the Institute for Environment and Sustainability of the EC Joint Research Centre (JRC) in the field of forestry. He is a leader of the JRC FOREST project (http://forest.jrc.it), which focuses on the development of methods for the assessment of the state of European forests (including e.g. forest resources, forest condition, forest fires). He received his Ph.D. and M.Sc. degrees (specialty in Remote Sensing and GIS) from the University of California, at Berkeley (in 1993 and 1989, respectively) and the Forest Engineering Degree (1987) by Polytechnic University of Madrid. Since 1997 he has been working at the JRC; he was (1995–1997) Associate

Professor and (1994–1995) Assistant Professor of Forest Inventory, Forest Mensuration and Remote Sensing at University of Cordoba, Spain.

David V. Sandberg, Ph.D., is an emeritus scientist with US Forest Service Research and sole proprietor of *Sam's FireWorks*, a consulting firm to conduct research, development, and policy analysis related to the role of wildland fire in global change, ecosystem health, and environmental quality. His specialty includes assessing changes in flammability and fire effects caused by climate change, land-use, and ecosystem management policy. Current research includes fire behavior modeling, prediction of environmental effects, and developing protocols to account for the carbon credits due to fuels and fire management.

Guido Schmuck is a Head of the Land Management and Natural Hazards Unit of the Institute for Environment and Sustainability, the European Commission-Joint Research Centre in Ispra, Italy. He completed his M.Sc. in 1984 and his Ph.D. in 1986 in biology studying vitality of trees and forest damage at the Technical University of Karlsruhe, Germany. He has been involved in development of the Pathfinder Phase (User requirement segment) Management of the Optical Systems Sector within the Advanced Techniques Unit of IRSA, development and implementation of the Human Capital and Mobility Network "Synergy of Remotely Sensed Data" and management of the EUREKA – project on "Laser Fluorescence Remote Sensing of vegetation (LASFLEUR).

Steve J. Seybold received a B.Sc. in Forest Resources from the University of Wisconsin-Madison in 1983, and a Ph.D. in Entomology from the University of California at Berkeley in 1992. He is currently a research entomologist with the Pacific Southwest Research Station, US Forest Service, in Davis, California. He specializes in the chemical ecology and biochemistry of pine bark beetles with an emphasis on invasive species in urban and wildland forests.

Allen M. Solomon is currently the US Forest Service National Program Leader for Global Change Research. He is a plant ecologist and paleoecologist who has studied the terrestrial ecology of the global carbon cycle for the past 30 years. He edited the Bulletin of the Ecological Society of America from 1992 to 2004 and was awarded the 2003 ESA Distinguished Service Citation. His B.A. (1965) is in Biology from the University of Michigan, Ann Arbor Michigan and Ph.D. (1970) in Botany from Rutgers University, New Brunswick New Jersey.

Milt Statheropoulos, Ph.D., is a Professor of Analytical Chemistry at the National Technical University of Athens (NTUA), Greece, Head of the Field Analytical Chemistry and Technology Unit at NTUA (FIACTU/NTUA), and a Director of the European Center for Forest Fires (Center in the framework of the Council of Europe). He is an Editor of the Forest Fire Net, a publication of the European Center for Forest Fires. His research activities are field chemical analysis in disasters, early location of entrapped people, air quality monitoring in forest fires, and air toxics.

Ryszard Szczygieł, Ph.D., is a senior research scientist in the Forest Research Institute (IBL) in Warsaw (Poland) and lecturer in the Main School of Fire Service in Warsaw. Between 1992 and 2005 he was a general director of the Science and Research Centre for Fire Protection. His professional interests are modelling of forest fires and methods of forest fires fighting and forest fire risk assessment.

Leland Tarnay is a physical scientist for Yosemite National Park, National Park Service. He earned his Ph.D. in Environmental Sciences in 2001 from the University of Nevada, Reno and a Bachelor of Science in 1995 from the University of California, Davis. His current work focuses on air resource issues as they relate to Yosemite National Park and similar Sierra Nevada Landscapes.

Robert G. Tissell is a computer and remote sensing specialist for the USDA Forest Service, Pacific Southwest Research Station, stationed at Seattle, Washington. He earned a Bachelor of Science degree in Biology from the University of California, Riverside in 1986 and has been employed by the Forest Service since that time. He has been a principal remote-sensing analyst for the Forest Service/IBAMA *Working Group on Fire and Environmental Change in Tropical Ecosystems* and for development and application of the FireMapper thermal imaging radiometer.

Barbara Ubysz, Ph.D., is a senior research scientist in the Forest Research Institute (IBL) in Warsaw (Poland), head of the Forest Fire Protection Department. His professional interests are studying the processes of the combustion in the forest environment, forest fire effects, their estimation and prognosis methods, and evaluation and forecasting of forest fire danger and risk.

Shawn P. Urbanski is an atmospheric chemist with the Fire, Fuels and Smoke Program at the US Forest Service, Rocky Mountain Research Station, Fire Sciences Laboratory in Missoula, Montana. Dr. Urbanski received his baccalaureate degree in meteorology from the University of Oklahoma in 1993 and his doctorate in atmospheric science from Georgia Institute of Technology in 1999. His doctorate research was a laboratory investigation of the atmospheric oxidation of dimethylsulfide. Dr. Urbanski enjoyed several years as postdoctoral fellow at Harvard University where he studied terrestrial carbon exchange and developed instrumentation for the measurement of atmospheric trace gases. His current research activities include field and laboratory studies characterizing wildland fire emissions and the development of biomass burning emission inventories.

Joseph K. Vaughan is a Research Assistant Professor with the Laboratory for Atmospheric Research in the Department of Civil and Environmental Engineering at Washington State University, in Pullman, WA. Joe has been a primary developer of two air quality modeling systems: the AIRPACT regional forecasting system and the ClearSky field-burning plume forecasting system. Joe has trained and worked with officials in Idaho and Washington as well as the Nez Perce and Coeur d'Alene tribes on applying the ClearSky system for management of crop residue disposal burning. Joe has an A.B. in Astronomy from Vassar College, an M.S. from Duke University in Environmental Studies, and a Ph.D. in Civil Engineering from the Washington State University.

Domingos X. Viegas, Ph.D., is a Full Professor at the Department of Mechanical Engineering of the Faculty of Science and Technology of the University of Coimbra, in Portugal. He has developed his research activity in the fields of Industrial Aerodynamics, Wind Engineering and Forest Fire propagation. He has been the Head of a research unit on forest fires at the University of Coimbra since 1986. He has coordinated various National and European research projects in this field. He is the author of many publications and Lecturer at several international meetings on the topic of forest fires. He has promoted five International Conferences on Fire Science, and has organized many other scientific meetings, training courses, and seminars about forest fires.

Alan Wain has been researching particulate transport since 1992. He obtained his Ph.D. from Monash University for a thesis examining air parcel transport over the South East Asian region. Employed since 1999 by the Bureau of Meteorology, Alan is currently engaged in the development of Smoke Dispersion Forecasting for Australia, part of the Bushfire Co-operative Research Centre's research program.

David R. Weise has been involved in fire research in the United States since 1980. He earned a B.S. in Forest Management (1984), M.S. in Forest Biometrics (1986) from Auburn University, and Ph.D. in Wildland

Resource Science (1993) from the University of California, Berkeley. Current research interests include fire spread in live fuels and application of models in fire management. He is one of a few individuals who have worked at all three of the US Forest Service's Fire Labs and has served as Project Leader of various fire research units at the Forest Fire Laboratory in Riverside, CA since 1994.

B. Mike Wotton is a Research Scientist with the Canadian Forest Service (Natural Resources Canada) and specializes in fuel moisture, fire occurrence, and fire behaviour modelling. His current research focuses on development of a new generation of models for the Canadian Forest Fire Danger Rating System and the development and implementation of fire occurrence prediction systems throughout Canada. He works frequently with forest fire management agencies in Canada to develop models for use as operational decision aids.

Haoruo Yi is a Research Professor with the Chinese Academy of Forestry and specializes in Fire Remote Sensing and Fire Danger Forecasting. His current research focuses on development of an operational system of fire monitoring and fire management for tropical forest in China. He manages the fire research projects.

Fengming Yuan is a Research Associate at the University of Arizona. He earned B.S. in Soil Sciences and Plant Nutrition from the Central-China Agricultural University (Wuhan, China) in 1990, M.S. in Soil Sciences from the Chinese Academy of Agricultural Sciences (Beijing, China) in 1993, and Ph.D. in Soil Sciences from the University of Wisconsin—Madison, in 2003. His main research interests include experimental and modeling studies of water, carbon, and nitrogen cycling in terrestrial ecosystems, to understand the complexity of energy, carbon, water, and nutrients in ecosystems and to aid in decision-making relevant to utilization and management at regional or global scales.

Tomasz Zawiła-Niedźwiecki, Ph.D., is a professor of remote sensing and GIS in the Faculty of Forest and Environment of the University of Applied Sciences in Eberswalde (Germany) and of the University of Ecology and Management in Warsaw (Poland). His professional interests are application of remote sensing in environmental protection, forestry and disaster management.

Shiyuan (Sharon) Zhong is an associate professor in the Geography Department of Michigan State University. She earned her Ph.D. from Iowa State University in 1992 and her M.S. from Institute of Atmospheric Physics, Chinese Academy of Sciences in 1985. She has authored/co-authored 50 research articles in the areas of boundary layer and mesoscale meteorology, atmospheric transport and dispersion and air pollution, fire–atmosphere interactions, and regional climate modeling. She has been an editor for Journal of Applied Meteorology and Climatology since 2003.

Sergiy Zibtsev, Ph.D., is an Associate Professor and Senior Researcher at the Institute of Forestry and Landscape Architecture, National Agricultural University of Ukraine in Kiev, Ukraine. He is an expert in understanding the radionuclide migration in forest ecosystem after the Chernobyl incident and has nine-year experience of forest monitoring in Ukraine. He was a Fulbright Fellow at Yale University in 2003–2004. Dr. Zibtsev received a Diploma Engineer degree in forestry from National Agricultural University of Ukraine in 1984 and a Ph.D. degree from Dnipropetrovs'k State University in 1990.

Acknowledgements

The editors would like to thank many people who have contributed to the success of this book. Elena Paoletti, Coordinator of the Research Group 7.01. ''Impacts of Air Pollution and Climate Change on Forest Ecosystems'' of the International Union of Forest Research Organizations has been a strong advocate of the symposium ''Forest Fires and Air Pollution Issues'' organized in Riverside, CA on September 11, 2006, and the book that resulted from that meeting. Erik Berg, Manager of the Joint Fire Science Program has been instrumental in assuring financial support for the symposium and production of this book. Susan Schilling helped with various administrative and technical tasks during the entire cycle of the book production. Laurie Dunne provided highly professional and flexible editorial services. Linda Versteeg-Buschman of Elsevier with great patience and understanding supported the editors. Sincere thanks go to the reviewers of individual chapters: Paulo Barbosa, Tina Bell, Randall Benson, Richard Birdsay, Tina Boucher, Robert Burgan, Scott Chang, Shyh Chen, Roland Draxler, Jo Ann Fites-Kaufman, Mark Fenn, Francis Fujioka, Rick Graw, Warren Heilman, Cindy Huber, Chris Johnson, Robert Keane, Jacek Kozak, Bob Kremens, Yongqiang Liu, Rainer Matyssek, Kevin McKelvey, Donald McKenzie, Sylvia Mori, Max Moritz, Roger Ottmar, Jeanne Panek, David Peterson, Janice Peterson, Thomas Pierce, Brian Potter, Miriam Rorig, Lindsey Rustad, Hanna Sakowska, Jesus Santamaria, Martin Schultz, Uma Shankar, William Sommers, Alan Taylor, Jan Van Wagtendonk, David Weise, Christine Wiedinmyer and Ruixin Yang.

We extend our thanks to Professor Sagar V. Krupa, editor of the Elsevier series ''Developments in Environmental Sciences'' for his continuous support during the production of this book.

Financial support for the book has been provided by the Joint Fire Science Program and the US Forest Service Pacific Southwest Research Station.

This page intentionally left blank

Preface

Environment pollution has played a critical role in human lives since the early history of the nomadic tribes. During the last millennium industrial revolution, increased population growth and urbanization have been the major determinants in shaping our environmental quality.

Initially primary air pollutants such as sulfur dioxide and particulate matter were of concern. For example, the killer fog of London in 1952 resulted in significant numbers of human fatality leading to major air pollution-control measures. During the 1950s, scientists also began to understand the cause and atmospheric mechanisms for the formation of the Los Angeles photochemical smog. We now know that surface level ozone and photochemical smog are a worldwide problem at regional and continental scales, with specific geographic areas of agriculture, forestry and natural resources, including their biological diversity at risk. As studies continue on the atmospheric photochemical processes, air pollutant transport, their atmospheric transformation and removal mechanisms, so is the effort to control the emissions of primary pollutants (sulfur dioxide, oxides of nitrogen, hydrocarbons and carbon monoxide), mainly produced by fossil fuel combustion.

During the mid-1970s environmental concerns regarding the occurrence of "acidic precipitation" began to emerge to the forefront. Since then, our knowledge of the adverse effects of air pollutants on human health and welfare (terrestrial and aquatic ecosystems and materials) has begun to rise substantially. Similarly, studies have been directed to improve our understanding of the accumulation of persistent inorganic (heavy metals) and organic (polyaromatic hydrocarbons, polychlorinated biphenyls) chemicals in the environment and their impacts on sensitive receptors, including human beings. Use of fertilizers (excess nutrient loading) and herbicides and pesticides in both agriculture and forestry and the related aspects of their atmospheric transport, fate and deposition; their direct runoff through the soil impacts on ground and surface water quality and environmental toxicology have become issues of much concern.

In the recent times environmental literacy has become an increasingly important factor in our lives, particularly in the so-called developed nations. Currently the scientific, public and political communities are much concerned with the increasing global scale air pollution and the consequent global climate change. There are efforts being made to totally ban the use of chloro-fuorocarbon and organo-bromine compounds at the global scale. However, during this millennium many developing nations will become major forces governing environmental health as their populations and industrialization grow at a rapid pace. There is an on-going international debate regarding policies and the mitigation strategies to be adopted to address the critical issue of climate change. Human health and environmental impacts and risk assessment and the associated cost-benefit analyses, including global economy are germane to this controversy.

An approach to understanding environmental issues in general and in most cases, mitigation of the related problems requires a systems analysis and a multi- and interdisciplinary philosophy. There is an increasing scientific awareness to integrate environmental processes and their products in evaluating the overall impacts on various receptors. As momentum is gained, this approach constitutes a challenging future direction for our scientific and technical efforts.

The objective of the book series *Developments in Environmental Science* is to facilitate the publication of scholarly works that address any of the described topics, as well as those that are related. In addition to edited or single and multi-authored books, the series also considers conference proceedings and paperback computer-software packages of publication. The emphasis of the series is on the importance of the subject topic, the scientific and technical quality of the content and timeliness of the work.

Sagar V Krupa
Editor-in-Chief, Book Series

Introduction

Wildland fires are one of the most devastating and terrifying forces of nature. They are unpredictable and most of the time uncontrollable. They draw strength from the wind, and are particularly devastating in areas prone to drought. Old growth forest stands can be consumed in minutes leaving nothing but skeletal remains. Or the fire may leave the tree canopies untouched, but scour the forest floor consuming understory vegetation. Fires fill the sky with heat and gloom, raining ashes and brands of fire for miles. In a matter of hours wildland fires can change entire landscapes. While their effects are mostly destructive they also help with regeneration of forests and other ecosystems. Low-intensity fire can clear dangerously accumulating underbrush and duff preventing catastrophic crown fires, and allowing seeds of the sun-loving trees to germinate. Health and survival of such ecosystems as mixed conifer forest with giant sequoia and ponderosa pine or chaparral with various *Ceanothus* species depend on the re-occurrence of fires.

In North America the area and intensity of wildland fire has been growing alarmingly during the past decade. Our choice of the word ‘‘alarmingly’’ is deliberate. During the past 10 years almost every year has seen an increase in total numbers of wildfires and the surface area burned over the previous year. Correspondingly, each year has cost the United States federal, state and local governments more than during the previous one. This experience is also true for Australia, Europe and Asia. Increasingly scientists and land managers are viewing this as a global change in wildland fire. It is not only that fires are increasing in number. It is rather that the nature of wildland fire is changing. Over 90% of the area burned in North American in the past five fire seasons has been consumed by only 1% of the fires. This data demonstrates that a few large fires are burning over larger areas. Additionally, the intensity and spread rates of these fires are often beyond the accepted fire indices used by forest managers to describe fire danger and intensity. These huge fires that burn for weeks over whole landscapes have been given a new name – they are called MegaFires, a name that has frightening implications for managing forests in decades to come.

It is the role of the International Union of Forest Research Organizations (IUFRO) to be the champion of forests, squaring off against even the most difficult problems, using scientific exchange and cooperative research as its main tools. In September of 2006 the IUFRO Research Group 7.01 "Impacts of Air Pollution and Climate Change on Forest Ecosystems" held a meeting in Riverside, California, to discuss wildland fire and its role in the atmospheric environment. At the meeting a select group of distinguished scientists and resource managers was called together to share information and research concerning wildland fire. A challenging theme of the meeting was the feedback between wildfire and the Earth's climate system. This theme was additionally explored while considering the effects of air pollution on forest fire fuels and the effects of wildland fire smoke on air quality. Several ideas arose that are of note. First, that MegaFires are a result of primarily short-term climate fluctuations, often termed climate variability. This variability, combined with the effects of past management practices which tend to increase fuel loading in forest systems, has made these dramatically large and intense fires possible. Secondly, air pollution in the form of elevated ground-level ozone and atmospheric nitrogen deposition has been a contributing factor to MegaFires in areas of North America. Finally, wildland fire smoke is becoming an increasingly significant health hazard. Managing and regulating smoke, however, has only been successfully applied to small prescribed fires. At present there are neither techniques nor regulations to manage smoke hazards from MegaFires. These fires have potential to adversely affect the health of millions of people through smoke exposure at concentrations far beyond air quality regulatory standards.

The purpose of this book is to provide a deeper understanding of wildland fires and air quality by exploring their unknowns, paradoxes and challenges. In the book the reader will find the knowledge offered at that unique international conference. The book is purposed as a practical walk along a scientific path to new comprehension, leading from facts to reasoning, understanding, and finally, it is hoped – to action. In the first section of the book the basics of wildland fires and resulting emissions are presented from the perspective of changing global climate, air quality impairment and effects on environment and human health and security. In the second section, effects of wildland fires on air quality, visibility and human health in various regions of the Earth are discussed. The third section of the book deals with complex issues of the ecological impacts of fires and air pollution in forests and chaparral in North America. The fourth section discusses various management issues facing land and fire managers which are related to wildfires, use of prescribed fires and air quality. This section also presents various models and modeling systems used for describing fire dangers and behavior as well as smoke and air pollution predictions applied in the risk assessment analysis. Finally, the book concludes with a series of expert recommendations for wildland fire and atmospheric research both in North America and internationally.

The ancients viewed fire as one of the four elements or elementals of which all things, animate and inanimate, were composed. It was in the balance of the four elementals of earth, air, water and fire that life was possible. As you read this written record of the important IUFRO meeting it encapsulates, the authors hope that you will find both a balance of essential elements and a sure guide to their understanding. Through science modern man has increased his understanding from four ancient elementals to modern physics, from an Earth-centric cosmos to a new understanding of the Universe as a Multiverse. Now as we face a new era in wildland fire, the era of the MegaFire, we apply our best science as a world-embracing partnership under the banner of the IUFRO. By such humble yet hopeful steps we try to unravel various wildland fire enigmas and paradoxes strand by strand.

Andrzej Bytnerowicz, Michael Arbaugh,
Christian Andersen, and Allen Riebau

This page intentionally left blank

Section I:
General Information and Emissions

This page intentionally left blank

Developments in Environmental Science, Volume 8
A. Bytnerowicz, M. Arbaugh, A. Riebau and C. Andersen (Editors)

ISSN: 1474-8177/DOI:10.1016/S1474-8177(08)00001-6

Chapter 1

Impacts of Vegetation Fire Emissions on the Environment, Human Health, and Security: A Global Perspective

Johann G. Goldammer, Milt Statheropoulos and Meinrat O. Andreae*

Abstract

Air pollution generated by vegetation fire smoke (VFS) is a phenomenon that has influenced the global environment in prehistoric and historic time scales. Although historic evidence of the impacts of VFS on societies is scarce, there are indications that VFS has been a factor that influenced society significantly since the Middle Ages. In recent decades, increasing application of fire as a tool for land-use change has resulted in more frequent occurrence of extended fire and smoke episodes with consequences on human health and security. Some of these events have been associated with droughts that are attributed to inter-annual climate variability or possible consequences of regional climate change. In metropolitan or industrial areas, the impacts of VFS may be coupled with the emission burden from fossil fuel burning and other technogenic sources, resulting in increasing adverse affects on the human population. We review the character, magnitude, and role of pyrogenic gaseous and particle emissions on the composition and functioning of the global atmosphere, human health, and security. Special emphasis is given on radioactive emissions generated by fires burning in peatlands and on terrain contaminated by radionuclides. The transboundary effects of VFS pollution are a driving argument for developing international policies to address the underlying causes for avoiding excessive fire application, and to establish sound fire and smoke management practices and protocols of cooperation in wildland fire management at an international level.

*Corresponding author: E-mail: johann.goldammer@fire.uni-freiburg.de

1.1. Introduction

1.1.1. Vegetation fire–smoke pollution: Prehistoric and historic evidence

Prehistoric occurrence of fire smoke emissions and the deposition of fire–smoke aerosol in lakes and on ice have been documented by a large number of sediment and ice core studies, which provide important sources for reconstruction of fire activities (Clark et al., 1997). In addition to biogenic, marine, and soil-dust particles, the smoke from vegetation fires has determined the composition and functioning of the natural global atmosphere before the expansion of human populations and the industrial age (Fig. 1.1; Andreae, 2007).

In the history of land-use phenomena and problems, vegetation fire smoke (VFS) has been documented in a few cases. One example is the smoke pollution generated by land-use fires and land-use change in northern Germany since the 16th century. At that time, large uncultivated bogs and swamps dominated the region. With population growth, people were forced to enlarge the area under production and started to cultivate these areas by burning the bogs (Goldammer, 1998).

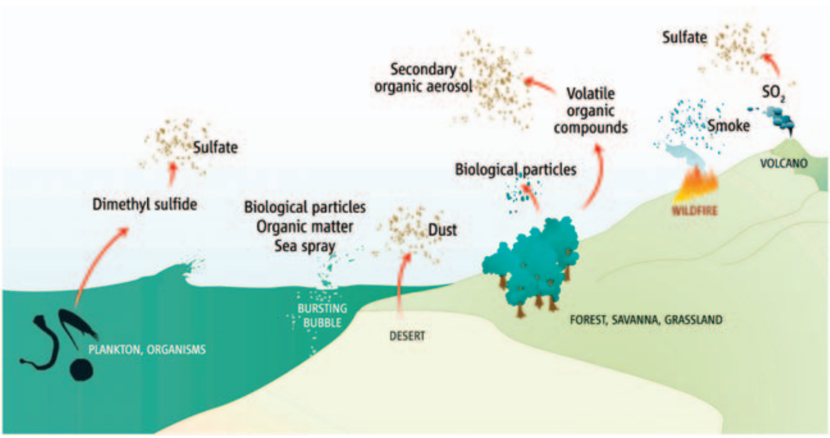

Figure 1.1. Sources of aerosol particles to the natural atmosphere: Primary particles—such as sea spray, soil dust, smoke from wildfires, and biological particles including pollen, microbes, and plant debris—are emitted directly into the atmosphere. Secondary particles are formed in the atmosphere from gaseous precursors; for example, sulfates are formed from biogenic dimethyl sulfide and volcanic sulfur dioxide (SO_2), as well as, secondary organic aerosol from biogenic volatile organic compounds. (Reprinted with the permission of Andreae 2007 and the American Association for the Advancement of Science (AAAS). Copyright: AAAS, 2007.)

Burning of bogs began usually in mid-May and ended in June. The drying of the organic material and the heat caused the break up of the normally barely accessible plant nutrients of the bog, enabling cultivation of oats and buckwheat on the freshly burned fields without fertilization. The burning of bogs was first noted in the year 1583. Smoke pollution from bog burning (Fig. 1.2) seemed to have an oppressive effect in northwestern Germany, even in areas far away. This effect, the ‘‘smell of burning’’ was known under the term ‘‘High Smoke’’. First historic evidence of an extended regional European fire–smoke episode dates back to the end of the 17th century. In 1657, the bog burnings began on May 6 in Northern Friesland, carried by strong easterly winds. On the next day, the smoke reached Utrecht (Netherlands), and a little bit later had changed direction, passing Leeuwarden towards Den Helder, and reaching the sea on May 15. There, the wind changed northwest and drove the bog smoke back, so that on May 16 it had reached Utrecht and Nijmwegen again. At the same time, the smoke was also noticed in Hanover, Münster, Köln, Bonn, and Frankfurt. On May 17, 1657, the smoke reached Vienna, on May 18 Dresden, and on May 19 Kraków (Poland).

Figure 1.2. Moor burning in Friesland (Frisia) around 1900. Sometimes smoke from these land-use fires covered large areas of Europe. (*Source*: Archive, Fire Ecology Research Group/Global Fire Monitoring Center.)

Other historic evidence is provided by the description of a large-scale fire–smoke pollution in Russia in 1915 (Shostakovich, 1925). Reports indicate the effects of a 50-day fire episode between June and August 1915, during which more than 140,000 km^2 of forest lands were affected by fire between Angara River and Nijnya Tunguska. Smoke pollution was reported on a total land area of about 6 million km^2 with extreme pollution, resulting in visibility of less than 20 m on more than 1.8 million km^2.

1.1.2. Contemporary trends in vegetation fire–smoke pollution

As a consequence of demographic developments and increasing pressure on vegetation resources in many developing countries, the application of fire as a land-clearing tool in large-scale land-use change projects, increased rapidly over the past three to four decades. In addition to traditional land clearing by small landholders shifting cultivation (slash-and-burn agriculture), the establishment of pastures and sugar cane plantations in Brazil, forest clearing for the establishment of palm oil plantations, or other cash crops in Southeast Asia, and other tropical regions involves massive burning of vegetation. During droughts, such as the dry spells associated with the El Niño-Southern Oscillation phenomenon, land-use fires also escape to large uncontrolled wildfires, reinforcing the fire–smoke burden at regional scales.

Other regions that are undergoing urbanization are experiencing an abandonment of the rural space. The rural exodus often results in an increase of wildfire hazard, due to decreasing land cultivation and utilization of vegetation resources. Increased fuel loads (combustible materials) are resulting in more severe and often uncontrollable fires. Portugal is one of the most impressive examples where land abandonment—coupled with the establishment of highly flammable eucalypt and pine plantations—has resulted in extended fire and smoke pollution episodes (Varela, 2006).

Other regions of the world are suffering an unhealthy combination of socioeconomic, political, and environmental drivers of ecosystem impoverishment and land degradation. In countries undergoing political and economic transition in Eurasia the institutional and political capabilities to practice efficient forest fire management have declined to an extent that fires are becoming almost uncontrollable. This is especially the case in the central Asian region (Goldammer, 2006a), where regional droughts associated with illegal forestry activities, arson, and negligence have resulted to extended severe fire episodes with smoke pollution affecting neighboring countries and long-range smoke transport in the Northern Hemisphere.

1.2. Fundamentals

1.2.1. VFS formation

Generally, vegetation fire can be considered as a four-phase process consisting of the pre-ignition, flaming, smoldering, and glowing phases. In the first phase (pre-ignition), heat from an ignition source or the flaming front evaporates water and the low molecular weight volatiles from the fuel and the process of pyrolysis begins. In the second phase (flaming), combustion of the pyrolysis products (gases and vapors) with air takes place. Flaming occurs if these products are heated to the ignition point (325–350°C) (US NWCG, 2001). The heat from the flaming reaction speeds the rate of pyrolysis and produces greater quantities of combustible gases, which also oxidize, causing increased flaming. The third phase (smoldering) is a very smoky process occurring after the active flaming front has passed. Combustible gases are still produced by the process of pyrolysis, but the rate of release and the temperatures are not high enough to maintain flaming combustion. Smoldering generally occurs in fuelbeds with fine packed fuels and limited oxygen flow. In the fourth phase (glowing), most of the volatile gases have been burned, and oxygen comes into direct contact with the surface of the charred fuel. As the fuel oxidizes, it burns with a characteristic glow, until the temperature is reduced so much that combustion cannot be continued, or until all combustible material is consumed (Johnson, 1999).

A vegetation fire is the result of interaction of three components—fuel, oxygen, and heat of combustion (fire triangle). The fuel is in principle the forest, or more generally, the vegetation. However, other types of fuels and/or materials may contribute to the VFS formation and composition during the flame-front expansion (Statheropoulos & Karma, 2007).

Vegetation fuels have specific characteristics, such as fuel moisture and fuel temperature, which contribute to the combustion process (see this volume, for a full discussion of weather and climatic influences on fire and combustion). Generally, vegetation fuel with high moisture content, such as big branches or tree trunks, produces water vapor that lowers the temperature of combustion and hence favors smoldering. The specific characteristics of the fuel, such as the amount and size burned, contribute mainly to the quantity of the smoke produced.

The oxygen-(O_2)-to-fuel ratio can be affected by wind speed and direction and also vegetation characteristics, such as vegetation density (packing ratio), shape, and arrangement (structure). The O_2-to-fuel ratio mainly contributes to the type of components in the VFS. For example, evolution of carbon monoxide (CO) and fine particles dominates in incomplete combustion (limited oxygen flow, smoldering phase), whereas in complete combustion (oxygen flow, flaming phase) the emission of carbon dioxide (CO_2) and H_2O is favored. However, O_2 flow also affects the amounts of smoke produced: the amount of particulate emissions generated per mass of fuel consumed during the smoldering phase is more than double that of the flaming phase (US NWCG, 2001).

The heat component of the fire triangle can contribute to the smoke components produced. An indicative example is that organic degradation of pine needles has been found to commence at 200–250°C, while maximum evolution rate of organic volatiles was found to occur in the temperature range 350–450°C (Statheropoulos et al., 1997); according to another source, peak production of combustible products was found to occur when the fuels were heated in the range of 300°C (Johnson, 1999). Recently, airborne measurement of sensible heat and carbon fluxes in fire plumes were combined with remote measurements of flame properties to provide consistent remote-sensing-based estimators of these fluxes. These estimators provide a mean to determine rates of fuel consumption and carbon emission to the atmosphere by wildland fires as required for assessments of fire impacts on regional air pollution or global emissions of greenhouse gases (Riggan et al., 2004).

1.2.2. VFS chemical composition

Generally, VFS is considered an aerosol, which is defined as a colloidal system in which the dispersed phase is composed of either solid or liquid particles in gas, usually air (Johnson, 1999).

VFS, basically, consists of water vapor, permanent gases, volatile organic compounds (VOCs), semi-volatile organic compounds (SVOCs), and particles (Andreae and Merlet, 2001). Permanent gases include CO_2, CO, nitrogen oxides (NO_x) (Muraleedharan et al., 2000; Radojevic, 2003). Sulfur oxides (SO_x) and ammonia (NH_3) have also been reported. SO_x are usually produced in small quantities, because in general vegetation fuel sulfur content is low (Ward & Smith, 2001). Concentrations of SO_2 identified in Brunei Darussalam during the 1998 smoke-haze episode were below World Health Organization (WHO) guidelines levels of 100–150 $\mu g m^{-3}$ (Radojevic, 2003). However, high amounts of sulfur-based compounds are created when sulfur-rich vegetation or soil are burned; for instance, significant quantities of SO_2 and hydrogen sulfide (H_2S) were produced by forest fires burning in Yellowstone National Park (Reh & Deitchman, 1992). NH_3 has been measured in forest and savannah fires (Hegg et al., 1988, 1990; Lacaux et al., 1995; Koppmann et al., 2005). However, the emission ratio of NH_3 relative to CO_2 has generally been found low; NH_3 is primarily emitted during the smoldering rather than during the flaming phase of combustion (Koppmann et al., 2005).

Methane (CH_4) and various VOCs have been found in VFS (Heil & Goldammer, 2001; Miranda, 2004; Ward, 1999). Hydrocarbons identified were aliphatic, such as alkanes, alkenes, and alkynes. Representative compounds included ethane, heptane, decane, propene, 1-nonene, 1-undecene, and acetylene (McDonald et al., 2000; Shauer et al., 2001; Statheropoulos & Karma, 2007; Ward & Smith, 2001). Additionally, aromatic hydrocarbons, such as benzene and alkylbenzenes have been found; for example, toluene, xylene, and ethyl-benzene (Muraleedharan et al., 2000; Reh & Deitchman, 1992; Statheropoulos & Karma, 2007). Moreover, VOC mixtures included the following oxygenated compounds: alcohols (phenol, m-cresol, p-cresol, guaiacol) (McDonald et al., 2000; Shauer et al., 2001; Statheropoulos & Karma, 2007; Ward & Smith, 2001), aldehydes (formaldehyde, acetaldehyde, furfural, acrolein, crotonaldehyde, benzaldehyde) (Kelly, 1992; Reh & Deitchman, 1992; Reinhardt & Ottmar, 2004; Shauer et al., 2001; Statheropoulos & Karma, 2007), ketones (acetone, 2-butanone) (McDonald et al., 2000; Statheropoulos & Karma, 2007), furans (benzofuran), carboxylic acids (acetic acid), and esters (benzoic acid, methyl ester) (McDonald et al., 2000; Muraleedharan et al., 2000; Reh & Deitchman 1992; Statheropoulos & Karma, 2007; Ward & Smith, 2001). Also, it has been shown that during fireplace pine wood combustion experiments and in a pine forest fire incident, chloro-methane was detected in the smoke produced (McDonald et al., 2000; Statheropoulos & Karma, 2007). Chloro-methane has been identified as the most abundant halogenated hydrocarbon emitted during biomass burning, mainly consisting of dead and living vegetation (e.g., savannahs, fuel wood, agricultural residues; (Andreae et al., 1996; Koppmann et al., 2005; Urbanski et al., this volume). SVOCs found in the VFS were polyaromatic hydrocarbons (PAHs), such as benzo (a) pyrene (Booze et al., 2004; Kelly, 1992; Muraleedharan et al., 2000; Reh & Deitchman, 1992; Ward, 1999) (also see Urbanski et al., this volume).

Generally, VFS contains particulate matter (PM) (Reid et al., 2005). Particles can be coarse, with diameter up to 10 μm (PM_{10}), fine with diameter up to 2.5 μm ($PM_{2.5}$), or ultrafine with diameter smaller than 0.1 μm (Sandström et al., 2005). The PM can be primarily released to the atmosphere due to combustion or can be formed through physical or chemical transformations (molecular agglomeration of supersaturated vapors, nucleation). Primary particles can be elemental carbon or organic carbon particles. Inorganic or elemental carbon, also known as graphitic or black carbon (soot), is a product of the incomplete combustion of carbon-based materials and fuels (CEPA, 1999). Organic carbon can also be produced via secondary gas-to-particle conversion processes. Condensation of hot vapors (VOCs, SVOCs) during combustion processes (tars) and also nucleation of atmospheric species result in formation of new particles, usually below 0.1 μm in diameter. Generally, low-volatility products either nucleate or condense on the surfaces of pre-existing particles, yielding particles in the size range 0.1–1.0 μm (CEPA, 1999).

Trace elements can also be contained in particles produced from forest fires, such as sodium (Na), magnesium (Mg), aluminum (Al), silicon (Si), phosphorus (P), sulfur (S), chlorine (Cl), potassium (K), calcium (Ca), titanium (Ti), manganese (Mn), iron (Fe), zinc (Zn), vanadium (V), lead (Pb), copper (Cu), nickel (Ni), bromine (Br), and chromium (Cr) (Muraleedharan et al., 2000; Radojevic, 2003; Reh & Deitchman, 1992; Ward & Smith, 2001). These species are usually absorbed on the surface of fine particles.

Particles, as PM_{10} and $PM_{2.5}$ have been measured in different forest fires, such as during the Gestosa experimental fires in Portugal (Miranda et al., 2005), during the 1997 haze episode in Southeast Asia (Muraleedharan et al., 2000; Ward, 1999), in the U.S. state of Montana 2000 wildfire season (Ward & Smith, 2001), in Korea during May 2003 (aerosol impact due to forest fires in the Russian Federation) (Lee et al., 2005), and in a forest fire in Greece (Statheropoulos & Karma, 2007).

However, VFS can exist as a more complicated mixture depending on the flame-front pathway. If a vegetation fire is in the interface of an urban area, it is possible the flame-front will co-burn fuels other than vegetation, such as wastes. In this case, synthesis of VFS can be the additive or synergistic result of all the possible emission products due to the pyrolysis and combustion of the vegetation and the wastes; significant quantities of hazardous components, such as dioxines (polychlorinated dibenzo-p-dioxines/polychlorinated dibenzo-furans PCDDs/PCDFs), can also be contained in the resultant VFS. Additionally, when vegetation fires pass over rural fields or rural/urban constructions, then wood, plastics, or fertilizers can also be burned and materials, such as pulverized glass, cement, dust, asbestos, plaster, or other chemical compounds can be contained in the smoke produced. Various scenarios of forest flame-front pathways and the possible related VFS chemical composition have been integrated in a road map for air-quality assessment (Statheropoulos & Karma, 2007).

It has to be noted that radioactive species can, occasionally be found in VFS. Their origin can be from vegetation fuel radioactively contaminated, such as a forest in the site of the Chernobyl Nuclear Power Plant Exclusion Zone (Dusha-Gudym, 2005; Poyarkov, 2006). It has been reported that in 1992, severe wildfires that burned in the Gomel Region (Belarus) spread into the 30 km radius zone of the Chernobyl Power Plant and the level of radioactive cesium in aerosols was increased 10 times within the 30 km zone (Dusha-Gudym, 2005; WHO/UNEP/WMO, 1999) (see Section 1.4.1 of this chapter and Hao et al., this volume).

1.2.3. VFS components concentration and exposure limits

During vegetation fires, high peak concentrations of VFS components can be observed, especially near the flame-front. Table 1.1 presents mean concentrations of VFS components measured in "smoky" conditions in the field (sampling duration 20–30 min) that have been reported in the literature (Miranda et al., 2005; Pinto & Grant, 1999; Reinhardt et al., 2000; Statheropoulos & Karma, 2007), together with the short-term limits recommended by the National Institute for Occupational Safety and Health (NIOSH). In general, exposure limits given by various health organizations that are presented in this chapter for comparison should be considered as indicative and not as references because they refer to indoor occupational exposure.

Concentrations of PM_{10} as high as 47,600 $\mu g\,m^{-3}$ have been found (Reh & Deitchman, 1992), whereas the exposure limit for 24 h given by the American Conference of Governmental Industrial Hygienists (ACGIH) is 150 $\mu g\,m^{-3}$. Moreover, $PM_{2.5}$ levels measured in the field,

Table 1.1. Mean concentrations measured in smoky conditions in the field and short-term occupational exposure limits (STELs)

Compound	Concentration	Short-term exposure limits (NIOSH, 1997)
CO[a]	54 ppm	200 ppm
CO_2[b]	350 ppm	30,000 ppm
Benzene[b]	0.22 ppm	1 ppm
Toluene[b]	0.12 ppm	150 ppm
Xylene[b]	0.08 ppm	150 ppm
Acroleine[a]	0.071 ppm	0.3 ppm
Formaldehyde[a]	0.468 ppm	0.1 ppm
BenzoPyrene (BaP)[c]	7.1 $n\,gm^{-3}$	—
$PM_{2.5}$[a,d]	[a,b]7000 $\mu\,gm^{-3}$, [d]2300 $\mu\,gm^{-3}$	[e]65 $\mu\,gm^{-3}$ (24 h)

[a]Reinhardt et al. (2000).
[b]Statheropoulos and Karma (2007).
[c]Pinto and Grant (1999).
[d]Miranda et al. (2005).
[e]American Conference of Governmental Industrial Hygienists (ACGIH).

at a distance of approximately 70 m from the flame-front, were estimated to be 49,500 $\mu g\,m^{-3}$ (Statheropoulos & Karma, 2007); the respective ACGHI 24 h limit is 65 $\mu g\,m^{-3}$.

Airborne measurements of fire emissions at a distance of 200–1000 m above the flame-front have shown that CO concentration ranged between 100–600 ppb with an average and standard deviation of 310 ± 10 ppb (Yokelson et al., 2007).

1.3. VFS emissions from various vegetation types

National statistical databases on the spatiotemporal extent of wildland fires—numbers and size of fires occurring in forests, other wooded lands, and other lands—are not only important for fire management planning but also for environmental, economic, and humanitarian impact assessments. In the majority of the countries of the world, the data collected by agencies on the ground or by aerial monitoring do not reflect the full extent of wildland fires. In most countries the forestry agencies or other services are collecting data only for the protected forests and other protected vegetation under their respective jurisdiction. Only in a few countries, data of grassland, steppe, and peat bog fires are entering the statistical databases. The fire statistical data provided by the recent survey in the regions of the Global Wildland Fire Network within the Global Forest Resources Assessment 2005 reflect this general situation and therefore do not provide a complete picture (FAO, 2007).

Other data sets on spatial and temporal occurrence of vegetation fires have been produced, based on various spaceborne sensors, such as the National Oceanic and Atmospheric Administration Advanced Very High Resolution Radiometer (NOAA AVHRR), Moderate Resolution Imaging Spectroradiometer (MODIS), Medium-Resolution Imaging Spectrometer (MERIS), Advanced Spaceborne Thermal Emission and Reflection Radiometer (ASTER), and Satellite Pour l'Observation de la Terre or Earth-observing Satellite (SPOT) Vegetation instruments. These data sets include all vegetation types affected by fire. Active fires and area burned recorded from space include both the ecologically benign fires burning in fire-dependent or adapted ecosystems and the economically and environmentally detrimental fires burning in fire-sensitive systems. Thus, these satellite-derived data cannot be compared directly with the conventionally collected data of the forest agencies, which are generally restricted to wildfires occurring in production or protected forests.

One of the global satellite-derived assessments of land areas affected by fire in the year 2000 was conducted by the Global Vegetation

Monitoring (GVM) unit of the Joint Research Center (JRC), in partnership with other six institutions, using the medium-resolution (1 km) satellite imagery provided by the SPOT-Vegetation system (JRC, 2002). According to the data set, the global vegetated area affected by fire in the year 2000 was 350 million ha (details on the area burned by country can be downloaded at the JRC Web site (JRC, 2002)).

Based on such global satellite-derived data sets and/or published statistics and models, a number of studies have been conducted to estimate total global gaseous and aerosol emissions from vegetation fires, such as the most recent Global Wildland Fire Emission Model (GWEM) (Hoelzemann et al., 2004).

Table 1.2 provides an overview of global emission of selected species annually emitted from vegetation fires in the late 1990s, based on emission factors as summarized by Andreae (2004) (for more information on chemical emissions from different fuel types, see Ottmar et al., this volume).

1.4. Smoke dispersion

VFS produced by large vegetation fires is usually transported many kilometres away from the flame-front. Usually, fine particles can be transported to long distances (cross border transfer). Table 1.3 presents some of the VFS pollutants and their transfer through the environment are presented (Brauer, 1999). According to Nakajima et al. (1999), during the 1997 episode in Southeast Asia, the smoke-haze layer covered an area up to 10 million km^2. Moreover, during 2002, the Canadian forest fires in a province of Quebec affected the PM levels of the city of Baltimore in the United States, which is located hundreds of kilometres from the source (Sapkota et al., 2005). Fires in Canada were also found to cause high concentrations of CO and O_3 over a period of 2 weeks in the southeastern and eastern coastal United States during the summer of 1995 (Wotawa & Trainer, 2000).

1.4.1. Transport of radionuclides in VFS

As a result of the failure of the Chernobyl nuclear power plant, a total of 6 million ha of forest lands were polluted by radionuclides. The most polluted forest area covers over 2 million ha in the Gomel and Mogilev regions of Belarus, the Kiev region of Ukraine, and the Bryansk region of the Russian Federation. The main contaminator is caesium-137 (^{137}Cs); in the core zones of contamination, strontium-90 (^{90}Sr) and

Table 1.2. Global annual emission of selected chemical species in the late 1990s (in mass of species per year; $Tg\,a^{-1}$)

Compound[a]	Savanna and grassland	Tropical forest	Extra-tropical forests	Biofuel burning	Charcoal making and burning	Agricultural residues	Total pyrogenic	Fossil fuel burning
Tg dm burned[b]	3160	1330	640	2663	196	1190	9200	—
CO_2	5096	2101	1004	4128	169	1802	14,300	23,100
CO	206	139	68	206	19	110	750	650
CH_4	7.4	9.0	3.0	16.2	1.9	3.2	41	110
NMHC	10.7	10.8	3.6	19.3	0.4	7.6	53	200
Methanol	3.8	2.6	1.3	3.9	0.16	2.1	13.8	—
Formaldehyde	1.1	1.8	1.4	0.4	0.10	1.4	6.3	—
Acetaldehyde	1.6	0.86	0.32	0.36	0.05	0.68	3.9	—
Acetone	1.4	0.83	0.35	0.06	0.05	0.65	3.3	—
Acetonitrile	0.33	0.24	0.12	0.48	0.01	0.21	1.4	—
Formic acid	2.1	1.4	1.8	0.35	0.11	0.3	6.0	—
Acetic acid	4.2	2.8	2.5	2.4	0.30	1.0	13.1	—
NO_x (as NO)	12.2	2.2	1.9	2.9	0.16	3.0	22.3	45
N_2O	0.67	0.27	0.17	0.16	0.01	0.08	1.4	2.0
NH_3	3.4	1.7	0.88	3.5	0.06	1.5	11.0	0.4
SO_2	1.1	0.76	0.64	0.73	0.015	0.48	3.7	228

COS	0.05	0.05	0.02	0.11	0.01	0.07	0.31	—
CH_3Cl	0.24	0.10	0.03	0.14	0.0005	0.28	0.80	—
CH_3Br	0.006	0.010	0.002	0.008	0.00011	0.004	0.031	—
$PM_{2.5}$	16.1	12.0	8.3	19.1	0.34	4.6	60	—
TPM	26.2	11.3	11.3	25.1	1.1	15.5	91	—
TC	11.7	8.7	5.3	13.8	0.24	4.8	45	27
OC	10.6	7.0	5.8	10.5	0.18	3.9	38	20
BC	1.5	0.88	0.36	1.6	0.06	0.82	5.2	6.6
K	1.09	0.39	0.16	0.14	0.02	0.33	2.1	—
CN	1.1E+28	4.5E+27	2.2E+27	9.1E+27	1.3E+26	4.0E+27	3.1E+28	—
CCN (1% SS)	6.3E+27	2.7E+27	1.7E+27	5.3E+27	7.6E+25	2.4E+27	1.8E+28	—
$N_{(>0.12\,\mu m\ diameter)}$	3.7E+27	1.3E+27	6.4E+26	2.7E+27	3.8E+25	1.2E+27	9.6E+27	—

[a]Abbreviations: NMHC, non-methane hydrocarbons; N_2O, nitrous oxide; COS, carbonyl sulfide; CH_3Cl, methyl chloride; CH_3Br, methyl bromide; $PM_{2.5}$, particulate matter $<2.5\,\mu m$ diameter; TPM, total particulate matter; TC, total carbon; OC, organic carbon; BC, black carbon; CN, condensation nuclei; CCN, cloud condensation nuclei at 1% supersaturation; $N_{(>0.12\,\mu m\ diameter)}$: particles $> 0.12\,\mu m$ diameter; $E = 10^{20}$.
[b]1 Tg, 1 million metric tons; dm, dry matter.

Table 1.3. Indicative VFS compounds and how they are transported from the source (Brauer, 1999)

Compound	Example	Notes
Permanent gases	CO, CO_2	Transported over distances[a]
	O_3	Only present downwind of fire-transported over distances
	NO_2	Reactive concentrations decrease with distance from fire
Hydrocarbons	Benzene	Some transport, and react to form organic aerosols
Particles	PM_{10}	Coarse particles are not transported and contain mostly soil and ash
	$PM_{2.5}$	Fine particles transported over long distances

[a]CO measured in the smoke plume of a tropical forest fire was transported to a distance greater than 500 km (Yokelson et al., 2007).

plutonium-239 (^{239}Pu) are found in high concentrations. This region constitutes the largest area in the world with the highest contamination by radionuclides and is located in a fire-prone forest environment in the center of Europe.

Every year, hundreds of wildfires are occurring in the contaminated forests, peatlands, and former agricultural sites. Between 1993 and 2001 a total of 770 wildfires in the closed zone of Ukraine affected 2482 ha. In the period 1993–2000, 186 wildfires occurred in the closed zone of Belarus and affected an area of 3136 ha including 1458 ha of forest. In Ukraine in 2002 alone, a total area of 98,000 ha of wildland was burned in the contaminated region of Polissya.

Under average dry conditions, the surface fuels contaminated by radionuclides—the grass layer and the surface layer of peatlands—are consumed by fire. Most critical is the situation in peat layers, where the radionuclides are deposited. The long-range transport of radionuclides lifted in the smoke plumes of wildfires and their fallout on large areas were investigated in detail in 1992. Radioactive smoke plumes, containing caesium-137, were monitored several hundred kilometres downwind from the sites where fires occurred in May and August 1992 (Dusha-Gudym, 2005).

This risk of radioactive contamination has not decreased substantially and is particularly threatening the population living in the immediate environment of the accident site (4.5 million people). Radioactive emissions are also a high risk for firefighters. In addition, populations are affected by radioactive smoke particles transported over long distances (Dusha-Gudym, 2005; Poyarkov, 2006).

A similar situation is found in Kazakhstan. At the Semipalatinsk Nuclear Weapons Test Site, more than 450 nuclear tests, including about

100 atmospheric tests, were conducted for a period of 40 years between 1949 and 1989. Radioactive contamination is highest in Eastern Kazakhstan, including the fire-prone pine forests along the Irtysh River at the border to the Russian Federation (Gorno-Altay). A recent report reveals that radioactive emissions from fires burning in central Asia in 2003 were recorded in Canada (Wotawa et al., 2006).

1.4.2. Remote-sensing methods to monitor VFS

There are satellite systems with aerosol detection capability. The National Oceanic and Atmospheric Administrationolar Operational Environmental Satellite (NOAA POES) AVHRR and the NASA MODIS are such examples (Fig. 1.3a and b). The NASA Stratospheric Aerosol and Gas

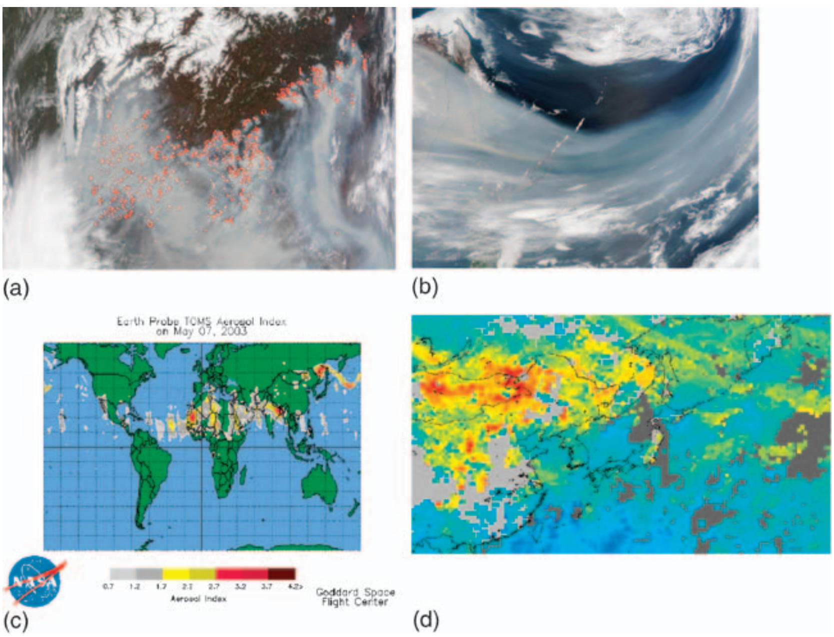

Figure 1.3. (a) Active fires in the Transbaikal Region (Russian Provinces Chita and Buryatia) depicted by the MODIS instrument on Terra, May 8, 2003 (courtesy: NASA). (b) Smoke plume from fires burning in the Transbaikal Region on May 8, 2003, stretching to Sakhalin and northern Japan (MODIS). (c) Smoke plume from fires burning in the Transbaikal Region stretching to Sakhalin and northern Japan (MODIS) on May 7, 2003 as depicted by NASA TOMS. (d) May 3–8, 2003, carbon monoxide concentration originated by VFS in the Transbaikal Region depicted by the MOPITT instrument on the Terra satellite (courtesy: NASA).

Experiment (SAGE) provides vertical resolution. The Total Ozone Mapping Spectrometer (TOMS) depicts aerosols at coarse resolution (Fig. 1.3c). A relationship between MODIS Aerosol Optical Thickness (AOT) and ground-based hourly fine particulate ($PM_{2.5}$) has been shown (Hutchison, 2003; Wang & Christopher, 2003). The Measurement of Pollution in The Troposphere (MOPITT) instrument aboard the NASA Earth-Observing System (EOS) Terra satellite is a thermal and near infrared (IR) gas correlation radiometer, designed specifically to measure CO profiles and total column CH_4 (Figs. 1.3d and 1.4). The CO pollutant can also be used as a tracer for other pollutants, such as ozone at or near ground level (Edwards et al., 2003).

1.5. Environmental impacts

VFS can have impacts on the air, water, and soil. The long-term effects of vegetation fire emissions on atmospheric composition and global processes have been presented and discussed (Houghton et al., 1992). Short-term effects of forest fires include elevated trace gases, aerosol, and CO_2 levels, nitrogen deposition, acid precipitation, and local climatic changes (Bazzaz, 1990; Fan et al., 1990; Vitousek et al., 1997). Environmental impacts of VFS include the increase of the ground-level ozone, due to photochemical reactions of VFS components in the

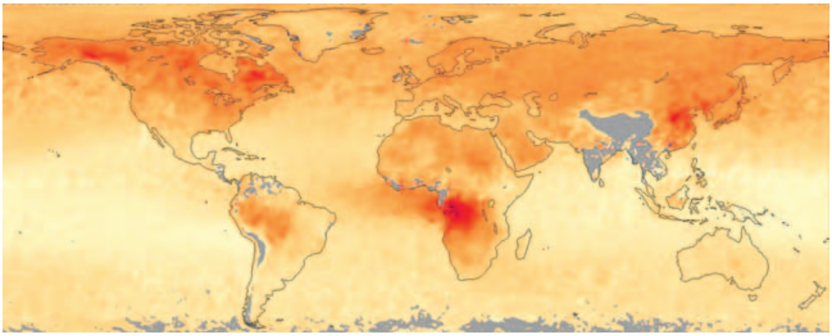

Figure 1.4. Global carbon monoxide (CO) concentrations in the Northern Hemispheric summer of 2004 depicted by the MOPITT sensor. A record fire season in Alaska in 2004 spread smoke across the Northern Hemisphere and elevated CO levels across North America and Europe. Red indicates high concentrations, while yellow indicates low concentrations. The high levels over China are caused by industrial and urban pollution. The high CO concentrations in sub-Saharan Africa are generated by savanna fires. The Alaskan fires released approximately 30 Tg (teragrams: 1 Tg = 1 million metric tons) of CO (NASA Earth Observatory, 2006).

presence of NO_2, CO, and VOCs, the ground-level O_3 precursors (Hogue, 2005). It has been reported that the big wildfires in Alaska and the Canadian Yukon during the summer of 2004 generated huge plumes of CO and other pollutants and affected large areas of the Northern Hemisphere by increasing ground-level O_3 (Barry, 2005). Moreover, according to another study, there was evidence that Canadian forest fires in 1995 changed the photochemical properties of air masses over Tennessee on days during the fire period (USDA, 2002). During the 1997–1998 SE Asia fire–smoke episode, enhanced concentrations of CO_2, and CH_4 were observed throughout the troposphere from eastern Java to the South China Sea (Heil & Goldammer, 2001). Additionally, it has been reported that photosynthesis of three tree species was reduced by the smoke-haze of 1997 in Indonesia, due to elevated aerosol and atmospheric pollutant levels (Davies & Unam, 1999). VFS particles can pollute surface water directly, by deposition, or can become part of the soil. In this case and after a rainfall, suspended soil particles, as well as dissolved inorganic nutrients and other materials, can be transferred into adjacent streams and lakes, reducing water quality and disturbing aquatic ecosystems balance. In sandy soils, leaching may also move minerals through the soil layer into the ground water (USDA, 1989) (also see Section III of this volume).

Recent research reveals that, as a consequence of climate change, mercury deposits once protected in cold northern forests and wetlands will increasingly become exposed to burning. Mercury is released to the atmosphere with fire smoke. Turetsky et al. (2006) quantified organic soil mercury stocks and burned areas across western boreal Canada; it was assumed that, based on ongoing and projected increases in boreal wildfire activity due to climate change, atmospheric mercury emissions will increase and contribute to the anthropogenic alteration of the global mercury cycle and to the exacerbating mercury toxicities for northern food chains.

1.6. Peatland fires

The recurring regional VFS pollution in Southeast Asia, a phenomenon largely resulting from application of fire in land-use change and extended wildfires, has been observed since the 1980s. Despite the 2001 Association of Southeast Asian Nations (ASEAN) Agreement on Transboundary Haze Pollution that aimed at reducing regional smoke-haze caused by VFS, the inappropriate and illegal use of fire land vegetation conversion, especially on drained peatlands, is still practiced (Goldammer, 2006b). Recent public interest on emissions from peatland conversion fires is based on the controversial debate about the increasing conversion of peatlands to establish oil palm plantations as a source of "bioenergy".

While much public attention has been given to regional VFS pollution in Southeast Asia, there is limited scientific and public coverage on the transboundary transport and impacts of peat fire smoke on human health and security in the Northern Hemisphere.

The fact of the matter is that fires burning in drained or desiccated peatlands are an important source of extended fire smoke pollution in formerly cultivated and currently abandoned regions of northern Eurasia. In the western Russian Federation, peatlands have been drained and used for agricultural purposes since the early 19th century. The fen peatlands were used as agricultural fields but are out of use now. According to the Wetlands International Russia Program, peatland fires are a common phenomenon in the Russian Federation (Minaeva, 2002) and may contribute to about 10% of the total area burned (Shvidenko & Nilsson, 2000). In most cases, the fires are started outside the peatlands, caused by forest visitors, hunters, tourists, or by agricultural burning and burning activities along roads. In Fig. 1.5a, a satellite image of the western Russian Federation with heat signatures of peat and forest fires in 2002 is presented.

In September 2002, the VFS from peat and forest fires in the Moscow region reduced the visibility to less than 100 m in Moscow, where the concentration of CO exceeded the permissible values by more than three

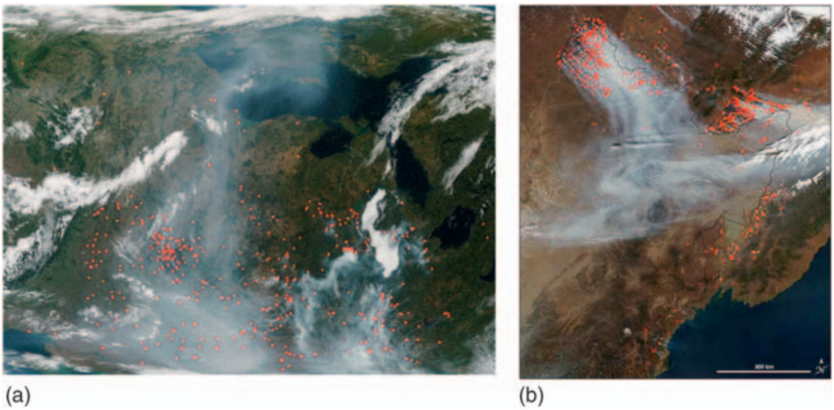

Figure 1.5. (a) Satellite scene of the western Russian Federation on September 4, 2002. The heat signatures of the peat and forest fires are given in red. The smoke plumes (light blue haze) stretch from the Western Russian Federation to Belarus, Poland, and the Baltic Sea. (b) Smoke transport from fires (marked in red) in northern China (top left) and the southeast of the Russian Federation (right) on October 15, 2004. (*Source*: True color image by Moderate-Resolution Imaging Spectroradiometer (MODIS), resolution 2 km.)

times (European Water Management News, 2002). The smoke pollution did not only cause a dramatic reduction of visibility but also had detrimental impacts on the health of the population and resulted in an increase of hospital admissions (also see Chubarova et al., this volume). In spring 2006, smoke from peat and forest fires in the western Russian Federation was noted in the United Kingdom. In summer 2006, VFS from fires burning in the Russian Federation persisted over Finland for weeks (GFMC, 2006). In Fig. 1.5b, transboundary transport of smoke due to fires in the northern China and the southeast of the Russian Federation during October 2004 is shown.

Short- to long-distance transport of smoke has also been noted within central and east Asia during the last 10 years. The fire episodes of 1998 (Far East), 2003 (Transbaikal region), and 2004 (Northeast China, Jewish Autonomous Region) caused severe smoke pollution in the Far East of the Russian Federation. The consequences of regional smoke pollution in 2004 were recorded in Khabarovsk and revealed that both aerosol and carbon monoxide concentrations exceeded the maximum permissible concentrations (Goldammer et al., 2004).

1.7. Impacts of VFS on visibility

Reduced visibility is the main impact of VFS on critical infrastructures. For instance, in 1994, VFS from fires in Sumatra (Indonesia) initially reduced the average daily minimum horizontal visibility over Singapore to less than 2 km. Later, the visibility in Singapore dropped to 500 m. At the same period, the visibility in Malaysia dropped to 1 km in some parts of the country (WHO/UNEP/WMO, 1999). Other impacts on infrastructures included the irregularities in operation of airports (reduced or cancelled flights), highways and hospitals, and even army camps. For example the regional airports in Indonesia were closed during the haze period of 1997. In 1982–1983, 1991, 1994, and 1997–1998, the smog episodes in Southeast Asia resulted in closing of airports and marine traffic. In addition, accidents in the highways or possible airplane crash and human losses can be the result of reduced visibility. Several smoke-related marine and aircraft accidents occurred during late 1997 (WHO/UNEP/WMO, 1999). From 1979 to 1988, 28 fatalities and more than 60 serious injuries were attributed to smoke that drifted across roadways in the southern United States (Mobley, 1990). According to a study concerning the 1998 smoke episode in Brunei Darussalam, it was found that the haze impact on areas where a school and a hospital were situated was significant (Muraleedharan et al., 2000). In Fig. 1.6, people

Figure 1.6. People exposed to VFS in East Kalimantan, Indonesia, during the 1997–1998 fire–smoke episode. (*Source*: A. Hoffmann, GFMC.)

exposed to VFS in East Kalimantan, Indonesia, during the 1997–1998 fire-smoke episode are presented.

Generally, limited data and case studies exist regarding VFS impacts on critical infrastructures for risk management (Dokas et al., 2007). In Fig. 1.7, reduced visibility in an urban area of Russian Federation due to transboundary smoke-haze transfer is shown.

1.8. Human health impacts of Vegetation Fire Smoke

1.8.1. Toxicity of VFS

Generally, toxicity is defined as the deleterious or adverse biological effects caused by a chemical, physical, or biological agent. Toxicity can be acute, defined as any poisonous effect produced within a short period of time, or chronic, defined as the capacity of a substance to cause adverse human health effects as a result of chronic exposure. To assess the risks

Figure 1.7. VFS pollution in Khabarovsk in the Far East of the Russian Federation caused by forest and peat fires in northeast China/Far East of the Russian Federation (March 11, 2008). (*Source*: L. Kondrashov, Pacific Forest Forum.)

from toxic substances, toxicity indicators can be used, such as the LC_{50} (concentration of a substance in the air at which 50% of the tested population is killed) or the EC_{50} (concentration of a substance in the air at which 50% of the tested population are affected (ContamSites, 2007). For evaluating chronic toxicity, the lowest observable effect concentration (LOEC) can be used. Although by themselves LC_{50} values are of limited significance, acute lethality studies are essential for characterizing the toxic effects of chemicals and their hazard to humans. The most meaningful scientific information derived from acute lethality tests comes from clinical observations and postmortem examination of animals rather than from the specific LD_{50} value (Eaton & Klaassen, 2001).

The toxic effects due to chemicals are also related to the duration of the exposure. Generally, exposure is defined as the contact made between a chemical, physical, or biological agent and an organism. Acute exposure is defined as exposure to the oral, dermal, or inhalation route for 24 h or less. Chronic exposure is the repeated exposure to the oral, dermal, or inhalation route for more than approximately 10% of the human life span. Risk assessment under specific exposure conditions is defined as the identification and evaluation of the human population exposed to a toxic agent, describing its composition and size, as well as the type, magnitude, frequency, route, and duration of exposure (EPA IRIS, 2007).

Toxicity of the VFS mixture can be the additive or the synergistic result of all the possible hazardous smoke components, depending on the fuel types burned and the possible materials contained in the VFS. Additive toxicity is defined as the toxicity of a mixture of contaminants that is equal to the summation of the toxicities of the individual components. Synergistic toxicity is defined as the toxicity of a mixture of contaminants that may result in a total toxicity greater than the summation of the toxicities of the individual components (ContamSites, 2007).

VFS may contain toxic compounds such as:

- *Respiratory irritants:* Irritants can cause inflammation of mucous membranes. Ammonia (NH_3) and nitrogen dioxide (NO_2) are indicative examples. Irritants can also cause changes in respiration and lung function, such as sulfur dioxide, formaldehyde, and acrolein (MSU, 2005). According to specific studies, formaldehyde and acroleine were suspected of causing respiratory problems to the exposed firefighters (Reinhardt & Ottmar, 2004; Reinhardt et al., 2000).
- *Asphyxiants:* Asphyxiants prevent or interfere with the uptake and transport of oxygen. An example is carbon monoxide, which in high concentrations can result in immediate collapse and death (MSU, 2005). Methane and carbon dioxide are also considered asphyxiants. Even beneficial gases can be asphyxiants: a 17% inhaled oxygen content is the safe limit for prolonged exposure. A 5% oxygen content is the minimum compatible with life. Concentrations of 1% produce stupor and memory loss (Stefanidou-Loutsidou, 2005).
- *Carcinogens:* A carcinogen is a chemical, known or believed to cause cancer in humans. The number of proven carcinogens is comparatively small, but many more chemicals are suspected to be carcinogenic (PTCL, 2007). Weight-of-evidence (WOE) for carcinogenicity is a system (U.S. EPA) for characterizing the extent to which the available data (human or animal data) support the hypothesis that an agent can cause cancer to humans. WOE descriptors are classified from A to E: group A are known human carcinogens, whereas group B are probable human carcinogens, group C possible human carcinogens, group D are not classifiable as human carcinogens, and E are compounds with evidence of non-carcinogenicity (EPA IRIS, 2007). Carcinogens can be of three categories: Category 1 are substances known to be carcinogenic to humans, for which there is sufficient evidence to cause

cancer development; Category 2 are substances for which there is sufficient evidence of causing cancer to humans, based on long-term animal studies and other relevant information; Category 3 are substances that can possibly have carcinogenic effects but for which available information is not adequate to make satisfactory assessments (UB, 2007). According to the above, benzene is considered as A, formaldehyde as B1, acetaldehyde as B2, crotonaldehyde as C, toluene and phenol as D (EPA IRIS, 2007).

- *Mutagens:* A mutagen is an agent that changes the hereditary genetic material. Such a mutation is probably an early step to the development of cancer, for example, formaldehyde, acroleine (PTCL, 2007). Teratogens may cause non-heritable genetic mutations or malformations in the developing fetus, for example, toluene (PTCL, 2007).
- *Systemic Toxins:* These are chemicals, which can cause toxic effects, as a result of their absorption and distribution to a site distant from their entry point (EPA IRIS, 2007). Examples are heavy metals, such as lead, mercury, and cadmium (Stefanidou-Loutsidou, 2005), which may be contained in the VFS particles, especially when the flame-front expands to waste disposals (landfills) (Statheropoulos & Karma, 2007).

1.8.2. Exposure

Exposure to VFS can be quantified as the concentration of the smoke components in the subject in contact integrated over the time duration of that contact. In order to have a more representative assessment of VFS health impacts, it should be considered that exposure to VFS is simultaneous exposure to multiple substances, such as gases, liquids, solids (mixed exposure). A potential synergism may exist among various VFS components.

Exposure can be characterized as point, area/surface or network; such exposure characteristics should be taken into account for addressing exposure limits. Temporal/averaged, discrete/sporadic or continuous/cumulative exposures have to be taken into account in order to calculate an averaged, sporadic, or cumulative exposure, respectively (Seyenaeve, 2006).

Firefighters' exposure to VFS is characterized mostly by a standard periodicity (every summer) and high frequency (e.g., long-lasting fires). Hence, the ability to measure online their exposure is considered critical. Exposure of the firefighters to CO and formaldehyde can exceed legal and short-term exposure limits, occasionally, in smoky conditions; CO level has been noted as exceeding the 200 ppm ceiling set by the NIOSH (Reinhardt et al., 2000).

Exposure of general populations to VFS is not a continuous situation. However, susceptibility of the receptors should also be taken into consideration during exposure assessment, as sensitive groups, such as children, pregnant women, people with respiratory problems, and the elderly are considered more vulnerable (USEPA, 2001).

Different organizations have evaluated compounds that are considered hazardous for the exposed populations. The WHO, European Union (EU), United Nations Economic Commission for Europe (UNECE), and United States Environmental Protection Agency (USEPA) are some of those organizations. In that scope, terms such as standards, guidelines, and limit values are used. EU limit values are mandatory, while guide values give only guidance. Standards (or EU Directives) can contain both limit and guide values (Colls, 2002). Additionally, the ACGIH has established Threshold Limit Values (TLVs), the Occupational Safety and Health Administration has addressed Permissible Exposure Limits (PELs), and the NIOSH has addressed Recommended Exposure Limits (RELs). These limits are referred to as the occupational exposure of 8 h or 24 h, and for some compounds the Short-Term Exposure Limits (STELs) of 15 min exposure are also given.

However, these Occupational Exposure Limits (OELs) need further investigation. For example, TLVs are based on a young and healthy worker, which might not be representative for the entire exposed population. Moreover, inhalation is considered the main route of exposure and the exposure pattern is 8 h/day/5 days/week (Seyenaeve, 2006). In emergency situations work-shifts of the firefighters are often extended.

For unusual schedules, adjustments of these limits to the extended work-shifts need to take place (Kelly, 1992; Reh & Deitchman, 1992). Threshold limits for the firefighters' exposure to VFS is an issue that needs further study. The time duration of the shifts varies, depending on the extension of the fire. In addition, the distance of the shift camping from the fire-front is usually not far enough for the firefighter to recover from smoke inhalation. Camping some distance from the fire and smoke front is a problem, especially in the case of forest fires in small islands, where dispatching means and personnel is difficult (Statheropoulos, 2005).

Especially for the exposure to particles, during a vegetation fire very high concentrations of particles at short-time duration may be observed; these short-term peaks may cause some of the most significant health implications. Fine particles, known as respirable, are not stopped by the cells of the respiratory tracts and can penetrate the lungs more easily than coarse particles. In this way, hazardous compounds absorbed by the fine particles can reach the air cells (Cesti, 2006; Dawud, 1999; Fowler, 2003; Malilay, 1998). Toxic effect of particles is related to the quantity of toxic substances that may be absorbed and the affinity for site of action (enzyme, membrane). In general, biological absorption of particles by the human body can take place by filtration through pores of membranes, simple diffusion, facilitated diffusion, active transport (against concentration gradient), or endocytose (pinocytose-phagocytose). Biological absorption can be oral, pulmonary, cutaneous, ocular, etc. Some of the health effects due to particles can be acute toxicity, skin corrosion/irritation, serious eye damage/eye irritation, sensitization (allergy), carcinogenicity, specific target organ systemic toxicity (TOST), respiratory irritation, and so forth (Seyenaeve, 2006). Hence, the 24 h assumption of particles for OELs might not be efficient for short-term risk assessment in a vegetation fire. It should be emphasized that official exposure limits for particles near the flame-front do not exist. However, there was an effort to provide some criteria, in order to assess the severity of the situation in a forest fire (USEPA, 2001). Adjustment of the existing exposure limits to the hostile conditions of vegetation fires has to be taken into consideration not only for the exposed population and its sensitive groups, but also for the firefighters of the front-line. In addition, exposure limits to VFS components should be addressed in the framework of field exposure, compared to occupational indoor exposure.

1.9. Conclusions and recommendations

VFS has serious impacts on the environment and human health, as well as the national economy (Rittmaster et al., 2006). Strategies and tactics exist to cope with its impacts. However, a number of issues are still open for further elaboration and decision making. Therefore, the Health Guidelines for Vegetation Fire Events (WHO/UNEP/WMO, 2000), dealing with potential risks to public health of emissions from vegetation fires, recommend that additional research be conducted to address:

- Quantification of resulting concentrations of ambient air pollutants in populated areas.
- Evaluation of likely exposure scenarios for affected populations (both indoors and outdoors).
- Assessment of consequent health risks posed by such human exposures.
- Special attention to fire-generated radioactive emissions.
- Physical/chemical factors contributing to the changes that occur over time and space during VFS transport.

- Compilation of information pertaining to levels of exposure and fire activity, in conjunction with past fire and smoke episodes.
- Mitigation approaches.
- Health impacts ofVFS.

In addition, a ''catalogue of ideas'' was prepared in the framework of a teleconference entitled ''Short- and long-term health impacts of forest fire smoke on the firefighters and the exposed population'' (FFNet, 2005), which was organized in 2005 by the European Center for Forest Fires (ECFF), a center that operates in the framework of the European Open Partial Agreement (EUROPA) on the prevention, protection against, and organization of relief in major natural and technological disasters. Some of these ideas are:

- Forest fire smoke is a complex mixture of chemical compounds produced from combustion of forest fuel. However, as fire expands, it may burn constructions, landfills, or crops. Asbestos, glass cement, and combustion products of plastics, pesticides, insecticides can potentially be found in forest fire smoke. Data need to be collected regarding this concept.
- Exposure limits for the firefighters need to be established, taking into consideration the complexity of smoke, the dynamic phenomena which occur during a forest fire, the nature of firemen's work, the duration of work-shifts, and the site of the shift camping. Research and studies, with strong operational components, might be the way for providing solutions.
- Exposure limits for the population and especially for the sensitive groups, such as infants, elderly people, pregnant women, and people with pre-existing cardiovascular and respiratory diseases have to be set and criteria of evacuation need to be considered. Evaluation of existing or similar studies needs to be carried out.
- Existing Personal Protective Equipment (PPE) needs to be benchmarked with careful experimentation.

1.10. Challenges ahead: Public policies addressing wildland fire smoke

The primary aim of this chapter was to provide a state-of-the-art report on the nature of VFS emissions. Exposure and vulnerability of humans to fire emissions, however, is a subject that needs more information on options for limiting smoke impacts on human health and security. A number of recent VFS pollution episodes have caused public concerns and alerted policy makers. Some responses, such as calls or laws for eliminating the use of fire in land management, have resulted in conflicts, contradicting effects, or are difficult — if not impossible — to enforce. Examples include the fire-use ban in Indonesia, which has been in force since the mid-1990s and has been proven to be ineffective. As discussed above, the ASEAN Agreement on Transboundary Haze Pollution, signed by the ASEAN member states in 2001 and aimed at reducing regional smoke-haze caused by VFS, has proven to be inefficient—largely because Indonesia was not willing and able to reduce inappropriate and illegal use of fire in land-use change, especially on drained peatlands (Goldammer, 2006b).

An example of contradicting effects is the reduction of prescribed burning in the U.S. due to limitations imposed by the U.S. Environmental Protection Agency standards. These limitations have resulted in a reduction of application of prescribed fire for various land management objectives in the 1980s and 1990s. Clearly, smoke products from prescribed fire are basically identical with those emitted from uncontrolled wildfires, even if differences have been revealed, such as ratios of oxidized/reduced compounds, for example, NO_x/NH_3 (Ward et al., 1993). The application of prescribed fire includes smoke management options, which will reduce smoke impacts on humans. The reduction of prescribed burning, however, results in the build-up of fuels, which in turn contributes to the risk of large, high-intensity and high-severity fires that are difficult to control, including uncontrollable and comparatively more severe impacts of smoke.

Besides the implications of fire bans on potentially uncontrolled fires and smoke production, it must be reminded that fire exclusion from fire-adapted or fire-dependent ecosystems, which require a regular influence of fire, can also result in dramatic changes of structure, biodiversity, stability, and productivity of such ecosystems. Therefore, a complete exclusion of fire from land-use systems would affect livelihoods of hundreds of millions of people worldwide.

However, the transboundary transport of VFS from one country to another country is increasingly the subject of public and political debates. Three recent cases may highlight this issue. In May 2006 western Europe including the United Kingdom was affected by fire smoke pollution generated and transported from vegetation burning in the western Russian Federation. As a consequence of the high concentration of PM_{10} monitored in the United Kingdom, the UK Department for Environment, Food and Rural Affairs (DEFRA) announced that the UK government was going to submit revisions to the United Nations Convention on long-range transboundary air pollution to prevent similar occurrences in the future (GFMC, 2006).

In August 2006, the VFS emissions from the western Russian Federation, Ukraine, and Belarus were transported to the Nordic countries. Smoke exposure was particularly severe in Finland where the air pollution exceeded the limits of the maximum permissible amount of airborne dust in city air of 50 micrograms per cubic meter of air for almost 2 weeks. In order to deal with this transboundary process, a joint Russian-Finnish wildland fire exercise was held in Karelia (Finland) soon after these events (GFMC, 2006).

In March–April 2007 the fire smoke generated by numerous land-use fires in northern Thailand, Myanmar, Laos, China, and Cambodia caused extremely severe regional smoke pollution. The situation was aggravated by a very strong inversion event, which trapped the smoke close to the ground. This resulted in a situation similar to the close-to-ground pollution in southern Malaysia and Singapore as a consequence of Indonesia's land-use fires. Tensions and international discussions on defining common solutions were reported from the region (GFMC, 2007a).

The consequences of fire burning on radioactively contaminated lands and its consequences on redistribution of radioactive particles lifted by fire smoke is another serious issue that needs to be addressed. In the case of the Chernobyl nuclear accident of 1986 and its implications on the redistribution of radioactivity by wildfires, a new initiative has been launched in 2007 by the Agricultural University of Kiev, Ukraine, to address the problem to reduce the contamination locally, nationally, and transnationally (GFMC, 2007b).

These examples reveal the transboundary and international nature of VFS emissions that can cause many problems, in an increasingly vulnerable global society. These problems have to be addressed cooperatively and collectively. Consequently, bilateral and multilateral agreements are necessary to address these issues. An international agreement—legally binding or voluntary—could be helpful to set standards for prevention and response to VFS pollution. The use of the WHO/UNEP/WMO Health Guidelines for Vegetation Fire Events (WHO/UNEP/WMO, 1999), the Voluntary Fire Management Guidelines (FAO, 2006), the Global Fire Monitoring Center (GFMC), and the mechanism of the UNISDR Global Wildland Fire Network (UNISDR, 2007) are available and could be applied to facilitate such an international approach.

REFERENCES

Andreae, M.O. 2004. Assessment of global emissions from vegetation fires. Int. For. Fire News 31, 112–121.

Andreae, M.O., Atlas, E., Harris, G.W., Helas, G., de Kock, A., Koppmann, R., Maenhaut, W., Manö, S., Pollock, W.H., Rudolph, J., Scharffe, D., Schebeske, G., and Welling, M. 1996. Methyl halide emissions from savanna fires in southern Africa. J. Geophys. Res. 101, 23,603–23,613.

Andreae, M.O., and Merlet, P. 2001. Emission of trace gases and aerosols from biomass burning. Global Biogeochem. Cycles, 15, 955–966.

Andreae, M.O. 2007. Aerosols before pollution. Science 315, 50–51.

Barry, D.A. 2005. Wildfire emissions totalled. Large area of Northern Hemisphere is affected by pollution from Alaska-Canadian blazes. Chem. Eng. News, 7 July 83, 27–28. http://pubs.acs.org/cen/news/83/i28/8328scic1a.html

Bazzaz, F.A. 1990. The response of natural ecosystems to the rising global CO_2 levels. Ann. Rev. Ecol. Syst. 2, 167–196.

Booze, T.F., Reinhardt, T.E., Quiring, S.J., and Ottmar, R.D. 2004. A screening—level assessment of health risks of chronic smoke exposure for wildland fire-fighters. J. Occup. Environ. Hyg. 1, 296–305.

Brauer, M. 1999. Health impacts of biomass air pollution. In: Goh, K.-T., Schwela, D., Goldammer, J.G., and Simpson, O., eds. Health guidelines for vegetation fire events-background papers, 6–9 October 1998. Lima, Peru, WHO/UNEP/WMO, pp. 186–257.

CEPA (Canadian Environmental Protection Act). 1999. National Ambient Air Quality Objectives of particulate matter Part 1, Science Assessment document. Minister Public Works and Government Services, ISBN 0-662-26715-X, Cat. No. H46-2/98-220-1E.

Cesti, G. 2006. Effects of forest fire smoke. FFNet 4, 113–126.

Clark, J.S., Cachier, H., Goldammer, J.G., and Stocks, B.J., eds. 1997. Sediment records of biomass burning and global change. Springer-Verlag, Berlin, NY, 489 pp.

Colls, J. 2002. Air Pollution, Clay's Library of Health and the Environment (second ed.). Taylor & Francis, p. 560.

ContamSites. 2007. Web site of project team for ecological risk assessment of contaminated sites in New Zealand. http://contamsites.landcareresearch.co.nz/glossary.htm

Davies, S.J., and Unam, L. 1999. Smoke-haze from the 1997 Indonesian forest fires: effects on pollution levels, local climate, atmospheric CO_2 concentrations, and tree photosynthesis. For. Ecol. Manag. 124, 137–144.

Dawud, Y. 1999. Smoke episodes and assessment of health impacts related to haze from forest fires: Indonesian experience. In: Goh, K.-T., Schwela, D., Goldammer, J.G., and Simpson, O., eds. Health guidelines for vegetation fire events-background papers, 6–9 October 1998. Lima, Peru, WHO/UNEP/WMO, pp. 313–333.

Dokas, I., Statheropoulos, M., and Karma, S. 2007. Integration of field chemical data in initial risk assessment of forest fire smoke. Sci. Total Environ. 376, 72–85.

Dusha-Gudym, S.I. 2005. Transport of radioactive materials by wildland fires in the Chernobyl accident zone: How to address the problem. Int. For. Fire News 32, 119–125.

Eaton, D.L., and Klaassen, C.D. 2001. Principles of toxicology. In: Klaassen, C.D., ed. Casarett and Doull's toxicology: The basic science of poisons. McGraw-Hill Medical Publishing Division, New York.

Edwards, D.P., Pétron, G., Lamarque, J.-F., Emmons, L.K., Gille, J.C., and Hauglustaine, D. 2003. Carbon monoxide measurements from Terra/MOPITT: Improving CO emissions (Invited), NARSTO Emission Inventory Workshop, Austin, TX, October, pp. 14–17.

EPA IRIS. 2007. Environmental protection agency, integrated risk information system. http://www.epa.gov/iris/

European Water Management News (EWMN). 2002. Peat fires raging around Moscow show need for swamp restoration. EWMN News, 6 September 2002. http://www.riza.nl

Fan, S.M., Wofsy, P.S., Jacob, D.J., and Fitzjarrald, D.R. 1990. Atmosphere-biosphere exchange of CO_2 and O_3 in the central Amazon forest. J. Geophys. Res. 95, 16.851–16.864.

FAO (Food and Agriculture Organization of the United Nations). 2006. Fire management: Voluntary guidelines. Principles and strategic actions. Fire Management Working Paper 17. FAO, Rome. www.fao.org/forestry/site/35853/en

FAO (Food and Agriculture Organization of the United Nations). 2007. Fire management – global assessment. A thematic study prepared in the framework of the Global Forest Resources Assessment 2005. FAO Forestry Paper 151, 121 pp.

FFNet (Forest Fire Net) 3. 2005. Special issue with the proceedings of the teleconference: Short and long term health impacts of forest fire smoke on the fire-fighters and the exposed population, October 2005, European Center for Forest Fires (ECFF), an initiative of the Council of Europe. http://www.coe.int/t/dg4/majorhazards/centres/presentation/ecff_en.asp, http://www.civilprotection.grecff/ecff.htm

Fowler, C.T. 2003. Human health impacts of forest fires in the Southern United States: A literature review. J. Ecol. Anthropol. 7, 39–59.

GFMC (Global Fire Monitoring Center). 2006. Reports on fire smoke pollution in Europe generated by wildland fires in the Russian Federation. http://www.fire.uni-freiburg.de/media/2006/05/news_20060518_uk.htm; http://www.fire.uni-freiburg.de/media/2006/08/news_20060825_fin.htm; http://www.fire.uni-freiburg.de/media/2006/06/news_20060608_fi.htm; http://www.fire.uni-freiburg.de/media/2006/06/news_20060608_fi4.htm; http://www.fire.uni-freiburg.de/media/2006/06/news_20060608_fi3.htm; http://www.fire.uni-freiburg.de/media/2006/06/news_20060608_fi2.htm; http://www.fire.uni-freiburg.de/GFMCnew/2006/05/0501/20060501_ru.htm

GFMC (Global Fire Monitoring Center). 2007a. Reports on fire smoke pollution in mainland Southeast Asia generated by land-use fires. http://www.fire.uni-freiburg.de/media/2007/04/news_20070405_thai.htm; http://www.fire.uni-freiburg.de/media/2007/03/news_20070330_thai2.htm; http://www.fire.uni-freiburg.de/media/2007/03/news_20070328_thai.htm; http://www.fire.uni-freiburg.de/media/2007/03/news_20070321_thai.htm; http://www.fire.uni-freiburg.de/media/2007/03/news_20070321_thai2.htm; http://www.fire.uni-freiburg.de/media/2007/03/news_20070313_thai.htm

GFMC (Global Fire Monitoring Center). 2007b. Statement of the international meeting on "Reducing Risk of Disaster from Catastrophic Wildfires in the Chornobyl Irradiated Forests" National Agricultural University, Kiev, Ukraine, 26–27 July 2007. http://www.fire.uni-freiburg.de/GlobalNetworks/SEEurope/Chornobyl-Wildfire-Conference-Report.pdf

Goldammer, J.G. 1998. History of fire in land-use systems of the Baltic Region: Implications on the use of prescribed fire in forestry, nature conservation and landscape management. Paper presented at the First Baltic Conference on Forest Fires, Radom-Katowice, Poland, 5–9 May 1998. http://www.fire.uni-freiburg.de/programmes/natcon/natcon_1.htm

Goldammer, J.G. 2006a. Global forest resources assessment 2005—thematic report on forest fires in the Central Asian region and adjacent countries. FAO Fire Management Working Paper 16, 45 p.

Goldammer, J.G. 2006b. History of equatorial vegetation fires and fire research in Southeast Asia before the 1997–98 episode. A reconstruction of creeping environmental changes. Special Issue: Mitigation and Adaptation Strategies for Global Change 12, 13–32, doi:10.1007/s11027-006-9044-7.

Goldammer, J.G., Davidenko, E.P., Kondrashov, L.G., and Ezhov, N.I. 2004. Recent trends of forest fires in Central Asia and opportunities for regional cooperation in forest fire management. Paper prepared for the Regional Forest Congress. Forest

Policy: Problems and Solutions, 25–27 November 2004, Bishkek, Kyrgyzstan. Int. Forest Fire News, 31, 91–101.
Hegg, D.A., Radke, L.F., Hobbs, P.V., and Riggan, P.J. 1988. Ammonia emissions from biomass burning. Geophys. Res. Lett. 15, 335–337.
Hegg, D.A., Radke, L.F., Hobbs, P.V., Rasmussen, R.A., and Riggan, P.J. 1990. Emissions of some trace gases from biomass fires. J. Geophys. Res. 95, 5669–5675.
Heil, A., and Goldammer, J.G. 2001. Smoke-haze pollution: A review of the 1997 episode in Southeast Asia. Reg. Environ. Change 2, 24–37.
Hoelzemann, J.J., Schultz, M.G., Brasseur, G.P., Granier, C., and Muriel, S. 2004. Global wildland fire emission model (GWEM): Evaluating the use of global area burnt satellite data. J. Geophys. Res. 109, D14S04, doi:10.1029/2003JD003666.
Hogue, C. 2005. EPA guidance on exempting volatile organic compounds from regulation worries some environmental groups. Chemical and Engineering News 24 January, 83, 26.
Houghton, J.T., Callander, B.A., and Varney, S.K. 1992. Climate change 1992. The supplementary report to the IPCC scientific assessment. Cambridge University Press, Cambridge, UK, 205 pp.
Hutchison, K. 2003. Applications of MODIS satellite data and products for monitoring air quality in the state of Texas. Atmos. Environ. 37, 2403–2412
Johnson, R. 1999. Guidance on measures in forest fire emergency cases. In: Goh, K.-T., Schwela, D., Goldammer, J.G., and Simpson, O., eds. Health guidelines for vegetation fire events-background papers, 6–9 October 1998. Lima, Peru, WHO/UNEP/WMO, pp. 411–465.
JRC (Joint Research Center). 2002. Global burnt area tables with areas burned in 2000 and gridded files. http://www-gvm.jrc.it/tem/products_complete.htm
Kelly, J. 1992. U.S. Department of the Interior National Park Service, Health Hazard Evaluation Report, Heta 92-045-2260, NIOSH. http://www.cdc.gov/niosh/topics/firefighting/
Koppmann, R., Czapiewski, K.von., and Reid, J.S. 2005. A review of biomass burning emissions, part I: Gaseous emissions of carbon monoxide, methane, volatile organic compounds, and nitrogen containing compounds. Atmos. Chem. Phys. Discuss. 5, 10455–10516.
Lacaux, J.P., Brustet, J.M., Delmas, R., Menaut, J.C., Abbadie, L., Bonsang, B., Cachier, H., Baudet, J., Andreae, M.O., and Helas, G. 1995. Biomass burning in the tropical savannas of Ivory Coast: An overview of the field experiment fire of savannas (FOS/DECAFE 91). J. Atmos. Chem. 22, 195–216.
Lee, K.H., Kim, J.E., Kim, Y.J., Kim, J., and Hoyningen-Huene, W. 2005. Impact of the smoke aerosol from Russian forest fires on the atmospheric environment over Korea during May 2003. Atmos. Environ. 39, 85–99.
Malilay, J. 1998. A review, of factors affecting the human health impacts, of air pollutants from forest fires. In: Goh, K.-T., Schwela, D., Goldammer, J.G., and Simpson, O., eds. Health guidelines for vegetation fire events-background papers, 6–9 October 1998. Lima, Peru, WHO/UNEP/WMO 1999: Health Guidelines for Vegetation Fire Events, Lima, Peru, October 6–9, pp. 255–270.
McDonald, J.D., Zielinska, B., Fujita, E., Sagebiel, J., and Chow, J. 2000. Fine particle and gaseous emission rates from residential wood combustion. Environ. Sci. Technol. 34, 2080–2091.
Minaeva, T. 2002. News from Russia: Peat fires. International Mire Conservation Group (IMCG) Newsletter No. 3/2002.
Miranda, A.I. 2004. An integrated numerical system to estimate air quality effects of forest fires. Int. J. Wildland Fire 13, 217–226.

Miranda, A.I., Ferreira, J., Valente, J., Santos, P., Amorim, J.H., and Borrego, C. 2005. Smoke measurements during Gestosa-2002 experimental field fires. Int. J. Wildland Fire 14, 107–116.

Mobley, H.E. 1990. Summary of smoke-related accidents in the south from prescribed fire (1979–1988). Technical release 90-R-11. Forest Resources Association, Inc, Rockville, MD.

MSU (Michigan State University). 2005. Chemical hygiene plan. http://www.orcbs.msu.edu/chemical/programs_guidelines/chem_hygiene/chem_hygienE_plan/chp_full.pdf

Muraleedharan, T.R., Radojevic, M., Waugh, A., and Caruana, A. 2000. Chemical characterisation of the haze in Brunei Darussalam during the 1998 episode. Atmos. Environ. 34, 2725–2731.

Nakajima, T., Higurashi, A., Takeuchi, N., and Herman, J.R. 1999. Satellite and ground based study of optical properties of 1997 Indonesian forest fire aerosols. Geophys. Res. Lett. 26, 2421–2424.

NASA Earth Observatory. 2006. Carbon Monoxide, Fires, and Air Pollution, NASA Earth Observatory website. http://earthobservatory.nasa.gov/Newsroom/NewImages/Images/co_jja2004.jpg

Pinto, J.P., and Grant, L.D. 1999. Approaches to monitoring of air pollutants and evaluation of health impacts produced by biomass burning. Health guidelines for vegetation fire events-background papers, Lima, Peru, 6–9 October 1998. WHO/UNEP/WMO, pp. 147–185.

Poyarkov, V. 2006. Using a radioactive marker for verification of dynamic models of forest fires at an experimental site located in the chernobyl exclusion zone. FFNet 4, 127–130.

PTCL (The Physical and Theoretical Chemistry Laboratory). 2007. Oxford University. Chemical and Other Safety Information. http://ptcl.chem.ox.ac.uk/MSDS/glossary/carcinogen.html

Radojevic, M. 2003. Chemistry of forest fires and regional haze with emphasis on Southeast Asia. Pure Appl. Geophys. 160, 157–187.

Reh, C.M., and Deitchman, S.D. 1992. U.S. Department of the Interior National Park Service, Health Hazard Evaluation Report, Heta 88-320-2176, NIOSH. http://www.cdc.gov/niosh/topics/firefighting/

Reid, J.S., Koppmann, R., Eck, T.F., and Eleuterio, D.P. 2005. A review of biomass burning emissions part II: intensive physical properties of biomass burning particles. Atmos. Chem. Phys. 5, 799–825.

Reinhardt, T.E., and Ottmar, R.D. 2004. Baseline measurements of smoke exposure among wildland fire-fighters. J. Occup. Environ. Hyg. 1, 593–606.

Reinhardt, T.E., Ottmar, R.D., and Hanneman, A.J.S. (2000), Smoke exposure among firefighters at prescribed burns in the Pacific Northwest. Res. Pap. PNW-RP-526. Portland, OR: U.S. Department of Agriculture, Forest Service, Pacific Northwest Research Station, 45 pp.

Riggan, P.J., Tissell, R.G., Lockwood, R.N., Brass, J.A., Pereira, J.A.R., Miranda, H.S., Miranda, A.C., Campos, T., and Higgins, R. 2004. Remote measurement of energy and carbon flux from wildfires in Brazil. Ecol. Appl. 14, 855–872.

Rittmaster, R., Adamowicz, W.L., Amiro, B., and Pelletier, R.T. 2006. Economic analysis of health effects from forest fires. Can. J. For. Res. 36, 868–877.

Sandström, T., Nowak, D., and Van Bree, L. 2005. Health effects of coarse particles in ambient air: messages for research and decision-making. Eur. Respir. J. 26, 187–188.

Sapkota, A., Symons, J.M., Kleissl, J., Wang, L., Parlange, M.B., Ondov, J., Breysse, P.N., Diette, G.B., Eggleston, P.A., and Buckley, T.G. 2005. Impact of the 2002 Canadian forest fires on particulate matter air quality in Baltimore City. Environ. Sci. Technol. 39, 24–32.

Seyenaeve, G. 2006. Exposure limits for particles. FFNet 4, 79–105.

Shauer, J.J., Kleeman, M.J., Cass, G., and Simoneit, B.T. 2001. Measurement of emissions from air pollution sources. 3. C1–C29 organic compounds from fireplace combustion of wood. Environ. Sci. Technol. 35, 1716–1728.

Shostakovich, V.B. 1925. Forest conflagrations in Siberia. J. For. 23, 365–371.

Shvidenko, A.Z., and Nilsson S. 2000. Extent, distribution, and ecological role of fire in Russian forests. In: Kasischke, E.S., and Stocks, B.J., eds. Fire, climate change, and carbon cycling in the Boreal Forest, Ecological Studies 138. Springer-Verlag, Berlin, NY, pp. 132–150.

Statheropoulos, M. 2005. Exposure limits in regard to fire-fighters shift duration and fire-fighters camping. FFNet 3, p. 23.

Statheropoulos, M., and Karma, S. 2007. Complexity and origin of the smoke components as measured near the flame-front of a real forest fire incident: A case study. J. Anal. Appl. Pyrolysis 78, 430–437.

Statheropoulos, M., Liodakis, S., Tzamtzis, N., Pappa, A., and Kyriakou, S. 1997. Thermal degradation of *Pinus halepensis* pine-needles using various analytical methods. J. Anal. Appl. Pyrolysis 43, 115–123.

Stefanidou-Loutsidou, M. 2005. Toxicology of forest fires smoke components. FFNet 3, p. 11.

Turetsky, M.R., Harden, J.W., Friedli, H.R., Flannigan, M.D., Payne, N., Crock, J., and Radke, L.F. 2006. Wildfires threaten mercury stocks in northern soils. Geophys. Res. Lett. 33, L16403, doi:10.1029/2005GL025595.

UB (University of Bristol). 2007. Chemical hazards. http://www.chm.bris.ac.uk/safety/chemicalhazards.htm#carcinogens

UNISDR (United Nations International Strategy for Disaster Reduction). 2007. The UNISDR Global Wildland Fire Network. http://www.unisdr.org/eng/task%20force/tf-working-groups4-eng.htm; http://www.fire.uni-freiburg.de/GlobalNetworks/globalNet.html

USDA (US Department of Agriculture, Forest Service Southern Region). 1989. Environmental Effects. Technical Publication R8-TP 11, February 1989.

USDA (US Department of Agriculture). 2002. Wildland fire on ecosystems: effects of fire on air. In: Sandberg, D.V., Ottmar, R.D., Peterson, J.L., and Core, J., eds. Gen. Tech. Rep. RMRS-GTR-42- vol. 5. Ogden, UT: U.S. Department of Agriculture, Forest Service, Rocky Mountain Research Station, 79 pp.

USEPA. 2001. Wildfire smoke: A guide for public health officials. With contributions by Ammann, H., Blaisdell, R., Lipsett, M., Stone, S.L., Therriault, S., Waldman, J., Jenkins, P., In: Lynch, K., ed. University of Washington (June 2001), 27 p. http://www.epa.gov/ttn/amtic/smoke.html

US NWCG (US National Wildfire Coordination Group, Fire Use Working Team). 2001. Smoke management guide for prescribed and wildland fire. In: Hardy, C.C., Ottmar, R.D., Peterson, J.L., Core, J.E., Seamon, P., eds. December 2001, 226 pp.

Varela, M.C., 2006. The deep roots of the 2003 forest fires in Portugal. Int. For. Fire News (IFFN), 34, 2–22.

Vitousek, P.M., Aber, J.D., Howarth, R.W., Likens, G.E., Matson, P.A., Schindler, D.W., Schlesinger, W.H., and Tilman, D.G. 1997. Human alteration of the global nitrogen cycle: sources and consequences. Ecol. Appl. 3, 737–750.

Wang, J., and Christopher, S.A. 2003. Intercomparison between satellite-derived aerosol optical thickness and PM2.5 mass: Implications for air quality studies. Geophys. Res. Lett. 30(21), 2095, doi:10.1029/2003GL018174.

Ward, D.E., 1999. Smoke from wildland fires. In: Goh, K.-T., Schwela, D., Goldammer, J.G., and Simpson, O., eds. Health guidelines for vegetation fire events-background papers, 6–9 October 1998. Lima, Peru, WHO/UNEP/WMO, pp. 70–85.

Ward, D.E., Peterson, J., and Hao, W. M. 1993. An inventory of particulate matter and air toxic emissions from prescribed fire in the USA for 1989. Air and Waste Management Association 86th Ann. Meeting & Exhibition, Denver, Colorado, 13–18 June 1993, 93-MP-6.03, p. 19.

Ward, T.J., and Smith, G.C., 2001. Air sampling study of the 2000 Montana Wildfire Season. Paper No 113. In: Proceedings of the Air and Waste Management. Conference, Orlando, Florida, USA.

WHO/UNEP/WMO. 1999. Health guidelines for vegetation fire events-guideline document. In: Schwela, D.H., Goldammer, J.G., Morawska, L.H., and Simpson O., eds. Lima, Peru, 6–9 October 1998, 219 pp.

WHO/UNEP/WMO. 2000. Health Guidelines for Vegetation Fire Events, IFFN No. 22-January 2000, pp. 91–101.

Wotawa, G., De Geer, L.-E., Becker, A., D'Amours, R., Jean, M., Servranckx, R., and Ungar, K. 2006. Inter- and intra-continental transport of radioactive cesium released by boreal forest fires. Geophys. Res. Lett. 33, L12806, doi:10.1029/2006GL026206.

Wotawa, G., and Trainer, M. 2000. The influence of Canadian forest fires on pollutant concentrations in the United States. Science 288, 324–328.

Yokelson, R.J., Karl, T., Artaxo, P., Blake, D.R., Christian, T.J., Griffith, D.W.T., Guenther, A., and Hao, W.M. 2007. The tropical forest and fire emissions experiment: Overview and airborne fire emission factor measurements. Atmos. Chem. Phys. Discuss. 7, 6903–6958.

Developments in Environmental Science, Volume 8 37
A. Bytnerowicz, M. Arbaugh, A. Riebau and C. Andersen (Editors)

ISSN: 1474-8177/DOI:10.1016/S1474-8177(08)00002-8

Chapter 2

Climatic and Weather Factors Affecting Fire Occurrence and Behavior

Randall P. Benson, John O. Roads and David R. Weise*

Abstract

Weather and climate have a profound influence on wildland fire ignition potential, fire behavior, and fire severity. Local weather and climate are affected by large-scale patterns of winds over the hemispheres that predispose wildland fuels to fire. The characteristics of wildland fuels, especially the moisture content, ultimately determine fire behavior and the impact of fire on the landscape. The physical processes related to combustion, fire, and plume behavior are largely affected by both daily weather and long-term climate.

2.1. Introduction

Both human-caused and lightning-caused fires result from changing climate and weather factors. After ignition, fire behavior is largely affected by ambient atmospheric factors including wind, atmospheric stability, fuel moisture, and topographic influences. In this chapter we will discuss the differences between climate and weather, how climate and weather affects fire, what the future implications may be for fire and climate change, and how the important atmospheric factors interact with fuel properties to determine fire behavior. In Section 2.2 we will discuss the impact of climate (climate anomalies, teleconnections and climate change) on fire and in Section 2.3 we will demonstrate the importance of weather (temperature, lightning, moisture and wind) on fire occurrence and fire behavior.

*Corresponding author: E-mail: randall.benson@sdsmt.edu

2.2. Climate

This section provides an overview of climate and its effects on fire. Climate is defined by the variability in weather and results from numerous non-linear processes and interactions between the atmosphere, the hydrosphere, the biosphere, and the geosphere. Any change in one of these spheres affects the other realms and these linked changes eventually result in changes to fire behavior. It is unclear how future fire behavior will be affected with anticipated changes in climate but it is clear that extreme weather conditions occurring over sufficient time periods will affect the moisture content of wildland fuels and thus fire regime characteristics. Most research indicates that future global temperatures will be warmer than current levels and that drought areas will increase making wildfire activity more likely (IPCC, 2007).

2.2.1. Defining climate

The climate we associate with a particular area involves the entire range of weather conditions that together combine to produce what is considered normal or average for that location. Climate may be defined as the statistical properties of the atmosphere that include both the frequency and variability of weather events. Climate zones, such as those found in the Koeppen system (McKnight & Hess, 2000), link the world distribution of vegetation types to various combinations of monthly mean temperature and precipitation. Each climate zone is distinguished across Earth's surface relative to latitude, degree of continentality, and location relative to major topographic features. Wildland fuel type characteristics such as fuel loading, fuel volume, continuity, moisture content, and size and shape are intimately associated with various climate zones. Accordingly, fire regime characteristics such as fire frequency, fire intensity, and season of occurrence are largely defined by climate. Possible changes in climate will affect the characteristics of wildland fuels and fire regimes.

The ranges in climate, along with variations in vegetative conditions, produce differences in climate from one region to the next. In both the Northern and Southern Hemisphere, fire seasons commence in lower latitude regions and progress poleward as the warm season develops and as Earth continues its orbit about the sun. Annual changes in climatic features of a region, such as snowpack and spring snowmelt or the lengths of growing seasons, are all important considerations to the start and the length of fire seasons (Westerling et al., 2006).

2.2.2. *Climate anomalies*

The fire climate is a synthesis of daily fire weather conditions averaged over a long period of time. The range of weather conditions over time helps determine fire season characteristics along with the normal or expected conditions. Daily extremes in the climate record profoundly affect fire occurrence and fire behavior. It is widely regarded that large wildfires requiring significant suppression resources are associated with weather anomalies that act to shape the climate record. The majority of the area burned by wildfires, which may be underestimated in some regions (Soja et al., 2002), is frequently associated with a very small number of the observed fires each year and has been attributed to changing climate and increasing fuel hazards (Stephens, 2005).

Anomalies of temperature are experienced over days and may persist for seasons and are observed over large regions of continents. Precipitation deficits may be observed over similar time periods but often display more complex patterns due to the factors that contribute to the development of rain and snow. The near random distribution of warm season convective precipitation often leads to irregularities in spatial patterns of precipitation on short time scales. Over longer time scales, precipitation patterns may become more evident as reflected in areas of flooding and drought. Geographic nonuniformity in precipitation patterns frequently occurs over continents, which allows for a region to be dry adjacent to a region experiencing above-normal precipitation. At middle and high latitudes, the geographic nonuniformity is linked to the direction of the prevailing upper-atmospheric winds that govern the strength and direction of travel of storms.

Lack of moisture over an extended period of time may lead to drought. Droughts are associated with persistent departures of the large-scale weather pattern from its normal pattern. It is believed that ocean surface temperatures contribute to the persistent weather patterns that are associated with drought (Cayan et al., 1998; Herweijer et al., 2007; Seager et al., 2005; Ting & Wang, 1997). Droughts are also commonly linked to increased wildfire occurrence (Girardin et al., 2006; Swetnam & Betancourt, 1998) and to increased fire size (Maingi & Henry, 2007). Westerling et al. (2003) found that seasonal fire severity may be predicted with some skill based on moisture anomalies from antecedent seasons.

2.2.3. *Teleconnections*

Teleconnection is a term used to describe the tendency for atmospheric circulation patterns from one location on the globe to be related either directly or indirectly to another that spans a significantly large area. Teleconnections play a vital role in the study of air–sea interactions and global climate processes. They often prove useful in understanding climate patterns that occur across the world.

Probably the most well-known teleconnection is the El Niño Southern Oscillation (ENSO). It is a phenomenon with global teleconnections and is observed in the tropical Pacific Ocean in which there is either a cooling or warming from the average sea surface temperature (Bridgman & Oliver, 2006). The relationship between ENSO and climate include drought frequency in Africa (Bekele, 1997), upper-atmospheric height anomalies over western Canada and the eastern United States (Horel & Wallace, 1981), summer precipitation in the Northern Plains of the United States (Bunkers et al., 1996), and temperature and precipitation patterns observed across Canada (Shabbar et al., 1997). Simard et al. (1985) studied the relationship between ENSO and fire occurrence in the United States. Their results indicate a strong correlation between El Niño (the warm phase of ENSO) and decreased fire occurrence in the southern United States. However, the results from other areas of the United States were less robust and indicated that ENSO effects are probably best characterized as regional in scale. Hotter and drier conditions favoring increases in wildfire occurrence and behavior typically occur in Australia during El Niño years than occur in La Nina years (Power et al., 2006).

An important intraseasonal variation, known as the Madden Julian Oscillation, has a 30–60 day oscillation period and is dominant in the western Pacific. However, like the ENSO phenomenon, this oscillation is sometimes thought to have far-reaching global teleconnections and has been linked to adversely affecting the forecast skill of numerical models used to predict weather not only in the Tropics but also in the extratropics of the Northern Hemisphere (Hendon et al., 2000).

The northern and tropical Pacific Ocean likely contributes to weather patterns that affect fire occurrence and behavior. The North Pacific Oscillation (NPO) or Pacific Decadal Oscillation (PDO) is a long-lived phenomenon of cyclical changes in ocean temperatures that have a great influence on climate anomalies in North America. In fact, research indicates that there is a correlation between North Pacific sea surface temperatures and El Niño events (Deser & Blackmon, 1995; Reynolds & Rasmussen, 1983; Trenberth, 1990). Flannigan et al. (2000) showed that significant correlations exist between the winter season sea surface temperature and provincial seasonal area burned (May–August) in Canada by separating the analysis by NPO phase.

2.2.4. Climate change

There is a consensus in the scientific community that global warming is occurring and that human activities are responsible for at least some of the increase in temperatures. Whether the warming is originating from anthropogenic or natural causes, it appears that radiatively-active gases in the atmosphere, such as carbon dioxide and methane, are contributing to a warmer global climate. General Circulation Models (GCMs) are used by scientists to simulate the future climate. These models are three-dimensional characterizations of the atmosphere, land, and ocean surfaces that incorporate the uncertainties in the effects of clouds and their radiative effects, the hydrologic balance over land, and ocean heat flux rates. Most model projections indicate that the greatest observed warming will occur at high latitudes in winter. Most models also indicate greater moisture deficits, particularly in the center of continents, during summer. Notaro et al. (2007) have found that future climates will be warmer due mainly to the elevated levels of carbon dioxide. However, these researchers suggest a positive feedback on the climate system that involves disruptions in the hydrologic cycle due to decreased rates of evapotranspiration. The physiological effect from plants' lower evapotranspiration rates will produce drying in tropical climates but increased precipitation in high latitudes due to warming from the combined physiological (less evapotranspiration) and radiative effects. A poleward shift in the boreal forest is expected as both the radiative and physiological effects enhance vegetation growth in the northern tundra and the radiative effect induces drying and summertime heat stress on the central and southern boreal forest. Vegetation feedbacks substantially impact local temperature trends through changes in albedo and evapotranspiration. The physiological effect increases net biomass across most land areas, while the radiative effect results in an increase over the tundra and decrease over tropical forests and portions of the boreal forest.

Some studies indicate universal increases in fire frequency with climatic warming with perhaps significant regional changes in fire activity and area burned (Flannigan et al., 2005; IPCC, 1996; Overpeck et al., 1990; Tymstra et al., 2007). Other studies indicate uncertainty regarding future fire occurrence and behavior associated with the effects of future climate change. Beer and Williams (1994) found that fire activity in Australia is expected to increase but that models may be underpredicting relative humidity, which, in turn, may overestimate fire activity.

2.3. Weather

The meteorological variables relevant to affecting fire behavior result from synoptic scale forcing of weather occurring at the microscale where fire, weather, fuels, and topography interact. Diurnal changes in relative humidity, temperature, and wind speed and direction may dramatically influence fire behavior (Flannigan & Harrington, 1987; Hirsch & Flannigan, 1990). Atmospheric instability, normally computed daily by the Haines Index (Haines, 1988), extended dry spells, and cold front passages are other examples of weather conditions important to managing wildfires and maintaining safety for firefighters (Brotak & Reifsnyder, 1977; Johnson & Miyanishi, 2001). In addition, the electrical properties of clouds cause lightning that affects the ignition of forest fires (Latham & Williams, 2001; MacGorman & Rust, 1998).

2.3.1. Defining weather

Weather is defined as the state of the atmosphere at some place and time, described in terms of such quantitative variables as temperature, humidity, cloudiness, precipitation, and wind speed and direction. Weather is dynamic and differs from the climate of a location, since observed weather over a time period constitutes climate. Fire weather, collectively, is the weather variables, especially wind, temperature, relative humidity, and precipitation that influence fire starts, fire behavior, or fire suppression (Pyne et al., 1996). Kasischke et al. (2002) used geographic analyses to show that the most relevant weather factors affecting fire occurrence in Alaska were growing season temperature, precipitation, and lightning frequency. Short-term local weather, particularly unusual dry spells, low relative humidities, and windy weather generally associated with cold fronts, predispose wildland fuels to fire (Johnson & Miyanishi, 2001).

2.3.2. Temperature

The fraction of the incoming solar radiation that is not reflected from Earth's surface is absorbed and converted to heat. Temperature is the average kinetic energy or energy of motion exhibited by the atoms and molecules composing a substance and is important in determining the ease of combustion of wildland fuels. Heat, an important aspect of the fire triangle, is the energy transferred between an object of greater temperature to an object of lower temperature. It is this heat energy that is crucial in beginning the evaporative or preheating phase of combustion

(Johnson & Miyanishi, 2001). Therefore, higher temperatures heat forest fuels and predispose them to ignition provided that an adequate ignition source becomes readily available (lightning or some anthropogenic source). Ambient temperature undergoes a daily or diurnal cycle that allows for increased fire behavior during the warmest part of the day and less fire activity during the coolest part of the day.

Temperature inversions typically occur during nighttime and usually lead to a decrease in fire activity. Warmer air at some small distance above Earth's surface creates a stable environment such that the smoke-filled air is more dense than the surrounding air and thus spreads horizontally. Temperature inversions may, however, lead to the development of thermal belts whereby sloped valleys in contact with the warm stable layer of air burn more actively than do the cooler slopes either above or below the stable inversion layer.

An important aspect of temperature that relates to fire behavior is the horizontal and vertical distribution of temperature. Vertical temperature contrasts in the atmosphere are described by the degree of atmospheric stability. An unstable atmosphere is one that cools to some degree with increasing height from Earth's surface and can lead to thunderstorm or cloud development as air is allowed to move upward from the surface. Unstable air leads to increased fire behavior in two ways: first, it allows for a well-defined convective plume or column that may produce fire whirls and/or spotting; second, unstable air allows for stronger winds to mix down to the surface, which can lead to higher fire spread rates, and horizontal roll vortices (Haines, 1982). A Lower Atmospheric Stability Index (LASI) was developed (Haines, 1988) and then modified (Potter, 1995) to help determine the potential for wildfires to become large and/or erratic.

2.3.3. Lightning

Lightning contributes to wildfires worldwide but only leads to ignition when fuel type and fuel moisture are favorable. There is some debate as to whether the positive cloud-to-ground (CG) lightning strikes produce more ignitions than do their negatively charged counterpart. It is believed that most lightning-caused wildfires are caused by more energetic lightning strokes. Approximately 90% of CG lightning flashes worldwide transfer negative electric charge to the ground. These negative flashes tend to be multi-stroked compared to the 10% of CG flashes that transfer positive charge to the ground in single-stroke flashes. It is thought that single-stroke flashes allow for a longer continuing current and thus are more apt to cause fire initiation. Only approximately half of the negative flashes contain continuing currents (Uman, 1969). This commonly regarded method of fire initiation has been questioned, however, by Flannigan and Wotton (1991), who found large numbers of negative CG flashes with continuing currents.

Fuel type and fuel state are also important to the occurrence of wildfires. Latham and Williams (2001) found that some fuel types are more efficient in lightning-caused ignition, based on a 7-year study utilizing geographic information system (GIS) layers of fuel type with lightning occurrence. The study indicates that trees including both coniferous and deciduous (0.03–0.05 fires/flash) are more apt to ignite compared to grass, shrubs, and croplands (0.003–0.02 fires/flash). Lightning fire efficiency rates are dependent upon a multitude of factors that include synoptic weather conditions, fuel types, thunderstorm characteristics including rainfall and lightning rates, lightning characteristics, and fuel state that primarily describes the moisture content of fuels (Johnson & Miyanishi, 2001).

2.3.4. Moisture

Atmospheric moisture in the form of water vapor and precipitation plays a significant limiting factor on fire occurrence and fire behavior by affecting fuel moisture in both dead and living plants. Evidence suggests that increasing amounts of fuel moisture act to retard the rate of combustion, preheating of fuels, and ease of ignition. When the air is saturated, there exists an equilibrium between evaporation and condensation. Much of the time in areas that are prone to fire, evaporation is greater than condensation, and wildland fuels lose their moisture to the ambient air through the process of evapotranspiration. Ambient air evaporation rates are known to change based on the difference between the vapor pressure between the adjacent air and a water surface (Johnson & Miyanishi, 2001). Relative humidity refers to the amount of water vapor in the air at one time relative to the maximum amount of water vapor the air could hold at the same temperature. It undergoes a diurnal cycle linked to the normal rising and falling of the ambient temperature and dew point temperature.

Indirectly, existing moisture on Earth's surface that is in contact with the air is related to the ease of temperature changes. During times of moisture pooling or ponding, available energy from incoming solar radiation is used in evaporation. Otherwise, when surface moisture is scarce, the energy from incoming solar radiation is converted to heat. Precipitation varies widely in time and space in both hemispheres, and these patterns also exhibit seasonal shifts depending upon factors such as proximity to large bodies of water, prevailing upper-atmospheric wind patterns, and storm tracks.

2.3.5. Wind

Air moves in response to pressure differences in Earth's atmosphere and as a result of frictional effects near Earth's surface. Wind affects fire occurence and especially fire behavior at the synoptic, regional, and microclimate scales. Fast-moving air at high altitudes or the jet stream level has been observed to enhance wildland fire behavior by allowing drier and warmer stratospheric air to penetrate to the lower part of the troposphere (Carlson, 1980; Danielsen, 1968; Keyser & Shapiro, 1986). Regionally, both warm and cold surface fronts are linked to jet stream behavior and both create challenges for wildland fire management. Weather changes that occur on a daily basis from air mass changes can have a considerable impact on fire occurrence and fire size. Brotak and Reifsnyder (1977), studying the relationship between major fires in the eastern United States, found that nearly 80% of large fires were associated with a cold front, and were predominantly associated with the passage of dry cold fronts. Winds associated with cold fronts are also important to smoke dispersal from large fires (Freitas et al., 2005).

There are also a number of important local wind circulations that are observed on the microclimate scale. Sea breezes and land breezes, occurring both during the day and night respectively, result from pressure differences induced by the heating and cooling rate of the land compared to the ocean. Mountain and valley winds are also related to the relative diurnal heating of the valley and mountaintops.

Mountain winds can sometimes have devastating effects when air is forced to descend through narrow mountain passes. Not only does the wind speed become excessive, the descending air tends to warm adiabatically, resulting in warm, dry, and fire-prone conditions. Examples of such föhn winds include the Santa Ana in southern California, the Chinook in the lee of the U.S. Rocky Mountains, the Bergwind in South Africa, the Terral in Spain, and the Nor'wester in New Zealand (see Whiteman, 2000).

2.4. Fire, climate, and weather

Many scientific studies of wildland fire have been conducted that describe the interactions between climate, weather, and wildland fire (Chandler et al., 1983; Cheney & Sullivan, 1997; Davis, 1959; Johnson & Miyanishi, 2001; Pyne et al., 1996; Schroeder & Buck, 1970). This section presents a brief glimpse at the rich knowledge of wildland fire and its interactions with weather and climate that have been described over the past century.

2.4.1. Wildland fire

Weather and climate influence a fire's ignition, the fuels that burn, and the environment in which the fire burns. Climate is one of the principal determinants of vegetation distribution and productivity (Fig. 2.1). Vegetation in similar climates has adapted similar characteristics that influence fire. For example, in Mediterranean areas, vegetation growth occurs in the spring, and plants have developed mechanisms to conserve moisture during the long drought (Naveh, 1975). Similarly, coniferous forests have developed in the boreal regions of the world in response to the long winters with subfreezing temperatures and short summer growing seasons typical of the subarctic and cold continental climate. The boreal forest is located in the northern regions of North America in Canada and Alaska, and in Eurasia in Sweden, Norway, Finland, Russia, Kazakhstan, and Siberia. Precipitation is low but exceeds evaporation. As in the Mediterranean regions of the world, naturally occurring fire often results in the combustion and consumption of the aboveground vegetation.

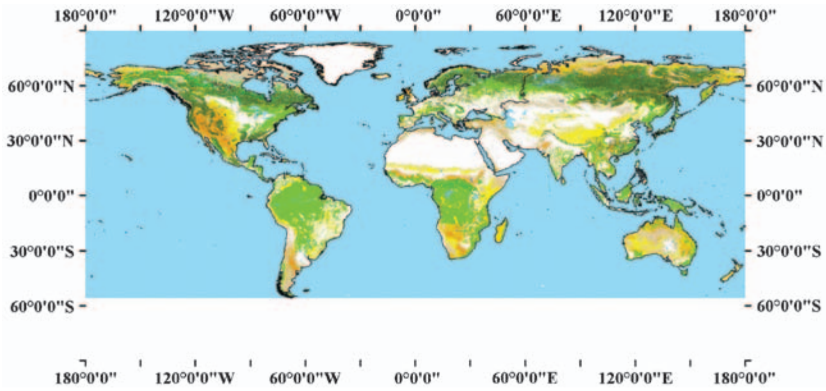

Figure 2.1. Global distribution of tree, shrub, and herbaceous vegetation, which is a result of climate. Herbaceous vegetation indicated by yellow, shrub by orange, broadleaved trees by light green, needle-leaved trees by dark green, and mixed trees by olive. Sparse vegetation is indicated by tan. (Modified from source map (European Commission Joint Research Centre, 2003)).

Globally, humans have used fire as a tool that has largely shaped the current status of the world's forests. This has been accomplished by both the introduction of fire into areas previously immune to it and the suppression of fire in large areas where fire has burned naturally on a regular basis. Humans and fire have a long history whereby prescribed fires are designed and used as a management tool to accomplish specific objectives. Wildland fires, however, are caused primarily by human carelessness and may be a destructive force to forest ecosystems (Pyne et al., 1996).

Lightning is a major cause of ignition throughout the world. In Christian et al. (2003), lightning occurrence ranged from 1 to 50 flashes $km^{-1}\,yr^{-1}$; however, all flashes did not result in a fire. The relative importance of lightning versus human-caused ignition varies around the world and is linked to human-population density. Lightning-caused fires often occur in mountainous areas. One of the important factors that determine the success of lightning ignition (as well as all other types of ignition) is the moisture content of the fuel where the ignition occurs (Latham & Williams, 2001).

2.4.2. Fuel moisture

Fuel moisture content is defined as the mass of water present in a fuel and is typically expressed as a fraction of the oven-dry mass of the fuel. Because of the importance of moisture in determining the ability of wildland fuels to burn, fuel moisture content is used in most fire hazard assessment and prediction systems (Fujioka et al., this volume; Roads et al., 2005) and has been correlated with area burned by wildfire in many countries (Flannigan & Harrington, 1988; for an in-depth discussion of fuel moisture and water relations in live and dead fuels, Nelson, 2001).

The cellular structure of plants contains void spaces that can contain water. In addition to playing an important role in photosynthesis and cellular metabolism, water also provides structural support to living plants. The cellular structure is maintained in the castoff foliage and branches that comprise dead wildland fuels until the dead material has decomposed. As a result, dead fuels are porous so that water is absorbed and desorbed much like a sponge; diffusion is the primary process governing the adsorption and desorption. Three weather factors strongly influence the amount of water contained within a dead fuel: temperature, relative humidity, and precipitation. A fourth factor, incident solar radiation, is important when considering the effects of ambient heating on the dead fuel (Chandler et al., 1983). Under constant temperature and relative humidity, a dead fuel particle will eventually reach an equilibrium moisture content (EMC) that is a function of the immediate environmental conditions surrounding the fuel particle. The time required for a cylindrical fuel particle to reach equilibrium with its surroundings increases as the diameter increases. EMC is seldom achieved in most wildland situations, as temperature and relative humidity are constantly changing; however, EMC is a useful concept when developing models to predict fuel moisture content (Catchpole et al., 2001; Viegas et al., 1992). Wildland fuels that are less than 0.63 cm in diameter are referred to as fine fuels and respond quickly to changes in relative humidity and temperature. Fuels of this size are often the primary carriers of wildland fire. Of the two weather variables, relative humidity is more important in determination of fuel moisture content, as it determines the moisture gradient between the air and the fuel particle. As air temperature increases, fuel moisture of dead fuels will decrease. Precipitation increases fuel moisture content; however, some dead cellulosic fuels such as grass may more readily absorb slight amounts of precipitation than similar-sized woody fuels (Weise et al., 2005a, 2005b). Reservoirs of accumulated precipitation in the form of snowpack and soil moisture also affect fuel moisture content of surface fuels (Hatton et al., 1988; McCammon, 1976).

Living plants have developed processes and mechanisms that regulate the intake of water from the soil and air and the release of water into the atmosphere. Many of these mechanisms are designed specifically to conserve water. Climatic conditions, notably relative humidity and temperature, have influenced the degree to which a plant needs to conserve water. In climates where water is deficit, plants have adapted mechanisms designed to conserve water. Among these adaptations are thick cutin (waxy coating) and hairs on leaf surfaces, sunken stomata, and the ability to store water (succulent plants). Many plants enter a form of dormancy to minimize water usage during drought periods. During this drought period, the moisture content of the plants decreases, increasing the likelihood that the vegetation will burn. Fire occurrence has been linked with drought throughout the world. In addition to the increased hazard presented by dry living vegetation, drought also causes plant mortality, increasing the amount of dead wildland fuels.

2.4.3. Types of wildland fire

Two types of combustion occur in wildland fires: flaming and smoldering (Pyne et al., 1996). Flaming combustion results when the gases released by the heating of a fuel come in contact with oxygen and ignite to produce the familiar flame of a fire. Due to the temperature of the gases and particulate matter (800–1000 °C), the gases and particles emit energy radiantly in the visible wavelengths. The flame is buoyant and forms a plume of hot gases that rise, expand, entrain ambient air, and eventually cool.

Wildland fires can be classified based on the location of the fuel that is burning. Perhaps the most common type of fire burns in live and dead vegetation that is in close proximity to the soil surface. This type of fire is known as a surface fire; oxygen is typically not a limiting factor. Some fires spread through layers of decomposing organic material and organic soils. This type of fire is called a ground fire; conduction and radiation from glowing fuel particles play a significant role in spread. Because oxygen is often limiting in this situation, smoldering combustion is often the dominant mode in these ground fires. Flames are not present. The third class of fire is called a crown fire because the fire spreads through the crowns and canopies of the shrubs or trees. In this situation, the fuels are elevated and the flame zone may or may not extend completely to the ground. Due to the depth of the fuels in shrub and tree crowns, crown fire typically has the greatest flame lengths compared to the other types of fire (also see Ottmar et al., this volume).

2.4.4. Wind and fire

Wind is arguably the most important weather and climate factor that influences the behavior of a fire (Albini, 1982; Beer, 1991; Taylor et al., 2004). There are three types of wind that are associated with wildland fire: general winds resulting from atmospheric activity, local winds resulting from unequal heating of land and sea surfaces, and winds resulting from a fire's buoyancy (also called entrainment). Most wildland fires move in one or more directions depending on the availability of fuels, wind direction, and topography. If fuels are discontinuous (e.g., as in deserts), then a fire may not spread successfully unless wind velocity and direction are sufficient to cause a fire to ''leap'' the gap between fuels.

Much research has been devoted to wind flow in urban and vegetated environments. A recent book compiles much of the material on the flow characteristics through these porous environments (Gayev & Hunt, 2007). Meroney (2007) discusses the effects of these porous environments on fire spread in both the urban and forested environments. These flow regimes also influence the distribution and transport of pollutants and smoke within urban and wildland–urban interface settings.

Wildland fires are often described by the direction the fire is spreading relative to the direction of the wind. A fire that spreads in the direction that the wind is blowing is called a heading fire, a fire that spreads in the direction the wind is blowing from is called a backing fire, and a fire that spreads perpendicular to the wind direction is called a flanking fire. The rates and completeness of combustion often differ as a function of fire spread, which in turn influences the production of smoke.

In addition to influencing the size of flames, wind and slope also influence the rate at which a fire will spread. It is generally agreed that the spread rate of a backing fire is relatively constant in surface fuels. Rates of spread of heading fires are several orders of magnitude greater than backing fire spread rates in litter (0.02–0.04 $km\,h^{-1}$). Under the influence of high-velocity winds or steep slopes, head fire spread rates can be 0.5 $km\,h^{-1}$ for logging residue fuels, 5–15 $km\,h^{-1}$ for brush fuels, and 22 $km\,h^{-1}$ for grass fuels (Pyne et al., 1996). Noble (1991) reported that the highest observed spread rates in grasslands in southeastern Australia were 23 $km\,h^{-1}$. Under high wind speeds and in deep fuels, flame lengths of 20–30 m are not uncommon.

Potter (2002) developed a conceptual model of plume and fire dynamics. This model describes dynamics in three layers: surface, mixing, and stable. The interaction of a fire and its plume varies in these layers, and influential atmospheric variables may change between layers. The interaction between the energy and mass released by a fire and the fire environment results in a highly turbulent region of complex fluid flows. The presence of wind further complicates these fluid flows. Various phenomena that are collectively termed "extreme" fire behavior result from this interaction. Extreme fire behavior includes long-range transport of flying embers (spotting), crown fires (Albini & Stocks, 1986; Grishin & Gruzin, 1990), fire whirls (Graham, 1957), horizontal roll vortices (Haines & Smith, 1987), blowup fires (Potter, 2002), and mass fire (Countryman, 1964). Mass fires result when a large area experiences multiple ignitions. McArthur (1967) reported that transport of burning embers of eucalyptus bark 8–10 km is commonplace in eucalyptus forests and that there are well-documented cases of spot fires occurring 19–24 km in advance of the main fire. Transport of partially combusted forest fuels has been recently reported from a crown fire in Switzerland; however, no subsequent fire was ignited, suggesting that the firebrands were extinguished before landing (Tinner et al., 2006).

While radiation and conduction are important modes of heat transfer, convection plays a significant role in transitions in fire behavior (Finney et al., 2006; Weise et al., 2005a, 2005b;). High wind speeds are linked with severe fire behavior in many regions of the world (Bureau of Meteorology, 1984; Kutiel & Kutiel, 1991; Moravec, 1990; Thomas, 1971; van Wilgen et al., 1985; Wilson, 1962). As wildland fires grow in size and energy release, their interaction with the fire environment modifies local wind flows and other components of the local environment. Under certain conditions, the water vapor that is released in combustion will condense, form a cumulus-type cloud at the top of the fire plume, and rain. If the plume collapses, downdrafts may result that cause the fire to spread in several different directions. Recent modeling and reconstruction of significant wildfires suggest that dry air introduced from high in the atmosphere can cause erratic fire behavior (Mills, 2005; Zimet et al., 2007).

Byram (1959) presented a model of the interaction between a fire and the atmosphere based on plume theory. The derivation of this model (Nelson, 1993), which assumed a neutrally stable atmosphere and no entrainment, was extended to an unstable atmosphere with entrainment (Nelson, 2003). The model essentially looked at the balance between the ''the rate of conversion of thermal energy to kinetic energy in the convection column'' (''power of the fire'') and the ''the rate of flow of kinetic energy in the atmosphere due to the wind field'' (''power of the wind''). When the rate of energy release by the fire into the convection column above the fire dominates the atmospheric winds (power of the fire is greater than the power of the wind), the fire is called a ''plume-dominated fire'' (Ingalsbee, 2005). A plume-dominated fire can behave erratically, and the entrainment winds caused by the buoyancy of the convection column can be very strong and occur from many directions.

The energy release and fluid flows associated with wildland fire are complex. Topography further complicates the fluid flows (Viegas, 2005). Until fairly recently, scientists who studied and modeled these phenomenon had to simplify the problems so that they could be analytically or empirically solved. Today, complex computer codes in computational fluid dynamics and radiative energy transport enable many of the complex fire behavior phenomena to be modeled and compared with experimental data. Instruments such as lidar and radar can be used to describe characteristics of fire plumes, including the fluid flows within the plume (Banta et al., 1992). Crown fire spread (Albini, 1996), fire spread in the solid and gas phases (Porterie et al., 2000), fire whirls (Battaglia et al., 2000), transition from surface to crown fire (Cruz et al., 2006), transition from no-spread to spread (Zhou et al., 2005), and firebrand generation and transport (Sardoy et al., 2007) are just some of the complex problems now being studied by fire scientists throughout the world. One of the current frontiers in fire behavior modeling is modeling the coupling between a fire and the atmosphere (Coen, 2005; Linn et al., 2002).

Interaction between a fire and the local weather determines the transport of the combustion products. Wildfire smoke is buoyant because it is released from the combustion zone at a temperature that is much greater than the ambient air temperature. Because of this buoyancy, smoke in the buoyant plume will rise, disperse, and cool until it reaches a height in the atmosphere at an equivalent temperature. The presence of temperature inversions in the lower atmosphere will restrict smoke dispersion. Temperature inversions result when cooler air becomes trapped under warmer air; this phenomenon often occurs in mountainous terrain. As a result of the temperature inversion, smoke can become trapped under the inversion resulting in unhealthful conditions. A fire of sufficient size and energy release rate has the ability to ''break through'' an inversion layer, which results in increased venting, smoke dispersion, and fire behavior.

Nocturnal smoke transport resulting from low-intensity fires in relatively flat terrain is strongly influenced by micrometeorological conditions and topography. Smoke can flow significant distances along small drainage channels, ending up in areas such as highways, creating local visibility hazards (Achtemeier, 2005; Achtemeier & Paul, 1994). In the southern United States, clear skies and light winds are critical to the movement of smoke in this manner.

The transport of smoke from wildfires can be long range, occurring at global scales (Bertschi & Jaffe, 2005; Damoah et al., 2004). In this instance, smoke from fires becomes mixed into the lower atmosphere at heights up to 6 km. In some instances, fires have been energetic enough to inject smoke into the upper troposphere/lower stratosphere but this has generally been considered a rare occurrence (Fromm & Servranckx, 2003). The long-range transport of smoke from wildfires may have political implications, as the world becomes a global community. The large-scale deforestation and fires associated with land clearing in the tropics have been implicated in climate change (Hao & Liu, 1994; Levine, 1991), and biomass burning has been shown to impact atmospheric chemistry and dynamics (also see Goldammer et al., this volume).

2.5. Conclusion

At the global scale, climate, vegetation, and fire interact to produce a complex pattern of fire occurrence. While we have had an understanding locally of weather and fire occurrence at the scale of individual countries, we have only recently been able to view fire occurrence globally (Fig. 2.2). Satellite imagery has greatly improved our ability to look at large-scale connections between wildfire occurrence, vegetation, and climate. The planned use of fire at smaller scales may not be as readily detected by these sensors, suggesting that fire is a complex phenomenon globally. As Pyne so eloquently stated, Earth is a fire planet (Pyne et al., 1996).

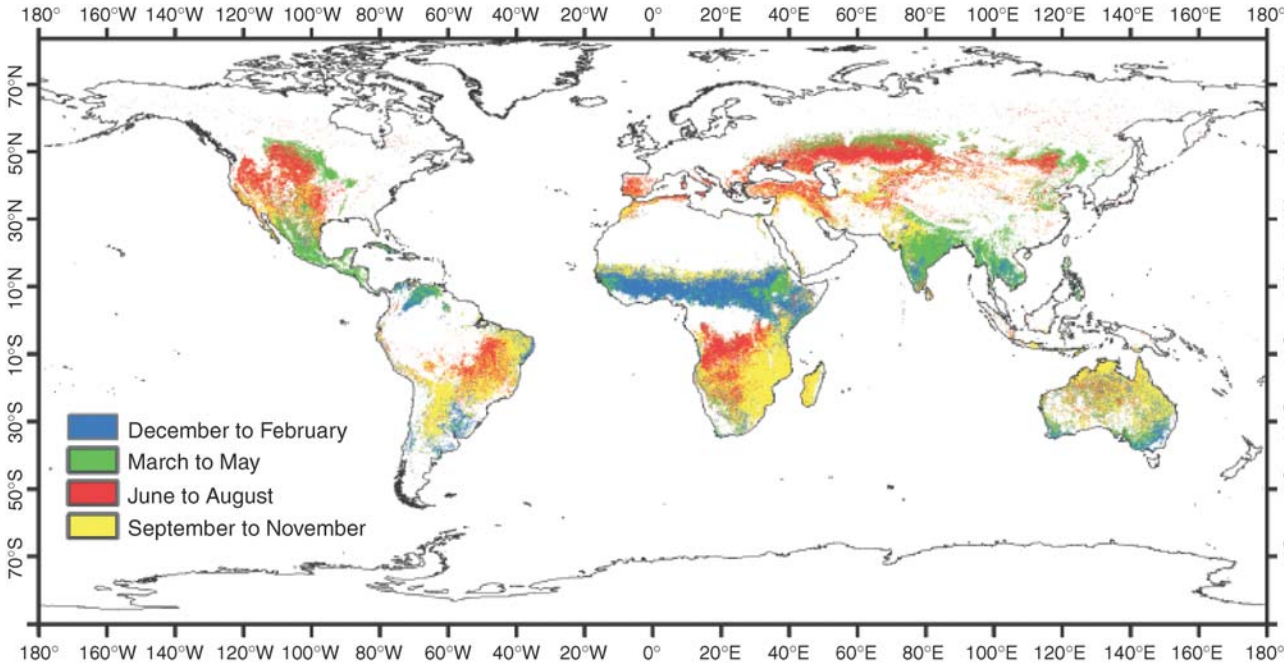

Figure 2.2. Global seasonal fire activity estimated using data from the space-based AVHRR sensor for the period 1982–1999. (From Carmona-Moreno et al., 2005.)

REFERENCES

Achtemeier, G.L. 2005. Planned burn-Piedmont. A local operational numerical meteorological model for tracking smoke on the ground at night: Model development and sensitivity tests. Int. J. Wildland Fire 14, 85–98.

Achtemeier, G.L., and Paul, J.T. 1994. A computer model for predicting smoke movement. South. J. Appl. For. 18(2), 60–64.

Albini, F.A. 1982. Response of free-burning fire to nonsteady wind. Comb. Sci. Technol. 29, 225–241.

Albini, F.A. 1996. Iterative solution of the radiation transport equations governing spread of fire in wildland fuel. Comb. Explo. Shock Waves 32(5), 534–543.

Albini, F.A., and Stocks, B.J. 1986. Predicted and observed rates of spread of crown fire in immature jack pine. Comb. Sci. Technol. 48, 65–76.

Banta, R.M., Olivier, L.D., Holloway, E.T., Kropfli, R.A., Bartram, B.W., Cupp, R.E., and Post, M.J. 1992. Smoke-column observations from two forest fire using Doppler lidar and Doppler radar. J. Appl. Meteorol. 31, 1328–1349.

Battaglia, F., McGrattan, K.B., Rehm, R.G., and Baum, H.R. 2000. Simulating fire whirls. Comb. Theor. Model. 4(2), 123–138.

Beer, T. 1991. The interaction of wind and fire. Bound. Lay. Meteorol. 54, 287–308.

Beer, T., and Williams, A. 1994. Estimating Australian forest fire danger under conditions of doubled carbon dioxide. Clim. Change 29(2), 169–188.

Bekele, F. 1997. Ethiopian use of ENSO information in its seasonal forecasts. Int. J. African Stud. 2. www.brad.as.uk/research/ijas/ihasno2/ijasno2.html

Bertschi, I.T., and Jaffe, D.A. 2005. Long-range transport of ozone, carbon monoxide, and aerosols to the NE Pacific troposphere during the summer of 2003: Observations of smoke plumes from Asian boreal fires. J. Geophys. Res. 110, D05303 doi:10.1029/2004JD005135

Bridgman, H.A., and Oliver, J.E. 2006. The global climate system. Cambridge University Press, Cambridge.

Brotak, E.A., and Reifsnyder, W.E. 1977. An investigation of the synoptic situations associated with major wildland fires. J. Appl. Meteorol. 16, 867–870.

Bunkers, M.J., Miller, J.R. Jr., and deGaetano, A.T. 1996. An examination of El Niño-La Niña related precipitation and temperature anomalies across the northern plains. J. Climatol. 9, 147–160.

Bureau of Meteorology, Australia. 1984. Report on the Meteorological Aspects of the Ash Wednesday Fires. 16 February, 1983, Australian Government Publishing Service, Canberra.

Byram, G.M. 1959. Combustion of forest fuels. In: Davis, K.P., ed. Forest fire: Control and use. McGraw-Hill, New York, 61–89 (584 pp.).

Carlson, T.N. 1980. Airflow through midlatitude cyclones and the comma cloud pattern. Mon. Wea. Rev. 108, 1498–1509.

Carmona-Moreno, C., Belward, A., Malingreau, J.-P., Hartley, A., Garcia-Alegre, M., Antonovskiy, M., Buchshtaber, V., and Pivovarov, V. 2005. Characterizing interannual variations in global fire calendar using data from Earth observing satellites. Glob. Chang. Biol. 11, 1537–1555.

Catchpole, E.A., Catchpole, W.R., Viney, N.R., McCaw, W.L., and Marsden-Smedley, J.B. 2001. Estimating fuel response time and predicting fuel moisture content from field data. Int. J. Wildland Fire 10, 215–222, doi:10.1071/WF01011.

Cayan, D.R., Dettinger, M.D., Diaz, H.F., and Graham, N.E. 1998. Decadal variability of precipitation over western North America. J. Clim. 11(12), 3148–3166.

Chandler, C., Cheney, P., Thomas, P., Traband, L., and Williams, D., eds. 1983. Fire in forestry, Vol. 1: Forest fire behavior and effects. Wiley, 450 pp.

Cheney, P., and Sullivan, A. 1997. Grassfires: Fuel, weather and fire behavior. CSIRO Publishing, Collingwood, Australia, 102 pp.

Christian, H.J., Blakeslee, R.J., Boccippio, D.J., Boeck, W.L., Buechler, D.E., Driscoll, K.T., Goodman, S.J., Hall, J.M., Koshak, W.J., Mach, D.M., and Stewart, M.F. 2003. Global frequency and distribution of lightning as observed from space by the optical transient detector. J. Geophys. Res. 108(D1), 4005, doi:10.1029/2002JD002347.

Coen, J.L. 2005. Simulation of the Big Elk Fire using coupled atmosphere-fire modeling. Int. J. Wildland Fire 14, 49–59.

Countryman, C.M. 1964. Mass fires and fire behavior. Research Paper PSW-19, Pacific Southwest Forest and Range Experiment Station. Forest Service, U.S. Department of Agriculture, Berkeley, CA. 53 pp.

Cruz, M.G., Butler, B.W., Alexander, M.E., Forthofer, J.M., and Wakimoto, R.H. 2006. Predicting the ignition of crown fuels above a spreading surface fire. Part 1: Model idealization. Int. J. Wildland Fire 15(1), 47–60.

Damoah, R., Spichtinger, N., Forster, C., James, P., Mattis, I., Wandinger, U., Beirle, S., Wagner, T., and Stohl, A. 2004. Around the world in 17 days—hemispheric-scale transport of forest fire smoke from Russia in May 2003. Atmos. Chem. Phys. 4, 1311–1321.

Danielsen, E.F. 1968. Stratospheric–tropospheric exchange based on radioactivity, ozone and potential vorticity. J. Atmos. Sci. 25, 502–518.

Davis, K.P. 1959. Forest fire: Control and use. McGraw-Hill, New York, 61–89, 584 pp.

Deser, C., and Blackmon, M.L. 1995. On the relationship between tropical and North Pacific sea surface temperature variations. J. Climatol. 8, 1677–1680.

European Commission Joint Research Centre. 2003. Global Land Cover 2000 database. www-gem.jrc.it/glc2000.

Finney, M.A., Cohen, J.D., Grenfell, I.C., and Yedinak, K.M., 2006. Experiments on fire spread in discontinuous fuelbeds. Proceedings, 5th International Conference on Forest Fire Research. 27–30 November 2006, Figueira da Foz, Portugal.

Flannigan, M.D., and Harrington, J.B. 1987. Synoptic conditions during the Porter Lake burning experiment. Climatol. Bull. 21, 19–40.

Flannigan, M.D., and Harrington, J.B. 1988. A study of the relation of meteorological variables to monthly provincial area burned by wildfire in Canada (1953–80). J. Appl. Meteorol. 27(4), 441–452.

Flannigan, M.D., Logan, K.A., Amiro, B.D., Skinner, W.R., and Stocks, B.J. 2005. Future area burned in Canada. Clim. Change 72, 1–16.

Flannigan, M.D., Todd, B., Wotton, B.M., Skinner, W.R., Stocks, B.J., and Martell, D.L. 2000. Pacific sea surface temperatures and their relation to area burned in Canada. Preprints, Third Symposium on Fire and Forest Meteorology. Amer. Meteorol. Soc. 151–157.

Flannigan, M.D., and Wotton, B.M. 1991. Lightning-ignited fires in northwestern Ontario. Can. J. For. Res. 21, 277–287.

Freitas, S.R., Longo, K.M., Silva Dias, M.A.F., Silva Dias, P.L., Chatfield, R., Prins, E., Artaxo, P., Grell, G.A., and Recuero, F.S. 2005. Monitoring the transport of biomass burning emissions in South America. Environ. Fluid Mech. 5, 135–167.

Fromm, M.D., and Servranckx, R. 2003. Transport of forest fire smoke above the tropopause by supercell convection. Geophys. Res. Lett. 30(10), 1542 49-1 to 49-4, doi:10.1029/2002GL016820.

Fujioka, F.M., Gill, A.M., Viegas, D.X., and Wotton, B.M. 2008. Fire danger and fire behavior modeling systems in Australia, Europe, and North America. In: Bytnerowicz, A., Arbaugh, M., Riebau, A. and Andersen, C., eds. Wildland fires and air pollution. Elsevier, Oxford, UK, pp. 469–497.

Gayev, Y.A., and Hunt, J.C.R., eds. 2007. Flow and transport processes with complex obstructions. NATO Science Series II-Vol. 236. Springer, New York.

Girardin, M.P., Bergeron, Y., Tardif, J.C., Gautheir, S., Flannigan, M.D., and Mudelsee, M. 2006. A 229-year dendroclimatic-inferred record of forest fire activity for the Boreal Shield of Canada. Int. J. Wildland Fire 15(3), 375–388.

Graham, H.E. 1957. Fire whirlwind formation as favored by topography and upper winds. Fire Control Notes 18(1), 20–24, Forest Service, U.S. Department of Agriculture, Washington, D.C.

Grishin, A.M., and Gruzin A.D., 1990. Investigation of the spread of the two-dimensional front of a crown forest fire initiated by a center of finite size. Fizika goreniya i vzryva (Combustion, Explosion, and Shock Waves) 26(4), 377–382. Russian Academy of Sciences, Novosibirsk, Siberia.

Haines, D.A. 1982. Horizontal roll vortices and crown fires. J. Appl. Meteorol. 21, 751–763.

Haines, D.A. 1988. A lower atmosphere severity index for wildland fires. Nat. Weath. Digest 13(2), 23–27.

Haines, D.A., and Smith, M.C. 1987. Three types of horizontal vortices observed in wildland mass and crown fires. J. Clim. Appl. Meteorol. 26(12), 1624–1637.

Hao, W.M., and Liu, M.-H. 1994. Spatial and temporal distribution of tropical biomass burning. Global Biogeochem. Cycles 8(4), 495–504.

Hatton, T.J., Viney, N.R., Catchpole, E.A., and De Mestre, N.J. 1988. The influence of soil moisture on eucalyptus leaf litter moisture. For. Sci. 34(2), 292–301.

Hendon, H.H., Liebmann, B., Newman, M., Glick, J.D., and Schemm, J.E. 2000. Medium-range forecast errors associated with active episodes of the Madden-Julian oscillation. Mon. Wea. Rev. 128, 69–86.

Herweijer, C., Seager, R., Cook, E.R., and Emile-Geay, J. 2007. North American droughts of the last millennium from a gridded network of tree-ring data. J. Clim. 20(7), 1353–1376.

Hirsch, K.G., and Flannigan, M.D. 1990. Meteorological and fire behavior characteristics of the 1989 fire season in Manitoba, Canada. International Conference on Forest Fire Research, Coimbra, B.06-1-B.06-16. Springer, New York.

Horel, J.D., and Wallace, J.M. 1981. Planetary-scale atmospheric phenomena associated with the southern oscillation. Mon. Wea. Rev. 109, 813–829.

Ingalsbee, T. 2005. A reporter's guide to wildland fire. FUSEE (Firefighters United for Safety, Ethics, and Ecology), Eugene, OR. www.fusee.org/content_pages/docs/Reporters_guide.pdf

Intergovernmental Panel on Climate Change. 1996. Climate change 1995 impacts, adaptations, and mitigation of climate change: Scientific-technical analyses. Cambridge University Press, Cambridge.

Intergovernmental Panel on Climate Change. 2007. Climate change 2007 impacts, adaptations, and mitigation of climate change: Scientific-technical analyses. Cambridge University Press, Cambridge.

Johnson, E.A., and Miyanishi, K., eds. 2001. Forest fires: Behavior and ecological effects. Academic Press, San Diego, CA, 594 pp.

Kasischke, E.S., Williams, D., and Barry, D. 2002. Analysis of the patterns of large fires in the boreal forest region of Alaska. Int. J. Wildland Fire 11(2), 131–144, doi:10.1071/WF02023.

Keyser, D., and Shapiro, M.A. 1986. A review of the structure and dynamics of upper-level frontal zones. Mon. Wea. Rev. 114, 452–499.

Kutiel, H., and Kutiel, P. 1991. The distribution of autumnal easterly wind spells favoring rapid spread of forest wildfires on Mount Carmel, Israel. GeoJournal 23(2), 17–152.

Latham, D., and Williams, E. 2001. Lightning and forest fires. In: Johnson, E.A., and Miyanishi, K., eds. Forest fires: Behavior and ecological effects. Academic Press, San Diego, CA, 375–418 (594 pp.).

Levine, J.S., ed. 1991. Global biomass burning: Atmospheric, climatic, and biospheric Implications. MIT Press, Cambridge, MA, 599 pp.

Linn, R., Reisner, J., Colman, J.J., and Winterkamp, J. 2002. Studying wildfire behavior using FIRETEC. Int. J. Wildland Fire 11(4), 233–246.

MacGorman, D.R., and Rust, W.D. 1998. The electrical nature of storms. Oxford University Press, New York, NY.

Maingi, J.K., and Henry, M.C. 2007. Factors influencing wildlife occurrence and distribution in eastern Kentucky, USA. Int. J. Wildland Fire 16, 23–33.

McArthur, A.G. 1967. Fire behaviour in eucalypt forests. Commonweath Forestry and Timber Bureau Leaflet No. 107. Department of National Development, Canberra, ACT, Australia, 36 pp.

McCammon, B. 1976. Snowpack influences on dead fuel moisture. For. Sci. 22(3), 323–328.

McKnight, T.L., and Hess, D. 2000. Climate zones and types: The Köppen System, physical geography: A landscape appreciation. Prentice Hall, Upper Saddle River, NJ, 200–201

Meroney, R.N. 2007. Fires in porous media: Natural and urban canopies. In: Gayev, Y.A., and Hunt, J.C.R. eds. Flow and Transport Processes with Complex Obstructions, 271–310. Springer, Netherlands.

Mills, G.A. 2005. A re-examination of the synoptic and mesoscale meteorology of Ash Wednesday 1983. Australian Meteorol. Mag. 54(1), 35–55.

Moravec, J. 1990. Regeneration of N.W. African *Pinus halepensis* forests following fire. Vegetatio 87, 29–36.

Naveh, Z. 1975. The evolutionary significance of fire in the Mediterranean region. Plant Ecol. 29(3), 199–208, doi: 10.1007/BF02390011.

Nelson, R.M. Jr. 1993. Byram derivation of the energy criterion for forest and wildland fires. Int. J. Wildland Fire 3, 131–138, doi: 10.1071/WF9930131.

Nelson, R.M. Jr. 2001. Water relations of forest fuels. In: Johnson, E.A., and Miyanishi, K., eds. Forest fires: Behavior and ecological effects. Academic Press, San Diego, CA, pp. 79–149. 594 pp.

Nelson, R.M. Jr. 2003. Power of the fire—a thermodynamic analysis. Int. J. Wildland Fire 12, 51–65.

Noble, J.C. 1991. Behaviour of a very fast grassland wildfire on the Riverine plain of southeastern Australia. Int. J. Wildland Fire 1(3), 189–196.

Notaro, M., Vavrus, S., and Liu, Z. 2007. Global vegetation and climate change due to future increases in CO_2 as projected by a fully coupled model with dynamic vegetation. Ontario. Can. J. For. Res. 21, 277–287.

Overpeck, J.T., Rind, D., and Goldberg, R. 1990. Climate-induced changes in forest disturbance and vegetation. Nature 343, 51–53.

Porterie, B., Morvan, D., Loraud, J.C., and Larini, M. 2000. Firespread through fuel beds: Modeling of wind-aided fires and induced hydrodynamics. Phys. Fluids 12(7), 1762–1782.

Potter, B.E. 1995. Regional analysis of Haines' LASI. Fire Manage. Notes 55, 30.

Potter, B.E. 2002. A dynamics based view of atmosphere–fire interactions. Int. J. Wildland Fire 11, 247–255.

Power, S., Haylock, M., Colman, R., and Wang, X. 2006. The predictability of interdecadal changes in ENSO activity and ENSO teleconnections. J. Clim. 19(19), 4755–4771.

Pyne, S.J., Andrews, P.L., and Laven, R.D. 1996. Introduction to wildland fire (second ed.). Wiley, 769 pp.

Reynolds, R.W., and Rasmussen, E.M. 1983. The North Pacific sea surface temperature associated with El Niño events. Proceedings of the Seventh Annual Climate Diagnostics Workshop. U.S. Department of Commerce, National Oceanic and Atmospheric Administration, Washington, D.C.

Roads, J., Fujioka, F., Chen, S., and Burgan, R. 2005. Seasonal fire danger forecasts for the USA. Int. J. Wildland Fire, Special Issue: Fire and Forest Meteorology, 14, 1–18.

Sardoy, N., Consalvi, J.-L., Porterie, B., and Fernandez-Pello, A.C. 2007. Modeling transport and combustion of firebrands from burning trees. Comb. Flame 150, 151–169, doi:10.1016/j.combustflame.2007.04.008.

Schroeder, M.J., and Buck, C.C. 1970. Fire weather. Agricultural Handbook No. 360. Forest Service, U.S. Department of Agriculture, Washington, D.C., 229 pp.

Seager, R., Kushnir, Y., Herweijer, C., Naik, N., and Velez, J. 2005. Modeling of tropical forcing of persistent droughts and pluvials over Western North America: 1856–2000. J. Clim. 18(19), 4065–4088.

Shabbar, A., Bonsal, B., and Khandekar, M. 1997. Canadian precipitation patterns associated with the southern oscillation. J. Clim. 10, 3016–3027.

Simard, A.J., Haines, D.A., and Main, W.H. 1985. Relations between El Nino/southern oscillation anomalies and wildland fire activity in the United States. Agric. For. Meteorol. 36, 93–104.

Soja, A.J., Sukhinin, A., Cahoon, D.R., Shugart, H.H., Stackhouse, P.W., and Conard, S.G. 2002. Fire frequency, distribution, and area burned in Siberia described using AVHRR-derived products. American Geophysical Union, Spring Meeting 2002, abstract #A22E-09.

Stephens, S.L. 2005. Forest fire causes and extent on United States Forest Service lands. Int. J. Wildland Fire 14, 213–222.

Swetnam, T.W., and Betancourt, J.L. 1998. Mesoscale disturbance and ecological response to decadal climatic variability in the American Southwest. J. Clim. 11(12), 3128–3147.

Taylor, S.W., Wotton, B.M., Alexander, M.E., and Dalrymple, G.N. 2004. Variation in wind and crown fire behaviour in a northern jack pine—black spruce forest. Can. J. For. Res. 34, 1561–1576.

Thomas, P.H. 1971. Rates of spread of some wind-driven fires. Forestry 44, 155–175.

Ting, M., and Wang, H. 1997. Summertime U.S. precipitation variability and its relation to Pacific sea surface temperature. J. Clim. 10(8), 1853–1873.

Tinner, W., Hofstetter, S., Zeugin, F., Conedera, M., Wohlgemuth, T., Zimmermann, L., and Zweifel, R. 2006. Long-distance transport of macroscopic charcoal by an intensive crown fire in the Swiss Alps-implications for fire history reconstruction. The Holocene 16(2), 287–292.

Trenberth, K.E. 1990. Recent observed interdecadal climate changes in the Northern Hemisphere. Bull. Amer. Meteorol. Soc. 71, 988–993.

Tymstra, C., Flannigan, M.D., Armitage, O.B., and Logan, K. 2007. Impact of climate change on area burned in Alberta's boreal forest. Int. J. Wildland Fire 16, 153–160.

Uman, M.A. 1969. Lightning. McGraw-Hill, New York.

Van Wilgen, B.W., Le Maitre, D.C., and Kruger, F.J. 1985. Fire behaviour in South African fynbos (macchia) vegetation and predictions from Rothermel's fire model. J. Appl. Ecol. 22(1), 207–216.

Viegas, D.X. 2005. A mathematical model for forest fires blowup. Comb. Sci. Technol. 177, 27–51.

Viegas, D.X., Viegas, M.T.S.P., and Ferreira, A.D. 1992. Moisture content of fine forest fuels and fire occurrence in central Portugal. Int. J. Wildland Fire 2, 69–86, doi:10.1071/WF9920069.

Weise, D.R., Fujioka, F.M., and Nelson, R.M. Jr. 2005a. A comparison of 3 models of 1-hr timelag fuel moisture in Hawaii. Agric. For. Meteorol. 133, 28–39, doi:10.1016/j.agrformet.2005.03.012.

Weise, D.R., Zhou, X., Sun, L., and Mahalingam, S. 2005b. Fire spread in chaparral—"go or no-go?". Int. J. Wildland Fire 14, 99–106, doi: 10.1071/WF04049.

Westerling, A.L., Gershunov, A., Brown, T.J., Cayan, D.R., and Dettinger, M.D. 2003. Climate and wildfire in the Western United States. Bull. Amer. Meteorol. Soc. 84(5), 595–604.

Westerling, A.L., Hidalgo, H.G., Cayan, D.R., and Swetnam, T.W. 2006. Warming and earlier spring increase western U.S. forest wildfire activity. Science 313, 940–943.

Whiteman, C.D. 2000. Mountain meteorology: Fundamentals and applications. Oxford University Press, New York, NY.

Wilson, R. 1962. The Los Angeles Conflagration of 1961—the devil wind and wood shingles. NFPA Quarterly, National Fire Protection Association, Boston, MA, 242–289.

Zhou, X., Mahalingam, S., and Weise, D. 2005. Modeling of marginal burning state of fire spread in live chaparral shrub fuel bed. Comb. Flame 143, 183–198, doi: 10.1016/j.combustflame.2005.05.013.

Zimet, T., Martin, J.E., and Potter, B.E. 2007. The influence of an upper-level frontal zone on the Mack Lake Wildfire environment. Meteorol. Appl. 14, 131–147.

This page intentionally left blank

Developments in Environmental Science, Volume 8 61
A. Bytnerowicz, M. Arbaugh, A. Riebau and C. Andersen (Editors)

ISSN: 1474-8177/DOI:10.1016/S1474-8177(08)00003-X

Chapter 3

Characterizing Sources of Emissions from Wildland Fires

*Roger D. Ottmar**, *Ana Isabel Miranda and David V. Sandberg*

Abstract

Smoke emissions from wildland fire can be harmful to human health and welfare, impair visibility, and contribute to greenhouse gas emissions. The generation of emissions and heat release need to be characterized to estimate the potential impacts of wildland fire smoke. This requires explicit knowledge of the source, including size of the area burned, burn period, characteristics and condition of the fuels, amount of fuel consumed, and emission factors for specific pollutants. Although errors and uncertainties arise in the process of estimating emissions, the largest errors are related to the characteristics of the fuels and amount of fuel consumed during the combustion phase. We describe the process of characterizing emissions and review the knowledge and predictive models currently available for performing the calculations. The information can be used by scientists, regulators, and land managers to improve the approach needed to define the emissions source strength for improved air quality and impact assessments.

3.1. Introduction

All wildland fires release various amounts of carbon dioxide (CO_2), carbon monoxide (CO), methane (CH_4), nitrogen oxides (NO_X), ammonia (NH_3), particulate matter (PM), nonmethane hydrocarbons (NMHC), sulfur dioxide (SO_2), and other chemical species into the atmosphere (Crutzen & Andreae, 1990; Holzinger et al., 1999; Yokelson et al., 1996). These particulates and gaseous compounds can be hazardous to human health, threaten human welfare and ecosystems, degrade

*Corresponding author: E-mail: rottmar@fs.fed.us

visibility, affect biogeochemical cycles, and contribute to greenhouse gas emissions (Battye & Battye, 2002; Bertschi et al., 2003; Hardy et al., 2001; Miranda et al., 1993, 2005a; Miranda & Borrego, 2002; Sandberg & Dost, 1990; Sandberg et al., 1999, 2002). The impacts are related to chemical reactions, and to transport and deposition processes, and can occur at both global and local scales (Borrego et al., 1999; Crutzen & Andreae, 1990; Crutzen & Carmichael, 1993; Miranda, 1998; Miranda et al., 1994; Reinhardt et al., 2001; Valente et al., 2005; Ward & Radke, 1993).

To acquire a better understanding of the potential impacts of these combustion by-products, the heat release rate and emissions generated by the fire must be characterized (Pouliot et al., 2005). This requires explicit knowledge of the source, including area burned, burning period, fuel characteristics, fire behavior, fuel consumption, and pollutant-specific emission factors (Battye & Battye, 2002; Hardy et al., 2001; Peterson, 1987; Peterson & Sandberg, 1988; Sandberg et al., 2002). Although errors and uncertainties arise during each step of the process of estimating emissions, the largest errors are related to the characteristics of the fuels and fuel consumption (Fig. 3.1) (Hardy et al., 2001; Peterson, 1987; Peterson & Sandberg, 1988), providing the area burned reported is area actually blackened and not total area within the perimeter of the fire.

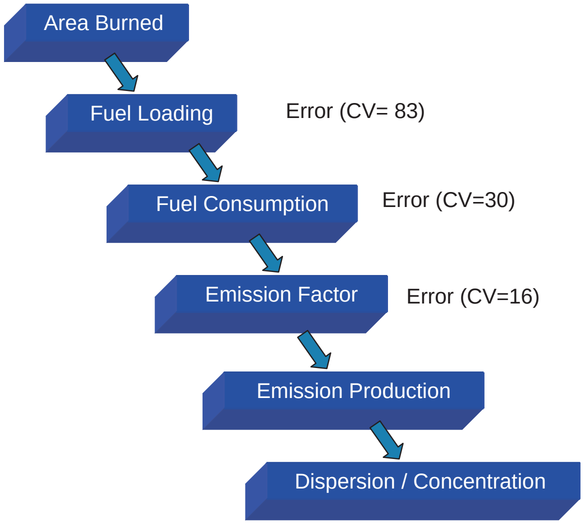

Figure 3.1. Information required for estimating emission production. The largest errors are associated with fuel loading and fuel consumption inputs (Peterson, 1987) unless the area burned is total acres within the perimeter of the fire. (CV = coefficients of variation.)

If this is the case, the area burned input value could have the largest uncertainty (Peterson, 1987). This chapter presents the process of characterizing emissions, source strength, and heat release from wildland fires and discusses several of the current models and approaches available to calculate these data.

3.2. Area burned

The area burned by a wildland fire is one of the more difficult parameters to accurately obtain when calculating fire emissions (Battye & Battye, 2002). At first glance, the amount of area burned seems relatively easy to determine. However, large systematic errors may exist depending on the quality of the reporting system (Peterson, 1987). Individual estimates of fire size tend to be exaggerated and fires are frequently double-counted in inventories (Sandberg et al., 2002). For example, the entire landscape within a fire perimeter is often reported burned although nonuniform fuels, geographic barriers, or changes in the weather can cause a fire to burn in a mosaic pattern with unburned patches. In other instances, poor reporting systems may miss a large number of fires, thus underestimating the number of acres burned. Although large-scale inventories of area burned are often derived from remotely sensed data, the technique has limited precision and is inadequate in landscapes with variable slope and fuel characteristics (Crutzen & Andreae, 1990; French et al., 2004; Levine, 1994; Sandberg et al., 2002).

Burned area measurements can be obtained from three sources: wildfire reports, prescribed fire or smoke management reports, and aerial or satellite imagery data (Battye & Battye, 2002). All three procedures have problems associated with the information. For example, wildfire reports are often difficult to obtain, fire location and vegetation data associated with the fire may be incorrect, and the daily perimeter growth is rarely included. Prescribed fire and smoke management reports often provide correct project size; however, the fuel loading and actual area burned may be incorrect. Aerial and satellite imagery are expected to provide improved temporal and spatial resolution in the near future, but procedures need further refinement and the imagery often lacks the ability to detect fire under canopies.

3.3. Burning period

The burn period (minute) is the length of time combustion is occurring for a particular area and is required for calculating emission source strength ($g\,min^{-1}$) and heat release rate ($J\,t^{-1}$). Source strength and heat release rate are critical inputs to dispersion models for assessing air quality impacts (Hardy et al., 2001; Sandberg et al., 2002).

The burn period for a wildland fire event may extend for several minutes or several months. It will often include periods of large, high intensity fire growth interspersed with periods of low intensity, slow growth. The periods may be marked with well-developed convection columns that entrain emissions and heat from large areas interspersed with periods with low, buoyant smoke with little or no spatial organization. The burn area is seldom all combusting at one time, but rather is an ever-changing perimeter that experiences successive ignitions, flaming spread, and smoldering/residual smoldering combustion periods. Although it is often convenient to characterize a wildland fire as a uniform event having a constant fire behavior and source strength for the entire period, such characterization overlooks the extreme spatial and temporal variation that normally exists over a burn area.

Burn period is not directly entered into wildfire or prescribed fire reports, but can be estimated based on known ignition time and information that indicates when consumption ceased. Satellite or aerial imagery over time could be assessed and used to estimate burning period.

3.4. Fuel characteristics

Fuel characteristics can vary widely across regions (Fig. 3.2). For instance, fuel loads can range from less than 0.6 $t\,ha^{-1}$ for a perennial grassland in the central part of the United States with no rotten woody material or duff (organic material that includes Oe horizon and Oa horizon), to 35 $t\,ha^{-1}$ in a cerrado denso woodland in central Brazil with a grass and shrub understory and a litter layer, to 195 $t\,ha^{-1}$ in a mixed-conifer forest with insect and disease mortality in the U.S. Rocky Mountains that has dead and down sound and rotten woody material, snags, litter and duff, and to 381 $t\,ha^{-1}$ in a black spruce (*Picea mariana*) forest of northern Canada with a deep moss and organic forest floor layer (Hardy et al., 2001; Ottmar & Vihnanek, 1998, 1999; Ottmar et al., 1998a, 2001, 2007; Sandberg et al., 2002). Human activities have also created an impressive mosaic of forest, shrublands, and grasslands across Occidental Europe also. Fuel loads can range from 2 $t\,ha^{-1}$ within a Mediterranean community of *Rosmarinus officinalis* garrigue to 160 $t\,ha^{-1}$ within a temperate beech forest of *Fagus silvatica* (Trabaud et al., 1993). The large variation in fuel loading across regions can contribute up to 80% of the error associated with estimating emissions (Peterson, 1987; Peterson & Sandberg, 1988).

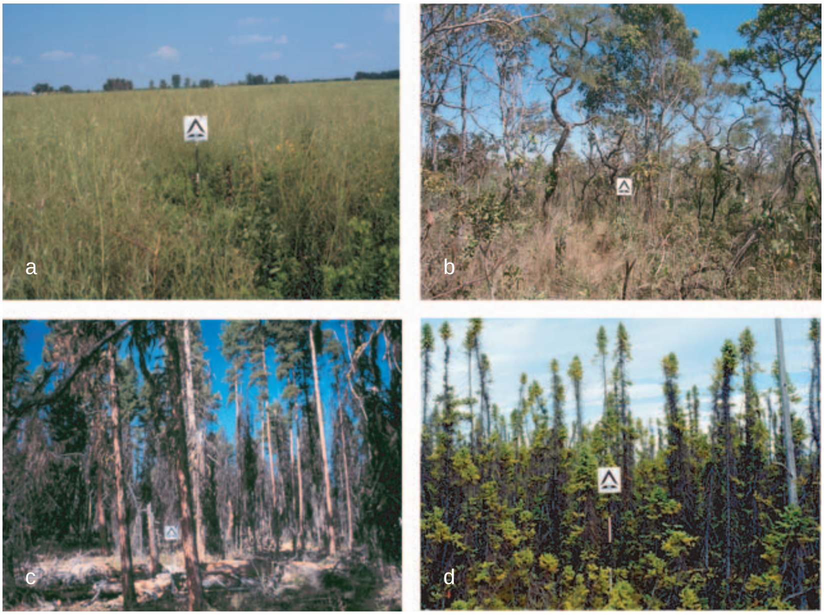

Figure 3.2. Fuelbed types and fuel loads can vary widely ranging from (a) grasslands in the midwestern United States (0.6 t ha^{-1}), (b) cerrado denso (woodland) in Brazil (35 t ha^{-1}), (c) mixed-conifer forest with insect mortality in the Rocky Mountain region of the United States (195 t ha^{-1}), and (d) black spruce forest with a deep organic layer in Canada (381 t ha^{-1}).

It would be prohibitively difficult to inventory loadings for all fuelbeds every time an assessment of emissions or management decision was necessary (Ottmar et al., 2004; Sandberg et al., 2001). Attempts have been made during the past 30 years to develop systems to construct and classify fuelbeds for loading in several countries with various degrees of success. These include the original and standard Fire Behavior Fuel Models (U.S.) (Anderson, 1982; Andrews & Chase, 1989; Scott & Burgan, 2005), National Fire Danger Rating System Fuel Models (U.S.) (Deeming et al., 1977), Fuel Condition Class System fuelbeds (U.S.) (Ottmar et al., 1998b; Schaaf, 1996), First Order Fire Effects Model (FOFEM) fuelbeds (U.S.) (Reinhardt et al., 1997; Reinhardt & Crookston, 2003), Canadian Fire Danger Rating System (Canada) (Hirsch, 1996), Australian Fire Danger Rating System fuel models (Australia) (Cheney & Sullivan, 1997; Cheney et al., 1990); Photo Series (U.S.) (Ottmar et al., 2004), the Fuel Load Models (U.S.) (Keane, 2005, Landscape Fire and Resource Management Planning Tools Project (LANDFIRE), 2005), and the

European Fire Management Information System (PROMETHEUS) (PROMETHEUS, 1999). Many of these systems were designed for specific software applications and therefore include only the fuelbed components required by the program they were designed to support. Consequently, the systems did not capture all fuel components required to estimate air pollutants (Ottmar et al., 2007; Sandberg et al., 2001). Although progress has been made in assessing fuel characteristics using Light Detection and Ranging (LIDAR) and other remote sensing techniques, large errors are evident when fuel loading is inferred from vegetation type when deriving biomass emissions from remotely sensed data (Crutzen & Andreae, 1990; Levine, 1994; Molina et al., 2006).

The Fuel Characteristic Classification System (FCCS) is a tool that is applicable worldwide, although the current fuelbed database contained in the system is robust only for the United States. The tool enables users to create and catalogue fuelbeds. Fuelbed characteristics from this tool will provide inputs to current and future wildland fire emission production models. The FCCS contains a set of fuelbeds representing the United States that were compiled from scientific literature, fuels photo series, fuels data sets, and expert opinion. The system enables modification and enhancement of these fuelbeds to represent a particular scale of interest. The FCCS then reports assigned and calculated fuel characteristics for each existing fuelbed stratum including the canopy, shrubs, nonwoody, woody, litter/lichen/moss, and duff (Fig. 3.3; Riccardi et al., 2007). FCCS outputs have been used to generate a fuelbed map for the United States, and these data are being used in a national wildland fire emissions inventory (Fig. 3.4; McKenzie et al., 2007) and in the development of fuelbed, fire hazard, and treatment effectiveness maps on several national forests.

The LANDFIRE Project (Rollins & Frame, 2006) will develop digital maps of wildland fuel loadings to be applied across the entire United States at a 30 m spatial resolution. The project will also map FCCS fuelbeds, thus allowing additional fuelbed characteristics to be available for improved estimation of emissions from wildland fires.

In addition, the Euro-Mediterranean Wildland Fire Laboratory European Commission Project (www.eufirelab.org) compiled and listed (Allgower et al., 2006) the different systems used to estimate and map fuelbeds across Europe.

3.5. Fire behavior

Fire behavior is defined as the reaction of fine fuels available for burning (Debano et al., 1998) and is dependent on fuelbed type, condition and

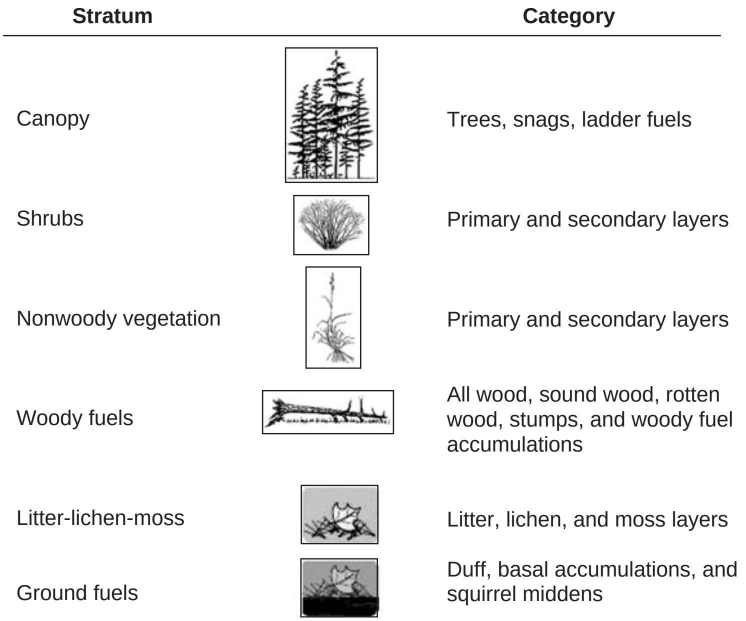

Figure 3.3. Horizontal stratification of an FCCS fuelbed by strata and categories in the United States.

arrangement of the fuels, local weather conditions, topography, and in the case of prescribed fire, ignition period and pattern. Important aspects of fire related to the production of emissions include fire intensity ($J\,m^{-2}$), rate of spread ($m\,min^{-1}$), and residence time (minute) in the flaming, smoldering, and residual stages of combustion (Sandberg et al., 2002). These aspects of fire behavior influence the combustion efficiency of burning fuels and the resulting pollutant chemistry and emission strength.

The Fire Emissions Production Simulator (FEPS) (Fire and Environmental Research Applications Team, 2006) and a fire growth simulator called FARSITE (Finney, 1998) take into account fire behavior and ignition period and pattern to estimate emission production rates. Both tools model the flaming and smoldering combustion and duration in down woody fuels and duff, although FEPS is better parameterized to predict flaming versus smoldering (Sandberg et al., 2004).

3.6. Fuel consumption

Fuel consumption ($t\,ha^{-1}$) is the amount of biomass consumed during a fire and is another critical component for estimating the amount and

Figure 3.4. A 1 km resolution map of FCCS fuelbeds for the contiguous 48 states in the United States.

source strength of emissions and the rate of heat release generated from wildland fire. Fuels are consumed in a complex combustion process that varies widely among fires and is dependent on fuel type, arrangement of the fuel, condition of the fuel, and in the case of prescribed fires, the way the fire is applied. As with fuel loading, extreme variations associated with fuel consumption and the data can contribute errors of 30% or more when emissions are estimated for wildland fires (Peterson, 1987; Peterson & Sandberg, 1988).

Equations for predicting consumption by combustion phase are widely available in two major software packages, Consume 3.0 (Ottmar et al., 2005) and the FOFEM (Reinhardt, 2003; Reinhardt et al., 1997). Consume 3.0 uses a set of theoretical models based on empirical data to predict the amount of fuel consumption from all material that can potentially burn in a fuelbed, including tree crowns, shrubs, grasses, woody fuels, moss, lichen, litter, and duff. The model also separates the consumption into flaming, smoldering, and residual phases. Input variables include the amount of fuel, moisture content of woody fuel and duff, length of ignition, and meteorological data. The system incorporates the FCCS for assigning default fuel loadings. FOFEM 5.0 relies on Burnup, a theoretical model of fuel consumption (Reinhardt et al., 1997). The software computes duff and woody fuel consumption for many forests and rangeland systems of the United States. Both Consume 3.0 and FOFEM 5.0 are updated on a regular basis as new consumption models are developed.

3.7. Emission factors

An emission factor ($g\,kg^{-1}$) for a particular pollutant of interest is defined as the mass of pollutant produced per mass of fuel consumed. Emission factors vary depending on type of pollutant, type and arrangement of fuel, and combustion efficiency (combustion phase). The average emission factors for the flaming and smoldering period of a fire have a relatively small range and contribute to about 16% of the total error associated with predicting emissions (Peterson, 1987; Peterson & Sandberg, 1988). The important distinction between fires is the ratio of flaming to smoldering/residual consumption. This is governed by the fuel characteristics in the burn area and the fuel condition during the burn period. Fires that burn primarily in smoldering combustion can produce several times the mass of pollutants (not including carbon dioxide) as compared to a fire in which a majority of the fuel is consumed during the flaming phase.

Emissions from wildland fires have been measured extensively by researchers since about 1970. The result is a relatively complete set of emission factors for criteria pollutants and many hazardous air pollutants for most important fuel types in the United States (Andreae & Merlot, 2001; Battye & Battye, 2002; Environmental Protection Agency, 1996; Hardy et al., 2001; Ward et al., 1989). Miranda (2004) and Miranda et al. (2005a) present a selection of emission factors to be applied to south-European forest conditions. Less complete compilations of emission factors are available for PM size class distribution, elemental and organic carbon fractions, particulate hazardous air pollutants, methane, ammonia, aldehydes, compounds of nitrogen, volatile organic compounds, and volatile hazardous air pollutants (Battye & Battye, 2002; Goode et al., 1999, 2000; Lobert et al., 1991; McKenzie et al., 1994; Sandberg et al., 2002; Yokelson et al., 1996).

3.8. Total emissions, source strength, and heat release

Total emissions from wildland fires can be calculated by the equation

$$\begin{aligned}\text{Total emissions (g)} &= \text{fuel consumed (kg ha}^{-1}) \times \text{emission factor (g kg}^{-1}) \\ &\quad \times \text{area burned (ha)}\end{aligned}$$

However, much better estimates of emissions can be made if the amount of fuel consumption in the flaming and smoldering/residual combustion periods is known. The fuels consumed during the flaming and smoldering stages are multiplied by the appropriate flaming and smoldering emission factor for an average fuelbed. Consume 3.0 (Ottmar et al., 2005) and FOFEM 5.0 (Reinhardt, 2003; Reinhardt et al., 1997) use this approach to improve the estimates of total emissions produced from wildland fire, as compared with using a fire average fuel consumption and emission factor. Currently, both fuel consumption models provide fuel consumption by fuelbed component, although emission factors by fuelbed component are not available at this time. Emission factor research is ongoing to fill in this gap (Hao, 1998; Ottmar, 2003).

Source strength is the rate of air pollutant emissions in mass per unit of time or in mass per unit of time per unit area and is the product of rate of biomass consumption and emission factor for the pollutant of interest. Source strength can be calculated by the equation

$$\begin{aligned}\text{Source strength (g min}^{-1}) &= \text{fuel consumption (kg ha}^{-1}) \\ &\quad \times \text{emission factor (g kg}^{-1}) \\ &\quad \times \text{rate of area burned (ha min}^{-1})\end{aligned}$$

The consumption of biomass produces thermal energy, and this energy creates buoyancy to lift smoke particles and other pollutants above the fire. Heat release rate is the amount of thermal energy generated per unit of time or per unit of time per unit area. It can be calculated by the equation

$$\begin{aligned}\text{Heat release rate } (\text{J min}^{-1}) = {} & \text{fuel consumption } (\text{t ha}^{-1}) \\ & \times \text{heat output } (\text{J t}^{-1}) \\ & \times \text{rate of area burned } (\text{ha min}^{-1})\end{aligned}$$

Both source strength and heat release rate are required by most sophisticated smoke dispersion models (Breyfogle & Ferguson, 1996; Miranda, 2004).

FEPS (Fire and Environmental Research Applications Team, 2006) predicts hourly emissions, heat release, and plume rise values for wildland fires. The program requires area burned, ignition period, fuel characteristics, and fuel moisture conditions as input variables. Fuel consumption may be added as an input or calculated internally. Although the system provides default input values for fuel characteristics, fuel condition, and ignition period to calculate source strength, heat release rate, and plume rise, FEPS can also import consumption and emissions data from Consume 3.0 and FOFEM. FEPS can be used for any forest, shrub, and grassland or piled-fuel types throughout the world.

3.9. Implementation

Several large-scale wildland fire emissions inventories and assessments have been conducted over the past several years using variations of the protocols discussed in this chapter. Peterson and Ward (1993) addressed historic emissions in 1989 for the United States using fire reports and expert opinion to determine burned area, fuelbed type, and fuel consumption. Fire average emissions factors were assigned to the fuelbeds and emissions calculated. In 1995, the Grand Canyon Visibility Transport Commission began a more comprehensive emission inventory for 10 states in the western United States. Reports were used to determine area burned; however, the FCC fuelbeds and Consume were used to determine fuel characteristics, fuel consumption, and emissions (Grand Canyon Visibility Transport Commission, 1996). During the Interior Columbia Basin Ecosystem Management Project (Quigley & Arbelbide, 1997) modeled smoke production was compared for recent historical and current time periods based on vegetative attributes determined from aerial photographs (Ottmar et al., 1998b). The vegetation type was assigned an FCC fuelbed, and Consume was used to calculate the emissions for each time period.

The European Commission Project called SPREAD estimated forest fire emissions for the year 2001 in southern Europe. Two approaches were used. The first approach acquired fire reports to determine area burned and used a European variation of the National Fire Danger Rating System to estimate emissions. The second approach also used fire reports to determine area burned but applied the model called EMISPREAD (Miranda et al., 2005b) to calculate emissions. The study found that of the southern European countries, Portugal was the major contributor of wildland fire emissions in 2001 (Miranda, 2005a, 2005b). It was also determined that the emissions from each approach were in reasonable agreement.

The approach to emissions calculations has improved over the years as new research and better models have made been created. Considering current available knowledge and models, a relatively accurate estimate of emissions can be generated (Fig. 3.5). Additional improvements

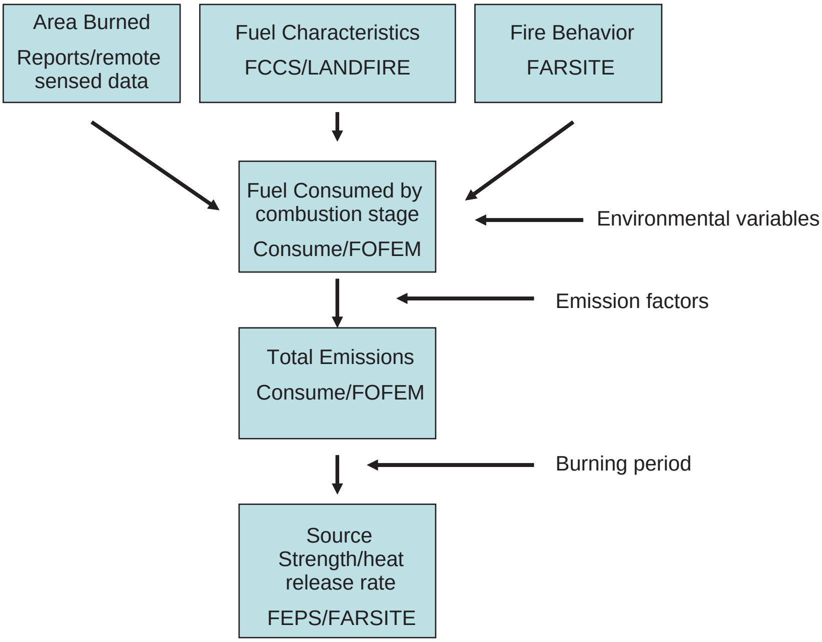

Figure 3.5. Flow diagram of one approach to estimating emissions.

in estimating smoke emissions will require better fire reporting or remote sensing of fire perimeters and period of burning; improved ability to assign fuelbed characteristics to the landscape, and development of more robust fuel consumption models that account individually for all combustion phases and all fuelbed components that have a potential to burn. Unless there are important hazardous compounds that do not have emission factors associated with them, additional emission factor research is not the most important science effort to pursue (Hardy et al., 2001; Peterson, 1987). There are well-accepted emission factor numbers (Hardy et al., 2001) available at this time, and the values do not vary greatly by fuelbed type (Sandberg et al., 2002), but rather primarily by the combustion efficiency and the fuel consumption by combustion stage.

The uncertainity associated with the approach described in this chapter to estimate emissions from wildland fire may change in the future. New and improved reporting and sensing methodologies will provide improved burned area data reducing the uncertainty associated with this estimation. Climate change may also cause fuelbed components to be more or less complex and consume differently, increasing or decreasing the associated uncertainty. For example, an increasing temperature and drought climatic pattern for a region may result in a less complex fuelbed, reducing uncertainty. However, the fuelbed will be drier, increasing the amount of fuel available to consume and changing the ratio of flaming and smoldering combustion by fuelbed component. This may result in an increase in uncertainty of this variable.

Although research characterizing fuels and modeling fuel consumption has progressed over the past 20 years (Brown et al., 1991; Ottmar et al., 2005), more studies are needed, especially as climate changes. Future emission production research would be best served by concentrating efforts in the area of burn area assessment, fuelbed characterization, and fuel consumption modeling.

ACKNOWLEDGMENTS

We thank the Joint Fire Science Program, National Fire Plan, and the USDA Forest Service, Pacific Northwest Region and Pacific Northwest Research Station, for financial assistance in the development of scientific models that have improved our ability to assess wildland fire emissions. We also greatly appreciate Ellen Eberhardt, David L. Peterson, and Clint Wright who provided helpful comments during the preparation of the manuscript. The European Commission is also acknowledged under the framework of the Projects SPREAD (EVGI-CT-2001-0043) and

EUFIRELAB (EVR1-CT-2002-40028). Finally, we would like to thank Andrzej Bytnerowicz and IUFRO for the organization of the conference and facilitating the book preparation.

REFERENCES

Allgower, B., Calogine, D., Camia, A., Cuiñas, P., Fernandes, P., Francesetti, A., Hernando, C., Koetz, B., Koutsias, N., Lindberg, H., Marzano, R., Molina, D., Morsdorf, F., Ribeiro, L.M., Rigolot, E., and Séro-Guillaume, O. 2006. Methods for wildland fuel description and modeling: Final version of the state-of-the art. Deliverable D-02-06, EUFIRELAB Project EVR1-CT-2002-40028, 57 pp.

Anderson, H.E. 1982. Aids to determining fuel models for estimating fire behavior. General Technical Report, GTR-INT-122. USDA Forest Service, Intermountain Forest and Range Experiment Station. Ogden, UT.

Andreae, M.O., and Merlot, P. 2001. Emissions of trace gases and aerosols from biomass burning. Global Biogeochem. Cycles 15, 955–966, 2000GB001382.

Andrews, P.L., and Chase, C.H. 1989. BEHAVE: Fire behavior prediction and fuel modeling system–BURN subsystem, part 2. General Technical Report, GTR-INT-122. USDA Forest Service, Intermountain Forest and Range Experiment Station. Ogden, UT.

Battye, W.B., and Battye, R. 2002. Development of emissions inventory methods for wildland fire. Prepared for Thompson G. Pace, D205-01 of the U. S. Environmental Protection Agency, Final report. www.epa.gov/ttn/chief/ap42/ch13/related/firerept.pdf

Bertschi, I.T., Yokelson, R.J., Ward, D.E., Babbitt, R.E., Susott, R.A., Goode, J.G., and Hao, W.M. 2003. Trace gas and particle emissions from fires in large diameter and below ground biomass fuels. J. Geophys. Res. 108(D13), 8472, doi: 10.1029/2002J?oo2100.

Borrego, C., Miranda, A.I., Carvalho, A.C., and Carvalho, A. 1999. Forest fires and air pollution: A local and global perspective. In: Brebbia, C., Jacobson, M., and Power, H., eds. Proceedings of the 7th International Conference on Air Pollution. WIT Press, Southampton, Boston, 741–750.

Breyfogle, S., and Ferguson, S. 1996. User assessment of smoke dispersion models for wildland biomass burning. General Technical Report, PNW-GTR-379. USDA Forest Service, Pacific Northwest Research Station. Portland, OR, 30 pp.

Brown, J.K., Reinhardt, E.D., and Fischer, W.C. 1991. Predicting duff and woody fuel consumption in northern Idaho prescribed fires. For. Sci. 37, 1550–1566.

Cheney, N.P., and Sullivan, A. 1997. Grassfires fuel, weather and fire behavior. CSIRO Publishing, Collingwood, Australia.

Cheney, N.P., Wilson, A.A.G., and McCaw, L. 1990. Development of an Australian fire danger rating system. RIRDC Project No. CSF-35A Report (unpublished), 24 pp.

Crutzen, P.J., and Andreae, M.O. 1990. Biomass burning in the tropics: Impacts on atmospheric chemistry and biogeochemical cycles. Science 250(4988), 1669–1678.

Crutzen, P.J., and Carmichael, G.R. 1993. Modeling the influence of fires on atmospheric chemistry. In: Crutzen, P.J., and Goldammer, J.G., eds. Fire in the environment: The ecological, atmospheric, and climatic importance of vegetation fires. Wiley, Chichester, England, pp. 90–105.

Debano, L.F., Neary, D., and Folliott, P.F. 1998. Fire's effects on ecosystems. Wiley, New York, 333 pp.

Deeming, J.E., Burgan, R.E., and Cohen, J.D. 1977. The national fire-danger rating system—1978. General Technical Report, GTR-INT-39. USDA Forest Service, Intermountain Forest and Range Experiment Station. Ogden, UT.

Environmental Protection Agency. 1996. Wildfire and prescribes fire emissions. AP-42. U.S. Environmental Protection Agence, Research Triangle Park, NC. 13.1.1-14.

Finney, M.A. 1998. FARSITE: Fire area simulator-model development and evaluation. Research Paper, RMRS-RP-4. USDA Forest Service, Rocky Mountain Research Station. Ft. Collins, CO, 47 pp.

Fire and Environmental Research Applications Team. 2006. Fire emission production simulator web page. www.fs.fed.us/pnw/fera/feps

French, N.H.F., Goovaerts, P., and Kasischke, E.S. 2004. Uncertainty in estimating carbon emissions from boreal forest fires. J. Geophys. Res. 09, D14S08, doi:10.1029/2003J?003635.

Goode, J.G., Yokelson, R.J., Susott, R.A., Babbitt, R.E., Ward, D.E., Davies, M.A., and Hao, W.M. 2000. Measurement of excess O_3, CO_2, CO, CH_4, C_2H_4, C_2H_2, HCN, NO, NH_3, HCOOH, CH_3COOH, HCHO, and CH_3OH in 1997 Alaskan biomass burning plumes by airborne Fourier transform infrared spectroscopy (AFTIR). J. Geophys. Res. 105, 22,147.

Goode, J.G., Yokelson, R.J., Susott, R.A., and Ward, D.E. 1999. Trace gas emissions from laboratory biomass fires measured by open-path Fourier transformation infrared spectroscopy: Fires in grass and surface fuels. J. Geophys. Res. 104, 21,237–21,245.

Grand Canyon Visibility Transport Commission. 1996. Report of the Grand Canyon Visibility Transport Commission to the United States Environmental Protection Agency (1996). Western Governors' Association, Denver, CO, 85 pp.

Hao, W.M. 1998. Smoke produced from residual combustion. Ongoing project, Joint Fire Science Progam, National Interagency Fire Center, Boise, ID. http://jfsp.nifc.gov/JFSP_Active_Projects_1.htm

Hardy, C.C., Ottmar, R.D., Peterson, J.L., Core, J.E., and Seamon, P. 2001. Smoke management guide for prescribed and wildland fire: 2001 edition. PMS 420-2. National Wildfire Coordinating Group, Boise, ID, 226 pp.

Hirsch, K.J. 1996. Canadian forest fire behavior prediction (FBP) system: User's guide. Special Report 7. Natural Resources Canada, Canadian Forest Service, Northern Forestry Centre, Edmonton, Alberta.

Holzinger, R., Warneke, C., Hansel, A., Jordan, A., Lindinger, D.H., Scharfe, G., Schade, G., and Crutzen, P.J. 1999. Biomass burning as a source of formaldehyde, acetaldehyde, methanal, acetone, acetonitrile, and hydrogen cyanide. Geophys. Res. Lett. 26, 1161–1164.

Keane, R. 2005. Fuel loading models. www.landfire.gov/National/ProductDescriptions18.php

Landscape Fire and Resource Management Planning Tools Project (LANDFIRE). 2005. Landfire. www.landfire.gov.

Levine, J.S. 1994. Biomass burning and the production of greenhouse gases. In: Zepp, R.G., ed. Climate-biosphere interactions: Biogenic emissions and environmental effects of climate change. Wiley, New York, pp. 139–160.

Lobert, J.M., Scharffe, D.H., Hao, W.M., Kuhlbusch, T.A., Sweuwen, R., Warnesk, P., and Crutzen, P.J. 1991. Experimental evaluation of biomass burning emissions: Nitrogen carbon containing compounds. In: Levin, J.S., ed. Global biomass burning: Atmospheric, climatic, and biospheric Implications. MIT Press, Cambridge, 569 pp.

McKenzie, L., Hao, W.M., Richards, G., and Ward, D. 1994. Quantification of major components emitted from smoldering combustion of wood. Atmos. Environ. 28(20), 3285–3292.

McKenzie, D., Raymond, C.L., Kellogg, L.-K.B., Norheim, R.A., Andreu, A.G., Bayard, A.C., Kopper, K.E., Elman, E. 2007. Mapping fuels at multiple scales: Landscape application of FCCS. Can. J. For. Res. 37(12), 2421–2437.

Miranda, A.I. 1998. Forest fire effects on the air quality. Ph.D. Thesis (in Portuguese only). Department of Environmental and Planning, University of Aveiro, Portugal. 213 pp.

Miranda, A.I. 2004. An integrated numerical system to estimate air quality effects of forest fires. Int. J. Wild. Fire 13, 1–10.

Miranda, A.I., and Borrego, C. 2002. Air quality measurements during prescribed fires. In: Viegas, D.X., ed. Forest Fire Research and Wildland Fire Safety: Proceedings of IV International Conference on Forest Fire Research 2002 Wildland Fire Safety Summit, Luso, Coimbra, Portugal, 18–23 November 2002. Millpress Science Publishers, Rotterdam, 205.

Miranda, A.I., Borrego, C., and Viegas, D. 1994. Forest fire effects on air quality. In: Baldasano, J., Brebbia, C., Power, H., and Zannetti, P., eds. Proceedings of the 2nd International Conference on Air Pollution, Vol. 1: Computer simulation. Computacional Mechanics Publications, Southampton, pp. 191–199.

Miranda, A.I., Coutinho, M., and Borrego, C. 1993. Forest fire emissions in Portugal: A contribution to global warming? Environ. Pollut. 83(1,2), 121–123.

Miranda, A.I., Ferreira, J., Valente, J., Santos, P., Amorim, J.H., and Borrego, C. 2005. Smoke measurements during Gestosa-2002 experimental fires. Int. J. Wild. Fire 14, 107–116.

Miranda, A., Borrego, C., Valente, J., Sousa, M., Santos, P., and Carvalho, A. 2005a. Smoke production report. Deliverable D254 of the European Commission Project SPREAD (Forest fire spread prevention and mitigation). EVG1-CT-2001-0043. AMB-QA-10/2005. 43 pp.

Miranda, A., Borrego, C., Sousa, M., Valente, J., Barbosa, P., and Carvalho, A. 2005b. Model of forest fire emission to the atmosphere. Deliverable D252 of the European Commission Project SPREAD (Forest fire spread prevention and mitigation), EVG1-CT-2001-0043. AMB-QA-07/2005, 48 pp.

Molina, M., Alvarez, A., Allgower, B., Kotz, B., Koutsias, N., Fernandes, P., Loureiro, C., Hernando, C., Cohen, M., Rigolot, E., Vigy, O., and Valette, J.C. 2006. Characteristics of wildland fuel bed. EUFIRELAB Project EVR1-CT-2002-40028, Deliverable D-02-04, 52 pp.

Ottmar, R.D. 2003. Forest floor consumption and smoke characterization in boreal forest fuelbed types of Alaska. Ongoing project, Joint Fire Science Progam, National Interagency Fire Center, Boise, ID. jfsp.nifc.gov/JFSP_Active_Projects_3.htm

Ottmar, R.D., Alvarado, E., and Hessburg, P.F. 1998b. Linking recent historical and current forest vegetation patterns to smoke and crown fire in the Interior Columbia River basin. In: Proceedings of 13th Fire and Forest Meteorology Conference. International Association of Wildland Fire, Moran, WY, 523–533.

Ottmar, R.D., Prichard, S.J., and Anderson, G.A. 2005. Consume 3.0. www.fs.fed.us/pnw/fera

Ottmar, R.D., Sandberg, D.V., Riccardi, C.L., and Prichard, S.J. 2007. An overview of the fuel characteristic classification system (FCCS)—quantifying, classifying, and creating fuelbeds for resource planning. Can. J. For. Res. 37, 1–11.

Ottmar, R.D., and Vihnanek, R.E. 1998. Stereo photo series for quantifying natural fuels. Volume II: Black spruce and white spruce types in Alaska. PMS 831. National Wildfire Coordinating Group, National Interagency Fire Center, Boise, ID, 65 pp.

Ottmar, R.D., and Vihnanek, R.E. 1999. Stereo photo series for quantifying natural fuels. Volume V: Midwest red and white pine, northern tallgrass prairie, and mixed oak types in the Central and Lake States. PMS 834. National Wildfire Coordinating Group, National Interagency Fire Center, Boise, ID, 99 pp.

Ottmar, R.D., Vihnanek, R.E., and Wright, C.S. 1998a. Stereo photo series for quantifying natural fuels. Volume I: mixed-conifer with mortality, western juniper, sagebrush, and grassland types in the interior Pacific Northwest. PMS 830. National Wildfire Coordinating Group, National Interagency Fire Center, Boise, ID, 73 pp.

Ottmar, R.D., Vihnanek, R.E., Miranda, H.S., Sato, M.N., and Andrade, S.M.A. 2001. Stereo photo series for quantifying cerrado fuels in central Brazil—Volume I. General Techical Report PNW-GTR-519. USDA Forest Service, Pacific Northwest Research Station. Portland, OR.

Ottmar, R.D., Vihnanek, R.E., Wright, C.S., and Olson, D.L. 2004. Stereo photo series for quantifying natural fuels. Volume VII: Oregon white oak, California deciduous oak, and mixed-conifer with shrub types in the Western United States. National Wildfire Coordinating Group, National Interagency Fire Center, Boise, ID.

Peterson, J.L. 1987. Analysis and reduction of the errors of predicting prescribed burn emissions. Thesis. University of Washington, Seattle, 70 pp.

Peterson, J.L., and Sandberg, D.V. 1988. A national PM10 emissions inventory approach for wildland fires and prescribed fires. In: Mathai, C.V., and Stonefield, D.H., eds. Transactions PM-10 Implementation of Standards: An APCA/EPA international specialty conference. Air Pollution Control Association, Pittsburgh, pp. 353–371.

Peterson, J., and Ward, D. 1993. An inventory of particulate matter and air toxic emissions from prescribed fire in the United States for 1989. Final report. IAG-DW 12934736-01-1989. Prepared by the USDA Forest Service for the U.S. EPA Office of Air Quality Programs and Standards.

Pouliot, G., Pierce, T., Benjey, W., O'Neill, S.M., and Ferguson, S.A. 2005. Wildfire emission modeling: Integrating BlueSky and SMOKE. www.epa.gov/ttn/chief/conference/ei14/session12/pouliot.pdf

PROMETHEUS S.V. Project. 1999. Management techniques for optimization of suppression and minimization of wildfire effects. System validation. European Commission, Contract number ENV4-CT98-0716. http://cardis.europa.eu/data/PROJ_ENV/ACTIONeqDndSESSIONeq8548200595ndDOCeqgndTBLeqEN_PROJ.htm

Quigley, T.M., and Arbelbide, S.J. 1997. An assessment of ecosystem components in the interior Columbia Basin and portfolios of the Klamath and Great Basins. General Technical Report PNW-GTR-405. USDA Forest Service, Pacific Northwest Research Station. Portland, OR.

Reinhardt, E.D. 2003. Using FOFEM 5.0 to estimate tree mortality, fuel consumption, smoke production and soil heating from wildland fire. In: Proceedings of the Second International Wildland Fire Ecology and Fire Management Congress. P5.2. ams.confex.com/ams/FIRE2003/techprogram/paper_65232.htm

Reinhardt, E.D., and Crookston, N.L. 2003. The fire and fuels extension to the forest vegetation simulator. General Technical Report RMRS-GTR-116. USDA Forest Service, Rocky Mountain Research Station, Ft. Collins, CO.

Reinhardt, E.D., Keane, R.E., and Brown, J.K. 1997. First order fire effects model: FOFEM 4.0, user's guide. General Technical Report INT-GTR-344. USDA Forest Service, Intermountain Research Station. Ogden, UT.

Reinhardt, T.E., Ottmar, R., and Castilla, C. 2001. Smoke impacts from agricultrual burning in a rural Brazilian town. J. Air Waste Ma., 51, 443–450.

Riccardi, C.L., Ottmar, R.D., Sandberg, D.V., Andreu, A.G., Elman, E., Kopper, K., and Long, J. 2007. The fuelbed: A key element of the fuel characteristic classification system. Can. J. For. Res. 37(12), 2394–2412.

Rollins, M.G., and Frame, C.K. Tech., eds. 2006. The LANDFIRE prototype project: Nationally consistent and locally relevant geospatial data for wildland fire management. General Technical Report RMRS-GTR-177. USDA Forest Service, Rocky Mountain Research Station, 416 pp.

Sandberg, D.V., and Dost, F.N. 1990. Effects of prescribed fire on air quality and human health. In: Walstad, J.W., Radosevich, S.R., and Sandberg, D.V., eds. Natural and prescribed fire in the Pacific Northwest Forests. Oregon State University Press, Corvallis, pp. 191–218.

Sandberg, D.V., Anderson, G.K., and Norheim, R.A. 2004. Fire emission production simulator [software] ver. 1.1. www.fs.fed.us/pnw/fera/feps/index.shtml

Sandberg, D.V., Hardy, C.C., Ottmar, R.D., Snell, J.A.K., Acheson, A., Peterson, J.L., Seamon, P., Lahm, P., and Wade, D. 1999. National strategic plan: modeling and data systems for wildland fire and air quality. General Technical Report PNW-GTR-450. USDA Forest Service, Pacific Northwest Research Station. Portland, OR, 60 pp.

Sandberg, D.V., Ottmar, R.D., and Cushon, G.H. 2001. Characterizing fuels in the 21st century. Int. J. Wildland Fire 10(4), 381–387.

Sandberg, D.V., Ottmar, R.D., Peterson, J.L., and Core, J. 2002. Wildland fire on ecosystems: Effects of fire on air. General Technical Report RMRS-GTR-42-vol. 5. USDA Forest Service, Rocky Mountain Research Station, Ft. Collins, CO, 79 pp.

Schaaf, M.D. 1996. Development of the fire emissions tradeoff model (FETM) and application to the Grande Ronde River Basin, Oregon. Final report. Contract 53-82FT-03-2 for USDA Forest Service, Pacific Northwest Region, Portland, OR.

Scott, J.H., and Burgan, R.E. 2005. Standard fire behavior fuel models: A comprehensive set for use with Rothermel's surface fire spread model. General Technical Report, RMRS-GTR-153. USDA Forest Service, Rocky Mountain Research Station. Ft. Collins, CO.

Trabaud, L., Christensen, N., and Gill, A. 1993. Historical biogeography of fire in temperate and Mediterranean ecosystems. In: Crutzen, P., and Goldammer, J., eds. Fire in the environment: The ecological, atmospheric, and climatic importance of vegetation fires. Wiley, pp. 277–295.

Valente, J., Miranda, A.I., Lopes, A.G., Borrego, C., and Viegas, X. 2005. A local-scale modelling system to simulate smoke dispersion. The Joint Meeting of the Sixth Symposium on Fire and Forest Meteorology and the 19th Interior West Fire Council Meeting, 25–27 October, Canmore, Canada. Proceedings on CD-ROM.

Ward, D.E., Hardy, C.C., Sandberg, D.V., and Reinhardt, T.E. 1989. Part III-emissions characterization. In: Sandberg, D.V., Ward, D.E., and Ottmar, R.D., comp., eds. Mitigation of Prescribed Fire Atmospheric Pollution through Increased Utilization of Hardwoods, Piled Residues, And Long-Needled Conifers. Final report. U.S. DOE, EPA. USDA Forest Service, Pacific Northwest Research Station. Seattle.

Ward, D., and Radke, L. 1993. Emissions measurements from vegetation fires: A comparative evaluation of methods and results. In: Crutzen, P., and Goldammer, J., eds. Fire in the environment: The ecological, atmospheric and climatic importance of vegetation fires. Wiley, Chichester, England.

Yokelson, R.J., Griffith, D.W.T., and Ward, D.E. 1996. Open-path fourier transform infrared studies of large scale laboratory biomass fires. J. Geophys. Res. 101(D15), 20,167–21,080.

Developments in Environmental Science, Volume 8 79
A. Bytnerowicz, M. Arbaugh, A. Riebau and C. Andersen (Editors)

ISSN: 1474-8177/DOI:10.1016/S1474-8177(08)00004-1

Chapter 4

Chemical Composition of Wildland Fire Emissions

Shawn P. Urbanski, Wei Min Hao and Stephen Baker*

Abstract

Wildland fires are major sources of trace gases and aerosol, and these emissions are believed to significantly influence the chemical composition of the atmosphere and the earth's climate system. The wide variety of pollutants released by wildland fire include greenhouse gases, photochemically reactive compounds, and fine and coarse particulate matter. Through direct emissions and secondary chemical and physical processes, wildland fire can have a significant impact on tropospheric chemistry and serve as a major source of air pollution. We provide a synthesis of emission factor data from the literature and previously unpublished research for use in global, continental and regional scale studies investigating the role of wildland fire emissions in atmospheric chemistry and climate. The emission factor data is presented by geographic zones (boreal, temperate, and tropical) and vegetation group (forest and savanna/ rangeland), allowing researchers to account for the different emission characteristics exhibited by biomass burning in these disparate regions. A brief overview of the wildland fuel combustion process as related to emissions production is also provided. The atmospheric fate of wildland fire emissions is briefly discussed and related to the production of secondary air pollutants. Previously unpublished results from a series of fire emission studies in the United States and Canada are presented in an appendix.

*Corresponding author: E-mail: surbanski@fs.fed.us

4.1. Introduction

Wildland fires emit large amounts of trace gases and particles (Ito & Penner, 2004; Michel et al., 2005; van der Werf et al., 2006; Wiedinmyer et al., 2006), and these emissions are believed to significantly influence the chemical composition of the atmosphere (Lapina et al., 2006; Simpson et al., 2006) and the earth's climate system. The wide variety of pollutants released by wildland fire include greenhouse gases (carbon dioxide (CO_2), methane (CH_4), nitrous oxide (N_2O)), photochemically reactive compounds (e.g., carbon monoxide (CO), nonmethane volatile organic carbon (NMVOC), nitrogen oxides (NO_x)), and fine and coarse particulate matter (PM). Wildland fires influence climate both directly, through the emission of greenhouse gases and aerosols, and indirectly, via secondary effects on atmospheric chemistry (e.g., ozone (O_3) formation) and aerosol and cloud microphysical properties and processes (e.g., the "Twomey" cloud albedo effect; Lohmann & Feichter, 2005; Naik et al., 2007). Wildland fire emissions contribute to air pollution by increasing the atmospheric levels of pollutants that are detrimental to human health and ecosystems and degrade visibility, leading to hazardous or general nuisance conditions. The air quality impacts occur through the emission of primary pollutants (e.g., PM, CO, NO_x) and the production of secondary pollutants (e.g., O_3, secondary organic aerosol (SOA)) when NMVOC and NO_x released by fires undergo photochemical processing. Air quality can be degraded through local (Muhle et al., 2007; Phuleria et al., 2005), regional (DeBell et al., 2004; Sapakota et al., 2005), and continental (Morris et al., 2006) scale transport and transformation of fire emissions.

The air quality impact of wildland fires depends on meteorology, fire plume dynamics, the amount and chemical composition of the emissions, and the atmosphere into which the emissions are dispersed. Fresh smoke from burning wildland fuel is a complex mixture of gases and aerosols. The amount and composition of fire emissions depends on a wide range of variables related to fuel characteristics (type, structure, loading, chemistry, moisture) and fire behavior (Christian et al., 2003). Fuel characteristics are ecosystem-specific properties that are heavily influenced by land use history and environmental conditions (e.g., seasonal weather patterns that drive fuel moisture or anthropogenic nitrogen and sulfur deposition that impact fuel chemistry). It is fuel characteristics in conjunction with meteorology and topography that control fire behavior (Albini, 1976; Anderson, 1983; Rothermel, 1972).

This chapter provides an overview of the wildland fuel combustion process as related to emissions production and provides a synthesis of emissions data from the literature and previously unpublished research for global and continental scale studies of atmospheric chemistry and climate. We also briefly discuss the atmospheric fate of wildland fire emissions and how it is related to the production of secondary air pollutants. Last, we include an appendix of previously unpublished results from a series of fire emission studies in the United States and Canada.

4.2. Wildland fuel combustion process and emissions

Given an ignition, wildland fire propagates through heat transfer from the open flame and burning region of a fuelbed to the unburned components of the fuelbed. Heat transfer can occur through direct flame contact, convective heating, radiative heating, and firebrand contact (Morvan & Dupuy, 2001). The unburned material is thermally degraded producing volatile gases that mix with air to form a combustible mixture ahead of the flaming front. Ignition of the combustible mixture by the flame spreads the flaming front (Benkoussas et al., 2007; Morvan & Dupuy, 2001). In the wake of the flaming front, combustion continues in the fuelbed, with regions of intermittent open flame. The combustion of wildland fuels may be divided into several phases: distillation/drying, pyrolysis, char oxidation, and flaming combustion (Benkoussas et al., 2007).

Laboratory studies investigating the combustion of wildland fuels and biomass provide valuable insight into the relationship between the character of fire emissions and the combustion process. Distillation involves volatilization of compounds stored in liquid pools as the vegetation is heated. Distillation of freshly harvested live foliage has been observed to emit a variety of volatile organic compounds (VOC; Greenberg et al., 2006). Greenberg et al. (2006) measured emission rates of terpenes, methanol, acetaldehyde, acetic acid, and methyl acetate from five different vegetation species when heated from 60°C to 200°C.

Minimal thermal decomposition of lignocelluosic biomass occurs prior to about 200°C, where pyrolysis begins ($\sim$250 °C for whole wood; Rowell & LeVan–Green, 2005). Below 300 °C, pyrolysis mainly leads to the production of volatile gases and the formation of reactive char (Rowell & LeVan–Green, 2005). Low temperature pyrolysis (200–300 °C) of freshly harvested live foliage and woody tissue produces CO, CO_2, and a host of oxygenated-VOC (OVOC), including methanol, acetic acid, acetone, 1,3-butadione, furan, and 2-furyladehyde (Greenberg et al., 2006). Oxidation of the reactive char leads to smoldering or glowing combustion. Pyrolysis and char oxidation create flammable gas mixtures that form the flame. The flaming combustion process produces gas-phase emissions that are dominated by highly oxidized compounds (CO_2, NO_x, sulfur dioxide (SO_2)) (Lobert et al., 1991; Yokelson et al., 1997) and aerosol with a significant, but highly variable fraction of elemental carbon (Chen et al., 2007; Radke et al., 1991; Reid et al., 2005).

After flaming combustion has ceased, oxidation of residual char results in glowing combustion. As the heat intensity decreases and the levels of combustible gases decrease, char oxidation initiates smoldering combustion (Rowell & LeVan–Green, 2005). Large scale, open fires in laboratory combustion chambers have identified several products of pyrolysis and char oxidation occurring following the cessation of open flame; these incomplete combustion products include CO, CH_4, ammonia (NH_3), C2–C3 hydrocarbons, methanol, formic and acetic acids, and formaldehyde (Bertschi et al., 2003; Yokelson et al., 1996, 1997).

During a wildland fire event, the complex thermal degradation processes (distillation, pyrolysis, char oxidation, and the oxidation of the resultant gas products in flaming combustion) occur simultaneously and often in close proximity. Thermal degradation of fuels occurs ahead and along the fireline, while pockets of intermittent open flame often persist well behind the flaming front. However, for purposes of characterizing emissions, wildland fire behavior is usually described based on the presence or absence of an open flame: ‘‘flaming’’ or ‘‘smoldering’’ combustion. While this taxonomy is imperfect, it does provide a basis for objectively describing the fire behavior associated with emission measurements. The relative amount of flaming and smoldering combustion in a wildland fire may be described using the combustion efficiency (CE) or modified combustion efficiency (MCE) indices (see Section 4.3). Numerous laboratory studies demonstrate flaming combustion is characterized by high CE and MCE (Chen et al., 2007; Goode et al., 1999; Yokelson et al., 1996). These studies demonstrate that values of CE and MCE approach 1 when flaming combustion dominates—for a bed of fine fuels (grass or conifer needles) completely engulfed in flame, MCE is about 0.99 (Chen et al., 2007; Yokelson et al., 1996).

The presence of open flame—flaming combustion—has a significant impact on the chemical composition of emissions and the plume dynamics of the fire. Volatile gases created by thermal degradation of the fuels are oxidized in the flame, generating more highly oxidized emissions (Lobert et al., 1991; Yokelson et al., 1997). Flaming combustion is a highly exothermic process that produces high-temperature gases and subsequent convective lofting of emissions. Consumption of the fuel leads to a reduced rate of pyrolysis and eventual cessation of the open flame.

The continued thermal degradation of fuels in the postfrontal fuelbed is the phase of fire commonly labeled "smoldering combustion." During the smoldering phase, the reduced rate of pyrolysis results in lower heat production and fuel consumption rates (Freeborn et al., 2007; Lobert & Warnatz, 1993; Ottmar, 2002; Rowell & LeVan–Green, 2005). The energy available to drive convective lofting of emissions is greatly diminished, and the smoke often remains close to the ground (Ottmar, 2002; Ottmar et al., 2002).

The convective updraft of a fire's flaming front often entrains emissions from smoldering combustion along the fire front and in the postfrontal fuelbed, resulting in a smoke plume that is a mixture of emissions created by flaming and smoldering combustion. It is these convectively lofted emissions that have the greatest potential for impacting air pollution beyond the local vicinity of a fire. Most field studies of fire emissions have employed aircraft or towers as sampling platforms and have measured the fresh smoke plumes of fire convective updrafts. Smoldering combustion that is not entrained in the convective updraft or is sustained without open flame is referred to as residual smoldering combustion (RSC; Bertschi et al., 2003; Wade & Lunsford, 1989). RSC generally involves the combustion of large diameter fuels and belowground biomass (e.g., peat, duff, and roots) and may persist for days or weeks after flaming combustion has ceased (Ward et al., 1992). Emissions from RSC can be quite significant; in boreal and temperate forests RSC may comprise 50% or more of the biomass consumed in some fire events (Kasischke et al., 2000; Reinhardt et al., 1991).

4.3. Emission data

The standard metric employed in the measurement of fire emissions is the excess mixing ratio, ΔX, defined as

$$\Delta X = X_{\mathrm{plume}} - X_{\mathrm{bkgd}} \tag{4.1}$$

where X_{plume} and X_{bkgd} are the mixing ratio of compound X in the fresh smoke plume and the background air, respectively (Ward & Radke, 1993). Emission data is typically reported as emission ratios ($\mathrm{ER}_{\mathrm{X/Y}}$) or emission factors ($\mathrm{EF}_{\mathrm{X}}$). The $\mathrm{ER}_{\mathrm{X/Y}}$ is the excess mixing ratio of species X normalized to the excess ratio of a reference species Y, typically CO or CO_2:

$$\mathrm{ER}_{\mathrm{X/Y}} = \frac{\Delta X}{\Delta Y} \tag{4.2}$$

This chapter presents emission data as emission factors, calculated using the carbon mass balance method (Ward & Radke, 1993), and defined as the mass of a compound released per mass of dry fuel consumed, in units of $\mathrm{g\,kg^{-1}}$. The emission factor for compound X, $\mathrm{EF_X}$, may be estimated using

$$\mathrm{EF_X} = F_\mathrm{C} \times 1000 \times \frac{\mathrm{MM_X}}{12} \times \frac{\Delta X}{C_\mathrm{T}} \tag{4.3}$$

$$C_\mathrm{T} = \sum_{j=1}^{n} N_j \times \Delta C_j \tag{4.4}$$

where ΔX is the excess molar mixing ratio of compound X (Eq. (4.1)), C_T the total excess molar mixing ratio of carbon emitted, $\mathrm{MM_X}$ the molecular mass of compound X ($\mathrm{g\,mole^{-1}}$), 12 the molar mass of carbon ($\mathrm{g\,mole^{-1}}$), F_C the mass fraction of carbon in the dry fuel, and 1000 ($\mathrm{g\,kg^{-1}}$) a unit conversion factor (Yokelson et al., 1999). Elemental analysis of wildland fuels from a wide range of vegetation types and ecosystems shows F_C falls between 0.45 and 0.55 (Chen et al., 2007; Lobert et al., 1991; Susott et al., 1991, 1996). A detailed discussion on the elemental analysis of wildland fuels is provided by Susott et al. (1996). C_T may be calculated using Eq. (4.4), where n is the number of emitted species measured, N the number of moles of carbon in species j, and ΔC_j is the excess mixing ratio measured for species j.

The creation of wildland fire source terms for chemical transport or air quality modeling generally requires a mass emission estimate, which $\mathrm{EF_X}$ provides. Emission data reported as $\mathrm{ER_{X/Y}}$ can be converted to $\mathrm{EF_X}$ using

$$\mathrm{EF_X} = \mathrm{ER_{X/Y}} \times \frac{\mathrm{MM_X}}{\mathrm{MM_Y}} \times \mathrm{EF_Y} \tag{4.5}$$

where $\mathrm{ER_{X/Y}}$ is the molar emission ratio of compound X to a reference compound Y (as defined in Eq. (4.2), $\mathrm{MM_X}$ and $\mathrm{MM_Y}$ are the molecular mass of compounds X and Y ($\mathrm{g\,mole^{-1}}$), and $\mathrm{EF_Y}$ is the emission factor for reference compound Y (Eq. (4.3)).

The fire behavior associated with emissions is often characterized using the CE or the MCE, indices that describe the relative amount of flaming and smoldering combustion in a biomass fire (Ward & Radke, 1993). The CE is the molar ratio of CO_2 emitted to the total moles of carbon emitted. CE may be expressed as the ratio of excess moles of carbon emitted as CO_2 to the molar sum of carbon (C) emitted, C_T (Eq. (4.6)). MCE is defined as the ratio of CO_2 emitted to the sum of emitted CO and CO_2

(Eq. (4.7); Ward & Radke, 1993).

$$\mathrm{CE} = \frac{\Delta\mathrm{CO}_2}{C_\mathrm{T}} \tag{4.6}$$

$$\mathrm{MCE} = \frac{\Delta\mathrm{CO}_2}{\Delta\mathrm{CO}_2 + \Delta\mathrm{CO}} \tag{4.7}$$

4.4. Emissions factors for global and continental scale modeling

4.4.1. Introduction

In this section, we provide a synthesis of emissions data from the literature and previously unpublished research for use in global to continental scale studies investigating the role of wildland fire emissions in atmospheric chemistry and climate. Since the research of Andreae and Merlet (2001), knowledge of emissions from wildland fires in tropical regions has increased greatly through extensive field campaigns in southern Africa (SAFARI-2000) (Swap et al., 2003) and Brazil (e.g., The Tropical Forest and Fire Emissions Experiment; Yokelson et al., 2007). The synthesis presented here includes previously unpublished emissions data from field studies of 56 fires covering a broad range North American ecosystems. The emission data is presented by geographic zones (boreal, temperate, and tropical) and vegetation group (forest and savanna/rangeland), allowing modelers to account for the different emission characteristics exhibited by biomass burning in these disparate regions.

Numerous global to continental scale studies using global chemical transport models have sought to elucidate the role of biomass burning in atmospheric chemistry and climate. Recent studies include the role of African biomass burning on tropical O_3 in the Atlantic (Jourdain et al., 2007), the global impacts of aerosol emitted from major source regions (Koch et al., 2007), and the influence of biomass burning on radiative forcing via aerosol and O_3 production (Naik et al., 2007). These studies consider the large-scale influence of widespread, seasonal, regional burning. The coarse grids ($1^\circ \times 1^\circ$ to $6^\circ \times 6^\circ$) of global chemical transport models used in such studies integrate fire activity across a heterogeneous mix of ecosystems (e.g. grasslands, shrublands, and open woodlands; Hely et al., 2003; Sinha et al., 2003). Emission factors for generalized vegetation types (e.g., tropical savanna), which synthesize data from studies encompassing a broad range of geographic regions (e.g., western and southern Africa, Brazil, Australia), ecosystems, and land use modes, are appropriate for global to continental scale investigations using global chemical transport models.

Biomass burning in the tropics is dominated by anthropogenic activities associated with agriculture (Fearnside, 1990; Hao & Liu, 1994; Kauffman et al., 2003, Roberts & Wooster, 2007). In the tropics, fire activity occurs largely within a region's ‘‘burning season’’ (e.g., June through November in the southern Africa; Giglio et al., 2006). The tropical savanna vegetation group represents grassland, shrubland, and woodland savanna ecosystems found in South America, Africa, India, Mainland Southeast Asia, and Australia. The tropical savanna and tropical forest emission data synthesizes an extensive collection of studies conducted in Brazil, Africa, and Australia.

The wildland fire activity in temperate zones includes wildfire and prescribed burning (see Section 4.4.2). Prescribed fires are defined as fires ignited by management actions to meet specific, nonagricultural objectives, such as fuel reduction and ecosystem management and restoration (Finney et al., 2005; Hardy et al., 2002). Wildfires are unplanned wildland fires. The temperate zone emission data has been grouped as forest or rangeland (grassland/shrubland). Temperate zone wildfires often occur during a region's wildfire season when meteorological and fuel conditions favor high intensity, rapidly spreading fires (e.g., July through September in the interior mountain west of the United States and Canada). Conversely, prescribed fire is typically employed under meteorological and fuel conditions favorable for low-intensity fires and selective fuel reduction (Fernandes & Botelho, 2004; Finney et al., 2005; Hardy et al., 2002; Price et al., 2007; Smith et al., 2004). Published emission studies for wildland fire in Europe and Central Asia are extremely sparse. As a result, the temperate zone emission data draws mostly from field studies of wildfires and prescribed fires in the United States and southwestern Canada.

Wildfires occurring in the boreal regions of Russia, Canada, and Alaska are estimated to comprise about 20% of annual global biomass burning emissions (van der Werf et al., 2006). Due to the lack of published emission studies, boreal zone emission data is given only for forests, and relies largely on data collected in Canada and Alaska. Despite the significance of boreal fires in Russia, published emission studies for fires in this region are extremely limited.

4.4.2. Methods

The emission data is presented here as emission factors (see Section 4.3). Emission factors defined following Eq. (4.3) were used unchanged.

Emission factors given as the fraction of carbon burned were adjusted using the fuel carbon content (F_C) provided by the authors. In the absence of an author provided F_C, a value of 0.50 was used. The F_C value of 0.50 is consistent with F_C measurements for a wide range of vegetation types and ecosystems and is likely accurate to within $\pm 10\%$ (Chen et al., 2007; Lobert et al., 1991; Susott et al., 1991, 1996). When emission data was provided as $ER_{X/Y}$, the data was converted to EF_X using Eq. (4.5). When EF_Y was not supplied by the authors, it was either calculated from the reported data if possible (using Eqs. (4.1–4.4)) or estimated based on EF_Y data for the appropriate vegetation cover group.

Most of the available emission data was obtained from near source, airborne sampling that measures an integrated mixture of emissions from flaming and smoldering combustion. Because the different fire phases often occur simultaneously and in close proximity, differentiating emissions by phase is problematic, even for ground-based measurements. Therefore, we have not attempted to tabulate emission factors by fire phase. When emission data was reported by flaming and smoldering phases, average emission factors were calculated by weighting the phases to achieve an MCE equal to the average MCE of the appropriate vegetation cover group.

The combination of data from wildfires and prescribed fires for temperate zone EFs may seem inappropriate given their different fire behavior characteristics. Temperate zone wildfires are generally more intense than prescribed fires, exhibiting higher rates of spread, greater flame lengths and fire line intensities, and sometimes crown fire (Fernandes & Botelho, 2004; Finney et al., 2005). The greater intensity of wildfires might be expected to result in greater CE compared to lower intensity for prescribed burns. However, during the temperate zone wildfire season, the combination of low fuel moistures (in particular for large diameter woody surface fuels and duff) and high-intensity fire fronts facilitates postfrontal consumption of large woody surface fuels and duff (Albini & Reinhardt, 1995). While pockets of intermittent open flame do persists in postfrontal combustion, low-efficiency, smoldering combustion dominates fuel consumption (Albini & Reinhardt, 1995; Ottmar, 2002; Ottmar et al., 2002). Postfrontal combustion of woody fuels and duff may comprise a significant portion of the total fuel consumed in a fire event (Reinhardt et al., 1991). Conversely, prescribed burning in temperate zones of North America and Europe is generally typified by low-intensity fire occurring under conditions when large woody surface fuels and duff moistures are moderate (Fernandes & Botelho, 2004; Finney et al., 2005; Hardy et al., 2002). These conditions minimize consumption of the large woody fuels and duff, which limits the detrimental fire effects on the ecosystem (Reinhardt et al., 2001), a key management objective of prescribed fire.

In a wildfire event, the convective plume integration of emissions from the high-intensity flaming front and a portion of the emissions from postfrontal smoldering combustion result in fire average combustion efficiencies similar to those of prescribed fires, where flaming combustion comprises a larger fraction of the total fuel consumption. For example, airborne measurements of conifer forest wildfire smoke plumes in the western United States observed MCE of 0.89–0.94 (Babbit et al., 1994; Friedli et al., 2001) compared with an average MCE of 0.92 from studies of 21 prescribed fires in western conifer forests (see Appendix A). Numerous laboratory and field studies (both ground-based and airborne) have shown EFs for a wide range of compounds are linearly correlated with MCE, particularly within vegetation types (Hao et al., 1996; Korontzi et al., 2003; Sinha et al., 2003; Yokelson et al., 2003). Therefore, the similar MCE of wildfires and prescribed fires suggests the aggregation of emissions data from these fire events is appropriate for estimating EFs for use in global to continental scale modeling.

4.4.3. Results and discussion

Emission factor data has been compiled in Table 4.1 according to five generalized vegetation cover groups: temperate forest, temperate rangelands, tropical savanna, tropical forest, and boreal forest. In most instances, the values listed in Table 4.1 are the average of the values obtained from the cited literature and previously unpublished data presented in Appendix A. The scope of Table 4.1 has been limited to compounds that dominate wildland fire emissions or that have a significant potential to impact atmospheric chemistry. Table 4.1 is not an all inclusive list of species that have been observed in wildland fire emissions (e.g., halocarbons are known to be minor products of wildland fire; Andreae & Merlet, 2001 but are not included). For the species considered in our synthesis, the data coverage is thorough for temperate and tropical forests and tropical savannas. The boreal forest data lacks measurements of nonmethane hydrocarbons (NMHC) and heavy OVOC. The temperate rangeland data does not include emission factors for formic acid, acetic acid, and formaldehyde. These three compounds, along with methanol, comprise a large fraction of both OVOC emissions and total NMVOC emissions in the other vegetation cover groups. We report emissions factors for $PM_{2.5}$; however, a detailed discussion of the complex topic of aerosol properties (size distributions, chemistry, thermodynamics) is beyond the scope of this chapter. Reid et al. (2005)

Table 4.1. Emission factors data from wildland fires according to five generalized vegetation cover groups

Species	Temperate forest	Temperate rangeland	Tropical savannas	Tropical forest	Boreal forest	References[a]
	EF ($g\,kg^{-1}$)[b]					
MCE[c]	0.919 ± 0.017	0.939 ± 0.015	0.935 ± 0.019	0.897 ± 0.017	0.906 ± 0.044	1–6,8–13,29–33
Carbon dioxide (CO_2)	1619 ± 112	1684 ± 45	1661 ± 66	1604 ± 50	1604 ± 119	1–6,8–13,29–33
Carbon monoxide (CO)	89.6 ± 13.2	69 ± 17	75 ± 20	117 ± 19	105 ± 45	1–6,8–13,14–27,28,29–33
Methane (CH_4)	3.41 ± 0.90	2.31 ± 1.08	2.7 ± 1.1	6.7 ± 1.1	4.5 ± 2.3	1–7,8–13,14–27,29–33
Ethane (C_2H_6)	0.49 ± 0.24	0.27 ± 0.13	0.42 ± 0.20	0.75 ± 0.23	0.97 ± 0.69	1–3,5,7,8,13,14,16–21,23,24,29–33
Ethene (C_2H_4)	1.11 ± 0.13	1.11 ± 0.44	1.25 ± 0.49	1.20 ± 0.40	2.52 ± 1.02	1–4,7,8,13,14–21,23,24,29,32,33
Ethyne (C_2H_2)	0.29 ± 0.05	0.38 ± 0.15	0.38 ± 0.28	0.21–0.28	0.38 ± 0.23	1–3,5,7,8,13,14–20,22–24,29,32
Propane (C_3H_8)	0.19 ± 0.10	0.09 ± 0.06	0.20 ± 0.28	0.15–0.99	0.31 ± 0.20	1–3,5,7,8,13,14,16–21,23,24,29,33
Propene (C_3H_6)	0.48 ± 0.14	0.40 ± 0.25	0.41 ± 0.15	0.97 ± 0.60	1.05 ± 0.69	1–3,5,7,8,13,14,16–21,24,29,32,33
Propyne (C_3H_4)	0.06 ± 0.02	0.06 ± 0.02				1–3,13
n-butane (n-C_4H_{10})	0.019–0.104	0.03	0.040 ± 0.032	0.04		1,7,14,16,19,22,23
i-butane (i-C_4H_{10})	0.006–0.027	0.008	0.008 ± 0.002	0.02		1,7,14,16,19,23
1+i-butene (C_4H_8)	0.115–0.270	0.06				1,7
1-butene (C_4H_8)			0.075 ± 0.024	0.02–0.13		14,16,17,19,32
i-butene (C_4H_8)			0.062 ± 0.012	0.11		16,17,19
t-2-butene (C_4H_8)	0.018–0.051	0.02	0.026 ± 0.009	0.02–0.05		1,7,14,16,17,23,32
c-2-butene (C_4H_8)	0.014–0.131	0.04	0.020 ± 0.008	0.02–0.04		1,7,14,16,17,23,32
1,3 butadiene (C_4H_6)	0.059–0.065	0.037	0.065 ± 0.069			1,7,14,17,23
n-pentane (n-C_5H_{12})	0.009–0.051	0.011	0.015 ± 0.013	0.014		1,7,14,16,23
i-pentane (i-C_5H_{12})	0.026	0.006	0.075 ± 0.084	0.007		1,16,17,22,23
1-pentene (C_5H_{10})	0.068	0.02	0.020	0.059		7,17,23,28
cis-2-pentene (C_5H_{10})	0.010		0.027 ± 0.006			1,14
trans-2-pentene (C_5H_{10})	0.019	0.003	0.003			1
2-methyl-1-butene (C_5H_{10})			0.006–0.029	0.031		14,17,28
2-methyl-2-butene (C_5H_{10})	0.033	0.027	0.005–0.010	0.046		1,14,28
3-methyl-1-butene (C_5H_{10})	0.019	0.01	0.005			1,14
Cyclopentene (C_5H_8)	0.019	0.005				1
Isoprene (C_5H_8)	0.044–0.114	0.03	0.011–0.042	0.02–0.37		1,7,14,16,17,32

Table 4.1. (Continued)

Species	Temperate forest	Temperate rangeland	Tropical savannas	Tropical forest	Boreal forest	References[a]
	EF ($g\,kg^{-1}$)[b]					
1,3-pentadiene (C_5H_8)	0.028	0.01				1
1,3-cyclopentadiene (C_5H_6)	0.025	0.03				1
Hexane (C_6H_{14})	0.005–0.033	0.006	0.010–0.013	0.067		1,7,14,23,28
Methylcyclopentane (C_6H_{12})	0.006					1
1-hexene (C_6H_{12})	0.102	0.03	0.030–0.046	0.042		1,23,28
trans-2-hexene (C_6H_{12})	0.014					1
cis-2-hexene (C_6H_{12})	0.004					1
2-methylpentene (C_6H_{12})	0.009		0.004			1
Heptane (C_7H_{16})	0.004–0.032	0.005	0.007	0.013		1,7,14,28
Octane (C_8H_{18})	0.017	0.003		0.012		1,28
1-octene (C_8H_{16})	0.018	0.003	0.009			1,14
1-nonene (C_9H_{18})	0.019	0.003				1
Decane ($C_{10}H_{22}$)	0.027	0.002				1
Benzene (C_6H_6)	0.250–0.440	0.22	0.29 ± 0.10	0.38 ± 0.08		1,7,14,16,20–23,28,32
Toluene (C_7H_8)	0.150–0.510	0.13	0.15 ± 0.04	0.23 ± 0.04		1,7,14,16,20,23,28,32
m+p-xylene (C_8H_{10})	0.171	0.039	0.04	0.050		1,16,23
o-xylene (C_8H_{10})	0.051	0.009	0.009–0.012	0.014–0.017		1,16,28
Xylenes (C_8H_{10})				0.13		32
Ethylbenzene (C_8H_{10})	0.020–0.051	0.02	0.009–0.024	0.04 ± 0.03		1,7,16,28,32
Methanol (CH_4O)	0.31–2.03	0.14	1.17	2.57	1.23–1.57	1,4,15,29,32
Phenol				0.01–0.37		32
Formic acid (CH_2O_2)	1.17		0.62	0.59	0.71–1.57	4,15,29,32
Acetic acid (CH_4O_2)	3.11		2.42	3.43	1.61–3.38	4,15,29,32
Formaldehyde (CH_2O)	2.25		0.24–1.10	1.66	1.50–2.38	4,15,21,29,32
Acetaldehyde (C_2H_4O)	0.24	0.25	0.53–0.97	1.38		1,21,22,32
Propanal (C_3H_6O)	0.035	0.01		0.09		1,32
Propenal (C_3H_4O)	0.123	0.08		0.58		1,32
2-methylpropanal (C_4H_8O)	0.206			0.01–0.16		1,32
2-methylbutanal ($C_5H_{10}O$)	0.015					1

Acetone (C_3H_6O)	0.347	0.25		0.57		1,32
2-butanone (C_4H_8O)	0.40	0.26				1
2,3-butanedione ($C_4H_6O_2$)	1.5			0.66		1,32
2-pentanone ($C_5H_{10}O$)	0.079	0.01		0.07		1,32
Cyclopentanone (C_5H_8O)	0.014					1
Furan (C_4H_4O)	0.445	0.1	0.36	0.27–0.33		1,20,32
2-methyl-furan (C_5H_6O)	0.521		0.051–0.24	0.11 ± 0.07		1,20,28,32
3-methyl-furan (C_5H_6O)	0.052		0.012	0.03–0.28		1,28,32
2-ethylfuran (C_6H_8O)	0.006		0.001	0.004		1,28
2,5-dimethyl-furan (C_6H_8O)	0.053					1
2-vinyl-furan (C_6H_6O)	0.013					1
Benzofuran (C_8H_6O)	0.038		0.015	0.016		1,28
Nitrogen oxides (as NO)	1.7		2.3 ± 1.0	1.77	1.1–3.3	5,15,21,22,27,32
Nitric oxide (NO)			1.1	0.74–1.8	1.5–2.3	25,29,32
Nitrous oxide (N_2O)	0.16	0.32	0.12–0.18		0.14–0.41	5,10,22,26,30,33
Ammonia (NH_3)	0.56–1.13		0.26–1.77	1.08	0.10–0.49	4,5,15,21,22,29,32
Hydrogen cyanide (HCN)			0.03–0.53	0.68		15,21,22,32
Aectonitrile (CH_3CN)			0.03–0.13	0.37		21,22,32
Sulfur dioxide (SO_2)			0.43			14
Carbonyl sulfide (OCS)	0.03	0.01		0.02		1,32
$PM_{2.5}$	11.7 ± 5.0	9.7 ± 4.3	4.4	8.5	1.5–7.2	2,3,6,13,24,25,31

Notes: $\mu \pm \sigma$ (mean $\pm$ one standard deviation).

[a]References: a. temperate forest, b. temperate rangeland, c. tropical savanna, d. tropical forest, e. boreal forest; 1. Friedli et al. (2001) (a, b); 2. Appendix A, western U.S. conifer forests (a); 3. Appendix A, southeastern U.S. conifer forests (a); 4. Yokelson et al. (1999) (a); 5. Nance et al. (1993) (a,b,e); 6. Babbit et al. (1994) (a); 7. Lee et al. (2005) (a); 8. Radke et al. (1991) (a, b, e); 9. Cofer et al. (1998) (e); 10. Cofer et al. (1990) (b); 11. Hardy et al. (1996) (b); 12. Ward and Hardy 1989 (b); 13. Appendix A, U.S. grassland and shrublands (b); 14. Sinha et al. (2003) (c); 15. Yokelson et al. (2003) (c); 16. Ferek et al. (1998) (c,d); 17. Bonsang et al. (1991) (c); 18. Rudolph et al. (1995) (c); 19. Bonsang et al. (1995) (c); 20. Greenberg et al. (1984) (c,d); 21. Hurst et al. (1994A) (c); 22. Hurst et al. (1994B) (c); 23. Hao et al. (1996) (c); 24. Ward et al. (1996) (c); 25. Ward et al. (1992) (c,d); 26. Cofer et al. (1996) (c); 27. Lacaux et al. (1996) (c); 28. Koppmann et al. (1996) (c,d); 29. Goode et al. (2000) (e); 30. Cofer et al. (1998) (e); 31. Appendix A, Alaska boreal forest (e); 32. Yokelson et al. (2007) (d); 33. Cofer et al. (1990) (b).

[b]Emission factors are in units of gram of compound emitted per kilogram of dry fuel consumed.

[c]MCE (modified combustion efficiency) = $\Delta CO_2/(\Delta CO+\Delta CO_2)$.

provide a thorough review of biomass burning aerosol. Due to the lack of published data for coarse aerosol (e.g., diameter < 10 μm or total particulate matter) emissions from wildland fire, we have not included EF for coarse aerosol.

Emissions are dominated by CO_2 and CO, which comprise 92–95% (87–92% of C burned) and 4–7% (6–10% of C burned) of total emissions, respectively. As discussed in Section 4.2, the MCE provides a measure of the relative amount of flaming and smoldering combustion in a wildland fire. The MCE is highest for tropical savannas and temperate rangelands and lowest for tropical forests. The high MCE of the savanna and rangeland vegetation cover groups reflects the dominance of flaming combustion in the burning of herbaceous fuels. The heat required for ignition of a fuel element depends on the fuel element's surface area-to-volume ratio (a larger surface area-to-volume ratio requires less heat for ignition) and the moisture content of the fuel (Rothermel, 1972). The large surface area-to-volume ratio of grasses makes these fuels prone to ignition and favors rapid and thorough consumption in open flames. Low-fuel moistures also favor flaming combustion in herbaceous fuels. During a region's dry season, herbaceous vegetation, especially annual grasses, typically have very low moisture content.

Boreal forests exhibited the greatest variability in MCE (0.78–0.95) (Cofer et al., 1998; Nance et al., 1993). The lower end of this range reflects the contribution of smoldering duff in the postfrontal fuelbed, which burns with a low MCE (Bertschi et al., 2003; Goode et al., 1999; Yokelson et al., 1997) and can be a significant component of fuel loading in boreal ecosystems (French et al., 2004). The strong convective updrafts often accompanying boreal crown fires can effectively entrain emissions from postfrontal combustion (Trentmann et al., 2006). The low MCE observed for some boreal fires may reflect significant entrainment of postfrontal duff combustion into the convective plumes sampled in airborne studies. Based on their observations of high CO emissions from extremely intense (overall fire intensity of 38,400 $kW\,m^{-1}$) flaming crown fires, Cofer et al. (1998) have suggested that intense crown fires may behave as a fuel-rich combustion system with an associated low combustion efficiency.

After CO_2 and CO, the species accounting for the next largest share of emissions is $PM_{2.5}$, followed by CH_4. The $EF_{PM2.5}$ in Table 4.1 is based on tower measurements obtained in the convective updrafts of fires at 3–15 m above the surface (see Appendix A). Numerous airborne studies provide aerosol emission data for a wide range of ecosystems (Reid et al., 2005). However, the EFs measured in these studies encompass aerosol with diameters up to 3.5 or 4 μm. Because these measurements include aerosol with diameters outside the traditional definition of fine aerosol (diameter $< 2.5\,\mu m$), these studies are not included in Table 4.1.

Emissions of CH_4 from wildland fires appear to have a significant impact on the global levels of this important greenhouse gas (Simpson et al., 2006). Tropical forests have the highest EF_{CH_4} and the highest CH_4:CO EF ratio (0.056 vs. 0.033–0.043). The high CH_4 emissions for tropical forests may reflect the nature of deforestation burns, which typically involve slashed and dried vegetation with large woody fuels being a significant portion of the vegetation consumed (Fearnside, 1990; Kauffmann et al., 2003). Boreal fires involving similar, intentionally arranged fuelbeds, such as slash/tramp or chained fuels (Cofer et al., 1998; Nance et al., 1993; Radke et al., 1991), exhibit similar CH_4:CO EF ratios. Unlike burning in tropical forests, fires in intentionally arranged fuels is not a significant fraction of boreal fire activity (French et al., 2004).

Total emissions of NMVOC exceed that of $PM_{2.5}$ and CH_4 combined and account for 1–2% of fuel C burned (excluding temperate rangelands for which the lack of OVOC measurements prohibits a meaningful assessment). OVOC account for ~60–70% of NMVOC emission and exceed NMHC emissions even on a carbon mass basis. Methanol, acetic acid, formic acid, and formaldehyde dominate OVOC; emissions of these four compounds alone equals or surpasses emissions of NMHC. Figure 4.1 gives the emissions of NMVOC functional classes as a percent of total NMVOC emissions on a carbon basis.

NMVOC of importance in tropospheric chemistry may be grouped into four major classes: alkanes, alkenes, aromatic hydrocarbons, and oxygenated compounds. Oxygenated compounds encompass a diverse range of chemical species that include aldehydes, ketones, alcohols, furans, and acids. In the atmosphere, NMVOC are subjected to a number of physical and chemical processes that lead to their transformation or removal. Wet and dry deposition remove NMVOC from the atmosphere (Seinfeld & Pandis, 1998). Transformation of NMVOC occurs through photochemical processing, initiated by photolysis or reaction with OH radical, NO_3 radical, or O_3 (Atkinson & Arey, 2003). The atmospheric oxidation of NMVOC is an extremely complex process that is closely coupled with the formation of both O_3 and SOA (Ito et al., 2007; Tsigaridis & Kanakidou, 2003; reviews of tropospheric VOC chemistry and SOA can be found in Atkinson & Arey, 2003 and Kanakidou et al., 2005, respectively).

The NMVOC emitted by wildland fires is dominated by oxygenated compounds and unsaturated hydrocarbons (Fig. 4.1). This mix of

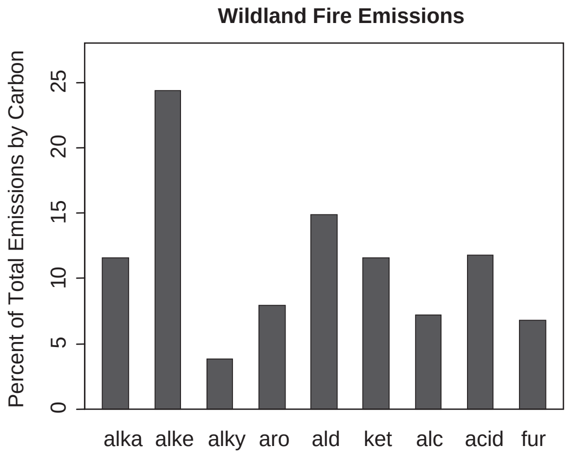

Figure 4.1. Wildland fire emissions aggregated by compound class and given as a percent of total emissions on a carbon basis. Based on an average of temperate and tropical forests and tropical savanna data from Table 4.1. Boreal forest and temperate rangeland data was not included due to insufficient data coverage. Compound classes listed on the *x*-axis are defined as follows: alka, alkanes; alke, alkenes; alky, alkynes; aro, aromatic hydrocarbons; ald, aldehydes; ket, ketones; alc, methanol; acid, formic and acetic acids; and fur, furans.

emissions is highly reactive, as demonstrated by the relatively short atmospheric lifetimes of many of these compounds with respect to gas phase reaction or photolysis (Table 4.2). The highly reactive nature of wildland fire emissions gives wildland fires a significant potential to influence tropospheric chemistry and degrade air quality. Through VOC–NO_x photochemistry, wildland fire emissions lead to O_3 formation on time scales of hours to days and over local to intercontinental distances (Real et al., 2007; Sudo & Akimoto, 2007; Trentmann et al., 2005). In addition to O_3 formation, the gas-phase oxidation of NMVOC can generate semivolatile oxygenated compounds. These semivolatile oxygenated compounds contribute to atmospheric aerosol loading through the formation of new aerosol via gas-to-particle conversion and by condensation on preexisting aerosol (de Gouw et al., 2005; Heald et al., 2005; Tsigaridis & Kanakidou, 2003). SOA formation resulting from the photochemical processing of wildland fire emissions can be quite significant relative to other sources (Heald et al., 2006). The formation of SOA can be quite rapid: wildland fire aerosol mass has been observed to increase by a factor of 1.5–2 over a period of a few days (Reid et al., 1998, 2005).

Table 4.2. Estimated lifetimes of dominant emissions from wildfire[a]

Lifetime due to reaction or photolysis[b]	OH[c]	NO_3[d]	O_3[e]	Photolysis[f]
Ethene	1.4 days	225 days	10 days	
Formaldehyde	1.2 days	80 days	>4.5 years	4 hours
Methanol[g]	12 days	1 year		
Acetic acid[h,i]	14.5 days			
Ethane	46.7 days			
Propene	5.3 hours	4.9 days	1.6 days	
Ethyne	13.2 days			
Acetadehyde	8.8 hours	17 days	>4.5 years	6 days
Propane	10 days	~7 years	>4500 years	
2,3-butadione	49 days			1 hour
Formic acid[h,i]	25.7 days			
Benzene	9.4 days	>4 years	>4.5 years	

Notes: The compounds listed comprise ~80% of the total emissions on a molar basis.
[a]Wildland fire emissions are an average of temperate and tropical forest and tropical savanna data from Table 4.1, following conversion to moles.
[b]All lifetime data from Atkinson (2000), or estimated based on rate coefficients from Atkinson and Ayer (2003), unless otherwise noted.
[c]For a 12-hour daytime average OH concentration of 2.0×10^6 molec cm^{-3}.
[d]For a 12-hour daytime average NO_3 concentration of 5.0×10^8 molec cm^{-3}.
[e]For a 24-hour daytime average O_3 concentration of 7.0×10^{11} molec cm^{-3}g.
[f]For overhead sun.
[g]In a study of the global budget of methanol, Jacob et al. (2005) estimate the atmospheric lifetime of methanol is 7 days with removal processes being: 63% reaction with OH, 26% dry deposition, 6% wet deposition, 5% ocean deposition.
[h]Rate coefficient data from Atkinson et al. (2001).
[i]Dry and wet deposition is believed to be an important removal process for formic and acetic acids. Sanhueza et al. (1996) report similar atmospheric lifetimes for formic and acetic acids: ~5 days for dry deposition and ~5 days for wet deposition.

4.5. Conclusions

Wildland fire emissions data from the literature and an extensive series of previously unpublished field experiments has been synthesized according to generalized vegetation cover groups, providing a dataset for use in global to continental scale studies of atmospheric chemistry and climate. Emissions from wildland fires are a rich and complex mixture of gases and aerosols. Primary pollutants emitted from wildland fires include greenhouse gases (CO_2, CH_4), NMVOC, NO_x, and aerosol. The NMVOC mixture produced by wildland fires is highly reactive. Participation of NMVOC fire emissions in VOC–NO_x photochemistry leads to the formation of O_3 and SOA. Through direct emissions and secondary chemical and physical processes, wildland fire can have a significant impact on tropospheric chemistry and serve as a major source of air pollution.

REFERENCES

Albini, F.A. 1976. Estimating wildfire behavior and effects. General Technical Report, INT-30. USDA Forest Service, Intermountain Forest and Range Experiment Station, Ogden, Utah.

Albini, F.A., and Reinhardt, E.D. 1995. Calibration of a large fuel burnout model. Int. J. Wildland Fire 5, 173–192.

Anderson, H.E. 1983. Predicting wind–driven wildland fire size and shape. Research Paper INT–305. USDA Forest Service, Intermountain Forest and Range Experiment Station, Ogden, Utah.

Andreae, M.O., and Merlet, P. 2001. Emissions of trace gases and aerosol from biomass burning. Global Biogeochem. Cy. 15, 955–966.

Atkinson, R. 2000. Atmospheric chemistry of VOC's and NOx. Atmos. Environ. 34, 2063–2101.

Atkinson, R., and Arey, J. 2003. Atmospheric degradation of volatile organic compounds. Chem. Rev. 103, 4605–4638.

Atkinson, R., Baulch, D.L., Cox, R.A., Crowley, J.N., Hampson, R.F. Jr., Kerr, J.A., Rossi, M.J., and Troe, J. 2001. In: Carver, G.D., and Cox, R.A., eds. Summary of evaluated kinetic and photochemical data for atmospheric chemistry. IUPAC Subcommittee on Gas Kinetic Evaluation for Atmospheric Chemistry, University of Cambridge, Cambridge, pp. 1–56.

Babbit, R.E., Ward, D.E., Susott, R.A., Hao, W.M., and Baker, S.P. 1994. Smoke from western wildfires, 1994. In: Proceedings, annual meeting of Interior West Fire Council. November, 1994, Coeur d'Alene, Idaho.

Benkoussas, B., Consalvi, J.-L., Porterie, B., Sarody, N., and Loraud, J.-C. 2007. Modelling thermal degradation of woody fuel particles. Int. J. Therm. Sci. 46, 319–327.

Bertschi, I.T., Yokelson, R.J., Ward, D.E., Goode, J.G., Babbitt, R., Susott, R.A., and Hao, W.M. 2003. The trace gas and particle emissions from fires in large–diameter and belowground biomass fuels. J. Geophys. Res. 108, 8472.

Bonsang, B., Boissard, C., Le Cloarec, M.F., Rudolph, J., and Lacaux, J.P. 1995. Methane, carbon monoxide and light non methane hydrocarbon emissions from African savanna burnings during the FOS/DECAFE experiment. J. Atmos. Chem. 22, 149–162.

Bonsang, B., Lambert, G., and Boissard, C.C. 1991. Light hydrocarbons emissions from African savanna burnings. In: Levine, J.S., ed. Global biomass burning: Atmospheric, climatic and biospheric implications. MIT Press, Cambridge, pp. 155–161.

Chen, L.-W.A., Moosmüller, H., Arnott, W.P., Chow, J.C., Watson, J.G., Susott, R.A., Babbitt, R.E., Wold, C.E., Lincoln, E.N., and Hao, W.M. 2007. Emissions from laboratory combustion of wildland fuels: Emission factors and source profiles. Environ. Sci. Technol. 41, 4317–4325.

Christian, T.J., Kleiss, B., Yokelson, R.J., Holzinger, R., Crutzen, P.J., Hao, W.M., Saharjo, B.H., and Ward, D.E. 2003. Comprehensive laboratory measurements of biomass–burning emissions: 1. Emissions from Indonesian, African, and other fuels. J. Geophys. Res. 108, 4719.

Cofer, W.R. III, Levine, J.S., Winstead, E.L., Cahoon, D.R., Sebacher, D.I., Pinto, J.P., and Stocks, B.J. 1996. Source composition of trace gases released during African savanna fires. J. Geophys. Res. 101, 23597–23602.

Cofer, W.R. III, Levine, J.S., Winstead, E.L., Lebel, P.J., Koller, A.M. Jr., and Hinkle, C.R. 1990. Trace gas emissions from burning Florida wetlands. J. Geophys. Res. 95, 1865–1870.

Cofer, W.R. III, Winstead, E.L., Stocks, B.J., Goldammer, J.G., and Cahoon, D.R. 1998. Crown fire emissions of CO_2, CO, H_2, CH_4, and TNMHC from a dense jack pine boreal forest fire. Geophys. Res. Lett. 25, 3919–3922.

DeBell, L.J., Talbot, R.W., Dibb, J.E., Munger, J.W., Fischer, E.V., and Frolking, S.E. 2004. A major regional air pollution event in the northeastern United States caused by extensive forest fires in Quebec, Canada. J. Geophys. Res. 109, D19305.

de Gouw, J.A., Middlebrook, A.M., Warneke, C., Goldan, P.D., Kuster, W.C., Roberts, J.M., Fehsenfeld, F.C., Worsnop, D.R., Canagaratna, M.R., Pszennym, A.A.P., Keene, W.C., Marchewka, M., Bertman, S.B., and Bates, T.S. 2005. Budget of organic carbon in a polluted atmosphere: Results from the New England Air Quality Study in 2002. J. Geophys. Res. 110, D16305.

Fearnside, P.M. 1990. Fire in the tropical rain forest of the Amazon basin. In: Goldhammer, J.G., ed. Fire in the Tropical Biota: Ecosystem Processes and Global Challenges. Springer–Verlag, Berlin, pp. 106–116.

Ferek, R.J., Reid, J.S., Hobbs, P.V., Blake, D.R., and Liousse, C. 1998. Emission factors of hydrocarbons, halocarbons, trace gases, and particles from biomass burning in Brazil. J. Geophys. Res. 103, 32107–32118.

Fernandes, P., and Botelho, H. 2004. Analysis of the prescribed burning practice in pine forest of northwestern Portugal. Environ. Manage. 70, 15–26.

Finney, M.A., McHugh, C.W., and Grenfell, I.C. 2005. Stand– and landscape–level effects of prescribed burning on two Arizona wildfires. Can. J. For. Res. 35, 1714–1722.

Freeborn, P.H., Wooster, M.J., Hao, W.M., Ryan, C.A., Nordgren, B.L., Baer, S.P., and Ichoku, C. 2007. Relationships between energy release, fuel mass loss, and trace gas and aerosol emissions during laboratory biomass fires. J. Geophys. Res., 113, D01301.

French, N.H.F., Goovaerts, P., and Kasischke, E.S. 2004. Uncertainty in estimating carbon emissions from boreal forest fires. J. Geophys. Res. 109, D14S08.

Friedli, H.R., Atlas, E., Stroud, V.R., Giovanni, L., Campos, T., and Radke, L.F. 2001. Volatile organic trace gases emitted from North American wildfires. Global Biogeochem. Cy. 15, 435–452.

Giglio, L., Csiszar, I., and Justice, C.O. 2006. Global distribution and seasonality of active fires as observed with the terra and aqua moderate resolution imagining spectro-radiometer (MODIS) sensors. J. Geophys. Res. 111, G02016.

Goode, J.G., Yokelson, R.J., Susott, R.A., and Ward, D.E. 1999. Trace gas emissions from laboratory biomass fires measured by open–path Fourier transform infrared spectroscopy: Fires in grass and surface fuels. J. Geophys. Res. 104, 21237–21245.

Goode, J.G., Yokelson, R.J., Ward, D.E., Susott, R.A., Babbitt, R.E., Davies, M.A., and Hao, W.M. 2000. Measurements of excess O_3, CO_2, CO, CH_4, C_2H_4, C_2H_2, HCN, NO, NH_3, HCOOH, CH_3COOH, HCHO, and CH_3OH in 1997 Alaskan biomass burning plumes by airborne Fourier transform infrared spectroscopy (AFTIR). J. Geophys. Res. 105, 22147–22166.

Greenberg, J.P., Zimmerman, P.R., Heidt, L., and Pollock, W. 1984. Hydrocarbon and carbon monoxide emissions from biomass burning in Brazil. J. Geophys. Res. 89, 1350–1354.

Greenberg, J.P., Friedli, H., Guenther, A.B., Hanson, D., Harley, P., and Karl, T. 2006. Volatile organic emissions from the distillation and pyrolysis of vegetation. Atmos. Chem. Phys. 6, 81–91.

Hao, W.M., and Liu, M.H. 1994. Spatial and temporal distribution of tropical biomass burning. Global Biogeochem. Cy. 8, 495–503.

Hao, W.M., Ward, D.E., Olbu, G., and Baker, S.P. 1996. Emissions of CO_2, CO and hydrocarbons from fires in diverse African savanna ecosystems. J. Geophys. Res. 101, 23577–23584.

Hardy, C.C., Conard, S.G., Regelbrugge, J.C., and Teesdale, D.R. 1996. Smoke emissions from prescribed burning of Southern California Chaparral. Research paper, PNW-RP-486, Pacific Northwest Research Station, USDA Forest Service, Seattle, Washington.

Hardy, C.C., Hermann, S.M., and Mutch, R.E. 2002. The wildland fire imperative. In: Hardy, C.C., Ottmar, R.D., Peterson, J.L., Core, J.C., and Seamon, P., eds. Smoke management guide for prescribed and wildland fire: 2001 edition. National Wildfire Coordination Group, National Interagency Fire Center, Boise, 11–19.

Heald, C.L., Jacob, D.J., Park, R.J., Russell, L.M., Huebert, B.J., Seinfeld, J.H., Liao, H., and Weber, R.J. 2005. A large organic aerosol source in the free troposphere missing from current models. Geophys. Res. Lett. 32, L18809.

Heald, C.L., Jacob, D.J., Turquety, S., Hudman, R.C., Weber, R.J., Sullivan, A.P., Peltier, R.E., Atlas, E.L., de Gouw, J.A., Warneke, C., Holloway, J.S., Neuman, J.A., Flocke, F.M., and Seinfeld, J.H. 2006. Concentrations and sources of organic carbon aerosols in the free troposphere over North America. J. Geophys. Res. 111, D23S47.

Hely, C., Dowdy, P.R., Alleaume, S., Caylor, K.K., Korontzi, S., Swap, R.J., Shugart, H.H., and Justice, C.O. 2003. Regional fuel load for two climatically contrasting years in southern Africa. J. Geophys. Res. 108, 8375.

Hurst, D.F., Griffith, D.W.T., Carras, J.N., Williams, D.J., and Fraser, P.J. 1994a. Measurements of trace gases emitted by Australian savanna fires during the 1990 dry season. J. Atmos. Chem. 18, 33–56.

Hurst, D.F., Griffith, D.W.T., and Cook, G.D. 1994b. Trace gas emissions from biomass burning in tropical Australian savannas. J. Geophys. Res. 99, 16441–16456.

Ito, A., and Penner, J.E. 2004. Global estimates of biomass burning emissions based on satellite imagery for the year 2000. J. Geophys. Res. 109, D14S05.

Ito, A., Sillman, S., and Penner, J.E. 2007. Effects of additional nonmethane volatile organic compounds, organic nitrates, and direct emissions of oxygenated organic species on global troposhperic chemistry. J. Geophys. Res. 112, D06309.

Jacob, D.J., Field, B.D., Li, Q., Blake, D.R., de Gouw, J., Warneke, C., Hansel, A., Wisthaler, A., Singh, H.B., and Guenther, A. 2005. Global budget of methanol: Constraints from atmospheric observations. J. Geophys. Res. 110, D08303.

Jourdain, L., Worden, H.M., Worden, J.R., Bowman, K., Li, Q., Eldering, A., Kulawik, S.S., Osterman, G., Boersma, K.F., Fisher, B., Rinsland, C.P., Beer, R., and Gunson, M. 2007. Tropospheric vertical distribution of tropical Atlantic ozone observed by TES during the northern Africa biomass burning season. Geophys. Res. Lett. 34, L04810.

Kanakidou, M., Seinfeld, J.H., Pandis, S.N., Barnes, I., Dentener, F.J., Facchini, M.C., Van Dingenen, R., Ervens, B., Nenes, A., Nielsen, C.J., Swietlicki, E., Putaud, J.P., Balkanski, Y., Fuzzi, S., Horth, J., Moortgat, G.K., Winterhalter, R., Myhre, C.E.L., Tsigaridis, K., Vignati, E., Stephanou, E.G., and Wilson, J. 2005. Organic aerosol and global climate modelling: A review. Atmos. Chem. Phys. 5, 1053–1123.

Kasischke, E.S., O'Neill, K.P., French, N.H.F., and Bourgeau–Chavez, L.L. 2000. Controls on patterns of biomass burning in Alaskan boreal forests. In: Kasischke, E.S., and

Stocks, B.J., eds. Fire, climate change, and carbon cycling in the North American boreal forest. Springer–Verlag, New York, 173–196.

Kauffman, J.B., Steele, M.D., Cummings, D.L., and Jaramillo, V.J. 2003. Biomass dynamics associated with deforestation, fire, and conversion to cattle pasture in a Mexican tropical dry forest. For. Ecol. Manage. 176, 1–12.

Koch, D., Bond, T.C., Streets, D., Unger, N., and van der Werf, G.R. 2007. Global impacts of aerosols from particular source regions and sectors. J. Geophys. Res. 112, D02205.

Koppmann, R., Khedim, A., Rudolph, J., Helas, G., Welling, M., and Zenker, T. 1996. Airborne measurements of organic trace gases from savanna fires in southern Africa during SAFARI–92. In: Levine, J.S., ed. Global biomass burning: Atmospheric, climatic and biospheric implications. MIT Press, Cambridge, pp. 309–319.

Korontzi, S., Ward, D.E., Susott, R.A., Yokelson, R.J., Justice, C.O., Hobbs, P.V., Smithwick, E.A.H., and Hao, W.M. 2003. Seasonal variation and ecosystem dependence of emission factors for selected trace gases and PM2.5 for southern African savanna fires. J. Geophys. Res. 108, 4758.

Lacaux, J.-P., Delmas, R., Jambert, C., and Kuhlbusch, T.A.J. 1996. NOx emissions from African savanna fires. J. Geophys. Res. 101, 23585–23596.

Lapina, K., Honrath, R.E., Owen, R.C., Val Martín, M., and Pfister, G. 2006. Evidence of significant large–scale impacts of boreal fires on ozone levels in the midlatitude Northern Hemisphere free troposphere. Geophys. Res. Lett. 33, L10815.

Lee, S., Baumann, K., Schauer, J.J., Sheesley, R.J., Naeher, L.P., Meinardi, S., Blake, D.R., Edgerton, E.S., Russell, A.G., and Clements, M. 2005. Gaseous and particulate emissions from prescribed burning in Georgia. Environ. Sci. Technol. 39, 9049–9056.

Lobert, J.M., and Warnatz, J. 1993. Emissions from the combustion process in vegetation. In: Crutzen, P.J., and Goldammer, J.G., eds. Fire in the environment: The ecological, atmospheric, and climatic importance of vegetation fires. Wiley, New York, pp. 15–37.

Lobert, J.M., Scharffe, D.H., Hao, W.M., Kuhlbusch, T.A., Seuwen, R., Warneck, P., and Crutzen, P.J. 1991. Experimental evaluation of biomass burning emissions: Nitrogen and carbon containing compounds. In: Levine, J.S., ed. Global biomass burning: Atmospheric, climatic and biospheric implications. MIT Press, Cambridge, pp. 289–304.

Lohmann, U., and Feichter, J. 2005. Global indirect aerosol effects: A review. Atmos. Chem. Phys. 5, 715–737.

Michel, C., Liousse, C., Gregoire, J.M., Tansey, K., Carmichael, G.R., and Woo, J.H. 2005. Biomass burning emission inventory from burnt area data given by the SPOT–VEGETATION system in the frame of TRACE–P and ACE–Asia campaigns. J. Geophys. Res. 110, D09304.

Morris, G.A., Hersey, S., Thompson, A.M., Pawson, S., Nielson, J.E., Colarco, P.R., McMillan, W.W., Stohl, A., Turquety, S., Warner, J., Johnson, B.J., Kucsera, T.L., Larko, D.E., Oltmans, S.J., and Witte, J.C. 2006. Alaskan and Canadian forest fires exacerbate ozone pollution over Houston, Texas, on 19 and 20 July 2004. J. Geophys. Res. 111, D24S03.

Morvan, D., and Dupuy, J.L. 2001. Modeling of fire spread through a forest fuel bed using a multiphase formulation. Combust. Flame 127, 1981–1994.

Muhle, J., Lueker, T.J., Su, Y., Miller, B.R., Prather, K.A., and Weiss, R.F. 2007. Trace gas and particulate emissions from the 2003 southern California wildfires. J. Geophys. Res. 112, D03307.

Naik, V., Mauzerall, D.L., Horowitz, L.W., Schwarzkopf, M.D., Ramaswamy, V., and Oppenheimer, M. 2007. On the sensitivity of radiative forcing from biomass burning aerosols and ozone to emission location. Geophys. Res. Lett. 34, L03818.

Nance, J.D., Hobbs, P.V., Radke, L.F., and Ward, D.E. 1993. Airborne measurements of gases and particles from an Alaskan wildfire. J. Geophys. Res. 98, 14873–14882.
Ottmar, R.D. 2002. Smoke source characteristics. In: Hardy, C.C., Ottmar, R.D., Peterson, J.L., Core, J.C., and Seamon, P., eds. Smoke management guide for prescribed and wildland fire: 2001 edition. National Wildfire Coordination Group, National Interagency Fire Center, Boise, 89–106.
Ottmar, R.D., Peterson, J.L., Leenhouts, B., and Core, J.E., 2002. Smoke management techniques. In: Hardy, C.C., Ottmar, R.D., Peterson, J.L., Core, J.C., and Seamon, P., eds. Smoke management guide for prescribed and wildland fire: 2001 edition. National Wildfire Coordination Group, National Interagency Fire Center, Boise, 141–160.
Phuleria, H.C., Fine, P.M., Zhu, Y., and Sioutas, C. 2005. Air quality impacts of the October 2003 Southern California wildfires. J. Geophys. Res. 110, D07S20.
Price, O.F., Edwards, A.C., and Russell–Smith, J. 2007. Efficacy of permanent firebreaks and aerial prescribed burning in western Arnhem Land, Northern Territory, Australia. Int. J. Wildland Fire 16, 295–307.
Radke, L.F., Hegg, D.A., Hobbs, P.V., Nance, J.D., Lyons, J.H., Laursen, K.K., Weiss, R.E., Riggan, P.J., and Ward, D.E. 1991. Particulate and trace gas emissions from large biomass fires in North America. In: Levine, J.S., ed. Global biomass burning: Atmospheric, climatic and biospheric Implications. MIT Press, Cambridge, pp. 209–224.
Real, E., Law, K.S., Weinzierl, B., Fiebig, M., Petzold, A., Wild, O., Methven, J., Arnold, S., Stohl, A., Huntrieser, H., Roiger, A., Schlager, H., Stewart, D., Avery, M., Sachse, G., Browell, E., Ferrare, R., and Blake, D. 2007. J. Geophys. Res. 112, D10S41.
Reid, J.S., Hobbs, P.V., Ferek, R.J., Blake, D.R., Martins, J.V., Dunlap, M.R., and Liousse, C. 1998. Physical, chemical and optical properties of regional hazes dominated by smoke in Brazil. J. Geophys. Res. 103, 32059–32080.
Reid, J.S., Koppmann, R., Eck, T.F., and Eleuterio, D.P. 2005. A review of biomass burning emissions part II: Intensive physical properties of biomass burning particles. Atmos. Chem. Phys. 5, 799–825.
Reinhardt, E.D., Brown, J.K., Fischer, W.C., and Graham, R.T. 1991. Woody fuel and duff consumption by prescribed fire in northern Idaho mixed conifer logging slash. Research Paper INT–443. USDA Forest Service, Intermountain Research Station, Ogden, Utah.
Reinhardt, E.D., Keane, R.E., and Brown, J.K. 2001. Modeling fire effects. Int. J. Wildland Fire 10, 373–380.
Roberts, G., and Wooster, M.J. 2007. New perspectives on African biomass burning dynamics. EOS Transactions 88, 369–370.
Rothermel, R.C. 1972. A mathematical model for predicting fire spread in wildand fuels. Research Paper INT–115. USDA Forest Service, Intermountain Forest and Range Experiment Station, Ogden, Utah.
Rowell, R.M., and LeVan–Green, S.L. 2005. Thermal properties. In: Rowell, R.M., ed. Handbook of wood chemistry and wood composites. CRC Press, Boca Raton, FL, pp. 121–138.
Rudolph, J., Khedim, A., Koppmann, R., and Bonsang, B. 1995. Field study of the emissions of methyl chloride and other halocarbons from biomass burning in western Africa. J. Atmos. Chem. 22, 67–80.
Sanhueza, E., Figueroa, L., and Santana, M. 1996. Atmospheric formic and acetic acids in Venezuela. Atmos. Environ. 30, 1861–1873.
Sapakota, A., Symons, J.M., Kleissl, J., Wang, L., Parlange, M.B., Ondov, J., Breysse, P.N., Diette, G.B., Eggleston, P.A., and Buckley, T.J. 2005. Impact of the 2002 Canadian forest fires on particulate matter air quality in Baltimore City. Environ. Sci. Technol. 39, 24–32.

Seinfeld, J.H., and Pandis, S.N. 1998. Atmospheric chemistry and physics: from air pollution to climate change. Wiley, New York.

Simpson, I.J., Rowland, F.S., Meinardi, S., and Blake, D.R. 2006. Influence of biomass burning during recent fluctuations in the slow growth of global tropospheric methane. Geophys. Res. Lett. 33, L22808.

Sinha, P., Hobbs, P.V., Yokelson, R.J., Bertschi, I.T., Blake, D.R., Simpson, I.J., Gao, S., Kirchstetter, T.W., and Novakov, T. 2003. Emissions of trace gases and particles from savanna fires in southern Africa. J. Geophys. Res. 108, 8487.

Smith, M.A., Grant, C.D., Loneragan, W.A., and Koch, J.M. 2004. Fire management implications for fuel loads and vegetation structure in jarrah forest restoration on bauxite mines in Western Australia. For. Ecol. Manage. 187, 247–266.

Sudo, K., and Akimoto, K. 2007. Global source attribution of tropospheric ozone: Long–range transport from various source regions. J. Geophys. Res. 112, D12302.

Susott, R.A., Ward, D.E., Babbit, R.E., and Latham, D.J. 1991. The measurement of trace emissions and combustion characteristics for a mass fire. In: Levine, J.S., ed. Global biomass burning: Atmospheric, climatic and biospheric implications. MIT Press, Cambridge, pp. 245–257.

Susott, R.A., Olbu, G.J., Baker, S.P., Ward, D.E., Kauffmann, J.B., and Shea, R.W. 1996. Carbon, hydrogen, nitrogen, and thermogravimetric analysis of tropical ecosystem biomass. In: Levine, J.S., ed. Biomass burning and global change. MIT Press, Cambridge, Vol. 1, pp. 249–259.

Swap, R.J., Annegarn, H.J., Suttles, J.T., King, M.D., Platnick, S., Privette, J.L., and Scholes, R.J. 2003. Africa burning: A thematic analysis of the Southern African Regional Science Initiative (SAFARI 2000). J. Geophys. Res. 108, 8465.

Trentmann, J., Yokelson, R.J., Hobbs, P.V., Winterrath, T., Christian, T.J., Andreae, M.O., and Mason, S.A. 2005. An analysis of the chemical processes in the smoke plume from a savanna fire. J. Geophys. Res. 110, D12301.

Trentmann, J., Luderer, G., Winterrath, T., Fromm, M.D., Servranckx, R., Textor, C., Herzog, M., Graf, H.-F., and Andreae, M.O. 2006. Modeling of biomass smoke injection into the lower stratosphere by a large forest fire (part I): Reference simulation. Atmos. Chem. Phys. 6, 5247–5260.

Tsigaridis, K., and Kanakidou, M. 2003. Global modelling of secondary organic aerosol in the troposphere: A sensitivity analysis. Atmos. Chem. Phys. 3, 1849–1869.

van der Werf, G.R., Randerson, J.T., Giglio, L., Collatz, G.J., Kasibhatla, P.S., and Arellano, A.F. Jr. 2006. Interannual variability in global biomass burning emissions from 1997 to 2004. Atmos. Chem. Phys. 6, 3423–3441.

Wade, D.D., and Lunsford, J.D. 1989. A guide for prescribed fire in southern forests. Technical Report, R8–TP–11. USDA Forest Service, Southern Region, Atlanta, Georgia.

Ward, D.E., and Hardy, C.C. 1989. Emissions from prescribed burning of chaparral. In: Programs and Abstracts, 1989 Annual Meeting of the Air Waste Management Association. June, 1989, Anaheim, California.

Ward, D.E., Hao, W.M., Susott, R.A., Babbitt, R.A., Shea, R.W., Kauffman, J.B., and Justice, C.O. 1996. Effect of fuel composition on combustion efficiency and emission factors for African savanna ecosystems. J. Geophys. Res. 101, 23569–23576.

Ward, D.E., and Radke, L.F. 1993. Emission measurements from vegetation fires: A comparative evaluation of methods and results. In: Crutzen, P.J., and Goldammer, J.G., eds. Fire in the environment: The ecological, atmospheric, and climatic importance of vegetation fires. Wiley, New York, pp. 53–76.

Ward, D.E., Susott, R.A., Kauffman, J.B., Babbitt, R.E., Cummings, D.L., Dias, B., Holben, B.N., Kaufman, Y.J., Rasmussen, R.A., and Setzer, A.W. 1992. Smoke and fire characteristics for cerrado and deforestation burns in Brazil: BASE–B experiment. J. Geophys. Res. 97, 14601–14619.

Wiedinmyer, C., Quayle, B., Geron, C., Belote, A., McKenzie, D., Zhang, X., O'Neill, S., and Wynne, K.K. 2006. Estimating emissions from fires in North America for air quality modeling. Atmos. Environ. 40, 3419–3432.

Yokelson, R.J., Bertschi, I.T., Christian, T.J., Hobbs, P.V., Ward, D.E., and Hao, W.M. 2003. Trace gas measurements in nascent, aged, and cloud–processed smoke from African savanna fires by airborne Fourier transform infrared spectroscopy (AFTIR). J. Geophys. Res. 108, 8478.

Yokelson, R.J., Goode, J.G., Ward, D.E., Susott, R.A., Babbitt, R.E., Wade, D.D., Bertschi, I., Griffith, D.W.T., and Hao, W.M. 1999. Emissions of formaldehyde, acetic acid, methanol, and other trace gases from biomass fires in North Carolina measured by airborne Fourier transform infrared spectroscopy. J. Geophys. Res. 104, 30109–30125.

Yokelson, R.J., Griffith, D.W.T., and Ward, D.E. 1996. Open–path Fourier transform infrared studies of large–scale laboratory biomass fires. J. Geophys. Res. 101, 21067–21080.

Yokelson, R.J., Karl, T., Artaxo, P., Blake, D.R., Christian, T.J., Griffith, D.W.T., Guenther, A., and Hao, W.M. 2007. The tropical forest and fire emissions experiment: Overview and airborne fire emission factor measurements. Atmos. Chem. Phys. 7, 5175–5196.

Yokelson, R.J., Susott, R., Ward, D.E., Reardon, J., and Griffith, D.W.T. 1997. Emissions from smoldering combustion of biomass measured by open–path Fourier transform infrared spectroscopy. J. Geophys. Res. 102, 18865–18877.

Appendix A. Emission factors for North America ecosystems

This appendix presents previously unpublished results from emission studies of prescribed fires in the southeastern, mid-western, and western United States, western Canada, and Alaska. The prescribed fire emissions data may be used to estimate emissions of several key primary pollutants from fires in a broad range of North American ecosystems for which prescribed fire is an essential land management tool. The prescribed fire studies indicate emission factors for many pollutants exhibit significant variability across vegetation types. These findings suggest modeling studies to assess the air quality impact of wildland fire at the local to regional scales may benefit from data that captures interecosystem variations in EFs. This may be particularly important for quantifying the incremental contribution of wildland fire emissions to air pollution in urban areas.

The coarsely grouped EFs in Table 4.1 will often be adequate for continental and global scales studies of atmospheric chemistry, biogeochemical cycling, and climate. However, the generalized nature of the data synthesis may not provide the differentiation among ecosystems that is necessary to accurately assess and predict the impact of wildand fire on air quality at the local to regional scale. The ecosystem specific emissions data presented in this section is representative of the information land management agencies and air quality managers may find necessary to successfully address the air quality issues presented by wildland fire.

A.1. Field sites and methods

Emission data was obtained for 56 prescribed fires in 9 states and 1 province (Table A1). The emission studies cover a wide range of ecosystems types, but may be aggregated as southeastern conifer forest (mostly pine, a few pine-hardwood mix), interior mountain west conifer forest (ponderosa pine and Douglas-fir), grassland (mostly wetland grasses) shrubland (southeastern), and boreal forest vegetation groups. The prescribed burns in southeastern and interior mountain west were low- to moderate-intensity understory burns. The two boreal forest fires sampled in Alaska were high-intensity burn-out fires employed as a fire suppression tactic during the intense Alaska fire season of 2004. The burn-out fires involved surface and canopy fuels. These high-intensity crown fires were representative of the fire activity during June and July of 2004 when 6 million acres were burned in Alaska.

The emission studies used the Fire Atmosphere Sampling System (FASS) (Hao et al., 1996). Briefly, the FASS instrument uses a 3–15 m tower to obtain in situ measurements of gases, particulate matter, vertical velocity, and air temperature. The FASS collects integrated $PM_{2.5}$ filter and gas canister samples for background air, primarily flaming combustion, the transition from flaming to smoldering combustion, and mostly smoldering combustion. The $PM_{2.5}$ filter samples are analyzed for total mass, organic and elemental carbon. The canister samples are analyzed for CO_2, CO, CH_4, and C2–C3 alkanes, alkenes, and alkynes. The FASS also provides continuous measurements of CO, CO_2, vertical velocity, and air temperature, which gives a unique, useful time-series of the fire from a point ''within'' the burn.

Two to six FASS instrument towers were deployed within the burn perimeter for each prescribed fire. The carbon mass balance method (Ward & Radke, 1993) was used for calculating EFs with an assumed fuel

Table A1. Fire weighted average emission factors (g of compound emitted per kg of dry fuel consumed)

Fire ID	Vegetation type	Location[a]	MCE[b]	CO_2	CO	CH_4	C_2H_6	C_2H_4	C_2H_2	C_3H_8	C_3H_6	C_3H_4	$PM_{2.5}$
		Grasslands and shrublands of southeastern and mid-western United States											
EB1	Sandhill shrub	Eglin AFB, FL	0.921	1652	89.7	2.62	0.32	1.01	0.23	0.11	0.47	0.03	11.9
EB2	Palmetto, turkey oak	Eglin AFB, FL	0.938	1695	71.1	1.65	0.18	1.13	0.49	0.02	0.31	0.05	6.9
FL5	Palmetto	Okefenokee NWR, FL	0.933	1665	76.4	2.13	0.23	1.12	0.35	0.08	0.45	0.05	15.7
NC3	Pacosin	Camp Lejune, NC	0.943	1683	64.2	1.84	0.22	1.35	0.36	0.11	0.46	0.06	16.7
SC9	Pacosin	Savannah River Site, SC	0.935	1682	75.0	2.66	0.30	0.98	0.34	0.10	0.39	0.05	8.9
EP1	Sawgrass	Panther WR, FL	0.914	1635	98.3	4.12	0.59	1.60	0.49	0.23	0.79	0.08	9.1
EP2A	Sawgrass	Big Cypress NWP, FL	0.936	1689	73.5	2.27	0.25	1.61	0.63	0.09	0.40	0.06	5.9
EP2B	Muley grass	Big Cypress NWP, FL	0.961	1743	45.5	1.54	0.19	0.95	0.36	0.08	0.30	0.05	3.7
MI1	Sawgrass	Merrit Island NWR, FL	0.97	1752	34.7	0.90	0.07	0.52	0.21	0.02	0.10	0.02	9.9
MN1	Freshwater grass	Bluestern Prarie, MN	0.948	1716	59.7	1.50	0.21	1.16	0.39	0.05	0.37	0.07	5.3
MN2	Freshwater grass	Bluestern Prarie, MN	0.933	1652	75.6	2.68	0.44	2.07	0.60	0.14	1.03	0.10	18.8
MN3	Freshwater grass	Sherburne NWP, MN	0.95	1705	57.1	1.53	0.15	1.22	0.46	0.07	0.23		11.8
MN4	Freshwater grass	Camp Ripley, MN	0.962	1750	44.4	1.07	0.12	0.55	0.20	0.02	0.04		3.6
FS1	Wiregrass	Fort Stewart, GA	0.936	1681	73.5	2.16	0.21	1.42	0.64	0.06	0.42	0.07	9.7
ICI3	Wiregrass	Ichuway, GA	0.912	1626	99.5	3.34	0.44	1.15	0.25	0.20	0.64	0.05	15.3
		Mean	0.939	1688	69.2	2.13	0.26	1.19	0.40	0.09	0.43	0.06	10.2
		Standard deviation	0.017	40	18.9	0.86	0.14	0.40	0.15	0.06	0.35	0.02	4.8
		Conifer forests of southeastern United States											
FL1	Longleaf pine, palmetto	Osceola NF, FL	0.952	1712	55.3	1.41	0.18	1.34	0.74	0.01	0.37	0.09	10.0
FL2	Longleaf pine, palmetto	Osceola NF, FL	0.94	1690	68.5	1.26	0.14	0.94	0.40	0.01	0.35	0.00	11.3
FL4	Longleaf pine, palmetto	Osceola NF, FL	0.934	1681	75.2	1.45	0.13	0.97	0.45		0.37	0.04	11.1

		Conifer forests of southeastern United States (continued)											
ICI1	Loblolly pine, wiregrass	Ichuway, GA	0.942	1687	66.5	1.78	0.26	1.27	0.42	0.10	0.45	0.05	13.2
ICI2	Loblolly pine, wiregrass	Ichuway, GA	0.928	1657	81.5	2.31	0.28	1.19	0.33	0.11	0.46	0.07	15.6
NC1	Mixed pine, wax myrtle	Camp Lejune, NC	0.904	1621	109.4	3.00	0.23	0.83	0.28	0.06	0.38	0.04	10.4
SC1	Oak, pine, grass	Piedmont WR, SC	0.921	1647	90.2	2.15	0.25	1.17	0.36	0.09	0.49	0.06	14.1
SC12a	Oak, pine, grass	Piedmont WR, SC	0.942	1688	65.9	1.75	0.21	0.97	0.32	0.08	0.40	0.05	14.4
SC12b	Oak, pine, grass	Piedmont WR, SC	0.923	1651	87.5	2.26	0.28	1.01	0.28	0.10	0.46	0.05	14.5
SC3	Mixed pine, wiregrass	Camp Lejune, NC	0.936	1682	73.1	1.99	0.22	0.86	0.23	0.09	0.37	0.09	11.4
SC4	Loblolly pine	Savannah River Site, SC	0.936	1679	73.3	1.64	0.21	1.13	0.41	0.05	0.42	0.07	12.2
SC5	Longleaf pine	Savannah River Site, SC	0.941	1683	66.9	1.59	0.14	0.74	0.24	0.05	0.28	0.04	15.4
SC6	Loblolly pine	Savannah River Site, SC	0.932	1651	77.2	2.04	0.26	1.12	0.29	0.08	0.47	0.04	21.9
SC7	Mixed pine, hardwood	Sumter NF, SC	0.915	1630	96.4	2.89	0.37	1.13	0.24	0.14	0.59	0.05	16.2
SC8	Longleaf pine	Savannah River Site, SC	0.918	1653	94.0	3.39	0.39	0.95	0.30	0.11	0.50	0.05	11.5
		Mean	0.931	1667	78.7	2.06	0.24	1.04	0.35	0.08	0.42	0.05	13.5
		Standard Deviation	0.013	25	14.4	0.62	0.08	0.17	0.13	0.04	0.08	0.02	3.07
		Interior west mountain conifer forests of United States and southwestern Canada											
AZ1	Ponderosa pine	Chimney Springs, AZ	0.941	1698	67.7	3.20							6.1
AZ2	Ponderosa pine	Limestone Flats, AZ	0.890	1605	126.7	4.86							21.4
AZ3	Ponderosa pine	Mormon Lake RD, AZ	0.924	1658	86.8	2.26	0.33	0.92	0.27	0.07	0.48	0.02	11.9
AZ4	Ponderosa pine	Limestone Flats, AZ	0.932	1668	77.9	2.29	0.31	0.99	0.28	0.12	0.49	0.08	13.4
AZ5	Ponderosa pine	Chimney Springs, AZ	0.910	1607	100.6	4.37	0.55	1.27	0.34	0.23	0.69	0.08	20.9
AZ6	Ponderosa pine	Peaks RD, AZ	0.924	1648	86.6	3.12	0.49	1.03	0.30	0.22	0.57	0.12	14.5
AZ7	Ponderosa pine	Chimney Springs, AZ	0.918	1640	93.1	3.53	0.55	1.07	0.32	0.22	0.60	0.11	13.0
AZ8	Ponderosa pine	Chimney Springs, AZ	0.926	1650	84.2	3.32	0.49	1.06	0.25	0.20	0.57	0.07	15.4
AZ9	Ponderosa pine	Peaks RD, AZ	0.919	1639	92.3	3.53	0.45	1.09	0.31	0.11	0.56		14.4
AZ10	Ponderosa pine	Limestone Flats, AZ	0.938	1678	70.1	2.49	0.34	0.87	0.26	0.07	0.41		14.8

Table A1. (*Continued*)

Fire ID	Vegetation type	Location[a]	MCE[b]	CO_2	CO	CH_4	C_2H_6	C_2H_4	C_2H_2	C_3H_8	C_3H_6	C_3H_4	$PM_{2.5}$
		Interior west mountain conifer forests of United States and southwestern Canada (continued)											
AZ11	Ponderosa pine	Chimney Springs, AZ	0.948	1717	59.4	1.62	0.22	0.87	0.29		0.34		6.2
AZ12	Ponderosa pine	Chimney Springs, AZ	0.916	1622	94.2	3.22	0.43	1.19	0.34	0.14	0.56	0.03	20.8
BC1	Ponderosa pine	Clearwater, BC, Canada	0.894	1542	116.9	5.71	0.92	2.13	0.51	0.33	1.11	0.17	29.0
BC2	Ponderosa pine	Clearwater, BC, Canada	0.889	1568	125.1	6.47	1.19	1.62	0.30	0.55	1.27	0.10	16.0
MT1	Ponderosa pine	Bitteroot NF, MT	0.914	1632	97.4	4.02	0.60	1.10	0.24	0.24	0.66	0.08	12.7
MT2	Ponderosa pine	Bitteroot NF, MT	0.904	1584	107.1	3.26	0.48	1.04	0.24	0.22	0.58	0.06	15.3
MT3	Ponderosa pine	Bitteroot NF, MT	0.918	1640	92.9	4.38	0.64	1.19	0.20	0.16	0.45	0.05	11.7
MT4	Ponderosa pine	Bitteroot NF, MT	0.910	1610	101.4	4.44	0.63	1.23	0.31	0.12	0.44	0.05	19.5
OR1	Ponderosa pine Douglas-fir, white fir	Hepner RD, OR	0.906	1601	106.0	3.85	0.57	1.33	0.41	0.24	0.70	0.14	20.3
OR2	Ponderosa pine Douglasfir, white fir	Hepner RD, OR	0.900	1603	113.6	5.23	0.63	1.16	0.33	0.23	0.67	0.08	14.5
OR3	Ponderosa pine Douglasfir, white fir	Hepner RD, OR	0.916	1609	93.7	4.01	0.61	1.35	0.45	0.22	0.69	0.12	15.7
		Mean	0.916	1629	94.9	3.77	0.55	1.19	0.31	0.21	0.62	0.07	15.6
		Standard deviation	0.016	42	17.7	1.18	0.22	0.29	0.08	0.11	0.23	0.04	5.2
		Boreal forest of southeastern Alaska											
AK1	Black spruce	Chicken, AK	0.91	1616	105.0	4.39	1.12	1.74	0.26	0.34	1.04	0.03	7.23
AK2	Black spruce	Tetlin Junction, AK	0.92	1671	86.0	9.43	2.00	3.61	0.66	0.58	2.05	0.10	2.97
		Pine-oak forests of mid-western United States											
MN4	Oak savanna	Camp Ripley, MN	0.953	1716.6	54.0	1.50	0.20	0.89	0.23	0.03	0.37	0.02	10.1
MN5	Oak	Chippewa NF, MN	0.936	1684.3	72.8	2.28	0.31	0.93	0.22	0.09	0.43	0.04	10.0
MN6	Redpine	Chippewa NF, MN	0.942	1692.9	65.9	2.07	0.26	0.87	0.23	0.08	0.41	0.04	11.5

[a]AFB, air force base; NWR, National Wildlife Refuge; NWP, national wildlife preserve; NF, national forest; WR, wildlife refuge; RD, ranger district.
[b]MCE (modified combustion efficiency) = $\Delta CO_2/(\Delta CO+\Delta CO_2)$.

carbon content of 50%. The F_C value of 0.50 is consistent with in situ F_C measurements for a wide range of vegetation types and is likely accurate to within $\pm 10\%$ (Lobert et al., 1991; Susott et al., 1991, 1996). Particulate matter was assumed to be 60% carbon by weight. The simultaneous measurements of plume vertical velocity, flux of emissions, and carbon were used to determine the rate of fuel consumption, which provides the weighting factors applied to the integrated $PM_{2.5}$ filter and canister samples to obtain fire average EFs for each FASS tower. The mean of the EFs produced from each FASS tower deployed during the fire were averaged to obtain an EF value for the fire as a whole.

A.2. Results

Emission factors were measured for $PM_{2.5}$, CO_2, CO, CH_4, and C2–C3 hydrocarbons. MCE and EFs for each fire are given in Table A1. Following CO_2 and CO, $PM_{2.5}$ is the dominant species emitted from prescribed fires, consistent with previous findings for a wide range of ecosystems, fire types, and measurement techniques (see references from Table 4.1). Fire weighted average $EF_{PM2.5}$ exhibits significant variability within vegetation groups. The $EF_{PM2.5}$ for the grassland and shrub cover group is lowest (10.2 g kg^{-1}) and differs significantly from the average values of the forest cover groups ($p < 0.001$ or better for Welch two sample *t*-test and Wilcoxon rank sum test). Emissions of C2 and C3 hydrocarbons equal 78–114% of CH_4 emissions. Alkene emissions exceed emissions of their respective alkanes for all individual fires, which appears to be a common characteristic of biomass burning (see Table 4.1 and related references). These light hydrocarbons (C2–C3) typically comprise about half of the total NMHC emissions from wildland fire (see Table 4.1).

The CH_4, C_2H_6, C_3H_6, and C_3H_8 emissions for the interior mountain west conifer forests are significantly higher than those for the southeastern conifer forests and the grassland/shrubland vegetation groups ($p < 0.05$ or better for Welch two sample *t*-test and Wilcoxon rank sum test). The lower MCE of the interior mountain west conifer fires suggests this difference may be a function of fire behavior. Emission factors for CH_4 and many hydrocarbons often exhibit a strong linear relationship with MCE (Sinha et al., 2003; Yokelson et al., 2003). The EFs for C_2H_2, C_2H_4, and C_3H_4 are not statistically different across the vegetation groups.

This page intentionally left blank

Developments in Environmental Science, Volume 8 109
A. Bytnerowicz, M. Arbaugh, A. Riebau and C. Andersen (Editors)

ISSN: 1474-8177/DOI:10.1016/S1474-8177(08)00005-3

Chapter 5

Effects of Wildland Fire on Regional and Global Carbon Stocks in a Changing Environment

Susan G. Conard and Allen M. Solomon*

Abstract

Every year tens of millions of hectares of forests, woodlands, and grasslands burn globally. Some are burned intentionally for land conversion, pasture renewal or hazard reduction, or wildlife habitat improvement, but most are burned by uncontrolled wildfire. Estimates of burned area available in the literature vary widely, but satellite-based remote sensing data are increasing the accuracy of monitoring active fire and estimating burned areas. Recent data suggest that global wildfire emissions vary substantially from year to year. Nonetheless, average annual carbon emissions from wildfire are 20–40% of those from fossil fuel combustion and cement production. Results of field studies and modelling efforts indicate that changing climate is likely to increase the extent and frequency of wildfires, highlighting the importance of accurately quantifying the regional and global effects of wildfire on carbon stocks and on atmospheric carbon compounds. The nature and strength of feedbacks between fire and climate will depend not only on changes in the area that is burned annually, but perhaps more importantly, on how those fires burn and how ecosystems respond and recover. Changes in burn severity can result in large differences in the amount of fuel consumed, emissions to the atmosphere, and the capacity of ecosystems to recover carbon after a fire. Recent work also indicates that even low-severity surface fire may cause significant changes in soil respiration, and these changes may either increase or decrease the net effects of fire on atmospheric carbon. Postfire recovery to a different vegetation type—which may occur in response to changing climate, unusually high burn severities, or other factors—also has the

*Corresponding author: E-mail: sconard@fs.fed.us

potential to affect the amount and rate of carbon storage on the landscape. Past and future vegetation and fire management activities also play a role in ecosystem condition and carbon storage, although the nature and magnitude of these impacts vary greatly among regions and ecosystems. Improved understanding of the extent and severity of fire, the feedbacks between fire and climate, and the effects of changing fire regimes on all aspects of the carbon cycle is needed before we can fully predict the magnitude, or perhaps even the direction, of the effect of changing fire regimes on global carbon balance and atmospheric chemistry.

5.1. Introduction

Global carbon (C) stores in vegetation and the top meter of soil are about 2500 gigatons (Gt), with 81% of this in soils and the balance in aboveground vegetation (Bolin & Sukumar, 2000). This terrestrial carbon storage is slightly over three times the amount of carbon in the atmosphere (760 Gt C). About 1146 Gt (46%) of this global terrestrial carbon storage is in tropical, temperate, and boreal forests (Bolin & Sukumar, 2000; Dixon et al., 1994); with 34% in grasslands and savannahs, and the balance in tundra (5%), wetlands (10%), and croplands (5%) (Bolin & Sukumar, 2000). In many of these systems, fire has long been a common disturbance event, whether started by lightning or intentionally or accidentally by humans. Fires in forests, savannahs, and grasslands release large amounts of carbon to the atmosphere annually, primarily as carbon dioxide (CO_2) but also in the form of other gases (such as carbon monoxide (CO) and methane (CH_4)) and aerosols, such as soot particles (Crutzen et al., 1979).

The recent report of the Intergovernmental Panel on Climate Change (IPCC, 2007) documents that climate has warmed over much of the earth in recent years. This warming, which is generally strongest in the boreal and temperate zones of the Northern Hemisphere, is expected to continue to accelerate over the next century, leading to more severe droughts and likely to more frequent and more severe fires in many parts of the world (IPCC, 2007). Such changes in fire patterns can be expected to lead to changes in atmospheric chemistry and in terrestrial carbon storage. This makes accurate estimates of effects of fire on carbon cycle and atmospheric chemistry increasingly critical.

As data sources and models improve, estimates of global and regional burned areas and of biomass emissions are changing and undoubtedly becoming more accurate. In a seminal paper, Crutzen et al. (1979) brought to the attention of the scientific community the potential importance on atmospheric chemistry of the impacts of global emissions from biomass burning. Seiler and Crutzen (1980) estimated global biomass emissions of 2.2–4.0 Gt C per year, with about 5% coming from forest fires. These estimates have been revised and refined as data and analysis techniques improve. A recent paper that integrated satellite data with ecosystem models estimated an average annual global emission from biomass burning of about 2.5 Gt C per year between 1997 and 2004, with a third to half of that from forest fires (van der Werf et al., 2006). Other recent estimates (generally for single years) have ranged from about 1.3 to 3.4 Gt C per year (Arellano et al., 2004; Hoelzemann et al., 2004; Ito & Penner, 2004; see Table 5.1 for additional examples). There is considerable research underway to validate and improve the accuracy of satellite-based estimates of burned areas (Barbosa et al., 1998; Fraser et al., 2000; Giglio et al., 2006; Roy et al., 2002, 2005).

It is reassuring that a number of recent global and regional fire emission[s] estimates are similar, given the great variability in earlier estimates (Conard and Ivanova, 1997; French et al., 2004; Ito and Penner, 2004; Soja et al., 2004a, 2004b). Considerable improvement is still needed before estimates of biomass emissions will reach the level of accuracy required for local or regional carbon accounting or estimating impacts of fire on atmospheric chemistry. Furthermore, emission components other than CO_2, such as CH_4, black carbon, and other aerosols, while emitted in smaller amounts, can have much stronger climate forcing coefficients per unit mass (IPCC, 2007). These other compounds are also not taken up through photosynthesis as vegetation regrows, although net uptake or release of methane by soils can be significant in some ecosystems (Conrad, 1996). Bousquet et al. (2006) concluded that interannual variability in atmospheric methane levels is influenced strongly by methane emissions from wetlands and less strongly by direct methane emissions from fires.

Recent estimates suggest that current average annual emissions from biomass burning are in the range 20–40% of the global annual average of about 7.3 Gt C emitted from fossil fuel combustion and cement production between 2000 and 2004 (Marland et al., 2007). Interest in the role of fire and changing fire regimes on the global carbon cycle has grown considerably in recent years as a result of evidence that unusually severe fire seasons in 1997 and 1998 in Indonesia (Page et al., 2002; Schimel and Baker, 2002), the tropics (Cochrane, 2003), and Russia (Dlugokencky et al., 2001; Kasischke et al., 2005) produced pulses of carbon into the atmosphere equivalent to close to half of annual fossil

Table 5.1. Sample estimates of fire emissions and burned areas from the literature for various years and regions. Note the wide variation in estimates from similar regions and among years and sources

Region	Year(s)	Emissions Tg C per year	Burn area 10^6 ha per year	Emissions t C/ha	Comment	Source
Indonesia	1997	810–2570	2.4–6.8	320–378	Ground sampling; fire scar analysis	Page et al. (2002)
Indonesia, New Guinea, Malaysia	1997	1090	16.7	65.6	Remote sensing; ecosystem-specific fuel consumption estimates	van der Werf et al. (2006)
Boreal zone		20–30	1.3		Very limited data available on burned area at that time	Seiler and Crutzen (1980)
Boreal zone	1998	212–422	29.0	7.3–14.5		Kasischke et al. (2005)
Boreal zone	1998	530	24.7	21.5		van der Werf et al. (2006)
Russia	Average	194	12	16.2	Based on fire return intervals and estimated consumption of available fuels	Conard and Ivanova (1997)
Russia	1998	135–190	13.3	10.2–14.3	Based on remote sensing and fuel consumption estimates	Conard et al. (2002)
Siberia	1998–2002	153–413	9.1	16.8–45.4	Annual. Average (low to high consumption)	Soja et al. (2004a, 2004b)
Eastern Russia	1998–2002	107–205	9.6	11.2–21.4	Annual. Average (low to high consumption)	Kasischke et al. (2005)
US and Canada	2002–2004	92–173	NA	NA	Low to high years	Wiedinmyer et al. (2006)
US and Canada	2002–2004	65–100	3.8–5.2	17.1	Low to high years	van der Werf et al. (2006)

US and Canada	2000	179–210	7.0–7.7		Means from two slightly different models; C emissions estimated assuming that 8% derived from CO	Hoelzemann et al. (2004)
Tropics		1800–4700			Includes deforestation, agricultural burning, savanna fire, and fuelwood	Crutzen and Andreae (1990)
Tropics	1970s	2245			Includes tropical and subtropical regions; deforestation, shifting cultivation, and savanna fires	Hao and Liu (1994)
Tropics	1997–2004	1944			Includes South America, Africa, Australia, SE and equatorial Asia, Central America	van der Werf et al. (2006)
Global		1250–2565	630–690		600 million ha of this in savannas and brushlands; not including agricultural waste and fuelwood	Seiler and Crutzen (1980)
Global	2000	1300			Satellite burned areas	Ito and Penner (2004)
Global	2000	1741	170	10.2	Satellite burned areas; excludes 0.3 million ha agricultural land	Hoelzemann et al. (2004)
Global	2000	2038	358	5.6	Satellite burned areas, regional emission factors and modelling	van der Werf et al. (2006)
Global	2000	3400			Satellite CO measurements and atmospheric modeling	Arellano et al. (2004)

fuel emissions. It is becoming increasingly clear, that these large pulses of biomass emissions are not rare or isolated instances, as the advent of improved satellite sensors has made fires easier to document and quantify.

Smoke from wildfires can move long distances, both at upper and lower levels in the atmosphere, and may affect air quality in areas thousands of miles from the source (Damoah et al., 2004; Fishman, 1991; Fromm et al., 2000; Kajii et al. 2002; Park et al., 2003; Wotawa and Trainer, 2000). This can have important implications for the effects of fires on local or regional weather and for atmospheric profiles of carbon monoxide, ozone, and other compounds. For example, Wotawa and Trainer (2000) estimated that smoke transport from Canadian fires into the United States in 1995 led to substantial increases in tropospheric CO and ozone levels across much of the eastern United States. Damoah et al. (2004) reported that smoke from 2003 fires in eastern Russia traveled completely around the Northern Hemisphere and back to Russia over a period of 17 days. While important, these effects are generally outside the scope of this chapter, which will focus on the interactions of fire with global and landscape-scale balance of carbon.

In the absence of natural or human disturbance, all forest and grassland systems would be carbon sinks, as indeed they were during Paleozoic and Mesozoic time, when much of today's fossil fuels were sequestered. As forests establish and grow, annual carbon (C) sequestration reaches a maximum rate some 30–100 or more years of age, and then the rate begins to decline. Even mature forests continue to store carbon in vegetation, litter, and soils, although the rate of sequestration may decrease greatly in older forests (Dixon & Krankina, 1993; Dixon et al., 1994; Kasischke et al., 1995; Kurz & Apps, 1999). Of course disturbance by fire, insects, or severe weather events is ubiquitous. For most forests and other ecosystems, fires have occurred for millennia, although the typical frequency and severity of fires have changed over time and vary greatly from one vegetation type to another. In a stable environment, the cycle of disturbance and regrowth can be expected to result in relatively constant levels of carbon storage in vegetation and soils, as vegetation regrowth at landscape and regional scales balances carbon losses through fire emissions, decomposition, and other processes.

General estimates of long-term trends in vegetation carbon stocks may be made from national inventories. Because such data are not available for all countries, and the intensity, frequency, and methods of data collection vary widely, inventories are not sufficient for developing global estimates. Where these data exist, they can provide an excellent overall picture of long-term trends in disturbance regimes and carbon storage, but they are less useful for determining mechanisms, evaluating changes within a landscape, determining interannual variability, or developing projections of future impacts. Furthermore, most inventory systems have also focused until quite recently on inventory of timber species, rather than on changes in soil carbon, understory plants, grassland vegetation, or other factors necessary for determining effects of fire regimes (see Birdsey & Lewis, 2003; Burrows et al., 2002; Heath et al., 2003; Kurz & Apps, 1999; Shvidenko & Nilsson, 2000, 2003, for examples of use of inventory data for analysis of long-term trends in carbon storage and impacts of disturbance on forested systems).

In this chapter we focus on the long- and short-term effects of fire on carbon fluxes revealed through remote sensing and *in situ* measurements that can provide sufficient detail to detect interannual differences in carbon storage at local to global scales. We also address the potential effects of direct fire emissions and indirect fire-related emissions on atmospheric chemistry and climate. Our primary objective is to discuss the kinds of information that are needed to develop reasonably accurate estimates of the impacts of wildland fire on carbon stocks and emissions in a changing environment. This will require a creative combination of outputs of climate models with models of vegetation dynamics that incorporate the effects of fire and with data from laboratory and field experiments that will enable researchers to accurately parameterize and evaluate their models. Some of the major areas of investigation that are needed include: improved understanding of variability in fire regimes; the drivers of and effects of variability in fire behavior; quantification of fuel consumption and emissions under a range of ecosystem and environmental conditions; and better data and models concerning processes such as soil respiration, decomposition and forest regrowth under changing environments. We will discuss a number of these issues and then provide some synthesis.

5.2. The importance of fire regime for carbon dynamics

The role of wildfire in the storage and release of carbon is largely a function of the fire regime (frequency, size, seasonality, and severity of fires, as well as the variability in these parameters) typical of a given ecosystem (see Brown et al., 2000 and Ryan, 2002 for excellent discussions of fire regime types and classification). The characteristics of individual fires may vary widely within a given ecosystem as a function of weather, fuel structure, fuel moisture, and terrain characteristics. These differences in fire regimes are a function of the combination of weather, topography, stand structure (fuels), and occurrence of ignitions that characterize specific ecosystems (Pyne et al., 1996). For example, many prairies and grasslands historically burned every few years, or even annually; dry pine forests in areas as diverse as the western United States and central Siberia burned, primarily in low-intensity surface fires, every 10–30 (or even 50) years; while cool moist conifer forests, such as coastal Douglas-fir in the Pacific Northwest of the United States burned in high-intensity stand-replacement fires only every few hundred years (Agee, 1993; Heinselman, 1978; Leenhouts, 1998; Schmidt et al., 2002).

Because vegetation that burns eventually grows back, the overall effects on carbon cycle need to be understood for individual stands over time, but ultimately integrated to a landscape level. Net effects on C storage come primarily from *changes* in fire regimes over time. In general fires that cause the most severe ecosystem effects release the most C and lead to the longest delays in recovery of ecosystem C (Fig. 5.1). These fires also tend to occur in ecosystems with the highest potential for net C storage.

In forest systems, the highest severity fires are termed *stand-replacing fires*, which typically kill all or most of the living vegetation, and burn deeply into surface litter and duff layers. These fires may release a great deal of carbon

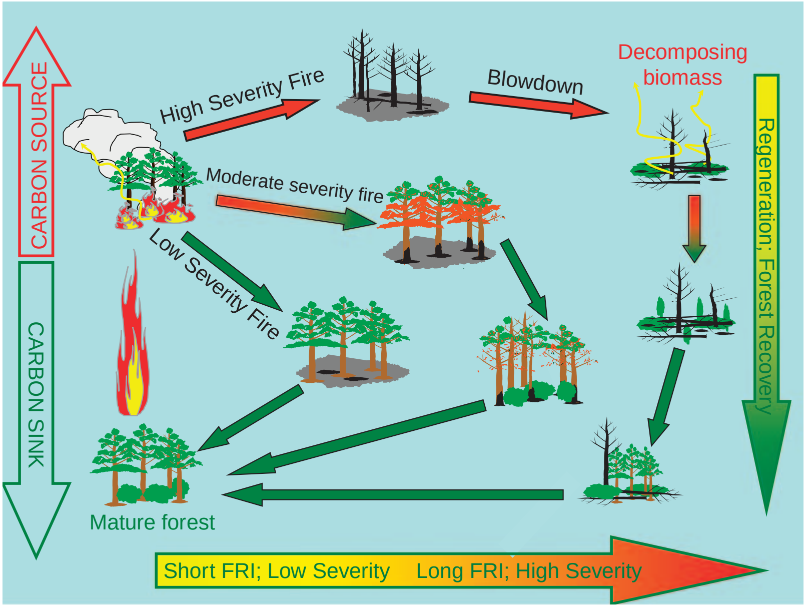

Figure 5.1. Carbon source/sink relationships in fires of varying severity as might occur in pine forest of the western United States or central Siberia (FRI, fire return interval).

and other compounds to the atmosphere, and ecosystem recovery, including return to prefire levels of carbon storage and fuel loading, is generally slow (100–300 years) (Kasischke et al., 1995; Kurz et al., 1995; Schmidt et al., 2002; Wirth et al., 2002a). Therefore, forest and shrubland systems that experience primarily stand-replacing fires tend to have relatively long intervals between fires. In some forest and shrub systems, as well as in perennial grasslands and savannas, fires may top-kill most of the above-ground biomass, but local species are adapted to recover rapidly through regrowth from live roots, basal sprouting, or other means. Such systems recover biomass (and therefore stored carbon) much more rapidly—and typically undergo a shorter interval between fires, although emissions over multiple fire cycles may be similar to those from longer interval systems.

Low-severity fires in forest systems may burn only surface fuels and low-growing vegetation, and have little impact on overstory trees beyond sometimes a brief reduction in growth rates. Such *surface fires* release relatively small amounts of carbon, but they are likely to occur more frequently, with the result that cumulative carbon release over time may be similar to that where fires are less frequent. These systems tend to have a lower potential for carbon storage than systems with less frequent, but higher-severity fires. Recent analyses and field studies have shown, however, that there can be a large range in fuel consumption and carbon emissions from even these relatively low-severity fires as a function of prefire weather conditions and details of fuel structure and consumption (Conard & Ivanova, 1997; McRae et al., 2006; Ottmar et al., 1993; Reinhardt et al., 1997; Sparks et al., 2002).

In *mixed-severity fire regimes*, relatively frequent surface fires may be interspersed with less frequent stand-replacement fires, or with patches of high-severity fire that are a function of either unusually severe weather or reduced fire frequency that leads to greater than normal fuel accumulation. This appears to be the pattern in many conifer forests in the western United States (Agee, 1998; Heinselman, 1981; Schmidt et al., 2002; Schoennagel et al., 2004), as well as the extensive Scots pine forests of northern Eurasia (Sannikov & Goldammer, 1996). In Scots pine forests in central Siberia, for example, the typical interval between low-severity surface fires is 35–50 years, with widespread stand-replacement fires occurring every 120–150 years (McRae et al., 2006).

5.3. Fire dynamics

Our understanding of the nature of fire and its effects on forests and other ecosystems comes from a combination of experimental studies (often using prescribed fire) and observations before, during, and after wildfires. These observations can occur at a range of scales using techniques such as satellite remote sensing of fires and burned areas, aircraft-based remote sensing or smoke sampling, and measurements of fluxes or changes in ecosystem properties made on the ground.

Fire effects on carbon storage and release are highly variable within and among wildfires as a function of fuel structure, fuel condition (e.g., moisture), weather at the time of burning, terrain effects, and internal fire dynamics (Pyne et al., 1996). Some of the most important differences involve the intensity (energy release) and speed of burning, which depend on the weather conditions before and during the fire, the structural properties of the vegetation, and the physical environment in which the fire occurs (Baeza et al., 2002; Brown et al., 2000; Ryan, 2002; Sandberg et al., 2002). The rate of fire spread can range over several orders of magnitude (Ryan, 2002), with the slowest spread rates in smoldering ground fires and low-intensity surface fires (e.g., less than $0.3\,\mathrm{m\,min^{-1}}$), and the fastest in crown fires (up to around $200\,\mathrm{m\,min^{-1}}$). Fires with more rapid spread rates also tend to exhibit higher energy release (intensity) and to have deeper (wider) actively burning zones (McRae et al., 2005; Ryan, 2002). The overall result, in the absence of extensive residual combustion behind the fire front, is higher fuel consumption per unit area. Residual or smoldering combustion can change this picture, particularly in areas of deep organic soils, thick humus layers, or peats—where smoldering may continue for days or even months, depending on weather conditions. Fuel consumption is more directly related to the total energy release per unit area during a fire than to other parameters, since the energy released per unit of dry biomass consumed is relatively constant. While these relationships have been evaluated in laboratory settings and from some aircraft measurements (Riggan et al., 2004; Wooster, 2002; Wooster et al., 2003), quantification of energy release from fires over large areas is just beginning to be feasible with remote sensing. Most estimates of fuel consumption in the literature are based on experimental data involving the difference between prefire and postfire fuel loading. These data show a high variability from site to site as a function of available fuels and the conditions of burning.

5.4. Fire effects on carbon dynamics

There are several components to and stages of ecosystem carbon release and uptake related to fire (Fig. 5.2). The intensity and timing of these

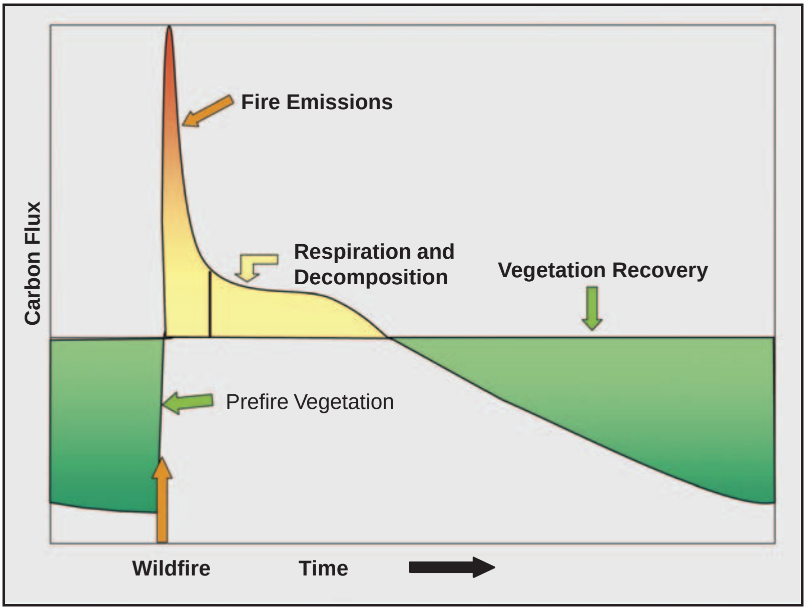

Figure 5.2. Change in net carbon emissions and storage relative to the atmosphere over time through a single fire cycle. The time scale may range from a few years to many decades depending on the ecosystem type and the severity of the fire.

fluxes is a function of the prefire fuel loading and vegetation structure, environmental conditions, and other factors that control the type of fire and the burn severity, as well as the specific ecosystem characteristics (such as adaptations to rapid recovery following fire) and the biophysical setting. The general climate and weather patterns in the months and years following the burn can strongly influence both rate and patterns of recovery.

The four major processes that drive these postfire dynamics are: (1) direct fire emissions, (2) postfire changes in soil respiration, (3) decomposition of material killed in or following the fire, and (4) postfire vegetation recovery (Fig. 5.2). Depending on the type and severity of the fire, and the ecosystem conditions before and after fire, these phases may be relatively discrete or may overlap considerably in time. Regardless, as the system recovers, at some point within months to several years the system becomes a carbon sink as carbon uptake by growing vegetation begins to dominate over carbon release from decomposition and soil respiration.

5.4.1. Direct fire emissions

The initial impact of fire on carbon flux is from the direct emissions that derive from consumption of live and dead fuels by a fire. Large fires may burn over many days or weeks. At any given point on the landscape most emissions occur during a relatively brief period of flaming combustion as the fire front passes, although there may be considerable residual combustion. Despite the common misconception that wildfires consume large amounts of tree branches and boles, most of the fuels consumed in fires are fine fuels primarily in the duff and litter layers, with additional contributions from consumption of foliage and fine twigs of living vegetation. There is typically little consumption of coarse fuels in tree canopies, even in a crown fire. This pattern is reflected in commonly used models for estimating fuel consumption (Ottmar et al., 1993; Reinhardt et al., 1997). Depending on spatial variability in fuels, terrain and other factors, and in temporal variability in winds, the severity of a fire can vary considerably across the landscape (Cochrane & Schulze, 1999; Conard & Ivanova, 1997; Key, 2006; Morgan et al., 2001), with resultant high variability in the emissions per unit area. Similar variation can occur from one fire to another. For example, Hoffa et al. (1999), working on experimental fires in woodland and grassland vegetation in Zambia, reported ranges in combustion factors (percent of fuel consumed) depending on season of burning from 1% to 47% for woodland and from 44% to 98% for grassland as fuel moisture decreased. McRae et al. (2006) reported threefold variation in fuel consumption from six experimental surface fires burned under different conditions in a relatively homogeneous stand of Scots pine in Siberia, with estimated range in emissions from 4.8 to 15.4 t C ha^{-1}. Based on allometric analysis of tree canopies, a crown fire on the same site might be expected to produce an additional 3–7.1 t C ha^{-1}; so within the Scots pine/lichen vegetation types common across central Siberia, the emissions from a given fire may range from as low as 4.8 to as high as 22.5 t C ha^{-1}.

Unfortunately, similar published data are available for few vegetation types around the world. Furthermore, we are just beginning to develop accurate global and regional databases to quantify burned areas, and information on fire severity is available only for a small percentage of the forest area burned every year. As a result, most regional to global emission estimates assume an average emission factor, either for each major vegetation or fuel type, or over the entire burned area. Several recent papers have attempted to address this problem by combining low, medium, and high surface fuel consumption estimates with estimated seasonal trends in proportions of crown fire versus surface fire (boreal zone: Kasischke et al., 2005); modelling fuel consumption based on expected seasonal trends in fire severity combined with a process-based model of ecosystem carbon stocks (global and regional: van der Werf et al., 2006); using literature-based estimates of fuel loadings and combustion factors for individual fuel types (North America: Wiedinmyer et al., 2006); or extrapolating from limited ground-based sampling to satellite-observed burned areas or hot spots (Indonesia: Page et al., 2002; some of these and other estimates are summarized in Table 5.1). There is a clear need for better data and models on which to base emission estimates from wildland fires.

5.4.2. Soil processes

It is often assumed that soil respiration will increase following fire because microbial activity would be encouraged by the increased insolation and soil moisture available after moderate to high-severity fires, along with increased availability of minerals and organic materials from dead roots (Amiro et al., 2003; Dixon & Krankina, 1993). It appears, however, that the net effect of fire on soil respiration varies widely among ecosystems. Several recent studies have reported significant decreases in soil respiration following fire in North American boreal aspen, spruce, and pine forests (Amiro et al., 2003; O'Neill et al., 2002), Siberian Scots pine forests (Baker & Bogorodskaya, 2007), and larch forests (46% decrease on year-old mild burn and 64% decrease on severe burn 5 years after fire; Sawamoto et al., 2000). Amiro et al. (2003) suggest this is a consistent pattern in many boreal forests. The magnitude of reported effects varies greatly from study to study and apparently among ecosystems. This variability likely represents real ecosystem differences as well as differences in study design, interannual variability in climate and soil moisture, and timing of sampling after fire.

In boreal forests, a number of studies have shown that depressed soil respiration may persist for several years after fire (Amiro et al., 2003). In Scots pine and larch forests of Siberia, the greatest decreases and longest periods of recovery seem to occur following higher-severity fires (Conard et al., 2004; Sawamoto et al., 2000). Several studies have suggested that decreased postfire respiration is mainly due to changes in root respiration following severe fires rather than decreases in soil microbial activity. However, a number of studies have shown substantial decreases in soil microorganism activity following even low-severity fires (Amiro et al., 2003). This is not necessarily caused by direct effects of soil heating, as the immediate postfire soil respiration in forested systems may be just about the same as the prefire respiration.

In prairie grasslands of the central United Sates, however, spring burning increased soil respiration by 38–51% relative to unburned sites (Knapp et al., 1998). Postfire increases in both soil microorganisms and soil respiration were small but significant in African savanna, although the effects of soil moisture and added organic matter were larger than those of the fire alone (Andersson et al., 2004). In ponderosa pine forests of the southwestern United States, Kaye and Hart (1998) found that restoration thinning decreased soil respiration relative to controls, while thinning along with prescribed burning increased respiration slightly, but only in the late summer. Soil respiration was the same on a burned site as on the control following surface fires in a chestnut forest in Switzerland, but increased 100–150% where surface fuel loads were artificially doubled before the fire (Wuthrich et al., 2002).

Thus, observed postfire changes in soil respiration have ranged from strong decreases in respiration on many boreal forest sites to insignificant changes or increases in respiration-related CO_2 emissions after fires in certain grassland, woodland, or dry pine ecosystems. Unfortunately, there are few studies of postfire respiration where data on fuel consumption are available. Two examples illustrate the range of potential impacts. On annually burned tallgrass prairie sites in the United States, Knapp et al. (1998) estimated that total yearly soil CO_2 emissions were equivalent to 1.3–1.4 $kg\,C\,m^{-2}$ higher than for unburned prairie. On these same sites, aboveground fuel loads (Abrams et al., 1986) suggest potential direct fire emissions of about 0.2 $kg\,C\,m^{-2}$, a mere 15% of the increase in soil respiration resulting from the burning. On Scots pine sites in Siberia, on the other hand, total C emissions from three experimental surface fires conducted in 2001 ranged from 0.44 to 0.57 $kg\,C\,m^{-2}$ (McRae et al., 2006). Soil respiration on these sites a year after the fires was an estimated 0.2–0.3 $kg\,C\,m^{-2}yr^{-1}$ lower than that on unburned control plots (Conard et al., 2004). Such a reduction in soil respiration would effectively cancel out about half of the fire emissions in just one year. Due to the potential magnitude of changes in soil respiration after fire, and the uncertainty in the direction of these changes in different systems, this is an area that clearly needs further study. In particular, assessments of impacts of fire on carbon balance require better data on how respiration changes compare with fire emissions.

Release or uptake of methane by soils and wetlands may also substantially affect the influence of fires on atmospheric emissions. Methane uptake appears highly variable as a function of ecosystem type, degree of soil moisture saturation, and other conditions (Brumme & Borken, 1999). Fiedler et al. (2005) reported methane fluxes ranging from annual emissions of 248–318 $kg\,C\,ha^{-1}$ (68–87 $mg\,C\,m^{-2}\,day^{-1}$) to CH_4

uptake of 0.1–5 kg C ha^{-1} (0.03–1.4 mg C m^{-2} day^{-1}) along a black spruce hydrosequence in Germany. They concluded that the magnitude of landscape-scale uptake of methane may often be underestimated because of exclusion of wetlands and water bodies (which emit methane) in studies of forest uptake. Gulledge and Schimel (2000) reported uptake of 0–0.5 mg C m^{-2} day^{-1} for spruce sites in Alaska. For deciduous forests in Michigan, Suwanwaree and Robertson (2005) reported average CH_4 oxidation rates of about 30 μg C m^{-2} hr^{-1} (0.7 mg C m^{-2} day^{-1}). Singh et al. (1997) reported methane uptake rates of 0.36–0.57 mg m^{-2} hr^{-1} (6.5–10.3 mg C m^{-2} day^{-1}) for dry tropical forests and savannas in India, with the lowest uptake in the wet season. In one of the few papers on effects of fire on methane uptake, Burke et al. (1997) found that carbon uptake as methane on burned upland boreal forest sites in Canada was about three orders of magnitude less than C release from soil respiration. Additional research is needed to determine the importance of soil methane fluxes to the overall impacts of fire on carbon and atmospheric chemistry.

5.4.3. Postfire carbon dynamics

Because consumption of aboveground litter, dead wood, and living biomass is seldom complete, fires leave behind varying amounts of dead organic matter, which gradually decomposes over time or may be consumed in subsequent fires. The remaining biomass is minimal following grassland fires or low-severity surface fire in forests. As forest fires increase in severity, larger trees or shrubs are killed. However, even in very intense fires, most standing woody material over 1 cm diameter is not consumed, although occasional dead trees will continue to smolder for many days. Large woody material on the ground, or that falls during the fire, may also be consumed by residual smoldering combustion. Dead trees that remain standing after a fire often decompose very little until they fall to the ground, which may take many years. Thus, the bulk of the dead material remaining after a severe fire can take a few years to centuries to decompose, as new vegetation grows to replace it. The exact time trajectory of transition from carbon source to sink following fire will be specific to the ecosystem characteristics and a function of fire severity.

Kashian et al. (2006) provide an excellent overview of the process of shifting from dominance by carbon emission to dominance by carbon sequestration and storage following stand-replacement fires in lodgepole pine forests of the western United States (Fig. 5.3). In this system standing dead trees slowly deteriorate, collapse, and then rot on the ground from 5 to 15 years after the fire. Hence, the first one or two

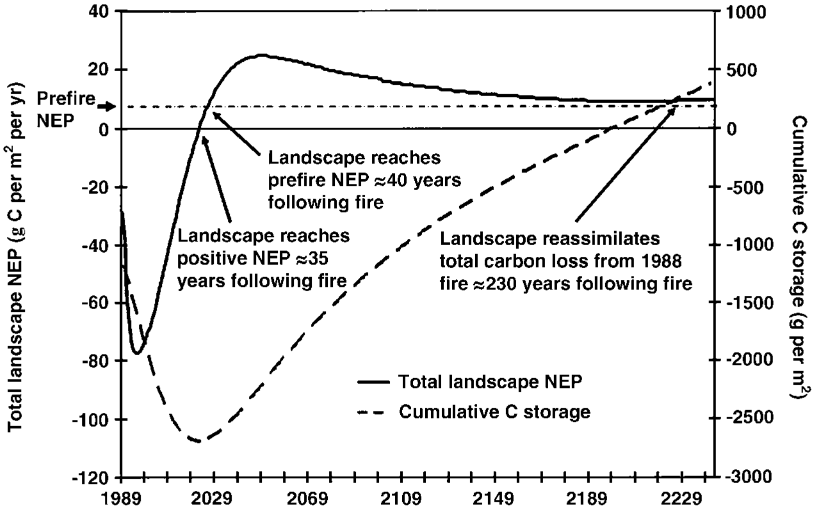

Figure 5.3. Predicted total net ecosystem production (NEP; solid line) and cumulative carbon (C) storage (dashed line) for lodgepole pine forests on the entire 525,000-hectare Yellowstone landscape following the 1988 fires. The landscape is expected to recover all C lost during and after the 1988 fires over the course of the fire interval. (*Source*: Kashian et al., 2006, Copyright, American Institute of Biological Sciences)

decades after fire are dominated by carbon release. While decomposition of dead tissue continues, annual and perennial herb and shrub species soon cover the landscape, fixing a small amount of new carbon. Tree seedlings from fire-adapted species may appear the growing season following fire or may take several growing seasons to germinate and establish. The saplings eventually outgrow the shade of the initial perennial herbs and shrubs, and at that point, the annual increment of photosynthetic tissue increases almost geometrically (Turner et al., 2004). Only after saplings are large enough to carry a leaf area index of 4 or $5\,\mathrm{m\,m^{-2}}$ or reach a height of 3 or 4 m (three to five decades) will fixation of new carbon finally predominate over emission of carbon derived from the burn. While the rate of carbon fixation (sequestration) is at a maximum at 30–50 years, the amount of carbon stored may reach its *minimum* at 20–30 years (Fig. 5.3). In lodgepole pine forests subjected to stand-replacement fires, carbon storage may not reach prefire levels for one to several centuries under stable climate (Kashian et al., 2006).

Both the timing and the magnitude of changes in ecosystem carbon fluxes may vary greatly for different ecosystems, as illustrated by Campbell et al. (2004) in a comparison of time trajectories in net ecosystem production (NEP) of western hemlock, Douglas-fir, and ponderosa pine forests in Oregon following stand-replacement disturbances. Working in Scots pine forests of central Siberia, Wirth et al. (2002b) concluded that the net postfire carbon flux was a function both of the initial amounts of coarse woody debris and the site conditions as represented by understory vegetation. Moister stands with *Vaccinium* species in the understory became net carbon sinks within 12 years after stand-replacing fire, while stands on drier sites with lichen understory took 24 years to recover to a net carbon accumulation. Fires of lower severity, or those in grassland and shrubland ecosystems, follow a similar but generally shorter chronology. Chronic climate change, especially as it reduces tree establishment and growth, or leads to changes in vegetation composition and structure, may increase the time span needed to replace emitted carbon, or may keep landscapes from ever storing as much carbon as did prefire landscapes.

5.5. Role of weather and climate on wildfire occurrence and effects

5.5.1. Interactions between ocean circulation patterns, regional climate, and fire

In mountainous areas of the western United States one of the key factors associated with severe fire seasons is the timing of snowmelt in the spring, with earlier snowmelt often being a precursor to longer summer drought periods (Westerling et al., 2006). High temperatures and low rainfall (or longer dry seasons) together produce increases in area burned and in numbers of large, intense fires (*ibid.*). Annual and multiyear weather patterns (such as those resulting from changes in El Niño/La Niña or other ocean circulation patterns) are highly correlated to the severity of fire seasons in different parts of North America, Brazil, Australia, and Eurasia.

The El Niño-Southern Oscillation (ENSO), for example, provides the southwestern United States with abundant winter rains every 3–7 years, supporting luxuriant growth of grasses and forbs the following growing season. If this pattern is followed by drought, the abundant surface fuels support development of stand-replacing fires in open woodlands, parklands, and dry pine (ponderosa) forests (Swetnam & Baisan, 1996; Swetnam & Betancourt, 1990, 1998). Recent research shows that the warm phase of the Atlantic Multidecadal Oscillation (AMO) has coincided with 40–60 year periods of increased fire frequencies throughout the western United States, and that the region appears to be entering such a period now (Kitzberger et al., 2007). These multiyear cycle effects may well amplify greenhouse gas-induced impacts of changing seasonal precipitation and temperature patterns that drive both fuel development (e.g., growth of shrubs and herbaceous species) and the severity of drought (which leads to increased fire hazard as fuel moisture decreases). In addition, the prediction of drought conditions resembling those that led to the 1930s Dust Bowl for much of the 21st century in the Southwest (Seager et al., 2007) suggests cause for serious concern regarding impending releases of carbon from these temperate zone forests and woodlands.

Similar relationships have been observed among ocean circulation patterns, drought, and fire in other regions of the world, including interactions of ENSO patterns and drought-related fire hazard in the Amazon (Nepstad et al., 2004), Arctic Oscillation patterns and fire occurrence in Siberia (Balzter et al., 2005), and the relation of ENSO to the unusually extensive fires in Indonesia in 1997–1998 (Page et al., 2002). Van der Werf et al. (2004) reported that a large anomaly in atmospheric CO, CO_2, and other compounds from August 1997 to September 1998 could be attributed largely to increased fire activity. This increase was associated with extensive droughts related to a strong El Niño, which caused unusually severe fire seasons in Southeast Asia, Central and South America, and boreal Eurasia and North America. Van der Werf et al. (2004) estimated that global fire emissions for 1997–1998 were about 1.17 (to 2.1) Gt above the 1997–2002 average of 3.53 Gt per year and accounted for as much as two-thirds of the global CO_2 anomaly for that period. The average emissions reported by van der Werf et al. (2004) for 1997–2002 are over half the 6.3 Gt C in global annual emissions from fossil fuel combustion and cement production cited earlier (Bolin & Sukumar, 2000). Although there are considerable uncertainties in the accuracy of various emission estimates, it is clear that biomass burning makes a significant contribution to global atmospheric chemistry as well as to interannual variability in global atmospheric carbon.

Drought and high temperatures interact to increase the moisture stress on vegetation. Initially this increased stress will lead to a decrease in fuel moisture that increases fire hazard and the probability of high-severity fires. As drought stress increases, trees and shrubs may lose their foliage or die. Drought stress also increases susceptibility of shrub and tree species to a number of insects (most notably bark beetles) and some pathogens. Furthermore, warmer temperatures increase the reproductive rates of some insect populations (Logan et al., 2003), permitting more intense infestations. Dried or drying foliage on trees subjected to insect attack and/or drought can increase fire hazard.

Many of the effects discussed above have occurred periodically over hundreds and even thousands of years (Kitzberger et al., 2007;

Swetnam & Baisan, 1996). However, regional climate models now project an increased frequency and intensity of fires, particularly in the boreal and temperate zones of the northern hemisphere (Bachelet et al., 2005; Brown et al., 2004; Stocks et al., 1998; Tchebakova et al., 2007; Wotton & Flannigan, 1993). Flannigan et al. (1998) point out that these effects will vary over wide regions in the boreal zone, with some areas (such as eastern Canada) expected to experience decreased fire hazard and others (such as central Canada) substantial increases in fire frequency and intensity. The recent report by IPCC (2007) projects global increases in surface temperatures particularly at high latitudes. It predicts longer growing seasons, increased heat waves, and greater high temperature extremes. Expectations for moisture pattern changes include increased heavy precipitation events, greater intensity and lengths of droughts in subtropical and lower latitude temperate regions, increased rainfall and flooding in higher latitude temperate and boreal regions, and reduced snow cover and increasing thaw of permafrost. The implications of these projections are obvious for increased boreal and temperate wildfire.

5.5.2. Potential interactions between fire and surface albedo

A more indirect effect of weather and climate involves the role of changes in surface albedo (reflectivity) from regional changes in fire regimes. Bonan et al. (1992) modelled the potential role of decreasing tree cover in boreal regions, as would occur if wildfire became more prevalent. The difference in a surface made dark by conifers masking snow, and a surface made light by snow covering the vegetation was large enough to lower temperatures in both winter and summer. Precise measurements and more intensive modelling by Randerson et al. (2006) in Alaska suggest that warming effects by release of carbon there by extensive wildfire would be entirely neutralized by cooling effects of increased albedo, at least until trees regrew.

A modelling exercise by Bala et al. (2007) projected that a temperate zone warming from carbon released by clearing all trees and forests would also be neutralized by the increased albedo of resulting grass and shrublands, although their climate model was incapable of correctly simulating the differences in evaporation that control the outcome of such an action (Thompson et al., 2004). While these studies on albedo effects are at best only somewhat indicative of potential system sensitivities, they make it clear that change in surface reflectance is an important factor to consider in determining the effects of changing fire regimes and associated changes in vegetation and land cover on climate.

5.5.3. Interactions between climate, fire regimes, and carbon

Climate change enters the fire cycle of carbon emission and carbon sequestration recovery at several points, but is particularly important in determining the fire regime and the nature of the recovery. Fire regime defines the frequency and intensity of fire across the spectrum from very frequent and moderate intensity fires that burn off accumulations of duff and kill seedlings through very infrequent but intense stand-replacing fires. Fire regime therefore determines the nature of the resulting forest ecosystem (savanna and open park-like forests to dense mesic forest) and its carbon-storage capacity. For example, Dezzeo and Chacon (2005) studied a gradient of increasing fire frequency in Venezuela that led to conversion of dense tropical forest to savanna. Along this gradient, ecosystem carbon storage decreased from 493 mg C ha^{-1} in undisturbed tall forest to 94 mg C ha^{-1} in sites that had been converted to savanna through frequent fire.

Although a mixed fire regime of 150–250 years between crown fires and 5–50 years between surface fires, such as that in Scots pine or ponderosa pine, might be expected to maintain a neutral carbon balance at the landscape scale, any change in frequency or severity of fires will alter this balance. A decline in fire return interval for crown fires can produce a severe decline in carbon carrying capacity, as time is shortened for regrowth by forests at the same time that forests may grow increasingly slowly under a climate that is chronically more stressful. An increase in surface fire severity or frequency also can generate a decline in carbon stocks, though perhaps not as great as that for crown fires (Wirth et al., 2002a).

Although we cannot predict with precision how fire regimes will be affected as climate changes, increasing frequency of drought, earlier snowmelt, decreases in permafrost, and longer fire seasons can all be expected to lead to increased fire hazard as the climate warms. A number of authors have suggested that a warming climate will cause increases in the annual area burned as well as in the severity of the fires that do occur (Fosberg et al., 1996; Stocks et al., 1998). Brown et al. (2004) used climate model projections of regional meteorology to predict a substantial increase in fire hazard by 2089 in areas of the northern Rockies, Great Basin, and the Southwest under a business as usual emissions scenario, which assumes no changes in energy policies or practices. Future changes in fire regimes can be expected to both facilitate and force changes in the structure and composition of ecosystems in a changing environment, with feedbacks that are largely unknown (Lavorel et al., 2007). Both burn severity and area burned can be expected to significantly increase, leading to higher levels of emissions from wildland fires (Overpeck et al., 1990), as well as to decreases in the amount of carbon stored in terrestrial ecosystems. In some systems in North America (such as many ponderosa pine forests) fuels have been accumulating for many years due to reduced fire frequency in the late 19th and 20th centuries (Schmidt et al., 2002). This stored carbon increases fire hazards and large, intense crown fires, a condition exacerbated by warming climate and longer fire seasons (Westerling et al., 2006).

5.6. Conclusions

Wildfire is increasingly recognized as a potentially important factor in regional and global carbon balance as well as radiative forcing in the atmosphere. Fire-related feedbacks to climate change can also be expected to occur through climate-induced impacts on vegetation structure and distribution and on fire regimes. While uncertainties remain in estimates of the level of emissions from wildfire, it is clear that global wildfire emissions are in the same order of magnitude as those from burning fossil fuels or clearing forests for agriculture. Therefore, interannual variability in burned area or changes over time in the average annual burned area or in fire severity can be expected to significantly impact overall global emissions of carbon to the atmosphere. While most of the emissions from fire are in the form of CO_2, fires also produce substantial amounts of CO, methane, carbon particulates, and other compounds that have stronger radiative forcing effects than CO_2. It is critical to consider these effects in evaluating the feedbacks between fire and changing fire regimes and climate.

The processes we must quantify to predict how wildfire will affect terrestrial *carbon stocks* are complex: fuel (carbon) consumption and fire emissions, composition of smoke, decomposition processes, soil respiration, rates of vegetation recovery, and the respective interactions of all these factors. The outcome is not as predictable as a simple increase in burning with warming that translates into more wildfire and carbon emissions. Instead, the local nature of wildfire and of ecological responses by vegetation must be understood, quantified, and modelled through research carried out at a range of scales and using a range of methods. To predict outcomes will require good field data on the range and variability of fire processes, fire effects, and fire/climate interactions in different ecosystems. The accuracy and value of modelling the climate-fire-carbon (interactions) system can be greatly improved with better understanding of ecosystem-specific responses, comprehensive data for parameterizing models, and site-specific data for evaluating their predictions.

The estimates of burned area available in the literature vary widely (Table 5.1), but accuracy is increasing as interpretations from satellite data are improved and validated. Accurate data on burned areas, their location, and the burn severity or fuel consumption for different fires are essential to improving these estimates.

Changes in burn severity can result in large differences in the amount of fuel consumed and in the capacity of the ecosystem to recover carbon rapidly after a fire. Recent work also indicates that even surface fire may cause significant changes in soil respiration—these changes can either increase or decrease the net effects of fire on atmospheric carbon. Postfire recovery to a different vegetation type—which may occur in response to changing climate, invasive species, unusually high burn severities, or other factors—also has the potential to affect the amount of carbon storage on the landscape. Past and future vegetation management and fire management activities also play a role in ecosystem condition and carbon storage, although the nature and magnitude of these impacts is a source of considerable debate.

In some years and in some regions, the carbon emissions from wildfire can exceed those from all fossil fuel sources combined. General circulation models predict that climate will get warmer and as a result, fire hazard and severity will increase over much of the globe. Studies and modelling efforts published over the past several years indicate that, especially in the boreal zone and some tropical areas, changing climate is likely to increase the extent and frequency of wildfires. As fire regimes change, we can expect that fires will be more resistant to suppression, that burned areas will increase, and that emissions per unit area will go up. As fires become more frequent, we can expect that carbon storage in terrestrial ecosystems will decrease over time.

All of this is important information to consider in evaluating the regional and global effects of wildfire on carbon stocks and on atmospheric carbon compounds. Most importantly, the intensity of feedbacks between fire and climate will depend not only on changes in the area that is burned annually, but on how those fires burn and on how the ecosystems respond and recover after the fires.

Improved understanding of the effects of changing fire regimes on all aspects of the carbon cycle is needed before we can fully predict the magnitude, or even the direction, of the effect of changing fire regimes on global carbon balance.

As a result of the uncertainties in these processes, we can define certain key research needs relative to interactions between wildfire and carbon as:

- Better historical and current data on burned area and on fire severity to help researchers analyze patterns in the past and to better project how fire regimes may change in the future.
- Improved regional projections of potential changes in climate from which to calculate changes in fire regime and in expected fuel loadings.
- Continued development of remote sensing methods to the point that they accurately measure wildfire energy release from flaming fronts and residual or smoldering combustion under the broad range of burning conditions that occur in many ecosystems.
- Increased understanding of the balance between carbon uptake and carbon emission through soil respiration over the fire cycle.
- Much greater understanding of the overall impacts of fire on radiative forcing so that the effects on the global climate of even very accurate predictions of future wildfire distributions and intensities can be assessed.
- Continued improvement of wildfire-vegetation models to validate model outputs and burned area algorithms, especially those based on analysis of remote sensing data.

ACKNOWLEDGMENTS

We thank two anonymous reviewers, whose comments greatly improved this chapter. We gratefully acknowledge financial support of the National Aeronautics and Space Administration Land Cover Land Use Change Science Program for Conard's research in Siberia, as well as the many fruitful discussions with collaborators in Russia, Canada, and the United States that fostered development of concepts presented in this chapter. Thanks to Douglas McRae and Tom Blake for developing an earlier version of the graphic in Fig. 1.

REFERENCES

Abrams, M.D., Knapp, A.K., and Hulbert, L.C. 1986. A ten-year record of aboveground biomass in a Kansas tallgrass prairie: Effects of fire and topographic position. American Journal of Botany, 73, 1509–1515.

Agee, J.K. 1993. Fire ecology of Pacific Northwest Forests. Island Press, Covelo, CA, 493 pp.

Agee, J.K. 1998. The landscape ecology of western fire regimes. Northwest Sci. 72, 24–34.

Amiro, B.D., MacPherson, J.I., Desjardins, R.L., Chend, J.M., and Liu, J. 2003. Post-fire carbon dioxide fluxes in the western Canadian boreal forest: Evidence from towers, aircraft and remote sensing. Agric. For. Meteorol. 115, 91–107.

Andersson, M., Michelsen, A., Jensen, M., and Kjøller, A. 2004. Tropical savannah woodland: Effects of experimental fire on soil microorganisms and soil emissions of carbon dioxide. Soil Biol. Biochem. 36, 849–858.

Arellano, A.F. Jr., Kasibhatla, P.K., Giglio, L., van der Werf, G.R., and Randerson, J.T. 2004. Top-down estimates of global CO sources using MOPITT measurements. Geophys. Res. Lett. 31(L01104), 5.

Bachelet, D., Lenihan, J., Neilson, R., Drapek, R., and Kittel, T. 2005. Simulating the response of natural ecosystems and their fire regimes to climatic variability in Alaska. Can. J. For. Res. 35, 2244–2257.

Baeza, M.J., De Luís, M., Raventós, J., and Escarré, A. 2002. Factors influencing fire behaviour in shrublands of different stand ages and the implications for using prescribed burning to reduce wildfire risk. J. Environ. Manage. 65, 199–208.

Bala, G., Caldeira, K., Wickett, M., Phillips, T.J., Lobell, D.B., Delire, C., and Mirin, A. 2007. Combined climate and carbon-cycle effects of large-scale deforestation. Proc. Nat. Acad. Sci. 104, 6550–6555.

Baker, S.P., and Bogorodskaya, A. 2007. The effect of fire on soil respiration rates in Siberia Scotch Pine Forest. EOS Trans., AGU, 88(52), Fall Meet. Suppl., Abstract B43D-1589.

Balzter, H., Gerard, F.F., George, C.T., Rowland, C.S., Jupp, T.E., McCallum, I., Shvidenko, A., Nilsson, S., Sukhinin, A., Onuchin, A., and Schmullius, C. 2005. Impact of the arctic oscillation pattern on interannual forest fire variability in Central Siberia. Geophys. Res. Lett. 32, L14709.

Barbosa, P.M., Cardoso Pereira, J.M., and Gregoire, J.-M. 1998. Compositing criteria for burned area assessment using multitemporal low resolution satellite data. Remote Sens. Environ. 65, 38–49.

Birdsey, R.A., and Lewis, G.M. 2003. Carbon in U.S. forests and wood products, 1987–1997: State-by-state estimates. USDA Forest Service, N.E. Res. Sta., Gen. Tech. Rep., NE-310, 42 p.

Bolin, B., and Sukumar, R. 2000. Global perspective. Ch. 1. In: Watson, R.T., I.R. Noble, B. Bolin, N.H. Ravindrath, D.J. Verardo, and D.J. Dokken, eds. Land use, land-use change, and forestry, Special Report of the Intergovernmental Panel on Climate Change. Cambridge University Press, Cambridge, England, pp. 23–51.

Bonan, G., Pollard, D., and Thompson, S.L. 1992. Effects of boreal forest vegetation on global climate. Nature 359, 716–718.

Bousquet, P., Ciais, P., Miller, J.B., Dlugokencky, E.J., Hauglustaine, D.A., Prigent, C., Van der Werf, G.R., Peylin, P., Brunke, E.-G., Carouge, C., Langenfelds, R.L., Lathiere, J., Papa, F., Ramonet, M., Schmidt, M., Steele, L.P., Tyler, S.C., and White, J. 2006. Contribution of anthropogenic and natural sources to atmospheric methane variability. Nature 443, 439–443.

Brown, J.K., and Smith, J.K., eds. 2000. Wildland fire in ecosystems: Effects of fire on flora. USDA For. Serv., Rocky Mountain Research Station, Ogden, UT., Gen. Tech. Rep., RMRS-GTR-42, vol. 2, 257 p.

Brown, T.J., Hall, B.L., and Westerling, A.L. 2004. The impact of twenty-first century climate change on wildland fire danger in the western United States: An applications perspective. Clim. Change 62, 365–388.

Brumme, R., and Borken, W. 1999. Site variation in methane oxidation as affected by atmospheric deposition and type of temperate forest system. Gobal Biogeochem. Cycles 13, 493–501.

Burke, R.A., Zepp, R.G., Tarr, M.A., Miller, W.L., and Stocks, B.J. 1997. Effect of fire on soil-atmosphere exchange of methane and carbon dioxide in Canadian boreal forest sites. J. Geophysical Res. 102(D24), 29289–29300.

Burrows, W.H., Henry, B.K., Back, P.V., Hoffmann, M.B., Tait, L.J., Anderson, E.R., Menke, N., Danaher, T., Carter, J.O., and McKeon, G.M. 2002. Growth and carbon stock change in eucalypt woodlands in northeast Australia: Ecological and greenhouse sink implications. Glob. Chang Biol. 8, 769–784.

Campbell, J.L., Sun, O.J., and Law, B.E. 2004. Disturbance and net ecosystem production across three climatically distinct forest landscapes. Global Biogeochem. Cycles 18(GB4017), 11.

Cochrane, M.A. 2003. Fire science for rainforests. Nature 421, 913–919.

Cochrane, M.A., and Schulze, M.D. 1999. Fire as a recurrent event in tropical forests of the Eastern Amazon: Effects on forest structure, biomass, and species composition. Biotropica 31, 2–16.

Conrad, R. 1996. Soil microorganisms as controllers of atmospheric trace gases (H_2, CO, CH_4, OCS, N_2O, and NO). Microbiol. Rev. 60, 609–640.

Conard, S.G., and Ivanova, G.A. 1997. Wildfire in Russian boreal forests—potential impacts of fire regime characteristics on emissions and global carbon balance estimates. Environ. Pollut. 98, 305–313.

Conard, S.G., Sukhinin, A.I., Stocks, B.J., Cahoon, D.R. Jr., Davidenko, E.P., and Ivanova, G.A. 2002. Determining effects of area burned and fire severity on carbon cycling and emissions in Siberia. Clim. Change 55, 197–211.

Conard, S.G., Sukhinin, A.I., Ivanova, G.A., Hao, W.M., and McRae, D.J. 2004. Modeling and monitoring effects of area burned and fire severity on carbon cycling, emissions, and forest health and sustainability in Central Siberia: February 2004 Progress Report, 36 p. http://lcluc.umd.edu/products/pdfs/2003AnPrgRp/AnPrgRp_ConardS_2003.pdf.

Crutzen, P.J., and Andreae, M.O. 1990. Biomass burning in the tropics: Impact on atmospheric chemistry and biogeochemical cycles. Science 250, 1669–1678.

Crutzen, P.J., Heidt, L.E., Krasnec, J.P., Pollock, W.H., and Seiler, W. 1979. Biomass burning as a source of atmospheric gases CO, H_2, N_2O, NO, CH_3Cl and COS. Nature 282, 253–356.

Damoah, R., Spichtinger, N., Forster, C., James, P., Mattis, I., Wandinger, U., Beirle, S., Wagner, T., and Stohl, A. 2004. Around the world in 17 days—hemispheric-scale transport of forest fire smoke from Russia in May 2003. Atmos. Chem. Phys. 4, 1311–1321.

Dezzeo, N., and Chacon, N. 2005. Carbon and nutrient loss in aboveground biomass along a fire induced forest-savanna gradient in the Gran Sabana, southern Venezuela. For. Ecol. Manage. 209, 343–352.

Dixon, R.K., and Krankina, O.N. 1993. Forest fires in Russia: Carbon dioxide emissions to the atmosphere. Can. J. For. Res. 23, 700–705.

Dixon, R.K., Brown, S., Houghton, R.A., Solomon, A.M., Trexler, M.C., and Wisniewski, J. 1994. Carbon pools and flux of global forest ecosystems. Science 263, 185–190.

Dlugokencky, E.J., Walter, B.P., Masarie, K.A., Lang, P.M., and Kasischke, E.S. 2001. Measurements of an anomalous global methane increase during 1998. Geophys. Res. Lett. 28, 499–502.

Fiedler, S., Holl, B.S., and Jungkunst, H.F. 2005. Methane budget of a black forest spruce ecosystem considering soil pattern. Biogeochemistry 76, 1–20.

Fishman, J. 1991. Identification of widespread pollution in the Southern Hemisphere deduced from satellite analysis. Science 252, 1693–1696.

Flannigan, M.D., Bergeron, Y., Engelmark, O., and Wotton, B.M. 1998. Future wildfire in circumboreal forests in relation to global warming. J. Vegetation Sci. 9, 469–476.

Fosberg, M.A., Stocks, B.J., and Lynham, T.J. 1996. Risk analysis in strategic planning: Fire and climate change in the boreal forest. In: Goldammer, J.G., and Furyaev, V.V., eds. Fire in ecosystems of Boreal Eurasia. Kluwer Academy Publisher, Norwell, MA, pp. 481–494.

Fraser, R.H., Li, Z., and Cihlar, J. 2000. Hotspot and NDVI differencing synergy (HANDS): A new technique for burned area mapping over boreal forest. Remote Sens. Environ. 74, 362–376.

French, N.H., Goovaerts, F.P., and Kasischke, E.S. 2004. Uncertainty in estimating carbon emissions from boreal forest fires. J. Geophys. Res. 109, D14S08.

Fromm, M., Alfred, J., Hoppel, K., Hornstein, J., Bevilacqua, R., Shettle, E., Servranckx, R., Li, Z.Q., and Stocks, B. 2000. Observations of boreal forest fire smoke in the stratosphere by POAM III, SAGE II, and LIDAR in 1998. Geophys. Res. Lett. 27, 1407–1410.

Giglio, L., van der Werf, G.R., Randerson, J.T., Collatz, G.J., and Kasibhatla, P. 2006. Global estimation of burned area using MODIS active fire observations. Atmos. Chem. Phys. 6, 957–974.

Gulledge, J., and Schimel, J.P. 2000. Controls on soil carbon dioxide and methane fluxes in a variety of taiga forest stands in interior Alaska. Ecosystems 3, 269–282.

Hao, W.M., and Liu, M.-H. 1994. Spatial and temporal distribution of tropical biomass burning. Global Biogeochem. Cycles 8, 495–504.

Heath, L.S., Smith, J.E., and Birdsey, R.A. 2003. Carbon trends in U.S. forestlands: A context for the role of soils in forest carbon sequestration. Ch. 3, In: Kimble, J.M., Heath, L.S., Birdsey, R.A., and Lal, R., eds. The potential of U.S. forest soils to sequester carbon and mitigate the greenhouse effect. CRC Press, pp. 35–45.

Heinselman, M.L., 1981. Fire intensity and frequency as factors in the distribution and structure of northern ecosystems. In: Mooney, H.A., Bonniksen, J.M., Christensen, N.L., Lotan, J.E., and Reiners, W.A., eds. Fire regimes and Ecosystem Properties. USDA Forest Service, Washington, DC, General Technical Report WO-26, pp. 7–57.

Hoelzemann, J.J., Schultz, M.G., Brasseur, G.P., Granier, C., and Simon, M. 2004. Global wildland fire emission model (GWEM): Evaluating the use of global area burnt satellite data. J. Geophys. Res. 109(D14S04), 18.

Hoffa, E.A., Ward, D.E., Hao, W.M., Susott, R.A., and Wakimoto, R.H. 1999. Seasonality of carbon emissions from biomass burning in a Zambian savanna. J. Geophys. Res. 104(D11), 13,841–13,853.

IPCC (Intergovernmental Panel on Climate Change). 2007. Climate Change 2007: The physical science basis. Summary for policymakers. IPCC Secretariat, Geneva Switzerland, 18 p.

Ito, A., and Penner, J.E. 2004. Global estimates of biomass burning based on satellite imagery for the year 2000. J. Geophys. Res. 109, D14S05.

Kajii, Y., Kato, S., Streets, D.G., Tsai, N.Y., Shvidenko, A., Nilsson, S., McCallum, I., Minko, N.P., Abushenko, N., Altyntsev, D., and Khodzer, T.V. 2002. Boreal forest fires in Siberia in 1998: Estimation of area burned and emissions of pollutants by advanced very high resolution radiometer satellite data. J. Geophys. Res. 107, D244745.

Kashian, D.M., Romme, W.H., Tinker, D.B., Turner, M.G., and Ryan, M. 2006. Carbon storage on landscapes with stand replacing fires. Bioscience 56, 598–606.

Kasischke, E.S., Christensen, N.L., and Stocks, B.J. 1995. Fire, global warming, and the carbon balance of boreal forests. Ecol. Appl. 5, 437–451.

Kasischke, E.S., Hyer, E.J., Novelli, P.C., Bruhwiler, L.P., French, N.H.F., Sukhinin, A.I., Hewson, J.H., and Stocks, B.J. 2005. Influences of boreal fire emissions on Northern Hemisphere atmospheric carbon and carbon monoxide. Global Biogeochem. Cycles 19(GB1012), 16.

Kaye, J.P., and Hart, S.C. 1998. Restoration and canopy-type effects on soil respiration in a ponderosa pine-bunchgrass ecosystem. Soil Sci. Soc. Am. J. 62, 1062–1072.

Key, C.H. 2006. Ecological and sampling constraints on defining landscape fire severity. Fire Ecol. 2, 34–59.

Kitzberger, T.P., Brown, M., Heyerdahl, E.K., Swetnam, T.W., and Veblen, T.T. 2007. Contingent Pacific-Atlantic Ocean influence on multicentury wildfire synchrony over western North America. Proc. Natl. Acad. Sci. 104, 543–548.

Knapp, A.K., Conard, S.L., and Blair, J.M. 1998. Determinants of soil CO_2 flux from a subhumid grassland: Effect of fire and fire history. Ecol. Appl. 8, 760–770.

Kurz, W.A., and Apps, M.J. 1999. A 70-year retrospective analysis of carbon fluxes in the Canadian forest sector. Ecol. Appl. 9, 526–547.

Kurz, W.A., Apps, M.J., Stocks, B.J., and Volney, W.J.A. 1995. Global climate change: Disturbance regimes and biospheric feedbacks of temperate and boreal forests. In: Woodwell, G.M., and MacKenzie, F.T., eds. Biotic feedbacks in the global climate system: Will the warming feed the warming? Oxford University Press, New York, pp. 119–133.

Lavorel, S., Flannigan, M.D., Lambin, E.F., and Scholes, M.C. 2007. Vulnerability of land systems to fire: Interactions among humans, climate, the atmosphere, and ecosystems. Mitig Adapt. Strat. Glob. Change 12, 33–53.

Leenhouts, B. 1998. Assessment of biomass burning in the conterminous United States. Conserv. Ecol. [online] 2(1), 1. http://www.consecol.org/vol2/iss1/art1/

Logan, J.A., Regniere, J., and Powell, J.A. 2003. Assessing the impacts of global warming on forest pest dynamics. Front. Ecol. Environ. 1, 130–137.

Marland, G., Boden, T.A., and Andres, R.J., 2007. Global, regional, and national CO_2 emissions. In trends: A compendium of data on global change. Carbon Dioxide Information Analysis Center, Oak Ridge National Laboratory, U.S. Department of Energy, Oak Ridge, Tenn., U.S.A. http://cdiac.ornl.gov/trends/emis/tre_glob.htm

McRae, D.J., Jin, J.-Z., Conard, S.G., Sukhinin, A.I., Ivanova, G.A., and Blake, T.W. 2005. Infrared characterization of fine-scale variability in behavior of boreal forest fires. Can. J. For. Res. 35, 2194–2206.

McRae, D.J., Conard, S.G., Ivanova, G.A., Sukhinin, A.I., Baker, S.P., Samsonov, Y.N., Blake, T.W., Ivanov, V.A., Ivanov, A.V., Churkina, T.V., Hao, W.M., Koutzenogij, K.P., and Kovaleva, N. 2006. Variability of fire behavior, fire effects, and emissions in Scotch pine forests of Central Siberia. Mitig. Adapt. Strat. Glob. Change Biol. 11, 1381–2386.

Morgan, P., Hardy, C.C., Swetnam, T.W., Rollins, M.G., and Long, D.G. 2001. Mapping fire regimes across time and space: Understanding coarse and fine-scale fire patterns. Int. J. Wildland Fire 10, 329–342.

Nepstad, D., Lefebvre, P., Da Silva, U.L., Tomasella, J., Schlesinger, P., Solorzano, L., Moutinho, P., Ray, D., and Benito, J.G. 2004. Amazon drought and its implications for forest flammability and tree growth: A basin-wide analysis. Glob. Change Biol. 10, 704–717.

O'Neill, K.P., Kasischke, E.S., and Richter, D.D. 2002. Environmental controls on soil CO_2 flux following fire in black spruce, white spruce, and aspen stands of interior Alaska. Can. J. For. Res. 32, 1525–1541.

Ottmar, R.D., Burns, M.F., Hall, J.N., and Hanson, A.D. 1993. CONSUME Users Guide. USDA Forest Service, Pacific Northwest Research Station, Portland, OR. Gen. Tech. Rep. PNW-GTR-304.

Overpeck, J.T., Rind, D., and Goldberg, R. 1990. Climate-induced changes in forest disturbance and vegetation. Nature 343, 51–53.

Page, S.E., Siegert, F., Rieley, J.O., Boehm, H.-D.V., Jayak, A., and Limin, S. 2002. The amount of carbon released from peat and forest fires in Indonesia during 1997. Nature 420, 61–65.

Park, R.J., Jacob, D.J., Chin, M., and Martin, R.V. 2003. Sources of carbonaceous aerosols over the United States and implications for natural visibility. J. Geophys. Res. 108(D12), 4355.

Pyne, S.J., Andrews, P.L., and Laven, R.D. 1996. Introduction to wildland fire. Wiley, 769 p.

Randerson, J.T., Liu, H., Flanner, M.G., Chambers, S.D., Jin, Y., Hess, P.G., Pfister, G., Mack, M.C., Treseder, K.K., Welp, L.R., Chapin, F.S., Harden, J.W., Goulden, M.L., Lyons, E., Neff, J.C., Schuur, E.A.G., and Zender, C.S. 2006. The impact of boreal forest fire on climate warming. Science 314, 1130–1132.

Reinhardt, E.D., Keane, R.E., and Brown, J.K., 1997. First order fire effects model: FOFEM 4.0, User's Guide. USDA For. Serv., Intermountain Research Station, Ogden, UT. Gen. Tech. Rep. INT-GTR-344, 65 p.

Riggan, P.J., Tissell, R.G., Lockwood, R.N., Brass, J.A., Raposo-Pereira, J.A., Miranda, H.S., Miranda, A.C., Campos, T., and Higgins, R. 2004. Remote measurement of energy and carbon flux from wildfires in Brazil. Ecol. Appl. 14, 855–872.

Roy, D.P., Lewis, P.E., and Justice, C.O. 2002. Burned area mapping using multi-temporal moderate spatial resolution data—a bi-directional reflectance model-based expectation approach. Remote Sens. Environ. 83, 263–286.

Roy, D.P., Jin, Y., Lewis, P.E., and Justice, C.O. 2005. Prototyping a global algorithm for systematic fire-affected area mapping using MODIS time series data. Remote Sens. Environ. 97, 137–162.

Ryan, K.C. 2002. Dynamic interactions between forest structure and fire behavior in boreal ecosystems. Silva Fennica 36, 13–39.

Sandberg, D.V., Ottmar, R.D., Peterson, J.L., and Core, J. 2002. Wildland fire in ecosystems: Effects of fire on air. USDA For. Serv. Rocky Mountain Research Station, Ogden, UT. Gen. Tech. Rep. RMRS-GTR-42, 5, 79.

Sannikov, S.N., and Goldammer, J.G. 1996. Fire ecology of pine forest of northern Eurasia. In: Goldammer, J.G., and Furyaev, V.V., eds. Fire in ecosystems of Boreal Eurasia. Kluwer Academic Publishers, Netherlands, pp. 151–167.

Sawamoto, T., Hatano, R., Yajima, T., Takahashi, K., and Isaev, A.P. 2000. Soil respiration in Siberian taiga ecosystems with different histories of forest fire. Soil Sci. Plant Nutr. 46, 31–42.

Schimel, D., and Baker, D. 2002. Carbon cycle: The wildfire factor. Nature 420, 29–30.

Schmidt, K.M., Menakis, J.P., Hardy, C.C., Hann, W.J., and Bunnell, D.L. 2002. Development of coarse-scale spatial data for wildland fire and fuel management. USDA For. Serv. Rocky Mountain Research Station, Fort Collins, CO. Gen. Tech. Rep. RMRS-GTR-87, 41 p.+CD.

Schoennagel, T., Veblen, T.T., and Romme, W.H. 2004. The interaction of fire, fuels, and climate across Rocky Mountain Forests. BioScience 54, 661–676.

Seager, R., Ting, M., Held, I., Kushnir, Y., Lu, J., Vecchi, G., Huang, H.-P., Harnik, N., Leetmaa, A., Lau, N.-C., Li, C., Velez, J., and Naik, N. 2007. Model projections of an imminent transition to a more arid climate in Southwestern North America. Science 316, 1181–1184.

Seiler, W., and Crutzen, P.J. 1980. Estimates of gross and net fluxes of carbon balance between the biosphere and the atmosphere from biomass burning. Clim. Change 2, 207–247.

Shvidenko, A.Z., and Nilsson, S. 2000. Fire and the carbon budget of Russian forests. In: Kasischke, E.S., and Stocks, B.J., eds. Fire, climate change, and carbon cycling in the boreal forest. Springer-Verlag, New York, pp. 289–311.

Shvidenko, A., and Nilsson, S. 2003. A synthesis of the impact of Russian forests on the global carbon budget for 1961–1998. Tellus 55B, 391–415.

Singh, J.S., Singh, S., Raghubanshi, A.S., Singh, S., Kashyap, A.K., and Reddy, V.S. 1997. Effect of soil nitrogen, carbon and moisture on methane uptake by dry tropical forest soils. Plant Soil 196, 115–121.

Soja, A.J., Cofer, W.R., Shugart, H.H., Sukhinin, A.I., Stackhouse, P.W. Jr., McRae, D.J., and Conard, S.G. 2004a. Estimating fire emissions and disparities in boreal Siberia (1998–2002). J. Geophys. Res. 109(D14S06), 22.

Soja, A.J., Sukhinin, A.I., Cahoon, D.R. Jr., Shugart, H.H., and Stackhouse, P.W. Jr. 2004b. AVHRR-derived fire frequency, distribution and area burned in Siberia. Int. J. Remote Sens. 25, 1939–1960.

Sparks, J.C., Masters, R.E., Engle, D.M., and Bukenhofer, G.A. 2002. Season of burn influences fire behavior and fuel consumption in restored shortleaf pine-grassland communities. Restoration. Ecol. 10, 714–722.

Stocks, B.J., Fosberg, M.A., Lynham, T.J., Mearns, L., Wotton, B.M., Yang, Q., Jin, J.Z., Lawrence, K., Hartley, G.R., Mason, J.A., and McKenney, D.W. 1998. Climate change and forest fire potential in Russian and Canadian boreal forests. Clim. Change 38, 1–13.

Suwanwaree, P., and Robertson, G.P. 2005. Methane oxidation in forest, successional, and no-till agricultural ecosystems: Effects of nitrogen and soil disturbance. Soil Sci. Soc. Am. J. 69, 1722–1729.

Swetnam, T.W., and Baisan, C.H. 1996. Historical fire regime patterns in the southwestern United States since AD 1700. In: Allen, C.D., ed. Fire effects in southwestern forests. USDA For. Serv. Rocky Mountain Research Station, Ogden, CO. Gen. Tech. Rept. RM-GTR-286, pp. 11–32.

Swetnam, T.W., and Betancourt, J.L. 1990. Fire–southern oscillation relations in the southwestern United States. Science 249, 1017–1020.

Swetnam, T.W., and Betancourt, J.L. 1998. Mesoscale disturbance and ecological response to decadal climatic variability in the American southwest. J. Clim. 11, 3128–3147.

Tchebakova, N.M., Parfenova, E.I., and Soja, A.J. 2007. Potential climate-induced vegetation change in Siberia during the 21st century. EOS Trans. AGU, 88(52), Fall Meet. Suppl., Abstract GC23A-0995.

Thompson, S., Govindasamy, L.B., Mirin, A., Caldeira, K., Delire, C., Milovich, J., Wickett, M., and Erickson, D. 2004. Quantifying the effects of CO_2-fertilized vegetation on future global climate and carbon dynamics. Geophys. Res. Lett. 31, L23211.

Turner, M.G., Tinker, D.B., Romme, W.H., Kashian, D.M., and Litton, C.M. 2004. Landscape patterns of sapling density, leaf area, and aboveground net primary production in postfire lodgepole pine forests, Yellowstone National Park (USA). Ecosystems 7, 751–775.

van der Werf, G.R., Randerson, J.T., Collatz, G.J., Giglio, L., Kasibhatla, P.S., Arellano, A.F., Olsen, S.C., and Kasischke, E.S. 2004. Continental-scale partitioning of fire emissions during the 1997 to 2001 el Niño/la Niña period. Science 303, 73–76.

van der Werf, G.R., Randerson, J.T., Giglio, L., Collatz, G.J., Kasibhatla, P.S., and Arellano, A.F. Jr. 2006. Interannual variability in global biomass burning emissions from 1997 to 2004. Atmos. Chem. Phys. 6, 3423–3441.

Westerling, A.L., Hidalgo, H.G., Cayan, D.R., and Swetnam, T.W. 2006. Warming and earlier spring increase in western U.S. forest wildfire activity. Science 313, 940–943.

Wiedinmyer, C., Quayle, B., Geron, C., Belote, A., McKenzie, D., Zhang, X., O'Neill, S., and Wynne, K.K. 2006. Estimating emissions from fires in North America for air quality modeling. Atmos. Environ. 40, 3419–3432.

Wirth, C., Czimczik, C.I., and Schulze, E.-D. 2002a. Beyond annual budgets: Carbon flux at different temporal scales in fire-prone Siberian Scots pine forests. Tellus B 54, 611–630.

Wirth, C., Schulze, E.-D., Luhker, B., Grigoriev, S., Siry, M., Hardes, G., Ziegler, W., Backor, M., Bauer, G., and Vygodskaya, N.N. 2002b. Effect of fire and site type on the long-term carbon and nitrogen balance in pristine Siberian Scots pine forests. Plant Soil 242, 41–63.

Wooster, M.J. 2002. Small-scale experimental testing of fire radiative energy for quantifying mass combusted in natural vegetation fires. Geophys. Res. Lett. 29, 2027.

Wooster, M.J., Zhukov, B., and Oertel, D. 2003. Fire radiative energy for quantitative study of biomass burning: Derivation from the BIRD experimental satellite and comparison to MODIS fire products. Remote Sens. Environ. 86, 83–107.

Wotawa, G., and Trainer, M. 2000. The influence of Canadian forest fires on pollutant concentrations in the United States. Science 288, 324–328.

Wotton, B.M., and Flannigan, M.D. 1993. Length of the fire season in a changing climate. For. Chron. 69, 187–192.

Wuthrich, C., Schaub, D., Weber, M., Marxer, P., and Conedera, M. 2002. Soil respiration and soil microbial biomass after fire in a sweet chestnut forest in southern Switzerland. Catena 48, 201–215.

Developments in Environmental Science, Volume 8
A. Bytnerowicz, M. Arbaugh, A. Riebau and C. Andersen (Editors)

ISSN: 1474-8177/DOI:10.1016/S1474-8177(08)00006-5

Chapter 6

Airborne Remote Sensing of Wildland Fires

Philip J. Riggan and Robert G. Tissell*

Abstract

In wildland fire management, reliable fire intelligence is needed to direct suppression resources, maintain firefighter safety, predict fire behavior, mitigate fire effects in the environment, and justify and evaluate the effectiveness of fuel management. Fire intelligence needs to be synoptic, quantitative, consistent, and timely. Airborne remote sensing with specialized infrared radiometers is now providing an unprecedented level of information on fire behavior and effects. The temperature, radiant intensity, carbon and sensible heat fluxes, and fuel consumption associated with the flaming front of a wildland fire have been estimated by remotely measuring its radiance at short- and mid-wave infrared wavelengths. Measurements of upwelling long-wave or thermal-infrared radiation provide estimates primarily of ground-surface temperatures, even beneath flaming fronts, that reflect a local time course of energy release and fuel consumption. Characteristics of flames and hot ground can be discriminated from radiances measured at wavelengths near 1.6, 3.9, and 11.9 μm. Fire radiance at 3.9 μm appears to be a good estimator of radiant-flux density, which integrates across wavelengths. There are strong temperature gradients along and within flaming fronts, and although their temperatures are high—commonly exceeding 1000°C along the line of a savanna fire, for instance—flames may not be bright when compared with a blackbody radiator. The combination of that low bulk emissivity and uncertainty as to the composition and radiance of nonfire background within the sensor's instantaneous field of view dictates that fire properties are best estimated from measurements of high spatial resolution in comparison with the scale of a fire front. The USDA Forest Service is now applying a FireMapper™ thermal-imaging radiometer for fire research and support of incident

*Corresponding author: E-mail: priggan@fs.fed.us

command teams over high-priority wildland fires, especially those threatening cities and communities in southern California. Resulting data are providing insight into fire behavior in complex and changing fuels, fire interactions with the atmosphere and a changing climate, and large-scale fire processes.

6.1. Introduction

Large wildland fires burning under high winds in highly flammable fuels and with high values at risk—such as during the October 2007 fire emergency in southern California—demand sophisticated monitoring and communication of fire activity and spread. For tactical firefighting in such situations, reliable fire intelligence and an ability to understand and predict fire behavior are needed to effectively deploy resources—engines, personnel, and aircraft; to keep firefighters safe; and to tailor the allocation of resources to the fire, reducing the need to commit more resources than necessary and reducing costs of suppression. After the emergency, data on fire severity are needed to mitigate fire effects in the environment. On a strategic level, an ability to accurately predict fire behavior is requisite to design, justify, and evaluate approaches for fire management, including landscape-scale fuel treatments.

Modern remote sensing can supply the intelligence needed for fire management and the data required for understanding and modeling fire behavior and effects in the environment. Frequent, high-resolution remote sensing at infrared wavelengths can track fire-line rate of spread and acceleration, the location and rates of spotting ahead of a fire front, and structure ignition in residential communities. Together with global positioning system (GPS)-based asset tracking, remote sensing could improve firefighter safety by showing incident commanders the spatial relation of firefighters and equipment to the fire, and especially to regions of high fire intensity or activity. High-resolution imaging also has the potential to accurately quantify large-fire energy release or intensity, residence time, fuel consumption rate, carbon emissions, and soil heating (Riggan & Hoffman, 2003; Riggan et al., 2004). The challenge is to deduce meaningful and useful fire properties based on measurements of upwelling infrared radiation, which will penetrate smoke, with some attenuation depending on wavelength, but not condensed-water clouds.

At present in the United States, national airborne infrared mapping operations collect fire imagery at night with fire-perimeter maps made available for early morning briefings of the incident-management team.

Fire locations during active burning periods in daylight hours are generally known from flights by helicopter along a fire's perimeter and ad hoc ground-based observations and verbal descriptions obtained from low-level aircraft flights, both of which are hindered by obscuring smoke and terrain and a limited field of view. Perimeter maps have the disadvantage of showing where the fire has been, but not necessarily where it is active, intense, or spreading, especially if not provided in real time.

To realize the promise of infrared fire imaging, one must make the proper measurements, and infrared imagers and imaging spectrometers traditionally used for earth remote sensing typically are saturated by—and incapable of measuring—the very bright infrared light that radiates from large wildland fires (Fig. 6.1). Thus, they provide a limited or even

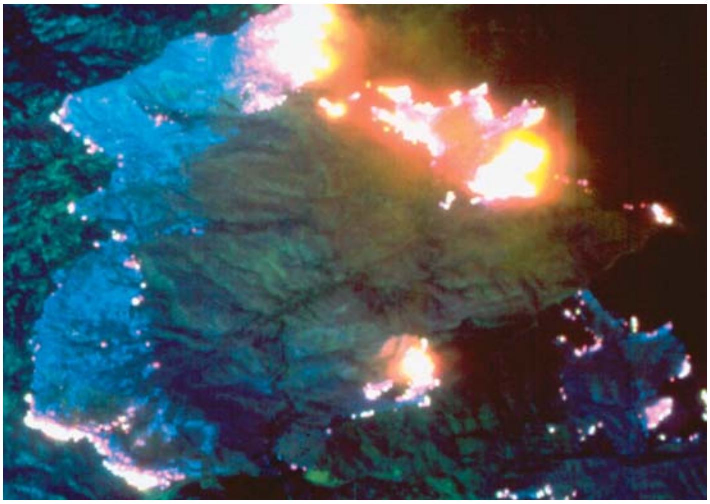

Figure 6.1. Color-composite infrared image of the 1985 Wheeler Fire, Los Padres National Forest, as viewed by the NASA Thematic Mapper Simulator aboard a high-altitude ER-2 aircraft (image courtesy of J.A. Brass, NASA Ames Research Center). In this depiction, using infrared channels nominally at 1.65-, 2.0-, and 8–12.5-μm wavelength, the fire line is comprised of an 8-km-long segment on the north, which generated a large plume reaching to over 19,000 ft altitude (top); burning in a riparian area (lower left); an inactive line (on the west); and a recent backfire north of Ojai, CA (lower right). Saturation of the preamplifiers in the Daedalus ADD 1268 line scanner at relatively low radiances caused a distorted view of fire activity, such as on the north where fire fronts appear to be over 1 km wide yet are likely much less than one-tenth that width. Even though the imager can map the fire through heavy smoke and show its location in terrain, it grossly distorts the magnitude of the fire activity and allows no estimates of fire intensity or impact (Riggan & Hoffman, 2003).

distorted view of fire activity. Furthermore, infrared line scanners, as currently used in fire operations in the United States, are expensive to procure and maintain, and require strong engineering support. They are typically deployed nationally, and thus may be infrequently available or unavailable to a given fire incident. Forward-looking infrared imagers designed for surveillance at common earth temperatures have also been used locally to map fire lines, but these also typically saturate at relatively low brightness values and may be even incapable of discriminating fire from warm ground or ash.

The USDA Forest Service's Pacific Southwest Research Station (PSW) and its partners, NASA Ames Research Center and Space Instruments, Inc., have developed and applied remote-sensing systems for airborne, high-resolution fire mapping and measurement. These have included an extended-dynamic-range imaging spectrometer, a line scanner operating in three regions of the infrared spectrum with channels centered at wavelengths of 1.63, 3.9, and 11.9 μm (Riggan et al., 1993, 2004), and the FireMapper™ thermal-imaging radiometer, which uses a modern micro-bolometer focal-plane array to image and measure thermal-infrared radiation at wavelengths from 8 to 12.5 μm (Riggan & Hoffman, 2003; Riggan et al., 2003).

In this chapter we will review the basis for quantifying large-fire properties by remote sensing and provide examples from airborne measurement with these instruments of fires in Mediterranean-type ecosystems in southern California and savanna and tropical forests of Brazil.

6.2. Estimating fire properties by remote sensing

6.2.1. Fire front temperatures and the emissivity-fractional area

Wildland fires present a complex remote-sensing target comprised of flaming fronts, ash, residual flaming combustion, smoldering of larger biomass elements, and unburned vegetation (Riggan et al., 2004), arrayed in a scene of complex spatial temperature gradients. Observations at high-resolution provide an opportunity of resolving these components and gradients. Low-resolution observations, as with some satellite-based sensors, such as the Moderate Resolution Imaging Spectrometer (MODIS) or Advanced Very High-Resolution Radiometer (AVHRR), will necessarily encompass radiation from a variety of these elements. In either case, atmospheric windows in the infrared, where radiation is not strongly absorbed by water vapor, dictate that observations may generally be made at wavelengths near 1.6, 2, and 4 μm in the short- and mid-wave infrared region and from 8 to 14 μm in the long-wave or thermal infrared.

To estimate fire properties by remote sensing it has been assumed that the radiant emissions from flames are primarily from entrained, glowing soot particles and that hot soot and ash approximate classic and highly efficient (or emissive) gray-body radiators whose properties are described by the Planck function (as given, e.g., by Liou (1980)). With these assumptions, the temperature, T, of a hot target within a flaming zone can be estimated by an iterative solution (Eq. 6.1) of two instances of the Planck function (referred to herein as the two-channel method), using the radiance, B, measured at each of two infrared wavelengths, λ_1 and λ_2 (Matson & Dozier, 1981; Riggan et al., 2004)

$$T = \frac{hc}{k\lambda_1 \ln\left[\left(\frac{B_2}{B_1}\right)\left(\frac{\lambda_2^5}{\lambda_1^5}\right)\left(\exp\left(\frac{hc}{k\lambda_2 T}\right) - 1\right) + 1\right]} \tag{6.1}$$

where h is the Planck constant, 6.63×10^{-34} (J.s); c is the speed of light, 3.00×10^8 (m s^{-1}); k is the Boltzmann constant, 1.38×10^{-23} (J K^{-1}); T is specified in Kelvin; λ is in meters, B_λ has units of J m^{-2} s^{-1} sr^{-1} μm^{-1}, and radiances are corrected for atmospheric transmittance and path radiance. Note that an iterative solution is required since T is found on each side of Eq. (6.1); the solution can begin with a temperature estimate (Eq. 6.2) derived from a simplification of Eq. (6.1)

$$T = \frac{hc\left(1/\lambda_2 - 1/\lambda_1\right)}{k \ln\left[(B_1\lambda_1^5/B_2\lambda_2^5)\right]} \tag{6.2}$$

A solution that converges to a temperature within 0.1 K is obtained within six iterations when wavelengths near 1.6 and 3.9 μm are used. These wavelengths are optimal for estimating flame temperatures since they fall on either side of the expected maximum in flame radiance.

The temperature and radiance at one wavelength can be used to estimate the product of the unitless *emissivity*, ε, and the *fractional area*, A_f, of the hot target within the instantaneous field of view of the sensor (Eq. 6.3)

$$\varepsilon A_f = \frac{B_i\lambda_i^5\left[\exp(hc/k\lambda_i T) - 1\right]}{2 \times 10^{-6} hc^2} \tag{6.3}$$

The latter parameter will be meaningful where the observations are of sufficient resolution that the radiance of the hot target is predominant in relation to unburned or cooled ground.

The fire's wavelength-integrated radiant-flux density, F_d (J m^{-2} s^{-1}), a measure of radiant fire intensity, can be estimated from the combined emissivity-fractional area and flame temperature as

$$F_d = \varepsilon A_f \sigma T^4 \tag{6.4}$$

where σ is the Stefan–Boltzmann constant, 5.67×10^{-8} J m^{-2} s^{-1} K^{-4}.

Riggan et al. (2004) mapped the apparent flame temperatures and radiant-flux density of large fires in Brazil by using this two-channel method and high-spatial-resolution remote-sensing observations with an extended-dynamic-range spectrometer at short- and mid-wave infrared wavelengths of 1.63 and 3.9 μm. Flame radiances at these wavelengths were sufficiently high so that contributions to the signal from reflected solar radiation could be ignored.

Among the most extensive measurements made were those of the Tapera prescribed fire on September 21, 1992, at the Reserva Ecológica of the Instituto Brasileiro de Geographia e Estatística (the Ecological Reserve of the Brazilian Institute of Geography and Statistics) in the Brazilian Federal District (Riggan et al., 2004). This fire burned within a watershed of low relief with vegetation comprised of three phases of the Cerrado ecosystem—campo cerrado, campo sujo, and campo limpo—which represent a gradient of tropical-savanna plant communities in which evergreen shrubs comprise a declining proportion of the plant cover in a grassland matrix. Biomass structure in these communities has been described by Ottmar et al. (2001).

Remote-sensing observations showed that 90% of the Tapera fire's radiant-flux density was associated with temperatures between 731°C and 1042°C with the 50th percentile for those radiant emissions associated with a temperature of 879°C. There were strong temperature gradients across and along fire lines, with temperatures at actively spreading fire fronts occasionally exceeding 1300°C (Fig. 6.2). The mean of *peak* temperatures observed along a fire front in one instance of the Tapera fire was 1050°C (SD = 108°C) with an associated emissivity-fractional area of 0.045 (SD = 0.021). Over a 40-minute course of burning, which encompassed most of the active spread by the fire, the mean radiometric fire temperature varied only from 824 to 852°C; thus a whole-fire temperature estimate, as might be obtained from low-spatial-resolution observations by satellite, would not provide much information regarding changes in fire activity. Temperature estimates from remote sensing of the fire compared favorably with temperatures measured with thermocouples in flames near the ground (Riggan et al., 2004).

Fire temperatures and radiant-flux densities associated with a fire burning in partially harvested and slashed tropical forest near Marabá,

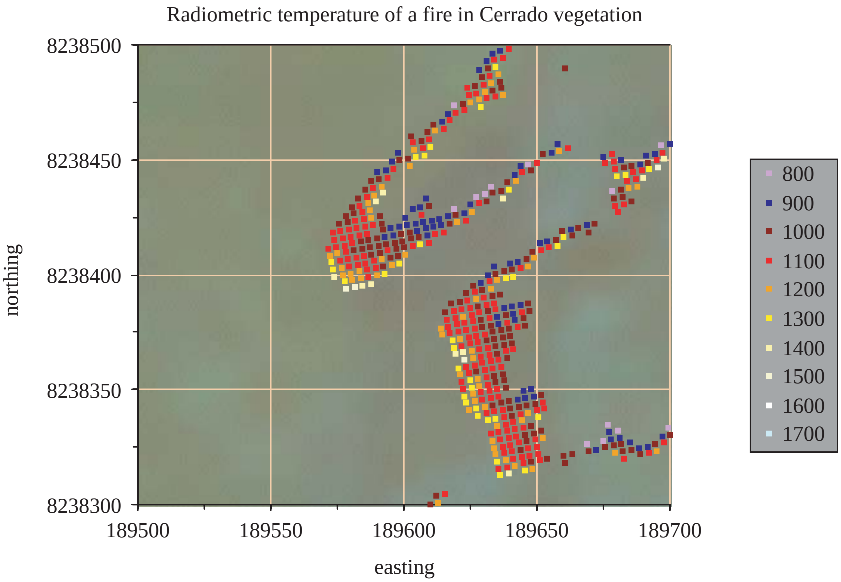

Figure 6.2. Radiometric temperatures (Kelvin) of a portion of the Tapera fire spreading in Cerrado vegetation, a form of tropical savanna, in central Brazil. Temperatures are estimated from radiances observed at 1.63- and 3.9-μm wavelengths by an extended-dynamic-range imaging spectrometer (Riggan et al., 2004). Here, fire is spreading with the wind from northeast to southwest. Temperatures are generally elevated along the leading edge of the two fire lobes and reduced behind the front and along the fire's flanks. Fire location is shown in Universal Transverse Mercator (UTM) coordinates.

Brazil, reflected a high-intensity front with extensive reaches of residual combustion of woody debris (Fig. 6.3a) (Riggan et al., 2004). The residual combustion was especially important to the overall radiant-flux density of the fire: only 17% of that measure for the slash fire was associated with temperatures greater than 800°C; 17% of the flux density from the Tapera fire was associated with temperatures *below* that value (Fig. 6.4). *Peak* temperatures, sampled at a 3.5-m interval along a 250-m flaming front spreading with low winds, had a mean value of 1021°C (SD = 284°C, $n = 250$), which was remarkably similar to that observed in the Tapera fire, which primarily burned grass.

Even though flames of Cerrado fires appeared quite hot, they were not especially bright when compared with a solid blackbody radiator. Observations from across the flaming front of the Tapera fire, for instance, showed that flames were optically thin: the mean value of the combined emissivity-fractional area was 0.091, so the radiant-flux density was on average less than one-tenth as great as that expected from a

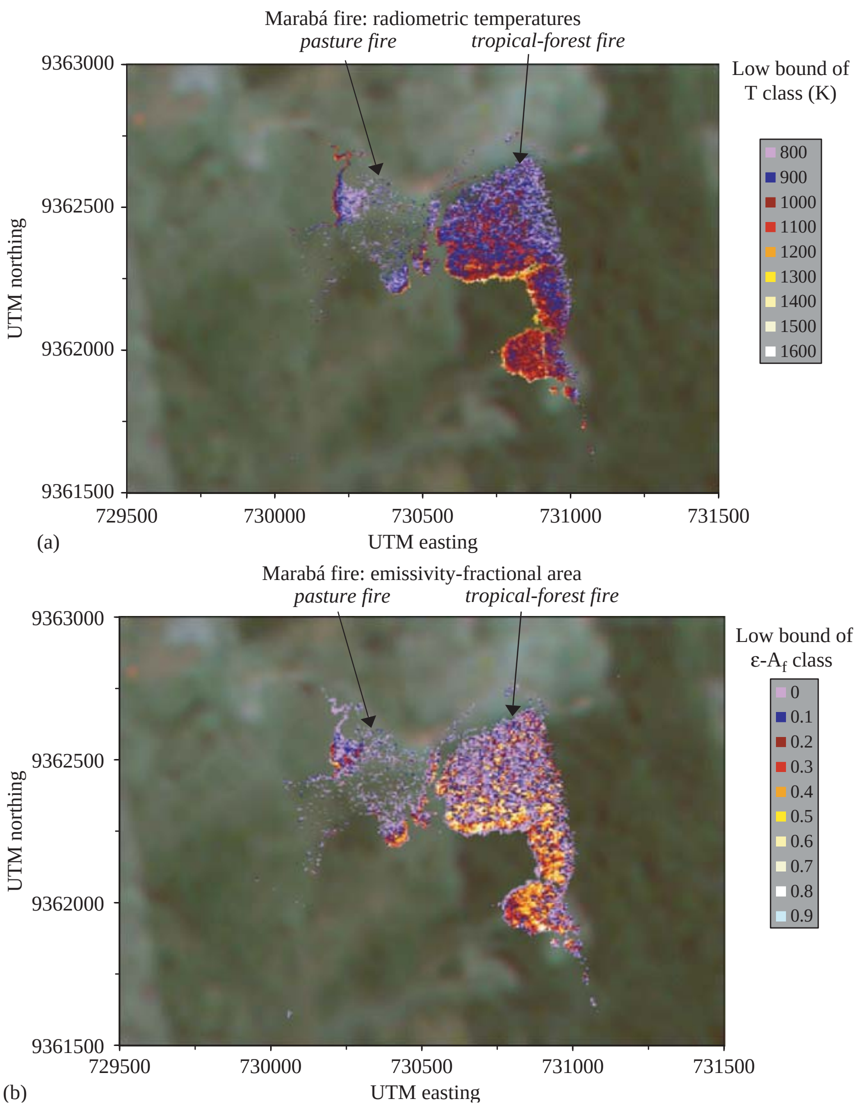

Figure 6.3. (a) Radiometric temperatures of a fire in partially slashed tropical forest and pasture in Brazil as estimated from radiances measured at 1.63- and 3.9-μm wavelengths with an extended-dynamic-range imaging spectrometer. The forest burning, which apparently consumed downed woody debris, was notable for its high-temperature front and extensive reach of cooler residual combustion. Temperatures along the fire line there were greatest where the fire spread with the northeast wind than where it generally spread to the north, unaided by the ambient wind. Tropical vegetation is shown here as imaged by the Landsat Thematic Mapper. (b) Values of the product of emissivity and fractional area for a fire as described in Fig. 6.3a. The forest burning was notable for relatively high values of the product behind the actively spreading, high-temperature, fire front. Pasture burning, west of an easting of approximately 730,600, showed moderate levels of the product at and near the fire front and very low values in residual burning in the interior of the fire area.

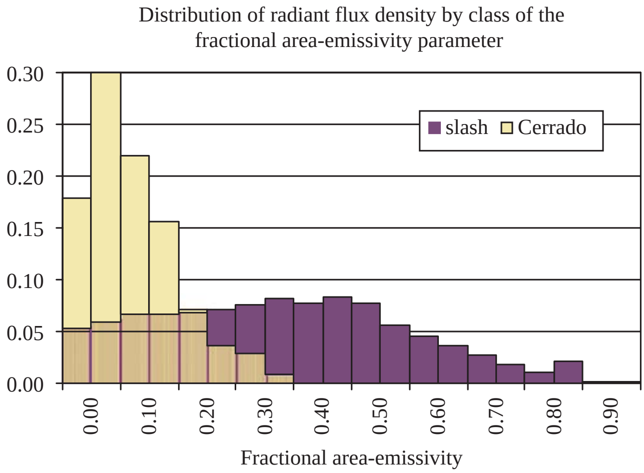

Figure 6.4. Distribution of radiant-flux density by class of the combined emissivity-fractional area for fires burning in slashed tropical forest (shown in purple) and Cerrado or tropical savanna vegetation (in yellow) in central Brazil (Riggan et al., 2004). A relatively large proportion of the emitted energy from burning in slash, which included a high-intensity fire front, was associated with large values of the emissivity-fractional area. Stippled areas in the graphic show overlap between the two histograms.

blackbody at comparable temperatures. Such a low value is suggestive that hot ash beneath a flaming front, which is expected to have an emissivity near 1.0 and is typically cooler than the peak flaming-front temperatures estimated from 1.63- and 3.9-μm radiances, may provide a substantial portion of the upwelling radiation from that front depending on the wavelength of the observation. The emissivity-fractional area observed in the Marabá slash fire obtained high values, approaching one, across a wide reach of ground behind the fire front (Fig. 6.3b).

Peak blackbody temperatures (median = 460°C, SD = 36°C) along flaming fronts in a September 19, 2000, Cerrado fire at the Reserva Ecológica, as estimated from radiances measured with the FireMapper at a *long-wave* infrared wavelength of 11.9 μm, were substantially less than those obtained from wavelengths of 1.63 and 3.9 μm at the nearby Tapera fire, which had burned in similar fuel. The long-wave radiometric temperatures were more consistent with temperatures obtained at the soil surface beneath flaming combustion in Cerrado vegetation (Miranda et al., 1996).

From these combined observations it appears that flames obtain maximum radiance in the short-wave infrared—temperatures observed in Cerrado fires correspond to a radiance peak at a wavelength of approximately 2.2 µm, and radiation from a high-emissivity, hot-ash surface, whose temperatures correspond with a peak radiance near 4 µm, dominates that from optically thin flames at long infrared wavelengths.

To demonstrate these points we modeled radiances for a Cerrado fire as follows: radiance of flames was assumed to be that of a gray-body radiator with a temperature of 1095°C and an emissivity-fractional area of 0.046, corresponding to an instance of peak fire-line temperatures estimated using measured radiances at 1.63- and 3.9-µm wavelength; the combined emissivity-fractional area of flames and subtending hot ground or ash was assumed to be 1.0; and an assumed temperature of the ash surface beneath the flames was adjusted to obtain the average peak radiometric blackbody temperature along fire lines as estimated under similar circumstances using FireMapper observations at 11.9-µm radiance in the long-wave infrared. An estimated temperature of the ground-surface beneath flames of 426°C results.

The model predicts for observations near the leading edge of a fire front in Cerrado that hot ground and ash contribute approximately 4% of the radiance at 1.63 µm; three-fifths of the radiance at 3.9 µm, and nearly nine-tenths of the radiance at 11.9 µm (Fig. 6.5). Since the 3.9-µm radiance is strongly influenced by both flames and the hot-ash surface beneath, fire temperature estimates obtained from the two-channel method of Eq. (6.1) and wavelengths of 1.63 and 3.9 µm must be influenced by both of these components as well; bulk temperature estimated by that method, 832°C, was intermediate to that of the two included model components. Radiant-flux density, $1.83 \times 10^4\,\mathrm{J\,m^{-2}\,s^{-1}}$, obtained from the bulk temperature, emissivity-fractional area, and an integration of radiance from 1 to 14 µm in this instance, was approximately nine-tenths of that obtained by integration of radiance from the two modeled components, flame, and hot ash. Thus, the two-channel method provided a modest underestimate of the radiant-flux density from the modeled system.

Because the 3.9-µm radiance of a wildland fire has substantial components from both flames and hot ash, we investigated the utility of that radiance alone in predicting the radiant-flux density of the bulk system. Whereas the 1.63-µm radiance provided only a poor predictor, the 3.9-µm radiance ($B_{3.9}$) showed a high and similar correlation with radiant-flux density (F_d) for both the Tapera and Marabá fires (Fig. 6.6). For one remote-sensing observation of the Tapera fire, linear regression with a no-intercept model gave the function $F_d = 17.87(B_{3.9})$, with $r^2 = 0.994$, $n = 712$, and the 95% confidence limit for the slope = {17.81, 17.93}, where n is the number of fire-associated pixels within the image. For the Marabá Fire, linear regression gave the function $F_d = 16.99(B_{3.9})$,

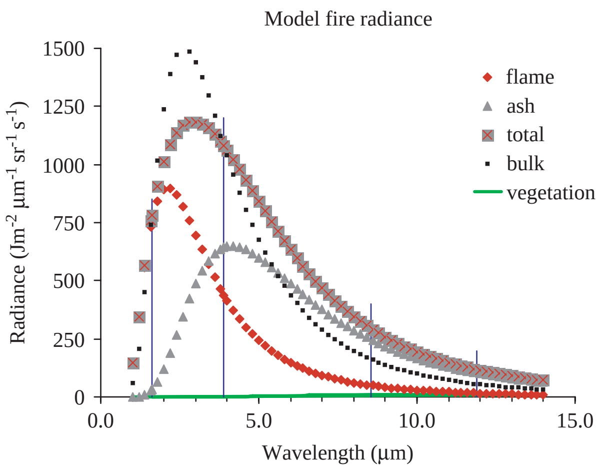

Figure 6.5. Modeled radiances ($\mathrm{J\,m^{-2}\,\mu m^{-1}\,sr^{-1}s^{-1}}$) of a fire in Cerrado or tropical savanna. Contributions from flames and hot ash are shown along with a "bulk" temperature computed from a two-channel estimator and measurements at wavelengths of 1.63 and 3.9 μm. The wavelength-integrated radiant-flux density ($\mathrm{J\,m^{-2}s^{-1}}$) for the bulk-temperature estimate is 0.89 of that obtained from the total of flame and ash radiances. The very low emitted radiance of vegetation is shown by comparison. Vertical blue bars indicate the wavelengths discussed in the text: 1.63 and 3.9 μm as measured with the NASA/Forest Service extended-dynamic-range imaging spectrometer and 8.6 and 11.9 μm as measured with the Forest Service FireMapper.

with $r^2 = 0.998$, $n = 33{,}333$, and the 95% confidence limit for the slope = {16.986, 16.998}. The small difference between the fires may be due to uncorrected differences in atmospheric transmittance involving the two channels.

6.2.1.1. A three-wavelength method

Our model of the radiances from the Tapera fire points to an improvement in the two-channel method of Eq. (6.1) in which component temperatures of flames and hot ash, emissivity-fractional area for flames, and their contributions to the upwelling radiation are estimated based on radiances measured at three wavelengths and a model where the emissivity-fractional areas of the two components sum to one (Riggan et al., 2000). The three-wavelength algorithm proceeds as follows:

1. Iteratively calculate approximate flame temperature and emissivity-fractional area using the two-channel method and observed radiances near 1.6 and 3.9 μm.

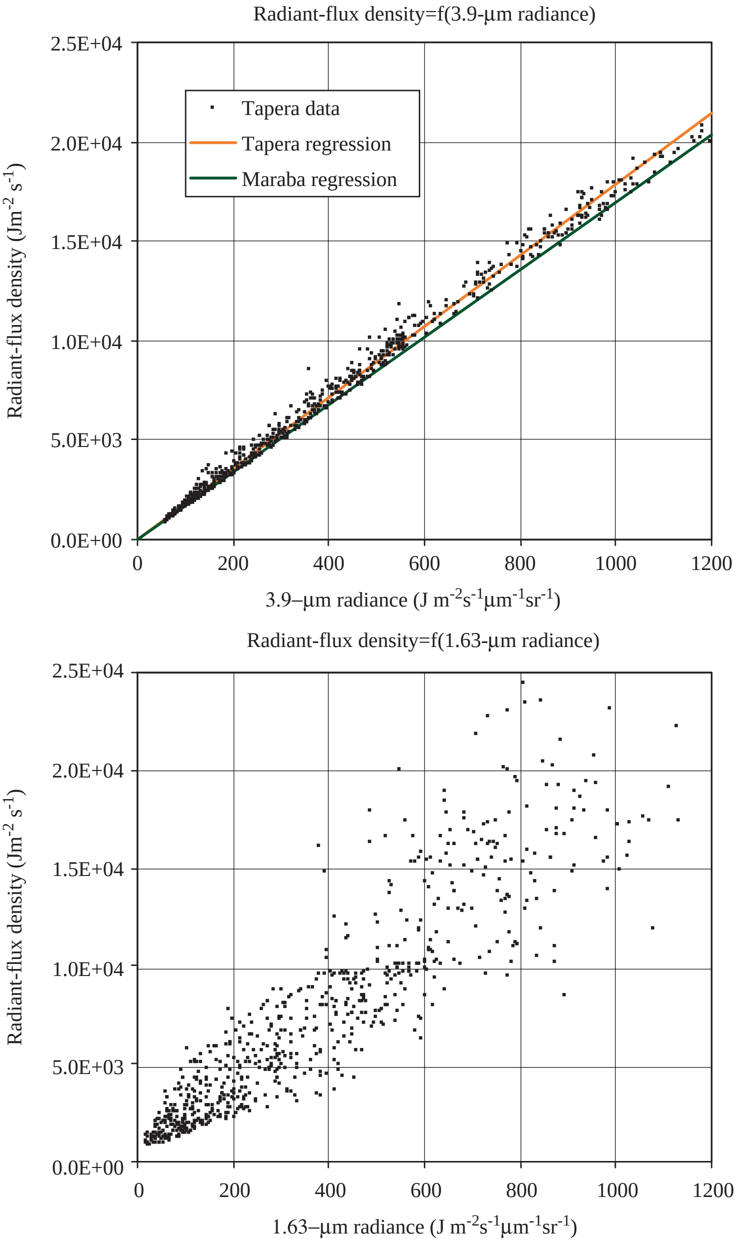

Figure 6.6. Radiant-flux density ($J\,m^{-2}\,s^{-1}$) as a function of single-channel radiances for the Tapera fire in Cerrado vegetation. The 3.9-µm radiance alone provides a good predictor of the flux density as determined by a two-channel solution for fire temperature (top). The 1.63-µm radiance (bottom) does not. The predictor based on the 3.9-µm radiance varies little with the fire situation as shown by the similarity of the two regression equations for the Cerrado and tropical forest fires (top).

2. Calculate the hot-ash or background contribution to the 11.9-μm radiance as the difference between the observed radiance and the flame radiance at that wavelength as estimated in step 1.
3. Estimate the background blackbody temperature and subtract the background contribution to radiances at 1.6 and 3.9 μm from the observed values at those wavelengths.
4. Iterate steps 1– 4 using successive estimates of flame and background radiance until stable estimates of flame temperature and emissivity-fractional area are achieved.

From the modeled two-component system above, the three-wavelength method achieves stable temperature estimates of flame and hot-ash to within 1°C within 10 iterations.

We applied the three-wavelength algorithm to a selection of data from across a fire front in Cerrado in Central Brazil (Riggan et al., 2000). In this case the measurement at 11.9 μm had a relatively low signal-to-noise ratio, so we estimated likely values for individual high-resolution point measurements based on a regression of radiance at 11.9 μm to that at 3.9 μm. The result was that estimated flame temperatures rose by an average of approximately 60°C over that estimated by two channels alone, and the mean background temperature from across the fire was estimated to be 170°C.

We conclude that high-resolution fire-radiance measurements at short- and mid-wave-infrared wavelengths describe the bulk properties of a combination of flame and hot ash, with the greatest contribution to the 1.6-μm radiance arising from flames and substantial contributions to the 3.9-μm radiance from both sources, and that partitioning the 3.9-μm radiance would be useful to account for hot background in the fire signal (Riggan et al., 2000). Measurements in the long-wave infrared, as with the FireMapper, primarily reflect the temperature of hot ash and ground beneath a flaming front.

These estimates provide useful and readily interpretable measures of fire activity that may be applied in fire management (Riggan et al., 2004; Riggan et al., 2003). Radiant-flux density from flames provides the intensity of the fire front and a measure of fuel consumption at the instant of observation, as described below. Integration with time of the radiant-flux density from the hot ground surface is expected to provide a correlative measure of fuel consumption during fire front passage.

6.2.2. Estimating fuel consumption and carbon flux to the atmosphere

Flame radiance and fire areal growth rate measured by remote sensing have provided a provisional but promising estimator for fuel consumption rate and the rates of carbon and sensible heat flux to the atmosphere (Riggan et al., 2004).

Sensible-heat and carbon fluxes from three large fires in central Brazil were estimated from *in situ* aircraft-based measurements of smoke-plume cross-sectional area and the vertical components of wind velocity, air temperature, and CO_2 mixing ratio within those plumes. Carbon and energy flux per unit area burned were estimated for one fire in Cerrado from the ratio of these whole-fire rates and the associated areal progression of the fire over time ($m^2\,s^{-1}$). The plume-based fuel consumption estimate so derived, 1.1 $kg\,m^{-2}$, compared well with nearby ground-based estimates of biomass loss during burning in somewhat lighter fuels (0.8–1.0 $kg\,m^{-2}$) (Miranda et al., 1996).

Whole-plume carbon and sensible heat fluxes were then related to *remotely sensed* flame properties by a simple model. The model set the sensible heat flux (Q_s) equal to the product of the density (ρ_{air}) and specific heat (C_p) of moist air, the eddy diffusivity of heat (K_H)—which was assumed proportional to flame temperature (T_f)—and the near-ground potential temperature gradient ($\partial\theta/\partial z$), which was taken as proportional to the difference between flame temperature and that of the overlying ambient air (T_{amb}). Thus,

$$Q_s = \rho_{air} C_p k_T T_f (T_f - T_{amb}) \tag{6.5}$$

With Q_s given in $J\,m^{-2}\,s^{-1}$, ρ_{air} in $g\,m^{-3}$, C_p in $J\,g^{-1}\,K^{-1}$, and T in K, application of the model to remote sensing observations of high-temperature, flaming combustion ($T_f > 1100\,K$) of the Tapera fire in Cerrado vegetation yielded a value of the proportionality constant $k_T = 0.0026$. When applied to observations of a free-burning fire in Cerrado vegetation at the Serra do Maranhão in the Brazilian Federal District and of the tropical-forest slash fire measured at Marabá, this remote-sensing-based model produced estimates of sensible heat flux that were consistent with *in situ* plume measurements from the two fires (Table 6.1). Furthermore, whole-plume carbon flux was strongly correlated with the flux of sensible heat (Riggan et al., 2004). Thus, the rate of fuel consumption by flaming fronts of entire large fires could be estimated from fire radiance at short- and mid-wave infrared wavelengths.

6.2.3. Satellite-based measurements of fire properties

Observations from sensors aboard the National Oceanic and Atmospheric Administration (NOAA) polar orbiting and geostationary environmental satellites and more recently from the NASA MODIS show that radiant

Table 6.1. Estimates of sensible-heat flux as derived from remotely sensed fire properties and from cross-plume airborne measurements for three wildland fires in Brazil (modified from Riggan et al., 2004)

	Cerrado		Tropical forest
	Tapera fire	Serra do Maranhão fire	Marabá slash fire
From remote sensing			
Radiant flux density ($J\,s^{-1}$) for $T > 1100\,K$	4.1×10^7	6.4×10^7	2.8×10^8
Modeled from remote sensing			
Sensible H flux ($J\,s^{-1}$) from fire radiance	8.7×10^8	*1.4×10^9*	**6.4×10^9**
From plume measurements			
Sensible H flux ($J\,s^{-1}$)	8.7×10^8	*1.4×10^9*	**6.7×10^9**

Note: Radiant-flux density is shown for comparison. A proportionality constant, $k_T = 0.0026$, from Eq. (6.5) was determined by setting the remote-sensing-based estimate for the Tapera fire equal to that from airborne measurements; the resultant model was applied to high-temperature remote-sensing data, with $T > 1100\,K$ (827°C), from the Serra do Maranhão and Marabá fires (see values in italic and bold.)

emissions of fires may be readily detected from space. These have usefully shown regions in which wildfires are common; provided a means of detecting and localizing fires; and for very large fires, identified general fire shape and reaches of active burning (Menzel & Prins, 1996; Morisette et al., 2005; Setzer & Malingreau, 1996). Quantitative measures of fire properties from these sensors may be more limited because of sensor saturation, the low resolution of the sensor, or uncertainty about the radiance of the surface outside of the fire front that contributes to a measurement. Low resolution furthermore limits understanding of fire behavior that is readily apparent in high-resolution airborne measurements (Fig. 6.7).

Riggan et al. (2000) considered the effect of observation scale by simulating the radiant properties of a reach of complex fire line, in the Brazilian Cerrado, as measured with an airborne extended-dynamic-range imaging spectrometer. The simulation considered the fire as viewed in isolation with differing amounts of background at temperatures typical of unburned Cerrado vegetation (at 30°C) or black ash warmed by solar heating (at 70°C). The question asked was: what scale of measurement is required to estimate a useful fire property such as the total fire radiant-flux density? The answer depends on the wavelengths chosen for observation.

The hot-pixel data from within a 50- by 50-m reach of the Serra do Maranhão fire (Riggan et al., 2004) were considered first in isolation: the

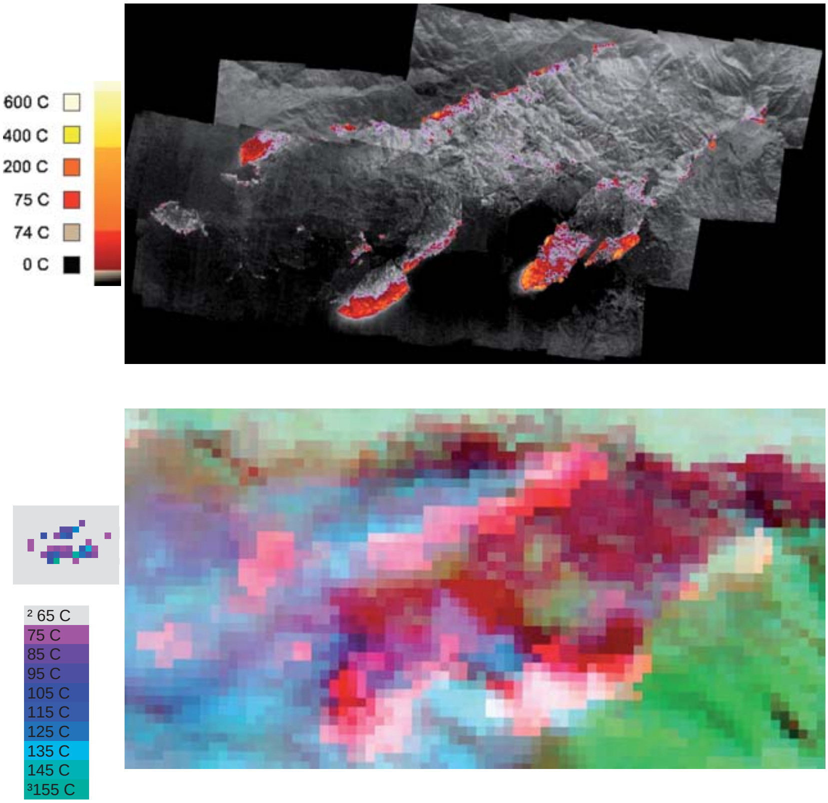

Figure 6.7. Esperanza Fire, Riverside County, CA, October 26, 2006. Color-coded surface temperatures (in Celsius), which reflect fire intensity, are presented as imaged at 14:12 Pacific Standard Time (PST) by the FireMapper at 11.9-µm wavelength in the thermal infrared (top) and compared with radiances at wavelengths of 2.1 µm (mapped in red), 0.85 µm (in green), and 0.65 µm (in blue) as measured at 14:05 PST by the NASA Moderate Resolution Imaging Spectrometer, MODIS (bottom). The MODIS 2.1-µm channel has a nominal resolution of 500 m. The MODIS band-21 fire channel at 3.96 µm, with nominal resolution of 1 km, is shown as a color-coded brightness temperature (inset at left). Here, a moderate Santa Ana wind is driving the fire to the southwest through light fuels and chaparral. By comparison to high-resolution FireMapper data, the MODIS provides approximate fire location and only a general sense of fire activity with little quantitative information regarding fire properties.

radiant-flux density, 3629 $\mathrm{J\,m^{-2}\,s^{-1}}$, estimated with the two-channel method from the summed radiances at wavelengths of 1.63 and 3.9 µm was a close approximation to that obtained by summing the radiant-flux density values from incorporated high-resolution pixels, 3638 $\mathrm{J\,m^{-2}\,s^{-1}}$.

A somewhat less successful estimate of $3537\,\mathrm{J\,m^{-2}\,s^{-1}}$ resulted from use of the summed radiances at 3.9 and 11.9 μm. Thus, considering fire-associated areas alone, a coarse-resolution measurement of radiances might produce a reasonable estimate of radiant-energy release given the diversity of incorporated temperatures and values of emissivity-fractional area.

As increasing amounts of relatively low-temperature background of either unburned vegetation or ash were included in the observation, the radiance was quickly elevated at wavelengths longer than 6 μm, but radiances at shorter wavelengths were little affected. Thus, use of radiances at 1.63 and 3.9 μm to estimate temperature, emissivity-fractional area, and radiant-flux density produced good estimates for pixels with a dimension less than approximately 100 m (Riggan et al., 2000). Daytime observations at scales greater than that dimension could incorporate substantial amounts of reflected solar radiation at 1.63 μm and require a correction for the background radiance. Composition of the background is not critical at scales less than 100 m; uncertainty therein produced only an additional 2% error in the estimated radiant-flux density.

Estimates of high-temperature properties from radiance of a low-resolution pixel using two wavelengths including the long-wave infrared will largely fail without some correction for the background. For a 75-m pixel, use of the 3.9 and 11.9 μm wavelengths produced an estimated bulk temperature, 435°C, that described neither the hot elements at 834°C nor the background at 30°C (Riggan et al., 2000). A background correction to the long-wave radiance is problematic since fires generate an ash layer that under solar heating may be at least 72°C (Riggan et al., 1994), 40–45°C warmer than unburned vegetation, and there is no way to know a priori the proportion of these differing targets within a low-resolution pixel. Since the background may be all ash or all unburned vegetation, and the magnitude of this uncertainty amounts to half of the simulated fire signal in a 125-m pixel and over twice the fire signal at 250-m resolution, this approach must fail when pixel sizes greater than about 50 m are used to view the fire. At that scale the uncertainty is only 3% of the fire signal.

6.2.4. High-resolution fire measurement with long-wave-infrared remote sensing

Whereas flame radiance provides an observation of the immediate character of a fire front, measurements at long-wave infrared wavelengths provide a longer-lived, integrating signal of heat absorbed and reradiated by the ground surface over the period from fire-front passage to the time of observation. This is readily apparent in successive FireMapper observations at 11.9 μm wavelength over the 2005 Woodhouse Fire in Riverside County, CA (Fig. 6.8). The Woodhouse Fire burned in the afternoon and evening of October 25, 2005, under moderate offshore winds, in a Mediterranean-type ecosystem with plant communities composed of chaparral and coastal sage scrub. Over the period of successive fire-line observations from 17:10 to 19:15 Pacific Daylight Time, the head of the fire spread with the wind to the west-southwest at a rate of $0.25\,\mathrm{m\,s^{-1}}$; the northern flank of the fire spread lateral to the ambient wind at $0.14\,\mathrm{m\,s^{-1}}$. Wind speed at nearby Beaumont, CA, 16 km east of the fire, averaged $5\,\mathrm{m\,s^{-1}}$ with gusts to $14\,\mathrm{m\,s^{-1}}$. Observed radiometric temperatures at and behind the fire front were affected by both the time since fire passage and the local fire intensity, which apparently reflected local fuel consumption. Based on the rate of spread, temperatures for 1–1.5 h remained elevated above those of black ash, which attained 60°C when heated only by insolation. Thermal data alone qualitatively reproduced the landscape vegetation patterns visible in prefire color-infrared photography, which depicts heavier fuel loadings in chaparral on north-facing aspects and along stream courses, and relatively low fuel loading in coastal sage and grass on ridgelines and south-facing aspects (Fig. 6.9).

6.3. FireMapper applications

The Forest Service's PSW Research Station is developing synoptic-scale fire and environmental data to understand and model the behavior and effects of large wildland fires, including the effects thereon of landscape-scale fuel patterns and treatment. The project supports a Forest Service initiative in which advances in our fundamental understanding of the behavior and immediate impacts of wildland fires are required to provide a firmer basis for fire and fuel management and to enhance public safety, ecosystem sustainability, and environmental quality. While conducting fundamental fire research, we are also developing means for rapid communication, dissemination, and application of the fire intelligence data, and applications of fire imaging in airborne fire operations.

The FireMapper thermal-imaging radiometer has been deployed aboard the PSW Airborne Sciences Aircraft, N70Z, a twin-engine Piper Navajo, since 2000. PSW acquired fire intelligence and provided data to the California interagency Southern Operations Coordination Center during the October 2003 fire emergency in southern California. Data from the FireMapper documented during critical periods the progress

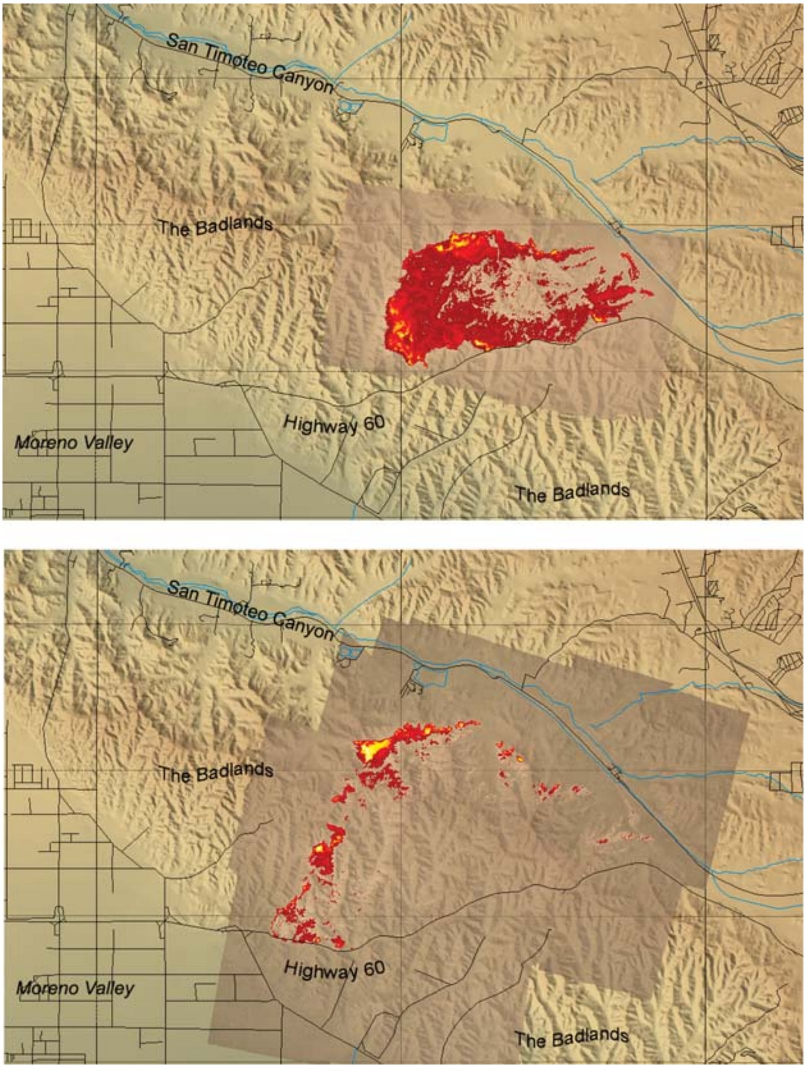

Figure 6.8. Ground temperatures behind the front of the October 5, 2005, Woodhouse Fire, Riverside County, CA, as estimated from radiances measured, at a wavelength of 11.9 μm, with the FireMapper thermal-imaging radiometer. The fire progression is shown from overflights at approximately 17:11 (top) and 19:15 Pacific Daylight Time (bottom). Such color-coded fire information is readily interpretable as to fire location, direction and rate of spread, and activity. Data are shown on shaded topographic relief as posted in near-real time to the Internet at http://www.fireimaging.com/.

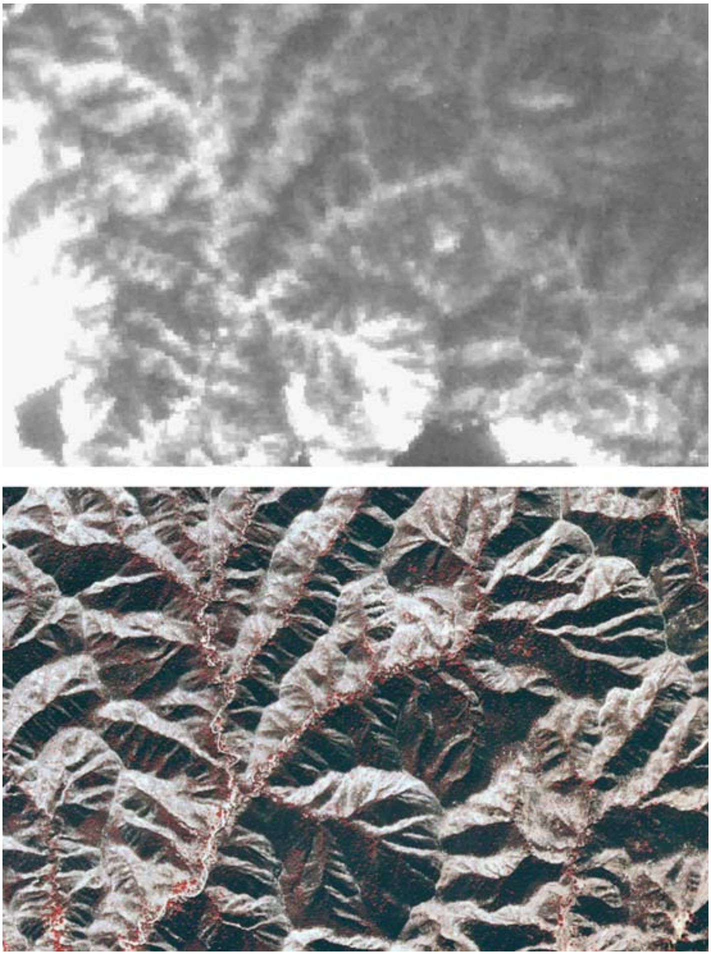

Figure 6.9. Ground-surface temperatures (top) behind the front of the October 5, 2005, Woodhouse Fire, Riverside County, CA, as estimated from radiances measured at 11.9 μm with the FireMapper thermal-imaging radiometer, shown with prefire color-composite photography (bottom) from a U.S. Geological Survey digital orthorectified quarter quadrangle. Images are oriented with north at the top. Residual heat from passage of the fire front, which is located to the west and south of the image, reflects local fuel loading and time since local ignition. Thermal patterns at the top appear to be dominated by fuel loading: bright, high-temperature areas correspond primarily to more north-facing aspects and riparian areas, both of which have relatively contiguous chaparral and woodland and higher fuel loading; dark, cool areas correspond to south-facing aspects with light vegetation, which is primarily annual grasses and coastal sage scrub.

and intensity of the 112,000-ha Cedar Fire and the Old, Grand Prix, Cedar, and Paradise fires, which collectively destroyed thousands of homes in San Bernardino and San Diego counties (Figs. 6.10a and 6.10b). Imagery from the Old and Cedar fires documented fire behavior in chaparral and forest fuels including effects of extensive forest mortality caused by drought and bark beetles. In conjunction with the Forest Service's Missoula Fire Sciences Laboratory, the PSW FireMapper system was deployed for wildfire measurements and intelligence gathering for the Multi-Agency Coordination Group in Missoula, Montana, during the Montana fire emergency in August 2003. Image mosaics depicting

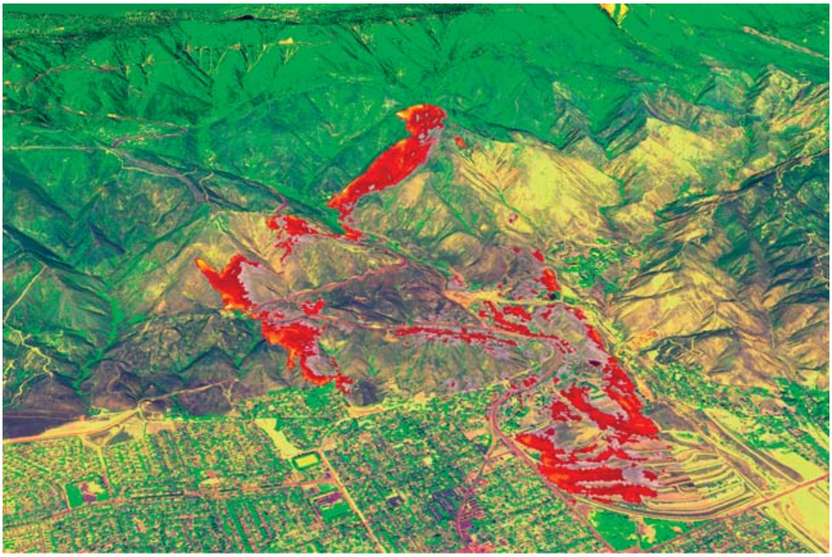

Figure 6.10a. Old Fire, San Bernardino County, CA, as viewed from the southwest at 11:14 Pacific Daylight Time, October 25, 2003, by the PSW FireMapper thermal-imaging radiometer. Color-coded surface temperatures, which reflect fire intensity, are presented as measured in the thermal infrared and posted as an off-nadir overlay on a prefire, multispectral image (with red, near-infrared, and thermal-infrared light shown in red, green, and blue) at http://www.fireimaging.com. Here, a moderate Santa Ana wind is driving the fire to the south and southeast through chaparral and light fuels on hillsides into urban vegetation and structures in the City of San Bernardino. Note the lack of fire activity where the Old Fire encountered the perimeter of the June 1–7, 2002, Arrowhead Fire (yellow vegetation at right of center). Fire at the lower right is burning on a spreading ground, which is used to recharge groundwater. At the time of this image there was little fire activity in the urban area below the burned foothills at lower center.

Figure 6.10b. Old Fire, Del Rosa neighborhood, City of San Bernardino, as viewed from the southwest at 13:56 PDT, October 25, 2003, by the PSW FireMapper. Color-coded surface temperatures are presented as an off-nadir overlay in Google Earth as shown as a standard product in near real time at http://www.fireimaging.com/. Here the fire has progressed into the urban area partly by wind-blown fire brands, a large portion of which apparently originated from eucalypts, palms, or other urban vegetation. A long fire incursion is visible along a flood-control facility at lower left-center. Fire-involved structures are readily identified in this image; rapid communication of such imagery could aid firefighters in showing the extent of the fire's incursion into the city and the location of newly involved structures.

fire activity of both small and large-scale incidents were created and disseminated via the Internet for use in strategic planning and operations by incident command teams. FireMapper data were incorporated into a geographic information system (GIS) database by a quick-response team from the Missoula Fire Laboratory and the University of Montana, and data were used to initialize and calibrate FARSITE simulations of behavior of active fires.

FireMapper data are typically acquired from a series of parallel, overlapping passes over a wildland fire. An absolute, through-the-lens calibration with a blackbody of known temperature is performed prior to each pass. Images are examined in flight and fire data are extracted, compressed with JPEG 2000 wavelet-compression software, and transmitted by File Transfer Protocol (FTP) to a dedicated FTP server via a Qualcomm, Inc., Medium Data Rate Satellite Communications System using the Globalstar network. Aircraft location and attitude data are provided at 20 Hz by a Northrop-Grumman LN-100GT inertial navigation system; these data are associated with imagery in postcollection processing aboard the aircraft. After transmission, fire imagery is decompressed and extracted by a ground-based analyst and orthorectified and associated into large-area mosaics using a Leica Fire Rectification Engine running the Leica Photogrammetry Suite Core software. The rectified thermal imagery is color coded by temperature and posted to the Internet at http://www.fireimaging.com. Products include fire visualizations on shaded relief in a Zoomify viewer based on Adobe Flash technology, in Google Earth, in Google Maps, and as downloadable Geo-TIFF imagery or shape files. The Zoomify viewer allows one to extract the precise location of spot fires or quickly map a fire perimeter over the Internet. Processed imagery from small fires has been posted to the Internet with a best delivery time of 10 min. This rate is sufficient to allow an incident command to use the data to take informed tactical actions, such as backfiring, that could affect the course of a fast-moving fire front. Imagery from large fires, such as the 16,000-ha Esperanza Fire in southern California (Fig. 6.7), has been processed and posted to the Internet within 45 min.

The FireMapper 2.0, a compact second-generation fire remote-imaging radiometer, has been developed by PSW and Space Instruments, Inc., as a commercially available product for routine use in fire research and management. The FireMapper 2.0 incorporates an uncooled BAE Systems, Inc., microbolometer focal-plane array; provides a broad-band thermal-infrared channel encompassing wavelengths from 8 to 12.5 μm and narrow-band channels at 8.8–9.1 μm and 11.3–12.4 μm that each provide unsaturated data over large wildland fires; and implements two levels of quantitative onboard thermal calibration that correct anomalies in image pattern and drift. A FireMapper 2.0 was first deployed in fire operations during the 2004 fire season aboard a firefighting aircraft employed as an aerial supervision module by the USDI Bureau of Land Management. The instrument's small size and weight, compared with the prototype FireMapper, allows it to be operated in a forward-looking, tactical mode to provide images of fire locations and retardant drops during lead-plane operations as well as in a nadir-looking, strategic mode for fire area and intensity mapping. Fire mapping data have been collected in the southwest United States and in Alaska.

6.4. Future missions

PSW is targeting FireMapper to address elements of the Forest Service strategic plan for fire research including (1) transitions and thresholds in fire behavior, (2) fire behavior in complex fuels including live vegetation, (3) physical interactions of fire with the atmosphere, (4) effects of fuel distribution and treatment on subsequent fire behavior, (5) landscape-scale fire processes, and (6) the role of wildland fire in global climate change.

6.4.1. Fire behavior transitions and thresholds

Potentially dangerous and unpredicted transitions in fire behavior, such as from ground-surface fire to crown fire, can compromise firefighter and public safety, tactical fire control, and the protection of communities and natural resources. Small and seemingly "well-behaved" fires may respond to changes in atmospheric conditions or encountered fuel loading and structure, and with little or no warning, become fast moving and highly energetic with catastrophic consequences. Operational fire behavior models are not now capable of successfully predicting these critical transitions in behavior. Transitions to extreme flammability—and potentially severe fire behavior and effects—could also result from prolonged drought stress in forests, woodlands, and chaparral. Qualitative changes in forest flammability are now a critical problem across several regions in the western United States, and especially in southern California, where the fire potential involves interactions of climate variability, forest stand density and structure, pathogens, air pollution, and population growth that place resources and communities at greater risk. Investigation of explosive fire growth requires synoptic fire measurements to document the rates of growth and effects of fuel condition in dynamic and altered ecosystems.

6.4.2. Fire in complex fuels

Fire and fuel management decisions are currently based in part on predictions from semi-empirical and computationally simple models of quasi-steady-state fire spread (Albini, 1976; Finney, 1998; Rothermel, 1972) that have been derived largely from observations of combustion in a laboratory with narrow, homogeneous fuel arrays and flame lengths on the order of 1 m. These models cannot be applied with confidence to simulate burning with high rates of energy release and conditions producing flames tens of meters in length in typically complex terrain and heavy forest or chaparral fuel, which are vertically stratified, spatially heterogeneous, and comprise a mixture of live and dead biomass. Observations of fire behavior under field conditions are required to validate or invalidate existing models and develop statistical models that describe fire behavior in macroscopic assemblages of fuels.

6.4.3. Interactions of fire with the atmosphere

Fire behavior at scales from a meter to several kilometers may be strongly influenced by the interaction of fire with atmospheric motions, specifically fire-generated winds and winds in complex terrain. At scales of one to tens of meters, fire spread is subject to wake effects (Rodman Linn, personal communication) and is a non-linear function of the length of the combustion zone perpendicular to the direction of spread (Fendell et al., 1990; Jean-Luc Dupuy, personal communication), possibly due to development of horizontal vortices above that zone. At larger scales, fire-modified winds and larger circulations in the atmospheric boundary layer, such as the waves that develop downstream of mountains, may locally accelerate or deform the fire front (Janice Coen, personal communication). Very long fire lines will develop multiple plumes and fire runs. Vorticity on the edges of large plumes can unexpectedly develop destructive fire whorls with strengths approaching those of tornados. Firefighters reportedly faced such extreme fire behavior during the 2003 fire emergency in southern California. Operational fire models do not account for such interactions of fire and the atmosphere, although there are general guidelines for anticipating dangerous fire behavior. More complex research models, such as the Firetec model developed at Los Alamos National Laboratory (Linn, 1997), numerically solve equations describing transport of mass, momentum, and energy in a fire environment. These explicitly describe interactions of fire with the atmosphere—including fire-generated winds—and provide a means to simulate fire behavior in nonhomogeneous fuels and terrain and rapidly changing weather. Direct and synoptic observation of wildland fires is needed to ascertain the importance of macroscale effects in fire behavior—above those of local conditions—such as the effects of long-range spotting in different fuel types or the influence of a fire plume on fire-line shape and to parameterize and validate the new class of fire–atmosphere models.

6.4.4. Fuel treatment influences on fire behavior

Land managers are often tasked to design and implement fuel treatments to mitigate or alter the consequences of wildland fire, yet evidence to document the effectiveness of treatments has been infrequent and largely anecdotal. We have been unable to objectively characterize changes in subsequent fire environments caused by such management practices as forest thinning, pruning, or harvesting or by prescribed burning in chaparral. Treatments should be designed with consideration of microclimate, fuel structure, and heterogeneity on the landscape, and the subsequent development of fuels, but such effects are not well known. Synoptic-scale, remote measurements of active fires give a means to test the ultimate efficacy of fuel treatments, but the remote sensing will have to largely provide a characterization of the fuels as well.

6.4.5. Landscape and large-scale fire processes

Landscape-scale mapping, assessment, and simulation of wildland fires is needed in order to predict and monitor the cumulative and interactive influences on wildland fire regimes of weather and climate, terrain, ecosystem and fuel development, and fire management. Current strategic planning is largely derived from simulation of fire behavior in static fuels conceptually removed from the landscape, vegetation patch dynamics, climate extremes, persistent fuel boundaries, or dynamic system considerations. This severely limits our ability to predict the resource or societal outcomes of different levels of intervention by fuel or fire management and thereby to defend such a program to the public or regulatory agencies. Large-scale direct impacts of fires are also important in issues of ecosystem response to environmental change, ecosystem restoration to a fire-resilient state, and management of regional air quality and carbon sequestration. Our present knowledge of large-scale dynamics is limited to such measures as decadal trends in cumulative burned area and historical or anecdotal observations of vegetation change. An improved understanding of these processes will require large-scale fire measurements of a large number of fires over time.

6.4.6. Wildland fires in global climate change

Wildland fires may now be contributing to climate change depending on their extent and the strength of their emissions. Best available estimates have considerable uncertainty but do show that biomass combustion is likely a globally important source of atmospheric aerosols, methane, hydrocarbons, carbon monoxide, carbon dioxide, methyl bromide, and nitrous oxide (Crutzen & Andreae, 1990; Radke et al., 1991).

Fires may contribute to global warming to the extent that they reduce the amount of carbon accumulated in standing biomass or soils, as occurs during burning of slashed forest for shifting agriculture or permanent conversion to pasture in the tropics or accelerated burning rates in Mediterranean or temperate climates. A substantial net carbon loss may also occur during dry-season burning of wetlands or due to progressive fire-associated loss of plant nutrients and productivity in ecosystems subject to frequent fires. Fires may also contribute to warming to the degree that they emit higher proportions of methane than would alternative pathways of organic matter decomposition since methane absorbs radiation more strongly than does carbon dioxide. Furthermore, combustion is a copious source of carbon monoxide; microbial decomposition is not. Carbon monoxide (CO) affects the atmospheric concentration of hydroxyl radical (Crutzen & Andreae, 1990), and thereby the residence time of methane and other radiatively important tropospheric species. Thus, increased carbon mineralization by fire yields CO emissions that also contribute to global warming.

High-resolution, remote measurement of wildland fires will be important in ascertaining the importance of global burning in climate change. Existing satellite-based remote sensing can track areas burned over large regions, but high-resolution monitoring will be required to estimate rates of carbon flux to the atmosphere and the degree of residual combustion that is related to emissions of carbon monoxide and other radiatively important trace gases.

6.5. Conclusions

A timely and synoptic view of wildland fire behavior is needed in fire management to efficiently allocate resources during fire-suppression operations; protect firefighters, the public, and our communities; reduce losses of natural resources; and develop our ability to predict the outcome of catastrophic fires. Modern airborne remote-sensing can provide needed quantitative mapping of fire properties including fire-front location, spread, and acceleration; flame temperature, emissivity, and areas; long-distance spotting; radiant-energy emissions; soil heating; residual combustion; and by inference, sensible heat and carbon fluxes to the atmosphere. Low-resolution fire observations at kilometer scale by satellite-based remote sensors readily detect fire radiant emissions and have been usefully applied to detect and localize fires, identify general fire shape and regions of active burning, and map the areas of large fires from changes in surface reflectance. High-resolution measurements at a scale of one to a few meters, as provided by specialized airborne sensors designed to accommodate the high radiance of wildland fires, are required to quantitatively measure thermal properties associated with active combustion.

Useful fire measurements can be made in high-transmittance atmospheric windows at wavelengths longer than 1.6 μm. Peak radiance from flames occurs at a wavelength of approximately 2.2 μm. Observations of wildland fires in Brazilian Cerrado or savanna vegetation suggest that hot ground and ash within flaming fronts contributes approximately 4% of the radiance at 1.63 μm, three-fifths of the radiance at 3.9 μm, and nearly nine-tenths of the radiance at 11.9 μm. Relative contributions of flames and hot ash to observed fire radiances can be resolved by an iterative method employing the solution of two Planck functions describing radiances at 1.6 and 3.9 μm (the two-channel method) with corrections derived from the long-wave or thermal infrared radiance at 11.9 μm. Single-channel radiance measurements using a wavelength of 11.9 μm have been usefully applied to map approximate ground-surface temperatures associated with burning; a highly resolved time course of this measurement provides a measure of soil heating and fire radiant-energy flux. Measurements of fire radiance at 1.6 and 3.9 μm alone have provided provisional but promising measures of whole-fire sensible energy flux and carbon flux to the atmosphere. Fire radiance at 3.9 μm alone was shown to provide a good estimator of the radiant-flux density estimated from the two-channel method.

PSW is applying synoptic measurements and mapping with its FireMapper thermal-imaging radiometer to characterize the behavior of wildland fires in California and the western United States. FireMapper data have provided the first quantitative and readily interpretable fire intelligence in near real time to interagency incident command teams and the public on major fires in the United States.

Measurements with the FireMapper are being applied to provide substantial new knowledge of wildland fire behavior, especially regarding fire behavior transitions and thresholds, fire in complex fuels, interactions of fire with the atmosphere, fuel treatment influences on fire behavior, landscape and large-scale fire processes, and the role of wildland fire in global climate change.

ACKNOWLEDGMENTS

Research reported herein has been supported by the U.S. National Fire Plan; the Joint Fire Sciences Program; the USDA Forest Service, Pacific

Southwest Research Station and International Programs; the U.S. Agency for International Development, Global Change Program; and the Instituto Brasileiro do Meio Ambiente e dos Recursos Naturais Renováveis. We acknowledge contributions to the research by NASA Ames Research Center, Space Instruments, Inc., and Qualcomm, Inc., and we appreciate reviews by James A. Brass, Nancy E. Grulke, and David Weise.

REFERENCES

Albini, F.A. 1976. Computer-based models of wildland fire behavior: A users' manual. U.S. Department of Agriculture, Forest Service, Intermountain Forest and Range Experiment Station, 68 pp.

Crutzen, P.J., and Andreae, M.O. 1990. Biomass burning in the tropics: Impact on atmospheric chemistry and biogeochemical cycles. Science 250, 1669–1678.

Fendell, F.E., Carrier, G.F., and Wolff, M.F. 1990. Wind-aided firespread across arrays of discrete fuel elements. Defense Nuclear Agency, Technical Report DNA-TR-89-193, Alexandria, VA, 131 pp.

Finney, M.A. 1998. FARSITE: Fire Area Simulator-Model development and evaluation. U.S. Department of Agriculture, Forest Service, Rocky Mountain Research Station, Research Paper RMRS-RP-4, 47 pp.

Linn, R.R. 1997. A transport model for prediction of wildfire behavior. Ph.D. Dissertation, New Mexico State University; also published as Los Alamos National Laboratory Report LA-13334-T.

Liou, K. 1980. An introduction to atmospheric radiation. Academic Press, International Geophysics Series, Vol. 26, London, England, p. 392.

Matson, M., and Dozier, J. 1981. Identification of subresolution high temperature sources using a thermal IR sensor. Photogrammetric Eng. Remote Sens. 47, 1311–1318.

Menzel, W.P., and Prins, E.M. 1996. Monitoring biomass burning with the new generation of geostationary satellites. In: Levine, J.S., ed. Biomass burning and global change, Vol. 2: Biomass burning in the tropical and temperate ecosystems. The MIT Press, Cambridge, MA, pp. 56–64.

Miranda, H.S., Rocha e Silva, E.P., and Miranda, A.C. 1996. Comportamento do fogo em queimadas de campo sujo. In: Anais do Simpósio Impacto das Queimadas sobre os Ecossistemas e Mudanças Globais. 3^0 Congresso de Ecologia do Brasil, 6 a 11 de outubro de 1996, Brasília-DF, 1–10.

Morisette, J.T., Giglio, L., Csiszar, I., and Justice, C.O. 2005. Validation of the MODIS active fire product over Southern Africa with ASTER data. Int. J. Remote Sens. 26, 4239–4264.

Ottmar, R.D., Vihnanek, R.E., Miranda, H.S., Sata, M.N., and Andrade, S.M. 2001. Stereo photo series for quantifying Cerrado fuels in central Brazil–volume 1. U.S. Department of Agriculture, Forest Service, Pacific Northwest Research Station, Portland, Oregon, USA.

Radke, L.F., Hegg, D.A., Lyons, J.H., Hobbs, P.V., Laursen, K.K., Weiss, R.E., Riggan, P.J., and Ward, D.E. 1991. Particulate and trace gas emissions from large biomass fires in North America. In: Levine, J.S., ed. Global biomass burning: Atmospheric, climate, and biospheric implications. The MIT Press, Cambridge, MA, pp. 209–224.

Riggan, P.J., Brass, J.A., and Lockwood, R.N. 1993. Assessing fire emissions from tropical savanna and forests of central Brazil. Photogrammetric Eng. Remote Sens. 59(6), 1009–1015.

Riggan, P.J., Franklin, S.E., Brass, J.A., and Brooks, F.E. 1994. Perspectives on fire management in Mediterranean ecosystems of southern California. In: Moreno, J., and Oechel, W., eds. Fire and Global Change in Mediterranean Ecosystems. Ecological Studies no. 107, Springer-Verlag, New York, 140–162.

Riggan, P.J., Weirich, F.H., DeBano, L.F., Jacks, P.M., Lockwood, R.N., Colver, C., and Brass, J.A. 1994. Effects of fire severity on nitrate mobilization in watersheds subject to chronic atmospheric deposition. Environ. Sci. Technol. 28(3), 369–375.

Riggan, P.J., Hoffman, J.W., and Brass, J.A. 2000. Estimating fire properties by remote sensing. Proceedings of the IEEE Aerospace Conference, Aspen, Colorado, Paper no. 519.

Riggan, P.J., and Hoffman, J.W. 2003. FireMapper™: A thermal-imaging radiometer for wildfire research and operations. Proceedings of the IEEE Aerospace Conference, Big Sky, Montana, Paper no. 1522.

Riggan, P.J., Tissell, R.G., and Hoffman, J.W. 2003. Application of the FireMapper™ thermal-imaging radiometer for fire suppression. Proceedings of the IEEE Aerospace Conference, Big Sky, Montana, Paper no. 1523.

Riggan, P.J., Lockwood, R.N., Tissell, R.G., Brass, J.A., Pereira, J.A.R., Miranda, H.S., Miranda, A.C., Campos, T., and Higgins, R. 2004. Remote measurement of wildfire energy and carbon flux from wildfires in Brazil. Ecol. Appl. 14(3), 855–872.

Rothermel, R.C. 1972. A mathematical model for predicting fire spread in wildland fuels: U.S. Department of Agriculture, Forest Service, Intermountain Forest and Range Experiment Station, 40 pp.

Setzer, A.W., and Malingreau, J.P. 1996. AVHRR monitoring of vegetation fires in the tropics: Toward the development of a global product. In: Levine, J.S., ed. Biomass burning and global change, Vol. 2: Biomass burning in the tropical and temperate ecosystems. The MIT Press, Cambridge, MA, pp. 25–39.

Section II:
Ambient Air Quality, Visibility and Human Health—Regional Perspectives

This page intentionally left blank

Developments in Environmental Science, Volume 8 171
A. Bytnerowicz, M. Arbaugh, A. Riebau and C. Andersen (Editors)

ISSN: 1474-8177/DOI:10.1016/S1474-8177(08)00007-7

Chapter 7

Effects of Forest Fires on Visibility and Air Quality

Douglas G. Fox and Allen R. Riebau*

Abstract

The U.S. Clean Air Act establishes the goal of preventing future and remedying existing visibility impairment in 156 Class I areas (national parks, wilderness areas, and wildlife refuges). A key element in implementing this goal is the Regional Haze Regulation (RHR). RHR is based on relating impaired visibility, using metrics of extinction (inverse megameters and/or "deciviews"), to concentration of ambient particulate matter (PM), especially the chemical components of particulates smaller than 2.5 μm in diameter, collectively known as $PM_{2.5}$. $PM_{2.5}$ itself is also subject to national ambient air quality standards. Forest, rangeland, and agricultural fires, both natural and human caused emit both primary and secondary (formed in the atmosphere from gaseous organic carbon (OC) emissions) $PM_{2.5}$. This chapter will review the RHR and what we know about relationships between fire emissions, their fate in the atmosphere, and their contribution to regional haze and $PM_{2.5}$.

7.1. Introduction

Since the implementation of the Clean Air Act in 1977, the United States has been using visibility in selected special federally managed rural areas—national parks, wilderness and wildlife reserves, designated as Class I areas—as a measure of air quality. In fact, the Act establishes a national goal of the "… prevention of any future, and the remedying of any existing, impairment of visibility in mandatory Class I federal areas in which impairment results from manmade air pollution." This goal, while simply stated, has proven difficult to quantify and to accomplish.

*Corresponding author: E-mail: Fox@cira.colostate.edu

(For further explanation see: http://vista.cira.colostate.edu/improve/Overview/hazeRegsOverview_files/frame.htm.)

In response, the U.S. Environmental Protection Agency (EPA) has promulgated a Regional Haze Program, providing States the responsibility to develop plans to reduce visibility impairment at federal Class I areas in their state. (http://www.epa.gov/ttn/oarpg/t1/fact_sheets/rh_girhp_fs.pdf). The Regional Haze Program has established a Regional Haze Regulation (RHR) stating that the appropriate measure of visibility is the haze index: a measure of visibility derived from calculated light extinction measurements that is designed so that uniform changes in the haze index correspond to uniform incremental changes in visual perception, across the entire range of conditions from pristine to highly impaired. The haze index (HI) is calculated in units of deciviews (dv) directly from the total light extinction (b_{ext} expressed in inverse megameters (Mm^{-1})] as follows (http://vista.cira.colostate.edu/IMPROVE):

$$\text{HI} = 10 \ln (b_{\text{ext}}/10)$$

In turn light extinction, b_{ext}, is caused by light being absorbed and scattered by both gases and aerosol particles. Atmospheric scattering by the gases and particles present in clean air is called Rayleigh scattering and is been assumed to have a constant value of $10\,\text{Mm}^{-1}$ by the RHP. Atmospheric gases absorb light, primarily by nitrogen dioxide, which is negligible in rural settings. Most atmospheric absorption is done by aerosols, primarily by their "elemental" carbon (EC or also called black carbon) component. Atmospheric scattering done by aerosols is complex. In the RHP, aerosol scattering is approximated by relating it to the concentrations of aerosol particles smaller than 2.5 μm in diameter ($PM_{2.5}$) because these particles are most effective in scattering visible light. $PM_{2.5}$ mostly consists of ammonium sulfate, ammonium nitrate, organic carbon (OC), EC, soil, and the total mass of "coarse" particles (those between 2.5 and 10 μm, $PM_{2.5-10}$). There are also effects of ambient humidity that must be included in this relationship because many of the aerosols, especially sulfates, are hygroscopic and scatter more light at higher humidity.

In the next section of this chapter, we will discuss the Clean Air Act and the Regional Haze Program. The third section will discuss how pollution is related to visibility degradation including how it is monitored by the IMPROVE network (Interagency Monitoring of PROtected Visual Environments). The fourth section will address the current understanding of contributions from various fire sources to U.S. regional visibility and specifically to $PM_{2.5}$ aerosol concentrations, especially the OC component of those aerosols. Developing an emissions inventory (EI) and some of the modeling steps needed to utilize the EI in a regional modeling context are discussed. The fifth section addresses the state of knowledge in assessing fire impacts on regional visibility and briefly reviews results to date from a variety of modeling efforts, including both source apportionment modeling and simulation modeling. The final section briefly reviews ongoing research needed in this area recommending next steps.

7.2. The U.S. Clean Air Act and regional haze regulations

The Clean Air Act authorizes regulations to protect visibility in Class I areas, specifically 156 federal wilderness and national park locations. The law and regulations require that all States and tribes:

- Develop implementation plans to achieve RHR goals by limiting emissions of visibility degrading aerosols (and their chemical precursors) from sources that contribute to impaired visibility at each of the 156 designated Class I areas.
- Formalize for each area where open burning is anticipated to make a significant contribution to air quality, a formal Smoke Management Program.

The regulations are based on data taken from the IMPROVE monitoring network. Since forest fire smoke is recognized as a significant contributor to regional haze but one that is different from other pollution sources (e.g., industrial and transportation activities), the States are also mandated in the regulations to implement Smoke Management Programs. The regulations specifically require States to identify for each Class I area the natural background for visibility and the mean of the 20% haziest and 20% cleanest days (based on a 5-year average), and to establish a program of emissions limitations to reduce the haziest days to natural background conditions (whilst not reducing the cleanest days) over the next half century, measuring progress in 10-year increments.

Natural background is a complex determination, but it is specifically identified in the regulations to be reflective of contemporary conditions and land use patterns (not historical or pre-European conditions); a long-term average condition analogous to the 5-year average best-and worst-day conditions that are tracked under the regional haze program; and estimated for each Class I area in the absence of human-caused impairment.

Specifically, the RHR require that natural background be developed as follows:

> derive regional estimates of natural visibility conditions by using estimates of natural levels of visibility-impairing pollutants in conjunction with the IMPROVE

> methodology for calculating light extinction from measurements of the five main components of fine particle mass (sulfate, nitrate, organic carbon, elemental carbon, and crustal material). (EPA Regional Haze Regulations 40 CFR 51.300-309.)

Default values of each of these components have already been established for the eastern and the western United States in the literature (Trijonis et al., 1990).

The EPA recommends natural background be determined by using default values for each of the aerosol components in the IMPROVE equation. The recommendation for OC mass (in micrograms per cubic meter) is 1.4 in the east and 0.47 in the west. Higher values in the east reflect hydrocarbon emissions from trees that can generate secondary organic aerosol (SOA).

EPA guidance also allows States to develop a refined approach essentially allowing different aerosol component values that the state can show more appropriately represent natural conditions. For example, this might include adding OC contributions from such an infrequent natural event as a wildfire, as long as the state can appropriately document the frequency and magnitude of its visibility impact (i.e., its contribution to OC and other aerosol components).

7.3. Relating pollution to visibility

The IMPROVE equation has been developed over a period of years based on radiation theory and empirical measurements from the IMPROVE network. The relationship that has been applied until 2006 is:

$$\begin{aligned} b_{\text{ext}} = {} & (e_{\text{sf}})f_{\text{s}}(\text{RH})[(\text{NH}_4)_2\text{SO}_4] + (e_{\text{nf}})f_{\text{n}}(\text{RH})[\text{NH}_4\text{NO}_3] \\ & + (e_{\text{ocmf}})f_{\text{ocm}}(\text{RH})[\text{OMC}] + (e_{\text{soilf}})[\text{SOIL}] \\ & (e_{\text{c}})[\text{Coarse Mass}] + (e_{\text{lacf}})[\text{lacf}] \end{aligned}$$

where: b_{ext} is the extinction coefficient, e the extinction efficiencies, f(RH) a relative humidity enhancement factor (bwet(RH)/bdry), [- - - -] the concentrations of species (24-hr averages), OMC the 1.4 $\times$ measured carbon mass, and lacf the light absorbing fraction of the aerosol or black carbon.

The IMPROVE network monitoring program measures mass concentrations of major aerosol species using filter-based measurement technologies. Estimates of extinction are made using this IMROVE equation. Dry mass scattering efficiencies are based on Trijonis et al. (1990). The f(RH) function represents the ability of the chemical aerosol in question to take up water, thus increasing its ability to scatter light.

Recently, Hand and Malm (2005) have reviewed and suggested slight alterations to the IMPROVE equation. The revised equation is:

$$\begin{aligned} b_{\text{ext}} = {} & 2.2 \times f_{\text{S}}(\text{RH}) \times [\text{small sulfate}] + 4.8 \times f_{\text{L}}(\text{RH}) \times [\text{large sulfate}] \\ & + 2.4 \times f_{\text{S}}(\text{RH}) \times [\text{small nitrate}] + 5.1 \times f_{\text{L}}(\text{RH}) \times [\text{large nitrate}] \\ & + 2.8 \times [\text{small organic mass}] + 6.1 \times [\text{large organic mass}] \\ & + 10 \times [\text{elemental carbon}] + [\text{fine soil}] + 1.7 \times f_{\text{SS}}(\text{RH}) \times [\text{sea salt}] \\ & + 0.6 \times [\text{coarse mass}] + \text{Rayleigh scattering (site-specific)} \\ & + 0.33 \times [\text{NO}_2\ (\text{ppb})] \end{aligned}$$

where,

$$[\text{large sulfate}] = ([\text{total sulfate}]/20\ \mu\text{g m}^{-3}) \times [\text{total sulfate}], \quad \text{for } [\text{total sulfate}] < 20\ \mu\ \text{gm}^{-3}.$$

$$[\text{large sulfate}] = [\text{total sulfate}], \ \text{for } [\text{total sulfate}] \geq 20\ \mu\text{g m}^{-3}$$

$$[\text{small sulfate}] = [\text{total sulfate}] - [\text{large sulfate}]$$

Currently, there are 165 sites around the U.S. where parameters for the IMPROVE equation are measured. At some of these sites there are also direct measurement of extinction and scattering to assure the validity of the aerosol component values and their relationship to visibility.

Figure 7.1 presents IMPROVE monitoring network results for the western United States, based on the original IMPROVE equation being used to estimate the worst 20% visibility days measured between 2000 and 2004, the baseline period for the RHRs.

7.4. How does fire contribute to regional visibility and aerosol loading?

Fire contributes to visibility in two fundamental ways: through direct emission of fine organic particles (PM2.5 emissions) and through gaseous emissions of organic hydrocarbons which in turn form SOA in the atmosphere.

In order to quantify the contributions of forest fire to regional air quality, the first step is to develop a fire EI. For retrospective analyses, since it varies much from year to year, the EI must be generated for a specified period of time (e.g., for 2002.) For real-time analyses or forecasts, the EI requires continuing input or a model forecast of fire activity and resulting emissions. Fire EIs are not trivial to develop; they

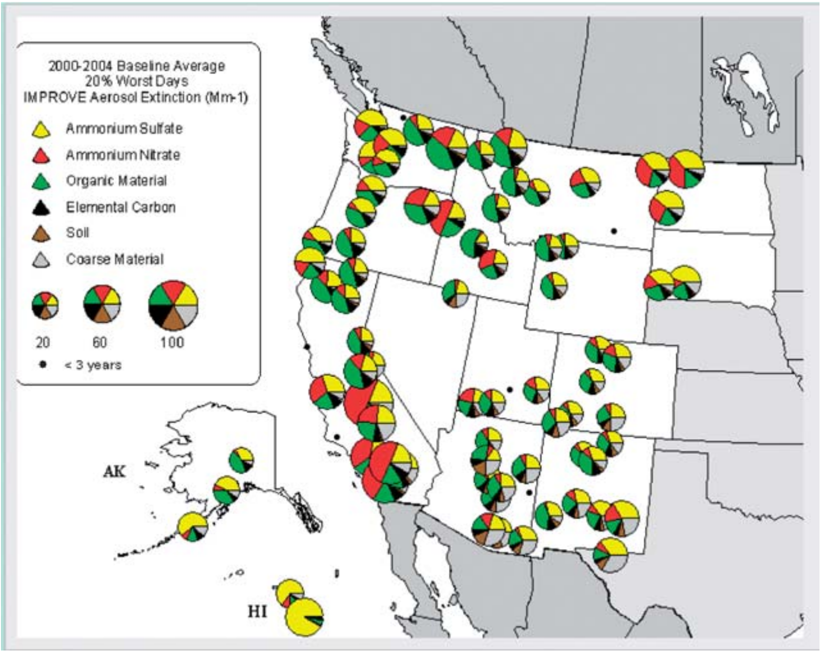

Figure 7.1. IMPROVE results for the Regional Haze Rule baseline period, 2000–2004. (http://vista.cira.colostate.edu/TSS/LinkBrowser/LinkBrowser.aspx?action = baseline)

require large data sets and complex analysis. Quality assurance of such large efforts is always a concern as well.

To create either type of fire EI, three fundamental types of data are needed: fire activity (location, start and end time, and area burned), fuel loadings (the nature of and amounts of fuels involved), and fire type (i.e., wildfire, different types of prescribed burning, agricultural burning.). Fire activity and fuel loadings then can be converted into a numerical estimate of emissions of the various chemical species that affect visibility, as follows:

$$\text{Emissions}_i = A \times B \times \text{CE} \times e_i$$

where emissions$_i$ is the emission of chemical species i (in mass units), A the area burned, B the fuel loading (biomass per area), CE the combustion efficiency, or fraction of biomass fuel burned, and e_i is an emission factor for species i (mass of species per mass of biomass burned.)

In practice there is great uncertainty associated with all the data used for this calculation. A, B, and CE are variables associated with fire activity. Fire activity is subject to significant uncertainty. In the

United States, there are different agencies involved in monitoring and recording fire activity, including federal land managers, state forestry agencies, and local firefighting resources. There are no standards for reporting fire activity: some agencies report total blackened acres and others report fire perimeters each using their own definitions. In addition, *A* depends on determining the actual area combusted, *B* depends upon quantifying the actual biomass complex engaged in the fire, a daunting task, and CE is likely a function of weather, fuel moisture, and a host of other fire dependent variables.

7.4.1. Area burned, A

Determining A, the area of the burn, is complicated by the fact that natural forest fires do not burn uniformly across the fuel bed. There are two different ways to determine the area burned: by ground observations from fire management personnel and from remote sensing, especially by satellite. Inaccuracies of the ground-based approach result from human errors and the priority of this data compared to other responsibilities. Satellite observations have the capability of indicating the actual fire boundaries if the fire is large enough to be resolved by the satellite A recent paper suggests that fires larger than on the order of 6 km^2 can be reliably detected by satellite sensors (about 92%), while those below this size cannot reasonably be detected accurately (Soja et al., 2006). A recent west wide demonstration project of the BlueSky smoke management tool suggested that there were significant errors in the ground-based reporting data associated with wildfires, the IS 209 reports (AirFire, 2006; BlueSky, 2006).

7.4.2. Fuel loading, B

The fuel loading or biomass is neither easily nor accurately estimated. In the United States, the National Fire Danger Rating System (NFDR) fuel models are often utilized to estimate fuel loading because they have been mapped based on data from satellite observation and a large ground-truth measurement program for the U.S. (Burgan et al., 1998; Cohen and Deeming, 1985).

Recently, USDA Forest Service researchers at the Pacific Northwest Research Station have refined the NFDR fuel models by developing a nationally mapped Fuel Characteristics Classification System (FCCS) (McKenzie et al., 2006; Sandberg et al., 2001), which is generated using a rule-based fuzzy classification system that is effectively a landscape fuel succession model allowing a default fuel loading to be approximated anywhere in the U.S.

7.4.3. Combustion efficiency, CE

Determining the specific amount of available fuel actually combusted is difficult. To date, most fire EIs have used the Emissions Production Model (EPM) (Ottmar et al., 1993; Sandberg & Peterson, 1984) which is an empirical relationship based on data collected from prescribed fire activities in the 1970s and 1980s as well as weather and fuel moisture. It has recently been updated with a more user-friendly system known as the Fire Emissions Production System (FEPS) (Sandberg et al., 2004).

7.4.4. Emission factor, e_i

An emission factor is a ratio of the mass of a chemical species released and the total mass of fuel consumed in a combustion process. It can be different for each chemical species and may also depend on the nature of the combustion process.

Table 7.1 summarizes the latest estimates of emissions factors for forest fires (Battye & Battye, 2002; U.S. EPA, 2003b). It is based largely on the research of the fire chemistry research group at the Forest Service's Fire laboratory in Missoula, Montana. Of course, there are added emission factors that are not included in this table, especially for primary and SOA emissions.

Table 7.1. Estimates of emission factors for forest fires in Montana, 2006

CO_2	1833∗CE
CO	961—(984∗CE)
CH_4	42.7—(43.2∗CE)
$PM_{2.5}$	67.4—(66.8∗CE)
PM_{10}	1.18∗$PM_{2.5}$
EC	0.072∗$PM_{2.5}$
OC	0.54∗$PM_{2.5}$
NO_x	16.8∗MCE—13.1
NH_4	0.012∗CE
VOC	0.085∗CO

Notes: Combustion Efficiency (CE) is defined as the difference of (CO_2) in the plume—[CO_2] outside the plume divided by the sum of the differences (between in and outside the plume) of CO+CO_2+CH_4+other organics. Modified Combustion Efficiency (MCE) is defined by the following equation: MCE = 0.15+0.86 CE.

7.5. Modeling fire emissions

The Community Smoke Emissions Model (CSEM) was developed to convert fire activity anywhere in the contiguous U.S. into emissions (Sestak et al., 2002; http://www.wrapair.org/forums/fejf/documents/emissions/JFEFWRAP_CSEM.ppt). Since its initial development, CSEM has been refined and improved by the BlueSky development team and others. The BlueSky emissions generator has been further developed to incorporate alternative fuel models, improved fuel consumption modeling (BlueSky, 2006).

7.5.1. Generating fire emissions inventories

Fire contributes to the $PM_{2.5}$ load in the atmosphere as well as to the specific burden of the various chemical species that make up regional air quality. In order to quantify the specific contribution that fire makes to regional visibility as well as other regional air pollution, it is necessary to use the tools described above to generate specific emissions inventories that can be used in an air quality simulation model. This activity is generally conducted by air quality regulators and managers seeking to estimate relative contributions from various pollution sources. For this purpose, it is helpful to recognize the differences between what, for lack of a better term, might be called natural and human caused fire emissions. Natural fire emissions are, of course, wildfire and prescribed fire done for the purpose of maintaining natural ecological conditions. Prescribed fire conducted to increase production or alter natural landscapes and agricultural burning clearly represents an example of human activities. Although the distinctions can become rather muddled when management practices have suppressed natural fire for decades, for the purpose here, inventories have been constructed based on distinguishing wildfire, wildland fire use (a conceptual category where a wildfire is not suppressed while accomplishing certain management objectives), prescribed fire, and agricultural burning.

A few recent projects have applied these concepts and the modeling approaches and other tools to develop specific fire emissions inventories. The most comprehensive fire EIs have been constructed for the Regional Haze Program's Regional Planning Organizations (RPOs) (http://www.epa.gov/oar/visibility/regional.html).

A national wildfire EI for 2002 for the entire United States has been developed by the RPOs. It is the best and the most comprehensive wildfire EI yet developed from a quality control standpoint. (The RPO inventory is available for download from the Western Regional Air Partnership

Web site at Inter-RPO National 2002 Wildfire Emissions Inventory, Final Work Plan, and the data can be found at http://www.wrapair.org/forums/fejf/tasks/FEJFtask7InterRPO.html.)

In addition to the national RPO wildfire EI, the Western Regional Air Partnership (WRAP) has generated more detailed fire emissions inventories for different types of fire (wildfire, wildland fire use fire, prescribed fire, and agricultural burning) for the western United States for the year 2002. WRAP has also generated hypothetical "baseline" or average-year fire emissions inventories and future average year fire emissions projections for the year 2018, assuming differing levels of prescribed fire and smoke management activities. (All of these fire emissions inventories are available from the WRAP Web site at http://www.wrapair.org/forums/fejf/tasks/FEJFtask7PhaseII.html for the 2002 inventory, and at http://www.wrapair.org/forums/fejf/tasks/FEJFtask7Phase3-4.html for the baseline and 2018 projection data.)

There have also been a few efforts to develop emissions inventories using satellite observations (Soja et al., 2004, 2006; Wiedinmyer et al., 2006). Alternative estimates of emissions such as these are useful in helping to bound EI uncertainties and improve the confidence one might wish to take in fire emissions estimates. These and related efforts have indicated that satellites are increasing in their ability to identify fire location and area burned. As new sensors are flown on satellites, more accurate determinations of smaller and smaller areas are possible.

Some of the results from these emissions inventories are informative. Figure 7.2a summarizes the emissions from all sources, including the contribution made by fire, to the total $PM_{2.5}$ emissions in the western United States. Clearly fire is a significant source in this region.

Figure 7.2b provides an illustration of the relative contribution made by fire (estimated from the 2002 inter-RPO fireEI) to the total $PM_{2.5}$ emissions in the United States from fuel combustion, transportation, and industrial process. Again, it is apparent that on a national basis, fire represents a major contribution to the total $PM_{2.5}$ loading in the U.S. atmosphere.

7.5.2. Processing the fire emissions inventories for use in air quality simulation models

The University of North Carolina's Environmental Program group has adapted the BlueSky emissions model to generate inputs for regional air quality models based on the SMOKE emissions processor (Pouliot et al., 2005). This code is available for anyone to use from the UNC Web site (http://www.cep.unc.edu/empd/products/smoke/bluesky/).

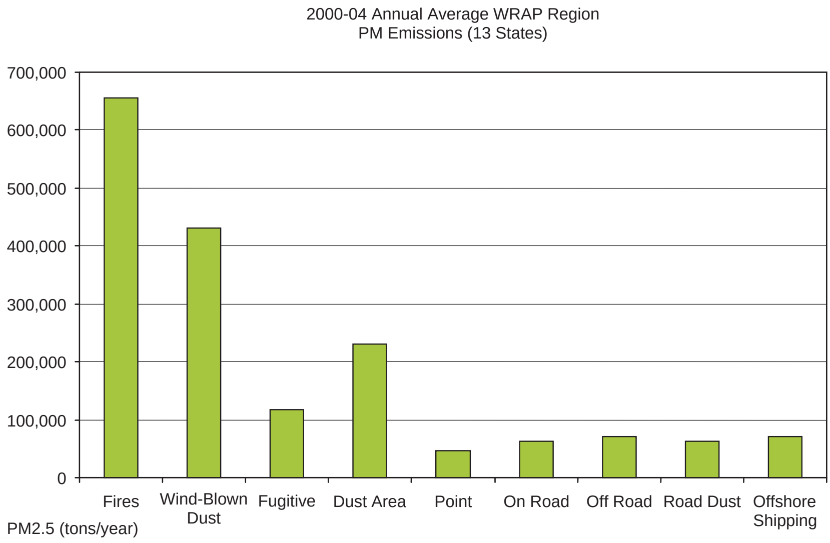

Figure 7.2a. WRAP emissions inventory developed as an annual average for the period from 2000 to 2004. (The inventory does not include out-of-region sources.) (http://wrapair.org/WRAP/meetings/060913m/Board_Tech_Talk_9_14_06_final.ppt)

The inventories have all been processed using the SMOKE model to generate model-ready emissions inventories. Details are available at the WRAP Web site (http://www.wrapair.org/forums/fejf/).

Model-ready fire EI results are detailed in two reports developed by Air Sciences, Inc. (Air Sciences, 2004; Air Sciences, 2005).

7.6. Assessing fire impacts on visibility

7.6.1. Using fire emissions inventory in air quality modeling

The Community Multiscale Air Quality model (CMAQ) is a standard for regional air quality simulation (U.S. EPA, 1999). For this reason, the RPOs have funded its development and application to simulate regional air quality and to realistically portray fire contributions.

Working under contract to the WRAP, the WRAP Regional Modeling Center (RMC) at the University of California, Riverside, conducted a set of simulations that were designed to illustrate the difference between the CMAQ-modeled visibility impacts with and without fire emissions. These model simulations isolate the effects of fire emissions on visibility from

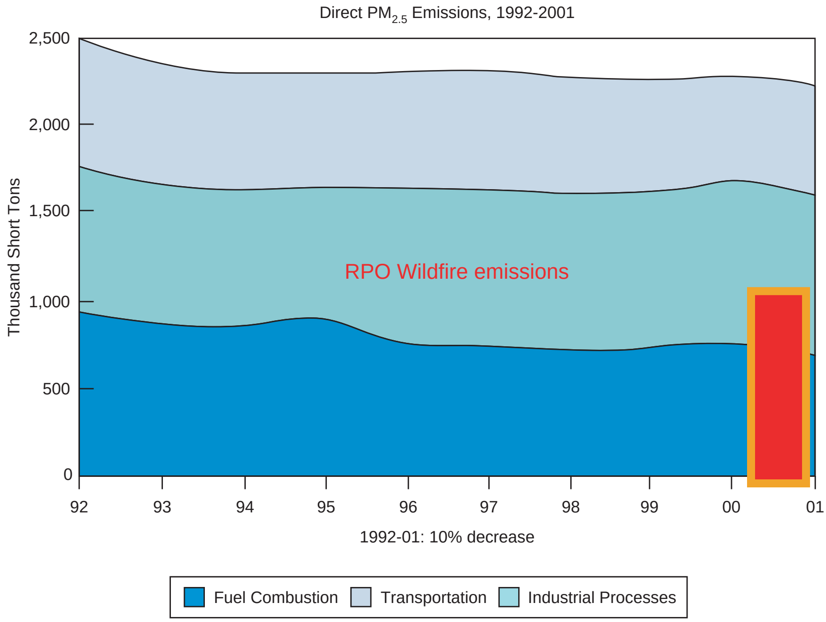

Figure 7.2b. EPA estimate of $PM_{2.5}$ national emissions inventory with the national RPO fire EI added for comparison. (http://www.epa.gov/air/airtrends/aqtrnd03/images/fig-2-45.gif and http://wrapair.org/WRAP/meetings/060913m/Board_Tech_Talk_9_14_06_final.ppt)

the effect of all other emissions sources in the model. It is important to realize that these figures only look at the isolated impact of fires on visibility. There are very large and significant anthropogenic emissions from industrial, mobile, and area sources that make a relatively larger contribution to visibility impact than does fire. However, for our purpose here we have isolated only the various forms of fire and look individually at their impacts. The WRAP RMC conducted three model sensitivity runs considering fire impacts on the WRAP region (Regional Modeling Center (RMC) 2005). These runs used 2002 fire emissions that included prescribed, agricultural and wildfire emissions in the region. The WRAP considers that wildfires, wildland-fire use fires, and prescribed burning used for resource management are natural, while agricultural burning and some prescribed burning are anthropogenic. (For more information regarding the definitions of specific fire activities see http://wrapair.org/forums/fejf/meetings/041208m/FEJF_N-A_EI_Approach_20040903.pdf and http://wrapair.org/forums/fejf/documents/nbtt/FirePolicy.pdf; and for results see http://wrapair.org/forums/aoh/ars1/report.html.)

Figure 7.3a presents the 2002 modeled annual average contribution to light extinction by the full set of emissions, including all fire emissions. However, the extinction values plotted for each grid cell represent modeled extinction due to fire activity only because the extinction due to other species has been subtracted out. Visibility impacts due to all fires are shown to have been generally less than $10\,\mathrm{Mm}^{-1}$ across WRAP, although some locations were impacted by as much as 25, 50, or $>100\,\mathrm{Mm}^{-1}$. Geographically, the largest impacts due to fire occur in southern Oregon, much of California, and isolated locations in Utah, Arizona, and Colorado. Figure 7.3b presents the modeled annual average contribution to light extinction by all natural fires for 2002. This map is not significantly different from Fig. 7.3a, indicating that natural fires contribute a large percentage of the impact of both fire categories combined. Figure 7.3c presents the modeled annual average contribution to light extinction by all anthropogenic fires for 2002. This map indicates that the most significant contributions by anthropogenic fires during 2002 occurred in the region around the panhandle of Idaho and California's Central Valley. The maximum modeled impact of anthropogenic fires is less than $5\,\mathrm{Mm}^{-1}$ (http://wrapair.org/forums/aoh/ars1/report.html and http://wrapair.org/forums/aoh/ars1/report.html).

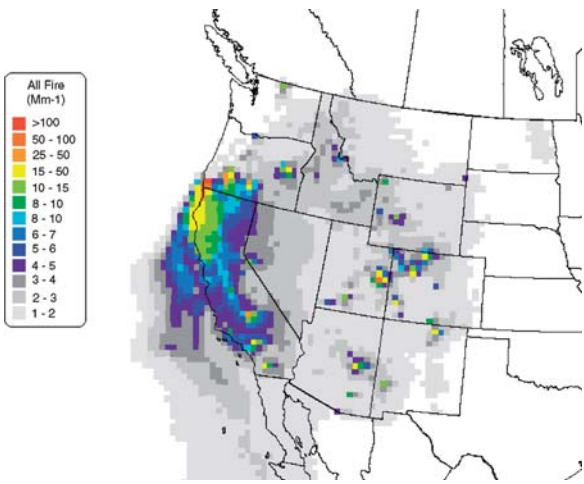

Figure 7.3a. CMAQ model results from a 36 km simulation of all 2002 emissions. However, only the light extinction attributed to fire emissions (all fire emissions, wildfire, wildland fire use fire, prescribed fire and agricultural burning) is presented. (http://www.wrapair.org/forums/aoh/ars1/documents/reports/Section_4.pdf)

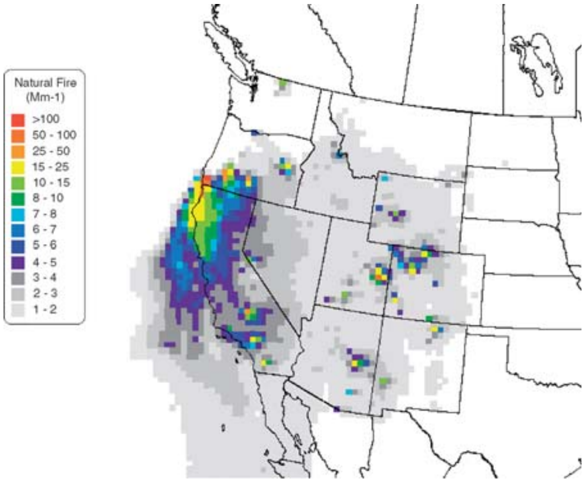

Figure 7.3b. CMAQ model results from a 36 km simulation of all 2002 emissions. However, only the light extinction attributed to "natural" fire emissions (wildfire, wildland fire use fire, and prescribed fire for ecosystem management purposes) is presented. Note this figure is nearly identical to Fig. 7.3a showing results of all fire emissions. (http://www.wrapair.org/forums/aoh/ars1/documents/reports/Section_4.pdf)

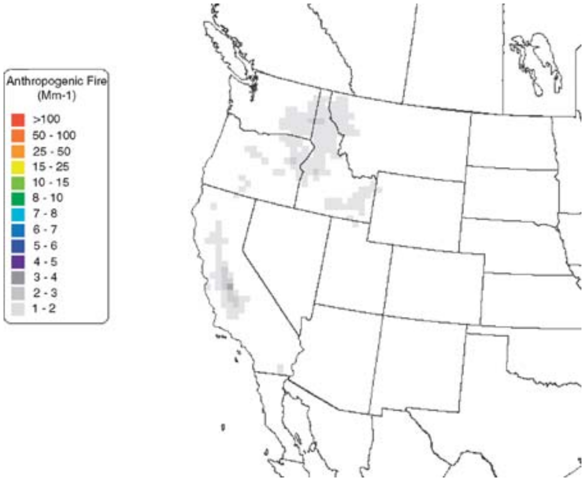

Figure 7.3c. CMAQ model results from a 36 km simulation of all 2002 emissions. However, only the light extinction attributed to "anthropogenic" fire emissions (some prescribed fire and agricultural burning) is presented. Note this figure illustrates that in the western United States, the contribution of this anthropogenic fire to regional haze appears to be quite limited. (http://www.wrapair.org/forums/aoh/ars1/documents/reports/Section_4.pdf)

7.6.2. Use of IMPROVE monitoring with modeling to quantify impacts of fire on regional visibility

In support of the RHR, two key Web sites have been developed: VIEWS presents details of regional air quality data and TSS provides a technical reference to help ascribe causes to impaired visibility in the western U.S. TSS also provides an array of tools that can help to quantify fire's contributions to regional visibility. However, none of these is completely satisfying by itself. Figure 7.1 illustrates the average results from the IMPROVE monitoring from 2000–2004, showing the relative contribution that each of the IMPROVE aerosol species makes to visibility on the 20% worst visibility days in the western United States. Figure 7.4 shows the same information for the entire United States in 2002. Note that the locations where the pie charts are predominantly green are locations where one might expect fire to be a significant contributor to regional visibility degradation.

7.6.3. Statistically apportioning visibility impacts to fire

Among the inferential ways to consider fire's impact are statistical analyses of the IMPROVE and other aerosol data. If there were a unique tracer of fire's contribution, then simply measuring the amount of that unique tracer would be possible. However, there is no such unique tracer, although this is the subject of ongoing research activities.

One approach that has been followed is to look at the ratio of OC to black (or elemental) carbon in the measurements (Malm et al., 2004). Ames et al. (2004) present results of this and an alternative approach aimed at bracketing the influence of fire. The ratio of organic carbon to elemental carbon (OC/EC) can be associated with significantly different forms of combustion. Combustion of fossil fuels (gasoline, diesel, etc.) is generally associated with an internal combustion engine characterized by a relatively efficient combustion. This combustion is enriched in EC such that the OC/EC ratio is on the order of 3. Urban organic fine particulate measurements often display ratios on this order. Open combustion is often less efficient, emitting a higher amount of OC relative to EC. Fine particulate measurements that can otherwise be related to wildland fire display OC/EC ratios on the order of 10 or more. Ames used this ratio to distinguish fire from urban sources in the IMPROVE measurements. However, there are sources of OC not associated with EC at all, namely atmospheric chemical reactions of natural hydrocarbon emissions from vegetation, termed biogenic emissions that generate SOAs. Wherever there is significant vegetative cover, there will be SOA formed. Since this

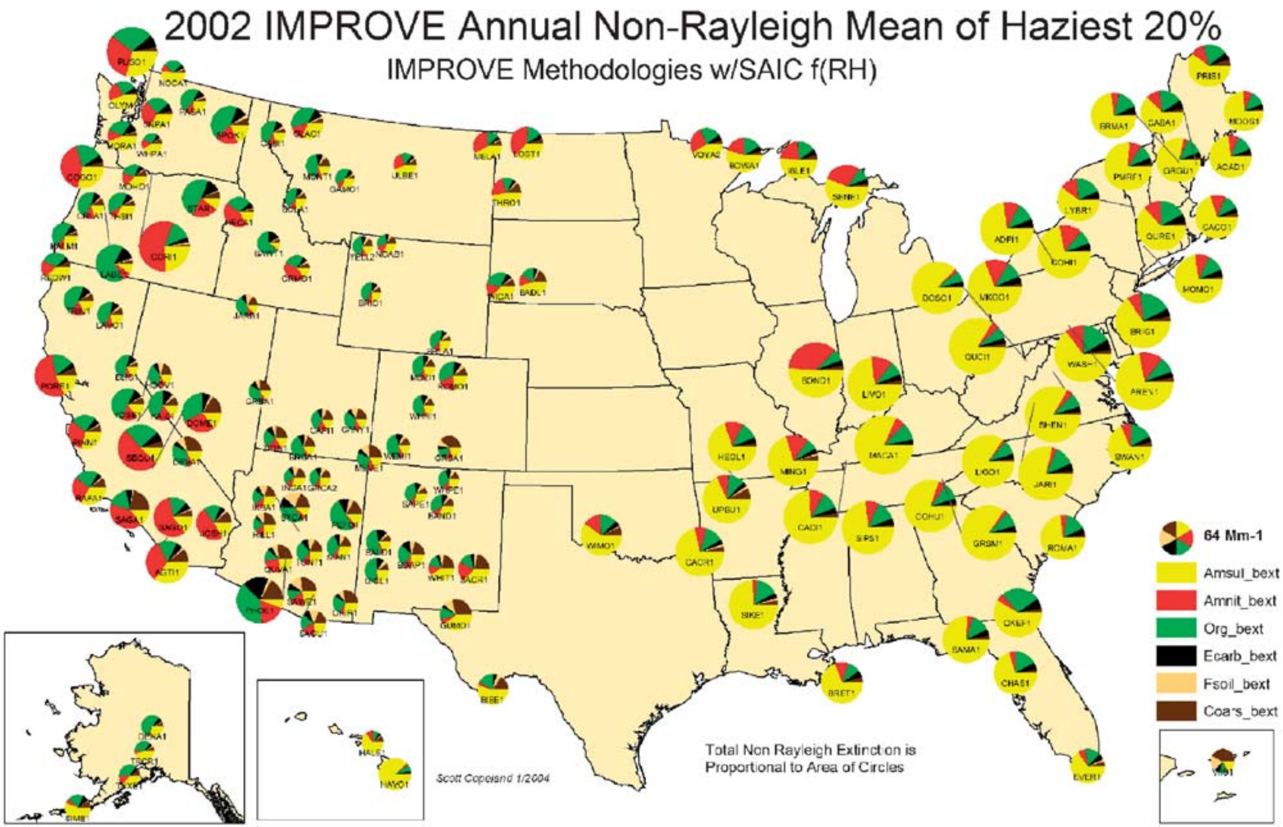

Figure 7.4. IMPROVE monitoring results from 2002 for the 20% worst visibility days. The pie charts illustrate the contribution that each of the IMPROVE aerosol components makes to the extinction. Note the distribution of values of OC (green) suggests locations where fire may have a potentially significant impact on regional visibility. (Unpublished graphic prepared by S. Copeland, CIRA, 2004 based on IMPROVE data from http://vista.cira.colostate.edu/improve/Publications/Reports/2006/PDF/Chapter3.SeasonalPatternsRegionalConcentrations.pdf)

source of OC is not considered in the analysis, the OC/EC ratio will be highly biased by the presence of this added OC; thus, this ratio is likely to overestimate the influence of fire on visibility. To bracket this, Ames considered a second apportionment method, namely using a fire occurrence database (Brown et al., 2002) and then looking at back trajectories (Heffter, 1980) from each IMPROVE monitor for a period of time leading up to and through the measurement and apportioning the fire influence based on the amount of time the air spent over fire locations. This approach has many potential errors, so many in fact, that the Joint Fire Sciences Program (JFSP) recently funded the National Park Service to investigate this and related methodologies further. Due to the facts that the fire activity database used does not include all fire and the inadequacies of trajectories, this method is likely to underestimate the influence of fire on visibility.

OC concentrations at IMPROVE monitoring sites (2000–2002 OC/EC analysis) are approximately 1.0 $\mu g/m^3$ in the western U.S. and 1.7 $\mu g/m^3$ in the east. Over the same time period and monitoring sites, OC apportioned to fire and SOA using the OC/EC ratio approach is about 0.6 $\mu g/m^3$ in the west, and 0.9 $\mu g/m^3$ in the east, or approximately 60% of observed OC in the west and 55% in the east. OC apportionments to U.S. wildland fires from the fire activity and trajectory method averaged about 0.3 $\mu g/m^3$ in the west and 0.4 $\mu g/m^3$ in the east, or approximately 30% of observed OC in the west and 20% in the east.

For reference, the RHRs assume that natural visibility in the U.S. is characterized by an OC concentration of approximately 1.1 $\mu g/m^3$ in the eastern U.S. and 0.4 $\mu g/m^3$ in the west (U.S. EPA, 2003a).

Recently, using a global air quality model, Park et al. (2003) have estimated OC values of approximately 0.7–1.1 $\mu g\,m^{-3}$ may be representative of natural conditions in the west, and OC concentrations of approximately 0.9 $\mu g\,m^{-3}$ to be characteristic of natural conditions in the eastern United States.

7.6.4. Compare model results to IMPROVE monitoring

Figures 7.5a–c present WRAP 2002 fire simulations and IMPROVE data developed from the TSS. Here, we present results at three of the more obviously fire-influenced sites in the western U.S.: the Flathead Lake IMPROVE site in Montana (Fig. 7.5a); Hells Canyon IMPROVE site in Oregon (Fig. 7.5b), and the Sequoia National Park IMPROVE site in California (Fig. 7.5c). The IMPROVE monitoring result is presented in the top panel, the second panel presents WRAP CMAQ modeling results

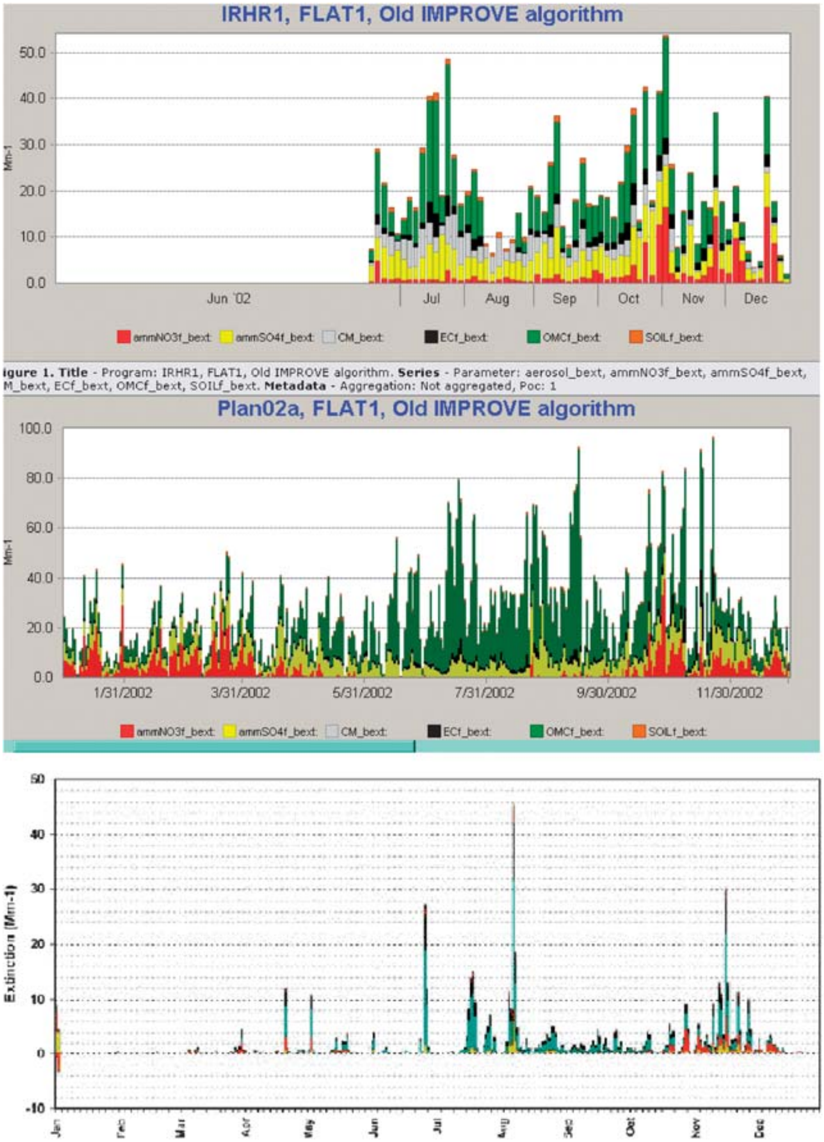

Figure 7.5a. Fire monitoring and modeling compared for the IMPROVE site at Flathead Lake, Montana, for 2002. Top panel represents the IMPROVE observations, the second panel the WRAP full emissions inventory modeling results and the third panel the WRAP fire emissions inventory modeling only. (http://vista.cira.colostate.edu/TSS/Results/HazePlanning.aspx)

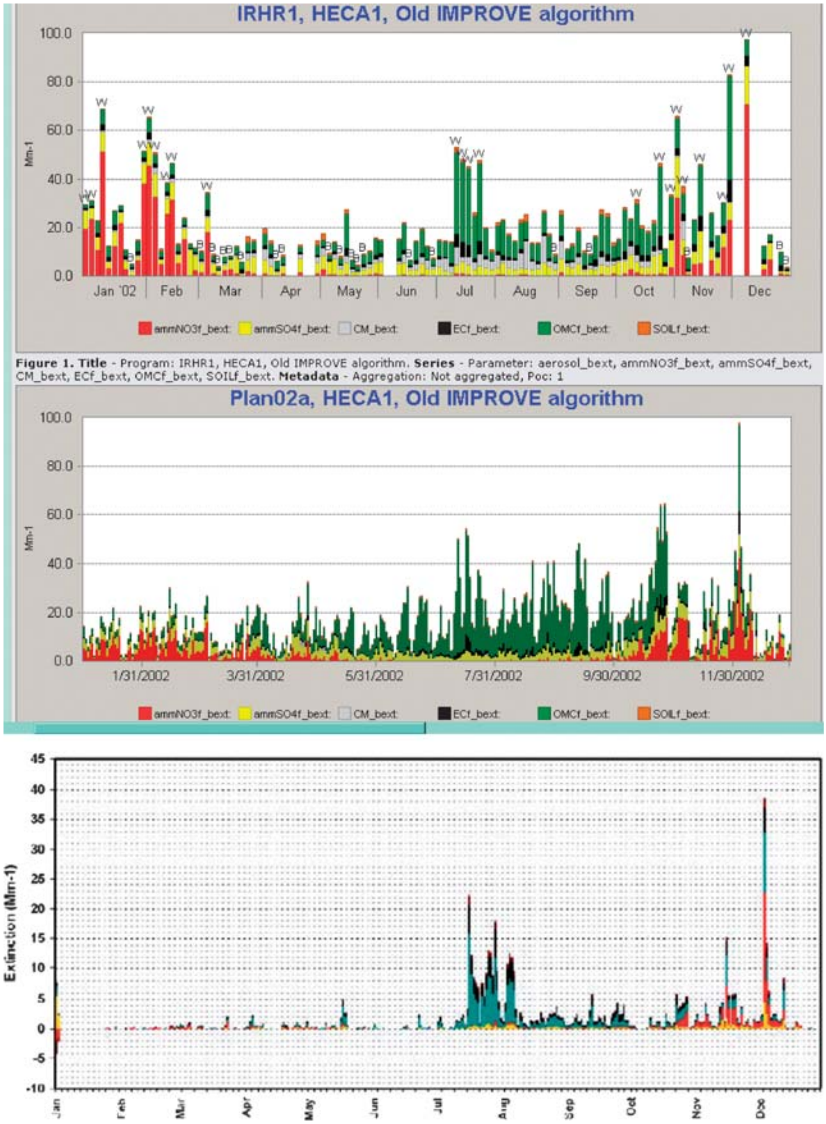

Figure 7.5b. Fire monitoring and modeling compared for the IMPROVE site at Hells Canyon, Oregon, for 2002. Top panel represents the IMPROVE observations, the second panel the WRAP full emissions inventory modeling results and the third panel the WRAP fire emissions inventory modeling only. (http://vista.cira.colostate.edu/TSS/Results/HazePlanning.aspx)

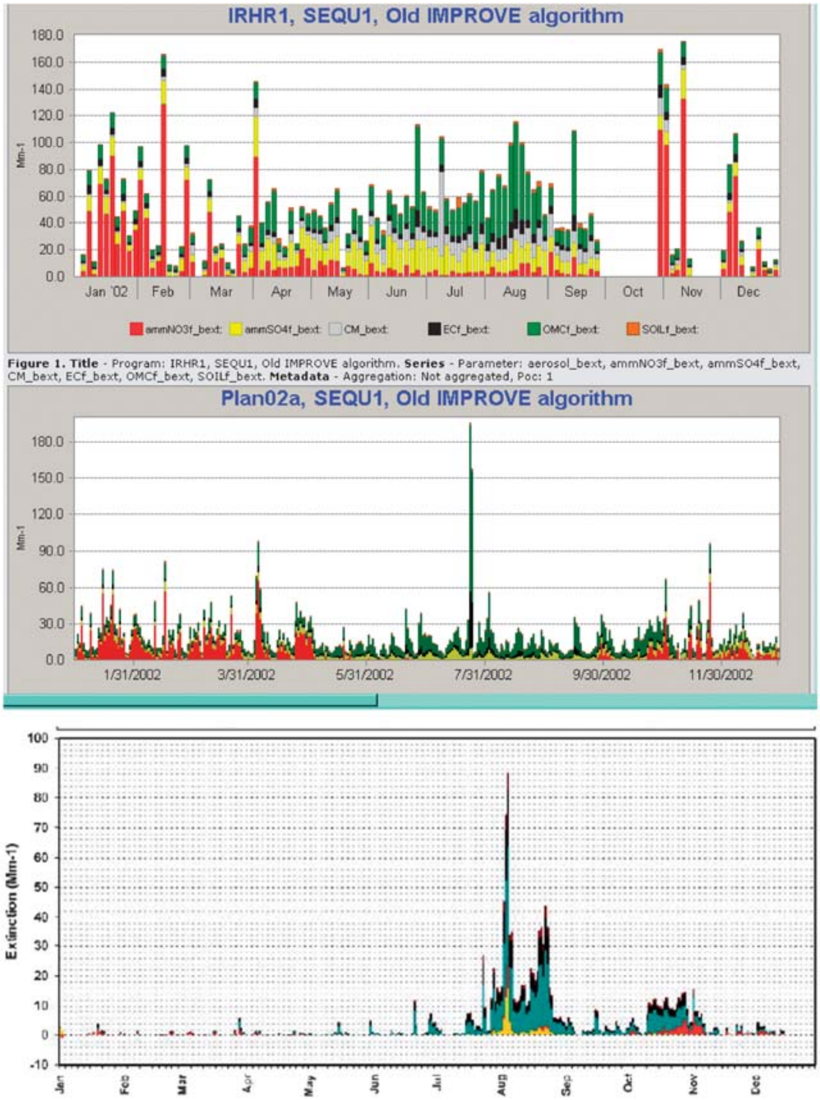

Figure 7.5c. Fire monitoring and modeling compared for the IMPROVE site at Sequoia National Park, California, for 2002. Top panel represents the IMPROVE observations, the second panel the WRAP full emissions inventory modeling results and the third panel the WRAP fire emissions inventory modeling only. (http://vista.cira.colostate.edu/TSS/Results/HazePlanning.aspx)

based on the full WRAP EI, and the third panel represents the fire only contribution to the extinction as calculated by the simulations.

It is clear from the results that the modeling appears to exhibit at least qualitative skill in simulating the impacts of fire on visibility. However, it is also clear that this represents only the beginning of what will be a continuing investigation into the influences of fire on regional haze (Rodriguez et al., 2006).

In July 2007 the WRAP engaged in an attribution of haze analysis utilizing the capabilities of the TSS (http://wrapair.org/forums/aoh/index.html). This project is scheduled for completion by the end of 2007. Figure 7.6 presents preliminary results illustrating the influences of different emissions types on visibility at the Hells Canyon Class I area. Specifically looking only at the impact of OC aerosol, this analysis involves combining source regions and the trajectories of air flows during the worst visibility conditions experienced in the 2000–2004 5-year baseline period as well as the simulated contributions from these sources in future inventories based on both planned and possible emissions reductions. Details of the analysis are found on the TSS web site (http://vista.cira.colostate.edu/tss). The results show that "anthropogenic fire" has a significant potential impact on this site.

7.7. Conclusions and next steps

By way of a preliminary conclusion, research to date suggests that somewhere between 25% and 60% of the OCM measured in ambient air is a result of smoke from wildfire. In relation to estimated natural background values, this suggests that the vast majority of the natural background of OC aerosol in the western U.S. results from fire and nearly 50% of it in the east may be due to fire. A significant portion of the remainder in the east is likely attributable to secondary aerosol formation from vegetation emissions of reactive hydrocarbons. These results are confounded by the presence of fine mass transported long distances, from Asia and Africa, which occasionally impact the United States. As regional air quality simulation modeling progresses, we should be better able to quantify these impacts.

We feel that the following six activities are among the most significant missing elements in any ongoing attempt to assess fire's contribution to regional air pollution and specifically to visibility degradation:

- *Develop a national fire activity database* system as a single, all-agency, all-area source of quality-assured information about the location, timing, and size of fires. This is the necessary first step in developing an

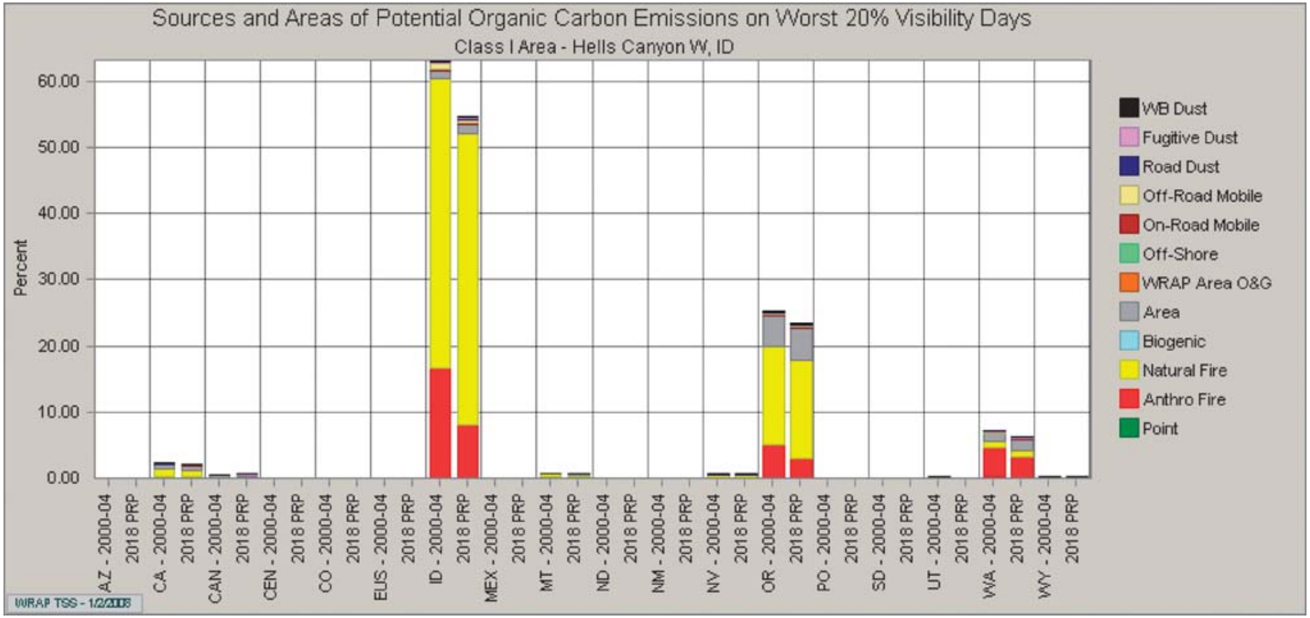

Figure 7.6. TSS results illustrating the influences of different emissions types on visibility at one IMPROVE site. Looking at only organic carbon aerosol, this analysis involves combining source regions and the trajectories of air flows during the worst visibility conditions experienced in the 2000–2004 5-year baseline period as well as planning inventories for future years. (http://vista.cira.colostate.edu/TSS/Results/HazePlanning.aspx)

accurate and continuing EI of fire emissions for not only air pollution but for climate change and CO_2 emissions issues as well.
- *Develop chemical tracers* to distinguish carbon from different types of fire and other sources in the measured regional aerosol mixture.
- *Improve emissions factors and secondary aerosol formation mechanisms* for primary and SOA resulting from different types of fires.
- *Continue apportionment* studies using multiple years of speciated PM data.
- *Apply improved regional scale simulation modeling including fire emissions.*
- *Apply satellite remote sensing* for fire impacts on Class I areas.

REFERENCES

Air Sciences, 2004. FINAL REPORT—1996 Fire Emission Inventory for the WRAP Region—Methodology and Emission Estimates. Project 178-1, March 2004. http://www.wrapair.org/forums/fejf/documents/emissions/FEJF1996EIReport_040325_final.pdf

Air Sciences, 2005. Integrated Assessment Update and 2018 Emissions Inventory for Prescribed Fire, Wildfire, and Agricultural Burning Report. Project 178-2. November 2005. Prepared for the Western Governor's Association/WRAP/Fire Emissions Forum. http://www.wrapair.org/forums/fejf/documents/emissions/WGA2018report20051123.pdf

AirFIRE, 2006. BlueSky and BlueSkyRAINS User's guide and Operating Manual. Version 1.1. February, 64 pp. http://marlin.airfire.org/BSUG_v1_1_020206.pdf

Ames, R.B., Fox, D.G., Malm, W.C., and Schichtel, B.A. 2004. Preliminary apportionments of carbonaceous aerosols to wild fire smoke using observations from the IMPROVE network. Regional Haze paper # 76; Air and Waste Management Association, Asheville, NC.

Battye, W., and Battye, R. 2002. Development of Emissions Inventory Methods for Wildland Fire. Prepared for the US Environmental Protection Agency, Research Triangle Park, North Carolina, 27711.

BlueSky, 2006. BlueSkyRAINS West (BSRW) Demonstration Project. Final report (unpublished). USDA Forest Service Pacific Northwest Research Station. Available from: http://www.fs.fed.us/pnw/airfire/

Brown, T.J., Hall, B.L., Mohrle, C.R., and Reinbold, H.J. 2002. Coarse Assessment of Federal Wildland Fire Occurrence Data. CEFA Report #02-04.

Burgan, R., Klaver, R.W. and Klaver, J.M. 1998. Fuel models and fire potential from satellite and surface observations. Int. J. Wildland Fire 8(3), 159–170.

Cohen, J.D., and Deeming, J.E. 1985. The national fire danger rating system: Basic equations. USDA For. Serv. Gen. Tech. Rep. PSW-82. Pacific Southwest Forest and Range Experiment Station, Berkeley, CA.

Hand, J.L., and Malm, W.C. 2005. Review of the IMPROVE equation for estimating ambient light extinction coefficients. CIRA Report, Colorado State University. ISN 0737-5352-71. Available at http://vista.cira.colostate.edu/improve/Publications/GrayLit/016_IMPROVEeqReview/IMPROVEeqReview.htm

Heffter, J.L. 1980. Air resources laboratories atmospheric transport dispersion model (ARL-ATAD). Technical Memo ERL ARL-81, NOAA, Rockville.

Malm, W.C., Schichtel, B.A., Pitchford, M.L., Ashbaugh, L.L., and Eldred, R.A. 2004. Spatial and monthly trends in speciated fine particle concentration in the United States. J. Geophys. Res. 109, doi:10.1029/2003 JD003739.

McKenzie, D., O'Neill, S.M., Larkin, N.K., and Norheim, R.A. 2006. Integrating models to predict regional haze from wildland fire. Ecol. Model. 199, 278–288.

Ottmar, R.D., Burns, M.F., Hall, J.N., and Hanson, A.D. 1993. CONSUME users guide. USDA Forest Service General Technical Report PNW-GTR-304. Pacific Northwest Research Station, Portland, OR.

Park, R.J., Jacob, D.J., Chin, M., and Martin, R.V. 2003. Sources of carbonaceous aerosols over the United States and implications for natural visibility. J. Geophys. Res. 108(D12),

Pouliot, G., Pierce, T., Benjey, W., O'Neill, S.M., and Ferguson, S.A. 2005. Wildfire emission modeling: Integrating Bluesky and SMOKE. Presentation at the 14th International Emission Inventory Conference, Transforming Emission Inventories Meeting Future Challenges Today, 4 /11 –4/14/05 Las Vegas, NV.

Regional Modeling Center (RMC), 2005. Fire sensitivity simulations. http://pah.cert.ucr.edu/aqm/308/cmaq.shtml#fire1

Rodriguez, M.A., Barna, M.G., and Schichtel, B. 2006. Using CAMx to model the potential impacts of a proposed power plant in the Four Corners region, presented at the 99th AWMA Annual Conference and Exhibition, New Orleans, LA, June 20–23.

Sandberg, D.V., and Peterson, J. 1984. A source-strength model for prescribed fires in coniferous logging slash. In: Proceedings, 21st Annual Meeting of the Air Pollution Control Association, Pacific Northwest International Section. Air Pollution Control Association, Pittsburgh, PA.

Sandberg, D.V., Ottmar, R.D., and Cushon, G.H. 2001. Characterizing fuels in the 21st century. Int. J. Wildland Fire 10, 381–387.

Sandberg, D.V., Anderson, G., and Norheim, R.A. 2004. Fire emission production simulator (FEPS): An upgrade of the emission production model (EPM). http://www.fs.fed.us/pnw/fera/feps/index.html

Sestak, M., O'Neill, S., Ferguson, S., Chang, J., and Fox, D.G. 2002. Integration of wildfire emissions into MODELS-3/CMAQ with the prototypes: Community smoke emissions modeling system (CSEM) and BlueSky. Extended Abstract presented at the First CMAS (Community Modeling and Analysis System) Models3 Workshop. October 21–22, 2002. Research Triangle Park, NC. http://www.cmascenter.org/conference/2002/session5/fox_abstract.pdf

Soja, A.J., Sukhinin, A.I., Cahoon, D.R. Jr., Shugart, H.H., and Stackhouse, P.W. Jr. 2004. AVHRR derived fire frequency, distribution and area burned in Siberia. Int. J. Remote Sensing 25, 22.

Soja, A., Al-Saadi, J., Pierce, B., Kittaka, C., Szykman, J., Williams, J., and Pace, T. 2006. How well does satellite data quantify fire and enhance biomass burning emissions estimates? EPA Conference proceedings. http://www.epa.gov/ttn/chief/conference/ei15/session10/soja.pdf

Trijonis, J.C., Malm, W.C., Pitchford, M., and White, W.H. 1990. Chapter 24. In: P.M. Irving, ed. Acidic deposition: State of science and technology, vol. 3. Terrestrial, materials, health and visibility effects, U.S. Natl. Acid Precip. Assess. Prog. (NAPAP), Washington, DC.

U.S. Environmental Protection Agency (EPA). 1999. Science algorithms of the EPA Models-3 community multiscale air quality (CMAQ) modeling system. EPA/600/R-99/030.

U.S. Environmental Protection Agency (EPA). 2003a. Guidance for estimating natural visibility conditions under the regional haze rule, Office of Air Quality Planning and Standards, Research Triangle Park, NC. EPA-454/B-03-005.

U.S. Environmental Protection Agency (EPA). 2003b. Data needs and availability for wildland fire emission inventories-short-term improvements to the wildland fire component of the national emissions inventory. June 5, 2003, prepared under EPA Contract No. 68-D-02-064, Work Assignment No. I-08.

Wiedinmyer, C.E., Quayle, B., Geron, C., Belote, A., McKenzie, D., Zhang, X., O'Neill, S., and Wynne K.K. 2006. Estimating emissions from fires in North America for air quality modeling. Atmos. Environ. 40, 3419–3432.

This page intentionally left blank

Developments in Environmental Science, Volume 8 197
A. Bytnerowicz, M. Arbaugh, A. Riebau and C. Andersen (Editors)

ISSN: 1474-8177/DOI:10.1016/S1474-8177(08)00008-9

Chapter 8

Assessment of Forest Fire Impacts and Emissions in the European Union Based on the European Forest Fire Information System

Paulo Barbosa, Andrea Camia, Jan Kucera, Giorgio Libertà, Ilaria Palumbo, Jesus San-Miguel-Ayanz and Guido Schmuck*

Abstract

An analysis on the number of forest fires and burned area distribution as retrieved by the European Forest Fire Information System (EFFIS) database is presented. On average, from 2000 to 2005 about 95,000 fires occurred annually in 23 European countries, burning almost 600,000 ha of forest land every year. Of these about two-thirds or 65,000 fires occurred in 5 European Union (EU) Mediterranean countries (France, Greece, Italy, Portugal, and Spain) where on average half a million hectares of forest land were burned every year. In addition, out of the 23 European countries, the total burned area was 86% within those 5 countries alone during the 6-year study period, and out of the 19 EU countries the total for the 5 countries was 96%. Estimates of atmospheric emissions of carbon dioxide (CO_2) and other trace gases were done for the 2000–2005 period in which burned area maps were retrieved using remote sensing imagery, and then combined with fuel load and burning efficiency figures, to estimate the quantity of burned biomass. Emission factors were further used to estimate trace gas and aerosol emissions produced by vegetation fires. Fuel load was estimated based on values found in the literature and from existing land cover maps of Europe. Average burning efficiency and emission factors were retrieved from the literature. The results obtained show that the forest fires atmospheric emissions of the 23 European countries considered in this study ranged from 8.4 to 20.4 Tg of CO_2/year.

*Corresponding author: E-mail: Paulo.BARBOSA@ec.europa.eu

8.1. Forest fires in Europe

Wildfires, often referred to as forest fires in Europe, have coexisted with human activities and have shaped the Mediterranean landscapes. Although fire has always existed as a natural phenomenon—inducing species regeneration and landscaped biodiversity—the use of fire for a number of activities such as grazing, agriculture, and hunting has significantly modified fire regimes, primarily in the Mediterranean region. More recently the increase of population density in Europe and the extensive use of natural and forest regions for recreation has increased the number of human-caused fires. In addition, the decrease of rural population and the abandonment of agricultural regions mainly in southern Europe have led to the build up of fire fuels on these areas and the consequent increase in fire risk. Nevertheless, although the number of fires has steadily increased in the last decades, on average the total area consumed has not increased. This is mostly due to the active fire suppression policy and the large economic investment in firefighting techniques of the European countries as well as the fire prevention measures. Lately, however, extreme fire danger meteorological conditions in 2003, 2005, and 2007 have contributed to an increased number of fires and burned area in Europe.

The European Commission Joint Research Centre (JRC) started a research activity in 1999 aimed at the development and implementation of advanced methods for the evaluation of forest fire risk and mapping of burnt areas at the European scale. The outcome was the development of the European Forest Fire Information System (EFFIS). In addition to producing daily meteorological fire danger forecast maps, and coordinating the harmonization of a European fire database, EFFIS has produced a number of burned area maps for the 2000–2005 period in five European Union (EU) Mediterranean countries: France, Greece, Italy, Portugal, and Spain (European Commission, 2001; European Commission, 2002; European Commission, 2003; European Commission, 2004; European Commission, 2005; European Commission, 2006). Since 2006 the burned areas of other European countries such as Croatia, Cyprus, and Turkey have also been mapped, and in 2007 due to the extreme fire season in the Balkans, the burned areas of the following additional countries were also mapped: Albania, Bosnia-Herzegovina, Bulgaria, Former Yugoslav Republic of Macedonia, Montenegro, and Serbia.

Although estimates of biomass burning emissions exist at the global and regional scales, no studies have ever been performed to specifically estimate the contribution of forest fires in the EU. This chapter presents the most current statistics for number of forest fires and burned area in the EU as well as estimates of biomass burning emissions for the 2000–2005 period. The burned area maps for each year were combined with fuel loads and burning efficiency figures, to estimate the quantity of burned biomass. Emission factors were further used to estimate the trace gas and aerosol emissions produced by vegetation fires.

8.2. Data sets

The burned area maps were produced using two different remote sensing images: the Indian Remote Sensing (IRS)–Satellite Wide Field Sensor (WiFS) for the 2000–2003 period and the TERRA/AQUA–MODerate-resolution Imaging Spectroradiometer (MODIS) images for the 2003–2005 period. A map of fuel types was used in order to obtain the fuel load information. The EU fire database managed by the JRC has also been used to further enhance the forest fire emissions and burned biomass estimates.

8.2.1. The EU fire database

The European Economic Community (EEC) regulation No. 804/94 (now expired) established a community system of information on forest fires for which a systematic collection of a minimum set of data on each fire, the ''common core'', had to be carried out by the member states participating in the system.

According to the current regulation (Forest Focus [EEC] No. 2152/2003) about monitoring forests and environment interactions in the community, the forest fire common core data should continue to be recorded and provided to the EC in order to collect comparable information on forest fires at community level. Within this new framework the database is being refined and an enhanced version is under development, with the support of the relevant forest services and civil protection services of the EU member states, to consolidate and implement the EU fire database in EFFIS (effis.jrc.it/EU_Fire_Database).

The forest fire data for the EU Fire Database are provided each year by individual member states, with the following primary data items recorded for each fire event

– Date and time of first alert, first intervention, and fire extinction.
– Fire location in terms of administrative units (local area units) and of geographical coordinates.

- Burned area detailed into the following four land cover categories: forest, other wooded land, other non-wooded natural land, agriculture, and other artificial vegetated land.
- Presumed fire cause as outlined in both the general EU fire causes category and the individual countries category.

At present the database covers 23 countries with information for 2000–2005 although some countries have information on a longer time period, such as Austria, Cyprus, Czech Republic, Estonia, Finland, France, Germany, Greece, Hungary, Italy, Latvia, Lithuania, Poland, Portugal, Romania, Slovakia, Slovenia, Spain, Sweden, Croatia, Switzerland, Turkey, and Norway.

The information from the EU fire database has been used to improve the estimations of forest fire emissions and burned biomass computed with the burned area maps for the five EU Mediterranean countries as well as to extend the estimations to the 23 countries currently included in the database.

8.2.2. Burned area maps

The burned area maps were obtained through the classification of two different types of satellite imagery, IRS–WiFS and MODIS. In both cases the minimum mapping unit used was set to 50 ha, meaning that only fires equal to or larger than 50 ha were mapped.

The WiFS camera is a multispectral-WiFS, whose spectral channels are optimized to determine vegetation indices. WiFS collects data in two bands that correspond to red and near infrared. The ground swath is around 810 km, and the spatial resolution is 180 m. The time of overpass is around 10:30 a.m. local time. The potential revisiting time is five days. Images were acquired at the end of the fire season, typically between middle of September to end of October, in order to map all the burned areas of the year. The burned areas were mapped using a multitemporal change-detection technique (Barbosa et al., 2002). Although no specific validation was done for the burned area maps, the maps were sent to the national Forest Services for quality assessment, which reported positive feedback.

MODIS instrument is carried both on the TERRA (morning pass) and AQUA (afternoon pass) satellites. MODIS data has two bands with spatial resolutions of 250 m (red and near-infrared bands) and five bands with spatial resolution of 500 m (blue, green, and three short-wave infrared bands). The time of overpass of TERRA is in the early morning, while AQUA overpass is in early afternoon, allowing for two images per day. Images are acquired every day, providing continuous monitoring of fires and mapping of burned areas. Although mainly the 250-meter bands were used to map the burned areas, the MODIS bands at 500 m resolution were sometimes used for confirmation. Mapping of the burned areas was done through visual classification, and the comparison of the estimated total burned area with the official statistics from the five countries analyzed showed high correlation (Barbosa et al., 2006).

8.2.3. Fuel map

Fuel types were classified using two databases: the COoRdinate Information on the Environment (CORINE) Land Cover 2000 (CLC2000; European Environment Agency, 2002) and the Map of Natural Vegetation of Europe (MNVE; Bohn & Neuhäusl, 2003). CLC2000 is an update for the reference year 2000 of the first CORINE Land Cover database that was finalized in the early 1990s as part of the European Commission CORINE program (European Commission, 1994). CLC2000 is based on the photo-interpretation of Landsat satellite images and has a fairly good spatial resolution, with a mapping scale of 1:100,000 and minimum mapping unit of 25 ha. However, thematically the CLC can be considered relatively poor, since only 44 classes are distinguished. On the other hand, the MNVE has a lower spatial resolution (mapping scale of 1:3,000,000) but depicts more than 100 vegetation associations. The CLC classes were stratified into subregions according to phytosociological criteria, which accounted for the floristic composition and other factors governing the distribution of the vegetation. These subregions were then linked to the U.S. National Fire Danger Rating System (NFDRS) fuel model map (Burgan, 1988; Sebastian et al., 2002) in order to assign a fuel type to each of the subregions. The NFDRS fuel load corresponding to each of the fuel model classes was then assigned to the European Fuel Model Map (Table 8.1).

8.3. Computation of burned biomass and atmospheric emissions

The NFDRS model divides each of the fuel classes into dead fuel (fine, small, and large) and live fuel (woody and herbaceous). Each of the components of the fuel classes are attributed a specific burning efficiency and emission factor for gas-phase or aerosol compounds, depending on if the fire is flaming or smoldering, which is related with the diameter of the fuel type (Leenhouts, 1998). The general equation for computing emission

Table 8.1. NFDRS fuel model corresponding to the fuel model classes assigned to the European fuel model map

NFDRS model	European fuel model model description
A	Grassland vegetated by annual grasses and forbs
C	Open pine stands with perennial grasses and forbs
D	Shrubland understory and pine overstory
F	Sclerophylous oakwood vegetation
H	Short-needled conifers with sparse undergrowth and thin layer of ground fuels
L	Grassland vegetated by perennial grasses
N	Inland and coastland marshes
O	Broadleaved forests of *Quercus ilex*, rotundifolia, and suber
P	Coniferous forest with Iberian-Atlantic oak-ash woods and Cantabrian beechwoods
R	Broadleaved forest
S	Sparsely vegetated areas
T	Transitional woodland shrub
X	Non forest class

(e.g., CO_2) from forest fires is the following:

$$CO_2 = \sum_f A_f \times B_f \times C \times E_f$$

A_f burned area (m^2)
B_f fuel load ($g\,m^{-2}$)
C burning efficiency ($g\,g^{-1}$)
E_f emission coefficient for CO_2
f fuel class

8.4. Results and discussion

According to the EU Fire Database, during the 2000–2005 period on average about 95,000 fires occurred annually in the 23 European countries (Fig. 8.1), burning almost 600,000 ha of forest land every year (Fig. 8.2).

Of these fires about two-thirds or 65,000 occurred in five EU Mediterranean countries (France, Greece, Italy, Portugal, and Spain) where on average half a million hectares of forest land were burned every year. In addition, out of the 23 European countries, the total burned area was 86% within those 5 countries alone during the 6-year study period, and out of the 19 EU countries the total for the 5 countries was 96%. Figure 8.3 shows the average burned area per year in the 23 European

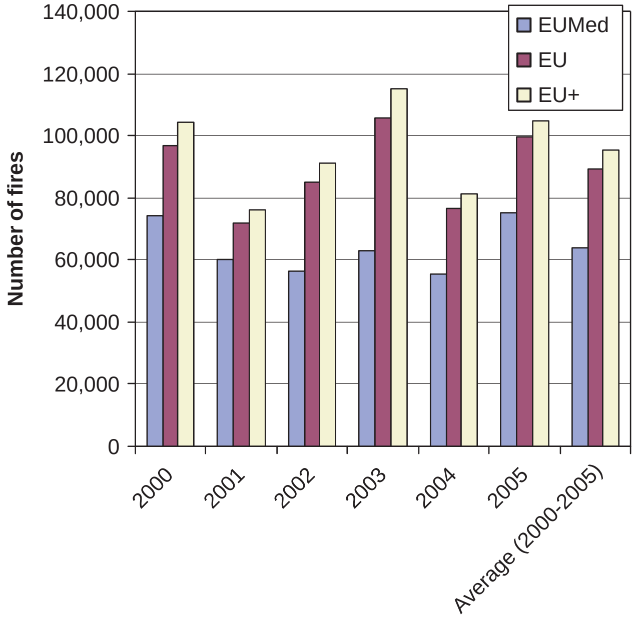

Figure 8.1. Number of fires in the 5 EU Mediterranean countries (EU Med: France, Greece, Italy, Portugal, and Spain) compared with the 19 countries for which data is currently available in the database of EU (Austria, Cyprus, Czech Republic, Estonia, Finland, France, Germany, Greece, Hungary, Italy, Latvia, Lithuania, Poland, Portugal, Romania, Slovakia, Slovenia, Spain, and Sweden) and with EU+ (19 EU countries + Croatia, Switzerland, Turkey, and Norway).

countries covered by the EU Fire Database for the period 2002–2005. (Note that possible discrepancies between the values in this chapter and in Szczygieł et al. (2009) in this book are due to the fact that the EU Fire Database does not include fires outside forest or shrubland (e.g., agriculture fires) except if these areas are part of a forest fire.)

The total area burned mapped from 2000 to 2005 for fires larger than 50 ha in the five EU Mediterranean countries was 1,828,663 ha. However, the burned area retrieved from the EU Fire Database, that includes also the fires smaller than 50 ha, was 2,942,924 ha. This means only 62% of the burned areas were mapped which is due to the fact that only fires larger than 50 ha can be detected with the satellite imagery used.

Taking into account this information and assuming that the relative distribution of fuel types remains the same in the burned areas that were not mapped, the total biomass burned annually for these five countries

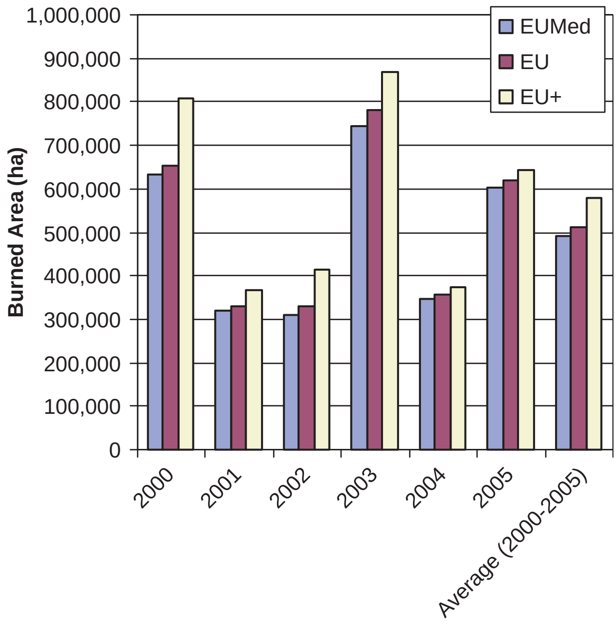

Figure 8.2. Burned area in the 5 EU Mediterranean countries (EU Med: France, Greece, Italy, Portugal, and Spain) compared with the 19 countries for which data is currently available in the database of EU (Austria, Cyprus, Czech Republic, Estonia, Finland, France, Germany, Greece, Hungary, Italy, Latvia, Lithuania, Poland, Portugal, Romania, Slovakia, Slovenia, Spain, and Sweden) and with EU+ (19 EU countries+Croatia, Switzerland, Turkey, and Norway).

was estimated between 4.0 and 10.5 Tg, while the CO_2 emitted was estimated between 6.6 and 17.5 Tg (Table 8.2).

Assuming that the relative distribution of fuel types remains invariable when including the remaining EU countries that did not have the burned area mapped, and considering that the total area burned increases to 3,023,293 ha, then the annual burned biomass for this 6-year period varied between 4.2 and 11.0 Tg, and the CO_2 between 7.1 and 18.4 Tg (Table 8.3). If all 23 countries covered by the EU Fire Database are included, further increases are found in the burned biomass values: from a minimum of 5.1 to a maximum of 12.2 Tg and from a minimum of 8.4 to a maximum of 20.4 Tg for CO_2 (Table 8.4).

Comparison of these results with average estimations for wildland fires in the conterminous United States (U.S.) show that although European forest fire emissions are normally smaller than those in the U.S., they can in some cases be larger than the average minimum in the U.S. (Table 8.5).

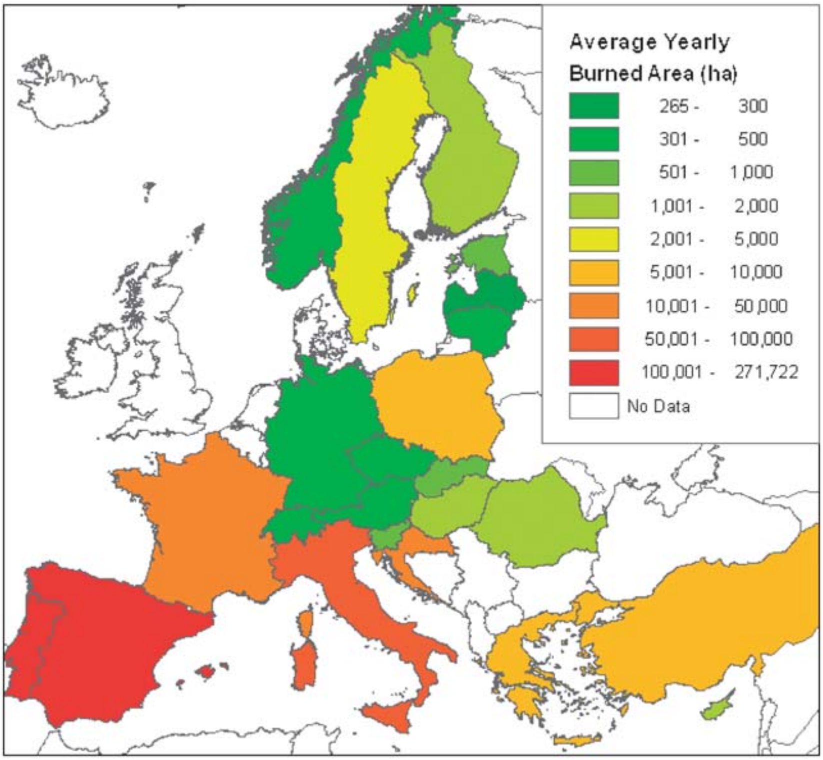

Figure 8.3. Average burned area per year in the European countries for the period 2000–2005, derived from the EU Fire Database.

Table 8.2. Burned biomass and emission estimates from forest fires in the five EU Mediterranean countries between 2000 and 2005. Values are given in Tg

	2000	2001	2002	2003	2004	2005	Average
Burned biomass	6.4	4.4	4.0	10.5	4.8	7.9	6.3
CO_2	10.7	7.4	6.6	17.5	8.0	13.2	10.6
CO	0.434	0.292	0.266	0.680	0.319	0.541	0.422
CH_4	0.023	0.015	0.014	0.036	0.017	0.028	0.022
PM2.5	0.043	0.029	0.027	0.069	0.032	0.054	0.042
PM10	0.051	0.035	0.031	0.081	0.038	0.063	0.050
NMHC	0.071	0.049	0.044	0.114	0.053	0.089	0.070
VOC	0.019	0.013	0.011	0.030	0.014	0.023	0.018
NO_X	0.022	0.015	0.014	0.036	0.017	0.028	0.022
OC	0.030	0.020	0.019	0.047	0.022	0.038	0.029
EC	0.026	0.017	0.016	0.041	0.019	0.032	0.025

Table 8.3. Burned biomass and emission estimates from forest fires in the 19 countries for which data is currently available in the database of EU (Austria, Cyprus, Czech Republic, Estonia, Finland, France, Germany, Greece, Hungary, Italy, Latvia, Lithuania, Poland, Portugal, Romania, Slovakia, Slovenia, Spain, and Sweden) between 2000 and 2005. Values are given in Tg

	2000	2001	2002	2003	2004	2005	Average
Burned biomass	6.6	4.6	4.2	11.0	5.0	8.1	6.6
CO_2	11.1	7.6	7.1	18.4	8.3	13.5	11.0
CO	0.448	0.302	0.286	0.717	0.329	0.555	0.439
CH_4	0.023	0.016	0.015	0.037	0.017	0.029	0.023
PM2.5	0.045	0.030	0.028	0.072	0.033	0.055	0.044
PM10	0.053	0.036	0.034	0.085	0.039	0.065	0.052
NMHC	0.074	0.050	0.047	0.120	0.055	0.091	0.073
VOC	0.019	0.013	0.012	0.031	0.014	0.024	0.019
NO_X	0.023	0.016	0.015	0.038	0.017	0.029	0.023
OC	0.031	0.021	0.020	0.050	0.023	0.039	0.031
EC	0.027	0.018	0.017	0.043	0.020	0.033	0.026

Table 8.4. Burned biomass and emission estimates from forest fires in EU+ (19 EU countries+Croatia, Switzerland, Turkey, and Norway) between 2000 and 2005. Values are given in Tg

	2000	2001	2002	2003	2004	2005	Average
Burned Biomass	8.2	5.1	5.3	12.2	5.2	8.5	7.4
CO_2	13.7	8.4	8.8	20.4	8.6	14.1	12.3
CO	0.555	0.333	0.358	0.795	0.342	0.577	0.493
CH_4	0.029	0.017	0.019	0.041	0.018	0.030	0.026
PM2.5	0.055	0.033	0.036	0.080	0.034	0.057	0.049
PM10	0.065	0.039	0.042	0.095	0.040	0.068	0.058
NMHC	0.091	0.055	0.059	0.133	0.057	0.094	0.082
VOC	0.024	0.014	0.015	0.034	0.015	0.025	0.021
NO_X	0.029	0.017	0.019	0.042	0.018	0.030	0.026
OC	0.039	0.023	0.025	0.055	0.024	0.040	0.034
EC	0.033	0.020	0.021	0.048	0.020	0.034	0.029

Table 8.5. Burned biomass (Tg) comparison between European union countries and USA with estimated maximum and minimum values in brackets

Regions	Tg
EU+	[5.1, 12.2]
EU 19 countries (2000–2005)	[4.2, 11.0]
EU Med (2000–2005)	[4.0, 10.5]
USA	[9, 59]

Analyzing forest fire emissions from the European countries in a wider context shows only a small contribution to the estimated emissions found in the literature. Estimates from Levine (1994) for burned biomass for savannas (3690 Tg/year), temperate and boreal forest (280 Tg/year), and tropical forest (1260 Tg/year) are in fact much higher than the results presented in this chapter. This is confirmed by more recent figures that estimate a total of 8903 Tg of CO_2/year at a global level (van der Werf et al., 2006).

8.5. Conclusions

The results of our study present an initial comprehensive and comparative picture of forest fire emissions in most of the EU countries. We found that the vast majority of the current emissions come from five EU Mediterranean countries (France, Greece, Italy, Portugal, and Spain). The relative importance of European forest fire emissions in a global context show that although their contribution is relatively small at the global scale, these emissions can have important implications for international commitments, such as the Kyoto protocol that has the objective of reducing greenhouse gases that cause climate change.

The most important uncertainties are mainly related to fuel load, since no specific fuel load or biomass maps exist at the European level. Burning efficiency is another factor that has to be studied in order to reduce uncertainties about forest fire emissions. Since the fuel map used was built using surface fire fuel models of the U.S. NFDRS model (Burgan, 1988), the estimates should be regarded as conservative because they do not include the emission contribution from tree-crown consumption in the case of crown-fire. In order to have more precise values of area burned, mainly for the fires smaller than 50 ha, higher spatial resolution satellite images should be used, depending on their availability. Efforts should also be made to develop a specific fuel map model for Europe, and specific studies should be conducted to quantify burning efficiency in different fuel types and in different fire-severity conditions.

REFERENCES

Barbosa, P., San-Miguel-Ayanz, J., Martinez, B., and Schmuck, G. 2002. Burned area mapping in southern Europe using IRS-WiFS. In: Viegas, X., ed. Forest fire research & wildland fire safety, 2002. Millpress, Rotterdam, ISBN 90-77017-72-0.

Barbosa, P., Kucera, J., Strobl, P., Vogt, P., Camia, A., and San-Miguel-Ayanz, J. 2006. European forest fire information system (EFFIS)-rapid damage assessment: Appraisal of burned area maps in southern Europe using modis data (2003–2005), Proceedings of the 5th International Conference on Forest Fire Research. 27–30 November, Figueira da Foz, Portugal, Elsevier Pub. ISSN 0378-1127.

Bohn, U., and Neuhäusl, R. 2003. Map of the natural vegetation of Europe, scale 1:2 500 000, Münster, Landwirtschaftsverlag, 656 pp.

Burgan, R.E. 1988. 1988 revisions to the 1978 national fire-danger rating system. Research Paper SE-273. Asheville, NC: U.S. Department of Agriculture, Forest Service, Southeastern Forest Experiment Station, 39 pp.

European Commission. 1994. CORINE land cover—Technical Guide. Publication EUR 12585 of the European Commission, EG, DG Environment, Nuclear Safety, and Civil Protection. Office for official publications of the European Communities, 144 pp.

European Commission. 2001. San-Miguel-Ayanz, J., Barbosa, P., Schmuck, G. and Schulte, E. eds. Report No. 1: Forest fires in southern Europe. Official Publication of the European Communities, SPI.01.95.EN.

European Commission. 2002. San-Miguel-Ayanz, J., Barbosa, P., Libertà, G., Schmuck, G., and Schulte, E. eds. Forest fires in Europe—2001 fire campaign. Official Publication of the European Communities, SPI.02.72.EN.

European Commission. 2003. San-Miguel-Ayanz, J., Barbosa, P., Libertà, G., Schmuck, G., and Schulte, E. eds. Forest fires in Europe—2002 fire campaign. Official Publication of the European Communities, SPI.03.83.EN.

European Commission. 2004. San-Miguel-Ayanz, J., Barbosa, P., Camia, A., Kucera, J., Libertà, G., Schmuck, G., Schulte, E., Bucella, P., Colletti, L., and Flies, R., eds. Forest fires in Europe—2003 fire campaign. Official Publication of the European Communities, SPI.04.124 EN.

European Commission. 2005. Schmuck, G., San-Miguel-Ayanz, J., Barbosa, P., Camia, A., Kucera, J., Libertà, G., Schulte, E., and Colletti, L., eds. Forest fires in Europe 2004. Official Publication of the European Communities, EUR 22 312 EN.

European Commission. 2006. Schmuck, G., San-Miguel-Ayanz, J., Barbosa, P., Camia, A., Kucera, J., Libertà, G., Schulte, E., Colletti, L., Martin, H., and Toussaint, M. eds. Forest fires in Europe 2005. Official Publication of the European Communities, EUR 22 312 EN.

European Environment Agency. 2002. CORINE Land Cover update 2000. Technical guidelines, 2002, 56 pp.

Leenhouts, B. 1998. Assessment of biomass burning in the conterminous United States. Conserv. Ecol. [online] 2(1), 1 http://www.consecol.org/vol2/iss1/art1

Levine, J.S. 1994. Biomass burning and the production of greenhouse gases. In: Righard, G.Z., ed. Climate biosphere interaction: Biogenic emissions and environmental effects of climate change. Wiley.

Sebastian, L. A., San-Miguel-Ayanz, J., and Burgan, R. 2002. Integration of satellite sensor data, fuel type maps, and meteorological observations for the evaluation of forest fire risk at the pan-European scale. Int. J. Remote Sens. 23(13), 2713–2719.

Szczygieł, R., Ubysz, B., and Zawiła-Niedźwiecki, T. 2009. Spatial and temporal trends in distribution of forest fires in central and eastern Europe (this volume).

van der Werf, G.R., Randerson, J.T., Giglio, L., Collatz, G.J., Kasibhatla, P.S., and Arellano, A.F. Jr. 2006. Interannual variability of global biomass burning emissions from 1997 to 2004. Atmos. Chem. Phys. Discuss. 6, 3175–3226.

Developments in Environmental Science, Volume 8
A. Bytnerowicz, M. Arbaugh, A. Riebau and C. Andersen (Editors)

ISSN: 1474-8177/DOI:10.1016/S1474-8177(08)00009-0

Chapter 9

Forest Fires and Air Quality Issues in Southern Europe

Ana Isabel Miranda, Enrico Marchi, Marco Ferretti and Millán M. Millán*

Abstract

Each summer forest fires in southern Europe emit large quantities of pollutants to the atmosphere. These fires can generate a number of air pollution episodes as measured by air quality monitoring networks. We analyzed the impact of forest fires on air quality of specific regions of southern Europe. Data from several summer seasons were studied with the aim of identifying air pollution episodes related to the occurrence of forest fires. Emissions from forest fires were estimated on the basis of vegetation burned and fire characteristics. Emissions from aircrafts used to fight forest fires were also calculated. It was possible to identify and quantify several particulate and photochemical air pollution episodes caused or enhanced by smoke from forest fires. A case study is described and a mesoscale air quality modelling system, specifically adapted to forest fires, was applied to simulate the fire impact on air quality. Results from the modeling exercise were considered to be reasonable when compared to air concentration values from monitoring networks, taking into account all the uncertainties inherent to this kind of simulation.

9.1. Introduction

Due to frequency of occurrence and the magnitude of effects on the environment, health, economy, and security, forest fires have increasingly become a major subject of concern for decision makers, firefighters, researchers, and citizens in general. According to the European Commission (2005), more than 12 million ha of forest have burned in

*Corresponding author: E-mail: miranda@ua.pt

the past 25 years in the five southern European Union (EU) member states alone, with an average value of nearly 500,000 ha/year. Moreover, approximately 60 million ha of forest, representing more than 50% of the former 15 EU member states forests, have been classified as high or medium fire risk areas (European Commission, 2004).

One of the consequences of forest fires is the atmospheric emissions of various environmentally significant gases and solid particulates that contribute to local, regional, and global phenomena in the biosphere. Pollutants emitted include atmospheric particulate matter (PM) and gaseous compounds, such as carbon dioxide (CO_2), carbon monoxide (CO), methane (CH_4), nonmethane hydrocarbons (NMHC), nitrogen oxides, (NO_X), and nitrous oxide (N_2O). Smoke pollution due to forest fire events can represent an important public health issue to the community, particularly for personnel involved in firefighting operations (Brustet et al., 1991; Miranda et al., 1994a, 2005a; Reinhardt et al., 2001; Valente et al., 2007; Ward et al., 1993). In addition, high levels of tropospheric ozone can occur at great distances from emission sources (Crutzen & Andreae, 1990; Crutzen & Carmichael, 1993). The environmental effects of these emissions are related to the transport and deposition processes involved.

Severe air pollution episodes caused by fires in Amazonia (Brazil), Indonesia, and Philippines in 1997–1998 and, more recently, in Australia and Russia have drawn worldwide attention to the problem of air quality due to forest fires. Increasingly, smoke pollution caused by wildland fires is considered an important health issue with major risks for the population and the environment. The World Health Organization (WHO) has even provided guidelines for forest fire episodic events to protect the public from adverse health effects (World Health Organization, 1999). This concern also applies to prescribed fires, especially in Australia and North America where this land management technique is frequently used.

The main purpose of this chapter is to provide an overview of the effects of forest fires on the air quality in southern European through two main approaches: the cross-analysis of air quality and forest fire behavior data, and the application of an air quality modelling system to a specific case study.

9.2. Forest fires and air quality in Europe

The link between forest fires and air quality is not commonly made. From the point of view of the community dealing with the fire, the main concerns are the direct effects of fire, such as human fatalities and property damage. In addition, air quality problems are usually analyzed in terms of the main anthropogenic sources, particularly the classic industrial and road transport sectors. However, forest fires can be a significant source of air pollutants, and air quality management strategies should consider these effects.

The extreme fire events that occurred in the summer 2003 in southern Europe highlighted the need to better analyze this phenomenon. In Portugal, for example, the firemen involved in these episodes regarded the summer of 2003 as the most important operational challenge of the past 30 years (Liga Bombeiros Portugueses, 2003). The decrease in the number of reported fires compared to the 1993–2002 period was not accompanied by a decrease in the area burned. On the contrary, fire area in 2003 was approximately four times higher than the annual average for the same period (Direcção Geral das Florestas, 2003). As a consequence, unusual air pollutant concentrations were registered at several monitoring stations in the national air quality network during 2003, most of them located inside urban areas (Monteiro et al., 2005). Moreover, increases in the number of hospital admissions and deaths due to respiratory and cardiovascular diseases were also reported either as a direct consequence of the fires or in association with the concomitant high air temperatures (Direcção Geral das Florestas, 2003). In Spain during the same year, deaths related to forest fires were caused not by the fire itself, but by smoke inhalation (Caballero, 2003).

9.2.1. Forest fires in southern Europe

Fire is the most important natural threat to forests and wooded areas of southern Europe. This area can be defined to include Spain, Portugal, Italy, Greece, and Mediterranean France (Corse, Provence–Alpes–Cote d'Azur, Languedoc–Roussillon, Rhone–Alpes). In the past decade (1996–2005), the average annual number of forest fires throughout southern Europe exceeded 61,000, which is 34% more than recorded during the previous decade (1986–1995) (Table 9.1). In particular, there has been an increase in the average number of annual fires in Portugal (94%), Spain (49%), and Greece (22%). Only in Italy was there a reduction (−26%) in the number of forest fires. On average, there were about 54 fires/100 km^2, with a maximum in Portugal (308 fires/100 km^2) and a minimum in Greece (14 fires/100 km^2). The average area burnt annually during the period 1996–2005 was approximately 423,000 ha, which was 19% less than in the previous decade (1986–1995) (Table 9.2). The mean total area burnt decreased in Spain (by 45%), Italy (by 35%), Mediterranean

Table 9.1. Number of forest fires in southern Europe (1996–2005)

Year	Forest fire (number)					
	Med. France	Greece	Italy	Portugal	Spain	Total
1996	1789	1508	9093	28,626	16,771	57,787
1997	2784	2273	11,612	23,497	22,320	62,486
1998	2586	1842	9540	34,676	22,448	71,092
1999	2995	1486	6932	25,477	18,237	55,127
2000	2430	2581	8595	34,109	24,118	71,833
2001	2788	2535	7134	26,533	19,099	58,089
2002	1677	1141	4601	26,488	19,929	53,836
2003	3490	1452	9697	26,195	18,616	59,450
2004	2028	1748	6428	21,870	21,396	53,470
2005	1871	1544	7951	35,697	26,269[a]	73,332
Total (1996–2005)	24,438	18,110	81,583	283,168	209,203	616,502
%	4.0	2.9	13.2	45.9	33.9	100.0
Total (1986–1995)	23,880	14,817	109,690	145,958	140,481	460,569
Difference	558	3293	−28,107	137,210	68,722	155,933
%	2.3	22.2	−25.6	94.0	48.9	33.9
Total national area km^2 [b]	113,249	131,957	301,333	92,040	505,960	1,144,539
No. fire/100 km^2	21.6	13.7	27.1	308.1	41.4	53.9

Sources: Promethee Database, France; Corpo Forestale dello Stato, Italy; Direcçao Geral dos Recursos Florestais, Portugal; Dirección General para la Biodiversidad, Ministerio de Medio Ambiente, Spain; Greece, European Commission (2006).

[a]Provisional data—lacking some data from Andalucia and Extremadura.

[b]Only Mediterranean area of France (Corse, Provence–Alpes–Cote d'Azur, Languedoc–Roussillon, Rhone–Alpes).

France (by 28%), and Greece (by 24%). Only Portugal experienced an increase of about 66% during the same period, mainly due to the 2003 and 2005 forest fire seasons.

9.2.2. Emissions

Air pollutant and precursor emissions in Europe are mainly due to combustion and energy transformation industries (SO_X), road transport (CO, NO_X, NMHC), solvents and other similar products (NMHC), and agriculture (NH_3) (Ritters, 1998). The major air pollutants emitted in southern Europe (France, Greece, Italy, Spain, and Portugal) over the period 1990–2003 are reported in Fig. 9.1. These data are based on a compilation of National Emission Inventories carried out according to

Table 9.2. Burnt area (ha) in southern Europe (1996–2005)

Year	Burnt area (ha)					
	Med. France	Greece	Italy	Portugal	Spain	Total
1996	3119	25,310	57,988	88,867	59,814	235,098
1997	12,250	52,373	111,230	30,535	98,503	304,891
1998	11,243	92,901	155,553	158,369	133,643	551,709
1999	12,782	8289	71,117	70,613	82,217	245,018
2000	18,860	145,033	114,648	159,605	188,586	626,731
2001	17,965	18,221	76,427	111,850	92,386	316,849
2002	6298	6013	40,791	124,411	107,464	284,977
2003	61,507	3517	91,805	425,716	148,173	730,718
2004	10,596	10,267	60,176	129,539	134,193	344,771
2005	17,356	6437	47,575	338,262	179,851[a]	589,481
Total (1996–2005)	171,976	368,361	827,310	1,637,767	1,224,829	4,230,242
%	4.1	8.7	19.6	38.7	29.0	100.0
Total (1986–1995)	237,681	485,902	1,278,521	988,107	2,214,973	5,205,184
Difference	−65,705	−117,541	−451,211	649,659	−990,144	−974,942
%	−27.6	−24.2	−35.3	65.8	−44.7	−18.7
Total national area (ha '000)[b]	11,325	13,196	30,133	9204	50,596	114,454
Total (1996–2005) burnt area/Total national area (%)	1.5	2.8	2.7	17.8	2.4	3.7

Sources: Promethee Database, France; Corpo Forestale dello Stato, Italy; Direcçao Geral dos Recursos Florestais, Portugal; Dirección General para la Biodiversidad, Ministerio de Medio Ambiente, Spain; Greece, European Commission (2006).
[a]Provisional data—lacking some data from Andalucia and Extremadura.
[b]Only Mediterranean area of France (Corse, Provence–Alpes–Cote d'Azur, Languedoc–Roussillon, Rhone–Alpes).

the Coordination of Information on Air Emissions (CORINAIR) methodology (European Environmental Agency, 2005a). In the year 2003, emissions amounted to 14,518 Gg (CO), 4614 Gg (NO_x), 4406 Gg (NMHC), and 3098 Gg (SO_X). Due to incomplete datasets, no estimate was available for NH_3 in 2003; in 2002, the estimate was 1786 Gg. There is clearly a decreasing trend in the emissions of NMHC, SO_X, and CO (Fig. 9.1). The trend is less pronounced for NO_X, while NH_3 emissions have remained fairly unchanged. Figure 9.2 shows the relative contribution of southern European emissions to the total emissions in the EU 15 member states.

It is worth noting that, despite the decreasing trend in emissions overall, the contribution from southern European countries has increased over the period 1990–2003. On average, this increase has been $11 \pm 6.5\%$, and driven primarily by SO_X in particular, a class of pollutant that has

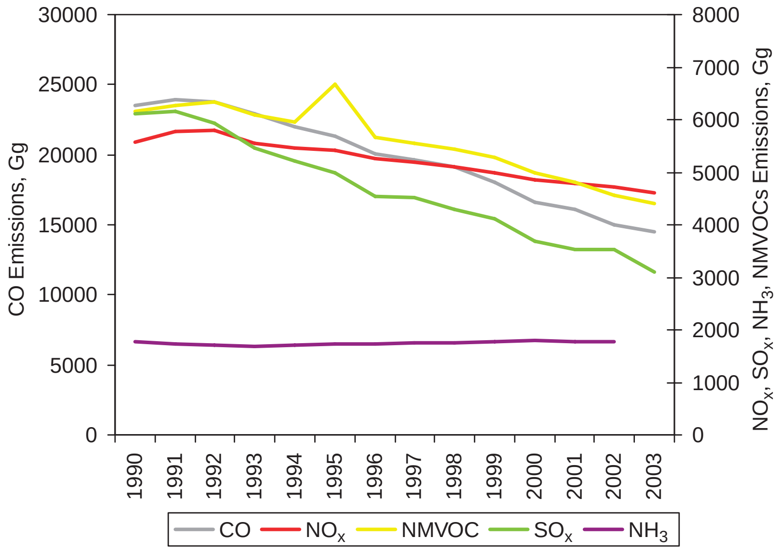

Figure 9.1. Emissions of CO (left *y* axis), NO_X, NMHC, SO_X, and NH_3 (right *y* axis) in southern Europe (France, Greece, Italy, Portugal, and Spain) for the period 1990–2003 (European Environmental Agency, 2005a).

had particularly effective reductions in countries that experienced very high emission rates in the past. For example, SO_X emissions in Germany were three times higher than in Italy in 1990.

Notwithstanding this trend, it is important to understand the contribution by forest fires to these total values. Of the pollutants analyzed, forest fires are major contributors of CO, NO_x, NMHC, and NH_3. In the European context and according to data from the European emission inventory CORINAIR (European Environmental Agency, 2004), forest fire emissions represent 0.2% of NO_2, 0.5% of NMHC, 1.9% of CO, and 0.1% of NH_3. For Portugal the contribution of forest fire emissions in 2003 to the total value (for the 1994 base year) equates to 14.1% CO, 5.2% NO_2, 2.7% NMHC, 2.2% CH_4, 1.3% NH_3, and 0.6% SO_2. These emissions were estimated using the national emission inventory for non-forest fire emissions and a model (EMISPREAD; Miranda et al., 2005b), which takes into account type of fuel and combustion phase, to estimate forest fire emissions from southern Europe.

Globally, fires are a significant contributor of CO_2 and other greenhouse gases (GHG) to the atmosphere. Fires account for approximately one-fifth of the total global emission of CO_2 (Sandberg

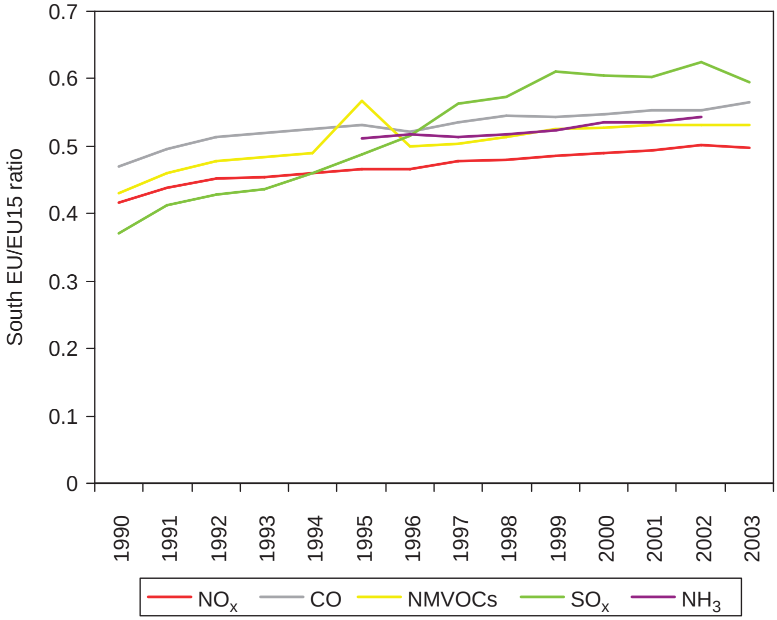

Figure 9.2. The ratio between the emissions in southern Europe and the EU 15 member states (European Environmental Agency, 2005a).

et al., 2002). Even taking into account the notion that fires in temperate ecosystems are minor contributors compared to biomass burning in savannas, boreal, and tropical forests, the contribution to total CO_2 equivalent emissions produced during forest fires can reach 7% if the annual area burned and exceeds 100,000 ha (Miranda et al., 1994b).

When assessing forest fire emissions, pollutants emitted during ground and air-fighting activities should also be evaluated. As with many vehicles, firefighting aircraft engines produce water vapor, unburned or partially combusted hydrocarbons, CO_2, CO, NO_X, SO_X, particulates (sulfur- and carbon-based), and other trace compounds. These emissions concentrate in the lower troposphere, as firefighting aircrafts do not exceed 3000 m.

Aircraft emissions are characterized in terms of emission index (EI; units of gram of emissions per kilogram of fuel burned), which is representative of a particular engine state, along with the time spent in that state performing the various operative modes (e.g., idling, taking off, climbing out, approaching, reverse thrust). The time that firefighting aircraft operates in each mode depends on a variety of factors including distance from airport to fire, distance from fire to water supply point and terrain morphology; however, no data are currently available to determine the time spent in the different operative modes.

Emission levels of H_2O, CO_2, and SO_2 are determined by the fraction of hydrogen (H), carbon (C), and sulfur (S) compounds contained in the fuel. In contrast, emissions of NO_X, CO, and HC vary according to the combustor conditions (Sutkus et al., 2003). It is likely that aircraft emissions are also modified by the presence of other atmospheric pollutants, including those from forest fires.

A preliminary analysis of the firefighting aircraft emission during the period 2000–2003 was carried out in Italy. Flight data were collected by the National Unified Aerial Operational Center (COAU) and included take off, in zone, off zone, and take on times. Travel (time to go and back from aircraft base to forest fire) and operative (time spent in active firefighting activities) times were then calculated. Since specific EIs for the engines used in the firefighting aircraft were not available, the average EI for the main pollutants were used according to Schumann (2002) and Penner et al. (1999). These EIs included ($g\,kg^{-1}$) 3150 for CO_2, 1260 for H_2O, 14 for NO_X, 4 for CO, 1 for SO_2, and 0.6 for HC. For NO_x, the emission index ($EI(NO_x)$) is given as gram equivalent NO_2.

On the basis of average fuel consumption, flight time, and EI, emissions from Italian firefighting aircrafts over the period 2000–2003 were calculated according to Draper et al. (1997).

The average annual emission was about 61 t NO_X, 3 t HC, 4 t SO_2, 18 t CO, 14,000 t CO_2, and 6000 t H_2O. According to the flight time distribution, over 60% of the emissions were concentrated close to the fire areas. In addition, forest fire emissions were estimated using the EMISPREAD model for Italy in 2001. Emissions from firefighting aircraft were compared with these values (Table 9.3), and it is obvious

Table 9.3. Forest fire and aircraft emissions in Italy in 2001

Source		Emissions (t)			
		CO_2	CO	HC	NO_X
Forest fires		950,769	46,417	5861	2632
	In zone	7906	10	2	35
Aircraft	Travel	5536	7	1	25
	Total	13,442	17	3	60
Total		964,211	46,434	5864	2692
Aircraft/forest fires	%	1.41	0.04	0.05	2.28

that aircraft emissions for some pollutants such as CO_2 and NO_X have to be considered when total emission values associated with forest fires are analyzed.

9.2.3. Air quality

The contribution of forest fires to total atmospheric emissions makes it clear that some relationship between forest fires and air quality is to be expected. However, it is not always easy to identify air pollution episodes caused or exacerbated by forest fires. Pollutants emitted from forest fires are transported and dispersed in the atmosphere, and their effects on air quality can occur far from the emitting source. Although major wildfires are limited to some hundreds of hectares, their impacts, with no natural or political boundaries, can be felt and reported far beyond the physical limits of the fire spread. Depending on meteorological conditions, smoke plumes and haze layers can persist in the atmosphere for long periods of time, and prevailing conditions will influence the chemical and optical characteristics of the plume. There is emerging evidence that smoke from widespread wildfires in Portugal in summer 2003 contributed to the high ozone levels measured at the air quality monitoring stations in Paris, France (Hodzic et al., 2006).

Air quality issues have changed with time in Europe. Early concern about sulfur compounds and acidification of ecosystems (freshwaters and forests) was particularly relevant in the 1970s and 1980s in central Europe. Today, concerns mostly include tropospheric ozone and PM_{10} (particles with mean aerodynamic diameter smaller than 10 µm) levels impinging on populations in urban environments (European Environmental Agency, 2005b; Lövblad et al., 2004; Percy & Ferretti, 2004). According to a recent report (European Environmental Agency, 2005b), the proportion of the population exposed to values exceeding EU protection values for PM_{10}, SO_2, and NO_2 or target values for O_3 is 25–55% (PM_{10}), 30% (O_3 and NO_2), and $<1\%$ (SO_2). These data have some limitations because the spatial coverage varies from year to year, and only populations in urban areas equipped with monitoring networks are considered. However, they are useful for making a qualitative estimate of the potential impact of the different air pollutants. In southern Europe, ozone and PM_{10} have been claimed as the most important air pollution problems.

Ozone, in particular, shows distinctly higher levels in southern Europe, which is also identified as the most critical area in terms of burnt area and forest fire risk, than in other regions of Europe (Beck et al., 1999). Ozone is a secondary photochemical pollutant, and its production depends on

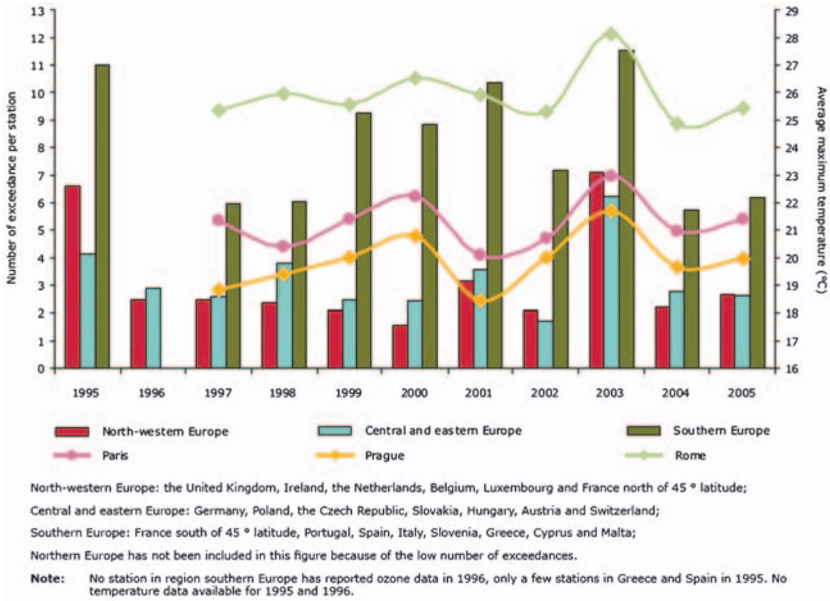

Figure 9.3. Average number of ozone exceedances per station for three European regions observed during each year for the period 1995–2005. The summer average maximum daily temperature in selected cities are also presented (European Environmental Agency, 2006).

levels of solar radiation and high temperatures. Figure 9.3 (European Environmental Agency, 2006) illustrates this relation between meteorological conditions and number of exceedances of permissible ozone levels in different regions of Europe—northwestern, central and eastern, and southern Europe. Daily maximum temperatures observed in three capital cities in these regions (Paris—northwestern region; Prague—central and eastern region; and Rome—southern region) averaged for the period April–September of a particular year are shown in Fig. 9.3. The ozone number of exceedances is based on data from the monitoring networks in Europe. Frequent occurrence of ozone exceedance was quite common in southern Europe, where the highest temperature values were also reported (city of Rome), compared to other temperature values measured in cities from northwestern, central, and eastern Europe.

Emissions from forest fires are also very dependent on weather conditions. An analysis of fire occurrence and burnt area per month in Italy, Greece, Mediterranean France, and Portugal can be used to evaluate the yearly distribution of forest fire emissions to the atmosphere. Two peaks are usually recorded: in spring (March/April) and in summer

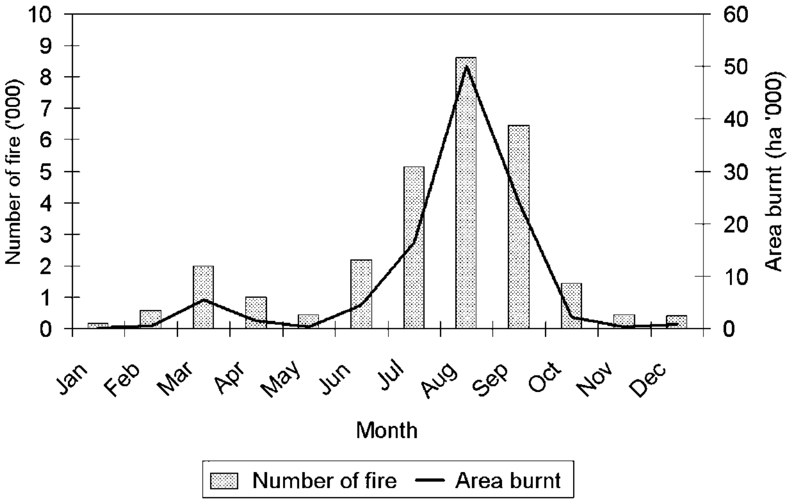

Figure 9.4. Fire number and burnt area per month (Portugal—average values 1997–2001). (Source: Direcção Geral dos Recursos Florestais, Portugal.)

(July, August, and September). The second peak is higher, with about 50–70% of the fires occurring annually, depending on year and country, and covering 70–90% of the annual area burnt. As an example, Fig. 9.4 shows the situation in Portugal.

The presence of ozone precursors emitted by forest fires, namely NO_X and NMHC, is also important. Southern European countries have good conditions for photochemical production (European Commission, 1999) and forest fire occurrence, namely very hot, dry, and sunny summers, and forested areas, both of which contribute to higher emissions of ozone precursors.

Weather conditions are also another possible link between forest fires and episodes of particulate air pollution in southern Europe, particularly where PM_{10} is a critical pollutant. During summer, low humidity and high wind speed values increase the risk of occurrence of large forest fires, while being related to high values of PM with the transport and resuspension of dust and pollen (Coutinho et al., 2005).

9.3. Air quality management and forest fires

Air quality is one of the areas in which Europe has been most active in recent years, namely focusing on the definition and implementation of air quality strategies, the improvement of air quality monitoring networks, and the development of scientific knowledge to better characterize and understand European air quality. The European Commission (EC) has aimed to develop an overall strategy through setting long-term air quality objectives. A series of directives has been introduced to control levels of certain pollutants and to monitor their concentration in air. In 1996, the Environmental Council adopted the Air Quality Framework Directive 96/62/EC (AQFD) on ambient air quality assessment and management. This Framework Directive, followed by its subsequent directives, presented several innovative aspects and concepts regarding air quality management strategies, such as the need to establish plans and programs for zones and urban agglomerations where the air quality thresholds are not met and the possibility of using simulation models as a tool to evaluate air quality. These two new aspects of the AQFD can be directly applied to forest fires, which are responsible for air pollution episodes.

9.3.1. Plans and programs

The AQFD establishes that if certain air quality standards are surpassed, member states have the obligation to prepare plans and programs (PPs) that must indicate measures to improve air quality and to comply with specified limit values.

Several member states have already delivered their plans and programs to the European Commission regarding air quality exceedances in 2001–2003, and stating how they intend to improve the air quality in a near future. These plans and programs mainly concern urban agglomerations, densely populated areas, and PM_{10} and NO_2 pollution.

In Portugal, Porto and Lisbon agglomerations are the only ones that submitted plans and programs to implement measures to reduce PM_{10} air pollution. According to EU Framework Directive PM_{10}, daily averaged values should not exceed $50\,\mu g\,m^{-3}$ more than 35 times/year (as of January 2005). The number of PM_{10} exceedances for the monitoring stations in the Porto agglomeration air quality monitoring network was analyzed (Coutinho et al., 2005). For the 3 years under study (2001–2003), all stations registered some exceedance of the annual average PM_{10} threshold value, and many stations did so more times than the 35 daily exceedances allowed by the directive.

The identification of PM_{10} sources was fundamental for the definition of plans and programs for the Porto agglomeration that has to ensure reaching the threshold value in 2005. Moreover, according to the European Commission, plans and programs should focus on anthropogenic sources, but forest fires are considered natural ones. For the analysis of the need to develop plans and programs, PM_{10} exceeding days due to natural sources (e.g., forest fires) can be deducted from the total exceeding days. However, due to the number of sources involved, the relation between forest fire emissions and PM_{10} values measured is not clear-cut. Therefore, a specific approach was developed to identify episodes of particulate pollution in the Porto agglomeration related to forest fires. To do this, days for which values were higher than the daily limit value for PM_{10} ($50\,\mu g\,m^{-3}$) at three or more monitoring stations simultaneously, plus a margin of tolerance for the specific year under analysis, were considered to be episodic days that could potentially be influenced by a forest fire smoke plume. For these days, the hybrid single-particle Lagrangian integrated trajectory model (HYSPLIT) was applied to estimate backward trajectories from the forest fires to the Porto agglomeration.

In very simple models, the trajectory and dispersion of the smoke plume can be simulated through straight-line trajectories. Other models assume that the atmosphere is neutrally buoyant to compute trajectories of air parcels that are transported by a tridimensional wind field, which is calculated by a numerical weather prediction model. This so-called ‘‘trajectory technique’’ is considered to be simple in its concept and only requires modest computer resources (Borrego et al., 2004). Trajectories can be run forward in time to determine receptor areas or backward in order to determine the pollutant source areas. In general, multiple trajectories are required due to instability of the atmospheric flow.

The HYSPLIT model, developed by the U.S. National Oceanic and Atmospheric Administration, is a system that can estimate trajectories and dispersion and deposition fields of gaseous and particulate pollutants (Draxler et al., 2005). It uses meteorological grid data from re-analysis of weather forecasting models. Figure 9.5 shows the estimated trajectories for August 3–4, 2003, when several forest fires were spreading through the center of Portugal. HYSPLIT was applied for air mass altitudes of 250, 500, and 750 m and for a period 1–2 days. Satellite photos for these days are also shown in Fig. 9.5.

This methodology, which was used for all the fires with a burned area larger than 100 ha, was applied for 3 years of air quality monitoring in the Porto agglomeration (Borrego et al., 2005). In this way, it was possible to calculate the contribution of forest fires to PM_{10} pollution episodes as 35%, 8%, and 18%, for 2001, 2002, and 2003, respectively. This information was used to differentiate between anthropogenic and forest fire contributions to particulate matter pollution episodes. After subtracting episodic days due to forest fires from the total exceeding days, the need to develop PPs still persisted.

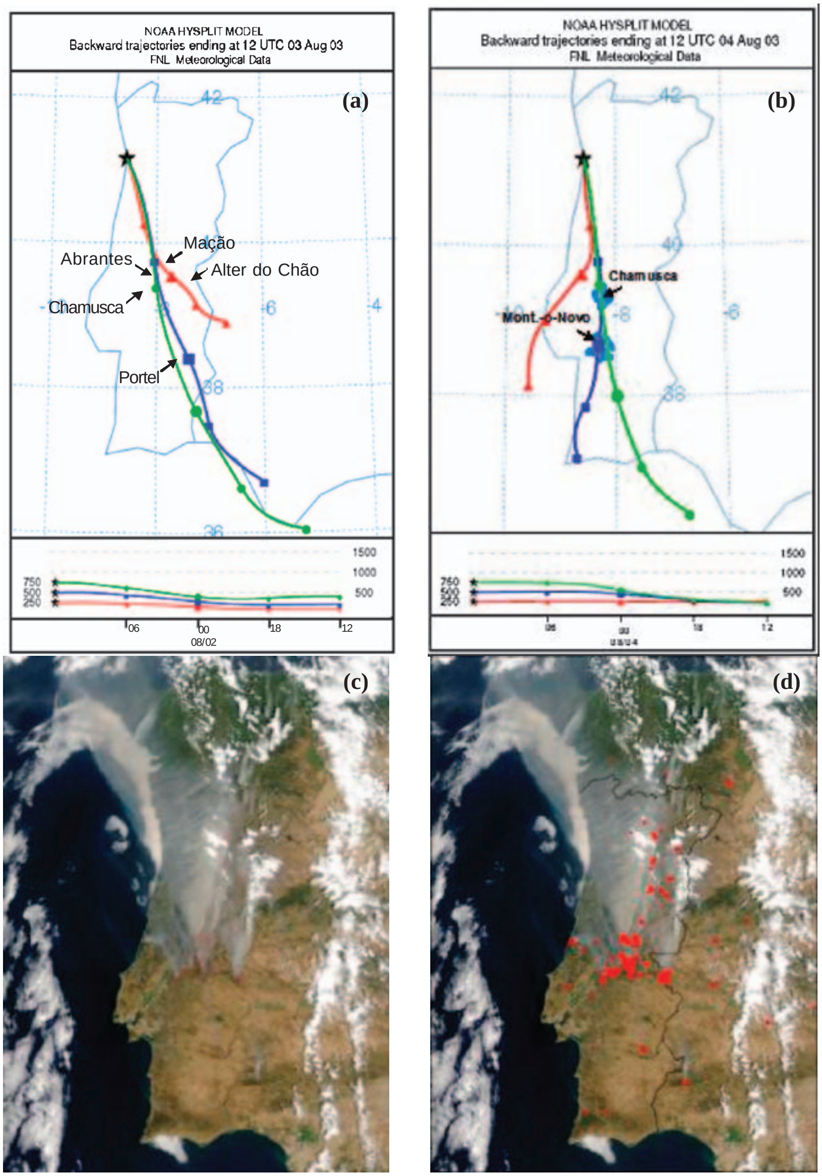

Figure 9.5. Backward trajectories (a, b) and satellite images (c, d) for August 3 (a, c) and August 4 (b, d), 2003, in Portugal. Blue areas correspond to burned areas, stars indicate the Porto agglomeration, and different colored lines indicate trajectories at different heights.

9.3.2. Modeling smoke plume impact on urban air quality in Lisbon

Smoke from forest fires can be a serious problem in cities and urban areas. In Portugal, forest fires in summer 2003 were considered the most devastating, and this is clearly reflected in the values measured by the air quality monitoring networks (Miranda et al., 2005c). Several air quality stations registered extremely high pollutant concentrations due to fire emissions and transport from surrounding areas. Ash from nearby fires reached many urban areas, reducing visibility, and depositing in urban areas.

Lisbon suffered the effects of smoke from forest fires north of its urban area in September 2003. This situation represents a very interesting case study for smoke dispersion and air pollutant concentration estimation because of the high population density involved and hence higher risk of human exposure to smoke. The Lisbon airshed, with a population of 3.5 million inhabitants, is the most important urban center in Portugal. It was built in a very complex topographic region, dominated by a large estuary and multiple hills and surrounded by small mountain ranges with elevations over 400 m above sea level.

The urban area of Lisbon has an air quality monitoring networking that includes several stations with different typologies (urban background or urban traffic), according to location and environmental criteria. Air quality data analysis enabled the identification of September 13, 2003 as the most critical day for high CO and PM_{10} concentration values in the Lisbon urban area. On this day, 33 fires were active in the Lisbon district, burning an area of about 400 ha of forest stands and shrubs. Figure 9.6 shows the location of the fires and the air quality monitoring stations in the Lisbon airshed. Figure 9.7 presents the hourly averaged PM_{10} (Fig. 9.7a) and CO (Fig. 9.7b) concentrations measured on September 13 at the monitoring stations indicated.

A dramatic increase in the concentration of PM_{10} measured at the end of the day was evident. The day was very warm, with temperatures reaching 35°C in Lisbon airport. Winds mainly blew from the east quadrant, changing towards southeast at the end of the afternoon, when the highest concentration values were measured. PM_{10} concentration values were generally high, but due to the fires, the average $50\,\mu g\,m^{-3}$ value was breached at all measuring stations except two (Quinta do Marquês and Mem-Martins), which are located west of Lisbon and were not affected by the smoke plumes. Avenida da Liberdade registered the highest daily averaged value of $150\,\mu g\,m^{-3}$.

The European Directive has established $10{,}000\,\mu g\,m^{-3}$ CO as the maximum eight-hour average allowable in a day. Even with a large

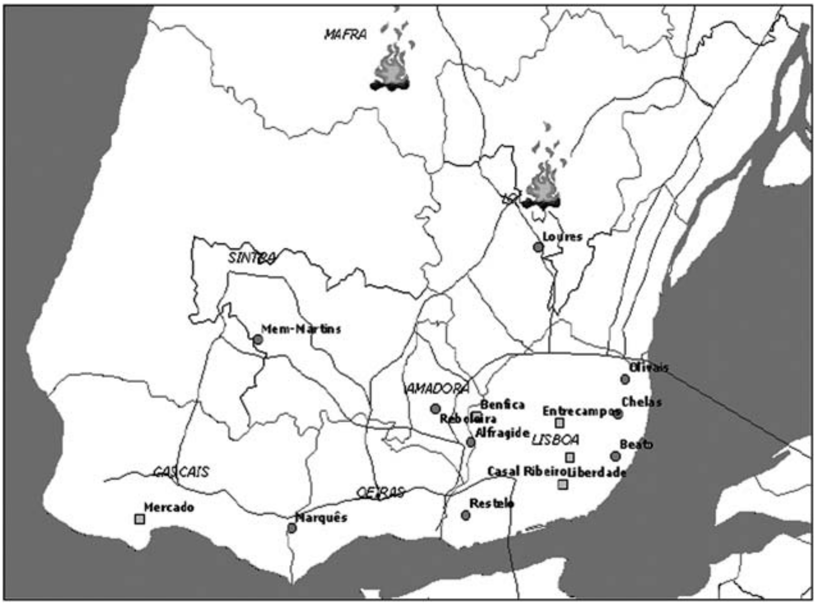

Figure 9.6. Location of the September 13, 2003, main forest fires and air quality monitoring stations in the Lisbon airshed (circles represent urban background stations, squares are urban traffic stations, and flame symbol represents forest fires).

increase in CO values at the end of the day (Fig. 9.7b), the values measured were not significant in terms of air pollution.

Numerical modeling of smoke dispersion allows us to understand how pollutants emitted by a forest fire are transported and dispersed in the atmosphere by estimating the resulting air pollutant concentration fields. AIRFIRE (Miranda, 2004) was developed to take into account the possible impact of forest fires on photochemical production. It integrates a modified version of the non-hydrostatic meteorological model (MEMO) (Moussiopoulos et al., 1993), the Rothermel fire progression model (Rothermel, 1972), and the atmospheric dispersion model for reactive species (MARS; Moussiopoulos et al., 1995). Using data available for September 13, 2003, AIRFIRE was applied to a modeling domain of 200 km $\times$ 200 km with a horizontal resolution of 4 km $\times$ 4 km. This domain was chosen in order to consider mesoscale circulations, such as sea breezes in the Lisbon area.

Carbon monoxide and PM_{10} emissions from forest fires were estimated using data relating to the area burnt and the type of vegetation. Average emission factors for the two main types of fuel, shrub, and forest were

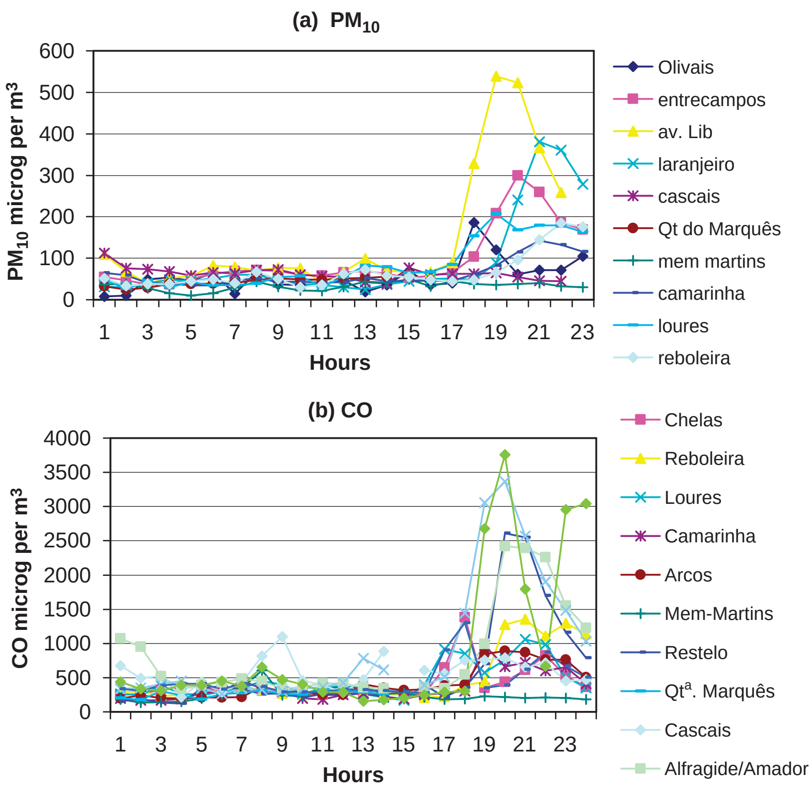

Figure 9.7. Measured PM_{10} (a) and CO (b) concentration values ($\mu g\,m^{-3}$) for September 13, 2003, at the different monitoring stations in Lisbon.

used, but these did not take into account differences in emissions due to smouldering and flaming combustion. These emission factors came from a selection of values for southern European forest fires (Miranda, 2004). The system was also applied considering only anthropogenic emissions from the national emission inventory (Instituto do Ambiente, 2006).

For meteorological conditions, MEMO used upper air data from the Lisbon airport as initial and boundary conditions. Aerological data, including temperature and wind speed and direction, obtained at 00.00, 12.00, and 24.00 LST (local standard time) were used as input data. Twenty vertical layers above the topography were considered, the first one (the surface layer) at a depth of 20 m. The top layer of the model was set at 6000 m.

The temporal evolution of the hourly averaged PM_{10} concentration fields during September 13 was estimated. Figure 9.8 shows the surface hourly averaged PM_{10} concentration patterns for 18.00 (Fig. 9.8a and b) and 22.00 LST (Fig. 9.8c and d) as estimated by AIRFIRE, considering all the sources in the simulation domain (Fig. 9.8b and d), which include forest fire emissions, and only considering the anthropogenic ones (Fig. 9.8a and c). Surface patterns of wind as estimated by AIRFIRE are also presented in Fig. 9.8. There is an obvious contribution by forest fires to the particularly high levels of PM_{10} measured in the urban area of Lisbon

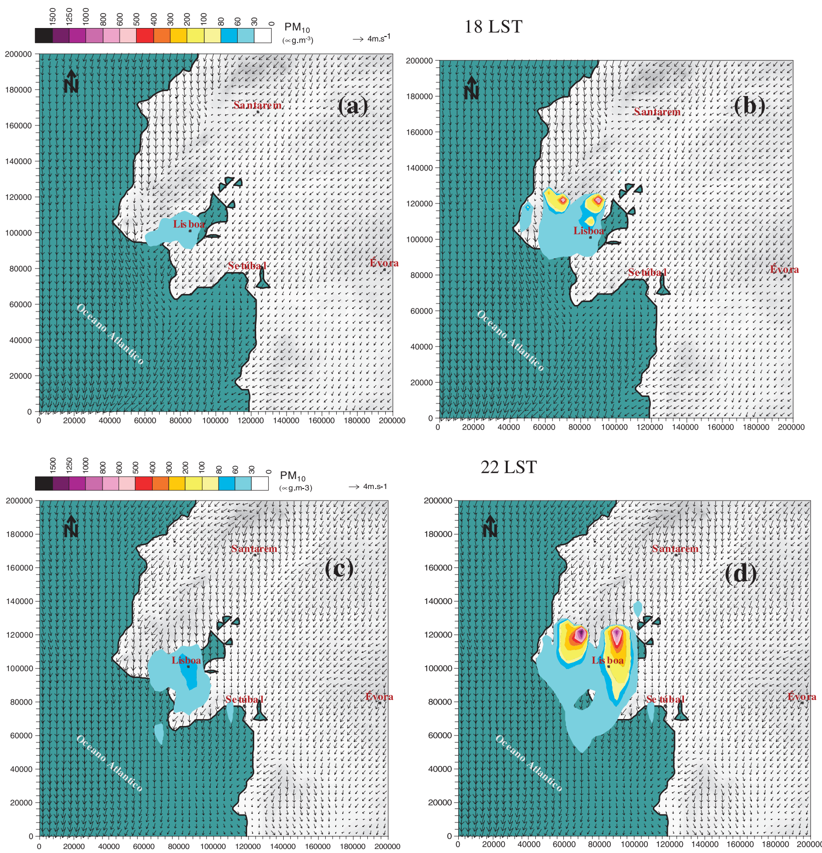

Figure 9.8. Hourly averaged surface PM_{10} concentration ($\mu g\,m^{-3}$) and wind values at 18.00 (a, b) and 22.00 (c, d) LST, both excluding forest fire emissions (a, c) and including forest fire emissions (b, d) in Lisbon.

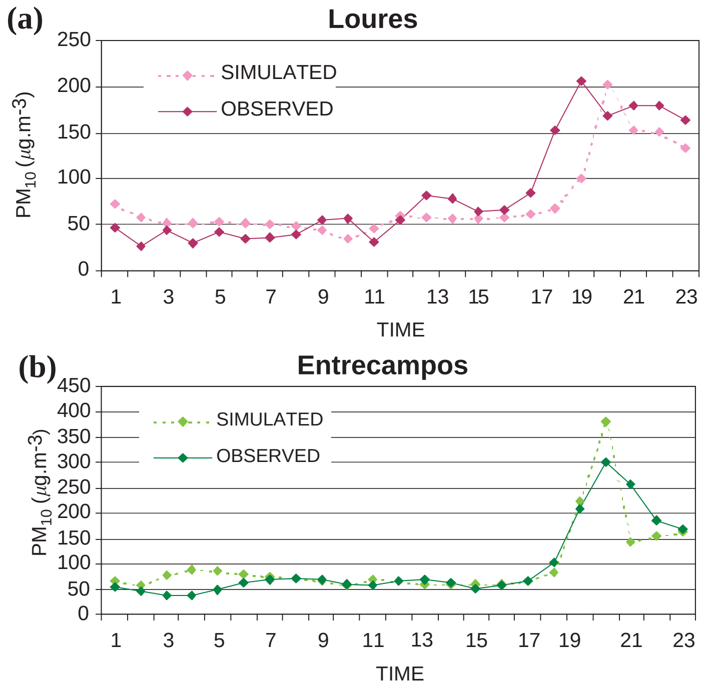

Figure 9.9. Qualitative comparison between measured and simulated hourly averaged concentration values of PM_{10} ($\mu g\,m^{-3}$) at Loures (a) and Entrecampos (b).

at night. More details regarding this Lisbon case study simulation can be found in Miranda et al. (2005c).

The accuracy of the modelling system was evaluated by directly comparing the simulated results with hourly averaged PM_{10} measurements from the Lisbon air quality monitoring network with Loures (Fig. 9.9a) and Entrecampos (Fig. 9.9b). There was reasonable agreement between simulated and observed values for most of the air quality monitoring stations (Miranda et al., 2005c). Taking into account the errors associated with this type of simulation, including those related to fuel load or fuel consumption, the simulation results can be considered an important source of information for managers of air quality. Currently, it is not a common procedure in Europe to model air quality by including forest fire emissions, but the use of this modelling tool can be extended to other European study cases.

9.4. Conclusions and future directions

The effect of forest fires on air quality is an issue of concern in many regions of the world, including the southern European countries. While pollution emissions are generally decreasing, the role of forest fires is becoming increasingly important. Emissions from forest fires may cause substantial exceedances of the air quality threshold, particularly in agglomerations with the high population densities. There is a strong need to take into account the role of forest fires when determining management strategies for air quality. To protect people, environmental policies must integrate the traditional pollution-oriented and land management issues into a unique system that can integrate both problems. Better land management can help to reduce both the number of air pollution episodes and the risk of unwanted fires.

This chapter illustrates how forest fires and air quality issues can be linked as we have shown by describing two case studies within different scopes and purposes. The quantification of forest fires' contribution to air pollution episodes is a fundamental stage of the development of plans and programs, particularly in southern European member states.

The application of numerical air quality modeling systems is also an added value when evaluating and assessing air quality levels in areas affected by forest fires. Fortunately, European researchers and managers are realizing the importance of forest fires to the degradation of air quality, and some modelling research has been developed and applied (e.g., Hodzic et al., 2007; Miranda et al., 2007). These studies are simulating larger areas—Europe and a European country—and longer periods (at least 1 month) than the one presented here. This different modelling scale implies the simulation of a larger number of fires and the use of a coarser grid resolution. It is a broader approach instead of the more specific approach presented in our case study. Both modelling approaches can be useful. The specific approach can be applied to simulate air pollution episodes related to the occurrence of forest fires. In this case the information from the numerical system, which can be applied almost in real time, can help to identify critical areas where people are exposed to high levels of air pollutants. The general approach is quite useful for the characterization and evaluation of air quality by each European member state or, at a higher level, by the EC.

ACKNOWLEDGMENTS

The authors are grateful to the Portuguese Foundation for Science and Technology for the project INTERFACE (POCI/AMB/60660/2004) funding. The Calouste Gulbenkien Foundation (CGF) and the Luso-American Foundation for the Development (FLAD) are also greatly acknowledged. Part of this work has been developed within the Emissions, Modeling and Climate Change Research Group at the University of Aveiro and to which we extend a special thanks to Carlos Borrego and Helena Martins. We also greatly appreciate the reviewers of this manuscript who provided helpful comments during its preparation.

REFERENCES

Beck, J.P., Krzyzanowski, M., and Koffi, B. 1999. Tropospheric ozone in the European Union: The consolidated report. ISBN 92-828-5672-0, Office for Official Publications of the European Union, Luxembourg, 74 pp.

Borrego, C., Miranda, A.I., Valente, J., and Amorim, J.H. 2004. A smoke dispersion model adapted to forest fire fighting using retardants. Deliverable D261 of the EC Project ERAS (Extension Retardant Application System). AMB-QA-05/04. University of Aveiro, Aveiro, Portugal.

Borrego, C., Miranda, A.I., Salmim, L., Monteiro, A., Ferreira, J., Martins, H., Coutinho, M., Pereira, M., and Ribeiro, C. 2005. Elaboração de Planos e Programas de Acção para a melhoria da qualidade do ar na região Norte. Relatório R3. AMB-QA-10/2005. University of Aveiro, Aveiro, Portugal. (Only Portuguese version available; English translation of the original title: "Elaboration of Action Plans and Programmes for the improvement of the northern region air quality. Report R3").

Brustet, J., Vickos, J., Fontan, J., Podaire, A., and Lavenu, F. 1991. Characterisation of active fires in West African savannahs by analysis of satellite data: Landsat thematic mapper. In: Levine, J., ed. Global biomass burning: Atmospheric, climatic, and biospheric implications. The Massachusetts Institute of Technology Press, Cambridge, MA, London, pp. 53–60.

Caballero, D. 2003. Synthetic report of some fires that affected WUI in Spain. Internal report of WARM project. www.eufirelab.org

Coutinho, M., Pereira, M., Ribeiro, C., and Borrego, C. 2005. Phenomenological interpretation of PM_{10} episodes occurring in the metropolitan area of Porto. In: Sokhi, R., Millán, M.M., and Moussiopoulos, N., eds. Proceedings of the 5th international conference on urban air quality, in CD-Rom.

Crutzen, P., and Andreae, M. 1990. Biomass burning in the tropics: Impact on atmospheric chemistry and biogeochemical cycles. Science 250, 1669–1678.

Crutzen, P., and Carmichael, G. 1993. Modelling the influence of fires on atmospheric chemistry. In: Crutzen, P., and Goldammer, J., eds. Fire in the environment: The ecological, atmospheric and climatic importance of vegetation fires. Wiley, Chichester, England.

Direcção Geral das Florestas. 2003. Incêndios florestais 2003 (1 Janeiro a 31 de Outubro). Relatório Provisório, Direcção Geral das Florestas (DGF), Divisão de Protecção e Conservação Florestal (DSVPF); Lisboa, Portugal (only Portuguese version available; english translation of the original title: "Forest Fires 2003 (1st January to 31st of October), Provisory Report, 3rd of November 2003").

Draper, J., Webb, A., Pernigotti, M., Plante, J., and Liang, D. 1997. Air quality procedures for civilian airports & air force bases. Federal Aviation Administration (U.S. Department of Transportation), U.S. Air Force, Washington.

Draxler, R., Stunder, B., Rolph, G., and Taylor, A. 2005. HYSPLIT User's guide. Version 4.7. http://www.arl.noaa.gov/readyopen/hysplit4.html

European Commission. 1999. Ozone Position Paper, ISBN 92-828-7865-1, Office for Official Publications of the European Union, Luxembourg, 171 pp.

European Commission. 2004. Forest Fires in Europe 2003 fire campaign. European Communities, Italy.

European Commission. 2005. Forest Fires in Europe 2004. European Communities, Italy.

European Commission. 2006. Forest Fire in Europe 2005. European Communities, Italy.

European Environmental Agency. 2004. EMEP/CORINAIR emission inventory guidebook, third ed. Technical Report no 30. European Environmental Agency. http://reports.eea.eu.int/EMEP/CORINAIR4/en/page002.html

European Environmental Agency. 2005a. Annual European Community CLRTAP Emission Inventory 1999–2003. EEA, Copenhagen, 30 pp.

European Environmental Agency. 2005b. The European Environment – State and Outlook 2005. EEA, Copenhagen, 584 pp.

European Environmental Agency. 2006. Air pollution by ozone in Europe in summer 2005. Overview of exceedances of EC ozone threshold values for April–September 2005. EEA Technical Report. No 3/2006. Copenhagen.

Hodzic, A., Madronich, S., Bohn, B., Massie, S., Menut, L., and Wiedinmyer, C. 2007. Wildfire particulate matter in Europe during summer 2003: Meso-scale modeling of smoke emissions, transport and radiative effects. Atmos. Chem. Phys. Discuss. 7, 4705–4760.

Hodzic, A., Vautard, R., Chepfer, H., Goloub, P., Menut, L., Chazette, P., Deuz, J., Apituley, A., and Couvert, P. 2006. Evolution of aerosol optical thickness over Europe during the August 2003 heat wave as seen from CHIMERE model simulations and POLDER data. Atmos. Chem. Phys. 6, 1853–1864.

Instituto do Ambiente. 2006. Portuguese National Inventory Report on Greenhouse Gases, 1990–2002. www.iambiente.pt

Liga Bombeiros Portugueses. 2003. Livro Aberto do Sistema de Protecção e Socorro em Portugal; September 2003. Liga dos Bombeiros Portugueses. Lisboa, Portugal. (Only Portuguese version available; English translation of the original title: "Open Book of the System of Protection and Rescue in Portugal; September 2003").

Lövblad, G., Tarrasón, L, Tørseth, K., and Dutchak, S. 2004. EMEP Assessment. Part I. European Perspective. EMEP, Oslo, 168 & Appendix.

Miranda, A.I. 2004. An integrated numerical system to estimate air quality effects of forest fires. Int. J. Wildland Fire 13(2), 217–226.

Miranda, A.I., Borrego, C., and Viegas, D. 1994a. Forest fire effects on the air quality. In: Baldasano, J., Brebbia, C., Power, H., and Zannetti, P., eds. Proceedings of the second international conference on air pollution. Computer Simulation, Barcelona, Spain, vol. 1, pp. 191–199.

Miranda, A.I., Coutinho, M., and Borrego, C. 1994b. Forest fire emissions in Portugal: A contribution to global warming? Environ. Pollut. 83(1,2), 121–123.

Miranda, A.I., Ferreira, J., Valente, J., Santos, P., Amorim, J.H., and Borrego, C. 2005a. Smoke measurements during Gestosa-2002 experimental field fires. Int. J. Wildland Fire 14, 107–116.

Miranda, A.I., Borrego, C., Sousa, M., Valente, J., Barbosa, P., and Carvalho, A. 2005b. Model of forest fire emissions to the atmosphere. Deliverable D252 of SPREAD Project (EVG1-CT-2001-00043). AMB-QA-07/2005. University of Aveiro, Aveiro, Portugal.

Miranda, A.I., Martins, H., Carvalho, A., and Borrego, C. 2005c. Modelling smoke effects on Lisbon air quality. In: Sixth fire and forest meteorology symposium and the 19th Interior West Fire Council meeting, October 25–27, 2005. Canmore, AB, Canada. Proceedings in CD-Rom.

Miranda, A.I., Monteiro, A., Martins, V., Carvalho, A., Schaap, M., Builtjes, P., and Borrego, C. 2007. Forest fires impact on air quality over Portugal. In: 29th NATO/CCMS international technical meeting on air pollution modelling and its applications, September 24–27, 2007. Aveiro, Portugal.

Monteiro, A., Vautard, R., Lopes, M., Miranda, A.I., and Borrego, C. 2005. Air pollution forecast in Portugal: A demand from the new Air Quality Framework Directive. Int. J. Environ. Pollut. 25(2), 4–15.

Moussiopoulos, N., Flassak, T., Sahm, P., and Berlowitz, D. 1993. Simulations of the wind field in Athens with the non-hydrostatic mesoscale model MEMO. Environ. Software 8, 29–42.

Moussiopoulos, N., Sahm, P., and Kessler, C. 1995. Numerical simulation of photochemical smog formation in Athens, Greece: A case study. Atmos. Environ. 29(24), 3619–3632.

Penner, J., Lister, D., Griggs, D., Dokken, D., and McFarland, M., eds. 1999. IPCC Special Report. Aviation and the Global Atmosphere. IPCC Working Groups I and III, Intergovernmental Panel on Climate Change, Switzerland.

Percy, K., and Ferretti, M. 2004. Air pollution and forest health: Toward new monitoring concepts. Environ. Pollut. 130, 113–126.

Reinhardt, E., Ottmar, R., and Castilla, C. 2001. Smoke impacts from agricultural burning in a rural Brazilian town. J. Air Waste Manage. Assoc. 51, 443–450.

Ritters, M. 1998. CORINAIR 1994 Inventory. EEA, Copenhagen, 49 pp.

Rothermel, R. 1972. A mathematical model for predicting fire spread in wildland fuels. USDA Forest Service, Intermountain Forest and Range Experiment Station Research Paper. INT-115. Ogden, UT, 40 pp.

Sandberg, D., Ottmar, R., Peterson, J. and Core, J. 2002. Wildland fire on ecosystems: Effects of fire on air. USDA For. Service Gen. Tech. Rep. RMRS-GTR-42-vol. 5, 79 pp.

Schumann, U. 2002. Aircraft emission. Causes and consequences of global environmental change. In: Douglas, I., ed. Encyclopedia of global environmental change, vol. 3, Munn, T. (editor-in-chief), Chichester, pp. 178–186.

Sutkus, D., Baughcum, S., and DuBois, D. 2003. Commercial aircraft emission scenario for 2020: Database development and analysis. National Aeronautics and Space Administration, Glenn Research Center, Washington.

Valente, J., Miranda, A.I., Lopes, A.G., Borrego, C., and Viegas, D.X. 2007. A local-scale modelling system to simulate smoke dispersion. In: 6th symposium on fire and forest meteorology, Canmore, Alberta, Canada, October 25–27, 2005. Proceedings of 6th symposium on fire and forest meteorology.

Ward, D., Rothermel, R., and Bushey, C. 1993. Particulate matter and trace gas emissions from the Canyon Creek Fire of 1988. In: Society of American Foresters, eds. Proceedings of the 12th fire and forest meteorology, Georgia, United States of America, pp. 62–76.

World Health Organization, 1999. In: Schwela, D., Goldammer, J., Morawska, L., and Simpson, O., eds. Health guidelines for vegetation fire events. World Health Organisation, Geneva.

This page intentionally left blank

Developments in Environmental Science, Volume 8 233
A. Bytnerowicz, M. Arbaugh, A. Riebau and C. Andersen (Editors)

ISSN: 1474-8177/DOI:10.1016/S1474-8177(08)00010-7

Chapter 10

Spatial and Temporal Trends in Distribution of Forest Fires in Central and Eastern Europe

Ryszard Szczygieł, Barbara Ubysz and Tomasz Zawiła-Niedźwiecki*

Abstract

Forest in Central and Eastern Europe (CEE) covers 56,285,000 ha (5% of European total forested area). Forest cover in CEE makes 30% of land use. Almost 50% of the forest under study is formed by coniferous species and only 30% by deciduous ones. Forest younger than 60 years old grows on 57% of that area. These factors, together with climate conditions cause that on the main part of CEE middle forest fire risk is noted. Between 1991 and 2001 some 387,680 fires burning 757,000 ha were noted in CEE. The most hazardous situation is observed in Poland where over 60% of fires and burns happen. Forest Research Institute in Warsaw has prepared a method of emission calculation based on the Polish experience. As the type of forest and environmental condition in the described area are similar, some calculations on emissions from neighbor countries, based on FAO's forest fire statistics were elaborated.

10.1. Characteristics of Central and Eastern European forests

For the purpose of this chapter the central and eastern European (CEE) countries are Austria, Belarus, Czech Republic, Estonia, Germany, Hungary, Latvia, Lithuania, Poland, Slovakia, and Ukraine (Fig. 10.1). Forests in CEE cover 56,285,000 ha (UNEP/FAO, 2000), which is about 5% of Europe's forested areas. Forestation of this part of the continent reaches 30% (it is about 46% on average throughout Europe).

Three types of temperate forest are the most common in the CEE countries: oceanic, continental, and mountain (UNEP/FAO, 2000).

*Corresponding author: E-mail: szczygiel@ibles.waw.pl

Figure 10.1. Central and eastern European countries.

Temperate oceanic forest is dominant in Germany (with the exception of a main part of the Land of Brandenburg) and northwestern Poland. Various types of European beech forests (*Fagus silvatica*) and its mixture are common here. However, large areas have been reforested with Norway spruce (*Picea abies*) and Scots pine (*Pinus sylvestris* L.). Apart from the mentioned species, the oak-ash (*Quercus* sp., *Fraxinus excelsior*) and oak-hornbeam (*Quercus* sp., *Carpinus betulus*) forests are also dominating locally. Temperate continental forests in CEE countries consist of Scots pine, Norway spruce, as well as oak-hornbeam and lime-oak (*Quercus* sp., *Tilia cordata*), while on permanently wet sites, black alder (*Alnus glutinosa*), and common ash (*Fraxinus excelsior*) appear. Temperate mountain forests formed by common beech, silver fir (*Abies alba*), and Norway spruce are not very sensitive to fire due to their specific climatic conditions (high precipitation and low temperature). In the CEE area the share of predominantly coniferous forest has been increasing over the past two centuries as a result of management practices oriented toward maximization of lumber production. Recently, this trend has slowed down; however, only in Hungary, Slovakia, and the Ukraine broad-leaved species predominate (UNEP/FAO, 2000).

In Austria 88% of the forest area is coniferous or mixed coniferous/broad-leaved; in Germany 50% of the forest area is coniferous and 20% is mixed coniferous/broad-leaved; while in Poland and Belarus these values are respectively 30%, 20%, and 40%. In the Czech Republic more than 50% of forest area is covered by mixed coniferous/broad-leaved, but as much as 80% of growing stock is coniferous (UNEP/FAO, 2000). Forest expansion is observed in Germany, Poland, Slovakia, Ukraine, and Belarus as a result of afforestation and conversion of other land to forest, as well as due to preservation of soil against erosion. The highest rate of forestation is over 45% and found in the CEE countries of Estonia, Latvia, Austria, Belarus, and Slovakia, and the lowest is less than 20% and found in Ukraine and Hungary (Table 10.1). The pattern of forest ownership varies from country to country as a result of historical, political, and social influences. Countries where the state owns the major share of forests are Baltic countries and Poland (81%), the Czech Republic (71%), Hungary (63%), Slovakia (43%), and Germany (33%).

10.2. Presence of forest fires in CEE

The forests in CEE should be classified as exposed to medium fire danger, with the exception of certain parts of Poland and eastern Germany, which are characterized by a potentially high risk of fire outbreaks.

Table 10.1. Forest area and volume in CEE countries (UNEP/FAO, 2000)

Country	Country area	Forested area		Volume and biomass	
	k ha		%	$m^3\,ha^{-1}$	$t\,ha^{-1}$
Austria	8273	3886	47.0	286	250
Belarus	20,748	9402	45.3	153	80
Czech Republic	7728	2632	34.1	260	125
Estonia	4227	2060	48.7	156	85
Germany	34,927	10,740	30.1	268	134
Hungary	9234	1840	19.9	174	112
Latvia	6205	2923	47.1	174	93
Lithuania	6258	1994	31.9	183	99
Poland	30,442	9047	29.7	213	94
Slovakia	4808	2177	45.3	253	142
Ukraine	57,935	9584	16.5	179	87[a]

[a]Assumed as mean value calculated from forest areas of Belarus and Poland.

Primarily, this risk is caused by the domination of coniferous stands, representing 57% of the surface area of forests. Contribution of mixed and broad-leaved forests is 30% and 13%, respectively. Moreover, 65% of forests are younger than 60 years, which causes them to be especially subject to initiating and spreading fires (FAO, 2001; UNEP/FAO, 2000).

Between 1991 and 2001, 387,680 forest fires occurred in CEE (Fig. 10.2, Table 10.2). As a result of these fires 757,071 ha forests and barren land burned down (Fig. 10.3, Table 10.3) (FAO, 2001), which comprised 37% of the total number of fires in Europe and 13% of the burned area.

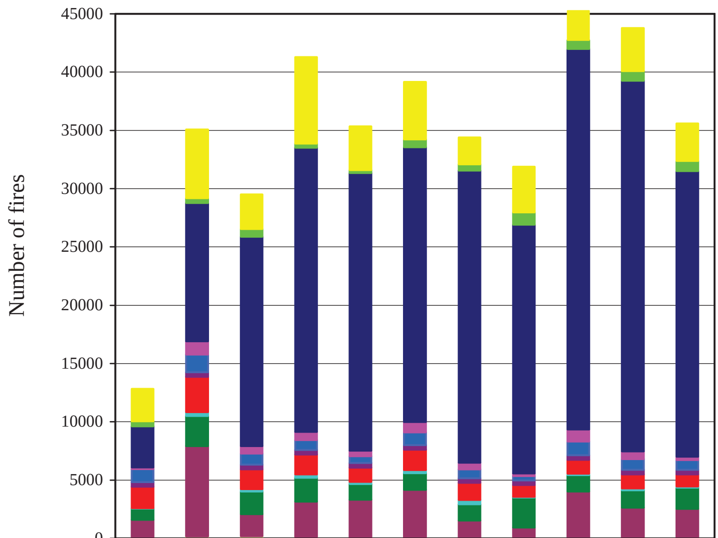

Year	1991	1992	1993	1994	1995	1996	1997	1998	1999	2000	2001
Ukraine	2771	5869	2967	7411	3754	4928	2309	3915	6070	3696	3205
Slovakia	431	431	674	366	254	662	535	1056	751	824	877
Poland*	3528	11,858	17,961	24,372	23,821	23,588	25,070	21,346	32,649	31,812	24,513
Lithuania	147	1154	635	714	472	889	565	231	1022	654	287
Latvia	1110	1510	965	854	582	1095	768	357	1196	915	823
Hungary	393	393	393	393	393	393	393	393	393	393	393
Germany	1846	3012	1694	1696	1237	1748	1467	1032	1178	1210	1032
Estonia	39	348	207	289	188	273	359	61	130	158	116
Czech Republic	961	2586	1951	2052	1331	1421	1398	2563	1403	1499	1822
Belarus	1517	7743	1887	3052	3257	4123	1466	876	3959	2569	2468
Austria	78	165	178	94	64	41	66	57	57	57	57

* In 1991–1993 without the wildland fires.

Figure 10.2. Number of forest and wildland fires in CEE countries in 1991–2001 (FAO, 2001, Forestry, 1991–2001, UNEP/FAO, 2002).

Table 10.2. Numbers of forest and wildland fires for Europe and only the CEE countries in 1991–2001 (FAO, 2001; Forestry, 1991–2001; UNEP/FAO, 2002)

Area	Years											
	1991	1992	1993	1994	1995	1996	1997	1998	1999	2000	2001	1990–2001
CEE countries	12,821	35,069	29,512	41,293	35,353	39,161	34,396	31,887	48,808	43,787	35,593	387,680
Europe	56,490	79,058	69,588	77,771	85,107	87,580	92,526	120,742	118,263	140,316	106,692	1,034,133

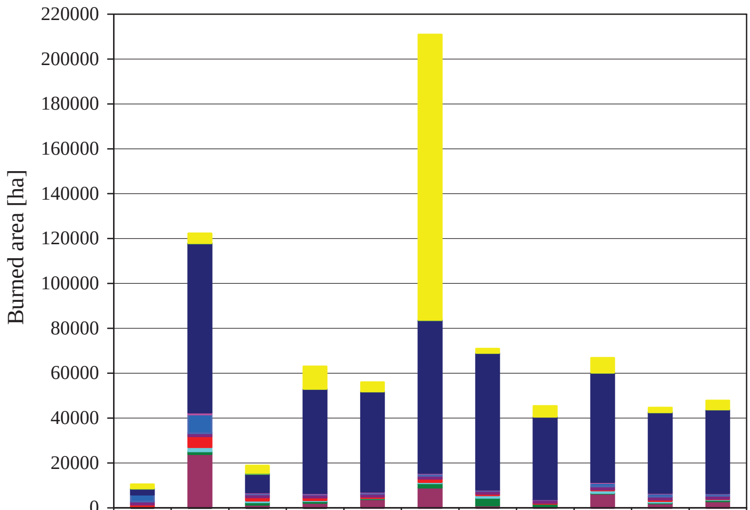

Year	1991	1992	1993	1994	1995	1996	1997	1998	1999	2000	2001
Ukraine	1781	4252	3214	10,040	3995	127,061	1835	4706	6494	1905	3860
Slovakia	233	233	518	96	85	220	35	32	96	105	78
Poland*	2567	75321	8290	46,379	44,681	68,039	60,967	36,814	48,687	35,956	37,386
Lithuania	54	863	305	301	321	385	139	93	494	352	112
Latvia	3096	8366	510	350	536	927	390	211	1544	1341	1032
Hungary	1349	1349	1349	1349	1349	1349	1349	1349	1349	1349	1349
Germany	920	4908	1493	1114	592	1381	599	397	415	581	122
Estonia	58	1787	647	456	158	528	1114	54	1103	684	314
Czech Republic	76	1278	1151	808	403	2043	3475	1132	336	375	614
Belarus	319	23,822	1253	2105	3780	8952	965	547	6261	1931	2913
Austria	53	132	112	57	32	28	39	33	33	33	33

* In 1991 and 1993 without wildland fires. In 1992 with peat burns (31,566 ha).

Figure 10.3. Forest and wildland burned areas in CEE countries in 1991–2001 (FAO, 2001, Forestry, 1991–2001, UNEP/FAO, 2002).

Table 10.3. Forest and wildland burned area ha in entire Europe and in CEE countries in 1991–2001 (FAO, 2001; Forestry, 1991–2001; UNEP/FAO, 2002)

Area	Years											
	1991	1992	1993	1994	1995	1996	1997	1998	1999	2000	2001	1991–2001
CEE countries	10,506	122,311	18,842	63,055	55,932	210,913	70,907	45,368	66,812	44,612	47,813	757,071
Europe	585,774	462,100	488,236	804,814	435,517	296,510	364,824	707,920	362,704	928,416	463,186	5,900,001

Majority of fires (over 60% of all fires registered in CEE) were in Poland, where 240,518 fires burned 465,087 ha (FAO, 2001; Forestry, 1991–2001; UNEP/FAO, 2002). Other countries highly threatened by fires were Ukraine (46,895 fires on the area of 169,143 ha in the analyzed period), Belarus (32,917 fires, 52,848 ha), Czech Republic (18,987 fires, 11,691 ha), and Germany (17,152 fires, 11,691 ha) (FAO, 2001; UNEP/FAO, 2002). Austria and Estonia were much less affected by forest fires (FAO, 2001; UNEP/FAO, 2002).

The largest number of fires in all countries occurred in 1999 (48,808 fires), in 2000 (43,787), and in 1994 (41,293) (FAO, 2001; Forestry, 1991–2001; UNEP/FAO, 2002). However, the largest burned area was in 1996, when 210,913 ha were affected by fires (with the main contribution of burned area in Ukraine) and in 1992 (122,311 ha) when a disastrous fire situation occurred in Poland (FAO, 2001; Forestry, 1991–2001; UNEP/FAO, 2002). Mean annual number of forest fires and the area burned by fires between 1991 and 2001 normalized to 10,000 ha of forest area is presented in Fig. 10.4. This objective index of fire and burned area density supports results of the fire occurrence statistics, showing that in Poland that index reached the highest values (24.17 fires and 46.73 ha of burned area). Other countries had much lower values of the fire density index, and among them the highest were Czech Republic (6.56), Ukraine (4.45), Belarus (2.18), and Latvia (3.16). However, while considering the burned area index, the sequence is slightly different and Poland is followed by Ukraine (16.04 ha), Hungary (7.33 ha), Latvia (5.69 ha), and Belarus (5.11 ha).

Every year the forest fires cause enormous economic losses, but their ecological damages are even more severe. Emission of gases and particles transported with smoke to the atmosphere, which contribute to the greenhouse effect, is one of the main impacts of fires on the natural environment. Emissions from burning biomass of boreal forests reach 3–5% of the total annual world value (Goldammer & Furayev, 1996). These emissions do not only contribute to the greenhouse effect and acid rain but also produce smoke aerosols, increasing the reflection of sun

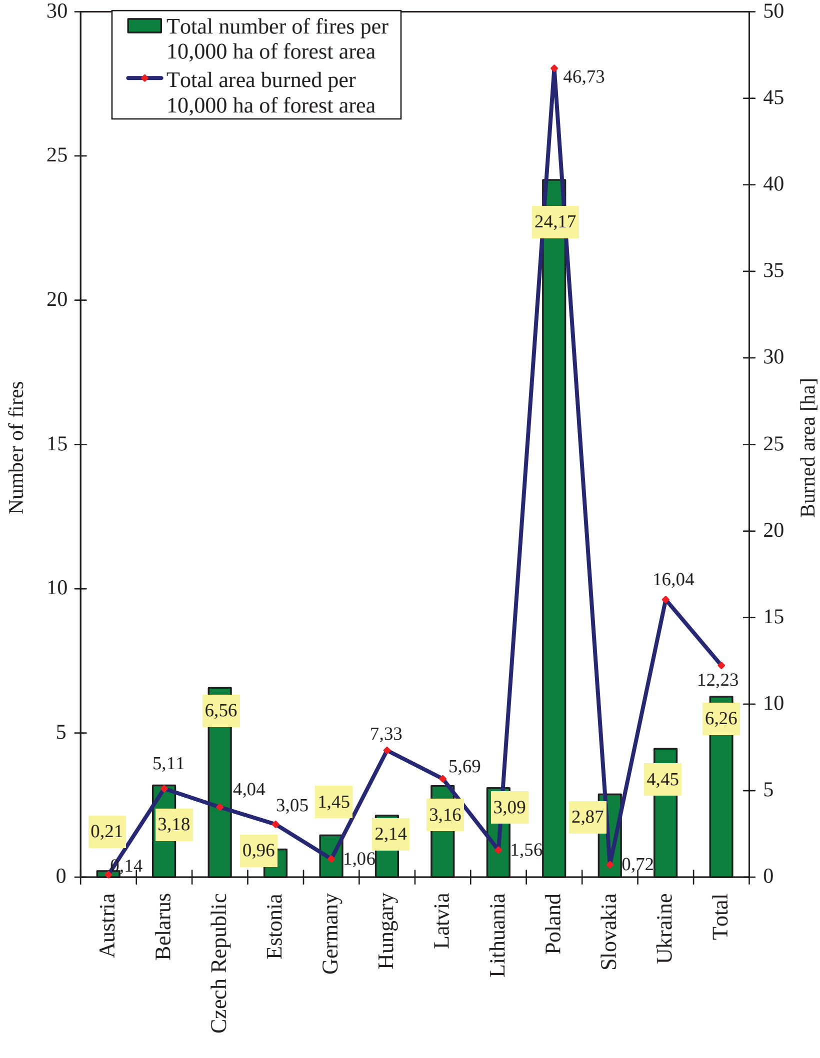

Figure 10.4. Mean annual number of fires and burned areas normalized by 10,000 ha of forest in CEE countries in 1991–2001.

radiation. During burning of vegetation, biomass carbon is released mainly as carbon dioxide (CO_2) and carbon oxide (CO), as these gases contribute to about 45% of the dry matter loss. When ground fires take place (and those are characterized by long-term processes of smoldering), methane (CH_4) as well as other hydrocarbons and organic acids are released (Goldammer et al., 1997). Currently, an awareness that emissions from forest fires have a strong impact on global and regional air pollution, which has deleterious effects on ecosystems and people, has increased.

10.3. Methods of determining amounts of fire emissions

In order to determine the amounts of substances emitted during forest fires and fires on barren land, the data on fires from 1991 to 2001 were analyzed. Data concerning fires and burned area were obtained from the Food and Agriculture Organization of the United Nations (FAO) reports (FAO, 2001; UNEP/FAO, 2002), and for Poland these were additionally verified on the basis of updated statistical data (Forest fires in Europe, 2004, 2005, 2006; Forestry, 1991–2001; Perlińska, 2000, Reports on the state of forests in 2001; Statistical tables for rescue operations for 1994, 1995, 1996, 1997, 1998, 1999, 2000, 2001; Ubysz, 2003; Ubysz and Szczygieł, 2002, 2005; Ubysz et al., 2005) and corrected in terms of the type of fire and its percentage in the total number of fires. This permitted a more accurate calculation of gas emissions generated by fires, by assuming an amount of biomass burnt corresponding to the type of fire. For Poland complete data concerning barren land since 1994 were available. For the remaining countries, the most complete data were for the Ukraine and Lithuania, followed by Latvia, Estonia, and Belarus, while for Germany and Hungary data were not available. Five types of emissions were taken into account for calculations, including carbon dioxide, solid and liquid particles (smoke), hydrocarbons, and nitrogen oxides (NO_x). Magnitudes of emissions were determined on the basis of amount of green biomass per unit area that was burned in forests and in barren land. Type of fire was also considered (surface fire, crown fire, and for Poland, ground fire), as well as the amount of burned green biomass. For 10 countries (except Poland), fixed percentages of surface fires (85%) and crown fires (15%) were assumed. For Poland the real annual values were used (e.g., contribution of fires of soil cover in the analyzed period varied from 74% in 1999 to 88% in 2001). Amounts of green biomass for 10 countries (except Poland) were used according to the FAO data (Table 10.1) (UNEP/FAO, 2000). For Poland data for analysis were taken from research on evaluation of amount of biomass predestinated to burning in local conditions (Fraszewski, 1997). Hence, for forests a value of 82 t ha^{-1} was used for surface fire and ground fire and 94 t ha^{-1} for crown fire. These values correspond to 55-year-old pine stands located on forest sites with soil covered with litter. For barren land, 55 t ha^{-1} was assumed as the amount of biomass for all countries. Magnitudes of emissions released as a result of burning of 1 t of forest combustible materials (Fraszewski, 1997; Goldammer, 1993) were assumed as follows: carbon dioxide: 1375.0 kg; carbon oxide: 125.0 kg; solid and liquid particles: 50.0 kg; hydrocarbons: 12.5 kg; nitrogen oxides: 2.5 kg.

10.4. Emissions from forest fires

Amounts of emissions released as a result of fires of forests and barren land for CEE countries between 1991 and 2001 are presented in Table 10.4, and Table 10.5 presents these data separately for Poland. According to the calculations during this period in the analyzed region of Europe, the following amounts of emissions were released due to the forest and barren land fires

- 46,416,000 t of CO_2
- 4,403,000 t of CO
- 1,689,000 t of solid and liquid particles
- 425,000 t of hydrocarbons
- 87,000 t of NO_x.

The maximum emission level of combustion products was recorded in 1996; in total, it amounted to as much as 8,793,000 t (without Poland), representing 45% of the total gas emissions caused by forest fires from 1991 to 2001. The magnitude of this release in 1996 was affected by the size of the area burnt in Ukraine, which was as much as 127,061 ha. Similarly, in Poland, the maximum emission level was recorded in 1996 (5,635,000 t); in addition, a very similar emission level (5,539,000 t) was recorded in 1992. The lowest levels of combustion products from forest and wildland fires were released in 1991, both in Poland and the other CEE countries. The mean annual emission level for Poland was 3,068,000 t, and it was 1,753,000 t for other countries. The specific situation in Poland is a result of a large number of arson cases, varying in different years from 35% to 47%, of all the causes of forest and wildland fires. Compared with other countries, there is also much burning of plant remains in the fields and uncultivated farmland (which is illegal under the law). This is a very frequent cause of forest fires, representing as much as a dozen percent of all the causes. After Poland's accession to the European Union (EU), the fires breaking out as a result of this were substantially limited by the threat that assistance grants from the EU resources would be withdrawn in the event of burning out fields and meadows.

Table 10.4. Emissions released due to forest and wildland fires in 10 CEE countries (except Poland) in 1991–2001

Year	Forests					Wildland					Total—forests and wildland				
	Amounts of the released emissions (thousands of tons)														
	CO_2	CO	Solid and liquid aerosols (smoke)	Hydro-carbons	NO_x	CO_2	CO	Solid and liquid aerosols (smoke)	Hydro-carbons	NO_x	CO_2	CO	Solid and liquid aerosols (smoke)	Hydro-carbons	NO_x
1991	495	47	18	4	1	[a]	[a]	[a]	[a]	[a]	495	47	18	4	1
1992	2042	193	74	19	4	871	82	32	8	2	2913	275	106	27	6
1993	656	62	24	6	1	60	6	2	1		716	68	26	7	1
1994	950	90	35	9	2	20	2	1			970	92	36	9	2
1995	471	45	17	4	1	244	23	9	4		715	68	26	8	1
1996	7536	713	274	69	14	156	21	8	2		7692	734	282	71	14
1997	491	45	18	4	1	119	11	4	1		610	56	22	5	1
1998	498	47	18	5	1	28	3	1			526	50	19	5	1
1999	758	72	28	7	1	345	33	13	3	1	1103	105	41	10	2
2000	453	43	16	4	1	84	8	3	1		537	51	19	5	1
2001	587	55	21	5	1	7	1				594	56	21	5	1
Total	14,937	1412	543	136	28	1934	190	73	20	3	16,871	1602	616	156	31
Mean	1357.9	128.4	49.4	12.4	2.5	193.4	19.0	8.1	2.9	1.5	1533.7	145.6	56.0	14.2	3.8

[a]No data.

Table 10.5. Emissions released due to forest and wildland fires in Poland in 1991–2001

Year	Forests					Wildland					Total—forests and wildland				
	Amounts of the released emissions (thousands of tons)														
	CO_2	CO	Solid and liquid particles (smokes)	Hydro-carbons	NO_x	CO_2	CO	Solid and liquid particles (smokes)	Hydro-carbons	NO_x	CO_2	CO	Solid and liquid particles (smokes)	Hydro-carbons	NO_x
1991	284	27	10	3	1	[a]	[a]	[a]	[a]	[a]	284	27	10	3	1
1992	4849	461	176	44	9	[a]	[a]	[a]	[a]	[a]	4849	461	176	44	9
1993	919	87	33	8	2	[a]	[a]	[a]	[a]	[a]	919	87	33	8	2
1994	1016	97	37	9	2	1453	137	53	13	3	2469	234	90	22	5
1995	574	55	21	5	1	1009	95	37	9	2	1583	150	58	14	3
1996	1547	148	56	14	3	3387	320	123	31	6	4934	468	179	45	9
1997	724	69	26	7	1	3162	299	115	29	6	3886	368	141	36	7
1998	440	42	16	4	1	2008	190	73	18	4	2448	232	89	22	5
1999	939	90	34	9	2	2078	197	76	19	4	3017	287	110	28	6
2000	784	74	28	7	1	1834	173	67	17	3	2618	247	95	24	4
2001	383	36	14	3	1	2155	204	78	20	4	2538	240	92	23	5
Total	12,459	1186	451	113	24	17,086	1615	622	156	32	29,545	2801	1073	269	56
Mean	1133	107.8	41.0	10.3	2.2	2135.8	201.9	77.8	19.5	4	2685.9	254.6	97.5	24.5	5.1

[a]No data.

10.5. Conclusions

The emission level of combustion products caused by forest and wildland fires in the CEE countries from 1991 to 2001 amounted to 53,020,000 t. Almost 64% of the emissions came from Poland; this resulted from both the particular fire danger posed to its forests (because of the species composition of stands, poor sites, and young stands) as well as arson, which were the primary causes of fires. As a result of this, 60% of all the fires recorded in the period in question in the CEE countries broke out in Poland. The progressive climate warming causes an increase in fire danger and the number of forest fire outbreaks. Therefore, it should be expected that the air pollution caused by emissions due to forest fires will grow. This situation can be significantly improved through application of preventive measures and education efforts, which should contribute to the reduction of forest fires. In turn, improvement of the effectiveness of firefighting, through application of new technical solutions, provides an opportunity to limit burned area of forests and volume of fire emissions.

REFERENCES

FAO. 2001. Global forest fire assessment 1990–2000. Forestry Department Food and Agriculture Organization of the United Nations. Forestry Resources Assessment Programme, Working Paper 55, Rome.

Forest fires in Europe. 2004. Report No 5, S.P.I.05.147 EN European Communities 2005. European Commission, Directorate General Joint Research Centre, Institute for Environment and Sustainability Land Management Unit, Directorate General for Environment Civil Protection Unit, Directorate General for Environment Forests Unit.

Forest fires in Europe. 2005. Report No 6, EUR 22312 EN European Communities 2006. European Commission, Directorate General Joint Research Centre, Institute for Environment and Sustainability Land Management Unit, Directorate General for Environment Civil Protection Unit, Directorate General for Environment Forests Unit.

Forest fires in Europe. 2006. Report No 7, EUR 22931 EN European Communities 2007. European Commission, Directorate General Joint Research Centre, Institute for Environment and Sustainability Land Management Unit, Directorate General for Environment Civil Protection Unit, Directorate General for Environment Forests Unit.

Forestry. 1991–2001. The series Information and Statistical Reports, GUS, Warsaw, pp 269–274.

Fraszewski, D. 1997. Economic, environmental and social consequences of catastrofic forest fires, Forest Reserche Institutes Report, Warsaw.

Goldammer, J.G. 1993. Feuer in Waldökosystemen der Tropfen und Subtropfen. Basel, Boston, Berlin.

Goldammer, J.G., and Furayev, V.V., eds. 1996. Fire in ecosystems of Boreal Eurasia. Forestry sciences vol. 48. Kluwer Academic Publisher, London, p. 528.

Goldammer, J.G., Prüter, J., and Page, H. 1997. Feuereinsatz im Naturschutz in Mitteleuropa. Ein Positionspapier. Alfred Toepfer Akademie für Naturschutz, Schneverdingen, NNA-Berichte 10, Heft 5, 2–17.

Perlińska, A. 2000. Analysis of the state of fire protection in State Forests in 1999. General Directorate of State Forests, Department of Forest Protection, Warsaw [in Polish].

Reports on the state of forests in 2001. Information Centre of State Forests [in Polish].

Statistical Tables for Rescue Operations for 1994, 1995, 1996, 1997, 1998, 1999, 2000, 2001. National Headquarters of the State Fire Service, National Centre for the Co-ordination of Rescue and Civil Protection 1994–2001, developed on the basis of the data from the programme EWID-93.

Ubysz, B. 2003. The influence factors on the forest fire danger in Poland. XII World Forestry Congress 2003, Québec, Canada, September 21 to 28, 2003, Forests, Source of Live. Congress Proceedings, B—Forests for the Planet, p. 230. www.fao.org/forestry/site/18509/en-2k/DOCREP/ARTICLE/WFC/XII/0009-B3.HTM

Ubysz, B., and Szczygieł, R. 2002. Fire situation in Poland. Int. For. Fire News, No. 27 – July 2002, p. 38–64, UN ECE/FAO.

Ubysz, B., and Szczygieł, R. 2005. Forest fires. In: Report on state of forests in Poland in 2004, pp. 46–48 and 67–68 [in Polish].

Ubysz, B., Szczygieł, R., and Piwnicki, J. 2005. Poland—Chapter 4.4. In: Forest Fires Report in Europe 2004, Report No 5, European Communities 2005, pp. 27–29.

UNEP/FAO. 2000. Forest resources of Europe, CIS, North, America, Australia, Japan and New Zealand (industrialized temperate/boreal countries). UN-ECE/FAO Contribution to the Global Forest Resources Assessment 2000. ECE/TIM/SP17. Geneva Timber and Forest Study Papers, No. 17. New York, Geneva.

UNEP/FAO. 2002. Forest fire statistics 1999-2001, Timber Bulletin 1999–2001, ECE/TIM/BULL/2002/4, Vol. LV (2002), No. 4, Geneva, 48 pp.

This page intentionally left blank

Developments in Environmental Science, Volume 8
A. Bytnerowicz, M. Arbaugh, A. Riebau and C. Andersen (Editors)

ISSN: 1474-8177/DOI:10.1016/S1474-8177(08)00011-9

Chapter 11

A Mega-Fire Event in Central Russia: Fire Weather, Radiative, and Optical Properties of the Atmosphere, and Consequences for Subboreal Forest Plants

Nataly Y. Chubarova, Nickolay G. Prilepsky, Alexei N. Rublev and Allen R. Riebau*

Abstract

In 2002, a major drought and prolonged high temperatures occurred in central Russia that resulted in unprecedented wildland fires. These fires occurred under extreme fire danger conditions and were impossible for the Russian authorities to extinguish. It is perhaps somewhat unique that the fires were first burning peat bogs and later forests, causing very massive smoke. Smoke was transported into Moscow itself for a period of almost 2 months, sometimes reducing visibility to below 60 m. Owing to the population size of Moscow and the duration of the event, these fires resulted in perhaps the most significant exposures of fire smoke to a major population center in recorded history. Significant reductions in solar radiation were observed during a course of measurements taken at the meteorological observatory at Moscow State University and at Zvenigorod Biostation located about 50 km west of the observatory. The fire smoke cloud was characterized by high aerosol optical thickness (AOT), high values of single scattering albedo in the visible spectral region (SSA $\sim$ 0.95), and high concentration of optically active gas species. Surface ozone levels were additionally elevated. At Zvenigorod Biostation changes in forest herbaceous plant development, flowering, and seeding were also observed. These changes may be explained as resulting from a combination of extreme weather, elevated surface ozone, and to a lesser extent changes in solar radiation.

*Corresponding author: E-mail: chubarova@imp.kiae.ru

11.1. Introduction

During July, August, and September of 2002, Moscow experienced periods of intense fire smoke. Massive amounts of smoke were generated by forest and peat bog fires, with the predominance of smoke coming from low-intensity smoldering fires. The fire smoke caused great public concern about health and well-being, especially for children and the elderly. Verbal accounts from people often described the situation as ''horrible'' or ''impossible.'' Health officials advised all residents to remain indoors whenever they could, with some health officials advising to soak bed sheets in water and nail them over windows to filter smoke from entering indoors.

The smoke event also soon caused international concern, as the duration stretched from days to weeks, and the fire smoke reached as far as Great Britain, causing violations of British air quality standards, and Moscow's international and domestic airports were closed several times due to reduced visibility. The cause for the fires was officially cited as a confluence of hot, dry conditions that went beyond those normally observed in the climate record, and a paucity of firefighters to extinguish the fires. Some reports cited an additional potential cause: the draining of peat bogs on a large scale to develop land for recreational housing may have also contributed to the peat bogs becoming more fire prone (from a news release of the World Wildlife Fund, 2002).

During the period of the fires, measurements of atmospheric aerosols and solar radiation were taken both at the meteorological observatory of Moscow State University (MOMSU, located on the Lenin Hills in the city proper) and at the MSU Zvenigorod Biostation (about 50 km west of MOMSU). From these measurements an assessment of atmospheric conditions during the fires was made, and several aspects of the observed fires were examined: the weather conditions in which they occurred, their direct and indirect influence on air quality, and specific features of solar radiation transmittance and radiative effects during dense fire smoke conditions. The radiative parameters of the atmosphere observed in 2002 were also compared with those measured during a similar period of intense Moscow region fires in 1972. Using assumed radiative characteristics of smoke aerosols and atmospheric gas species as input parameters for a model, smoke impacts on the attenuation of solar irradiance in different spectral ranges were simulated and compared with measurements. During the same time, a complex program of observations of forest herbaceous plant phenology and induced plant injury occurred at Zvenigorod Biostation. Thus, the unique smoke intrusion event and the region's extreme weather effects were compared from both an atmospheric and plant ecology consequence viewpoint.

11.2. Observations, simulation, and analysis

11.2.1. Meteorology, wildland fire danger, and visibility

The forest and peat bog fire events observed in the Moscow region in summer to fall 2002 were characterized by very high air temperatures and prolonged drought. During July, the Moscow region received 16 mm of rainfall, or only 17% of climatic norm (values based on 1960 through 1990 data). Air temperatures reached an absolute monthly mean maximum of 23.4°C in July which was about 5°C higher than the climatic average value (128% of the average). Rainfall for August and September were 65% and 114% of the regional climatic values, respectively, with the September rainfall at the end of the month increase and return to more normal air temperatures (monthly average only 1.4 degrees higher than norm) being the main factors that ultimately extinguished the wildfires. The July, August, and early September extreme fire weather conditions caused fire danger to be highly elevated over normal values.

In Russia, the intensity of fire danger is often determined by Nesterov's flammability indices. Fire indices are calculated according to Nesterov's equation: $G = \sum(T * d)$; which takes into account the day-to-day accumulation of the joint effect of maximum temperature at midday (T) and dew point depression ($d = T - Td$) in the absence of precipitation higher than 3 mm. Fire risks are classified with K fire class values from 0 to 5, where $K = 3$, 4, and 5 relate to dangerous, highly dangerous, and extremely dangerous fire conditions, respectively. Figure 11.1 shows the frequency distribution of these classes in a typical fire season situation (2001) as well as during 2002 and 1972 fire conditions. In 2002 there were much higher frequencies of the classes $K = 4$ and 5 during periods with fires, with $K = 5$ indices only occurring during the periods of extreme fire. It should be noted that these K values are higher and greater in frequency of occurrence even than those during the extreme Moscow fire event of 1972. Figure 11.2 shows the percent of fire numbers (occurrence) and the percent of increase in fire area in the Moscow region compared with values within the Central European Plain (with associated Nesterov's indices). An indication of the severity of the event is that approximately 55% fires in the entire Central European Plain occurred in the Moscow Region. The main forest and peat bog fires during early August of 2002 were located to the east of the city of Moscow. By late August they were distributed in other regions surrounding Moscow. Although loss of forest resources was of concern, the press and general public soon voiced more concerns about smoke than with direct damage from the fires.

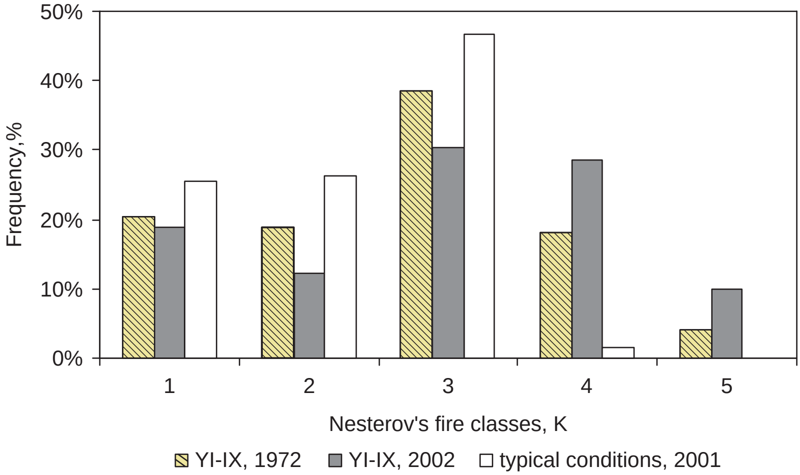

Figure 11.1. Frequency distribution of Nesterov's fire classes, *K*, in typical (2001) and in fire conditions (1972 and 2002, June–September period).

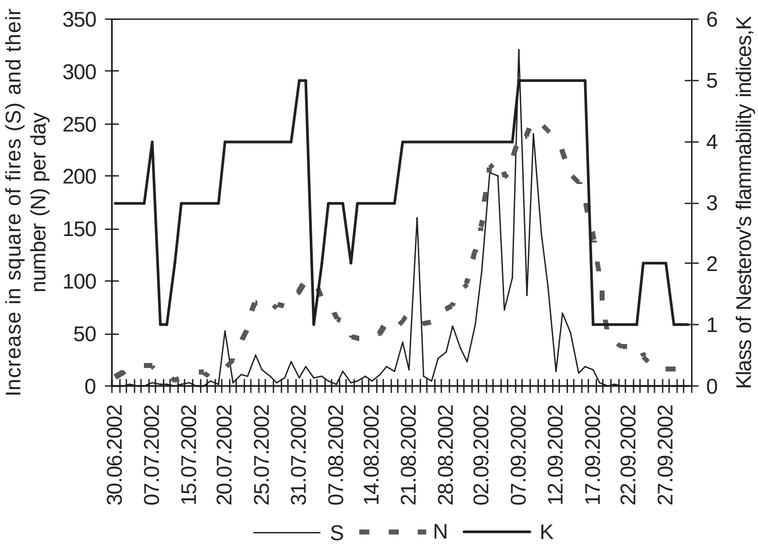

Figure 11.2. The percent of fire number (*N*) and the percent of increase in fire area (*S*) in Moscow region compared with totals in the Central European Plain, and Nesterov's fire indices (*K*) 2002.

Figure 11.3. Views of a Moscow city center region (Taganka) during fire smoke event (left) and in normal clear sky conditions (right) on August 1, 2002.

In the Moscow region the effects of forest fires led to an extraordinary decrease in visibility due to a very high aerosol loading from smoke (at times less than 60 m surrounding Red Square). This low visibility is shown in Fig. 11.3, which presents photographic evidence of the effects of fire smoke in the central part of Moscow city itself.

11.2.2. Geographic extent of smoke plumes and aerosols

Figure 11.4 is a high resolution satellite image of the Moscow region during the fires on July 30, 2002. It also includes 12-h backward trajectories at different heights for cloudless conditions and high aerosol optical thickness (AOT500 = 1.6). Most of the fires at this time were 50–100 km to the east of Moscow and produced strong heterogeneity over eastern regions but with well diffuse plumes over Moscow A high correlation ($r = 0.91$) between simultaneous AOT500 records at Zvenigorod Biostation (measured by handheld hazemeters) and in Moscow (measured by the National Aeronautics and Space Administration AERONET program Cimel sun photometer) demonstrated a homogeneous distribution of the fire smoke cloud 50–100 km to the west of the main fire locations.

The AOT500 distribution in typical conditions without fires during the Moscow summer period is characterized by the near absence of AOT500 > 0.4 (less than 1% of cases in May–June 2002;

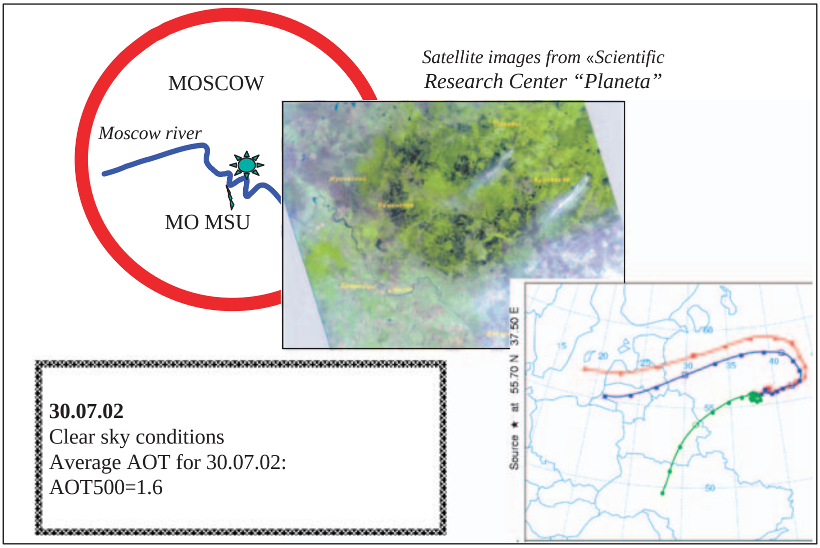

Figure 11.4. Satellite image of the fires over the eastern part of the Moscow region and 12-h National Oceanic and Atmospheric Administration NOAA backward trajectories at approximately 500 m (red), 1000 m (blue), and 1500 m (green) heights.

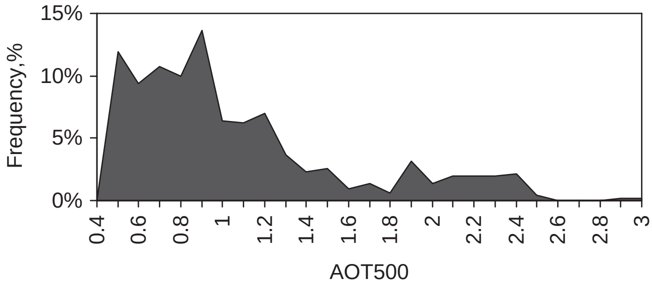

Figure 11.5. Frequency distribution of aerosol optical thickness at 500 nm (AOT500) in Moscow during fires in 2002 (from AERONET Cimel data).

Uliumdzhieva et al., 2005). To identify conditions with the presence of a fire smoke cloud, the study employed a simple math filter for AOT500 >0.4 on data collected at MOMSU. The distribution of AOT500 is presented in Fig. 11.5, which shows the occurrence of the extremely high AOT values up to 2.5–3 during the fire smoke event. Table 11.1 presents the statistics of optical parameters and concentration of different gases

Table 11.1. Statistics of some optical parameters in Moscow. 2002: Aerosol optical thickness AOT at 500 nm and at 380 nm, Angstrom parameters in two spectral intervals ($n = 513$), single scattering albedo and factor asymmetry at 440 nm (only clear sky cases, $n = 36$), and ground concentration of different gaseous species ($\mu g\,m^{-3}$, $n = 36$) in fire conditions

	Mean	Standard Deviation
AOT500	1.02	0.53
AOT380	1.43	0.66
Angstrom parameter (440–870 nm)	1.65	0.15
Angstrom parameter (340–380 nm)	0.99	0.28
SSA at 440 nm	0.95	0.01
Factor asymmetry at 440 nm	0.68	0.02
NO_2	99.7	49.9
O_3	62.6	63.8
SO_2	9.5	16.7
HCHO	21.4	16.8

measured during the fires at the meteorological observatory, which represent characteristics of the regional fire smoke cloud. High concentrations of nitrogen dioxide (NO_2), formaldehyde (HCHO), and sulfur dioxide (SO_2) were also observed during the fires at the observatory, with the maximum surface values of gas concentrations (except SO_2) being 1.5–3 times higher than instantaneous maximum concentrations allowable by the Russian Federation air quality standards.

Data on total aerosols were correlated with measured surface atmospheric gas concentrations in order to better understand the effects of the smoke plumes on Moscow air quality. The calculated correlations of elevated AOT500 values with high NO_2 and HCHO concentrations, as well as the daily maxima of surface ozone, all exceed correlation coefficient values of $r = 0.5$. However, the correlation of AOT500 with SO_2 concentrations was much lower ($r = 0.37$), indicating the existence of other anthropogenic sources for SO_2. The correlation between the concentration of optically active gases and aerosols may indicate additional attenuation of solar irradiance during the fires due to concurrent influence of both factors.

Volume aerosol size distributions retrieved by the method described in Dubovik and King (2000) were characterized by a distinct bimodal character (Fig. 11.6) with an increase in fine aerosols compared with typical Moscow conditions (61% and 56%, respectively). Figure 11.7 shows monthly mean values of real and imaginary aerosol refractive index fractions during typical and the "fire" months (July, August,

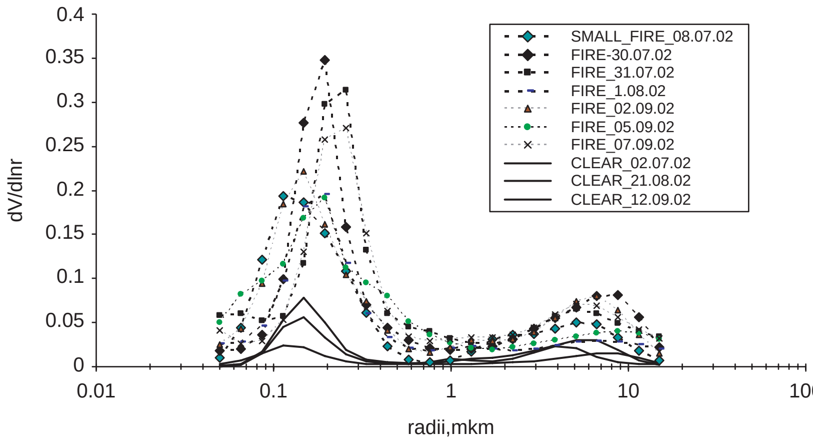

Figure 11.6. Aerosol size distribution in clear conditions (lines) and during fires (dots). For X axis, mkm = micrometer.

September). From this can be concluded that during fire conditions the real fraction of the refractive index tends to be higher, and the imaginary fraction (e.g., theoretical fraction) tends to be lower than those in typical situations. This leads to higher values of aerosol single scattering albedo (SSA) during fire events (Table 11.1, Fig. 11.8). These high values of SSA correlate well with the results obtained in other regions (i.e., fires in North America, Brazilian fires) where the smoldering phase prevailed over the flaming fire phase (Dubovik et al., 2002).

11.3. Changes in solar irradiance

The attenuation of surface solar irradiance during the fires (e.g., duration of the smoke event) had significant spectral features, with a dramatic mean loss of global (Q) irradiance. There was a loss of 23% for shortwave irradiance (300–4500 nm or QIR), 31% for visible irradiance (QVIS), and 36% for longwave UV irradiance (300–380 spectral range or QUV380). The most significant attenuation was observed in the UV-B region for erythemally weighted irradiance (Qer), which was measured at 58% of normal season values. Figure 11.9 presents QIR and QUV380 losses during the fires in 2002 and in 1972. As can be seen from the figure, there were larger attenuations of radiation fluxes in 2002 due to more severe and extensive fires (as supported by the higher Nesterov's *K* values in 2002; Fig. 11.1). Also one can see the same more pronounced attenuation of UV irradiance compared with shortwave irradiance.

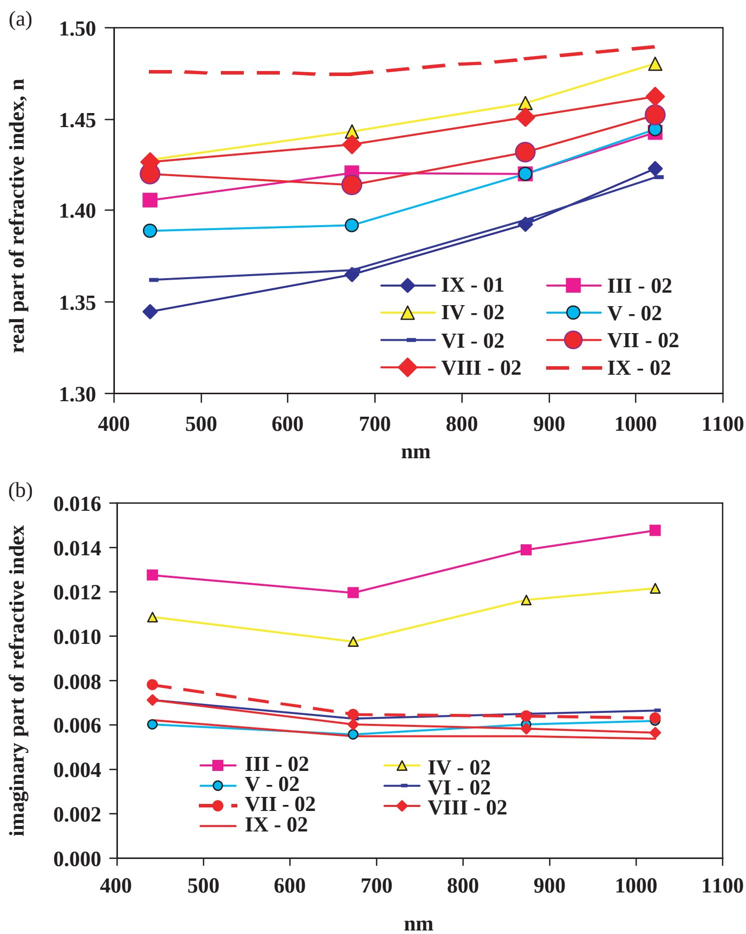

Figure 11.7. Real (a) and imaginary or ideal (b) refractive indices under typical and fire conditions in Moscow.

In order to understand the causes of more pronounced UV attenuation we have applied model radiative transfer calculations. Using the input parameters from aerosol and gaseous measurements and a TUV radiative transfer model (Madronich & Flocke, 1998) we calculated erythemally weighted UV irradiance Qer, UV irradiance 300–380 nm QUV380 and visible irradiance QVIS for different smoke and non-smoke cloudless conditions. The results were compared with the corresponding measurements. In addition to aerosol parameters, the concentrations of gas species optically active in UV and visible spectral regions were

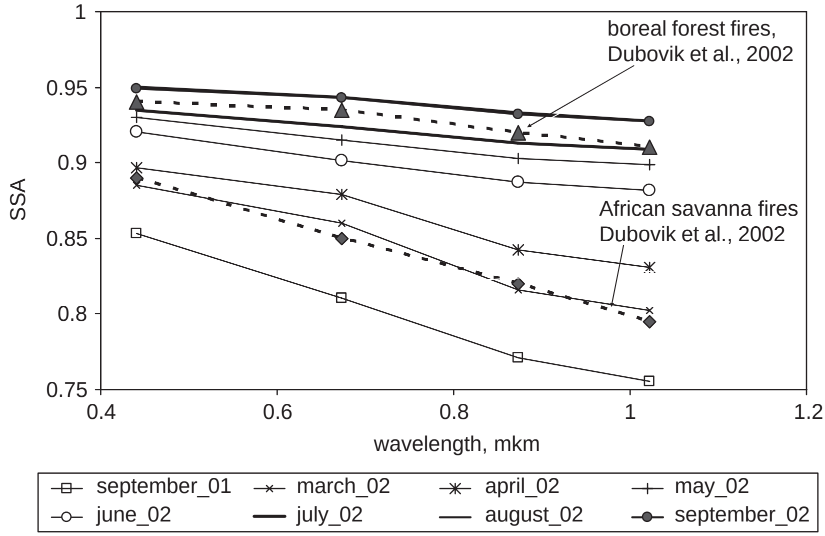

Figure 11.8. Aerosol single scattering albedo (SSA) in typical optical conditions in Moscow and in conditions with forest fires over different regions, 2001–2002. For X axis, mkm = micrometer.

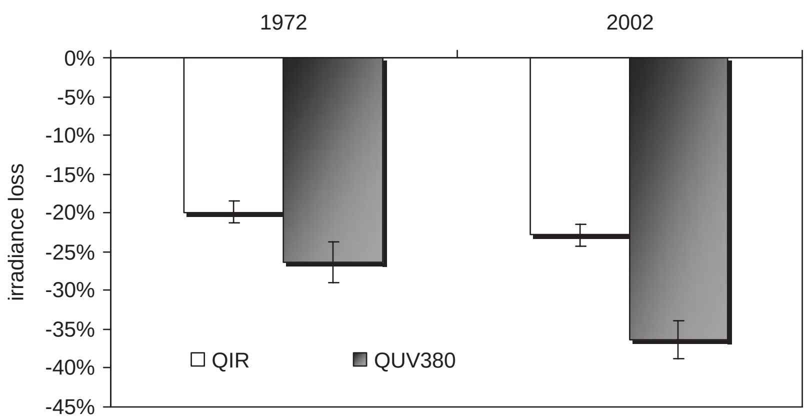

Figure 11.9. Attenuation of QUV380 and QIR during fire smoke events in 1972 and 2002 during cloudless conditions.

included in the calculations. The comparison between calculations and measurements for Qer is presented in Fig. 11.10. It was shown that for erythemally weighted UV irradiance, the rather high observed concentrations of SO_2 and HCHO do not play a vital role

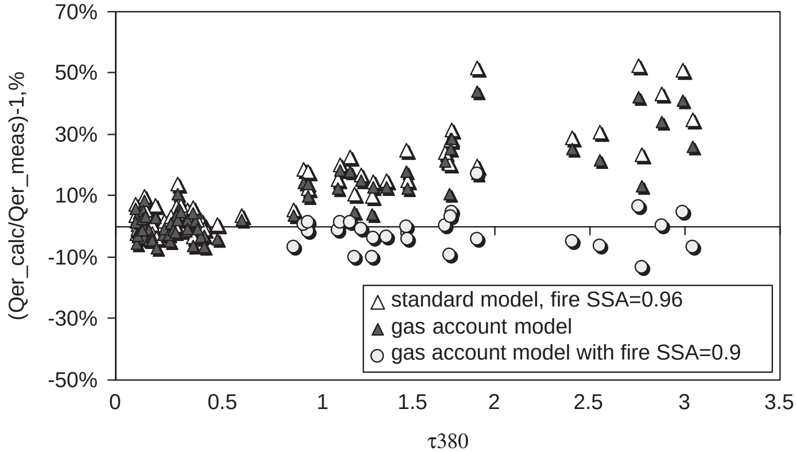

Figure 11.10. Relative difference between erythemally weighted irradiance (Qer) calculations, and measurements taking into account for gaseous absorption and without it as a function of AOT at 380 nm during cloudless conditions.

($<$1–2%), while surface ozone can attenuate by up to 2–3%. Extremely high concentrations of NO_2 can attenuate irradiance up to 10–15% in longwave UV and up to 5–6% in the visible region of the solar spectrum. Using observed gas species concentrations in the model improved the agreement with experimental data in all spectral regions, with standard deviations falling from 0.16 to 0.14 for Qer, from 0.11 to 0.08 for QUV380, and from 0.037 to 0.032 for QVIS. In the shortwave UV region, however, even with all gases accounted, the model overestimated, especially when AOT was high. One of the reasons for this may be the manner in which the model applied real and imaginary refractive indices in the visible spectral range (at 440 nm). The model's systematic discrepancies at high AOT could be eliminated by setting SSA = 0.92, QUV380 = 0.89, and a value of 0.9 set for Qer. These values are noticeably less than SSA retrievals at 440 nm (Table 11.1). The larger attenuation of UV is thus explained by both the effects of multiple scattering (especially at longer wave paths) and higher aerosol and gas species absorption in this spectral range.

While the attenuation of solar irradiance due to the advection of fire smoke was significant, there were not large effects in the total monthly sum values of solar irradiance reaching the earth's surface. This is explained by the almost complete absence of clouds during the drought period. Clouds naturally create large optical thickness values that significantly decrease the level of total solar irradiance reaching the earth's surface. Clear skies and cloudless days coincided with the absence of precipitation during the 2002 summer–fall period, which in turn led to the fire conditions. There was a measurable increase of the solar irradiance attenuation due to smoke aerosol effects that did reach levels of reduction from 40% to 70% (with stronger attenuation in the UV region). At the same time there were some spectral changes in solar irradiance reaching the ground from the perspective of monthly totals. For example, during July, August, and September 2002 the level of global shortwave irradiance was 14%, 7%, and 2% higher than the corresponding average values for 1958–1997, while the changes in UV irradiance were about +9%, −3%, and −10%, indicating much more significant loss in this portion of the solar spectrum. Lack of cloud cover thus compensated for reductions in solar radiation reaching the earth's surface due to fire smoke, at least when such radiation is viewed from the perspective of monthly averages.

11.4. Radiative forcing and radiation budget

To account for the Moscow smoke episode effects of aerosol and gas species, radiative forcing was calculated to evaluate changes in the shortwave radiation budget. In this case radiative forcing (R) and radiative forcing efficiency were calculated as:

$$R = Q_{\mathrm{net(gas,aerosol)}} - Q_{\mathrm{net(no\ gas,no\ aerosol)}} \tag{11.1}$$

$$R_{\mathrm{eff}} = R/d\mathrm{AOT500} \tag{11.2}$$

where R_{eff} characterizes relative changes in solar irradiance without and with gas and aerosol content for $d\mathrm{AOT500} = 1$.

To analyze the role of different atmospheric components on the radiation budget, 5 days with a fire smoke cloud situation were chosen, and the optical properties of atmospheric aerosols were recalculated, while specifically accounting for gaseous NO_2 absorption (Chubarova & Dubovik, 2004). Shortwave flux calculations used a Monte-Carlo model (developed by A. Rublev), which had been carefully validated against radiation measurements (Chubarova et al., 1999). It should also be noted that during the fires, surface albedo (A) was low. For example, in August the monthly mean A was 0.15 in 2002 and 0.17 in 1972, compared with A of 0.2 in typical nonfire smoke conditions. This is of importance because changes in reflectance of the surface during fires (possibly due to soot sedimentation on the ground and/or blackened patches from burning of grasses) will also affect estimates of radiative forcing. Applying a

Table 11.2. Statistics of shortwave radiative forcing in $W\,m^{-2}$ at the top of the atmosphere TOA and at the ground for fire smoke conditions in Moscow, July–September 2002. (Cos $\theta \approx 0.6$; $A = 0.17$)

	Ground model/measurements	TOA model
R_{mean}(AOT500 = 1.02)	−100/−82	−39
R_{max}(AOT500 = 0.4)	−49/−32	−12
R_{min}(AOT500 = 2.96)	−210/−239	−91
Average R_{eff}	$-90 \pm 10/-81 \pm 12$	−39

computed value for the molecular atmosphere $Q_{net(no\ gas,no\ aerosol)}$, we calculated measured and model radiative forcing at ground using $Q_{net(gas,aerosol)}$, respectively, from measurements and modeling in fire conditions. Table 11.2 shows mean, minimum, and maximum radiative forcing at the ground calculated using radiative forcing efficiency from measurements (R_{eff}_meas) with AOT variations as well as pure model R-values (to avoid R_{eff} nonlinear AOT dependence). One can see significant variation of the fire cloud radiation forcing at the ground reaching $-210/-240\,W\,m^{-2}$. Under typical conditions (mean AOT500 = 0.16) R at the ground is much smaller ($-25\,W\,m^{-2}$), and the calculated effect of NO_2 on R-values at ground levels is about $-6/-10\,W\,m^{-2}$; for R_{eff} it is close to $-5\,W\,m^{-2}$.

Radiative forcing at the top of the atmosphere (TOA) can reach $-91\,W\,m^{-2}$ at maximum AOT. Owing to the comparatively small effective diameters of smoke aerosols, AOT in the longwave (thermal infrared) region is not very high; therefore, aerosol longwave radiative forcing is small. Hence, there is a significant cooling effect at high smoke aerosol loading compared with typical conditions when R at TOA is $-10/-20\,W\,m^{-2}$.

The absorption in the atmosphere is calculated according to the following equation:

$$Q_a = S_0 \cos\theta - F_\lambda^{\uparrow} - \int F_\lambda^{\downarrow}(1 - A_\lambda)d\lambda$$

where S_0 is $1367\,W\,m^{-2}$, θ the zenith angle, $F_\lambda^{\uparrow}$ and $F_\lambda^{\downarrow}$ the upward and downward fluxes, and A_λ = surface albedo.

Figure 11.11 illustrates the sensitivity of absorption in the atmosphere due to different factors: aerosol loadings, NO_2 concentrations, and the sum of absorption by other gaseous species (H_2O, etc.). The calculations were done for mean, maximum, and minimum AOT in fire conditions. On average, the solar absorption due to both aerosol and NO_2 in the observed fire smoke cloud was about 28% but can reach almost 35% at

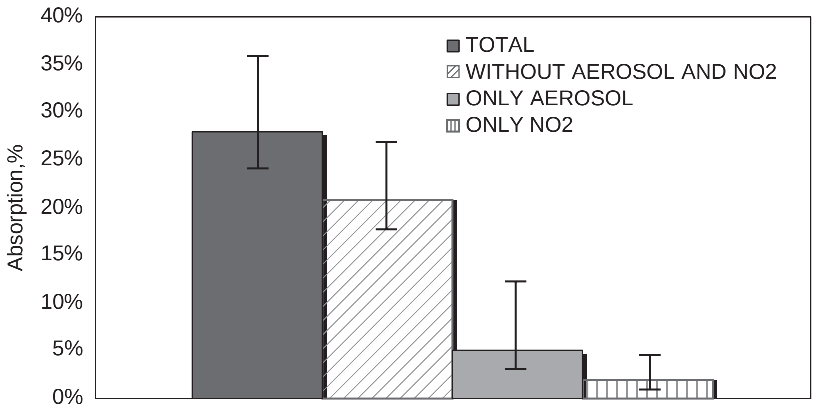

Figure 11.11. The solar absorption in the atmosphere in fire smoke conditions. Monte-Carlo simulations, $\cos\theta \approx 0.6$. Mean fire conditions are characterized by AOT500 = 1.02, $NO_2 = 3.8\,\text{matm} \cdot \text{cm}$. $1\,\text{matm}\,\text{cm}^{-1} = 1$ Dobson Unit (D. U.) $= 2.69 \times 10^{16}\,\text{mols/cm}^2$.

the highest AOT. The mean shortwave absorption by NO_2 is about 2% and can reach 4%.

On the whole, there was a distinct redistribution of radiation budget and changes in transmission in the atmosphere in the presence of the fire smoke cloud. Figure 11.12 illustrates the changes in the components of the radiation budget and transmission in conditions with total absence of aerosol, with continental aerosol at AOT500 = 0.16, and in the presence of a mean fire smoke cloud with AOT500 = 1.02 and $NO_2 = 3.8\,\text{matm}\,\text{cm}^{-1}$. The calculations were made for one month (August 2002) and reflect microclimatic changes in the radiation budget. These changes in radiation budget as well as the strong attenuation of radiation reaching the earth's surface, combined the spectral features of this radiation, may contribute to some extent to the observed adverse plant phenology changes at Zvenigorod Biostation. Such effects are difficult to quantify, however, due to the coincident effects of drought and high air temperatures on forest plants.

11.5. Wildland fire smoke and forest plant phenophases

The fire smoke and weather conditions of summer 2002 had a great impact on the city of Moscow itself. Many believed the smoke to be a significant health hazard, with concentrations of regulated air pollutants exceeding government air quality standards. It is believed that these

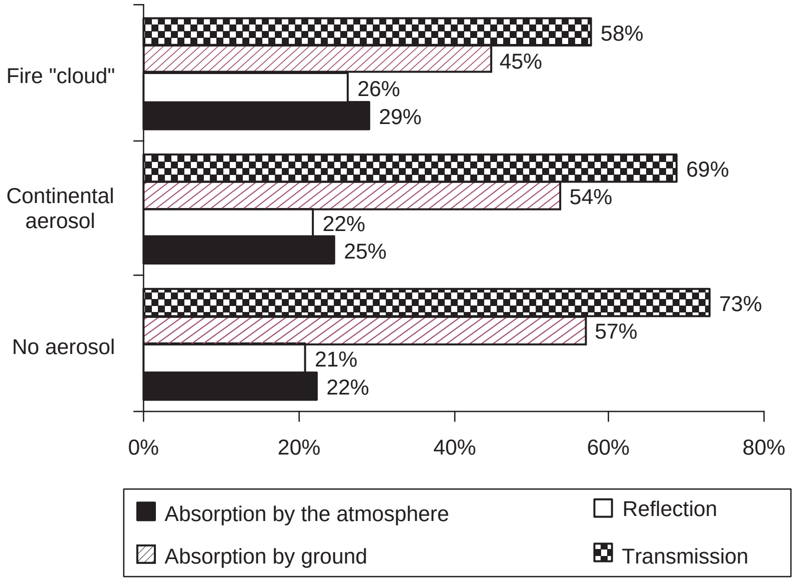

Figure 11.12. The redistribution of radiation budget and changes in transmission in different conditions in August 2002.

conditions also led to changes in forest herbaceous plant phenology and induced plant injury. This was mainly due to the drought conditions, high air temperatures, elevated surface ozone, and possibly to a lesser extent episodic reductions in available photosynthetic light. Several bioindicator plant species sensitive to ozone are widely spread throughout the Moscow region (Manning et al., 2002). During the fire events of 2002, corresponding high levels of surface ozone may have resulted in impact to bioindicator plants across the Moscow area. Ozone injury was directly observed during the smoke event, with measured impacts to *Alnus incana*, *Physocarpus opulifolia*, *Sambucus racemosa*, and *Crataegus sanguinea*. Figure 11.13 presents the traces of ozone injury (bronzing) for *Crataegus sanguinea* observed in early September 2002 in Moscow.

In addition to the ozone damage observed, changes in the seasonal development of central Russian subboreal forest plants were also observed. These changes are postulated to result from a combination of the hot, dry weather and to a lesser extent the smoke-impaired solar radiation regime, resulting in microclimatic drift at observation sites (at Zvenigorod Biostation), and made worse by possible synergistic direct ozone damage. Such effects were expressed in missing phenophases

Figure 11.13. Traces of surface ozone injury (bronzing) in the leaves of *Crataegus sanguinea* found at Zvenigorod Biostation during September 2002. (Courtesy of Robert Musselmann, USDA Forest Service.)

(absence of winter-annual shoots in *Carex digitata* and *Calamagrostis arundinacea* and practically total absence of flowering individuals in *Solidago virgaurea*) as well as in modified phenorhythmotypes (*C. arundinacea*, usually summer–winter green, was summer green only in 2002). Additionally plant mortality (in *Luzula pilosa*, *Galeobdolon luteum*, and *Asarum europaeum*) accompanied by a changed sequence of seasonal development phases during the next year after the drought (in 2003, the flowering stems in *C. digitata* developed after vegetative ones, while in normal years the sequence is reversed) was observed. Figure 11.14 illustrates the 2002 season compared with normal years for differences in vegetative shoot mortality in one of the species (*C. digitata*) under two types of forest at Zvenigorod Biostation. Further work will need to be done to prove even a minor causal relationship between reduced solar radiation and the phenophase changes cited above, especially if elevated ozone levels are also considered as a potentially additive stress factor. It is likely, however, that when such episodic reductions in solar radiation occur from wildland fire smoke, there will also be coincidental drought, high air temperatures, and increased ozone in the lower atmosphere. Thus, the suite of factors potentially causative for the observed forest plant phenology changes will naturally occur as an

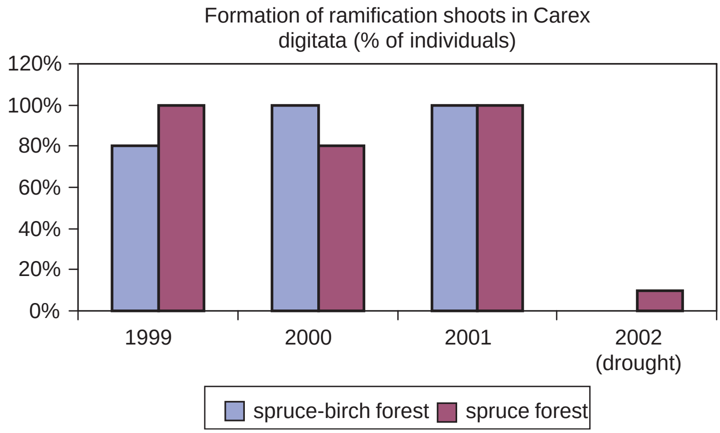

Figure 11.14. Percent of vegetative shoot mortality in *C. digitata* in differing drought condition years and under the two main forest types at Zvenigorod Biostation.

ensemble, with reductions in solar radiation as only one factor of the suite of measurable stressors.

11.6. Conclusions

The peat bog fires of 2002 had a significant impact on air quality in the Moscow region, with currently undetermined and undocumented public health consequences. From observations, the aerosol loading of the atmosphere combined with increased reflectance, lowered surface solar radiation levels in all spectra. Surface ozone levels were also increased as a result of the fire episode. Measurements of forest plants at Zvenigorod Biostation showed adverse growth impacts that were likely caused by a synergism between drought, temperature, lowered solar radiation, and surface ozone damage or stress. The fires did not consume all the peat in bogs in the Moscow region, and under similar climatic and wildland fire conditions—as expressed in Nesterov's indices or by other measures—more such smoke events will occur. Such large-scale extreme fire weather and smoke events would result in regional plant microsite changes during a fire season, and if repeated in areas such as boreal or subboreal peat bog regions with potential for generation of large amounts of smoke, they could contribute to observable ecological change. Although such speculations may be risky and should be further investigated through more observations, the potential for ecological change should be considered if fire seasons in northern latitudes become extreme under a warming climate.

ACKNOWLEDGMENTS

We thank the Mosecomonitoring Agency and the Institute of Atmospheric Physics for providing data on concentrations of some gas species. Alexei Rublev and Nataly Chubarova were partly supported by ISTC Project #3254 and RSFBR 06-04-48483A. Additionally, we wish to acknowledge the work of scientists of the biological faculty at the Moscow State University, especially, Pavel Zhmylev and Elizaveta Karpukhina.

REFERENCES

Chubarova, N. A., and Dubovik, O. 2004. The sensitivity of aerosol properties retrievals from AERONET measurements to NO_2 concentration over industrial region on the example of Moscow. Optica Pura y Aplicada 3, 3315–3319. http://www.sedoptica.es/indice.html

Chubarova, N.A., Rublev, A., Trotsenko, A., and Trembach, V. 1999. The comparisons between modeled and measured surface shortwave irradiances in clear sky conditions. Izvestiya, Atmos. Oceanic Phys. 2, 201–216.

Dubovik, O., and King, M.D. 2000. A flexible inversion algorithm for retrieval of aerosol optical properties from sun and sky radiance measurements. J. Geophys. Res. 105(D16), 20673–20696.

Dubovik, O., Holben, B.N., Eck, T.F., Smirnov, A., Kaufman, Y.J., King, M.D., Tanre, D., and Slutsker, I. 2002. Variability of absorption and optical properties of key aerosol types observed in worldwide locations. J. Atmos. Sci. 59, 590–608.

Madronich, S., and Flocke, S. 1998. The role of solar radiation in atmospheric chemistry. In: Boule, P., ed. Handbook of environmental chemistry. Springer-Verlag, Heidelberg, pp. 1–26.

Manning, W.J., Godzik, B., and Musselman, R. 2002. Potential bioindicator plant species for ambient ozone in forested mountain areas of central Europe. Environ. Pollut. 119, 283–290.

Uliumdzhieva, N., Chubarova, N., and Smirnov, A. 2005. Aerosol characteristics of the atmosphere over moscow from cimel sun photometer data. Meteorology and Hydrology 1, 48–57.

World Wildlife Fund. 2002. Moscow enveloped by smoke. News release at www.wwf.org

Developments in Environmental Science, Volume 8 265
A. Bytnerowicz, M. Arbaugh, A. Riebau and C. Andersen (Editors)

ISSN: 1474-8177/DOI:10.1016/S1474-8177(08)00012-0

Chapter 12

Vegetation Fires, Smoke Emissions, and Dispersion of Radionuclides in the Chernobyl Exclusion Zone

Wei Min Hao, Oleg O. Bondarenko, Sergiy Zibtsev and Diane Hutton*

Abstract

The accident of the Chernobyl nuclear power plant (ChNPP) in 1986 was probably the worst environmental disaster in the past 30 years. The fallout and accumulation of radionuclides in the soil and vegetation could have long-term impacts on the environment. Radionuclides released during large, catastrophic vegetation fires could spread to continental Europe, Scandinavia, and Russia. The potential for large fires occurring in the Chernobyl Exclusion Zone (EZ) was assessed based on vegetation conditions. We reviewed the composition of radionuclides in the soil and vegetation and in the particulate matter emitted by fires. The highest atmospheric radionuclide ^{137}Cs levels occurred in early spring and late fall, corresponding to the most intense periods of burning in the EZ. It is evident from satellite images that smoke plumes from the EZ and southern Ukraine dispersed several hundred kilometers from the active fires and reached a major metropolitan area. We propose to install a satellite receiving station to detect fires in real time. It is also essential to develop a smoke dispersion and air quality forecasting model to predict the radioactivity levels downwind from catastrophic fires in order to protect public health.

12.1. Introduction

The explosion of the No. 4 reactor of the Chernobyl nuclear power plant (ChNPP) in Pripyat, Ukraine, on April 26, 1986, created the worst nuclear accident in history. The reactor burned for 10 days and caused

*Corresponding author: E-mail: whao@fs.fed.us

high concentrations of radionuclides over most of Europe, especially in Ukraine, Belarus, and western Russia. The International Atomic Energy Agency of the United Nations reported that 56 deaths were directly caused by the accident and nearly 4000 deaths could be related to the accident.

The Chernobyl Exclusion Zone (EZ) covers an area of 2600 km^2. The EZ has a 154.5 km long international border adjacent to Belarus. About 70% of the territory is boreal forest, which is dominated by Scots pine, and the other 30% is mostly agricultural land. The forest provides multiple functions for the ecosystems of the EZ. It stores the radionuclides from the smoke plume fallout during the accident, absorbs the radionuclides from contaminated soil, and stabilizes the mobility of radionuclides. The concentrated radionuclides in the vegetation and soil would be emitted to the atmosphere during vegetation fires, which could lead to serious environmental damage. However, there was no active forest and fire management after the accident because the forest was contaminated by radionuclides and had limited commercial use. Scots pine stands became overstocked and stressed, predisposing them to attack by insects and diseases. The lack of fire management allowed the vegetation to overgrow, creating conditions favorable for fires to ignite and spread. About 12,000 hectares (ha) were burned in 1992, which led the Chernobyl State Enterprise to develop a fire surveillance system using lookout towers and reconnaissance planes. Hence, the region has not experienced a large fire in the past 15 years due to improved surveillance and aggressive, efficient fire suppression. During this period, fire activity has been largely limited to small fires in areas of formal agricultural land and settlement. The number of fires and total area burned have been declining since 1995. In 2005, only 36 ha were burned.

Since the nuclear accident, tremendous international efforts have been made to understand the impacts of radioactivity on ecosystems and human health. However, there are limited studies evaluating the potential risks of forest fires, the exposure levels of radionuclides from vegetation fires in the EZ, and the long-range transport of smoke plumes to large cities (e.g., Kiev) and across international borders to neighboring countries (e.g., Belarus, Russia, Poland). In this chapter, we will review the fire risks and the radioactivity levels in the soil, vegetation, and atmospheric particulate matter. We will show the satellite observation of long-range transport of smoke plumes from the EZ.

12.2. Fire risks

Although fire suppression in the Chernobyl EZ has been successful, budget limitation and the inability to utilize contaminated wood have inhibited implementation of an active forest management program to reduce the amount of fuel in the forest. The dense spacing of trees within the forest limits the growth of understory vegetation; the forest floor is largely litter. This fuel structure causes fires to remain close to the ground with relatively short flame lengths and without the means of transitioning to large crown fires except under extreme weather conditions. However, as mature trees die and more sunlight reaches the forest floor, small young trees and some shade-tolerant trees will grow in these spaces. This forest succession process will result in more ladder fuels on the forest floor, increasing the risks of large crown fires.

In the EZ, certain areas are especially vulnerable to fires. For instance, because of limited forest management, Scots pine stands are overstocked, stressed, and susceptible to insects and diseases. The gypsy moth (*Lymantria dispar*) has prospered causing root rot that has killed a large portion of trees, including a 400-ha stand. The infected forest is highly susceptible to fires. Many trees have fallen in areas that burned in 1995, creating openings in the forest canopy that have allowed sunlight to reach the forest floor. This progression has introduced new fuel in the understory from seedling and shrub establishment. The blend of new undergrowth vegetation with large, downed trees provides fires an avenue to reach the crowns of the canopy. Hence, future fires could be more intense than previous fires in the EZ with higher flame lengths, longer burning time, and more smoke emissions. Catastrophic fires of this magnitude are difficult to control and pose safety and health hazards for firefighters and the general public.

The fire risks found in the EZ are quite common in many parts of the world. More than 70 million ha of federal land in the United States are characterized by heavy accumulation of understory vegetation, downed logs, and regrowth of secondary forest; conditions similar to the landscape in the EZ. The lack of proper forest management and the focus on fire suppression in the United States has been the major cause of many large, uncontrollable catastrophic fires in the western U.S. in the past eight years. These megafires usually occur under hot, dry, and windy conditions, burn for several weeks, and spread over thousands of hectares. Such catastrophic fires could also occur in the Chernobyl EZ if effective forest management is not implemented in the near future.

12.3. Radioactivity in soil and vegetation

The radioactivity of radionuclides ^{90}Sr, ^{137}Cs, ^{238}Pu, and $^{239+240}$Pu is concentrated mostly in the top layer of soil in the forests and grasslands in Chernobyl (Yoschenko et al., 2006a). The radioactivity of each element varies considerably among the different components of the vegetation. The radioactivity of litter is higher than that in live foliage, bark, or live grasses.

The spatial distribution of ^{137}Cs radioactivity levels on the surface layer of contaminated soil in December 2002 is shown in Fig. 12.1. The radioactivity is the highest within a 10 km radius of the ChNPPs. The spatial distribution of the soil contamination closely follows the prevailing winds (easterly and southerly) during the accident. Seventy percent of the radioactivity was blown to Belarus, covering about a quarter of the area in Belarus and causing a high incidence rate of children's thyroid cancer.

12.4. Radioactivity of atmospheric particulate matter

There are two major sources of atmospheric radionuclides ^{90}Sr, ^{137}Cs, ^{238}Pu, and $^{239+240}Pu$ in Chernobyl: smoke particles and mineral dust. Construction and windy conditions are the major causes of dust from contaminated soil. Dust particles are usually large (range: 2–100 μm in diameter, mean: ~10 μm) (Brasseur et al., 1999) and redeposit close to the source. In contrast, forest and grassland fires emit fine particles with a bimodal size distribution of 0.04–0.07 μm and 0.1–0.3 μm (Chakrabarty et al., 2006). While large particles are usually repelled by the respiratory system, fine particles are inhaled into the lungs. Fine particles in smoke plumes often form large particles in aged plumes through coagulation with cloud droplets downwind from the fires.

The radioactivity levels of ^{90}Sr, ^{137}Cs, ^{238}Pu, and $^{239+240}Pu$ for atmospheric particulate matter near an experimental forest fire and two grassland fires in Chernobyl were found to be several orders of magnitude higher than the ambient levels (Yoschenko et al., 2006a). The estimation from an atmospheric transport model suggested that a small percentage of the radionuclides in the litter was emitted to the atmosphere during forest fires, and less than 1% of the radionuclides in the vegetation was emitted during grassland fires (Yoschenko et al., 2006b). The emitted radionuclides were concentrated in fine particles, which would increase the inhalation dosage to firefighters. The plutonium nuclides were the dominant radioactive elements of the fine particles.

The Chernobyl Radioecological Centre of the State Specialised Scientific and Industrial Enterprise (SSSIE "Ecocentre") has been operating an automated monitoring network to measure the ^{137}Cs radioactivity of particulate matter in the atmosphere within the EZ.

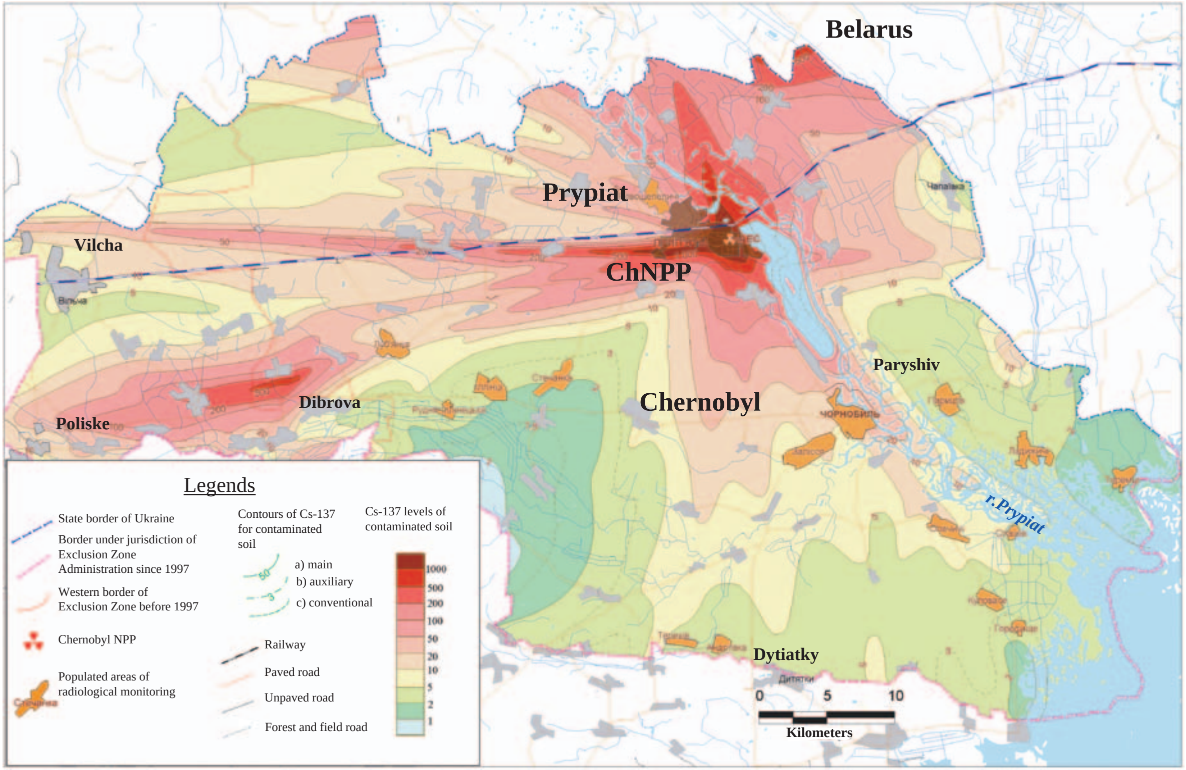

Figure 12.1. ^{137}Cs radioactivity on the surface layer of contaminated soil in the Chernobyl Exclusion Zone in December 2002 (scale in kilometers).

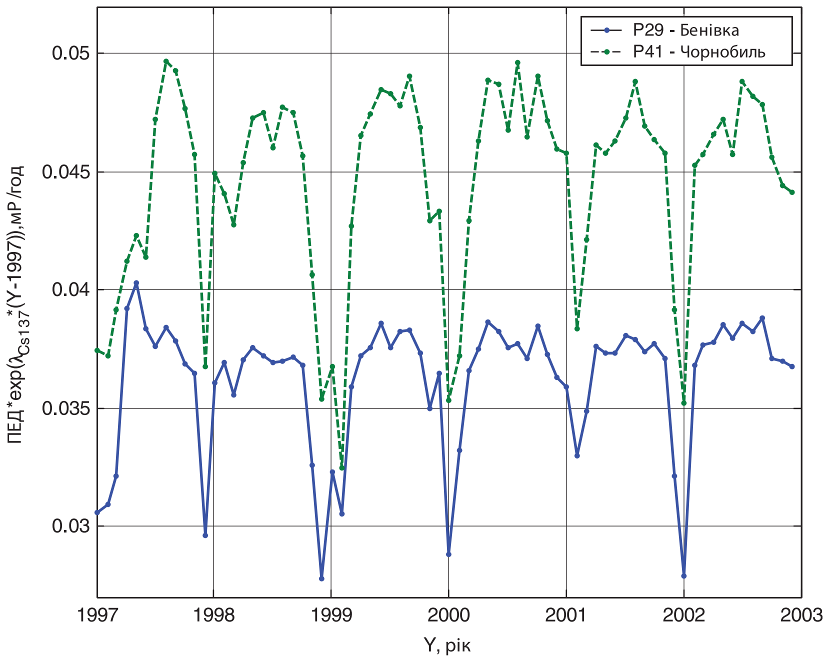

Figure 12.2. Monthly average ^{137}Cs radioactivity of atmospheric particulate matter at two monitoring stations of the Chernobyl Exclusion Zone from 1997 to 2003. P29: Benivka village; P41: Chernobyl; *x*-axis: years; *y*-axis: exposure rate (γ, ^{37}Cs since 1997), mP per year.

Figure 12.2 shows the monthly ambient cesium radioactivity measured at two stations in the SSSIE network: Benivka village (P29) and Chernobyl (P41). The ^{137}Cs radioactivity levels in Chernobyl are about 20–30% higher than those at the Benivka village. The radioactivities at both sites increased several times in the early spring and late fall of each year, corresponding to the periods of most intense burning. The ambient radioactivities at both stations remained relatively stable between 1997 and 2003.

12.5. Long-Range transport of smoke plumes

In addition to being inhaled by humans close to the fires, fine particles emitted from fires can be transported hundreds to thousands of kilometers from large fires. Smoke plume dispersion depends on the vegetation type burned, fire intensity, burned areas, duration of the fires, plume heights, and meteorological conditions. Cropland dominates the landscape in Ukraine, accounting for about 80% of the total area (Fig. 12.3) with mixed forests comprising the other 20%. Vegetation fires are widespread in Ukraine especially during the spring. These fires are often caused by human activities, such as clearing of agricultural residues before plowing the soil in the spring. Figure 12.4 shows the spatial distribution of fires and smoke in Ukraine and neighboring countries on April 16, 2006. Smoke plumes originating from active fires south of Kiev traveled north about 100 km.

The long-range transport of smoke plumes produced by fires in the Chernobyl EZ was observed by the U.S. National Oceanic and Atmospheric Administration's (NOAA) Advanced Very High Resolution Radiometer (AVHRR) satellite on May 8, 2003 (Fig. 12.5). The satellite image showed that the smoke plumes of a spring fire in the EZ reached Kiev, a city with a population of 2.7 million. The accumulation of understory vegetation and downed trees over the past 20 years has increased the probability of crown fires. Large, intense crown fires often

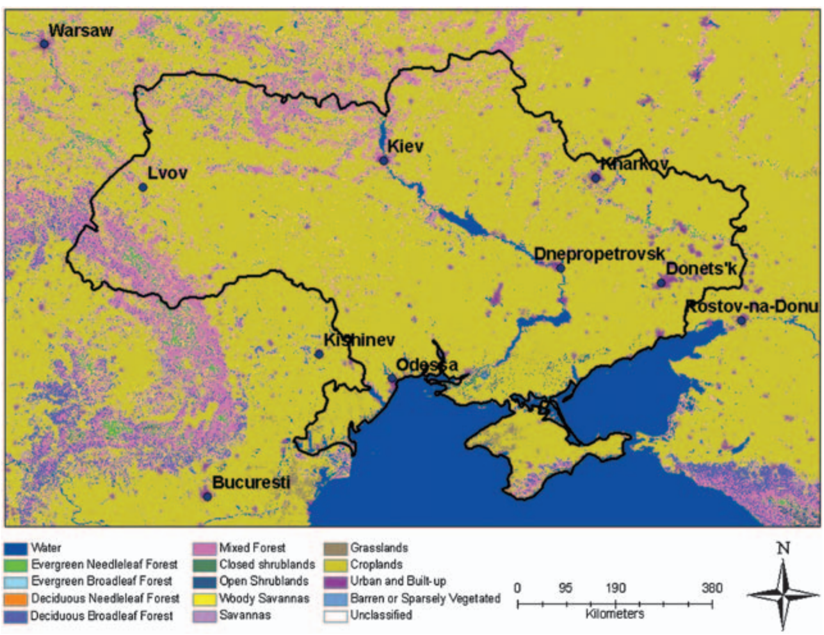

Figure 12.3. Land cover map in Ukraine and neighboring countries (The data are downloaded from NASA's Moderate Resolution Imaging Spectroradiometer (MODIS) MOD12 Land Cover and Land Cover Dynamics Products: www-modis.bu.edu/landcover/userguidelc/intro.html).

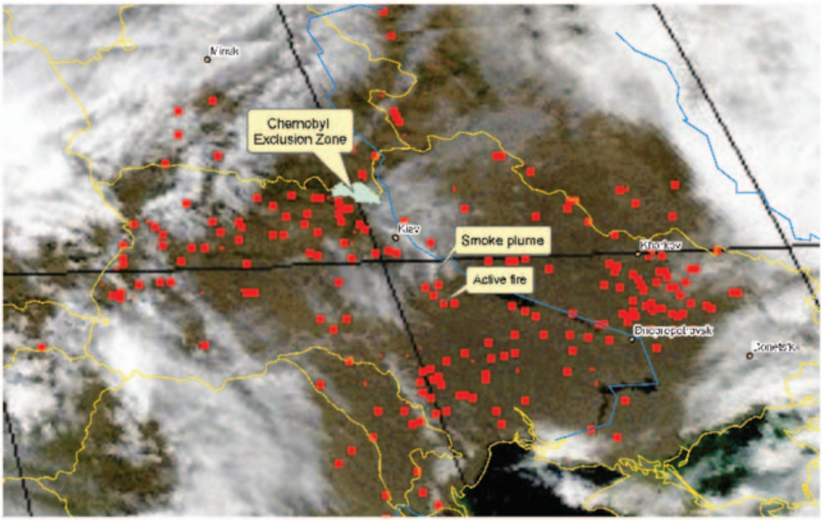

Figure 12.4. The MODIS satellite image of fire locations (red dots) and smoke in Ukraine and its neighboring countries, April 16, 2006.

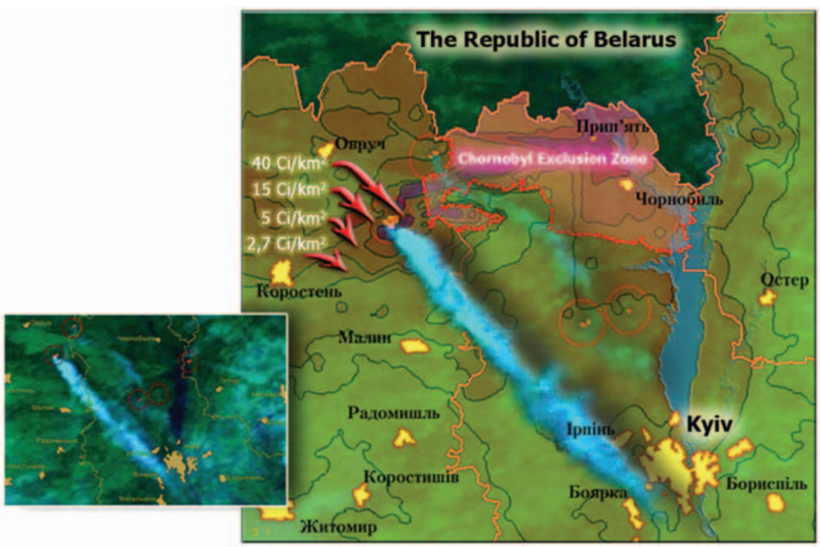

Figure 12.5. The NOAA Advanced Very High Resolution Radiometer (AVHRR) satellite image (small figure) of a smoke plume in western Ukraine, May 8, 2003, overlaid on a land cover map (large picture) (courtesy of the Ukrainian Land and Resource Management Center).

create highly buoyant smoke plumes which penetrate the free troposphere and undergo long-range transport (Fig. 12.5).

The long-range transport of Chernobyl's smoke plumes not only were observed by the satellites but also may be detected by the ground radioisotope monitoring stations in Sweden. During the 1972–1985 period, the monthly ^{137}Cs levels peaked in May, which were caused by the nuclear test fallout in the stratosphere (Kulan, 2006). However, during the 1987–2000 period, the ^{137}Cs levels peaked in April and October, which coincided with the periods of most intense burning in the EZ. The resuspension of mineral dust in Chernobyl may also have contributed to the elevated ^{137}Cs levels (Kulan, 2006).

12.6. Conclusion

The uncontrolled growth of understory vegetation, fallen trees, and the lack of forest management since the accident in 1986 have created conditions favorable for catastrophic fires in the Chernobyl EZ. These megafires are likely to occur under extremely dry and windy conditions, similar to the large fires that occurred in the western U.S. in the past eight years. Smoke plumes from these fires may spread radionuclides across continental Europe, Scandinavia, and Russia. To mitigate the impact of any future catastrophic fires in the EZ, we recommend the following improvements in fire detection and the development and implementation of a real-time smoke and radionuclide dispersion forecasting system.

12.6.1. Real-time fire detection

One of the major difficulties in monitoring and suppressing multiple fires over a large area is obtaining updated fire intelligence in real time. The information is essential for firefighters to locate fires and prioritize deploying firefighting equipment. We propose installing a Moderate Resolution Imaging Spectroradiometer (MODIS) direct broadcast satellite receiving station to monitor the fire locations, burned areas, and fire intensity. The system will complement the existing fire detection network.

The satellite receiving station automatically receives, processes, and archives MODIS data in real time from NASA's Terra and Aqua satellites. Data from the daily MODIS overpasses provide two daytime (13:00 and 14:30 local time) and two nighttime (1:30 and 23:00 local time) snapshots for each location in most of western Russia, continental Europe, and Scandinavia. It takes approximately 40 min to retrieve and process the original MODIS data and generate fire locations at a 1 km × 1 km resolution. The fire products can be posted on the web site shortly after the satellite overpasses, enabling fire managers to access the information online. The MODIS instrument on the Terra and Aqua satellites not only detects fires but also detects smoke plumes with a more accurate spatial resolution than the NOAA AVHRR satellite.

The MODIS system can be used for monitoring the spatial and temporal distribution of fires, smoke, vegetation, and flooding not only in the EZ but also in the entire Ukraine and parts of the neighboring countries.

12.6.2. Forecasting of smoke-radionuclide dispersion

We recommend developing and installing a smoke dispersion forecasting system in Kiev. One such forecasting system currently under development is the Weather Research and Forecasting–Smoke Dispersion model (WRF–SD). The WRF–SD system forecasts the emission, transport, and transformation of atmospheric pollutants from vegetation fires. The WRF–SD modeling system is composed of fire products derived from real-time MODIS satellite data, a fire growth prediction model, the First Order Fire Effects Model (FOFEM) fire emissions model, and the Weather Research and Forecasting model with photochemistry and particulate matter modules. MODIS observations will be used to identify active fire locations and perimeters and measure the growth of burn areas. The MODIS derived fire products are used in conjunction with data on fuel characteristics, pollutant emissions factors categorized by fuel type, and meteorological conditions as input for FOFEM and the fire growth prediction model. FOFEM simulations provide a history of estimated smoke emissions for all wildland fires observed by MODIS in the most recent 24-h period. The fire growth simulations will provide a 48-h forecast of hourly fire growth and smoke emissions for large wildland fires. The daily emission inventories and forecasts of fire behavior and smoke emissions will provide input for WRF–SD. Nationwide 24- to 36-h forecasts of smoke dispersion and pollutant concentrations resulting from active large fires will be generated using WRF–SD.

The accident of the ChNPP has tremendous implications in today's world. The rapid expansion of nuclear energy and the proliferation of nuclear power plants increase the likelihood of future nuclear accidents. The emissions of radionuclides during the accidents will have immediate, catastrophic damages to the environment. However, the fallout of the radionulcides from the accidents, which are deposited on the soil and vegetation, will have significant long-term environmental impacts. Subsequent vegetation fires, which may occur many years after the accidents, will release the radionuclides and potentially disperse the pollutants over a large area.

ACKNOWLEDGMENTS

We thank Dr. Shawn Urbanski at the Fire Sciences Laboratory and two reviewers for constructive comments and suggestions on the manuscript.

REFERENCES

Brasseur, G.P., Orlando, J.J., and Tyndall, G.S. 1999. Atmospheric chemistry and global change. Oxford University Press, New York, 118–119.

Chakrabarty, R.K., Moosmüller, H., Garro, M.A., Arnott, W.P., Walker, J., Susott, R.A., Babbitt, R.E., Wold, C.E., Lincoln, E.N., and Hao, W.M. 2006. Emissions from the laboratory combustion of wildland fuels: Particle morphology and size. J. Geophys. Res. 111, D07204, doi:10.1029/2005JD006659.

Kulan, A. 2006. Seasonal ^{7}Be and ^{137}Cs activities in surface air before and after the Chernobyl event. J. Environ. Radioactivity 90, 140–150.

Yoschenko, V.I., Kashparov, V.A., Protsak, V.P., Lundin, S.M., Levchuk, S.E., Kadygrib, A.M., Zvarich, S.I., Khomutinin, Yu.V., Maloshtan, I.M., Lanshin, V.P., Kovtun, M.V., and Tschiersch, J. 2006a. Resuspension and redistribution of radionuclides during grassland and forest fires in the Chernobyl exclusion zone: Part I. Fire experiments. J. Environ. Radioactivity 86, 143–163.

Yoschenko, V.I., Kashparov, V.A., Levchuk, S.E., Glukhovskiy, A.S., Khomutinin, Yu.V., Protsak, V.P., Lundin, S.M., and Tschiersch, J. 2006b. Resuspension and redistribution of radionuclides during grassland and forest fires in the Chernobyl exclusion zone: Part II. Modeling the transport processes. J. Environ. Radioactivity 86, 260–278.

This page intentionally left blank

Developments in Environmental Science, Volume 8 277
A. Bytnerowicz, M. Arbaugh, A. Riebau and C. Andersen (Editors)

ISSN: 1474-8177/DOI:10.1016/S1474-8177(08)00013-2

Chapter 13

Remote Sensing Applications of Wildland Fire and Air Quality in China

John J. Qu, Xianjun Hao, Yongqiang Liu, Allen R. Riebau, Haoruo Yi and Xianlin Qin*

Abstract

As one of the most populous and geographically largest countries, China faces many problems including industrial growth, economic sustainability, food security, climate change, and air pollution. Interwoven with these challenges, wildland fire is one of the natural hazards facing modern China, especially under a changing climate. From a national perspective, wildland fire information is a fundamental and yet challenging prerequisite for understanding forest ecology and hazards in China. In recent years, China has begun to use remote sensing (RS) as a tool for monitoring regional fire hazards, and to a lesser extent, air quality emissions. With the unique features of global coverage, high-resolution, and continuous operation, RS is able to obtain detailed information of fire occurrence, extent, structure, and temporal variation, together with some related fuel properties. Satellite instruments such as the Advanced Very High-Resolution Radiometer (AVHRR) and the Moderate Resolution Imaging Spectroradiometer (MODIS) have been used in Chinese field experiments and routine monitoring of wildfires and air quality emissions by scientists of the National Satellite Meteorology Center (NSMC) and Chinese Meteorology Agency (CMA). MODIS applications of fire monitoring have also been done by the Chinese Academy of Forestry Sciences. In addition, Landsat measurements have been used for land cover mapping by the Geography Institute, Chinese Academy of Sciences, with land cover being used to determine fuel type and loading and to estimate fire emissions. All of these measurements can be useful for

*Corresponding author: E-mail: jqu@gmu.edu

both forest management and air quality management in China, especially as air quality concerns and forest fires increase under a warming global climate.

13.1. Air quality in China

Air quality in China is illustrative of a set of environmental issues the country must address as coincident factors. In 2002, China was estimated as emitting 13% of the world's carbon dioxide (CO_2) from industrial sources, only 3% less than Western Europe. A report released in 1998 by the World Health Organization (WHO) noted that of the 10 most polluted cities in the world, seven can be found in China. Sulfur dioxide (SO_2) and particulate emissions caused by coal combustion are China's two major air pollutants. These sulfur and nitrogen emissions result in the formation of acid rain, which now falls on about 30% of China's total land area. Industrial boilers and furnaces consume almost half of China's coal and are the largest single point sources of urban air pollution (World Resources Institute, UNEP and World Bank, 1998). Additionally, rapid growth in the number of privately owned vehicles, especially in the larger cities, has increased emissions of nitrogen oxides (NO_x). A 15-year-old government policy to promote the growth of China's domestic car industry has spurred car ownership to staggering levels. China's roads are expected to be clogged with 130 million vehicles in 2020, by which time the country will have surpassed the United States in total car ownership. Nowhere is this more visible than in the national capital. The number of vehicles on Beijing roads soared by nearly one thousand a day in 2005 for a total of nearly 2.6 million (Bezlova, 2006).

China's national legislature, through its model of "cleaner production" and other attempts to reduce air pollution, has significantly altered the Law on the Prevention and Control of Air Pollution (revised in 2002). Although there have been reports of progress (e.g., reductions in total particulate, NO_x, and SO_2 emissions for the country as a whole during the 1990s according to the State Environmental Protection Administration of China or SEPA), China's major cities have been characterized by some of the highest surface concentration levels of criteria air pollutants in the world, with their annual mean ambient levels in these cities usually exceeding the Chinese urban air quality standards for total suspended particles (TSP), SO_2, and NO_x (Raufer et al., 2000). Sixty percent of the cities countrywide exceeded the second-class ambient standard for TSP in 1999, while 28.4% of the cities exceeded the SO_2 secondary standard.

NO_x has become a major pollutant in a number of metropolitan areas, such as Guangzhou, Beijing, and Shanghai, due to vehicular emissions. In 1997, the average annual NO_x concentration in Guangzhou was $140\,\mu g\,m^{-3}$, the highest value in all large cities of China (Raufer et al., 2000). Beijing's annual NO_x concentration was $133\,\mu g\,m^{-3}$, and Shanghai's was $105\,\mu g\,m^{-3}$. Acid deposition is mainly a problem in the southwest parts of China (such as the Sichuan Basin) and in central portions of the country (i.e., around Changsha, Nanchang, and Ganzhou). The strongest acidity of rainwater and the highest frequency of acid deposition occur in these regions. Acid rain is also found in southern China and in the coastal areas, causing serious environmental damage. Amongst the 106 cities with acid rain monitoring systems, 43 had rainfall pH values lower than 5.6 in 1999. The total area affected by acid precipitation is estimated to be approximately 30% of the country's territory. Changsha had the lowest pH value of 3.54, while Yibin, Ganzhou, and Xiamen had annually averaged pH values of rainfall less than 4.5 (Zhang, 1988).

China's air quality management is more difficult when smoke from wildland fire enters areas that experience problems from urban air pollution. In the United States forest fires are a major source of particulate matter, with most fine particulate matter generated each year from a small number of large wildfires (Riebau & Fox, 2006). These fires are mainly due to a very active program of fire suppression in the United States, which extinguishes small- or medium-sized fires. China has also been enacting a program of very active fire suppression. This program, coupled with the location and extent of Chinese forests and other management practices, has ameliorated wildfire smoke air quality issues in China to some extent. As in the United States, Chinese wildland fire suppression activities are unlikely to reduce the number of large fires, which ignite under severe fire weather conditions. There is also potential for China, just as in the United States, to experience significant amounts of fire smoke entering populated areas. Such additions would exacerbate China's air quality problems, if only for relatively short periods. Industrial areas close to large expanses of forest in the northeastern part of the country would be perhaps especially vulnerable to episodic smoke and air pollution episodes. At the present time no studies have been completed to assess either the past impacts or future potential for impacts from wildland fire smoke in China.

13.2. Forests in China

According to an estimate by the United Nations Food and Agriculture Organization (United Nations Food and Agriculture Organization

(UN FAO), 2005) of the United Nations, China has a forest area of 280,170,000 ha (692,315,143 acres). The percentage of Chinese forest cover is about 12% of the nation's area. Altogether, the land assigned to forestry in China includes 115,280,000 ha of rich forest land (rich forests, with a crown shadow rate of above 30%, whereas sparse forests have a crown shadow rate of 10–30%), 17,200,000 ha of sparse forest land, 27,730,000 ha of shrubs, and 119,960,00 ha of desolate mountains and land fit for planting trees. The geographical distribution of China's forests is very uneven, with greatest concentrations in the northeast and southwest. Additionally, there are some subtropical zone and tropical zone forests. The northeast, southwest, and combined subtropical and tropical zones account for 29.9%, 19.6%, and 41%, respectively, of the national forest area. Meanwhile, very few forests exist on the North China plain and the Northwest (altogether 9.6%). In the very arid northwest only 2% of China's forests can be found. The most notably forest-rich area close to mainland China is Taiwan (37%), followed by seven Chinese provinces having coverage above 30%, six provinces above 20%, and thirteen provinces and regions lower than 10%. The provinces with the lowest percentage of forest cover are the Xinjiang province with only 0.7% and in Qinghai province with only 0.3%.

13.3. Climate change and China's natural resources

China faces great threats from a warming and drying climate. It is a paradox for the country that to achieve a higher quality of life for Chinese, the country has been involved in industrial development that is similar to Western nations, which in itself may exacerbate environmental challenges and adversely impact the Chinese population. The Intergovernmental Panel on Climate Change in its recent report has voiced concern over climate change impacts for Asia. They cite potential adverse changes to biodiversity, water resources, deltas and coastal zones, and a potential for increases in forest fires (IPCC, 2001). Regional climate models developed by the UK's Hadley Centre for Climate Prediction and Research have predicted that as global warming events occur, Chinese winters will become warmer and there is a greater likelihood of high summer temperatures and a rise in the number of days of heavy rainfall. Average yearly temperatures could increase as much as 3–4°C. Such changes in climate would almost certainly increase forest fire events in China, especially if evapotranspiration rates increase in forested areas during the wildfire season.

13.4. Fire management in China

The occurrence of forest fires varies from year to year depending on interannual climate variability. Furthermore, the variations of fire occurrence, fire size, and fire severity are closely related to the accumulation of combustible material in the forest. The major portion of forest fire occurrence is concentrated in a small number of Chinese regions called "High Fire Occurrence Regions." The highest number and largest sizes of forest fires occur in five provinces: Heilongjiang, Inner Mongolia, Yunnan, Guangxi, and Guizhou. In these provinces, the number of forest fires accounted for 42.5% of the whole country, and the damaged area accounted for 75% of the area affected by fires in the whole country during the period 1950–1998. Within these provinces and in other forest zones the forest fire distribution is not even. The highest concentration is in more than 100 key counties of 16 key regions. This phenomenon results from the fact that these regions, which have a higher share of forest cover, are exposed to more climatic extremes, including extreme wind events, and are remote with limited access and fire management (prevention and control) facilities. In combination with the complexity of fire origins, the high combustibility of forests, and the difficulty in controlling wildfires, the probability of large forest fire occurrence in these regions is very high.

The number of forest fires is large in forests of the south of China while the damaged forest area is largest in the northeast and Inner Mongolia. Because of the gentle regional topography—featuring a broad geographic trench and with accompanying embankments that link (ecotones) between grassland and forest—and the influence of the monsoon in spring and autumn, forest fires in the northeast and Inner Mongolia spread quickly and over large areas. Due to the different characteristics of these varied forest regions, fire prevention methods and control measures are also different in the South and in the North.

Clearly defined responsibilities of governments at different levels and of the different units in the forest regions are an important aspect of forest fire prevention. Through this system, the fundamental and crucial problems in forest fire prevention have been addressed in recent years, resulting in strengthening of forest fire prevention and a visible reduction of forest fire occurrence and damages. In the period 1960–1987, about 16,000 forest fires damaged an area of 950,000 ha in the entire country, representing a forest damage rate of 8.5%. Compared with these figures, the number of forest fires, the damaged forest area, and the forest damage rate from 1988 to 1998 was reduced by 49%, 98%, and 95.4%, respectively (Figs. 13.1 and 13.2; IFFN, 2002). These reported reductions were after the occurrence of the large fires of 1987 (discussed in

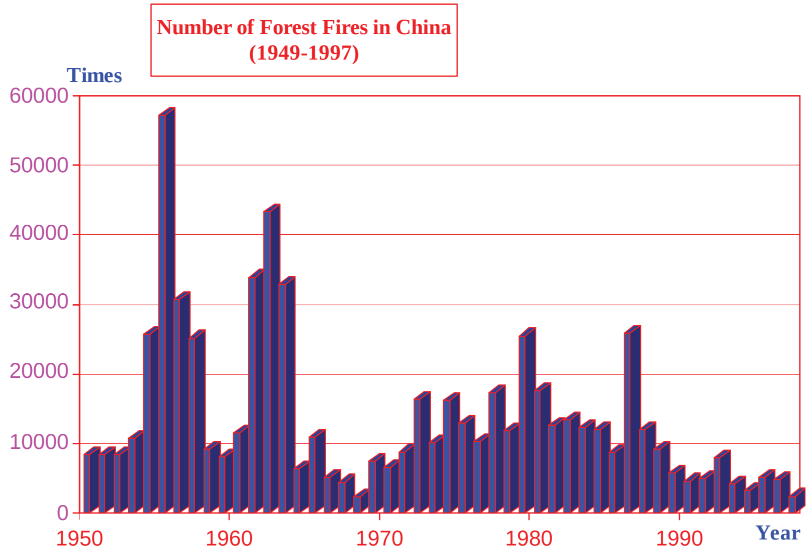

Figure 13.1. Number of forest fires in China have been decreasing over time. (*Source*: IFFN 2002.)

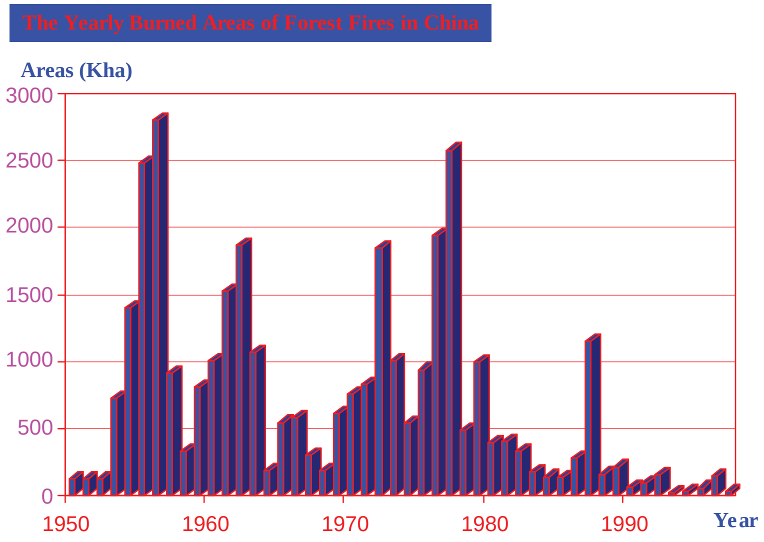

Figure 13.2. The yearly surface burned by wildland fires in China has been decreasing (*Source*: IFFN 2002.)

Section 13.6), and perhaps make fire suppression appear unrealistically successful in China. However, important steps were taken to revise and improve regulations on the use of fire in the agricultural and forestry sectors. Several important laws, decrees, regulations, and stipulations became effective after being passed by the local people's congress and promulgated by the governments. Many villages have developed community regulations and agreements and have strengthened forest fire management at the local level very successfully. Such measures may continue to be effective against smaller, low-intensity fires, but may be much less effective as protective measures during periods of prolonged drought and extreme fire weather conditions.

13.5. Remote sensing and wildland fire in China

Satellite remote sensing (RS) is a new technique for wildfire monitoring and fire danger assessment. Satellite instruments like the Advanced Very High-Resolution Radiometer (AVHRR) and the Moderate Resolution Imaging Spectroradiometer (MODIS) can be used to create global high-resolution products like the Normalized Difference Vegetation Index (NDVI) and Surface Temperature (ST) (Qu et al., 2002), which have been shown to be closely related to fuel moisture status. Thus, RS can overcome some problems facing the traditional fuels-based fire danger estimation techniques, including low spatial resolution and unavailability of meteorological data over parts of forest regions.

RS mapping and characterization of vegetation and fire fuels parameters and datasets were clearly defined as technology goals in strategic documents such as the U.S. National Fire Plan. They have also been required by international fire management and science communities. Applications of satellite RS have been made during many large wildland fires, including monitoring fire lines and total fire smoke. The Wildland Fire Assessment System (WFAS) developed by the USDA Forest Service, became operational in the mid-1990s, and has been providing useful information such as a "greenness" map using AVHRR-NDVI (Burgan et al., 1997).

Satellite RS also has great potential to provide information for calculating seasonal fire danger. The fuel moisture detected by satellite RS is mostly the moisture of live fuel, which predominately represents long-lag moisture (e.g., 1000 h fuel moisture), a determining factor of seasonal fire danger. Thus, it is possible to develop a capacity to assess the seasonal fire danger using RS of fuel moisture and other products. These products are limited by spatial resolution of 1 km or more and thus are generally only representative at meso or synoptic scales (Qu et al., 2003).

The estimation of forest fire danger from satellite RS data is an important research area, with potential for great practical application. Fuel moisture is an important index of fire potential. Over the past decade, research on fire danger estimation from RS data has concentrated on determining fuel moisture. The accurate estimation of fuel moisture using RS data is very difficult, as most of the approaches use proxy variables as indices of fuel moisture. Currently available techniques can be placed into two categories: methods based on the relationship of Land Surface Temperature (LSTs) and the NDVI, and methods based on regression analysis of vegetation indices directly.

As a key research instrument of the NASA Earth Observing System (EOS) missions, the MODIS instrument was launched onboard the NASA Terra and Aqua satellites. It has proven itself as a useful tool for wildland fire and smoke mapping worldwide (Fig. 13.3). Because the MODIS instrument senses the earth's entire surface in 36 spectral bands, it spans from the visible (0.415 μm) to infrared (14.235 μm) spectrum with spatial resolutions of 1 km, and 500 and 250 m at nadir, respectively. One strength of MODIS, especially important to fuel property estimation, is that strong absorbance of water in the middle infrared region (1.3–2.13 μm) makes this band 7 (2.13 μm) most suitable for the estimation of forest fuel moisture content. This band 7 is not included in most satellite systems, suggesting that MODIS should be useful for improving the capacity of applying satellite RS data to more accurately

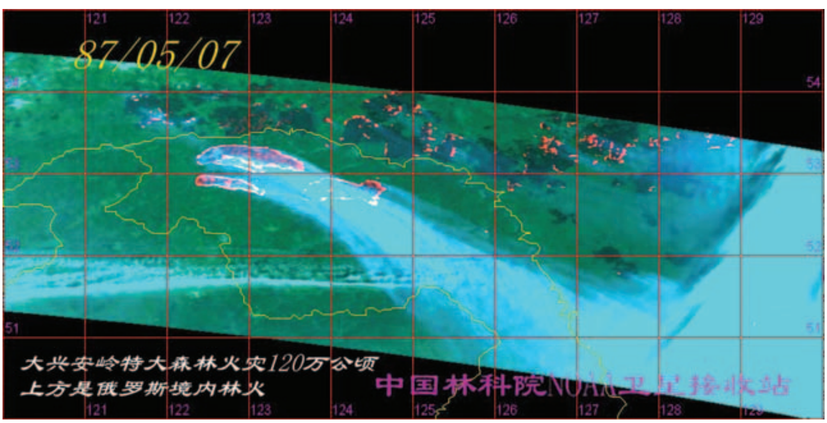

Figure 13.3. NOAA advanced very high-resolution radiometer (AVHRR) image of the black dragon fire taken on May 7, 1987.

estimate fuel moisture content and fire danger indices (Qu et al., 2003; Xinwen et al., 1998). Figure 13.4 shows the Aqua MODIS true color (RGB) image of forest fires around the China-Russia border at 04:20 UTC time. The smoke plumes and clouds can be seen clearly. The false color image shows the burnt areas clearly (Fig. 13.5).

In China, RS of wildland fire has been successfully implemented on a routine basis. This is especially true for fire detection using MODIS. Satellite data has been regarded as a primary information source by many

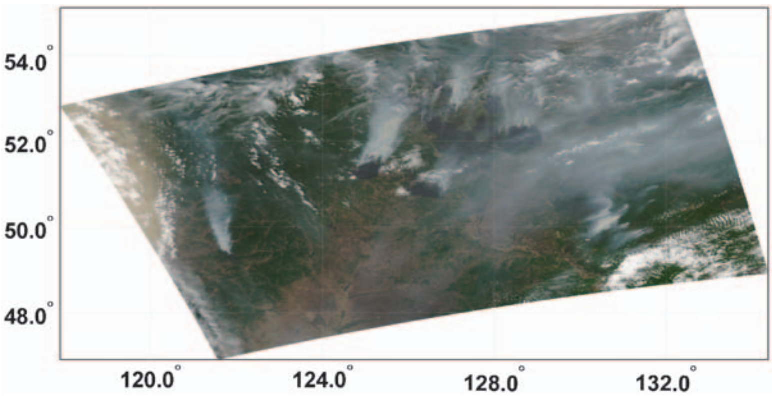

Figure 13.4. Aqua MODIS true color (RGB) image of forest fires around the China–Russia border (05/30/2006 04:20 UTC time). The smoke plumes and clouds can be seen clearly.

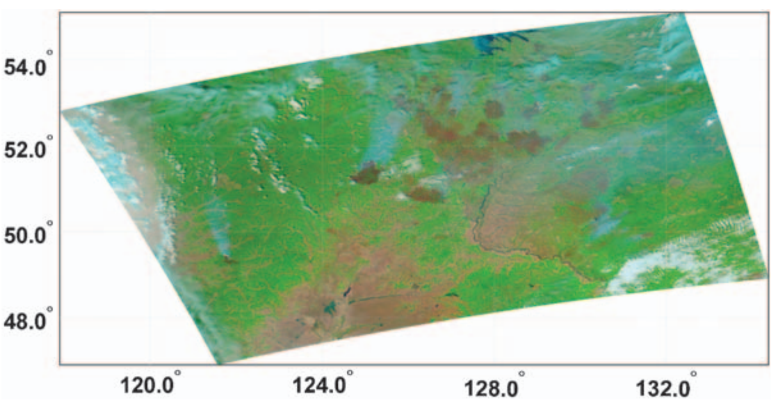

Figure 13.5. Aqua MODIS false color (Band 7, 2, and 1) image of forest fires around the China–Russia border (05/30/2006 04:20 UTC time). The burnt areas can be monitored.

key projects in forestry for the past 20 years; examples of such uses include comprehensive forest RS inventory, monitoring and assessment of forest fire, mapping evaluation of the Yunnan provincial tropical forest in southwestern China, assessing forest ecological impacts, preventing desertification, monitoring insects, and developing innovations over the current national forest resources survey system.

13.6. The black dragon fire

China is often not considered as a country in which large forest fires occur, which has been correct in most years in the recent past. However, this assumption does not hold true for years with extreme climate conditions. In terms of sheer destruction and ecological damage, the fires that swept the Hinggan forests of Manchuria and Siberia in May 1987 (Fig. 13.1) rank as one of the worst environmental disasters of the 20th or any other century (Salisbury, 1989). The fires were more than 10 times the size of the 1986 fires in Yellowstone National Park. Yet, little is known about them outside China and official circles in the Soviet Union. Even among experts, there is only sketchy information on possibly the world's largest forest fire in the past 300 years, a conflagration that blackened an area almost the size of New England (3,000,000 acres of land and killed 220 people).

The Greater Hinggan Forest was the world's largest stand of evergreens, stretching like a green velvet sea approximately 500 miles long and 300 miles wide. It is bisected by the Heilongjiang, or Black Dragon River (known in the West by its Russian name, the Amur), which forms the border between Chinese Manchuria and Soviet Siberia. Before the fires, the Manchurian part of the forest accounted for one-third of China's timber reserves. In 1987, there had been a prolonged period of dry weather, and the danger of fire was high on both sides of the river in the spring. At that time, Chinese fire prevention and detection methods and firefighting resources were primitive by American and Canadian standards. Despite the hazardous conditions, people smoked in the forest, built campfires, and used unsafe logging practices. From natural and accidental causes, a number of fires broke out about the same time in Manchuria and Siberia, quickly consolidating into several large ones.

The Black Dragon Fire had much significance for China's future under a changing climate. The specific weather conditions that allowed the fire to become such a large and intense complex event fit well with climate change scenarios depicted by the United Kingdom's Hadley Climate Center. Recently, even in areas of southern China where firefighting resources are considered good, climate variability has overwhelmed firefighters when fires start. For example, mobilized firefighters were unable to put out a forest fire that was spreading rapidly through the parched timberlands of the Chongqing Municipality on August 31, 2006. More than 4000 people were mobilized to fight the fire that began at 1 pm on a Wednesday in Yakou Village, 40 km northeast of downtown Chongqing. It soon spread to neighboring areas, ravaging 66 ha of forest. The cause of the fire was unclear, but the prolonged drought contributed to its spread. Officials cited a change in weather (rainfall) as the reason the fire was contained at 66 ha. Even with more than 4000 people to fight this fire, they were unable to extinguish it until fire weather conditions allowed. Thus, the Black Dragon Fire is perhaps an example that climate considerations need to be fully integrated into fire management not only in China but also worldwide.

13.7. Conclusions

China values its forest resources and wishes to increase forest cover. Although air pollution is a significant issue for China, at the present time Chinese fire suppression policies and available resources meet most normal fire challenges. By using satellite instruments, effective systems can detect large fires and assist in fire danger predictions. Climate change predictions for China suggest that wildland fires will increase in frequency, size, and intensity. Should this occur, the wildland fire smoke, especially in the north of China, may become a significant issue.

Thus, due to this predicted climate change in China, fire suppression as a management tool may itself need reassessment. In the United States, past policies of fire suppression have been postulated to have caused massive fuels build-up in forests, particularly in the western states. Recent evidence has shown, however, that due to a period of relative calm from drought, such suppression strategies were more successful than they perhaps might have been without the coincidence of this calm period (Westerling et al., 2006). Currently, China has entered into a fire suppression policy that parallels the policies employed in the 1950s and 1960s in the U.S. Climate variability and change, interacting with exclusion of fire from ecosystems, may prove to be as interesting a challenge for fire and air quality management in China as they are for the United States.

REFERENCES

Bezlova, A. 2006. China: Race to improve air quality for the 2008 Olympics. Inter Press News Agency.

Burgan, R.E., Andrews, P.L., Bradshaw, L.S., Chase, C.H., Hartford, R.A., and Latham, D.J. 1997. WFAS: Wildland fire assessment system. Fire Manag. Notes 57(2), 14–17.

International Forest Fire News (IFFN). 2002. Fire situation in china. IFFN 26, 9–14.

IPCC. 2001. Climate change 2001: Impact, adaptation and vulnerability. Cambridge University Press, Cambridge, UK.

Qu, J.J., Serafino, G., Teng, B., Ouzounov, D., Pollack, N., and Chiu, L. 2002. Responding to the challenge of producing and distributing MODIS data at the NASA/GES DISC via the remote sensing information partners (RSIP) program, Proceeding of IGARSS (CD-ROM publication).

Qu, J.J., Kafatos, M., Hao, X., Riebau, A.R., and Liu, Y. 2003. Estimating of fire danger potential using MODIS measurements. Proceedings of ISPRS (CD-ROM Publication).

Raufer, R., Zhuang, Y.H., and Tang, H., eds. 2000. Urban air pollution control in china: A sector review report. United Nations Development Program (UNDP).

Riebau, A.R., and Fox, D.G. 2006. Fire in forests, rangelands, and agricultural systems. World Meteorology Organization WMO/TD. 1313 Geneva.

Salisbury, H.E. 1989. The great black dragon fire: A Chinese inferno. Little, Brown & Company, Boston.

United Nations Food and Agriculture Organization (UN FAO). 2005. State of the world's forests. Rome. Available at http://www.fao.org/docrep/007/y5574e/y5574e00.htm

Westerling, A.L., Hidalgo, H.G., Cayan, D.R., and Swetnam, T.W. 2006. Warming and earlier spring increases western U.S. forest wildfire activity. Science DOI: 10.1126/science. 1128834.

World Resources Institute, UNEP and World Bank. 1998. World resources 1998–99: Environmental change and human health.

Xinwen, Z., Yuan, C., Green, R.O., and Tong, Q. 1998. Application of remote sensing in chinese forestry, hyperspectral remote sensing and application. Conference of China Optics & Optoelectronic Manufacturers Association. 19981988, 3502, 134–141. Beijing.

Zhang, H. 1988. Past, present and future development tendency of the forest resources in china. J. Nat. Resour. 3(3), 201–214.

Developments in Environmental Science, Volume 8 289
A. Bytnerowicz, M. Arbaugh, A. Riebau and C. Andersen (Editors)

ISSN: 1474-8177/DOI:10.1016/S1474-8177(08)00014-4

Chapter 14

Smoke from Wildfires and Prescribed Burning in Australia: Effects on Human Health and Ecosystems

Tina Bell and Mark Adams*

Abstract

Much of Australia is seasonally hot and dry, and fuel beds can become very flammable. Biomass burning ranges from annual savanna fires in the north to sporadic but extensive forest fires in the south. In addition, prescribed burning (the controlled application of fire) is being used more frequently as a means of reducing fuel loads, for maintenance of plant and animal biodiversity and in forestry practices. Despite this and in comparison to the Northern Hemisphere, there are few Australian studies of the production or composition of smoke from biomass burning. There is also relatively minimal Australian literature detailing the effect of wildfire smoke on human health and flora and fauna. Most of the literature dealing with smoke and human health issues in Australia outline epidemiological studies that document the incidence of hospital visits and admissions during wildfire events. The causal link between smoke and respiratory illness is yet to be established. The bulk of the publications dealing with ecological effects of smoke are concerned with germination of seed, with little information available on the direct effects of components of smoke on the physiology and biochemistry of plants, animals, invertebrates, or microorganisms. We will outline the knowledge of emissions and effects of smoke from prescribed and wildland fire in Australia on human health and the environment and will indicate potential areas for future research. In addition, a large proportion of the vegetation of Australia is composed of forests dominated by native species of *Eucalyptus* and *Acacia*, while large expanses of plantations are dominated by

*Corresponding author: E-mail: tlbell@unimelb.edu.au

single species of *Eucalyptus*, and the production of volatile organic compounds (VOCs) by such vegetation is substantial. Thus, we will also outline an emerging research area in which the links among the production of VOCs by native Australian species, environmental conditions, and VOCs found in smoke produced from burning native vegetation are explored.

14.1. Introduction

Australia is a fire-prone continent primarily because of increased aridity during the Pleistocene (1.8 million to 10,000 years BP). As Australian ecosystems became more sclerophyllous, fire became more frequent and accelerated the change in biota (Barlow, 1981). With the onset of human occupation 50,000 years BP, a wave of anthropomorphic burning followed and played a major role in altering the distributions of sclerophyll forests and assuring the dominance of *Eucalyptus* and *Acacia* in southern Australia (Bowman, 1998). Today, wildfires or bushfires have become more frequent and may be started naturally, accidentally, or intentionally. Controlled burning for fuel-reduction or biodiversity outcomes has also increased. An average area of 46.8 million hectares has been burnt annually during the period 1997–2003, and this area includes both planned and unplanned fires (Ellis et al., 2004). The need for specific Australian research into the effect of smoke on human health and ecosystems from both these types of fires has been recognized with the recent formation of targeted projects within a federally funded cooperative research center. Firefighter health and safety is also of considerable importance in Australia and has been funded under the same research scheme. Other consequences of smoke such as impairment of visibility or contribution to regional haze, while important to understand, do not have such a high priority for national study and will only be briefly commented on in this review.

This chapter reviews the body of knowledge concerning smoke from vegetation fires in Australia. The current state of knowledge of the effects of smoke on human health in Australian communities will be discussed briefly before turning to the effects of smoke on biota. Particular attention will be given to the production and effect of volatile organic compounds (VOCs) in smoke, as this is the current research interest of our research group. The natural production of large amounts of VOCs by native Australian vegetation will be described and used as a basis for tailoring our future studies of smoke composition.

14.2. The nature of smoke from vegetation fires

The production of smoke through the combustion of vegetation (also referred to here as biomass burning) is one of the most common of all chemical reactions, but it may well be the least understood (Radojevic, 2003). Smoke is a natural by-product of an integral natural process, but it is more often than not viewed and reported in a negative manner. Smoke, whether resulting from consumption of wood for energy, slash-and-burn agricultural practices, prescribed burning activities or wildfires, contains a complex mixture of the visible products of burning (particulates and water vapor), and primary and secondary gaseous products, many of which are air pollutants or greenhouse gases (Ward, 1999).

Components of smoke include gaseous aerosols, such as carbon monoxide (CO) and carbon dioxide (CO_2), methane (CH_4) and ammonia (NH_3), oxides of nitrogen (NO_X as nitrous oxide [NO] and nitrogen dioxide [NO_2]), sulfur dioxide (SO_2), VOCs, and polycyclic aromatic (or polynuclear) hydrocarbons (PAHs; Crutzen & Andreae, 1990; McKenzie et al., 1994; Ward, 1999). Smoke also includes aerosols that are stable solid or liquid suspensions and may vary in concentration, composition, and size distribution. Aerosols may also be formed from gaseous precursors by a variety of oxidation pathways (Koutrakis & Sioutas, 1996). As an indication of the complexity of emissions in biomass smoke, McKenzie et al. (1994) identified 26 oxygenated organic compounds in the condensable fraction of smoke from smouldering sapwood of ponderosa pine (*Pinus ponderosa*), and over 70 different compounds were listed by Andreae and Merlet (2001) as being produced by burning of various types of vegetation.

The composition and quantity of smoke produced during vegetation burning will differ depending on the chemistry and moisture content of the fuel, the amount and arrangement of fuel layers, and on the behavior of the fire and weather conditions (Ward, 1990; Ward & Hardy, 1991). For example, fires of low intensity (low heat and light emissions) tend to produce more particulate emissions than fires of higher intensities (high heat and light emissions), while smouldering (flameless) combustion produces more CO, NH_3, and particulates than flaming combustion (Ward, 1999). Different types and amounts of smoke can even be produced simultaneously within a single fire; for example, heading fires generally produce two to three times more emissions than backing fires (Ward, 1990). Fine fuels with a high moisture content will encourage smouldering, while drier fuels will produce flaming combustion (Lobert & Warnatz, 1993). Brushy vegetation with highly dissected leaves and branches produces more smoke per weight of fuel than non-brushy vegetation or dense wood (Lobert & Warnatz, 1993; Ward & Hardy, 1991). Fires in grassy savannah ecosystems may result in most of the vegetation being consumed in the flaming process, while in ecosystems with large amounts of peat, rotten logs, and deep duff, the majority of the biomass is burnt during smouldering combustion when the moisture content is low (Ward, 1999). Moisture content controls the amount of fuel consumed in a fire and has been used as a means of managing smoke production from larger logs and duff (Hardy et al., 2001). Carbon monoxide, methyl chloride, methyl bromide, and methyl iodide, together with amines and nitriles are formed predominantly in the smouldering stage of a fire, while NO_X and molecular N_2 are released during flaming combustion (Shirai et al., 2003). Volatile organic hydrocarbons are vaporized from fuels early in the combustion process and at later stages, as lignin and cellulose are decomposed through pyrolysis (Ward & Hardy, 1991). Smouldering combustion produces greater levels of VOCs than flaming combustion (Miranda et al., 2005). Ward (1990) and Lobert and Warnatz (1993) both describe the combustion process in relation to the smoke produced, and Gao et al. (2003) provide an excellent description of the basic chemistry involved.

Visibility is impaired when particulate matter (PM) and gases in the atmosphere absorb and scatter incoming radiation and reflect light (Garcia-Nieto, 2002; Malm, 1999). PM less than 2.5 μm in diameter has the greatest effect on visibility and radiation transfer and can act as condensation nuclei for fog formation (Ward & Hardy, 1991). Smoke from wildfires and prescribed burns and annual agricultural or forestry burning can produce a haze that may last for several days or months (Legg & Laumonier, 1999; Nichol, 1997; Robock, 1991). In much of Australia, prevailing winds are often unpredictable and capital cities and larger towns are occasionally covered in a haze of smoke (Packham & Vines, 1978; Vines et al., 1971). For example, smoke from the extensive wildfires in 1939 was observed in New Zealand several days later as it was blown eastward (Vines et al., 1971), and this was certainly the case during bushfires in New South Wales and the ACT in 2001–2002 and in Victoria in 2003.

Much of the early information relating to the general composition of smoke comes from studies of industrial emissions, tobacco smoke, residential combustion, and burning of biomass under controlled laboratory conditions. However, an increasing number of investigations of smoke emissions from wildfires and other types of vegetation fires have been published in recent years. Much of this research has been conducted in southern Africa where annual burning of large quantities of biomass from tropical and savannah ecosystems is common practice

(Scholes et al., 1996). Many more examples are from the United States where a great deal of federal funding has been provided for fire research, particularly in response to a recent increase in the number of wildfires and greater use of prescribed burning. In comparison, investigation of the smoke from biomass burning in Australia has received only moderate research attention. Regardless of location, most of the studies relating to composition of smoke from biomass burning have been concerned with the measurement of CO_2 and CO, as well as NO_X, O_3, and trace gases. Much less research attention has been paid to measurement of H_2, sulfides, VOCs, and PAHs. The literature suggests that continued and more comprehensive analyses of the compounds found in smoke from biomass burning is needed to advance the predictive capacity of smoke behavior and to determine the impacts of smoke (Sandberg et al., 2002).

14.3. Estimates of wildfire smoke emissions

Estimates of gaseous emissions from vegetation fires are largely constrained to the last 25 years with evidence emerging for long-range transport of smoke from large-scale slash burning and wildfires (Andreae & Merlet, 2001; Delmas et al., 1995). Severe air pollution caused by fires in Indonesia, the Philippines, and Brazil in 1997–1998 (bin Abas et al., 2004; Heil & Goldammer, 2001) and more recently in Australia have added to this increased profile (Simmonds et al., 2005). The demand for such information is increasing due to the following:

- Accountability by governments and companies for greenhouse gas emissions
- Increased capability for modelling of biogeochemistry, atmospheric processes, and global climate change
- Identification by health authorities of sources of air pollution affecting human health (Global Emissions Inventory Activity, 2002)
- Increased regional haze and impairment of visibility.

A number of large-scale, coordinated biomass burning experiments has allowed characterization of emissions from a range of vegetation types around the world (Andreae & Merlet, 2001; Delmas et al., 1995). Methods adopted in campaigns such as these and in other experimental work, were reviewed extensively by Ward and Radke (1993) and Delmas et al. (1995). Models of emissions from biomass burning using remote sensing data were recently reviewed by Palacios-Orueta et al. (2005).

Radke (1989) estimated that the worldwide total of biomass consumed by burning each year is 100,000 Tg (Teragram = 10^{12} g).

Table 14.1. Total annual worldwide emissions from all sources compared to emissions from burning biomass[a]

	Species	Worldwide (Tg)[b]	Biomass burning (Tg)
Gases	CO	600–1300 C	120–510 C
	CH_4	400–600 C	11–53 C
	NO	25–60 N	2.1–5.5 N
	HCN, CH_3CN	>0.4 N	0.5–1.7 N
	H_2	~36	5–16
	CH_3Cl	~2	0.5–2
	COS	0.6–1.5 S	0.04–0.20 S
Particulates	Organic C	~180	24–102
	Elemental C	20–30	6.4–28

[a]Data from Crutzen and Carmichael 1993.
[b]Teragram = 10^{12} g.

Gaseous emissions from burning of this vegetation represent only a small fraction of total emissions from all sources (Table 14.1). Other estimates indicate that 3800–4300 Tg of carbon (C) is released annually to the atmosphere from vegetation fires (Andreae, 1991; Andreae & Merlet, 2001), including 20,000–33,000 Tg of C as CO_2 (Seiler & Crutzen, 1980). In Australia, estimates of gross release of C from vegetation fires range from 80 to 250 Tg based on estimates of the area burnt that range from 40 to 130×10^6 ha (Cheney et al., 1980). In a low fire year (1992) in the Northern Territory, almost 30 Tg of biomass was burnt resulting in emission of 11.3 Tg of CO_2, 1.0 Tg of CO, 5.2×10^{-3} Tg of PM, and 26.1×10^{-3} Tg of NO_X (Beringer et al., 1995). According to the Darwin Air Emission Inventory (2001), wildfires in the same area caused 94% of annual emissions of PM, and some 83% of that of benzene, 78% of CO, and 46% of VOCs. In contrast, in southern Western Australia, wildfires caused only 3% of annual emissions of PM, no gaseous benzene, 39% of CO and only 3% of VOCs (Department of Environmental Protection, 2003). Differences among topography, climate, burning patterns, and fuel types make a significant difference to gaseous and particulate emissions from vegetation fires in Australia.

14.4. Smoke from vegetation fires and effects on human health

Smoke from any source is known to have significant deleterious effects on human health, particularly in children and the elderly and people with poor respiratory function (World Health Organisation, 1999). Much of the current knowledge about the impact of smoke on human health is derived from studies of tobacco smoke from cigarettes, smoke from wood fires and ovens ("indoor biomass smoke") and industrial smoke in densely populated cities (Larson & Koenig, 1994; World Health Organisation, 1999), rather than smoke from vegetation fires. In these studies, exposure to smoke is generally investigated at known concentrations and for a specified duration. In contrast, wildfires and prescribed burning expose humans to high levels of smoke episodically and only for short periods of time (Breysse, 1984; Pinto & Grant, 1999). In Australia, it has been recognized that emissions from both woodsmoke and smoke from bushfires or fuel-reduction burns are generally unknown and need to be monitored and assessed (Lewis & Corbett, 2002; Manins et al., 2001; Sim, 2002).

Smoke contains toxic compounds of both a gaseous and particulate nature, and while the effects of gas phase toxicants are of concern, most of the deleterious effects on human health are from the inhaled particulate phase (Schollnberger et al., 2002; Spengler & Wilson, 1996). Determining the effects of particulates is not straightforward, since it is the gaseous compounds, particularly VOCs and PAHs adsorbed onto the surfaces of PM that have the greatest effect on respiratory health (Dost, 1991). The composition of chemicals on the surface of PM will depend on the conditions under which they are generated (Hueglin et al., 1997; Malilay, 1999).

PM is generally classified by aerodynamic diameter, since this parameter governs the transport and gravitational settling of particles from the air and the deposition within the respiratory system. Smaller particles are deposited further into the lungs; therefore, in health studies a description of particle size is particularly important in determining exposure and human dose. Most of the PM produced by biomass burning has diameters less than 0.1 μm or between 0.1 and 2.5 μm (Phuleria et al., 2005; Schollnberger et al., 2002); however, ambient air quality standards were originally set to quantify PM with aerodynamic diameter equal to or less than 10 μm (PM_{10}; e.g., Pope et al., 1991). Annual average exposure to PM_{10} in the United States is recommended to be less than $50\,\mu m\,m^{-3}$ with a maximum 24-hour standard period set at $150\,\mu m\,m^{-3}$ (United States Environment Protection Agency, 1999). It is only relatively recently (July 1997) that guidelines determining exposure to finer PM ($PM_{2.5}$) have been established (Brauer, 1999), with an annual average limit of $15\,\mu m\,m^{-3}$ and a maximum 24-hour standard period set at $65\,\mu m\,m^{-3}$.

In Australia, health guidelines have taken even longer to be formulated, with air quality standards for PM_{10} only endorsed in June 1998. The Australian limits of exposure to PM_{10} are lower ($50\,\mu m\,m^{-3}$

within a 24-hour period) than that in the United States; however, there is an allowance for exceeding this limit for up to 5 days per year to allow for smoke emissions from bushfires (Australian National Environment Protection Council, 1998). The national Australian guidelines for exposure to $PM_{2.5}$ have recently been amended (July 2003), with data collection taking place until 2005 to facilitate a review of the Advisory Reporting Standards (Australian National Environment Protection Council, 2003). Maximum limits of exposure to $PM_{2.5}$ have been set at $25\,\mu m\,m^{-3}$ within a 24-hour period and $8\,\mu m\,m^{-3}$ over the course of a year.

Gaseous components of vegetation smoke such as SO_2, CO, NO_X, O_3, formaldehyde, acrolein (C_3H_4O), and benzene also cause health problems in humans. For example, SO_2 is a colorless gas that is readily soluble in water vapor forming sulfuric acid. Long-term exposure of animals to SO_2 produces damage to airways similar to chronic bronchitis in humans and the effects may be enhanced by simultaneous exposure to ultra-fine particles (World Health Organisation, 2000). Prolonged exposure results in a reduction in lung volume and capacity for gaseous diffusion. Another example is formic acid, which is one of the most abundant VOCs emitted from burning biomass and is produced when formaldehyde is oxidized in a moist environment or when low concentrations of oxygen are coupled with high concentrations of formaldehyde (Ciccioli et al., 2001). Formaldehyde is normally present in the atmosphere at concentrations of between 4 and $20\,\mu g\,m^{-3}$ depending on location of sampling and proximity to urban sources. Dost (1991) has reviewed the formation and toxicology of formic acid in detail. It can cause irritation to the nose, eyes and throat at concentrations of $100–3000\,\mu g\,m^{-3}$, with damage to cells occurring through exposure at this concentration for longer periods of time or at greater concentrations ($10{,}000–20{,}000\,\mu g\,m^{-3}$). The threshold concentration of formic acid for irritation is unknown but is thought to be higher than for formaldehyde. Acrolein is a more potent irritant than formaldehyde and can effect respiratory function at concentrations as low as $100\,\mu g\,m^{-3}$ (Ward, 1999) but is released in woodsmoke in much smaller quantities (Dost, 1991).

Worldwide, wildfires are becoming more prevalent and prescribed burning is being used more frequently as a means of reducing fuel loads. In addition, air quality regulations are becoming stricter, more people are living in the interface between urban and rural areas, and the general public is becoming less tolerant of air contamination (Sandberg et al., 2002). Despite this, the effects of smoke from biomass burning on human health at regional or global scales are unknown (Ward, 1999). There is a relatively large pool of information regarding the effect of smoke on firefighter health and safety (e.g., Brandt-Rauf et al., 1988; Mustajbegovic et al., 2001; Reinhardt & Ottmar, 1997; Slaughter et al., 2004), but little long-term health effects studies have been done in regard to firefighter exposure (Booze et al., 2004). There is a distinct lack of studies concerning the production of smoke at the "ground level" and the impact this smoke may have on localized human populations. Brauer (1999) highlights this inadequacy by recommending further studies on health impacts of large-scale fire-related episodes of air pollution by using standardized study protocols and over a range of locations.

The association between respiratory impairment and exposure of the general public to smoke from wildfires or prescribed burning has been noted in a number of epidemiological studies, but a causal link is yet to be established. For example, smoke from the 1997–1998 fires in Indonesia affected air quality (Aditama, 2000) and resulted in a significant increase in the number of people requiring clinic visits or hospital admission for smoke-related illnesses, and this has been reported as such in some studies (Phonboon et al., 1999), but not in others (Emmanuel, 2000). In the United States, smoke from large forest fires resulted in increased hospital visits in at least two studies (Duclos et al., 1990; Mott et al., 2002). Similarly, increased levels of particulates (PM_{10}) in smoke from biomass burning in northern Australia caused an increase in hospital visits or use of medication for asthma (Chen et al., 2006; Johnston et al., 2002) but not after a large wildfire event in New South Wales (Smith et al., 1996). A fourth Australian study did not find any reduction in lung function in symptomatic children during the same fires (Jalaludin et al., 2000). In comparison, exposure to high levels of particulates in anthropogenic air pollution is more strongly linked to respiratory illness and reduced lung function (Vedal et al., 1998), and exposure to smoke in indoor air generated from cooking and heating has been linked to respiratory disease and poor lung function (Brauer, 1999; Eisner et al., 2002; Larson & Koenig, 1994). These studies relate to exposure to particulates at very high levels (1000–2000 $\mu g\, m^{-3}$) for long periods of time (20 years or more) so comparisons with exposure to smoke from wildfires or prescribed burns are neither straightforward nor particularly valid.

14.5. Effects of smoke on Australian ecosystems

There is a small body of literature relating smoke from biomass burning to plant functioning and even less dealing with fauna (see Whelan, 1995). The literature concerning fauna reports of survival of mice in burrows with adequate ventilation or death of animals due to suffocation from smoke. There are no studies on the toxicology of smoke from biomass burning on any form of native fauna. The bulk of Australian publications are concerned with the effect of smoke on germination of seed, with little information available on the direct effects of smoke from biomass burning on plant or animal physiology or biochemistry. In contrast, the effect of air pollution (as opposed to vegetation smoke) on whole ecosystems, particularly vegetation, has long been noted and is a major topic of research worldwide. Thus, there are many books and review articles dealing with the effects of air pollution, and this topic is the subject of regular international symposia. Because many of the reactive chemicals found in air pollution are also common in smoke from vegetation fires, the literature dealing with air pollution is a potential source of information. However, several failings can be levelled at the majority of these pollution studies when considered in the context of the effects of smoke. These inadequacies are discussed below.

The first, a more general criticism, is that plant responses to air pollution are generally measured using seedlings and saplings of target species, with only a few extrapolations to mature field-grown trees (Bytnerowicz, 1996). Another general criticism is that many of the pollution studies are done in the laboratory under carefully controlled conditions, whereas pollutants in the free atmosphere (including those in smoke) are dynamic and can vary in concentration over a great range of time scales (Cape & Unsworth, 1988). A third failing is that many of the pollution studies have been from mesophytic or tropical environments and are therefore generally inappropriate for predicting the response of sclerophyllous vegetation from xerophytic communities (Wilson, 1995). A useful exception is the body of air pollution literature relating to *Pinus ponderosa*, *P. radiata*, and *P. halepensis*, species which are typically associated with fire-prone mediterranean climates (e.g., Momen et al., 2002; Takemoto et al., 2001).

A final inadequacy we might note is that air pollution studies are mostly concerned with long-term exposure to air pollution (months) whereas exposure to smoke from biomass burning is episodic and transitory (hours to days, occasionally weeks). In addition, the effects of the gaseous and particulate components of air pollution on plant growth and development are investigated at concentrations two to three times ambient, whereas this is generally not a realistic situation for vegetation fires. Despite these problems, the synthesis presented here draws heavily on studies of air pollution, as these often provide the only guide to what might be expected from exposure of flora and fauna to smoke from biomass burning. Similarly, the chemico-physical influences of smoke, such as high temperatures, low light and high vapor pressure deficit, are poorly studied, and information must be obtained from related fields.

The influence of air pollution on plants is a complex subject and dependent on the interactions of concentrations and types of pollutants involved and on biochemical and physiological properties of the vegetation (Fig. 14.1; Bytnerowicz, 1996). By extrapolation, the effect of smoke from biomass burning on vegetation must be equally complex. Unfortunately, much of the biochemistry involved in the interaction of plant tissues with pollution is not yet fully elucidated (Bytnerowicz, 2002; Polle, 1998), and little, if anything, is known about the biochemical reactions of smoke emissions in plant tissues. Effects of air pollution (and therefore smoke) on vegetation can be at cellular, whole plant, species, and ecosystem levels and can have both positive and negative effects on cells (Fig. 14.1; Bytnerowicz, 1996; Heck, 1973; Kozlowski, 1980).

As with general air pollution, smoke may impinge on plant organs (leaves, stems, trunks) and on soil surfaces. There is equal opportunity for smoke to promote cell growth as there is for it to be detrimental by causing cell injury or death (Fig. 14.1). Growth of plants would certainly be promoted if nutrients such as ammonium and nitrate were deposited or washed from a smoky atmosphere to soil surfaces in the course of a wildfire. However, reduced light conditions and lower vapor pressure deficit may temporarily alter the capacity for photosynthesis (environmental level effects, Fig. 14.1). However, unlike air pollution, separation of the effects of heat from fire from the effects of the smoke produced is a difficult task. As suggested earlier, air pollution is relatively long-lasting, whereas smoke from biomass burning is fairly transitory, and the effects of smoke from vegetation fires are likely to be short. Biotic factors such as mycorrhizas, pathogens, insects, competition, N_2-fixation, and genetic variability, and abiotic factors such as humidity, temperature, radiation (light and UV-B), wind, CO_2, water and nutrient availability, and soil type and condition can also interact with vegetation to modify physiological responses (Bytnerowicz, 1996; Krupa & Manning, 1988). The interaction of smoke from vegetation fires with this list of factors remains unclear.

14.6. Types of deposition

Air pollutants, including those from biomass burning, can reach plant and soil surfaces as PM and can enter through cuticular surfaces or stomata as gases (both often referred to as dry deposition) or dissolved in rain, snow, hail or fog (wet deposition; Bytnerowicz & Grulke, 1992;

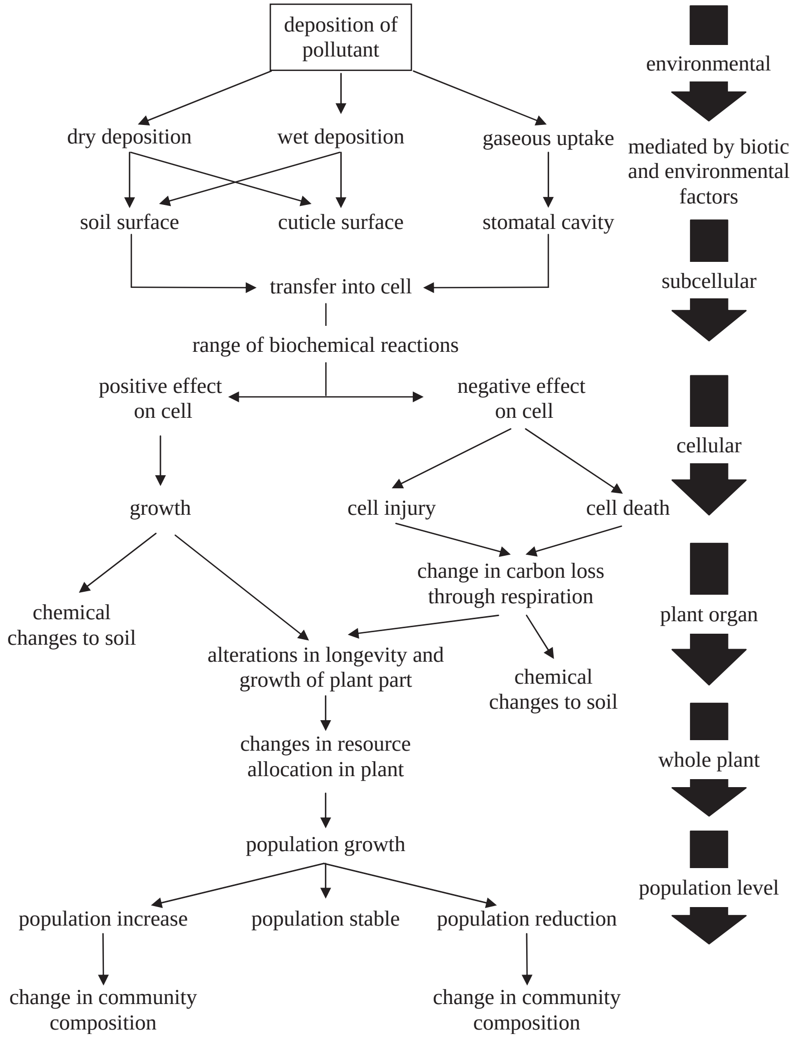

Figure 14.1. Deposition of air pollutants and the effects on plants at the ecosystem, individual, and cellular organizational levels. The range of biochemical reactions includes effects on enzymes, changes to metabolic pathways and cellular constituents, and alterations in the genetic code by transcription and translation. (Redrawn from Bytnerowicz, 1996; Heck, 1973; Kozlowski, 1980.)

Crutzen & Andreae, 1990; Grantz et al., 2003). These pathways are indicated in Fig. 14.1. Occult deposition is intermediate between wet and dry deposition and refers to deposition of small water droplets in fog or interception of cloud water at high altitudes (Cape & Unsworth, 1988). Logically, dry deposition of pollutants on vegetation and soil surfaces dominates in low rainfall regions, particularly during dry periods, and wet deposition dominates in more humid and mountainous regions (Cape & Unsworth, 1988; Crutzen & Andreae, 1990).

The type and location of deposition of pollutants on plants will cause different types and extent of interactions (Bytnerowicz & Grulke, 1992). For example, stomata might be expected to be the main point of entry for gaseous pollutants (Fig. 14.1), so regulation of the opening and closing of stomata will play a key role in determining plant sensitivity (Darrall, 1989). The molecular weight and permeability of a gas will determine how well it penetrates into plant tissue (Lendzian & Kerstiens, 1991). At the leaf surface there is generally little active uptake or exclusion of substances, including pollutants, but passive movement of solutes will be dependent on the physical and chemical nature of the leaf surface (Cape & Unsworth, 1988). Once water droplets are in contact with the leaf surface, organic and inorganic ions may diffuse from solution into the leaf (e.g., NO_3^- and NH_4^+) or are leached from within cells (e.g., SO_4^{-2}). The presence of epicuticular wax, trichomes, and hairs provide a barrier for water adhesion and wet deposition and consequently for solute transfer. Consequently, the morphological and anatomical adaptations of fire-prone, sclerophyllous vegetation are likely to confer different protection to airborne pollutants than that of mesophytic vegetation.

Plants generally respond differently to air pollution at different stages of their life cycle (Reiling & Davison, 1994). Young expanding leaves are likely to be more sensitive than older leaves, and seedlings may be more sensitive than established plants (Kozlowski, 1980). However, it is still a matter of dispute if seedlings are more susceptible than adult plants to pollution and most of the differences between seedlings and older plants, as well as between young and old foliage, can be attributed to differences in rates of uptake. Since much of the prescribed burning in Australia takes place during periods of active growth and flowering, there may be greater implication for response to components of combustion than at other times of the year. As Robinson et al. (1998) point out, a small disturbance in stomatal control during periods of stress may have considerable consequences for plant survival. Given that wildfires in Australia are most common in the hot dry months (i.e., periods of water-stress), vegetation may well be vulnerable to additional stress induced by the effects of smoke, albeit for a relatively short period of time.

The position of leaves within plant canopies largely determines the extent of their exposure to wet and dry deposition (Grantz et al., 2003). Modelling of large-scale deposition suggests that most aerosols are deposited on upper and outer surfaces of forests with exponentially lower transfer downwards into the canopy (Shaw et al., 1994). The canopy thus acts as a filter for tree seedlings and understory vegetation. Several studies have sampled leaves from outer edges and well within the canopy and herbaceous layer to try to quantify exposure to air pollution (Kozlowski, 1980; Steubing et al., 1989). This line of evidence suggests that understory vegetation in Australia in open woodlands with less crown cover is more likely to be exposed to smoke from prescribed burns and wildfires than the understorey in closed canopy forests.

Leaves of vegetation in unburnt areas surrounding a fire are likely to be coated in a layer of PM. Smoke from wildfires contains particulates that may range in size from 0.5 to 43 μm (Ward & Hardy, 1991), the smallest of which may have long residence times in the atmosphere and can be carried hundreds of kilometers in drifting smoke plumes (Crutzen & Andreae, 1990). Hirano et al. (1995) found that dust applied to leaves of cucumber and kidney bean decreased stomatal conductance under well-lit conditions, decreased photosynthetic rate by shading the leaf surface, and increased leaf temperature by greater absorption of incident radiation. Such physiological changes are likely to be similar for plants coated with fine ash from biomass burning. In addition, it seems likely that prevailing warm and dry conditions, that produce water and heat stress in plants and that are associated with the lack of rainfall for washing leaf surfaces, could well exacerbate the leaf-coating effects of fire-produced ash and particulates. Given that the variety of effects of PM on vegetation, soils, and whole ecosystems has been thoroughly reviewed by Grantz et al. (2003), investigation into the load and effect of PM on surrounding unburnt vegetation after prescribed burning and wildfires is clearly warranted.

It is obvious that plant responses to long-term exposure to gaseous pollutants are not always indicative of responses to short-term exposure. For example, in one of the few publications dealing directly with the effect of smoke on plants, Gilbert and Ripley (2002) found exposure to smoke for only 1 minute was enough to reduce stomatal conductance and intercellular levels and rates of assimilation of CO_2 of *Chrysanthemoides monilifera* for up to 5 h. Normal stomatal functioning was re-established after 24 h. Following a similar pattern, all populations of *Plantago major* showed reduced stomatal conductance within hours of coming in contact with high levels of O_3, but more sensitive populations showed different stomatal responses to that of less sensitive populations over the following

4 days of exposure (Reiling & Davison, 1995). Stomata of *Vicia faba* responded within 15 min of exposure to SO_2 regardless of the concentration of the pollutant, and the effect remained for several days after exposure (Black & Unsworth, 1980). Stomatal response to low concentrations of gaseous pollutants (particularly ozone) often includes loss of stomatal control so that stomata remain open under dry conditions, rendering plants more susceptible to drought and presumably, the effect of pollutants. This may be a more realistic scenario for short-term exposure to vegetation smoke during summer wildfires and should be investigated further.

14.7. Effects of smoke on soil, roots, and microorganisms

Along with the obvious effects of airborne pollutants on aboveground vegetation there may be indirect effect via the soil (Fig. 14.1). Several authors have concluded that induced changes in soil chemistry will have a greater impact than will direct action of pollution on foliage (Cape & Unsworth, 1988; Grantz et al., 2003). As an example, elevated CO_2 has also been shown to alter soil properties by promoting greater accumulation of carbon and nutrients in vegetation and soil horizons (Johnson et al., 2003). The impact of smoke from biomass burning on soil has yet to be considered.

Root growth can be used as an indirect yet sensitive indicator of the physiology of plant shoots, and changes in shoot–root ratios are often used as an indicator of changes in nutritional status of plants and reduced translocation of photosynthate (Ormrod, 1982). Using the milieu of pollution studies, root biomass of mature trees in natural stands of *Pinus ponderosa* was up to 16 times greater in unpolluted sites than polluted sites (Grulke et al., 1998). At a different scale, root initiation in mung bean (*Vigna radiata*) and tomato (*Lycopersicon esculentum*) can be promoted by application of aqueous extracts of smoke (Taylor & van Staden, 1996, 1998), but this research has yet to be extended to woody plants or natural environments. The interaction of coal-smoke and root-knot nematode infection on okra and eggplant suggests greater susceptibility for infection and reduced productivity in areas of high air pollution (Khan & Khan, 1994a, 1994b). This type of response is from plants with relatively long-term exposure to coal-smoke (3 months) and may or may not be translatable to the effect of smoke from vegetation fires. Changes in the availability of nutrients to vegetation and soil microorganisms may cause disruptions in ecosystem functioning, particularly in Australian ecosystems where balanced nutrient cycling is commonplace. Losses and additions of nutrients in soil during burning have been well-studied for Australian ecosystems (see Raison, 1979), but nutrient alterations via smoke from vegetation fires is yet to be fully elucidated.

Smoke has been shown to have variable impacts on microorganisms. In early studies, traditional preservative applications of smoke to fungal species produced a range of responses, with critical exposure time of spores and mycelium ranging from seconds to minutes (Parmeter & Uhrenholdt, 1975a, b; Zagory & Parmeter, 1984). At the other extreme, liquid condensates of smoke from beech wood killed spores of several common mold fungi (Wolkowskaja & Lapszin, 1962). Despite the well-known use of smoke as a sterilizing agent, there has been little research into smoke effects on soil microbes in natural ecosystems.

In a broader context, functional groups of fungi have been used as bioindicators of environmental pollution (e.g., Arnolds, 1991; Fellner, 1993; Lagana et al., 1999; Wallenda & Kottke, 1998). Similarly, lichens have been used as indicators of air quality (e.g., Conti & Cecchetti, 2001; Seaward, 2004). Decreases in the ratio of mycorrhizal to saprophytic fungi have been used to indicate forest decline due to anthropogenic contamination (Fellner, 1993; Rühling & Tyler, 1991), while nitrogen deposition appears to affect formation of fruiting bodies more readily than belowground structures (Wallenda & Kottke, 1998). Steubing et al. (1989) found the ratio of soil bacteria to fungi was depressed when exposed to SO_2, NO_2, and O_3 applied separately and in combination. Infection by mycorrhizal fungi is generally reduced with increased additions of nitrogen (Caporn et al., 1995), and simulation of long-term atmospheric deposition of nitrogen by Lee and Caporn (1998) demonstrated its potential to radically change above- and belowground processes. Microbial and fungal activities are essential to the efficient and healthy functioning of all ecosystems, and knowledge of how smoke affects their ecological processes would be productive.

14.8. Effects of smoke on seed germination and other processes

By far the most intensively studied effect of smoke on plants is the ability of combustion compounds from burnt vegetation to stimulate germination of seed. This research has been reviewed extensively by Brown (1993), Brown and van Staden (1997), and Vigilante et al. (1998) and will not be elaborated here. However, since the publication of these three major reviews, research has focussed on extending the range and type of species tested (e.g., Tang et al., 2003; Wills & Read, 2002).

Other recent research has concentrated on the interaction of smoke-promoted germination with other germination cues such as temperature, irradiance, hormones, mechanical and chemical scarification, seed burial and nitrogenous compounds. Smoke not only enhances seed germination but has also been found to stimulate flowering (Keeley, 1993; LeMaitre & Brown, 1992) and release of bulbs from dormancy (Tompsett, 1985).

14.9. Effects of volatile organic compounds on ecosystems

VOCs are a diverse group of compounds and include isoprene, terpenes, alkanes, alkenes, alcohols, esters, carbonyls, and acids (Ciccioli et al., 2001; Kesselmeier & Staudt, 1999; Owen et al., 2001). Acetic and formic acids are the most abundant VOCs emitted from burning biomass (Ciccioli et al., 2001), whereas isoprene and monoterpene constitute more than 50% of VOCs in natural plant emissions (Kesselmeier & Staudt, 1999). Detailed identification and chemical analysis of functional groups of particulates such as VOCs have the potential to be used as markers compounds, which could then be used to distinguish smoke from biomass burning from other sources (Brauer, 1999). This information would aid in tracing smoke plumes in both time and space and could be used to distinguish biomass smoke from other sources of pollution, thus improving emission quantifications (Sandberg et al., 2002).

There are limited studies on the effects of VOCs as primary pollutants on plants (Cape, 2003; Cape et al., 2003a). Several of these studies have suggested that plants may absorb and metabolize VOCs under different circumstances, but the effects on the plant, toxic or otherwise, is largely unknown (e.g., Binnie et al., 2002; Collins et al., 2000; Cornejo et al., 1999). The research that is available is generally concerned with the effects of ethylene as a plant hormone (Cape et al., 2003b) or the effect of VOCs as components of air pollution, such as in vehicle exhaust gases (e.g., Viskari et al., 2000). Responses to VOCs are variable; for example, exposure of herbaceous plants to a mixture of six VOCs caused changes (both reductions and increases) in seed production, leaf water content and photosynthetic efficiency in some species (Cape et al., 2003a). These and other relevant studies involve relatively short-term exposure (hours and days rather than months or years, see Cape, 2003), which, unlike most air pollution studies, can provide realistic comparisons for exposure of plants to VOCs in smoke from vegetation fires.

14.10. Biogenic production of volatile organic compounds

More often than not, research has been initiated to determine VOC emissions from plants rather than absorption from the atmosphere (see reviews by Cape, 2003; Penuelas & Llusia, 2001). Along with isoprene and monoterpene (Guenther et al., 1995), other VOCs emitted from plants included aromatic hydrocarbons such as toluene, xylenes, ethyl-, methyl- and propyl-benzenes and naphthalene (e.g., Viskari et al., 2000). Actual rates of VOC emission can equate to more than 10% of the carbon gained through photosynthesis (Holzinger et al., 2000). Plants can be categorised according to major VOC compounds produced and emitted (Harley et al., 1999; Lerdau & Gray, 2003; Owen et al., 2001). For example, the composition and concentration of terpenoids in plant tissue has been used to taxonomically separate certain species (Adams, 1994; Benjamin et al., 1996). Along similar lines, recent unpublished research by one of the authors has focused on environmental conditions associated with production and emission of VOCs in eucalypts. Intercepted radiation has a strong influence on emissions of isoprene but not monoterpenes or carbonyl compounds. Temperature strongly influenced emissions of all classes of terpenes but again had less influence over carbonyl compounds. Instead, factors such as atmospheric concentration and concentrations of the precursor compounds within tree sap appear to be better predictors for these compounds.

Many studies have identified and quantified monoterpenoids in plants, but only one study has made the link between this group of phytochemicals, seasonal conditions, and plant flammability (Owens et al., 1998; and see Bond & Midgley, 1995; Zedler, 1995). Most studies of plant flammability only concentrate on heat and ash content, temperature of ignition, and physical properties such as surface area-to-volume ratio and fuel particle density (e.g., Dimitrakopoulos, 2001; Mak, 1988; Papio & Trabaud, 1990). The line of study involving phytochemistry and flammability of plants may be useful in conjunction with distribution patterns of species and to predict the composition and production of VOCs.

Plant roots and other microorganisms in the rhizosphere also produce VOCs but in different patterns and responses from aboveground vegetation (Steeghs et al., 2004). Such exudates can have a wide variety of effects on the rhizosphere and soil microbial community, including changing chemical and physical properties of the soil, chemical communication, and inhibiting growth of competing organisms. For example, the effect of VOCs produced by soil bacteria on fungal growth and enzyme activity varied widely and depended on the species of fungi and bacteria involved and on the environment in which they interacted (Mackie & Wheatley, 1999). How these metabolic emissions may be affected by changes in simple parameters such as temperature and moisture is unknown, and information about more complex interactions such as the effect of smoke from biomass burning is yet to be acquired. Further studies investigating aspects of physiological responses of ecosystems to smoke including VOCs are needed in both practical (e.g., effect of smoke from prescribed fires on grape and soft fruit quality) and land management contexts (e.g., losses and gains of nutrients in smoke).

Eucalypts grow widely in the Australian landscape and are cultivated in large numbers in plantations here and around the world. In Australia, there are over 160 million hectares of native forests dominated by species of *Eucalyptus* and *Acacia* and 740,000 ha of plantations of *Eucalyptus globulus* (National Forest Inventory, 2007). The production of VOCs by such vegetation is estimated to be up to 60% of total VOC emissions (National Environmental Protection Council, 1997). For example, the characteristic blue haze in the Dandenong Ranges in Victoria and the Blue Mountains in New South Wales is associated with emissions of VOCs from eucalypts. Rates of emissions of monoterpene range from 0 to 5.4 $\mu g\, g^{-1}\, h^{-1}$ and from 5.3 to 69.0 $\mu g\, g^{-1}\, h^{-1}$ for isoprene (He et al., 2000). In this study, *E. globulus* was the greatest emitter of both VOCs. There is emerging evidence that emissions vary with changes in temperature and water availability (Guenther, 2001; Guenther et al., 1999) and may be exacerbated under extreme conditions of heat or drought (Llusià et al., 2006). Biogenic emissions from eucalypts are species-specific in both rates of production and composition (He et al., 2000; Maleknia et al., 2006). The age of the leaf is also important, with young eucalypt leaves often containing more oil than mature leaves (Silvestre et al., 1997) and with higher emission rates (Street et al., 1997). With eucalypts dominating the forested vegetation of Australia and increasing establishment of eucalypt plantations worldwide, it is important to understand the background emissions of VOCs from living trees and the potential for increased emissions with changes in environmental condition, particularly during fire events.

14.11. Summary

Advancing our knowledge of the composition of smoke—including its unique, hazardous, or reactive compounds—would have a number of advantages. First, detailed identification and chemical analysis of functional groups on particulates (e.g., VOCs) could be used to determine markers compounds that could then be used to distinguish smoke from biomass burning from other sources and aid in increasing the accuracy of quantification of worldwide emissions. Second, the quantification of hazardous compounds in smoke from biomass burning could be used in risk analysis of health and safety of firefighters and the general public during wildfire and prescribed burning activities and allow decision-making processes to be better informed. Third, studies involving phytochemistry and flammability of ecosystems may provide the potential to use distribution patterns of groups of species to predict the composition and production of VOCs and other important components in smoke. Knowledge of all aspects of smoke from biomass burning has developed steadily over the past 25 years and will continue to progress as governments, land management and health agencies, and researchers and the general community become more aware of the potential impacts of this source of air pollution on their surrounding environment.

REFERENCES

Adams, R.P. 1994. Geographic variation and systematics of monospermous *Juniperus* (Cupressaceae) from the Chihuahua Desert based on RAPDs and terpenes. Biochem. Syst. Ecol. 22, 699–710.

Aditama, T.Y. 2000. Impact of haze from forest fire to respiratory health: Indonesian experience. Respirology 5, 169–174.

Andreae, M.O. 1991. Biomass burning: Its history, use, and distribution and its impact environmental quality and global climate. In: Levine, J.S., ed. Global biomass burning—atmospheric, climatic, and biosphere Implications. The MIT Press, Cambridge, pp. 3–21.

Andreae, M.O., and Merlet, P. 2001. Emissions of trace gases and aerosols from biomass burning. Global Biogeochem. Cycles 15, 955–966.

Arnolds, E. 1991. Decline of ectomycorrhizal fungi in Europe. Agric. Ecosyst. Environ. 35, 209–244.

Australian National Environment Protection Council. 1998. National Environment Protection (Ambient Air Quality) Measure. http://www.ephc.gov.au/nepms/air/air_nepm.html

Australian National Environment Protection Council. 2003. National Environment Protection (Ambient Air Quality) Measure Variation. http://www.ephc.gov.au/nepms/air/air_nepm.html

Barlow, B.A. 1981. The Australian flora: Its origins and evolution. Flora of Australia, Introduction. Volume 1, Bureau of Flora and Fauna. Australian Government Publishing Service, Canberra, 25–75.

Benjamin, M.T., Sudol, M., Bolch, L., and Winer, A.M. 1996. Low-emitting urban forests: A taxonomic methodology for assigning isoprene and monoterpene emission rates. Atmos. Environ. 30, 1437–1452.

Beringer, J., Packham, D., and Tapper, N. 1995. Biomass burning and resulting emissions in the Northern Territory, Australia. Int. J. Wildland Fire 5, 229–235.

bin Abas, M.R., Oros, D.R., and Simoneit, B.R.T. 2004. Biomass burning as the main source of organic aerosol particulate matter in Malaysia during haze episodes. Chemosphere 55, 1089–1095.

Binnie, J., Cape, J.N., Mackie, N., and Leith, I.D. 2002. Exchange of organic solvents between the atmosphere and grass—the use of open top chambers. Sci. Total Environ. 25, 53–67.

Black, V.J., and Unsworth, M.H. 1980. Stomatal responses to sulphur dioxide and vapour pressure deficit. J. Exp. Bot. 31, 667–677.

Bond, W.J., and Midgley, J.J. 1995. Kill thy neighbour: An individualistic argument for the evolution of flammability. Oikos 73, 79–85.

Booze, T.F., Reinhardt, T.E., Quiring, S.J., and Ottmar, R.D. 2004. A screening-level assessment of the health risks of chronic smoke exposure for wildland firefighters. J. Occup. Health Environ. 1, 296–305.

Bowman, D.M.J.S. 1998. Tansley Review No. 101. The impact of Aboriginal landscape burning on the Australian biota. New Phytol. 140, 385–410.

Brandt-Rauf, P.W., Fallon, L.F., Tarantini, T., Idema, C., and Andrews, L. 1988. Health hazards of firefighters: Exposure assessment. Brit. J. Ind. Med. 45, 606–612.

Brauer, M. 1999. Health impacts of biomass air pollution. In: Goh, K.T., Schwela, D., Goldammer, J.G., and Simpson, O., eds. Health guidelines for vegetation fire events: Background papers. World Health Organisation, Lima, pp. 186–257.

Breysse, P.A. 1984. Health hazards of smoke. J. Forest. 82, 89.

Brown, N.A.C. 1993. Promotion of germination of fynbos seeds by plant-derived smoke. New Phytol. 123, 575–583.

Brown, N.A.C., and van Staden, J. 1997. Smoke as a germination cue: A review. Plant Growth Regul. 22, 115–124.

Bytnerowicz, A. 1996. Physiological aspects of air pollution stress in forests. Phyton 36, 15–22.

Bytnerowicz, A. 2002. Physiological/ecological interactions between ozone and nitrogen deposition in forest ecosystems. Phyton 42, 13–28.

Bytnerowicz, A., and Grulke, N.E. 1992. Physiological effects of air pollutants on western forests. In: Olson, R.K., Binkley, D., and Bohm, M., eds. The response of western forests to air pollution. Springer-Verlag, New York, pp. 183–233.

Cape, J.N., and Unsworth, M.H. 1988. Deposition, uptake ad residence of pollutants. In: Schulte-Hostede, S., Darrall, N.M., Blank, L.W., and Wellburn, A.R., eds. Air pollution and plant metabolism. Elsevier Applied Science, London, pp. 1–18.

Cape, J.N. 2003. Effects of airborne volatile organic compounds on plants. Environ. Pollut. 122, 145–157.

Cape, J.N., Fowler, D., and Davison, A. 2003a. Ecological effects of sulfur dioxide, fluorides, and minor air pollutants: Recent trends and research needs. Environ. Int. 29, 201–211.

Cape, J.N., Leith, I.D., Binnie, J., Content, J., Donkin, M., Skewes, M., Price, D.N., Brown, A.R., and Sharpe, A.D. 2003b. Effects of VOCs on herbaceous plants in an open-top chamber experiment. Environ. Pollut. 124, 341–353.

Caporn, S.J.M., Song, W., Read, D.J., and Lee, J.A. 1995. The effects of repeated nitrogen fertilization on mycorrhizal infection in heather (*Calluna vulgaris* (L) Hull). New Phytol. 129, 605–609.

Chen, L., Verrall, K., and Tong, S. 2006. Air particulate pollution due to bushfires and respiratory hospital admissions in Brisbane, Australia. Int. J. Environ. Health Res. 16, 181–191.

Cheney, N.P., Raison, R.J., and Khanna, P.K. 1980. Release of carbon to the atmosphere in Australian vegetation fires. In: Pearman, G.I., ed. Carbon dioxide and climate: Australian research. Australian Academy of Science, Canberra, pp. 153–158.

Ciccioli, P., Brancaleoni, E., Frattoni, M., Cecinado, A., and Pinciarelli, L. 2001. Determination of volatile organic compounds (VOC) emitted from biomass burning of Mediterranean vegetation species by GC-MS. Anal. Lett. 34, 937–955.

Collins, C.D., Bell, J.N.B., and Crews, C. 2000. Benzene accumulation in horticultural crops. Chemosphere 1(S2), 109–114.

Cornejo, J.J., Munoz, F.G., Ma, C.Y., and Stewart, A.J. 1999. Studies on the decontamination of air by plants. Ecotoxicology 8, 311–320.

Conti, M.E., and Cecchetti, G. 2001. Biological monitoring: Lichens as bioindicators of air pollution assessment: A review. Environ. Poll. 114, 471–492.

Crutzen, P.J., and Andreae, M.O. 1990. Biomass burning in the tropics: Impacts on atmospheric chemistry and biogeochemical cycles. Science 250, 1669–1678.

Crutzen, P.J., and Carmichael, G.R. 1993. Modeling the influence of fires on atmospheric chemistry. In: Crutzen, P.J., and Goldammer, J.G., eds. Fire in the environment: The ecological, atmospheric and climatic importance of vegetation fires. Wiley, Chichester, pp. 89–105.

Darrall, N.M. 1989. The effect of air pollutants on physiological processes in plants. Plant Cell Environ. 12, 1–30.

Darwin Air Emission Inventory. 2001. National Pollutant Inventory (NPI) in the Northern Territory. http://www.lpe.nt.au/enviro/poldoc/npi/dai.htm

Delmas, R., Lacaux, J.P., and Brocard, D. 1995. Determination of biomass burning emission factors: Methods and results. Environ. Monit. Assess. 38, 181–204.

Department of Environmental Protection. 2003. Aggregated emissions inventory of National Pollution Inventory substances for the Bunbury Regional Airshed. Final Emissions Inventory Report, Western Australia, 118 pp.

Dimitrakopoulos, A.P. 2001. A statistical classification of Mediterranean species based on their flammability components. Int. J. Wildland Fire 10, 113–118.

Dost, F.N. 1991. Acute toxicology of components of vegetation smoke. Rev. Environ. Contam. T. 119, 1–46.

Duclos, P., Sanderson, L.M., and Lipsett, M. 1990. The 1987 forest fire disaster in California: Assessment of emergency room visits. Arch. Environ. Health 45, 53–58.

Eisner, M.D., Yelin, E.H., Katz, P.P., Earnest, G., and Blanc, P.D. 2002. Exposure to indoor combustion and adult asthma outcomes: Environmental tobacco smoke, gas stoves, and woodsmoke. Thorax 57, 973–978.

Ellis, S., Kanowski, P., and Whelan, R. 2004. National Inquiry on Bushfire Mitigation and Management, Commonwealth of Australia, Canberra. http://www.coagbushfireenquiry.gov.au/findings.htm#response

Emmanuel, S.C. 2000. Impact to lung health of haze from forest fires: The Singapore experience. Respirology 5, 175–182.

Fellner, R. 1993. Air pollution and mycorrhizal fungi in central Europe. In: Pegler, D.N., Boddy, L., Ing, B., and Kirk, P.M., eds. Fungi of Europe: Investigation, recording and conservation. Royal Botanic Gardens, Kew, pp. 239–250.

Gao, S., Hegg, D.A., Hobbs, P.V., Kirchstetter, T.W., Magi, B., and Sadilek, M. 2003. Water-soluble organic components in aerosols associated with savanna fires in southern Africa: Identification, evolution and distribution. J. Geophys. Res. 108, D13 Article number 8491.

Garcia-Nieto, P.J. 2002. Study of visibility degradation due to coagulation, condensation and gravitational settling of the atmospheric aerosol. Aerosol Sci. Tech. 36, 814–827.

Gilbert, M.E., and Ripley, B.S. 2002. The effect of smoke on the photosynthetic gas exchange of *Chrysanthemoides monilifera*. S. Afr. J. Bot. 68, 525–531.

Global Emissions Inventory Activity. 2002. Improving global estimates of atmospheric emissions from biomass burning. Executive summary, Joint GOFC/GOLD and IGBP-IGAC/BIBEX workshop, Boulder, CO, 10 pp. http://geiacenter.org/

Grantz, D.A., Garner, J.H.B., and Johnson, D.W. 2003. Ecological effects of particulate matter. Environ. Int. 29, 213–239.

Grulke, N.E., Andersen, C.P., Fenn, M.E., and Miller, P.R. 1998. Ozone exposure and nitrogen deposition lowers root biomass of ponderosa pine in the San Bernardino Mountains, California. Environ. Poll. 103, 63–73.

Guenther, A. 2001. Review of the effects of drought and high temperature on biogenic emissions and future research efforts in Texas. National Center for Atmospheric Research, Texas natural Resource Conservation Commission, TX, 16 pp. http://www.tceq.state.tx.us/assets/public/implementation/air/am/contracts/reports/ei/EffectsOfDroughtHighTemperatureOnBiogenicEmissions.pdf

Guenther, A.B., Hewitt, C.N., Erickson, D., Fall, R., Geron, C., Graedel, T., Harley, P., Klinger, L., Jerdau, M., McKay, W.A., Pierce, T., Scholes, B., Steinbrecher, R., Tallamraju, R., Taylor, J., and Zimmerman, P. 1995. A global model of natural volatile organic compound emissions. J. Geophys. Res. 100, 8873–8892.

Guenther, A., Archer, J., Greenberg, P., Harley, D., Helmig, L., Klinger, L., Vierling, M., Wildermuth, P., Zimmerman, P., and Zitzer, S. 1999. Biogenic hydrocarbon emissions and landcover/climate change in a subtropical savanna. Phys. Chem. Earth 24, 659–667.

Hardy, C.C., Ottmar, R.D., Peterson, J.L., Core, J.E., and Seamon, P. 2001. Smoke management guide for prescribed and wildland fire. PMS 420-2, National Wildfire Coordination Group, Boise, ID, 226 pp.

Harley, P.C., Monson, R.K., and Lerdau, M.T. 1999. Ecological and evolutionary aspects of isoprene emission from plants. Oecologia 118, 109–123.

He, C., Murray, F., and Lyons, T. 2000. Monoterpene and isoprene emissions from 15 *Eucalyptus* species in Australia. Atmos. Environ. 34, 645–655.

Heck, W.W. 1973. Air pollution and the future of agricultural production. In: Naegele, J.A., ed. Air pollution damage to vegetation. Advances in chemistry, Series 122. American Chemical Society, Washington, DC, pp. 118–129.

Heil, A., and Goldammer, J.G. 2001. Smoke-haze pollution: A review of the 1997 episode in Southeast Asia. Reg. Environ. Change 2, 24–37.

Hirano, T., Kiyota, M., and Aiga, I. 1995. Physical effects of dust on leaf physiology of cucumber and kidney bean plants. Environ. Poll. 89, 255–261.

Holzinger, R., Sandoval-Soto, L., Rottenberger, S., Crutzen, P.J., and Kesselmeier, J. 2000. Emissions of volatile organic compounds from *Quercus ilex* L. measured by proton transfer reaction mass spectrometry under different environmental conditions. J. Geophys. Res. 105, 20573–20580.

Hueglin, C., Gaegauf, C.H., Kunzel, S., and Burtscher, H. 1997. Characterization of wood combustion particles: Morphology, mobility and photoelectric activity. Environ. Sci. Tech. 31, 3439–3447.

Jalaludin, B., Smith, M., O'Toole, B., and Leeder, S. 2000. Acute effects of bushfires on peak expiratory flow rates in children with wheeze: A time series analysis. Aust. New Zeal. J. Pub. Health 24, 174–177.

Johnson, D.W., Hungate, B.A., Dijkstra, P., Hymus, G., Hinkle, C.R., Stiling, P., and Drake, B.G. 2003. The effects of elevated CO_2 on nutrient distribution in a fire-adapted scrub oak forest. Ecol. Appl. 13, 1388–1399.

Johnston, F.H., Kavanagh, A.M., Bowman, D.M.J.S., and Scott, R.K. 2002. Exposure to bushfire smoke and asthma: An ecological study. Med J. Australia 176, 535–538.

Keeley, J.E. 1993. Smoke-induced flowering in the fire-lily *Cyrtanthus ventricosus*. S. Afr. J. Bot. 59, 638.

Kesselmeier, J., and Staudt, M. 1999. Biogenic volatile organic compounds (VOC): An overview on emission, physiology and ecology. J. Atmos. Chem. 33, 23–88.

Khan, M.R., and Khan, M.W. 1994a. Smoke pollution and the effects of root-knot nematodes on the growth of eggplants. Plant Path. 43, 683–693.

Khan, M.R., and Khan, M.W. 1994b. Single and interactive effects of root-knot nematode and coal-smoke on okra. New Phytol. 126, 337–342.

Koutrakis, P., and Sioutas, C. 1996. Physico-chemical properties and measurement of ambient particles. In: Wilson, R., and Spengler, J.D., eds. Particles in our air: Concentrations and health effects. Harvard University Press, Harvard, pp. 15–39.

Kozlowski, T.T. 1980. Impacts of air pollution on forest ecosystems. BioScience 30, 88–93.

Krupa, S.V., and Manning, W.J. 1988. Atmospheric ozone: Formation and effects on vegetation. Environ. Poll. 50, 101–137.

Lagana, A., Loppi, S., and de Dominicus, V. 1999. Relationships between environmental factors and the proportions of fungal trophic groups in forest ecosystems of the central Mediterranean area. Forest Ecol. Manag. 124, 145–151.

Larson, T.V., and Koenig, J.Q. 1994. Wood smoke: Emissions and noncancer respiratory effects. Ann. Rev. Pub. Health 15, 133–156.

Lee, J.A., and Caporn, S.J.M. 1998. Ecological effects of atmospheric reactive nitrogen deposition on semi-natural terrestrial ecosystems. New Phytol. 139, 127–134.

Legg, C.A., and Laumonier, Y. 1999. Fires in Indonesia, 1997: A remote sensing perspective. Ambio 28, 479–485.

LeMaitre, D.C., and Brown, P.J. 1992. Life cycles and fire-stimulated flowering in geophytes. In: van Wilgen, B.W., Richardson, D.M., Kruger, F.J., and van Hensbergen, H.J., eds. Fire in South African mountain fynbos. Springer-Verlag, Berlin, pp. 145–160.

Lendzian, K.J., and Kerstiens, G. 1991. Sorption and transport of gases and vapors in plant cuticles. Rev. Environ. Contam. T. 121, 65–128.

Lerdau, M., and Gray, D. 2003. Ecology and evolution of light-dependent and light-independent phytogenic volatile organic carbon. New Phytol 157, 199–211.

Lewis, P.R., and Corbett, S.J. 2002. Bushfires, air pollution and asthma. Med. J. Australia 176, 517.

Lobert, J.M., and Warnatz, J. 1993. Emissions from the combustion process in vegetation. In: Crutzen, P., and Goldammer, J., eds. The ecological, atmospheric and climatic importance of vegetation fires. Wiley, Chichester, pp. 15–37.

Llusià, J., Peñuelas, J., Alessio, G.A., and Estiarte, M. 2006. Seasonal contrasting changes of foliar concentrations of terpenes and other volatile organic compound in four dominant species of a Mediterranean shrubland submitted to a field experimental drought and warming. Physiol. Plantarum 127, 632–649.

Mackie, A.E., and Wheatley, R.E. 1999. Effects and incidence of volatile organic compound interactions between soil bacteria and fungal isolates. Soil Biol. Biochem. 31, 375–385.

Mak, E.H.T. 1988. Measuring foliar flammability with the limiting oxygen index method. Forest Sci. 34, 523–529.

Maleknia, S.D., Bell, T.L., and Adams, M.A. 2006. PTR-MS analysis of reference and plant-emitted volatile organic compounds. Int. J. Mass Spectrom. 262, 203–210.

Malilay, J. 1999. A review of factors affecting the human health impacts of air pollutants from forest fires. In: Goh, K.T., Schwela, D., Goldammer, J.G., and Simpson, O., eds. Health guidelines for vegetation fire events: Background papers. World Health Organisation, Lima, pp. 258–274.

Malm, W.C. 1999. Introduction to visibility. Cooperative Institute for Research in the Atmosphere: NPS Visibility Program. Colorado State University, Colorado, CA, 70 pp.

Manins, P.C., Beer, T., Fraser, P.J., Holper, P.N., Suppiah, R., and Walsh, K. 2001. Australia State of Environment Report 2001 Atmosphere. Commonwealth of Australia. http://www.ea/gov.au/soe/2001

McKenzie, L.M., Hao, W.M., Richards, G.N., and Ward, D.E. 1994. Quantification of major components emitted from smouldering combustion of wood. Atmos. Environ. 28, 3285–3292.

Miranda, A.I., Ferreira, J., Valente, J., Santos, P., Amorim, J.H., and Borrego, C. 2005. Smoke measurements during Gestosa-2002 experimental field fires. Int. J. Wildland Fire 14, 107–116.

Momen, B., Anderson, P.D., Houpis, J.L.J., and Helms, J.A. 2002. Growth of ponderosa pine seedlings as affected by air pollution. Atmos. Environ. 36, 1875–1882.

Mott, J.A., Meyer, P., Mannino, D., Redd, S.C., Smith, E.M., Gotway-Crawford, C., and Chase, E. 2002. Wildland forest fire smoke: Health effects and intervention evaluation, Hoopa, California, 1999. Western J.Med. 176, 157–162.

Mustajbegovic, J., Zuskin, E., Schachter, E.N., Kern, J., Vricic-Keglevic, M., Heimer, S., Vitale, K., and Nada, T. 2001. Respiratory function in active firefighters. Am. J. Ind. Med. 40, 55–62.

National Environmental Protection Council. 1997. Draft national environmental protection measure and impact statement for ambient air quality. National Environmental Protection Council, Canberra, 101–129.

National Forest Inventory. 2007. Australia's forests at a glance. Bureau of Rural Sciences, Department of Agriculture, Fisheries and Forestry, Canberra, 68 pp.

Nichol, J. 1997. Bioclimatic impacts of the 1994 smoke haze event in southeast. Asia. Atmos. Environ. 31, 1209–1219.

Ormrod, D.P. 1982. Air pollution interactions in mixtures. In: Unsworth, M.H., and Ormrod, D.P., eds. Effects of gaseous air pollution in agriculture and horticulture. Butterworths, London, pp. 307–331.

Owen, S.M., Boissard, C., and Hewitt, C.N. 2001. Volatile organic compounds (VOCs) emitted from 40 Mediterranean plant species: VOC speciation and extrapolation to habitat scale. Atmos. Environ. 35, 5393–5409.

Owens, M.K., Lin, C.-D., Taylor, C.A., and Whisenant, S.G. 1998. Seasonal patterns of plant flammability and monoterpeniod content in *Juniperus ashei*. J. Chem. Ecol. 24, 2115–2129.

Packham, D.R., and Vines, R.G. 1978. Properies of bushfire smoke: The reduction in visibility resulting from prescribed fires in forests. J. Air Poll. Control Assoc. 28, 790–795.

Palacios-Orueta, A., Chuvieco, E., Parra, A., and Carmona-Moreno, C. 2005. Biomass burning emissions: A review of models using remote-sensing data. Environ. Monit. Assess. 104, 189–209.

Papio, C., and Trabaud, L. 1990. Structural characteristics of fuel components of five mediterranean shrubs. Forest Ecol. Manag. 35, 249–259.

Parmeter, J.R., and Uhrenholdt, B. 1975a. Effects of smoke on pathogens and other fungi. Proc. Tall Timbers Fire Ecol. Conf. 14, 299–304.

Parmeter, J.R., and Uhrenholdt, B. 1975b. Some effects of pine-needle or grass smoke on fungi. Phytopath 65, 28–31.

Penuelas, J., and Llusia, J. 2001. The complexity of factors driving volatile organic compound emissions by plants. Biol. Plantarum. 44, 481–487.

Phonboon, K., Paisarn-Uchapong, O., Kanatharana, P., and Agsorn, S. 1999. Smoke episodes emissions characterization and assessment of health risks related to downward air quality—case study, Thailand. In: Goh, K.T., Schwela, D., Goldammer, J.G., and Simpson, O., eds. Health guidelines for vegetation fire events: Background papers. World Health Organisation, Lima, pp. 334–380.

Phuleria, H.C., Fine, P.M., Zhu, Y., and Sioutas, C. 2005. Air quality impacts of the October 2003 Southern California wildfires. J. Geophys. Res. 110, D07S20, doi:10.1029/2004JD004626.

Pinto, J.P., and Grant, L.D. 1999. Approaches to monitoring of air pollutants and evaluation of health impacts produced by biomass burning. In: Goh, K.T., Schwela, D., Goldammer, J.G., and Simpson, O., eds. Health guidelines for vegetation fire events: Background papers. World Health Organisation, Lima, pp. 147–185.

Polle, A. 1998. Photochemical oxidants: Uptake and detoxification mechanisms. In: De Kok, L.J., and Stulen, I., eds. Responses of plant metabolism to air pollution and global change. Backhuys Publishers, Leiden, pp. 95–116.

Pope, C.A., Dockery, D.W., Spengler, J.D., and Raizenne, M. 1991. Respiratory health and PM10: A daily time-series analysis. Am. Rev. Resp. Disease 144, 668–674.

Radke, L.F. 1989. Airborne observations of cloud microphysics modified by anthropogenic forcing. In: Proceedings of a Symposium on The Role of Clouds in Atmospheric Chemistry and Global Climate. American Meteorological Society, Anaheim, CA, 310–315.

Radojevic, M. 2003. Chemistry of forest fires and regional haze with emphasis on southeast Asia. Pure Appl. Geophys. 160, 157–187.

Raison, R.L. 1979. Modification of the soil environment by vegetation fires, with particular reference to nitrogen transformations: A review. Plant Soil 51, 73–108.

Reiling, K., and Davison, A.W. 1994. Effects of exposure to ozone at different stages in the development of *Plantago major* L. on chlorophyll fluorescence and gas exchange. New Phytol. 128, 509–514.

Reiling, K., and Davison, A.W. 1995. Effects of ozone on stomatal conductance and photosynthesis in populations of *Plantago major* L. New Phytol. 129, 587–594.

Reinhardt, T.E., and Ottmar R.D. 1997. Smoke exposure among wildland firefighters: A review and discussion of the current literature. PNW-GTR-373, United States Department of Agriculture, Forest Service, Pacific Northwest Research Station, Portland OR, 61 pp.

Robinson, M.F., Heath, J., and Mansfield, T.A. 1998. Disturbance in stomatal behaviour caused by air pollutants. J. Exp. Bot. 49, 461–469.

Robock, A. 1991. Surface cooling due to smoke from biomass burning. In: Levine, J.S., ed. Global biomass burning—atmospheric, climatic, and ciosphere implications. The MIT Press, Cambridge, pp. 463–476.

Rühling, A., and Tyler, G. 1991. Effects of simulated nitrogen deposition to the forest floor on macrofungal flora of a beech forest. Ambio 20, 261–263.

Sandberg, D.V., Ottmar, RD., Peterson, J.L., and Core, J. 2002. Wildland fire in ecosystems: Effects of fire on air. General Technical Report RMRS-GTR-42-V5, United States Department of Agriculture, Forest Service, Rocky Mountain Research Station Ogden, UT, 79 pp.

Scholes, R.J., Ward, D.E., and Justice, C.O. 1996. Emissions of trace gases and aerosol particles due to vegetation burning in southern hemisphere Africa. J. Geophys. Res. 101, 677–682.

Schollnberger, H., Aden, H., and Scott, B.R. 2002. Respiratory tract deposition efficiencies: Evaluation of effects from smoke released in the Cerro Grande forest fire. J. Aerosol Med. 15, 387–399.

Seaward, M.R.D. 2004. The use of lichens for environmental impact assessment. Symbiosis 37, 293–305.

Seiler, W., and Crutzen, P.J. 1980. Estimates of gross and net fluxes of carbon between the biosphere and the atmosphere from biomass burning. Clim. Change 2, 207–247.

Shaw, G., Farrington-Smith, J.G., Kinnersley, R.P., and Minski, M.J. 1994. Dry deposition of aerosol particles within model spruce canopies. Sci. Total Environ. 157, 17–23.

Shirai, T., Blake, D.R., Meinardi, S., Rowland, F.S., Russell-Smith, J., Edwards, A., Kondo, Y., Koike, M., Machida, T., Takegawa, N., Nishi, N., Kawakami, S., and Ogawa, T. 2003. Emission estimates of selected volatile organic compounds from tropical savanna burning in northern Australia. J. Geophys. Res. 108(D3), Article number 8406.

Silvestre, A.J.D., Cavaleiro, J.A.S., Delmond, B., Filliatre, C., and Bourgeois, G. 1997. Analysis of the variation of the essential oil composition of *Eucalyptus globulus* Labill. from Portugal using multivariate statistical analysis. Ind. Crops Prod. 6, 27–33.

Sim, M. 2002. Bushfires: Are we doing enough to reduce the human impact? Occup. Environ. Med. 59, 215–216.

Simmonds, P.G., Manning, A.J., Derwent, R.G., Ciais, P., Ramonet, M., Kazan, V., and Ryall, D. 2005. A burning question. Can recent growth rate anomalies in the greenhouse gases be attributed to large-scale biomass burning events? Atmos. Environ. 39, 2513–2517.

Slaughter, J.C., Koenig, J.Q., and Reinhardt, T.E. 2004. Association between lung function and exposure to smoke among firefighters at prescribed burns. J. Occup. Environ. Hygiene 1, 45–49.

Smith, M.A., Jalaludin, B., Byles, J.J., Lim, L., and Leeder, S.R. 1996. Asthma presentations to emergency departments in western Sydney during the January 1994 bushfires. Int. J. Epidemiol. 25, 1227–1236.

Spengler, J., and Wilson, R. 1996. Emissions, dispersion, and concentration of particles. In: Wilson, R., and Spengler, J.D., eds. Particles in our air: Concentrations and health effects. Harvard University Press, Harvard, pp. 41–62.

Steeghs, M., Bais, H.P., de Gouw, J., Goldan, P., Kuster, W., Northway, M., Fall, R., and Vivanco, J.M. 2004. Proton-transfer-reaction mass spectrometry as a new tool for real time analysis of root-secreted volatile organic compounds in *Arabidopsis*. Plant Physiol. 135, 47–58.

Steubing, L., Fangmeier, A., Both, R., and Frankenfeld, M. 1989. Effects of SO_2, NO_2, and O_3 on population development and morphological and physiological parameters of native herb layer species in a beech forest. Environ. Poll. 58, 281–302.

Street, R.A., Hewitt, C.N., and Mennicken, S. 1997. Isoprene and monoterpene emissions from a *Eucalyptus* plantation in Portugal. J. Geophys. Res. 102, 15875–15887.

Takemoto, B.K., Bytnerowicz, A., and Fenn, M.E. 2001. Current and future effects of ozone and atmospheric nitrogen deposition on California's mixed conifer forests. Forest Ecol. Manag. 144, 159–173.

Tang, Y., Boulter, S.L., and Kitching, R.L. 2003. Heat and smoke effects on germination of seeds from soil seed banks across forest edges between subtropical rainforest and eucalypt forest at Lamington National Park, south-eastern Queensland, Australia. Aust. J. Bot. 51, 227–237.

Taylor, J.L.S., and van Staden, J. 1996. Root initiation in *Vigna radiata* (L) Wilczek hypocotyl cuttings is stimulated by smoke-derived extracts. Plant Growth Regul. 18, 165–168.

Taylor, J.L.S., and van Staden, J. 1998. Plant-derived smoke solutions stimulate the growth of *Lycopersicon esculentum* roots *in vitro*. Plant Growth Regul. 26, 77–83.

Tompsett, A.A. 1985. Dormancy breaking bulbs by burning over. Plantsman 7, 40–52.

United States Environment Protection Agency. 1999. Compendium of methods for the determination of toxic organic compounds in ambient air (second ed.). OH, 11A–51.

Vedal, S., Petkau, J., White, R., and Blair, J. 1998. Acute effects of ambient inhalable particles in asthmatic and nonasthmatic children. Am. J. Resp. Critical Care Med. 157, 1034–1043.

Vigilante, T., Dixon, K.W., Sieler, I.M., Roche, S., and Tieu, A. 1998. Smoke germination of Australian plants, Report for the Rural Industries Research and Development Corporation, Canberra, 106 pp.

Vines, R.G., Gibson, L., Hatch, A.B., King, N.K., MacArthur, D.A., Packham, D.R., and Taylor, R.J. 1971. On the naturen properties, and behaviour of bush-fire smoke, CSIRO Division of Applied Chemistry Technical Paper No. 1, Melbourne, 32 pp.

Viskari, E.-L., Holopainen, J.K., and Kärenlampi, T. 2000. Responses of spruce seedlings (*Picea abies*) to exhaust gas under laboratory conditions. II. Ultrastructural changes and stomatal behaviour. Environ. Poll. 107, 99–107.

Wallenda, T., and Kottke, I. 1998. Nitrogen deposition and ectomycorrhizas. New Phytol. 139, 169–187.

Ward, D.E. 1990. Factors influencing the emissions of gases and particulate matter from biomass burning. In: Goldammer, J.G., ed. Fire in the tropical biota—ecosystem processes and global challenges. Springer-Verlag, Berlin, pp. 418–436.

Ward, D.E. 1999. Smoke from wildland fires. In: Goh, K.T., Schwela, D., Goldammer, J.G., and Simpson, O., eds. Health guidelines for vegetation fire events: Background papers. World Health Organisation, Lima, pp. 70–85.

Ward, D.E., and Hardy, C.C. 1991. Smoke emissions from wildland fires. Environ. Int. 17, 117–134.

Ward, D., and Radke, L. 1993. Emissions measurements from vegetation fires; a comparative evaluation of methods and results. In: Crutzen, P., and Goldammer, J., eds. The Ecological, atmospheric and climatic importance of vegetation fires. Wiley, Chichester, pp. 53–76.

Whelan, R.J. 1995. The ecology of fire. Cambridge University Press, Cambridge, 346 pp.

Wills, T.J., and Read, J. 2002. Effects of heat and smoke on germination of soil-stored seed in a south-eastern Australian sand heathland. Aust. J. Bot. 50, 197–206.

Wilson, S.A. 1995. Are Mediterranean plant species likely to have a distinctive response to SO_2 pollution? Agric. Ecosyst. Environ. 55, 71–93.

Wolkowskaja, I.L., and Lapszin, I.I. 1962. Bactericidal and fungicidal properties of smoke solution. Technol. Mesa special edition, 26–28.

World Health Organisation. 1999. In: Schwela, D.H., Goldammer, J.G., Morawska, L.H., and Simpson, O., eds. Health guidelines for vegetation fire events, guideline document. World Health Organisation, Singapore, 197 pp.

World Health Organisation. 2000. Air quality guidelines (second ed.). WHO Regional Office for Europe, Copenhagen, 288 pp.

Zagory, D., and Parmeter, J.R. 1984. Fungitoxicity of smoke. Phytopath 74, 1027–1031.

Zedler, P.H. 1995. Are some plants born to burn? Trends Ecol. Evol. 10, 393–395.

Section III: Ecological Impacts of Forest Fires and Air Pollution

This page intentionally left blank

Developments in Environmental Science, Volume 8
A. Bytnerowicz, M. Arbaugh, A. Riebau and C. Andersen (Editors)

ISSN: 1474-8177/DOI:10.1016/S1474-8177(08)00015-6

Chapter 15

Global Warming and Stress Complexes in Forests of Western North America

*Donald McKenzie**, *David L. Peterson and Jeremy J. Littell*

Abstract

A warmer climate in western North America will likely affect forests directly through soil moisture stress and indirectly through increased extent and severity of disturbances. We propose that *stress complexes*, combinations of biotic and abiotic stresses, compromise the vigor and ultimate sustainability of forest ecosystems. Across western North America, increased water deficit will accelerate the normal stress complex experienced in forests, which typically involves some combination of multi-year drought, insects, and fire. Four examples suggest how stress complexes are region-specific. Symptoms of prolonged drought and insects are currently manifested in extensive dieback of pine species in the pinyon-juniper forest of the American Southwest, an area where only a few tree species can survive. Air pollution and high stand densities from fire exclusion have compromised mixed-conifer forests of the Sierra Nevada. Bark beetles are proliferating and killing millions of hectares of dry forest in the northern interior of western North America, setting up the prospect of large and intense fires. Fire and insect mortality have also exceeded previously recorded levels in both interior and south-central Alaska, possibly precipitating extensive ecosystem changes, while extensive permafrost degradation is causing other changes. Increases in fire disturbance superimposed on forests with increased stress from drought and insects may have significant effects on growth, regeneration, long-term distribution and abundance of forest species, and short- and long-term carbon sequestration. The effects of stress complexes will be magnified given a warming climate.

*Corresponding author: E-mail: dmck@u.washington.edu

15.1. Introduction

Forests are rarely at dynamic equilibrium. Succession occurs even in relatively constant climate, punctuated by disturbance episodes that may or may not be associated with climatic variability. The principal disturbance regimes of western North America, wildfire and insect outbreaks, respond to short-term weather and annual decadal cycles in climate. For example, synchronous fire years are associated with the El Niño Southern Oscillation (ENSO) cycle in the Southwest and southern Rocky Mountains (Swetnam & Betancourt, 1998; Veblen et al., 2000), though less so in Oregon and Washington (Hessl et al., 2004). In higher-severity fire regimes, short-term weather anomalies associated with atmospheric blocking ridges of high pressure are responsible for extreme wildfire years (Gedalof et al., 2005; Johnson & Wowchuk, 1993; Skinner et al., 1999). Outbreaks of insect defoliators are associated with years of high vegetation productivity (Swetnam & Lynch, 1993; Weber & Schweingruber, 1995), whereas cambium feeders such as bark beetles are associated with drought years, in which tree defenses are compromised (Ferrell, 1996; Swetnam & Betancourt, 1998).

Steadily increasing global temperatures are expected to change the frequency, severity, and extent of natural disturbances (Littell, 2006; McKenzie et al., 2004; Westerling et al., 2006). Recently, hot dry conditions have led to large wildfires such as the Biscuit Fire (2002) in southwestern Oregon, the Hayman Fire (2002) on the Colorado Front Range, the Cerro Grande Fire (2000) in northern New Mexico, the Cedar Fire (2003) in southern California, and the complex of fires in interior Alaska (2004). Similarly, bark beetles, whose life cycles are accelerated by increased temperatures, particularly winter minima, are causing extensive mortality across the West (Logan et al., 2003; Swetnam & Betancourt, 1998; Veblen et al., 1991). Fire and insect disturbance clearly interact, often synergistically, compounding rates of change in forest ecosystems (Veblen et al., 1994). For example, fire severity in subalpine forests, though usually associated with weather anomalies, can be altered by a combination of bark beetles and annual-scale drought (Bigler et al., 2005). A third factor, air pollution, is not so much a function of increasing temperatures as of anthropogenic emissions, principally from vehicle use and industrial sources. However, in a warming climate, pollution acts as an additional stressor interacting synergistically with insects and fire.

In a warming climate, what will be the effects of increasing disturbance on forest ecosystems? Will disturbances act synergistically, and in conjunction with direct climatic stress (e.g., drought), air pollution, and perhaps pathogens and invasive species, to cause rapid or irreversible changes, or both, in species composition and ecosystem function? In this chapter we refer to these interacting stresses as *stress complexes* and suggest how they may bring about rapid ecosystem changes in a warming climate, using four examples that span a latitudinal gradient from the American Southwest to interior Alaska. We conclude by identifying challenges for land management and suggest potential adaptive strategies that may be of value when changes in stress complexes are not too abrupt or severe.

15.2. Models of stress complexes

15.2.1. The environmental niche space

Climate provides an overarching control on the distribution of tree species (Woodward, 1987; Woodward & McKee, 1991), in that species do not establish or persist outside a characteristic bioclimatic "envelope", sometimes referred to as the *fundamental niche* (Pearson & Dawson, 2003). Within the fundamental niche, areas of bioclimatic suitability are often identified probabilistically by either gradient modeling or machine-learning methods (Franklin, 1995; Cushman et al., 2007; Guisan & Zimmermann, 2000; McKenzie et al., 2003). Gradient modeling with carefully chosen predictor variables can identify specific limiting factors, where in a species' range they are most operative, and how they change among species (Cushman et al., 2007). For example, in the Pacific Northwest, USA, mountain hemlock (*Tsuga mertensiana*) growth is limited by winter snowpack at high elevations in the northern part of its range but limited by summer moisture in the southern part (Peterson & Peterson, 2001).

Climate-induced stress occurs in low-suitability areas within a species' fundamental niche, and as a consequence, shifts in climatic regime lead to compositional changes. In forests with long-lived dominant species, compositional changes could be slow even in a rapidly warming climate, because mature individuals can survive at the edges of their ranges. Disturbance is therefore expected to be the principal agent of change, operating at shorter time scales than the direct influences of climate (Fig. 15.1; McKenzie et al., 2004).

15.2.2. Energy- and water-limited systems

Climatic limiting factors operate mechanistically through the interface between organisms and their environment. Plant performance is

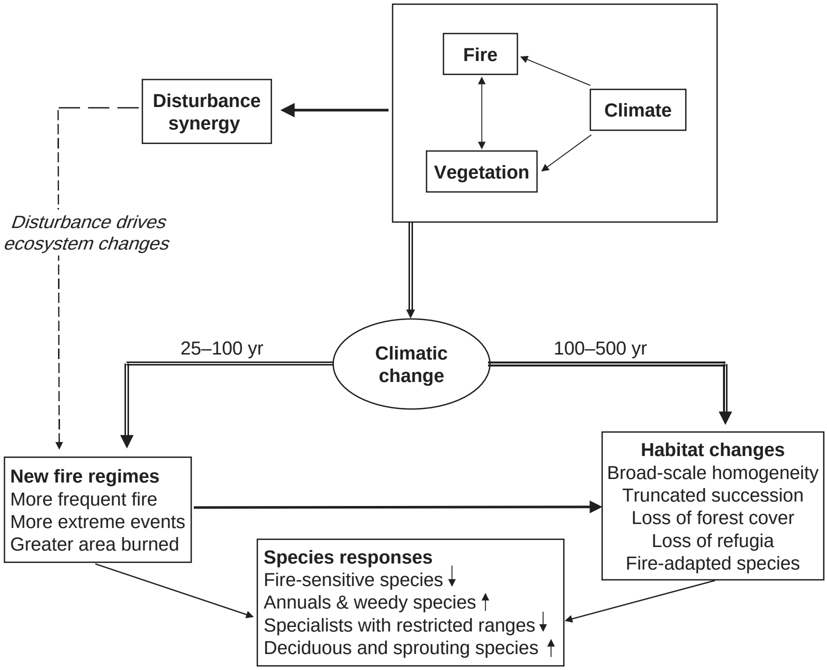

Figure 15.1. Conceptual model of the relative time scales for disturbance versus climatic change alone to alter ecosystems. Times are approximate. (Adapted from McKenzie et al., 2004.)

compromised when one or more resources (e.g., light/energy, water, nutrients) is limited. At broad scales, forests of western North America can be partitioned into energy-limited versus water-limited domains (Littell, 2006; Littell & Peterson, 2005; McKenzie et al., 2003; Milne et al., 2002). Energy-limiting factors are chiefly light (e.g., productive forests where competition reduces light to most individuals) and temperature (e.g., high-latitude or high-elevation forests). Tree growth in energy-limited ecosystems appears to be responding positively to warming temperatures over the past 100 years (McKenzie et al., 2001).

In contrast, productivity in water-limited systems is expected to decline with warming temperatures, as negative water balances constrain photosynthesis across more of the West (Hicke et al., 2002), although this may be partially offset if CO_2 fertilization significantly increases water-use efficiency in plants (Neilson et al., 2005). For example, Littell (2006) found that most montane Douglas-fir (*Pseudotsuga menziesii*) forests across the northwestern United States appear to be water-limited; under current climate projections these limits will increase in both area affected and magnitude, because temperatures are expected to increase while there is much uncertainty about precipitation and no indication of a trend (IPCC, 2007).

Limiting factors can of course shift within a species range (Peterson & Peterson, 2001), or between seasons, as water demands abate and energy needs increase (Stephenson, 1990, 1998). For example, in high-elevation or high-latitude arid forests (e.g., eastern slopes of the Sierra Nevada, Rocky Mountain Front Range, interior boreal spruce), short growing seasons limit energy inputs, but drought stress still occurs in summer.

15.3. Stress complexes and warmer climate

Temperature increases predispose forest ecosystems of western North America to often lethal stresses, acting both directly through increasingly negative water balances (Littell, 2006; Milne et al., 2002; Stephenson, 1998) and indirectly through increased frequency, severity, and extent of disturbances, chiefly fire and insect outbreaks (Logan et al., 2003; McKenzie et al., 2004). Here, we briefly present four examples of forest ecosystems whose species composition and stability are currently compromised by stress complexes precipitated by the recent period of warm dry weather. Two cases involve the loss of a single dominant species; the other two involve two or more dominant species.

15.3.1. Pinyon-juniper woodlands of the American Southwest

Pinyon pine (*Pinus edulis*) and various juniper species (*Juniperus* spp.) are among the most drought-tolerant trees in western North America. As such, pinyon-juniper ecosystems characterize lower treelines across much of the West. Although pinyon-juniper woodlands appear to be expanding in some areas, possibly due to fire suppression or cessation of Native American fuelwood harvesting (Samuels & Betancourt, 1982), they are clearly water-limited systems. At fine scales, pinyon-juniper ecotones are sensitive to feedbacks both from environmental fluctuations and existing canopy structure that may buffer trees against drought to some degree (Milne et al., 1996). Periodically, however, severe multi-year droughts cause massive dieback of pinyon pines, overwhelming any local buffering.

Dieback of pine species—both ponderosa and pinyon pine—occurred during and before the 20th century (Allen & Breshears, 1998; Breshears et al., 2005), but the current dieback is massive (Fig. 15.2), and its combination of low precipitation and high temperatures, indicative of global warming, is unprecedented (Breshears et al., 2005). Ecosystem

Figure 15.2. Massive dieback of pinyon pine in the Jemez Mountains, New Mexico. (Photo courtesy of Craig Allen, U.S. Geological Survey.)

change, possibly irreversible, comes from large-scale severe fires that lead to colonization of invasive species that further compromises the ability of pinyon pines to re-establish. This stress complex is illustrated in Fig. 15.3.

15.3.2. Mixed-conifer forests of the Sierra Nevada and southern California

These forests experience a Mediterranean climate. Summers are dry and long, with significant precipitation beginning around mid-October through most of the Sierra Nevada and later in the San Bernardino and San Gabriel Mountains of southern California. Increasing temperatures since 1850 contrast with a relatively cool (and dry) period from 1650 to 1850 (Briffa et al., 1992; Graumlich, 1993; Stine, 1996). Fire frequency and extent have not increased concomitantly with warmer temperatures (McKelvey et al., 1996), rather they have decreased to their lowest levels in the last 2000 years (Stine, 1996; Swetnam, 1993). Stine (1996) attributes this to decreased fuel loads from sheep grazing and decreased ignition from the demise of Native American cultures, leading to fire exclusion. Fire exclusion subsequently led to increased fuel loadings (McKelvey et al., 1996) and competitive stresses on individual trees as stand densities have increased (Ferrell, 1996; van Mantgem et al., 2004).

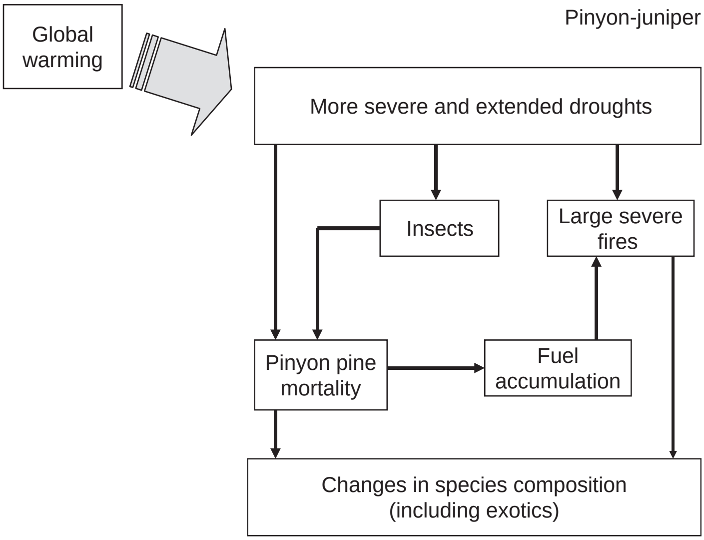

Figure 15.3. Stress complex in pinyon-juniper woodlands of the American Southwest. The effects of disturbance regimes (insects and fire) are exacerbated by global warming. Stand-replacing fires and drought-induced mortality both contribute to species changes and exotic invasions.

Elevated levels of ambient ozone (Fig. 15.4) have affected plant vigor in the Sierra Nevada and the mountains of southern California (Byternowicz & Grulke, 1992; Miller, 1992, 1996; Peterson & Arbaugh, 1988; Peterson et al., 1991). Ozone reduces net photosynthesis and growth (Peterson et al., 1991; Reich & Amundson, 1985), and ozone from vehicular and industrial sources in urban environments often concentrates at middle and upper elevations (Brace & Peterson, 1998) where mixed-conifer forests occur.

Sierra Nevada forests support endemic levels of a diverse group of insect defoliators and bark beetles, but bark beetles in particular have reached outbreak levels in recent years facilitated by protracted droughts (Ferrell, 1996). Ferrell (1996) refers to *biotic complexes* where bark beetles interact with root diseases and mistletoes. Dense stands, fire suppression, and new pathogens such as white pine blister rust (*Cronartium ribicola*) exacerbate both biotic interactions (van Mantgem et al., 2004) and drought stress. Figure 15.5 shows the stress complex associated with Sierra Nevada forest ecosystems, which is also likely applicable to the mountain ranges east and north of the Los Angeles basin. High stand densities and ozone generate more stress pathways than in the

Figure 15.4. Photochemical haze over Sequoia National Park, California, in October 2003. (Photo by Don McKenzie.)

southwestern pinyon-juniper complex, wherein drought, insects, and fire are the principal stressors.

15.3.3. Interior lodgepole pine forests

Lodgepole pine (*Pinus contorta* var. latifolia) is widely distributed across western North America. It is the dominant species over much of its range, forming nearly monospecific stands that are maintained either because poor soils preclude other species or through adapting to stand-replacing fires via cone serotiny (USDA, 1990). Lodgepole pine is the principal host of the mountain pine beetle (*Dendroctonus ponderosae*), and monospecific stands are vulnerable to massive mortality during beetle outbreaks.

Recent beetle outbreaks have caused extensive mortality across millions of hectares in western North America (Fig. 15.6; Logan & Powell, 2001), with large mature cohorts (age 70–80 yr) contributing to widespread vulnerability (Carroll, 2006). Warmer temperatures facilitate insect outbreaks in two ways: (1) drought stress makes trees more vulnerable to attack and (2) insect populations respond to increased temperatures by speeding up their reproductive cycles (e.g., to 1-year life

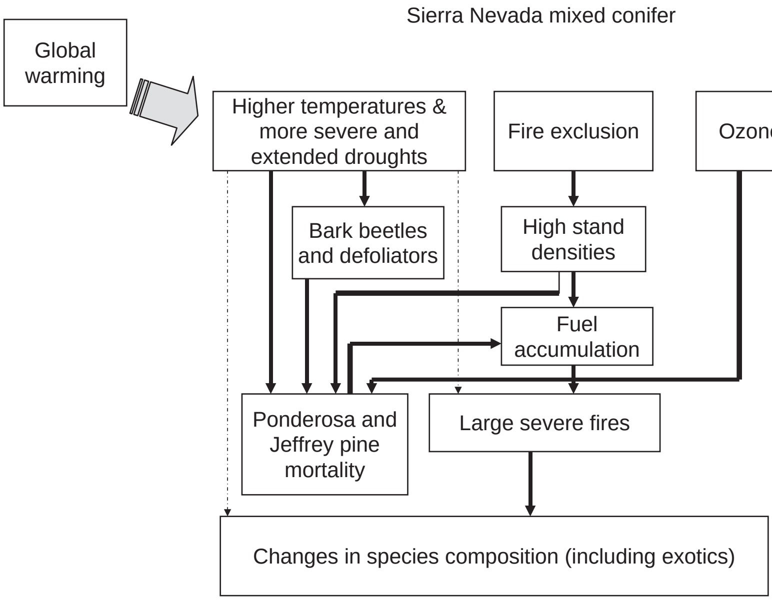

Figure 15.5. Stress complex in Sierra Nevada and southern Californian mixed-conifer forests. The effects of disturbance regimes (insects and fire) and fire exclusion are exacerbated by global warming. Stand-replacing fires and drought-induced mortality both contribute to species changes and exotic invasions.

cycles; Logan & Bentz, 1999; Logan & Powell, 2001; Werner & Holsten, 1985). Warming temperatures would be expected to exacerbate these already devastating outbreaks northward and even eastward across the continental divide (Logan et al., 2003, but see Hicke et al., 2006), but even at current levels of recent mortality lodgepole pine ecosystems may be poised for significant changes.

Figure 15.7 shows the stress complex for interior lodgepole pine forests. Warmer temperatures in combination with the greater flammability of dead biomass associated with beetle mortality sets up these ecosystems for extensive species conversion following stand-replacing fires plus a favorable environment for the establishment of species adapted to warmer temperatures, such as interior Douglas-fir or even ponderosa pine.

15.3.4. Alaskan forests

The state of Alaska has experienced massive fires in the last decade (Fig. 15.8), including the five largest fires in the United States (NIFC, 2006).

Figure 15.6. Massive lodgepole pine mortality from mountain pine beetles in south-central British Columbia, Canada. (Photo courtesy of Alan Carroll, Canadian Forest Service.)

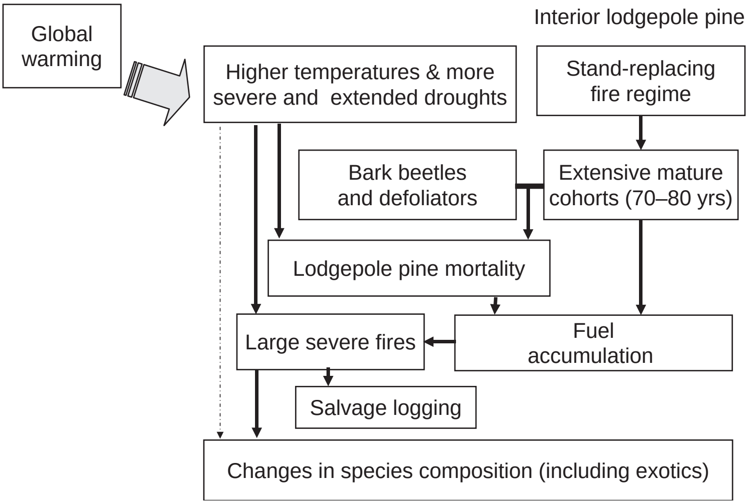

Figure 15.7. Stress complex in interior lodgepole pine forests (British Columbia and USA). The effects of disturbance regimes (insects and fire) are exacerbated by global warming. Stand-replacing fires, beetle mortality, and changes in environmental niche space contribute to species changes.

Over 2.5 million ha burned in the interior in 2004. Concurrently (1990s), massive outbreaks of the spruce bark beetle (*Dendroctonus rufipennis*) occurred on and near the Kenai Peninsula in south-central Alaska (Figs. 15.8, 15.9; Berg et al., 2006). Although periodic outbreaks have occurred throughout the historical record, both in south-central Alaska and the southwestern Yukon, these most recent outbreaks may be unprecedented in extent and percentage mortality (over 90% in many places; Berg et al., 2006; Ross et al., 2001).

Both these phenomena are likely associated with warmer temperatures in recent decades (Berg et al., 2006; Duffy et al., 2005; Werner et al., 2006). Summer temperatures in the Arctic have risen 0.3–0.4 °C per decade since 1961 (Chapin et al., 2005). Although fire-season length in interior Alaska is associated with the timing of onset of the late-summer monsoon, the principal driver of annual area burned is early summer temperature (Duffy et al., 2005). As with lodgepole pine, warmer temperatures have the same twofold effect on beetle outbreaks in spruce forests.

Disturbance regimes place unequal competitive stress on species most vulnerable to the particular disturbance. In the interior, conifer species—white spruce and black spruce (*Picea mariana*)—are more flammable than their sympatric deciduous species (chiefly paper birch (*Betula papyrifera*)). Similarly, conifers are the target of bark beetles, so in south-central Alaska they will be disadvantaged compared to deciduous species.

Permafrost degradation is widespread in central Alaska, shifting ecosystems from birch forests to wetland types such as bogs and fens (Jorgensen et al., 2001; T. Boucher, personal communication). The expected gain in area of deciduous forests from fire and insect mortality may be offset by the loss from permafrost degradation. If broad-scale water balances become increasingly negative, peatlands may begin to support upland forest species (Klein et al., 2005). Fire could play a major role in accelerating this ecosystem change by preparing seedbed for both conifer and deciduous tree species.

Figure 15.10 shows the stress complex for Alaska forest ecosystems, predicting a significant transition to deciduous life forms via more frequent and extensive disturbance associated with global warming, offset by the expected loss of some deciduous forests from permafrost degradation (Jorgensen et al., 2001), and subsequent or simultaneous potential conversion of peatlands to forests. These transitions would be unlikely without changes in disturbance regimes even under global warming, because both empirical and modeling studies suggest that warmer temperatures alone will not favor a life-form transition except in the case of permafrost loss (Bachelet et al., 2005; Boucher & Mead, 2006; Johnstone et al., 2004).

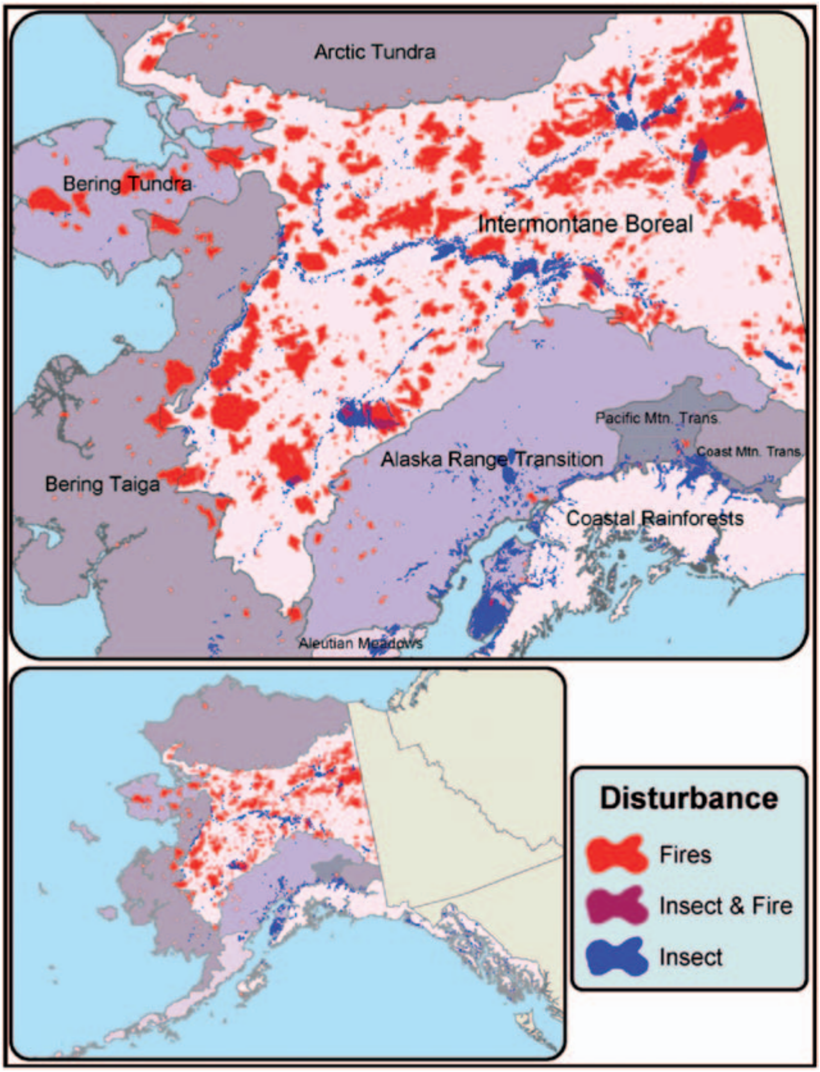

Figure 15.8. Recent wildfire and insect activity in Alaska. (Data from the Alaska Fire Service.)

15.4. Discussion

Rapid climatic change and qualitative changes in disturbance regimes may send ecosystems across thresholds into dominance by different life

Figure 15.9. Nearly complete stand mortality of white spruce (*Picea glauca*) from spruce bark beetle on the Kenai Peninsula, Alaska. (Photo courtesy of Diana Olson, USDA Forest Service.)

forms and significant changes in productivity and capacity for carbon storage. For example, in the Southwest, stand-replacing fires are becoming common in what were historically low-severity fire regimes (Allen et al., 2002), and protracted drought is killing species (ponderosa pine) that are adapted to low-severity fire (Allen & Breshears, 1998). If these trends continue, ponderosa pine may be lost from some of its current range in the Southwest, and productivity of these systems will decline. In contrast, if warming temperatures permit doubling of mountain pine beetle reproductive cycles (Logan & Powell, 2001) such that outbreaks are more frequent and more prolonged, lodgepole pine might be replaced by a more productive species such as Douglas-fir, at least on more mesic sites where conditions for establishment are favorable.

We expect that more ecosystems will become water-limited (Littell, 2006; Milne et al., 2002), more sensitive to variability in temperature, and prone to more frequent disturbance. Consequently, productivity may decline across much of the West (Hicke et al., 2002), and long-term carbon sequestration may be interrupted by an increasing area being subject to high-severity fire and insect-caused mortality. Species and ecosystems will be affected in various ways, and not all undesirable

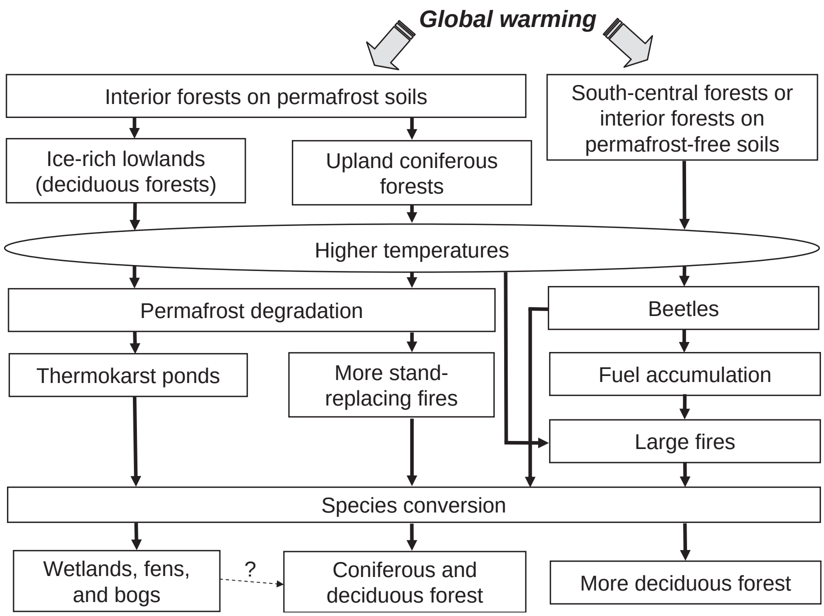

Figure 15.10. Stress complex in the interior and coastal forests of Alaska. Rapid increases in the severity of disturbance regimes (insects and fire) are triggered by global warming. Stand-replacing fires, massive mortality from insects, and permafrost degradation contribute to species changes and conversion to deciduous life forms.

changes will be preventable by management intervention (McKenzie et al., 2004).

The following adaptive strategies, however, may help in maintaining ecosystem resilience in some systems in which changes are not too abrupt or severe, although we caution that they are only suggestions whose value will have to be considered carefully for specific applications.

- *Use nursery stock tolerant to low soil moisture and high temperature*. With most systems moving toward being more water-limited, resistant individuals will be those from the drier and warmer provenances.
- *Use a variety of genotypes in nursery stock*. If we are unable to accurately predict local climatic trends, then the variety of genotypes will help maintain diversity when headed into an uncertain future that may include rapid climatic change.
- *Consider planting mixed-species stands*. This gives forests more ecological amplitude (i.e., the combined bioclimatic envelope is broader) to respond to climatic change.

- *Retain large downed logs on sites to moderate temperature and provide micro-refugia.* As landscape conditions become drier and warmer, interior habitat for mesic species will be lost and sensitive taxa will be more compromised (Carey & Alexander, 2003).

There is no historical or current analogue to the combination of climate conditions, disturbance regimes, and land-use changes expected for the next century. For example, tempering the idea of ''desired future conditions'' with ''achievable future conditions'' will facilitate more adaptive management and more efficient allocation of resources to maintain forest resilience. We have taken a small step here toward understanding potential disturbance interactions in forest ecosystems affected by global warming. Robust models are needed that can be tested with either simulation studies or ongoing natural ''experiments'' (Stephenson et al., 2006) to understand alternative future states in a rapidly changing world.

ACKNOWLEDGMENTS

We thank Constance Millar and Andrzej Byternowicz for providing the initial fora for the presentation of these ideas, and Tina Boucher and Kevin McKelvey for comments that substantially improved the manuscript. Alynne Bayard, Ellen Eberhardt, and Robert Norheim assisted with graphics. This research was funded by the USDA Forest Service, Pacific Northwest Research Station, the USGS Global Change Research Program, and the Joint Institute for the Study of the Atmosphere and Ocean under cooperative agreement NA178RG11232 of the National Oceanic and Atmospheric Administration. This is a contribution of the Western Mountain Initiative.

REFERENCES

Allen, C.D., and Breshears, D.D. 1998. Drought-induced shift of a forest-woodland ecotones: Rapid landscape response to climate variation. Proc. Nat. Acad. Sci., USA 95, 14839–14842.

Allen, C.D., Savage, M., Falk, D.A., Suckling, K.F., Swetnam, T.W., Schulke, T., Stacey, P.B., Morgan, P., Hoffman, M., and Klingeli, J.T. 2002. Ecological restoration of southwestern ponderosa pine ecosystems: A broad perspective. Ecol. Appl. 12, 1418–1433.

Bachelet, D., Lenihan, J., Neilson, R.P., Drapek, R., and Kittel, T. 2005. Simulating the response of natural ecosystems and their fire regimes to climatic variability in Alaska. Can. J. For. Res. 35, 2244–2257.

Berg, E.E., Henry, J.D., Fastie, C.L., de Volder, A.D., and Matsuoka, S.M. 2006. Spruce beetle outbreaks on the Kenai Peninsula, Alaska, and Kluane National Park and Reserve, Yukon Territory: Relationship to summer temperatures and regional differences in disturbance regimes. For. Ecol. Manage. 227, 219–232.

Bigler, C., Kulakowski, D., and Veblen, T.T. 2005. Multiple disturbance interactions and drought influence fire severity in Rocky Mountain subalpine forests. Ecology 86, 3018–3029.

Boucher, T.V., and Mead, B.R. 2006. Vegetation change and forest regeneration on the Kenai Peninsula, Alaska, following a spruce beetle outbreak, 1987–2000. For. Ecol. Manage. 227, 233–246.

Brace, S., and Peterson, D.L. 1998. Tropospheric ozone distribution in the Mount Rainier region of the Cascade Mountains, U.S.A. Atmos. Environ. 32, 3629–3637.

Breshears, D.D., Cobb, N.S., Rich, P.M., Price, K.P., Allen, C.D., Balice, R.G., Romme, W.H., Kastens, J.H., Floyd, M.L., Belnap, J., Anderson, J.J., Myers, O.B., and Meyer, C.W. 2005. Regional vegetation die-off in response to global-change-type drought. Proc. Nat. Acad. Sci., USA 102, 15144–15148.

Briffa, K.R., Jones, P.D., and Schweingruber, F.H. 1992. Tree-ring density reconstructions of summer temperature patterns across western North America since 1600. J. Climate 5, 735–754.

Byternowicz, A., and Grulke, N.E. 1992. Physiological effects of air pollutants on western trees. In: Olson, R.K., Binkley, D., and Böhm, M., eds. Response of Western forests to air pollution. Springer-verlag, New York, pp. 183–233.

Carey, C., and Alexander, M.A. 2003. Climate change and amphibian declines: Is there a link? Divers. Dist. 9, 111–121.

Carroll, A. 2006. Changing the climate, changing the rules: Global warming and insect disturbance in western North American forests. Paper presented at the 2006 MTNCLIM conference, Timberline, OR.

Chapin, F.S. III, Sturm, M., Serreze, M.C., McFadden, J.P., Key, J.R., Lloyd, A.H., McGuire, A.D., Rupp, T.S., Lynch, A.H., Schimel, J.P., Beringer, J., Chapman, W.L., Epstein, H.E., Euskirchen, E.S., Hinzman, L.D., Jia, G., Ping, C.-L., Tape, K.D., Thompson, C.D.C., Walker, D.A., and Welker, J.M. 2005. Role of land-surface changes in Arctic summer warming. Science 28, 657–660.

Cushman, S.C., McKenzie, D., Littell, J.S., and Peterson, D.L. 2007. Climatic change, fire, and ecosystems: A research agenda for landscape modeling. USDA Forest Service Research Paper RMRS-194, Rocky Mountain Research Station, Fort Collins, CO.

Duffy, P.A., Walsh, J.E., Graham, J.M., Mann, D.H., and Rupp, T.S. 2005. Impacts of large-scale atmospheric-ocean variability on Alaskan fire season severity. Ecol. Appl. 15, 1317–1330.

Ferrell, G.T. 1996. The influence of insect pests and pathogens on Sierra forests. In: Sierra Nevada Ecosystem Project: Final report to Congress, vol. II, Assessments and scientific basis for management options. University of California, Centers for Water and Wildland Resources, Davis, CA, 1177–1192.

Franklin, J. 1995. Predictive vegetation mapping: Geographical modeling of biospatial patterns in relation to environmental gradients. Prog. Phys. Geog. 19, 474–499.

Gedalof, Z., Peterson, D.L., and Mantua, N. 2005. Atmospheric, climatic, and ecological controls on extreme wildfire years in the northwestern United States. Ecol. Appl. 15, 154–174.

Graumlich, L.J. 1993. A 1000-year record of temperature and precipitation in the Sierra Nevada. Quatern. Res. 39, 249–255.

Guisan, A., and Zimmermann, N.E. 2000. Predictive habitat distribution models in ecology. Ecol. Modell. 135, 147–186.

Hessl, A.E., McKenzie, D., and Schellhaas, R. 2004. Drought and pacific decadal oscillation linked to fire occurrence in the Inland Pacific Northwest. Ecol. Appl. 14, 425–442.

Hicke, J.A., Asner, G.P., Randerson, J.T., Tucker, C., Los, S., Birdsey, R., Jenkins, J.C., and Field, C. 2002. Trends in North American net primary productivity derived from satellite observations. Glob. Biogeochem. Cycles 16,2,1018, 10.1029/2001GB001550.

Hicke, J.A., Logan, A., Powell, J.A., and Ojima, D.S. 2006. Changes in temperature influence suitability for modeled mountain pine beetle (*Dendroctonus ponderosae*) outbreaks in the western United States. JGR Biogeosciences. J. Geophys. Res. III, G02019, doi:10.1029/2005JG000101.

IPCC (Intergovernmental Panel on Climate Change). 2007. Climate change 2007: The physical science basis. Summary for policymakers. http://www.ipcc.ch

Johnson, E.A., and Wowchuk, D.R. 1993. Wildfires in the southern Canadian rocky mountains and their relationships to mid-tropospheric anomalies. Can. J. For. Res. 23, 1213–1222.

Johnstone, J.F., Chapin III, F.S., Foote, J., Kemmett, S., Price, K., and Viereck, L. 2004. Decadal observations of tree regeneration following fire in boreal forests. Can. J. For. Res. 34, 267–273.

Jorgensen, M.T., Racine, C.H., Walters, J.C., and Osterkamp, T.E. 2001. Permafrost degradation and ecological changes associated with a warming climate in central Alaska. Clim. Change 48, 551–579.

Klein, E., Berg, E.E., and Dial, R. 2005. Wetland drying and succession across the Kenai Peninsula Lowlands, south-central Alaska. Can. J. For. Res. 35, 1931–1941.

Littell, J.S. 2006. Climate impacts to forest ecosystem processes: Douglas-fir growth in northwestern U.S. mountain landscapes and area burned by wildfire in western U.S. ecoprovinces. Ph.D. dissertation, University of Washington, Seattle. 171 pp.

Littell, J.S., and Peterson, D.L. 2005. A method for estimating vulnerability of Douglas-fir growth to climate change in the northwestern US. For. Chron. 81, 369–374.

Logan, J.A., and Bentz, B.J. 1999. Model analysis of mountain pine beetle (Coleoptera: Scolytidae) seasonality. Environ. Entomol. 28, 924–934.

Logan, J.A., and Powell, J.A. 2001. Ghost forests, global warming, and the mountain pine beetle (Coleoptera: Scolytidae). Am. Entomol. 47, 160–172.

Logan, J.A., Regniere, J., and Powell, J.A. 2003. Assessing the impacts of global warming on forest pest dynamics. Fron. Ecol. Environ. 1, 130–137.

McKelvey, K.S., Skinner, C.N., Chang, C., Etman, D.C., Husan, S.J., Parsons, D.J., van Wagtendonk, J.W., and Weatherspoon, C.P. 1996. An overview of fire in the Sierra Nevada. In: Sierra Nevada Ecosystem Project: Final report to Congress, vol. II, Assessments and scientific basis for management options. University of California, Centers for Water and Wildland Resources, Davis, CA, 1033–1040.

McKenzie, D., Hessl, A.E., and Peterson, D.L. 2001. Recent growth in conifer species of western North America: Assessing the spatial patterns of radial growth trends. Can. J. For. Res. 31, 526–538.

McKenzie, D., Peterson, D.W., Peterson, D.L., and Thornton, P.E. 2003. Climatic and biophysical controls on conifer species distributions in mountain forests of Washington State, USA. J. Biogeogr. 30, 1093–1108.

McKenzie, D., Gedalof, Z.M., Peterson, D.L., and Mote, P. 2004. Climatic change, wildfire, and conservation. Conserv. Biol. 18, 890–902.

Miller, P.R. 1992. Mixed conifer forests of the San Bernardino Mountains, California. In: Olson, R.K., Binkley, D., and Böhm, M., eds. Response of Western forests to air pollution. Springer-Verlag, New York, pp. 461–497.

Miller, P.R. 1996. Biological effects of air pollution in the Sierra Nevada. In: Sierra Nevada Ecosystem Project: Final report to Congress, vol. II, Assessments and scientific basis for management options. University of California, Centers for Water and Wildland Resources, Davis, CA, 885–900.

Milne, B.T., Johnson, A.R., Keitt, T.H., Hatfield, C.A., David, J., and Hraber, P.T. 1996. Detection of critical densities associated with pinyon-juniper woodland ecotones. Ecology 77, 805–821.

Milne, B.T., Gupta, V.K., and Restrepo, C. 2002. A scale-invariant coupling of plants, water, energy, and terrain. EcoScience 9, 191–199.

Neilson, R.P., Pitelka, L.F., Solomon, A.M., Nathan, R., Midgley, G.F., Fragoso, J.M.V., Lischke, H., and Thompson, K. 2005. Forecasting regional to global plant migration in response to climate change. BioScience 55, 749–759.

NIFC (National Interagency Fire Center). 2006. http://www.nifc.gov.

Pearson, R.G., and Dawson, T.P. 2003. Predicting the impacts of climate change on the distribution of species: Are bioclimate envelope models useful? Global Ecol. Biogeogr. 12, 361–371.

Peterson, D.L., and Arbaugh, M.J. 1988. Growth patterns of ozone-injured ponderosa pine (*Pinus ponderosa*) in the southern Sierra Nevada. J. Air Pollut. Control Assoc. 38, 921–927.

Peterson, D.L., Arbaugh, M.J., and Robinson, L.J. 1991. Growth trends of ozone-stressed ponderosa pine (*Pinus ponderosa*) in the Sierra Nevada of California, USA. The Holocene 1, 50–61.

Peterson, D.W., and Peterson, D.L. 2001. Mountain hemlock growth responds to climatic variability at annual and decadal scales. Ecology 82, 3330–3345.

Reich, P.B., and Amundson, R.G. 1985. Ambient levels of ozone reduce net photosynthesis in tree and crop species. Science 230, 566–570.

Ross, D.W., Daterman, G.E., Boughton, J.L., and Quigley, T.M., 2001. Forest health restoration in south-central Alaska: A problem analysis. USDA Forest Service General Technical Report PNW-GTR-523, Pacific Northwest Research Station, Portland, OR.

Samuels, M.L., and Betancourt, J.L. 1982. Modeling the long-term effects of fuelwood harvest on piñon-juniper woodlands. Environ. Manage. 6, 505–515.

Skinner, W.R., Stocks, B.J., Martell, D.L., Bonsal, B., and Shabbar, A. 1999. The association between circulation anomalies in the mid-troposphere and area burned by wildfire in Canada. Theor. Appl. Climatol. 63, 89–105.

Stephenson, N.L. 1990. Climatic control of vegetation distribution: The role of the water balance. Am. Nat. 135, 649–670.

Stephenson, N.L. 1998. Actual evapotranspiration and deficit: Biologically meaningful correlates of vegetation distribution across spatial scales. J. Biogeogr. 25, 855–870.

Stephenson, N.L., Peterson, D.L., Fagre, D., Allen, C.D., McKenzie, D., Baron, J.S., and O'Brian, K. 2006. Response of western mountain ecosystems to climatic variability and change: The western mountain initiative. Park Sci. 24, 24–29.

Stine, S. 1996. Climate, 1650–1850. In: Sierra Nevada Ecosystem Project: Final report to Congress, vol. II, Assessments and scientific basis for management options. University of California, Centers for Water and Wildland Resources, Davis, CA, 25–30.

Swetnam, T.W. 1993. Fire history and climate change in giant sequoia groves. Science 262, 885–889.

Swetnam, T.W., and Lynch, A.M. 1993. Multicentury regional-scale patterns of western spruce budworm outbreaks. Ecol. Monogr. 63, 399–424.

Swetnam, T.W., and Betancourt, J.L. 1998. Mesoscale disturbance and ecological response to decadal climatic variability in the American Southwest. J. Climate 11, 3128–3147.

USDA (United States Department of Agriculture) Forest Service. 1990. Silvics of North America: Volume 1. Conifers. USDA Forest Service, Agriculture Handbook, vol. 54, Russell M. Burns and Barbara H. Honkala (Coordinators) USDA, Washington, DC.

van Mantgem, P.J., Stephenson, N.L., Keifer, M., and Kelley, J. 2004. Effects of an introduced pathogen and fire exclusion on the demography of sugar pine. Ecol. Appl. 14, 1590–1602.

Veblen, T.T., Hadley, K.S., Reid, M.S., and Rebertus, A.J. 1991. The response of subalpine forests to spruce beetle outbreak in Colorado. Ecology 72, 213–231.

Veblen, T.T., Hadley, K.S., Nel, E.M., Kitzberger, T., Reid, M., and Villalba, R. 1994. Disturbance regimes and disturbance interactions in a Rocky Mountain subalpine forest. J. Ecol. 82, 125–135.

Veblen, T.T., Kitzberger, T., and Donnegan, J. 2000. Climatic and human influences on fire regimes in ponderosa pine forests in the Colorado Front Range. Ecol. Appl. 10, 1178–1195.

Weber, U., and Schweingruber, F.H. 1995. A dendroecological reconstruction of western spruce budworm outbreaks (*Choristoneura occidentalis*) in the Front Range, Colorado, from 1720 to 1986. Tree 9, 204–213.

Werner, R.A., and Holsten, E.H. 1985. Factors influencing generation times of spruce beetles in Alaska. Can. J. For. Res. 15, 438–443.

Werner, R.A., Holsten, E.H., Matsuoka, S.M., and Burnside, R.E. 2006. Spruce beetles and forest ecosystems in south-central Alaska: A review of 30 years of research. For. Ecol. Manage. 227, 195–206.

Westerling, A.L., Hidalgo, H.G., Cayan, D.R., and Swetnam, T.W. 2006. Warming and earlier spring increase western U.S. forest wildfire activity. Science 313, 940–943.

Woodward, F.I. 1987. Climate and Plant Distribution. Cambridge University Press, London.

Woodward, F.I., and McKee, I.F. 1991. Vegetation and climate. Environ. Int. 17, 535–546.

This page intentionally left blank

Developments in Environmental Science, Volume 8

A. Bytnerowicz, M. Arbaugh, A. Riebau and C. Andersen (Editors)

ISSN: 1474-8177/DOI:10.1016/S1474-8177(08)00016-8

Chapter 16

A Probabilistic View of Chaparral and Forest Fire Regimes in Southern California and Northern Baja California

Richard A. Minnich and Ernesto Franco-Vizcaíno*

Abstract

Fire suppression in industrialized countries encourages massive smoke emissions from high-intensity fires as a result of two inextricably related processes under current suppression policies: the nonrandom occurrence of vegetation fires in extreme weather states and the anomalous accumulation of spatially homogenous fuels. We propose as an organizing idea that the natural long-term cumulative distribution of fires is focused by chance on modal weather states. Thus, while individual fires are each associated with unique combinations of weather and fuel conditions, vegetation mosaics are expressed in self-organized, stable distributions in the size, interval, and frequency of fires. Here we evaluate fire regimes by using spatially explicit data for chaparral and conifer forests and compare southern California (SCA) fire history under suppression with fire history produced by free-running fire (little or no suppression) in neighboring Baja California (BCA), Mexico. In SCA, suppression has reduced the number of fires, while increasing the size of old-growth patch elements and thus the spatial extent of subsequent fires. The selective dousing of fires starts nonrandomly limits extensive burning to rare periods of extreme weather. Free-running fires formerly spread in a broad spectrum of mostly normal weather over spans of months during summer and fall. This long forgotten property of fire regimes in California is still an ongoing property in BCA. Because plant response to perturbations depends on the cumulative effects of plant successions, those who study climatic relationships with fire regimes should consider the long-term dynamics of fuel accumulation as a source of outbreaks in vegetation mosaics. The development of fire

*Corresponding author: E-mail: richard.minnich@ucr.edu

management policies by the Mexican authorities should consider continued maintenance of the current fine-grained vegetation mosaic that is resistant to extensive fires.

16.1. Introduction

Wildland fire and smoke emissions occur in most of the world's vegetation (Golddammer, this volume; Moderate Resolution Imaging Spectroradiometer (MODIS) Rapid Response System: http://rapidfire.sci.gsfc.nasa.gov). While studies currently focus on possible increases in global ambient carbon from anthropogenic burning, fire suppression in industrialized countries also affects smoke emissions from vegetation fires. The systematic extinguishing of fire-starts exacerbates fire size and intensity. When fire cannot be contained, massive smoke emissions from high-intensity fires result from two inextricably related processes under current suppression policies: the nonrandom occurrence of vegetation fires in extreme weather states and the anomalous accumulation of spatially homogenous fuels.

In the southern end of the Mediterranean-climate (winter precipitation and summer drought) region of the North American Pacific coast, fire suppression in southern California (SCA), USA, has been associated with infrequent wind-driven fires (shallow mixing) that create coarse-grained burn mosaics. Dry, offshore Santa Ana winds advect smoke along surface air layers over urbanized coastal plains and valleys (Fig. 16.1). In neighboring Baja California (BCA), Mexico, which is rapidly urbanizing but still retains much of its original vegetation, free-running fire has been associated with frequent small blazes. These are pushed by prevailing onshore winds, resulting in fine-grained patch mosaics, with thin smoke layers that are often convected into the upper air layers (deep mixing). These smoke layers frequently disperse eastwards, away from population centers and toward the Sonoran Desert (Fig. 16.1; Minnich, 2006). In BCA, chaparral and mountain conifer forests burn two to three times per century (30- to 70-year intervals), but fires are nonrandomly constrained in self-organizing patch mosaics in which vegetation that has not burned over long periods is preferentially burned, in contrast to surrounding younger vegetation (Minnich, 1983; Minnich & Chou, 1997).

The self-organization of patch emplacement over long time scales can be understood from a probabilistic perspective, while recognizing the unpredictability of fires at short time scales. Large differences in fire outcomes can arise from the timing of fire-starts, becoming in effect a natural Monte Carlo experiment. While chaparral and forests gradually attain flammability at time scales of decades to centuries, fires are

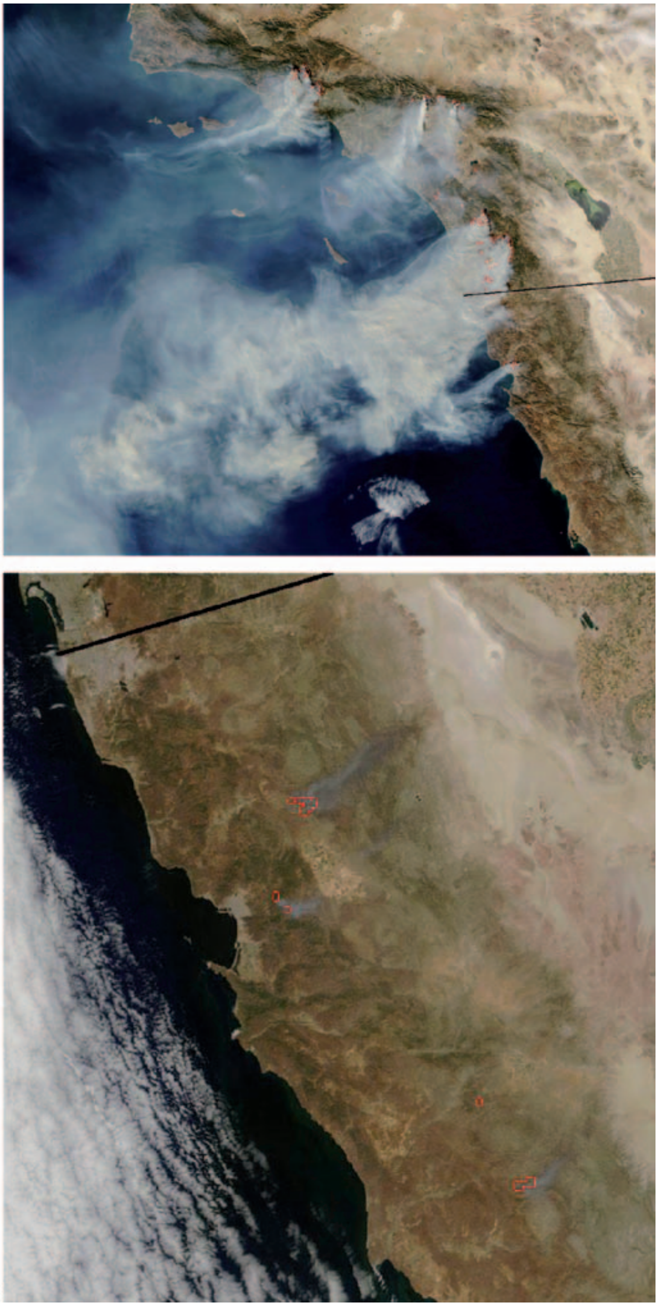

(a)

(b)

Figure 16.1. Smoke from chaparral fires in (a) southern California, October 26, 2003, and (b) Baja California, July 6, 2005. Areas in active burning are outlined in red. The U.S.–Mexico boundary is shown by black line. (Source: MODIS: rapidfire.sci.gsfc.nasa.gov)

triggered by "instantaneous" ignitions under a wide range of weather conditions, with divergent outcomes. This is the dilemma of fire ecologists seeking to discover the modal properties of fire regimes. It is also the dilemma of fire suppression policy. The nonrandom snuffing out of small fires, a selective process, causes unintended adjustments in the severity and size of subsequent fires, as well as to the structure of vegetation mosaics.

We propose as an organizing idea, that the natural long-term cumulative distribution of fires is focused by chance on modal weather states. Thus, while individual fires are each associated with unique combinations of weather and fuel conditions, vegetation mosaics are expressed in self-organized, stable distributions in the size, interval, and frequency of fires. The parameters that contribute to fire and patch dynamics include vegetation growth and fuel accumulation rates, stand-age thresholds for combustion, fuel properties and combustion of plant assemblages, ignition fluxes and fire establishment rates, fire weather, and self-organization of fire sequences.

In California, a research goal in fire ecology has been to develop databases on these properties of fire regimes prior to their alteration by land use and management. Currently, information on presuppression fire is fragmentary, site-specific, and retrospective because suppression has moved ecosystems away from presuppression states (see review in Minnich, 2007). Here we evaluate fire regimes by using spatially explicit data for chaparral and conifer forests and by comparing SCA fire history under suppression with fire history produced by free-running fires (little or no suppression) in BCA, Mexico. A divergence in fire regimes has persisted between these two otherwise similar regions since the early 20th century (Minnich & Chou, 1997). This "natural" experiment—caused by societal differences in land use and management—allows us to examine the response of fire and patch dynamics, as fire parameters have been changed by fire suppression policy.

16.2. Characteristic vegetation, patch mosaic dynamics, threshold of combustion, and fire weather window

Vegetation is similar from the east–west Transverse ranges north of Los Angeles and down the north–south Peninsular Range southward into BCA. Assemblages adapted to moist habitats gradually become less extensive and occur at higher elevations with decreasing latitude (Minnich, 2007; Minnich & Franco-Vizcaíno, 1998). Hillslopes from below 1500 to 2000 m are covered with extensive carpets of chaparral dominated by *Adenostoma fasciculatum* (chamise), *Adenostoma sparsifolium*, and members of *Ceanothus*, *Arctostaphylos*, and *Quercus*, with patches of serotinous conifer forests that include *Pinus coulteri*, *Pinus attenuata*, *Pinus muricata*, *Cupressus forbesii*, and *Cupressus arizonica*, as well as the nonserotinous pinyon *Pinus quadrifolia*. Basins and canyons contain woodlands of *Quercus agrifolia* and *Q. engelmannii*, with galleries of *Populus fremontii*, *Platanus racemosa*, *Alnus rhombifolia*, and *Acer macrophyllum* along streamcourses. Mixed evergreen forests of *Pseudotsuga macrocarpa* and *Q. chrysolepis* grow in canyons and north-facing slopes from near Santa Barbara to the mountains east of San Diego. *Q. chrysolepis* continues southward in canyons and rocky sites in BCA where it is joined by *Q. peninsularis*. Above 1500–2000 m chaparral gives place to mixed-conifer forest dominated by *Pinus jeffreyi*, *P. lambertiana*, *Abies concolor*, and *Calocedrus decurrens*. *P. ponderosa* is locally common in SCA, but does not occur in BCA, and conversely *Cupressus montana* is endemic to the Sierra San Pedro Mártir (SSPM) in BCA.

To explain differences in chaparral and forest fire regimes between SCA and BCA, a model that integrates fire weather and fuel-driven patch mosaics was proposed by Minnich (1983), Minnich and Chou (1997), and Minnich (2001). Self-organized mosaics composed of vegetation of different ages characterize the chaparral and mixed-conifer forest in BCA. In BCA chaparral, frequent stand-replacement fires produce fine-grained mosaics and discrete local-scale heterogeneity of fuels, with site-specific intervals of about two to three events per century. These mosaics are an outcome of time-dependent fuel accumulation within self-organized mosaics of patches that have burned at different times (Fig. 16.2). In SCA, suppression has reduced the number of fires, while increasing the size of old-growth patch elements and thus the spatial extent of subsequent fires. Fires nevertheless still spread in old stands, and site-specific fire intervals also average about two events per century (Wells et al., 2004). Self-organized mosaics develop from intense surface fires in mixed-conifer forest of BCA (Minnich et al., 2000). In SCA, suppression has excluded fire from most mixed-conifer forest since the late 19th century, resulting in massive increases in forest density and catastrophic stand-replacement fires (Goforth & Minnich, 2008; Minnich et al., 1995).

The threshold of flammability is coupled to fuel accumulation, increased leaf area, and greater transpiration in the later stages of plant successions. Fires consistently consume old stands, but are constrained in young stands because limited fuels narrow the "fire weather window" to the most extreme dry periods. The structure of shifting mosaics is locally modified in response to the unique weather states of individual fires (Minnich, 2006).

Nonrandom patch emplacement is explained from first principles of thermodynamics. Fires occur when the potential heat energy of

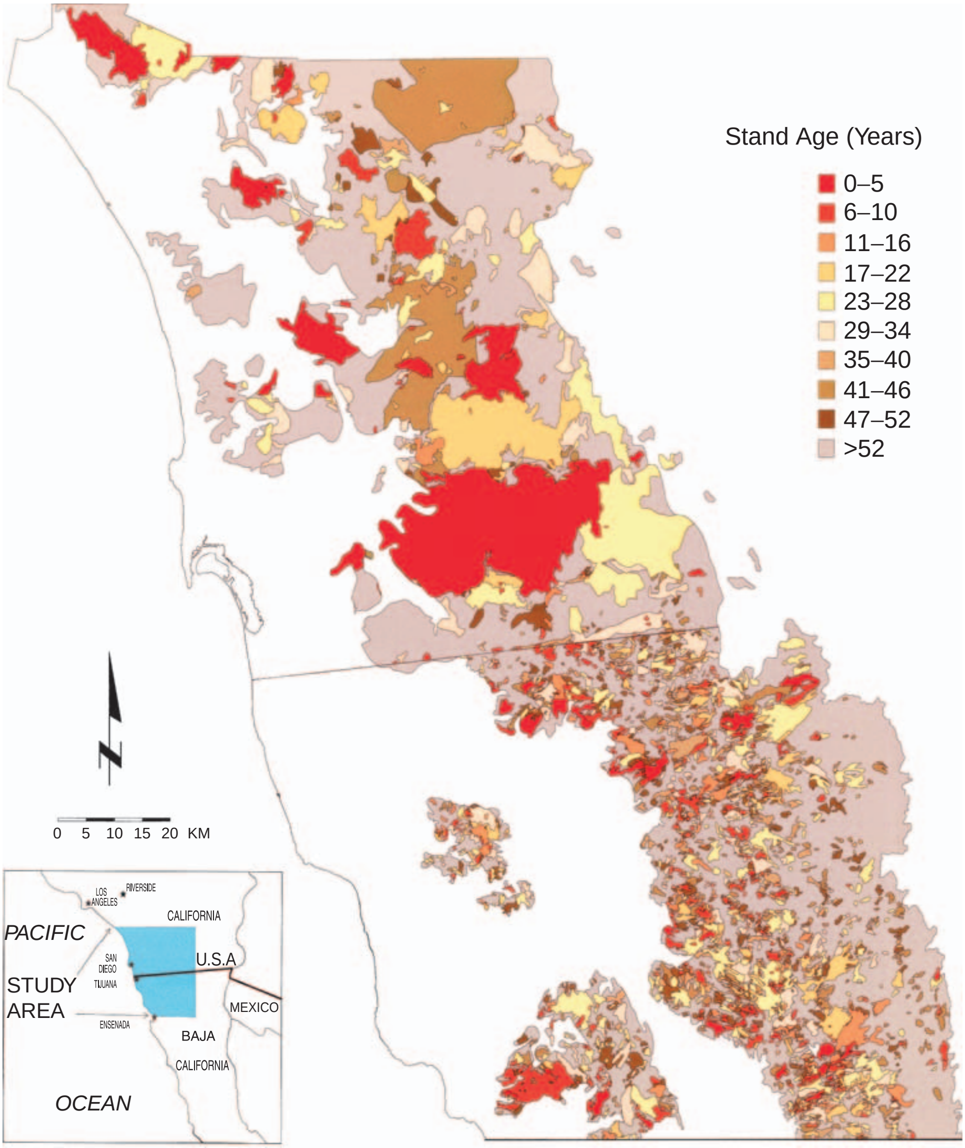

Figure 16.2. Chaparral patch mosaic in southern California and northern Baja California in 1971 (from Minnich & Chou, 1997). The current situation on the ground has been greatly altered by subsequent fires (see Fig. 16.1).

accumulated standing live and dead biomass exceeds the heat capacity of plant water content, i.e., the calorie-to-water ratio is >1 (Rothermel, 1972; Scott & Burgan, 2005). Riggan et al. (1988) proposed that, in chaparral, the expanding foliage area promotes seasonal drying, thus hastening the date of onset of seasonal drought stress with advancing stage of succession. This process increases the ratios of dead-to-live fuels in phase with fuel accumulation (Barro & Conard, 1991; Rundel, 1983; Sparks et al., 1993).

The fire weather window at a site is the full range of weather conditions capable of propagating fires, from a moist threshold to the driest weather of the climate (Fig. 16.3). Fire is unlikely in early successions because low biomass (available calories) coincides with low canopy leaf area and transpiration demand, thereby maximizing plant water. This results in a deficit in the ratio of carbohydrate calories to plant water calories as a heat sink (<1). The weather window enlarges gradually with time-since-fire due to cumulative fuel build-up, increasing dead fuel content, and increasing canopy transpiration that reduces live fuel moisture. The

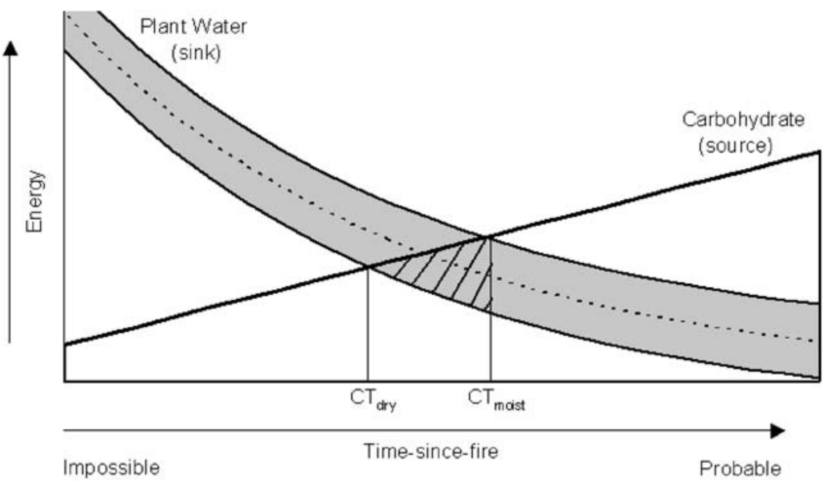

Figure 16.3. A conceptual model of carbohydrate (fuel) and plant-available water during postfire succession. The *y*-axis shows the biomass carbohydrate energy as a heat source and the energy of water as a heat sink. Carbohydrate increases linearly with cumulative growth of vegetation canopy. Average plant-available water (dashed line) decreases due to increasing leaf area and evapotranspiration demand but over a broad range (shaded belt) in response to short-term weather, seasonal drought, and interannual precipitation variability. Fires occur when carbohydrate as a heat source for combustion exceeds plant-available water as a heat sink. The fire weather window (hachured area) is limited to extreme weather states in early succession (CT dry) and expands into normal weather in later succession (CT wet). CT is the threshold of combustion.

different weather windows that result for each stand-age class contribute to the nonrandom turnover of patch mosaics. More extreme weather-risk states are required to burn vegetation in early successions than in later mature phases. Keeley et al. (1999) state that fires burn chaparral at any age, noting that fires overlap previous boundaries as young as a few years. However, local short-period overlap results from the momentum of fires crossing from old to young stands, and these incursions rarely extend far into young stands in transitions from older to younger stands (Minnich & Chou, 1997). In their work, edge effects are weighed instead of the whole landscape.

Rates of patch emplacement vary along climatic gradients. In BCA, chaparral on moist windward slopes of mountain ranges burns more frequently (high burn density per time with intervals of two to three events per century) than chaparral/pinyon woodlands on rain-shadowed leeward slopes (low burn density per time with <1 event per century) because productivity and fuel build-up rates are proportional to mean annual precipitation. Nearly contiguous burns from the coastal range to the crest of the interior range thin to scattered burns on the eastern escarpment (Fig. 16.2). Similarly, SCA chaparral has burned one to three times in the 20th century, while pinyon-juniper woodlands burned at rates of less than one per century in the same period (Minnich & Chou, 1997; Wangler & Minnich, 1996; Wells et al., 2004). The discontinuity in patch structure from BCA to SCA cannot be explained by climatic gradients because the fire regime discontinuity shifts from north-to-south, while gradients in temperature and precipitation run west-to-east in response to elevation gradients (Minnich & Chou, 1997). Alternatively, the transnational discontinuity is related to differences in fire establishment rates with management systems, which is seminal to differences in the size and number of fires, as well as fire weather.

The initial fire start is an intensely selective process. Suppression would have no effect (be random) on the weather of fires only if the firefighting system had a uniform capacity to influence the spread of flame lines, regardless of fire size or state of weather risk. This premise is unrealistic because the effectiveness of suppression energy produced to mitigate fire (clearing fuels, aerial placement of water drops or retardants) is dependent on the energy output of flame lines. Suppression influences fire primarily at the ignition phase (firefighting at the "initial attack" phase, i.e., surrounding fire-starts) when the fire is within the bounds of management. All fires begin at low rates of energy release, and then increase exponentially with increasing length of flame lines and rates of spread. Suppression forces extinguish practically all ignitions at <1 ha, but have little effect on escaped large fires because their energy release rates exceed the capacity for suppression by orders of magnitude. With free-running fire in BCA, random temporal fire occurrence in a modal weather state is a plausible assumption because lightning occurs in predictable atmospheric states. Deliberate burning does not produce nonrandom effects because human fire-starts take place at different times, with different effectiveness. Even circumstances of malicious burns timed to coincide with extreme weather would be mitigated by heterogeneous fuels of a fine-grained patch mosaic.

The probability that ignitions establish wildfires depends on the age and size of patch elements. Ignitions in recently burned patches not only have less chance of establishing fires than in old burns, but ignition success is also dependent on target size, as shown in the equation.

$$I_{\mathrm{p}} = (I_{\mathrm{ltg}} + I_{\mathrm{anth}})P\,F$$

where I_{p} is the patch ignition rate or number of ignitions in a patch per fire cycle (number of events $\mathrm{km}^{-2}\,\mathrm{yr}^{-1}$), I_{ltg} the lightning detection rate (number of events $\mathrm{km}^{-2}\,\mathrm{yr}^{-1}$), I_{anth} the anthropogenic ignition rate (number of human ignitions $\mathrm{km}^{-2}\,\mathrm{yr}^{-1}$), P patch size (km^2), and F the vegetation fuel threshold, or the time required for vegetation to become flammable (yr) (Minnich, 2006). The equation holds that the proportion of ignitions that initiate fires is proportional to patch size but inversely related to flammability thresholds. Few ignitions establish fires of significant size in early successional states, even without fire control, for lack of fuel. If we consider only natural ignitions, at lightning detection rates of $1.0\,\mathrm{km}^{-2}\,\mathrm{year}^{-1}$ over a 50-year fire cycle (Minnich, 2006), a 1000 ha patch—the modal size in BCA—is struck about 500 times. At this rate, large patch targets in SCA (e.g., 10,000 ha) would experience 5000 strikes because of their size.

A universal property of fire regimes is that most ignitions fail to grow into "large fires" because of insufficient fuel. In BCA the number of large fires (>15 ha) is nearly an order of magnitude greater than in SCA, but the fine-grained mosaic in BCA represents relatively few fires as a proportion of the total ignition flux, about 1% of the natural ignition frequency. In the San Bernardino and San Jacinto Mountains of SCA the ratio of lightning fires to lightning detection rates varies annually from 1–11%, with ratios inversely related to lightning detection rates (Minnich, 2006). Increases in ignition rates due to anthropogenic ignition sources or temporal fluctuations in thunderstorm activity may shorten fire intervals by reducing the time lag between the threshold of combustion and ignition, but with diminishing returns created by the vegetation threshold which is related to the time-since-burn and moisture content. Increasingly fine-grained mosaic fragmentation approaches a theoretical limit in which infinitely numerous small fires account for an infinitely small burn area, i.e., target size and ignition success approach zero.

The view that ignitions are a ''cause'' of fires is a valid perspective only at instantaneous time scales but represents an error in first-cause logic that biases human perception to short-term fire processes, rather than the long-term accumulation of fuel through photosynthesis. A broad view requires consideration of the reverse: large fires, by removing fuel, influence the success of future ignitions. Studies that associate fire ''cause'' with individual fire areas, using records of fire management agencies (e.g., Stephens, 2005) are narrow and simplistic because this approach does not account for vegetation status (long-term cumulative fuel build-up) at the ignition site. Individual fire-starts provide little explanation of fire regimes because most fail to establish large landscape fires. An analogy would be to evaluate snow avalanching by counting snowflakes. While any one snow crystal may produce the weight that initiates downslope movement, the energy release of the avalanche would have been triggered by any given snowflake of the moment. Likewise, fire-establishing ignitions are one of many that could have triggered large fires. The successful ignition, whether initiated by man or lightning, is meaningless in the generic explanation of fire regimes.

An important question in patch dynamics is the threshold of fire size necessary to achieve nonrandom turnover of patches. Clearly, infinitely small ignitions operate independently of one another, but the chance that fire patches constrain their spatial extent increases with fire size. This limit represents an important threshold in fire size distributions. The threshold of patch interaction is a function of the rate of ignitions, with increasing fire establishment rates lowering the size threshold. Below this threshold fires have trivial influence on ecosystems, no matter how numerous (cf. Keeley et al., 1999).

16.3. Nonrandom weather of fires

The selective dousing of fire-starts affects the weather conditions that lead to large fires escaping the ignition phase of firefighting. Satellite imagery and serial aerial photographs document burning in BCA under prevailing sea breezes/onshore winds in summer, but during fall offshore Santa Ana winds in SCA (Minnich, 1983; Minnich & Chou, 1997). The difference in the weather conditions of fires across the international boundary reflects the nonrandom occurrence of large fires during extreme weather states, as a result of suppression (see Minnich, 2006, Fig. 2.1.2). Fire spread rates increase as the weather becomes drier, but over long time scales these rates respond to fire climate, which is described as the proportion of time in weather states along a normal statistical distribution. In this distribution, days associated with modest rates of burning in mature vegetation are most frequent. Days with high spread rates in extreme weather of the distribution are rare. Likewise days too moist for fire are also rare. In BCA modest spread rates are phased with a large portion of time in the summer fire season, i.e., "slow burning" that consumes large areas of the landscape. This limits extensive burning in rare periods of extreme weather. In SCA the nonrandom elimination of fire-starts reduces slow burning in normal weather states, and thereby selects for increasing area burned during states of severe weather risk, e.g., Santa Ana winds.

The differences in fire weather in SCA and BCA, specifically the frequency and intensity of Santa Ana winds, is not due to regional shifts in synoptic global circulation structure, which operate at scales of thousands of kilometers, compared to the 200-km length of this wildfire analysis. At synoptic scales, lands on one side of the international boundary will have virtually the same chance of being affected by any mode of atmospheric circulation as the other. Santa Ana winds have been documented in BCA from case studies (Castro et al., 2003; Figueroa-Gonzaléz et al., 2004; Westerling et al., 2004) and QuikSCAT measures of ocean wind vectors (Hu & Liu, 2003). Smoke and dust frequently extend far out to the Pacific on both sides of the border (Fig. 16.1, see book cover). Climatic evidence for the prominence of Santa Ana winds in BCA is the accumulation of dune material from lacustrine deposits drifted to the west side of Laguna Chapala of the Central Desert (lat. 29°N 115°W) by offshore winds after the desiccation of the lake at 7.45 ka (Davis, 2003).

Transborder differences in fire weather have persisted through the 20th century. MODIS satellite data and fire report data for 2003–2006 (Table 16.1) show that the total burn area in SCA was six times greater (764,000 ha) than in BCA (133,000 ha). The proportion of burned area with offshore winds was 77% (576,000 ha) in SCA compared to 39% (31,000 ha) in BCA, where most fires took place with prevailing westerly winds from June to August.

Long-duration fires increase the probability of fire spread in normal weather because the integrated departure from average weather (climate) decreases with increasing time scale. A forgotten element of presuppression regimes in the 19th century is that free-running fires spread in a broad spectrum of weather over spans of months until they were extinguished by the first rains of autumn (Minnich 1987, 1988). When flame line expansion was not occurring, local fires were stored by glowing

Table 16.1. Fire data for southern California (SCA) and northern Baja California (BCA), 2003–2006.

Year	Location/ area (mha)	Days with fires	Tot. fire-days[a]	Max. fire-day/fire	Max. fire duration	Burn area (kha)[b]	Burn area/ fire day	Burn area offshore winds (kha)	Offshore wind burn area/total burn area (%)
	SCA								
2003	2.0	23	77	11	13	320	4.2	310	97
2004		27	39	4	4	20	0.5	0	0
2005		32	38	3	3	7	0.2	6	86
2006		27	53	23	25	115	1.9	60	52
2007		73	132	49	61,55	317	2.4	210	66
Tot./Max.		182	334	49	61	764	2.3	586	77
% burned						38.0			
	BCA								
2003	1.2	47	84	11	10	15	0.2	5	30
2004		39	52	5	5	3	0.1	0.1	2
2005		63	110	15	59,34	30	0.3	9	29
2006		53	85	9	15	9	0.1	0.4	5
2007		49	74	8	53,43	23	0.5	17	78
Tot./Max.		251	405	15	59	80	0.3	31	39
Area wt.[c]		418	675	—	—	133.3	—	—	—
% burned						11.1			

Source: MODIS Rapid Response System, http://rapidfire.sci.gsfc.nasa.gov/.
[a]Two separate fires in one day = 2 fire-days.
[b]Southern California: Fire and Resource Assessment Program, http://frap.cdf.ca.gov/. Baja California: File data, CONAFOR, Comisión Nacional Forestal, Gerencia Nacional I, Peninsula de Baja California, Ensenada, Baja California.
[c]Days with fire and fire days normalized to differences in vegetation area in BCA and SCA.

combustion (cf. Lobert & Warnatz, 1993) in large fuels (tree snags, logs, root crowns) as virtual season-long ''torches,'' that established new flame lines when weather and fuel conditions permitted. Torch frequencies multiplied in frequency and became more widely distributed with each successive flame line expansion, dissipating only when the region was soaked by autumn rains.

Nineteenth century newspaper reports of smoke in SCA document that at least one fire persisted 1 month or longer most years, with several burning 3–4 months (Table 16.2). Detailed accounts in the western San Gabriel Mountains near Pasadena in the late 1890s reveal that three fires near Mt. Wilson consumed chaparral and local forests over periods of days or weeks, and remained latent by storing in coarse fuels for weeks,

Table 16.2. Long duration fires in southern California.

Year	Mountain range/region	Duration (Newspaper dates)
1869	E. San Gabriel/Cucamonga Peak[a]	July–October 2
1869	S. Bernardino/San Bernardino Peak[a]	July–October 2
1872	W. San Gabriel[a]	June–September
1872	San Bernardino/Santa Ana River[a]	July 4–September 14
1878	San Gabriel, Cucamonga Peak[b]	July 20–September 21
1878	San Gabriel/Big Tujunga Canyon[b]	July–fall rains
1881	San Bernardino	August–September
1882	San Bernardino/Lake Arrowhead[a]	September 7–16 (several weeks), Dec 20
1883	San Gabriel/Placerita-Soledad Canyon	September 25–November 29
1887	Northern Santa Ana	October 6–October 30
1888	San Gabriel, north of Pasadena	July 8–August 22
1888	San Bernardino/San Gorgonio	July 23 (two weeks)
1889	Santa Barbara/Rincon-Carpenteria	July 28–September 22
1889	Santa Monica	July 23–September 28
1891	Santa Barbara-Ventura/Montecito, Rincon	October 3–November 25
1891	Santa Monica	August 19–September 26
1894	Santa Inez/Santa Barbara	August 26–November 15
1895	Santa Monica	September 23–November 15
1896	San Gabriel/west of Mt. Wilson[a]	July 11–October 20
1896	E. San Gabriel/San Antonio Mtn.–Cucamonga Pk.	June 14–October 14
1898	San Gabriel/Mt. Wilson[a]	July 30–October 23
1898	San Bernardino/Running Springs	August 30–October 8
1899	San Gabriel/San Antonio	August 30–October 2, February 25, 1900
1899	San Diego/Cuyamaca	October 3 (several weeks)
1899	San Diego/Palomar	September, 27, 29 (two weeks)
1900	San Gabriel/Santa Anita Can.–W. Fork S. Gabriel[a]	July 23–September 2
1900	San Bernardino/Running Springs	August 17–October 10

Source: Los Angeles *Times* unless otherwise indicated.
[a]Minnich (1987, 1988). Newspapers were published weekly before 1878.
[b]Los Angeles *Evening-Express*, Los Angeles *Star*.

resulting in intermittent expansion throughout the dry season (Minnich, 1987).

In the 20th century, fires in SCA lasted only for days, rarely a week, before being encircled by firefighting forces, further aggravating area-weighted burning toward extreme weather states. Fires in BCA still burn as long as 1–3 months (Minnich et al., 2000). MODIS imagery documents a fire in 2005 south of Ensenada from August 26 to September 10 that burned only 1750 ha. Another fire in the foothills of the Sierra San Pedro Mártir (SSPM) in 2005 burned 5789 ha from July 6–15, and an additional 1150 ha from August 30 to September 2. In 2002, MODIS and 1-km visible GOES imagery recorded a 10,000 ha forest fire in the central SSPM from August 29 to September 15 (file data, Comisión Nacional Forestal, CONAFOR).

Fires in SCA continue to have short durations, larger sizes, and greater rates of vegetation consumption compared to BCA. Normalizing for vegetation area, the frequency of fires in BCA is about 2.3 times greater than in SCA, while the number of fire-days is about twice that of SCA. During the megafires of October 2003 and 2007, most burning in SCA occurred during a 1-week period (300,000 and 210,000 ha, respectively), while the total annual range in burn areas in BCA varied from 3000 to 30,000 ha yr^{-1}. During the MODIS reference period, the average area burned per fire-day was 2300 ha in SCA compared to 300 ha per fire-day in BCA (Table 16.1). The higher rate in SCA reflects the larger size of fires (more perimeter length in expansion), as well as higher linear-spread rates. This suggests that fires under suppression in SCA are characterized by higher fire intensities and greater smoke production, as compared to free-running fires in BCA, because more fuel area is being burned per time. In SCA the Zaca fire burned from July 4 to September 5, 2007, an unprecedented duration in the region since the initiation of fire suppression. However, this fire burned 100,000 ha at daily rates comparable to the mean for the MODIS reference period.

Lower fire intensities in BCA are also suggested by landscape-scale patterns in fuel consumption. Fires leave reticulate patchiness in which separated flame lines merge and depart with fluctuations in terrain, fuels, and weather. "Islands" of unburned vegetation may constitute a major portion of the landscape. For this reason even single burns may contribute to complex patchiness of mosaics (Minnich, 2006). In SCA wind-driven fires denude virtually all chaparral within the perimeter, further homogenizing patch mosaics.

An example of a slow-moving, long-duration fire in BCA is illustrated by a blaze in 2006 in the western SSPM. The fire established during thunderstorms at the base of the range and spread upslope in 70-year-old chaparral with anabatic winds (2440 ha; Fig. 16.4, Table 16.3). Flame lines expanded in the afternoons of June 3–4 and June 12–17. Mostly passive smoke developed from smoldering during humid weather on June 5–11 and June 21. Daily burn areas ranged from 50 to 1000 ha. The perimeter on its south flank was constrained for a continuous length of 7 km by a large burn that occurred in 1974, and its northeast flank was limited by burns that occurred in 1975 and 1987. The GOES weather satellite Fog Product (emissivity differences between 11 and 3.9 μm bands used to estimate fog depth) detected smoke layers as late as July 4.

16.4. Phase-transition fire regime

What happens when fire control is launched on a free-running fire regime? The result is a new pattern of increasing fire size and severity like that now being experienced with the establishment of suppression in Spain (Díaz-Delgado et al., 2005) and the Mediterranean Basin since the 1980s (Chuvieco, 1999). In SCA, newspaper accounts in the early 20th century detail the onset of suppression in the San Gabriel Mountains, including the construction of fuel breaks and the extirpation of small fires (Minnich, 1987). From 1905 to 1918 only 8000 ha burned in an area of 120,000 ha of chaparral, a rate consistent with a fire rotation period of 225 years, four times longer than actual mean fire intervals. Clearly, a net aging of chaparral took place across the range. The hiatus ended precipitously with a 50,000 ha fire outbreak in 1919 and a 20,000 ha fire in 1924, which together consumed nearly 60% of chaparral in that mountain range.

The limited acreage burned in the San Gabriel Mountains before 1919 is remarkable given the period's ''low tech'' suppression, but foresters had inherited a ''well-managed'' mosaic like that in present-day BCA. Forest reserve reports, U.S.–Mexican boundary surveys, and Forest Service surveys between 1895 and 1905 describe intricate chaparral patchiness and numerous small fires across the southern California chaparral landscape (Minnich, 1987, 1988). We propose that the onset of suppression temporarily lengthens regional fire intervals by about one-third of a fire cycle in chaparral. This is approximately the time required for fine-grained mosaics to age to the levels that would permit the differences in the size of fires that are now seen across the international boundary. During this ''phase transition,'' the suppression of otherwise-rare viable ignitions postpones the establishment of mass fires in the oldest patches of an inherited fine-grained patch mosaic, as well as in younger stands that continue to resist ignitions. Eventually, the entire

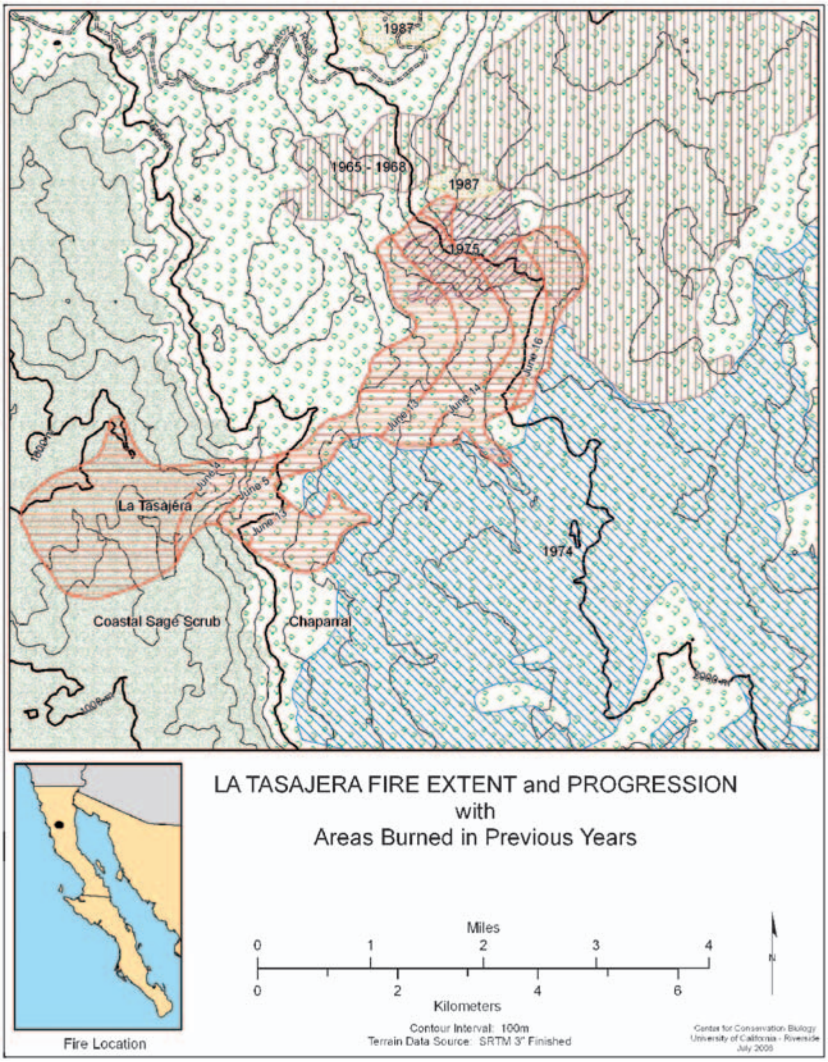

Figure 16.4. Fire perimeter and daily position of flame lines of a fire in 2006 fire in La Tasajera in the western Sierra San Pedro Mártir. Fire positions are mapped from daily true color (250 m resolution) and bands 7-2-1 imagery of the MODIS Rapid Response System (rapidfire.sci.gsfc.nasa.gov), from smoke in time-lapse animations of GOES 11-west weather satellite 1-km resolution visible channel, from "hot spot" animations in the GOES-west weather satellite 4-km resolution fog product archive in the National Weather Service, San Diego (animations by H.P. Wren, www.wrh.noaa.gov/sgx), and from ground photographs taken June 24–July 1, 2006. The fire perimeter is shown in relation to previous fire history mapped from aerial photographs in Minnich et al. (2000).

Table 16.3. Satellite and field data of the 2006 La Tasajera fire, Sierra San Pedro Mártir, northern Baja California, Mexico.

Date	Smoke (GOES 1-km visible)[a]	"Hot spot" (GOES 4-km fog product)[b]	Active flame lines (MODIS)[c]	Comments
June 2				Small thunderstorms
June 3	X	X	X	Small thunderstorms
June 4	X	X	X	
June 5		X		Thunderstorms
June 6		X		Thunderstorms
June 7		X		
June 8		X		
June 9		X		
June 10		X		
June 11		X		
June 12	X	X	X	
June 13	X	X	X	
June 14	X	X	X	
June 15	X	X	X	
June 16	X	X	X	
June 17	X	X	X	
June 18	X	X		
June 19		X	X	
June 20		X		
June 21	X	X		
June 22		X		
June 23				
June 24				
June 25				Thunderstorms
June 26				Thunderstorms
June 27				Smoke observed in field
June 28				Thunderstorms
June 29				Thunderstorms
June 30		X		Thunderstorms
July 1				Thunderstorms
July 2				Thunderstorms
July 3				Thunderstorms
July 4		X		Thunderstorms
July 5				Thunderstorms
July 6				

[a]http://archive.hpwren.ucsd.edu/SDW/VIS1/ANIMATIONS/.
[b]http://archive.hpwren.ucsd.edu/SDW/FOGREFL/ANIMATIONS/.
[c]MODIS Rapid Response System http://rapidfire.sci.gsfc.nasa.gov/.

mosaic ages so that both old and young patches reach flammable states, thus forming new, ever-larger aggregates of combustible patches, as well as ever-larger ignition targets. The large size of flammable patches eventually overwhelms initial attack capacity, leading to such anomalously large fires as those of 1919 and 1924. The evolution of coarse patch structure with suppression has since then predisposed the region to repeated cycles of excessively large burns. Such a transformation was recognized a century ago by William Mulholland, a perceptive engineer of the Los Angeles Water Department, who refused to allow his personnel to fight fire for the Forest Service in 1908 (Minnich, 1987).

Keeley et al. (1999, 2004, 2006) assert that fires were always large in SCA even into prehistory and at scales comparable to those recorded under suppression. This conclusion is based on the observation that fire sizes before 1950, when advanced suppression technology was introduced (airplanes, bulldozers, retardants), were as large as those thereafter. This model disregards the exclusive effectiveness of the initial attack phase of suppression, a process that triggered the onset of the phase transition in the early 1900s, when suppression resources were limited. Their model also disregards the fundamental observation that the energy release of large fires exceeds the energy produced by suppression technology, primitive or advanced, by orders of magnitude (Minnich, 2001). Hence, the 1950 time line is *ad hoc*. The model also suffers from the "shifting baseline syndrome" (Jackson et al., 2001). Only fire records under suppression are consulted. There was no concern to take official records until public policy and expenditures became committed to suppression about 1900 (Goforth & Minnich, 2007; Minnich, 1987). The stepwise shift in fire pattern along the international boundary was already conspicuous when the first aerial photographs were taken in 1938 (Fig. 16.5).

The October 2003 and 2007 firestorms in SCA have no historical precedent despite claims of "100-mile by 15-mile fire" (200,000 ha) near the town of Santa Ana in 1889 (Keeley, 2006; Keeley et al., 2004). Critical analysis of the 1889 fire using property tax records, voter registration rolls, claimed insurance, and place names (Goforth & Minnich, 2007) shows that the 1889 fire burned about 6500 ha of chaparral, or 40 times smaller than the 100-mile fire estimate. Goforth and Minnich (2007) also conclude that quantitative historical evidence is inadequate for reconstructing a statistical distribution of presuppression fire sizes.

From varved charcoal in the Santa Barbara Channel, Mensing et al. (1999) assert that the chaparral fires over the past 560 years were dominated by Santa Ana winds. The relationship between charcoal deposition, fire history, and discrete weather events is not constrained spatially or temporally. Ash deposits may arise from singular or multiple

Figure 16.5. Aerial photographs of the fire mosaic at Canada Verde on the international boundary east of Tecate, Baja California, in 1938. Black line delimits the international boundary. In BCA (below the boundary) is a fine-grained patch mosaic of recent burns (light areas of exposed granitic soil) and dark mature chaparral. Nearly all the area on the U.S. side is mature chaparral. The shift in patchiness along the international boundary at the time of these aerial photographs shows that differences in the chaparral fire regime between the U.S. and Mexico have prevailed since the early 20th century.

fire events. The transport of charcoal from watersheds, by wind or runoff long after fires, precludes specific correlation with discrete weather events operating at short time scales. For example, heavy ash deposition occurred in the Santa Barbara Channel with northerly Santa Ana winds on October 20, 2007 from the Zaca burn (Fig. 16.6), which occurred in July and August, with prevailing onshore winds, and at a season when Santa Ana winds are not part of the climate. The calibration data for varved charcoal are 20th century fire records that cannot account for the effects of fire suppression.

16.5. Fire and long-term climate change

Large fire outbreaks often coincide with short-term climatic perturbations such as extreme drought, moist periods with higher-than-normal fuel production, and sudden accumulations of dead fuel from dieback and pathogens. On the other hand, climatic relationships with fire regimes must also take stock of long-term dynamics of fuel accumulation in forest and brushland mosaics as a source of outbreaks, because plant response to perturbations depends on the cumulative effects of plant succession. We suggest that climatic variability as a forcing factor on burning in brushlands and forests is constrained by inertial forces of cumulative fuel build-up. This view can be addressed by a simple thought experiment. Does climate variability, especially precipitation, have the same effect on a 10-year old stand as on a nearby 100-year stand? If fires preferentially consume old-growth vegetation, then fuel build-up and transpiration demand linked to vegetation age may have more explanatory power in terms of fire outcomes than does climate variability. In addition, fluctuations in precipitation and plant-available water are also attenuated in areas where mean annual precipitation exceeds soil field capacities (Franco-Vizcaíno et al., 2002). Excess water tends to run off and does not affect the landscape evapotranspiration (ET).

In a hypothetical landscape with steady-state turnover of patches, regional calorie-to-water ratios and fire hazard would deviate mostly around a flat, long-term trend. This is due to negative feedbacks between fire hazard and vegetation (water) status. The response of the mosaic would depend on the time scale in relation to the mean fire interval of that vegetation type. In the short term, the lowering of fire thresholds during drought encourages the burning of ever-younger stands, increasing regional burn area. Moist years constrain fires to old stands, decreasing fire area. In the long term, large fire outbreaks from extreme drought lead

Figure 16.6. Ash plume pushed by Santa Ana winds over the Santa Barbara Channel from the Zaca burn on October 20, 2007. The fire burned in July and August with onshore winds. (Source: MODIS Rapid Response System, rapidfire.sci.gsfc.nasa.gov)

to reduction in age and fuel hazard of the landscape mosaic. Moist periods postpone burning, thus increasing regional fuel build-up.

Fire-scar dendrochronology (FSD) studies on changes in fire regime with climate variability rely on the assumption of covariance between the rates of tree scarring and landscape burning (Minnich, 2007). Spatial estimates of fire intervals using site-based FSD methods are equivocal and tend to underestimate, because mass burns that are responsible for most regional burning are accompanied by abundant microburns (ignition failures) symptomatic of long-tailed fire size frequency distributions (see also Baker & Ehle, 2001). It follows that transient fluctuations in the scarring record may also arise from site-specific microburns rather than rates of burning at the landscape scale.

For example, variable scarring rates due to the El Niño cycle (Swetnam & Betancourt, 1990) could also be reasonably explained by changing fuel moisture of the litter layer and microburn frequency, rather than changes in landscape-scale burning. The Pacific Decadal Oscillation (PDO; Chao et al. 2000; Minobe, 1997) is associated with the running precipitation means fluctuating 10% from the long-term mean in the western United States. However, such modest fluctuating means are attenuated by large-precipitation/field-capacity ratios. Landscape water demand may be more influenced by patterns of mosaic emplacement than by precipitation variability.

Westerling et al. (2006) posit that global warming has contributed to a substantial increase in large wildfires in the western U.S. beginning in the mid-1980s, with longer wildfire durations and wildfire seasons due to increasing spring/summer temperatures and earlier spring snow melt. The question remains as to what extent these trends affect plant-available water and fire hazard, especially if increases in plant transpiration and long-term changes in plant-available water are attenuated by precipitation/soil field-capacity ratios. The trend for longer duration fires must account for artificial effects of suppression that prevent secondary episodes of fire spread (Minnich 1987)—the selective effects for large fires coinciding with extreme weather states caused by the suppression of millions of fire-starts and aging mosaics of conifer forests from 1900 to 1985.

In the chaparral, long-term burning rates in SCA and BCA have not been in phase with climate perturbations. The total area burned at annual and subdecadal scales has been random, only with more amplified variability in SCA due to suppression (Minnich, 1983; Minnich & Chou, 1997). Short-term increases in flammability, due to unusually rapid build-up of dead fuel from pathogens or drought (e.g., Brooks & Ferrin, 1994; Davis et al., 2002; Riggan et al., 1994), have not been correlated with specific fire outbreaks. The question can be asked whether the recent

764,000 ha (38%) of chaparral burned in SCA since 2003 (MODIS) is a response to climatic forcing. However, MODIS also shows that burning rates in BCA remained within the range of burning rates during the previous 80 years (Table 16.1; cf. Minnich, 1983; Minnich & Chou, 1997). The frequent occurrence of landscape fires in BCA leads to modest interannual and interdecadal variability in burning. In SCA, transient fluctuations are dominated by rare enormous fire outbreaks (>50,000 ha, e.g., in 1970, 2003, 2007), even at decadal time scales (Minnich & Chou, 1997). The 2003 and 2007 fire sieges in SCA were an artifact of fire control policy, rather than an outcome of global climate change. A valid test of the global warming/fire hypothesis would be an examination of regions with free-running fire such as Mexico, northern Canada, or Russia (Webster, 2007), rather than ecosystems already contaminated by suppression.

16.6. Baja California is California's past

Fire regimes in forests and brushlands respond to vegetation dynamics over long time scales. To investigate modalities of fire regime properties, studies of landscapes need to adopt a probabilistic view of vegetation and fire using spatially explicit, historical approaches based on time-series data from aerial and space platforms, as well as ground-based sampling.

The U.S.–Mexican border region provides a fortuitous opportunity to study paired landscapes with differing land management and fire regimes for the development of policies that reintroduce fire in California ecosystems. The recent free-running fire history of BCA documents a mediated, self-organized fire regime that develops by chance. It also demonstrates that the potential for a "no management option" in California wildlands—no initial attack, no attempts to surround flame lines—would spontaneously produce more desirable fire outcomes than 20th century fire history under suppression in SCA with respect to fire size, intensity, ecological processes, and smoke dispersal. This fundamental finding gives support to new management options in which fire is allowed to burn at will in California wildlands, and firefighting is restricted to the wildland urban interface. Such policy change is rational only if it is assumed that continuation of suppression has trivial capacity to influence large fires. Baja California should continue to serve as a model of California's past, as well as a model for future fire management of the entire North American Mediterranean region.

The development of fire management policies by the Mexican authorities should consider continued maintenance of the current fine-grained vegetation mosaic that is resistant to extensive fire. Political will is required to resist public pressure to automatically "combat" all wildfires. Such momentary public pressure can only be dealt with by having clearly enunciated policy beforehand. The public's perception that fire results in the irretrievable loss of valuable forest resources should be addressed through education campaigns that point out the mountain forest's unaided survival through the millennia and their sudden vulnerability by the belated adoption of fire suppression policies that are already being abandoned in the developed world. The Comisión Nacional Forestal is currently developing wildfire management plans tailored to each state, and the draft plan for Baja California properly recognizes the region's unique characteristics that are very different from the rest of tropical Mexico.

Another concern relates to objections by astronomers to the degradation in atmospheric quality because of infrequent summer smoke over the National Astronomical Observatory (OAN) in the Sierra San Pedro Mártir. Minor reductions in observation time should be considered similar to disturbances due to weather and weighed against the inevitability of future firestorms like the 2003 and 2007 events just north of the border. The loss of Australia's Mount Stromlo Observatory during January 2003, in similar Mediterranean-type vegetation, should serve as a cautionary example. Detailed recommendations for the removal of fuels from areas adjacent to the OAN buildings have been provided by the authors and should be implemented. Fires—just like hurricanes, earthquakes, and other earth surface processes—should be seen as natural phenomena over which humans have little control in the long term.

REFERENCES

Baker, W.L., and Ehle, D. 2001. Uncertainty in surface-fire history: The case of ponderosa pine forests in the western United States. Can. J. For. Res. 31, 1205–1226.

Barro, S.C., and Conard, S.G. 1991. Fire effects on California chaparral systems: An overview. Environ. Internat. 17, 135–149.

Brooks, F., and Ferrin, D.M. 1994. Branch dieback in California chaparral vegetation caused by *Botryosphaeria dothidea*. Phytopathology 84, 78–83.

Castro, R., Parés-Sierra, A., and Marinone, S.G. 2003. Evolution and extension of Santa Ana winds of February 2002 over the ocean off California and the Baja California peninsula. Ciencias Marinas 29, 275–281.

Chao, Y., Ghil, M., and McWilliams, J.C. 2000. Pacific interdecadal variability in this century's sea surface temperatures. Geophys. Res. Lett. 27, 2261–2264.

Chuvieco, E., ed. 1999. Remote sensing of large wildfires in the European Mediterranean Basin. Springer, Berlin, 212 pp.

CONAFOR (Comisión Nacional Forestal), Gerencia Regional I, Peninsula de Baja California. Ensenada, Baja California. File data.

Davis, L.G. 2003. Geoarchaeology and geochronology of pluvial lake Chapala, Baja California, Mexico. Geoarchaeol: An Internat. J. 18, 205–223.

Davis, S.D., Ewers, F.W., Sperry, J.S., Portwood, K.A., Crocker, M.C., and Adams, G.C. 2002. Shoot dieback during prolonged drought in *Ceanothus* (Rhamnaceae) chaparral of California: A possible case of hydraulic failure. Am. J. Bot. 89, 820–828.

Díaz-Delgado, R., Lloret, F., and Pons, X. 2005. Spatial patterns of fire occurrence in Catalonia, NE, Spain. Landscape Ecol. 19, 731–745.

Figueroa-González, J., Ocampo-Torres, F., Durazo, R., and Terrill, E. 2004. Analysis of Santa Ana wind effects on surface circulation in the coastal region of the North West of Baja California. Geophys. Res. Abstracts 6, 00391 S. Ref-ID 1607-7962/gra/EGU04-A-00391.

Franco-Vizcaíno, E., Escoto-Rodríguez, M., Sosa-Ramírez, J., and Minnich, R.A. 2002. Water balance at the southern limit of the Californian mixed-conifer forest and implications for extreme deficit watersheds. Arid Land Res. Manage. 16, 133–147.

Goforth, B.R., and Minnich, R.A. 2007. Evidence, exaggeration, and error in historical accounts of Chaparral wildfires in California. Ecol. Appl. 17, 779–790.

Goforth, B.R., and Minnich, R.A. 2008. Densification, stand-replacement wildfire, and extirpation of mixed conifer forest in Cuyamaca Rancho State Park, southern California. For. Ecol. Manage. 17, 779–798.

Hu, H., and Liu, W.T. 2003. Oceanic thermal and biological responses to Santa Ana winds. Geophys. Res. Lett. 30(11), 1596, doi:10.1029/2003GL017208.

Jackson, J.B.C., Kirby, M.X., Berger, W.H., Bjorndal, K.A., Botsford, L.W., Bourque, B.J., Bradbury, R.H., Cooke, R., Erlandson, J., Estes, J.A., Hughes, T.P., Kidwell, S., Lange, C.B., Henihan, H.S., Pandolfi, J.M., Peterson, C.H., Steneck, R.S., Tegner, M.J., and Warner, R.R. 2001. Historical overfishing and the recent collapse of coastal ecosystems. Science 293, 629–637.

Keeley, J.E. 2006. South coast bioregion. In: Sugijara, N.G., Van Wagtendonk, J.W., Shaffer, K.E., Fites-Kaufman, J., and Thode, A.E., eds. Fire in California's ecosystems. University of California Press, Berkeley, pp. 350–390.

Keeley, J.E., Fotheringham, C.J., and Morais, M. 1999. Reexamining fire suppression impacts on brushland fire regimes. Science 284, 1829–1832.

Keeley, J.E., Fotheringham, C.J., and Moritz, M.A. 2004. Lessons from the October 2003 wildfires in southern California. J. Forest. 107, 26–31.

Lobert, J.M., and Warnatz, J. 1993. Emissions from the combustion process in vegetation. In: Crutzen, P.J., and Goldammer, J.G., eds. Fire in the environment: The ecological, atmospheric, and climatic importance of vegetation fires. Wiley, New York, pp. 15–37.

Mensing, S.A., Michaelson, J., and Byrne, R. 1999. A 560-year record of Santa Ana fires reconstructed from charcoal deposited in the Santa Barbara Basin, California. Quat. Res. 51, 295–305.

Minnich, R.A. 1983. Fire mosaics in southern California and northern Baja California. Science 219, 1287–1294.

Minnich, R.A. 1987. Fire behavior in southern California chaparral before fire control: The Mount Wilson burns at the turn of the century. Ann. Assoc. Am. Geogr. 77, 599–618.

Minnich, R.A. 1988. The biogeography of fire in the San Bernardino Mountains of California: A historical study. U. Calif. Publ. Geogr. 27, 1–121.

Minnich, R.A. 2001. An integrated model of two fire regimes. Conserv. Biol. 15, 1549–1553.

Minnich, R.A. 2006. California climate and fire weather. In: Sugijara, N.G., Van Wagtendonk, J.W., Shaffer, K.E., Fites-Kaufman, J., and Thode, A.E., eds. Fire in California's ecosystems. University of California Press, Berkeley, pp. 13–37.

Minnich, R.A. 2007. Southern California coniferous forest. In: Barbour, M.G., Keeler-Wolf, T., and Schoenherr, A., eds. Terrestrial vegetation of California. University of California Press, pp. 502–538.

Minnich, R.A., Barbour, M.G., Burk, J.H., and Fernau, R.F. 1995. Sixty years of change in Californian conifer forests of the San Bernardino Mountains. Conserv. Biol. 9, 902–914.

Minnich, R.A., and Chou, Y.H. 1997. Wildland fire patch dynamics in the chaparral of southern California and northern Baja California. Int. J. Wildland Fire 7, 221–248.

Minnich, R.A., and Franco-Vizcaíno, E. 1998. Land of chamise and pines: Historical accounts and current status of northern Baja California's vegetation. U. Calif. Publ. Bot. 80, 1–166.

Minnich, R.A., Barbour, M.G., Burk, J.H., and Sosa Ramírez, J. 2000. Californian mixed-conifer forests under unmanaged fire regimes in the Sierra San Pedro Mártir, Baja California, Mexico. J. Biogr. 27, 105–129.

Minobe, S. 1997. A 50-70 year climatic oscillation over the North Pacific and North America. Geophys. Res. Lett. 24, 683–686.

Riggan, P.J., Franklin, S.E., Brass, J.A., and Brooks, F.E. 1994. Perspectives on fire management in Mediterranean ecosystems in southern California. In: Moreno, J.M., and Oechel, W.C., eds. Ecological studies; the role of fire in Mediterranean ecosystems. Springer-Verlag, pp. 140–162.

Riggan, P.J., Goode, S., Jacks, P.M., and Lockwood, R.N. 1988. Interaction of fire and community development in chaparral of southern California. Ecol. Monogr. 58, 155–176.

Rothermel, R.C. 1972. A mathematical model for predicting fire spread in wildland fuels. USDA Forest Service Research Paper. INT-115. USDA Forest Service, Intermountain Forest and Range Experiment Station. Ogden, UT.

Rundel, P.W. 1983. Impact of fire on nutrient cycles in Mediterranean-type ecosystems with reference to chaparral. In: Kruger, F.J., Mitchell, D.T., and Jarvis, J., eds. Mediterranean-type ecosystems: The role of nutrients. Springer, New York, pp. 192–207.

Scott, J.H., and Burgan, R.E. 2005. Standard fire behavior fuel models: A comprehensive set for use with Rothermel's surface fire spread model. General Technical Report RMRS-GTR-153. Colorado. USDA Forest Service, Rocky Mountain Research Station. Fort Collins, Colorado.

Sparks, S.R., Oechel, W.C., and Maufette, Y. 1993. Photosynthate allocation patterns along a fire-induced age sequence in two shrub species from the California chaparral. Int. J. Wildland Fire 3, 21–30.

Stephens, S.L. 2005. Forest fire causes and extent on United States forest service lands. Int. J. Wildland Fire 14, 213–222.

Swetnam, T.W., and Betancourt, J.L. 1990. Fire-southern oscillation relations in the southwestern United States. Science 249, 1017–1020.

Wangler, M.J., and Minnich, R.A. 1996. Fire and succession in piñon-juniper woodlands of the San Bernardino Mountains, California. Madroño 43, 493–514.

Webster, P. 2007. Setting the forest alight. Science 317, 1854–1855.

Wells, M.L., O'Leary, J.F., Franklin, J., Michaelson, J., and McKinsey, D.E. 2004. Variations in regional fire regime related to vegetation type in San Diego County, California (USA). Landscape Ecol. 19, 139–152.

Westerling, A.L., Cayan, D.R., Brown, T.J., Hall, B.L., and Riddle, L.G. 2004. Climate, Santa Ana winds and autumn wildfires in southern California. EOS, Transact. Am. Geophys. Union 85(289), 296.

Westerling, A.L., Hidalgo, H.G., Cayan, D.R., and Swetnam, T.W. 2006. Warming and earlier spring increase western U.S. wildfire activity. Science 313, 940–943.

Developments in Environmental Science, Volume 8
A. Bytnerowicz, M. Arbaugh, A. Riebau and C. Andersen (Editors)

ISSN: 1474-8177/DOI:10.1016/S1474-8177(08)00017-X

Chapter 17

Air Pollution Increases Forest Susceptibility to Wildfires: A Case Study in the San Bernardino Mountains in Southern California

Nancy E. Grulke, Richard A. Minnich, Timothy D. Paine, Steve J. Seybold, Deborah J. Chavez, Mark E. Fenn, Philip J. Riggan and Alexander Dunn*

Abstract

Many factors increase susceptibility of forests to wildfire. Among them are increases in human population, changes in land use, fire suppression, and frequent droughts. These and other factors have been exacerbating forest susceptibility to wildfires over the past century in southern California. We report on the significant role that air pollution has had on increasing forest susceptibility to wildfires, based on a 1999–2003 case study in the San Bernardino Mountains. Air pollution, specifically ozone (O_3) and wet and dry deposition of nitrogenous (N) compounds as a by-product of fossil fuel combustion, has significantly increased since urbanization and industrialization of the region after 1945. Ozone and elevated N deposition cause specific changes in forest tree carbon (C), N, and water balance that enhance individual tree susceptibility to drought, bark beetle attack, and disease, and when combined, contribute to whole ecosystem susceptibility to wildfire. For example, elevated O_3 and N deposition increase leaf turnover rates, leaf and branch litter, and decrease decomposability of litter, creating excessively deep litter layers in mixed-conifer forests affected by air pollutants. Elevated O_3 and N deposition decrease the proportion of whole tree biomass in foliage and roots, thereby increasing tree susceptibility to drought and beetle attack. Because both foliar and root mass are compromised, carbohydrates are stored in the bole over winter. Elevated O_3 increases drought stress by significantly reducing plant control of

*Corresponding author: E-mail: ngrulke@fs.fed.us

water loss. The resulting increase in canopy transpiration, combined with O_3 and N deposition-induced decreases in root mass, significantly increases tree susceptibility to drought stress, likely contributing to successful host colonization and population increases of bark beetles. Phenomenological and experimental evidence is presented to support the role of these factors contributing to an increase in the susceptibility of forests to wildfire in southern California.

17.1. Introduction

Historically, the forests of southern California were created, adapted to, and maintained by regular episodes of wildfire. This agent of ecosystem disturbance paradoxically functioned to maintain forests in a resilient state by better preparing them to withstand severe episodes of wildfire, drought, and bark beetle colonization. However, periodic extreme drought stress (affecting an individual tree within a dense stand) and bark beetle outbreaks can also increase forest susceptibility to wildfire. Under particular current forest conditions, there are many compounding factors, some of which were set in motion decades ago, that increase the susceptibility of southern California forests to severe wildfire and often result in stand-replacing fires. These factors include a rapid increase in human population and resulting resource use, a shift in management goals during the early part of the 20th century from timber utilization to recreational use, and successful fire suppression with subsequent forest densification.

Despite the level of attention given to the causative factors for increased wildfire activity (Westerling et al., 2006), a largely ignored contributing factor is air pollution. Chronic nitrogen (N) deposition contributes to increased forest densification by stimulating aboveground biomass production and enhances litter accumulation through increased needle production, turnover rates, and depressed long-term decomposition rates (Fog, 1988). Elevated ozone (O_3) exposure increases tree susceptibility to drought stress through direct effects on loss of stomatal control with subsequent increased canopy transpiration, and increased successful bark beetle colonization through both increased tree drought stress and pollutant-induced redistribution of carbohydrates to the bole. The effects of these air pollutants, combined with the human and ecological changes in the fire-adapted ecosystem, have increased forest stand susceptibility to wildfire in southern California (Fig. 17.1). This chapter presents a case study for the San Bernardino Mountains in the

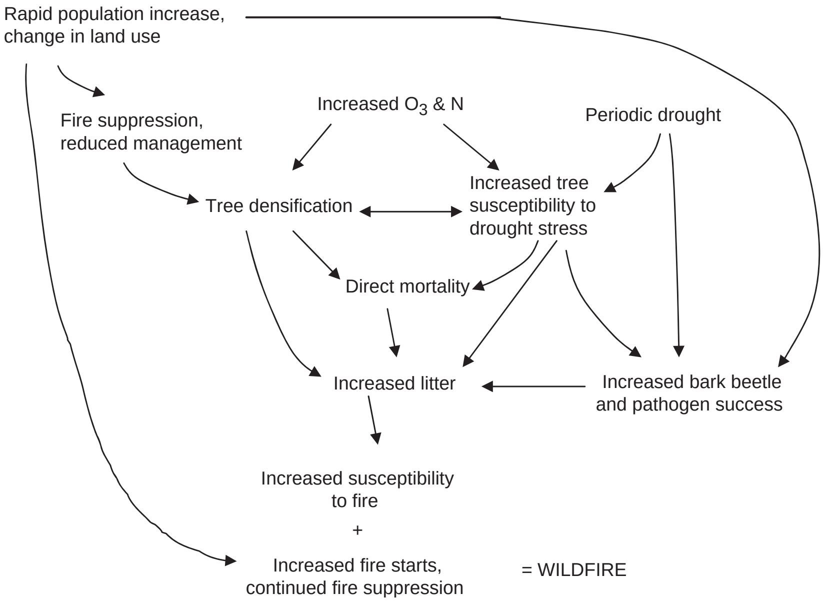

Figure 17.1. Diagram of multiple factors contributing to forest susceptibility to wildfire.

eastern Transverse Range, east of Los Angeles (LA), California that focuses on pollutant effects on ponderosa pine (*Pinus ponderosa* Laws)—an ecologically, socially, and economically important species throughout the western U.S.—that result in forest susceptibility to wildfire.

17.2. Historical effects of land development

The San Bernardino National Forest (SBNF) was established in 1908 and covers about 331,838 ha within San Bernardino and Riverside Counties in California. It includes the eastern end of the Transverse Range and the northern part of the Peninsular Range (San Jacinto Mountain and adjacent areas). Of this area, about 65,558 ha are in private, county, state, or other type of federal ownership.

During the late 19th century, settlers fundamentally altered the mountain landscape in southern California. Gold and other valuable minerals were discovered, and the population rapidly increased in surrounding low elevation areas as well as in the mountains (Minnich, 1988). The forest was logged to provide construction materials for buildings, mine shaft timbers, and for fuel. In 1899, a severe drought occurred (Fig. 17.2), water was rationed in the communities, and a premium was placed on reservoir development (Lake Gregory, Lake Arrowhead, and Big Bear Lake). As the reservoirs were established, they became the focus for recreational use in the 1920s. With the shift from resource utilization to recreation, forest thinning was suppressed, incursions of fire from the chaparral into the forest were repressed, and forest density increased on the mountaintop. In the 1950s, an attempt was made to thin the forests, but the mountain community councils were strongly opposed to both branch trimming and stand thinning for aesthetic reasons: these were now resort destinations for the rapidly increasing population in post-1945 LA. As a consequence, forest density continued to increase, and with in-growth and lateral canopy expansion, more trees were in physical contact with each other as well as structures, increasing fire hazard. An example of increasing canopy cover of individual trees through time can be observed in the sequence of aerial photos taken from 1938 through 1994 from the western San Bernardino Mountains (Fig. 17.3).

In 1980, the SBNF adopted a new set of forest plans, which addressed in part how to manage for fire on the National Forests surrounding and adjacent to the mountain communities. Due to the high percentage of private land ownership, National Forest personnel participated in community councils and solicited their support for fire-safe activities that would benefit both the private landowner and the National Forest. In response, mountain community councils, in conjunction with the SBNF, drew up their own plans, which included raking leaves, branch trimming, and thinning of trees within 30 m of valued structures (Asher & Forrest, 1982). The community's fire-safe plans were not implemented effectively, nor were they enforced. As a result of these human-induced changes over the past century, the region was, and is, highly susceptible to fire.

17.3. Mountain community behaviors related to fire-safe activities

The consensus of opinion is that either mountain community residents started to follow through on those practices and then stopped, or did not start at all, or did not implement these practices in a coordinated fashion so as to reduce the fire hazard on private property. There are a number of reasons why residents might not have implemented changes for their own (fire) safety. Some of the reasons have to do with demographic changes. Examination of California state census data (www.dof.ca.gov/html/demograp/calhist2a.xls) from 1980 to 2000 indicates population shifts in

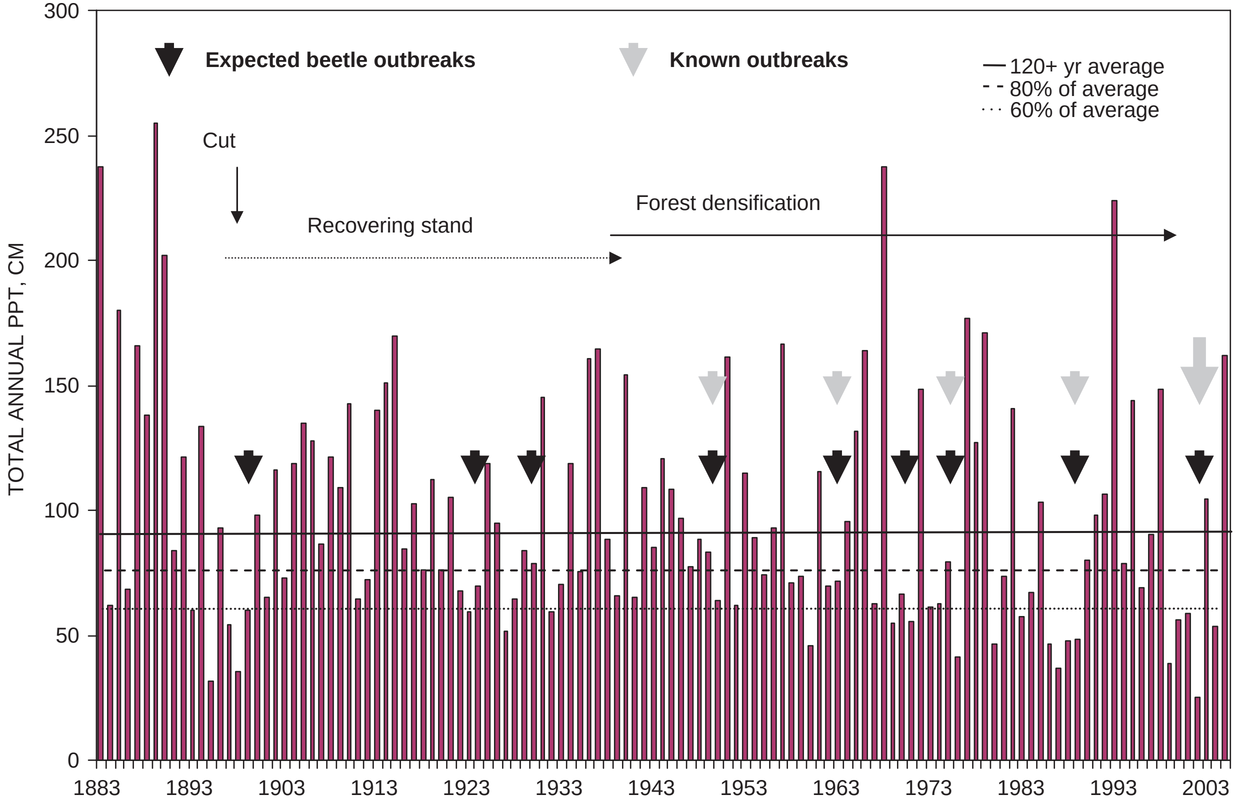

Figure 17.2. Long-term record of regional precipitation at Big Bear Dam, San Bernardino County, California. Total annual precipitation (*y*-axis in centimeters) from October 1 to September 30 was accumulated over each year and plotted. The overall average is denoted by a solid line (96 cm), with the 80% of average (below which moderate drought stress is incurred using physiological definitions) and the 60% of average (below which extreme drought stress is incurred) denoted by dashed and dotted lines, respectively.

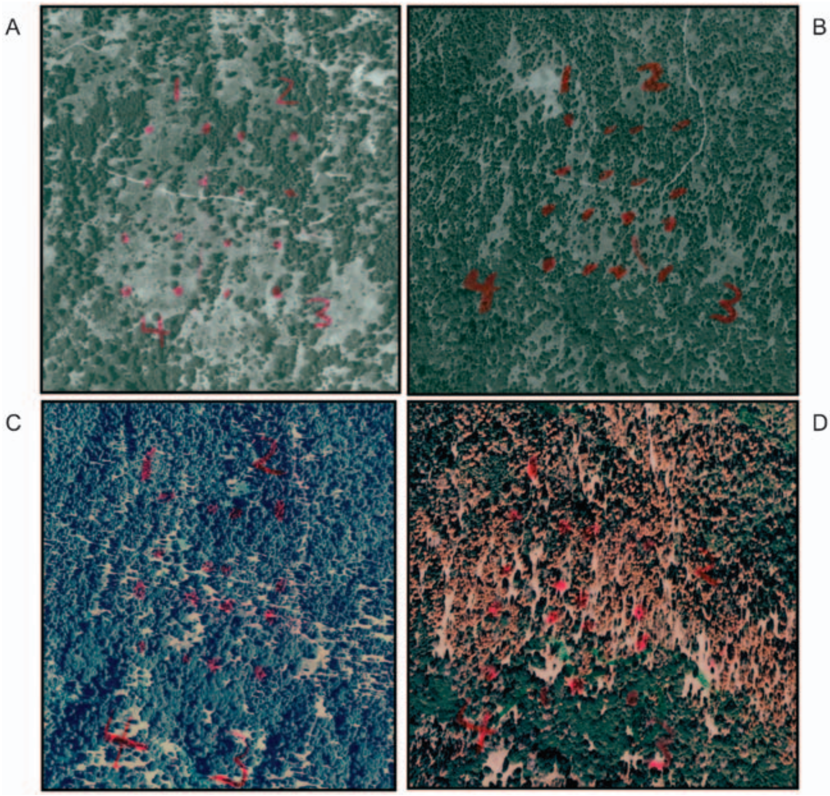

Figure 17.3. Repeat aerial photographs of mixed conifer forest dominated by *Pinus ponderosa* demonstrating forest densification (near site 1, western San Bernardino Mountains; see Fig. 17.5) in (A) 1938, (B) 1965, (C) 1994, and (D) 2003. Photograph sources are San Bernardino County Flood Control (A), San Bernardino National Forest (B,C), and the U.S. Geological Survey, SCAMP program, Department of Earth Sciences, University of California, Riverside (D).

several San Bernardino Mountain communities (Table 17.1). In mountain communities with population increases, some portion of the residents must have moved into the area and were never a part of the mid-1980s community council discussions on fire-safe actions for their property. New residents may have brought a different set of social values, such as the expectation of less, not more regulation, even if the activity improved their own survival or protection of property. New mountain residents arriving from urban areas often bring with them an expectation that fire is an emergency, not a way of life. The perception

Table 17.1. Population statistics for permanent residents in San Bernardino Mountain communities from 1980 to 2000

Place/Town/City	1980	2000	Change (%)
Big Bear City	11,151	5779	−52
Big Bear Lake	4896	5438	+11
Idyllwild-Pine Cove	2959	3504	+18
Lake Arrowhead	6272	8934	+42
Wrightwood	2511	3837	+53

that emergencies are handled by the fire department, not themselves, could have had an effect on their sense of control over the fire hazard. New residents may also have had a different level of trust in or experience with adjacent landowners (e.g., federal, state, or private) in carrying out fire-safe activities.

On the other hand, the population of Big Bear City was halved over the last two decades. If some of the reduction in residential population was due to seasonal use of homes, the level of property care by owners may have also declined, and some residents who originally agreed to participate may no longer reside in the area and are not on site to conduct or adequately maintain fire-safe activities. Interestingly, a single study (Vogt, 2003) suggests a moderate level of fire-safe activities among seasonal ($n = 176$) and permanent homeowners ($n = 119$) in the north-eastern U.S. In their study, permanent homeowners had a greater level of compliance of defensible space ordinances (68%) relative to seasonal homeowners (52%). If the age of the property owner has increased, this could also play a role in the reduced level of property care observed.

There are no data available to quantify what proportion of the residents participated in the 1980 mountain community forest plan discussions. The current residents in the San Bernardino Mountains may not have been involved in community decision making or agreements that were in place before their arrival. In the study in the northeastern U.S., only about one-third (30%) of the permanent and fewer (6%) seasonal homeowners attended a public meeting about wildland fire (Vogt, 2003). In another report on the same data set, Vogt and Cindrity (2003) found that the majority of respondents had purchased their property with the help of a realtor or sales office (75% of permanent and 70% of seasonal homeowners). Less than 2% of the permanent residents and 7% of the seasonal homeowners acquired their property through their family. Property transfer outside of the family could reduce the exchange of information on fire-safe activities that could occur from generation to generation, and this emphasizes the importance of the community in fire-safety education. Currently, efforts to educate new residents to mountain communities about fire-safe activities focus on delivering messages through communication tools that reach both permanent and seasonal, as well as long- and short-term residents.

There are other sociological and experiential reasons for not maintaining fire-safety practices. For example, some of the original participants may have initially agreed to implement fire-safe practices, but had a dispute with other participants, or the activities requested were perceived as ineffective, or ineffective relative to the magnitude of the risk. For example, if mountain residents observed a lack of fire-safe activities on adjacent properties, they may see no value in maintaining fire-safe activities on their own property. Perhaps the importance of peer pressure has declined in the past two decades. It is also possible that there are too many changes and burdens imposed on the residents. There could be other regulations that have been imposed that made fire-safe activities an overburden.

It is possible that homeowners may not have direct experience with wildfires. In one study from the northeastern U.S., 82% of permanent residents experienced smoke from a wildfire, compared to 45% of seasonal homeowners (Vogt, 2003). The homeowners were also questioned about their involvement in fire-education activities. Three-quarters of the permanent homeowners had read information on home protection from wildland fires, as had 70% of the seasonal homeowners. Residents who may have been motivated to implement fire-safe actions by the experience of living through a fire in recent history may be less likely to remain a resident of the community because of the experience itself. Fire is a motivating factor only for those who choose to stay in a fire-prone community. New residents may or may not have experienced a fire and thus have no context that would influence a decision to take action.

It is difficult or impossible to pinpoint the multiple causes for a lack of compliance with fire-safe actions on private land. Generally, mountain community residents and seasonal owners, historically and currently, influence the susceptibility of their properties to wildfire through knowledge, attitudes, observations and sense of risk, physical presence in the community, and level of action on community fire-safe activities. Regardless of causation, and whether intentional or not, private property owners in the San Bernardino Mountains have significantly contributed to the current state of high fire hazard that exists today. They have an equally significant opportunity to influence the future susceptibility of their properties and the forest as a whole to future wildfires through implementing fire-safe practices on their property.

17.4. Air pollution deposition

Pollutants generated by urban residents in the greater LA metropolitan area are transported 60–100 km downwind and affect mid-elevation forests in the San Bernardino Mountains (Bytnerowicz, et al., in press). The primary source of air pollution is fossil fuel combustion, whether it is from vehicular exhaust, residential production, or industry. Approximately half of the air pollution in the LA Air Basin is generated from mobile sources including trucks, trains, cars, ships, and buses (South Coast Air Quality Management District, 1997). On the western end of the San Bernardino Mountains, nearly half of the nitrogen deposition is in reduced forms (Fenn & Poth, 2004), most of which is believed to originate from dairy farms in the Chino/Norco area. Agricultural sources of ammonia are expected to decrease in coming years as farmland is converted to residential uses.

Fossil fuel combustion emits nitrogen oxide, which is converted to other nitrogen oxides (NO_x) and O_3 in the presence of high-energy ultraviolet (UV) light. Both NO_x and O_3 are strong oxidizing agents and damage living cells. These pollutants also react with biogenic volatile organic compounds like terpenes in the airspace of forested ecosystems facilitating the formation of organic aerosols (Atkinson & Arey, 2003; Cahill et al., 2006). Although O_3 is highly reactive and disintegrates through time, sufficient concentrations are generated in urban and agricultural areas (from NO_x emissions from fertilized soils) and transported long distances. For example, from west (nearer the pollutant source) to east (farther from the source) in the San Bernardino Mountains, O_3 concentrations were high at Camp Paivika (80 ppb h^{-1}, averaged over 24 h, from April 15 through October 15, from 1993 through 1995; Grulke et al., 1998), moderately high (72–74 ppb h^{-1}) 5 km further east near Rim Forest, and moderate (62–64 ppb h^{-1}) 45 km east of Camp Paivika at Barton Flats (Figs. 17.4, 17.5).

Because O_3 is a product of photolysis of nitrogen oxides, if O_3 is present at moderate concentrations, there is also concurrent N deposition. Deposition occurs from a wide variety of nitrogen species in gaseous, wet, and dry forms to vegetation and soil surfaces (nitric oxide [NO], nitrous oxide [NO_2], nitric acid vapor [HNO_3], nitrous acid vapor [HNO_2], particulate nitrate [NO_3^-]). Ammonium (NH_4^+) can also be transported moderate distances from feedlots for cattle and poultry (Bytnerowicz et al., 2002). Along the same west to east gradient in the San Bernardino Mountains (Fig. 17.5), N deposition averages 71 kg $ha^{-1} yr^{-1}$ at Camp Paivika and declines to 9 kg $ha^{-1} yr^{-1}$ at Barton Flats (Breiner et al., 2007). Because air pollution has been high since 1945 in the LA Air Basin (Lee et al., 2003), N deposition is in excess of plant and microbial

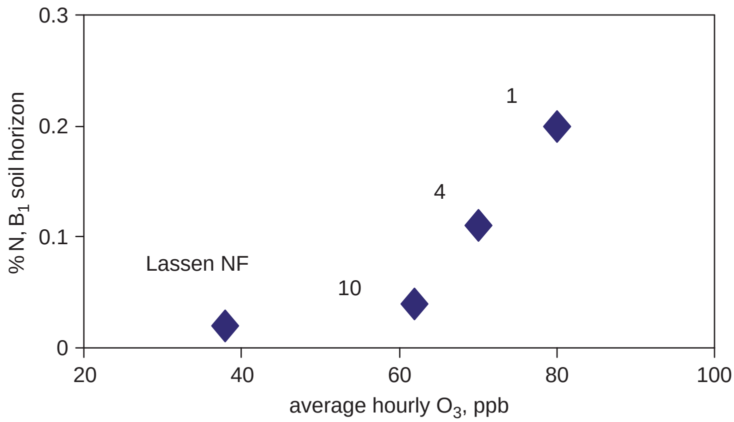

Figure 17.4. Relationship between O_3 exposure (averaged across the summers of 1993–1995; Grulke, 1999) and incorporation of long term, excess nitrogen deposition within the upper 5 cm of B_1 mineral soil (Grulke et al., 1998). Site numbers correspond to those given in Fig. 17.4. The atmospherically "clean" site is 1 mile west of the Guernsey Creek Campground (Hwy 38), Lassen National Forest, in northern California.

demand (Fenn et al., 1996). The cardinal symptom of excess N is the export of high nitrate levels in streamwater, which is well demonstrated for areas with N deposition above 15 kg $ha^{-1}yr^{-1}$ in the San Bernardino and San Gabriel Mountains (Breiner et al., 2007; Fenn & Poth, 1999; Michalski et al., 2004; Riggan et al., 1985).

In the mid 1990s, soil N in the mineral horizon was 0.2% at Camp Paivika, 0.1% near Rim Forest, and 0.04% in the Barton Flats area (Fig. 17.4; Grulke et al., 1998). This represents a considerable increase over background levels expected from weathered granitic bedrock substrates and when compared to atmospherically "clean" sites (e.g., 0.02% N, Lassen National Forest). The effects of O_3 and excess N deposition are evaluated here as contributing factors to forest susceptibility to wildfires. Although O_3 concentrations have declined in the last decade due to increased regulation (Lee et al., 2003), soil N is still in excess and continues to influence plant response (Tingey et al., 2004).

17.5. O_3 exposure and excess nitrogen deposition effects on forest health

17.5.1. Tissue, cellular, and subcellular levels

Ozone is primarily deposited and decomposes on surfaces in the forest such as leaves, branches, bark, soil, and litter. In a ponderosa pine

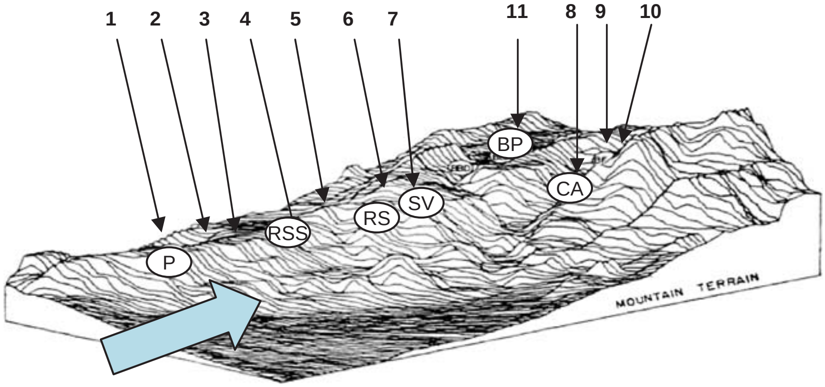

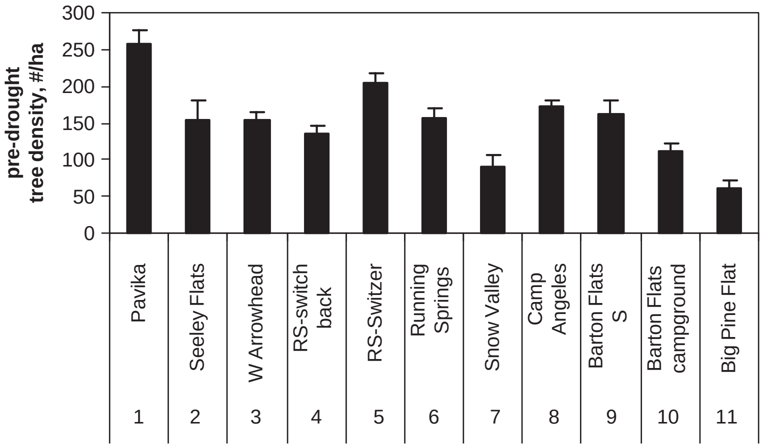

Figure 17.5. San Bernardino Mountains pollution gradient from west to east based on historic data (intermittent databases from 1977 to 1995). Recent data (2001; Grulke et al., 2004) suggest a more consistent, high O_3 concentration across these sites, with higher nighttime O_3 concentrations experienced in the area around sites 4 and 5 during the growing season. Since nitrogenous deposition is not transported as far (i.e., the west side of the San Bernardino Mountains has higher N deposition than the east side), and because it has accumulated in these ecosystems since post-1945, an N gradient in the soil still persists from west to east (see Fig. 17.3). Nitrogen deposition has contributed to significant densification of forest stands in the western San Bernardino Mountains.

plantation, approximately one-third of the O_3 was absorbed into the leaf via stomata (Bauer et al., 2000). When plants take up carbon dioxide (CO_2) during photosynthesis (the carbon capturing mechanism), they also inadvertently take up O_3 (from the air into the leaf, down a concentration gradient). Once O_3 enters the leaf, it reacts with a thin film of water (apoplastic water) that surrounds cells, where it may be decomposed by ascorbate to oxidative derivatives, which in turn initiate signaling of oxidative stress through receptors in the plasmalemma. The decomposition of O_3 in the apoplastic water requires energy, and the regeneration of oxidized ascorbate with glutathione in the cytosol (De Kok & Tausz, 2001). Once oxidative derivatives are formed, membrane pH and permeability is altered such that ions that should be retained by the cell leak out and other ions influx along a chemical as well as charge gradient (Zhang et al., 2001). Other mechanisms of ion transport such as calcium (Ca^{+2}) channeling can also be blocked with O_3 exposure (McAinsh et al., 2002). Also, the oxidative derivatives may initiate signaling of stress (Pei et al., 2000), which could stimulate a chain of metabolic steps that launch an antioxidative defense, or cell death if redox regulation in the cell is overwhelmed.

Drought stress that is sufficient to reduce stomatal conductance, while the leaf is experiencing moderately high light levels ($>1000\,\mu mol\,m^{-2}\,s^{-1}$), may also induce oxidative stress. Under these conditions, there is sufficient light to drive photosynthesis, but CO_2 may be limited by lower stomatal aperture. Instead of passing light-excited electrons to CO_2, it may be passed to O_2 (which is in abundance if photosynthetic rate is high under nonlimiting light levels), forming a highly reactive oxygen radical ($\bullet O$), which then reacts with O_2 to form O_3 within the chloroplast. An antioxidant signature of this process was presented for Jeffrey pine in xeric versus mesic microsites (Grulke et al., 2003b). When strong oxides degrade photosynthetic pigments in the chloroplast, the pigments must be reconstructed into functional arrays, requiring additional nutrients and energy.

One of the first measurable effects of O_3 in plants is a decrease in the efficiency of photosynthesis. Carbon–carbon bonds store energy in plants for later use. Because O_3 damages tissue, there is a metabolic cost in energy, C, and nutrient resources to repair tissues (Matyssek & Sandermann, 2003). That metabolic cost is reflected in an increase in respiration and decrease in the total C stored by the plant. Lower total C stored and greater requirements for N (to rebuild photosynthetic pigments) results in retranslocation of materials from older to younger needles.

In general, a reduction in leaf water loss (transpiration or stomatal conductance to water) accompanies the reduction in photosynthesis in low to moderate O_3 exposures (for ponderosa pine seedlings; Weber et al., 1993). Both moderate or lower O_3 exposure, and a low level of drought stress have been shown to reduce stand level O_3 uptake (for ponderosa pine; Panek & Goldstein, 2001). Although drought is considered to protect plants via a reduction in O_3 uptake, under moderate O_3 exposure and greater levels of drought stress, the two stresses were synergistically deleterious for C acquisition (for ponderosa pine in 1994 at Barton Flats; Grulke et al., 2002).

17.5.2. Whole tree and stand levels

At the whole plant (tree) level, O_3 exposure and excess N deposition results in premature senescence and loss of needles (within whorl loss of needles, fewer needle age classes) (Grulke, 2003; Grulke & Balduman, 1999). The greater the O_3 exposure and N deposition, the more needles are lost. One of the reasons this may occur is that with ample nitrogen availability, older needles may not be needed as storage organs for nitrogen. In a moderately polluted site such as Barton Flats, up to nine needle age classes were retained in ponderosa pine. At a high pollution site such as Camp Paivika, only four needle age classes were retained, but there were few needles retained in the older needle age classes. When air pollution was combined with moderate drought stress in the following year, less than three needle age classes were retained at Camp Paivika, whereas five were retained at Barton Flats (Grulke & Balduman, 1999). In an atmospherically "clean" site on the Lassen National Forest, seven needle age classes were retained even in a drought year. Because premature needle senescence of older needles can be extreme in high pollution sites (Camp Paivika), 95% of the total canopy biomass can be found in current-year foliage (Grulke & Balduman, 1999). In contrast, canopy foliar biomass was more or less evenly distributed across four to five needle age classes in Lassen National Forest.

Self-pruning of older (lower) branches is accelerated in O_3-exposed trees (Miller et al., 1996). First, lower branches are more likely to be shaded, and shaded branches have greater transpiration (water loss through stomata from foliage) per unit C uptake but inadvertently also take up more O_3. Second, because lower branches are more shaded and are more injured due to O_3 uptake, the net C balance is lower. Presumably when net C balance drops below zero, the branch is excised (Sprugel et al., 1991; but see Reiter et al., 2005).

As a result of the combined effects of O_3 exposure and chronic N deposition, needle and branch production and loss are increased and may contribute to greater litterfall (Fig. 17.6). In addition to pollutant stressors, other factors could contribute to differences in litterfall, such as stand density, composition, leaf area index, and differences in forest floor

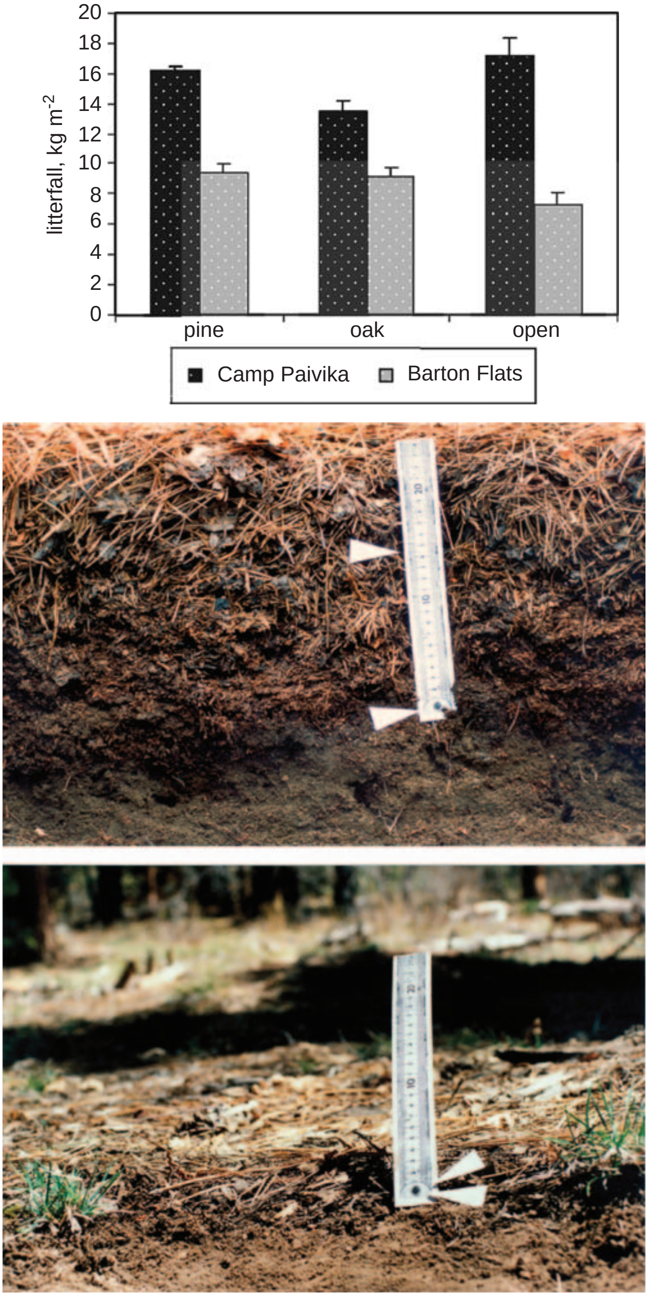

Figure 17.6. Difference in forest floor litter layer between a high and moderate pollution site (Camp Paivika [upper photo] and Barton Flats [lower photo], respectively). Arrows depict the decomposed O_2 litter layer. Annual litter accumulation ranged from 50 to 125% greater in the more polluted site. The large difference in litter build up at Camp Paivika was likely due to both higher litter deposition (O_3 exposure, N deposition, and drought) and lower litter decomposability due to O_3-induced high lignin content (Dizengremel, 2001) and the effects of N enrichment on long-term deposition (Fog, 1988; data from tabular data presented graphically from Fenn et al., 2005).

microenvironment (lower temperatures may be associated with higher stand density, and thus result in lower decomposition rate). Simulations using the CENTURY model predicted greater long-term needle fall with the combination of O_3 and N deposition (Arbaugh et al., 1999).

Litter accumulation is further enhanced by the retarding effects of these pollutants on litter decomposition. Higher lignin content is found in needles produced in high O_3 exposure environments (Dizengremel, 2001), and greater lignin content reduces decomposability (Kimmins, 1997). As a result of N deposition, litter N concentrations are significantly higher in the more polluted areas of the San Bernardino Mountains. The higher N levels in litter result in higher litter decomposition rates in the initial stages of decomposition (Fenn & Dunn, 1989; Persson et al., 2000). However, many studies have demonstrated that long-term decomposition rates are retarded by high N concentrations in litter (Berg, 2000; Fog, 1988; Persson et al., 2000; Swanston et al., 2004), particularly in high lignin content litters (Carreiro et al., 2000; Knorr et al., 2005), and that litter accumulates to a greater degree in N-enriched forests (Kuyper, 1994; Nilsson, 1995; Nohrstedt et al., 1989). In the western San Bernardino Mountains experiencing high pollution, the O_2 litter depth averaged 15 cm compared to 1 cm in the eastern San Bernardino Mountains experiencing moderate pollution (Fig. 17.6). The mass of litter in the forest floor is typically 50–125% greater in the more polluted site. The large difference in litter accumulation between the high and low pollution sites is a result of greater tree densities, high leaf turnover rates, and inhibited long-term decomposition at the high pollution site.

Perhaps because of the increased repair costs for aboveground tissues, less biomass is retained in roots of ponderosa pine exposed to high O_3 concentrations, which is exacerbated by lower allocation to root mass with N-enrichment (Haynes & Gower, 1995). From the western to the central San Bernardino Mountains, both O_3 and N deposition contributed to significantly lower fine and medium root biomass at depths of -10, -30, and -50 cm. Root biomass at these sites was 6–14 times lower than that at a moderate pollution site (Fig. 17.7; Grulke et al., 1998). Lower root biomass alone significantly increases the susceptibility of ponderosa pine to drought in this Mediterranean-type climate.

In addition to lower leaf and root mass (Grulke et al., 1998), ponderosa pine also had lower carbohydrate concentrations of both leaf and root tissue (Grulke et al., 2001) at the high pollution sites relative to the moderate pollution site. In general, carbohydrates for spring growth are stored in the roots over winter. However, because of the lower leaf and

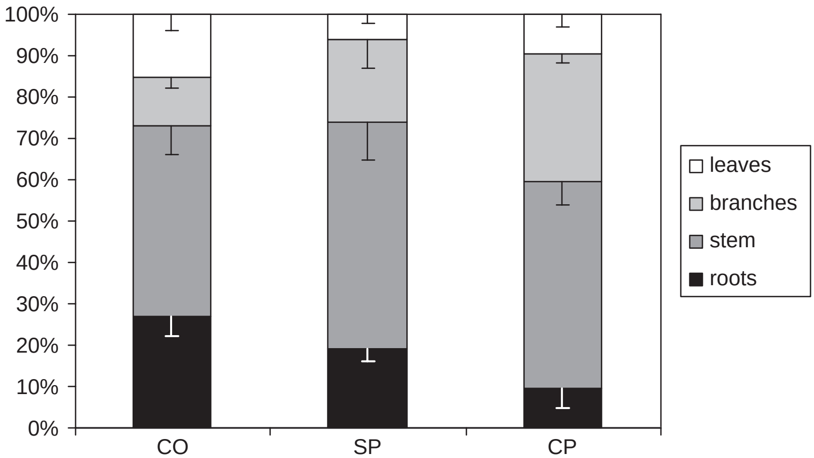

Figure 17.7. Exposure to high O_3 concentrations and excess N deposition alters biomass allocation (*y*-axis, in %) within ponderosa pine (Grulke & Balduman, 1999). CO is Camp Osceola, a site in eastern Barton Flats, in the eastern San Bernardino Mountains (less polluted site); Strawberry Peak is a site between sites 4 and 5 (see Fig. 17.4); and CP is Camp Paivika (highly polluted site).

root mass in ponderosa pine at highly polluted sites, overwintering carbohydrate was stored in tree boles, and potentially in branches (as seen in Fig. 17.7 at Camp Paivika). Hypothetically, increased carbohydrate storage as found in the bole subcortex, which includes phloem, cambium, and xylem, may enhance fecundity of bark beetles that feed and create galleries for their eggs and larvae in this area of the tree (see later).

At the scale of the stand, N deposition, associated with high to moderately high O_3 concentrations, increased stand density, as has been shown by Miller et al. (1989) for the period from 1973 to 1988, and subsequently by Arbaugh et al. (1999). Stand densification was especially promoted on north-facing slopes and in microsites with more water availability or lower evapotranspiration (topographic lows). When more stringent regulatory controls were imposed limiting O_3 concentrations in the early 1990s (Lee et al., 2003), ponderosa pine diameter growth increased in the western San Bernardino Mountains (Arbaugh et al., 1999; Tingey et al., 2004). In these stands, historically high O_3 exposure was also associated with high N deposition, which was not regulated and persists in the soil. Current N deposition fluxes in throughfall in the western San Bernardino Mountains are 30–470 kg N ha^{-1} yr^{-1} (Breiner et al., 2007). Excess N promotes tree growth, especially with reduced oxidant exposure. Dense forest stands and rapid canopy growth further increase susceptibility to drought because of the greater total demand for water at the stand level.

17.6. Air pollution effects on the incidence of forest tree diseases

Ozone injury has been shown to predispose ponderosa pine to annosus root disease (*Heterobasidion annosum*; James et al., 1980) and black stain root disease (*Leptographium wageneri*; Fenn et al., 1990). The effects of elevated soil N levels on disease has not been studied in the San Bernardino Mountains, although N-enrichment has been shown to increase fungal and bacterial diseases of foliage (Snoeijers et al., 2000). Annosus root disease was most severe in Norway spruce (*Picea abies* (L.) H. Karst.) in N-rich soils (Boyce, 1961). Nitrogen fertilization has also been shown to increase root rot of eucalyptus (Marks et al., 1973) and crown and root rot of apple trees (Utkhede & Smith, 1995), both caused by *Phytophthora* species.

Ponderosa and Jeffrey pine stands are frequently infected with Western dwarf mistletoe (*Arceuthobium campylopodum* Engelm.), but possible relationships between air pollution and the severity of mistletoe infestations in the San Bernardino Mountains have not been studied. It has long been assumed that reduced tree vigor from dwarf mistletoe infection, plus the debilitating effects of O_3, is additive in the least, and results in greater host mortality (Pronos et al., 1999). We hypothesize that greater allocation of plant carbohydrates and biomass aboveground as a result of O_3 exposure and N deposition may enhance mistletoe parasitism by providing a greater pool of available nutrients at infection points. Severe infections with mistletoe increase tree mortality rates and predispose trees to attack by insects (Hawksworth & Shaw, 1987), suggesting that if O_3 and N deposition do in fact predispose pine trees to more severe mistletoe infestations, the additional factor of air pollution stress will likely lead to enhanced tree mortality. Even though O_3 injury and possibly increased N fertility are known to increase tree diseases, including the major diseases occurring in the San Bernardino Mountains, it has not been shown that tree diseases are more common or severe in the more polluted sites within this mountain range (Pronos et al., 1999).

17.7. Effects of periodic extreme drought on forest health

Ponderosa pine frequently experiences drought stress in the Mediterranean-type climate of California. Although there is an increase in evapotranspiration from west to east, weather that results in precipitation in the San Bernardino Mountains is generally a regional phenomenon. The longest record of precipitation for the range has been collected over the past 123 years at Big Bear Dam (San Bernardino County Water Resources Division, www.sbcounty.gov/transprtn/psw/; Fig. 17.2) in the eastern San Bernardino Mountains. The seasonal distribution of precipitation begins with the onset of the hydrological year on October 1 (Fig. 17.8). Regardless of the total annual precipitation (low, average, or high), 90% of the annual precipitation accumulates by April 1. Summer precipitation occurs when occasional monsoonal incursions from the Gulf of California travel north into California, but these events are generally insufficient to relieve late summer drought stress in pine for more than a few days (Franco-Vizcaino et al., 2002). An exception was a mid-July precipitation event in 1992 that wetted soils to −15 cm and increased stomatal conductance for 10 d (Temple & Miller, 1998). Such events in 1993 and 1994 had little influence on stomatal conductance. By relating the level of physiological stress that develops in ponderosa pine to the total annual precipitation received in that year, we have a means for estimating how

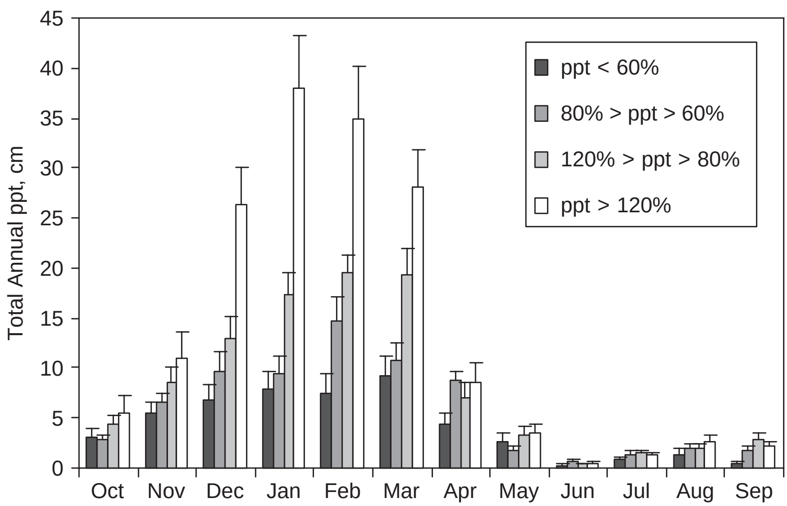

Figure 17.8. Seasonal distribution of annual precipitation in extreme drought years (<60%), drought (61–80%), average precipitation (81–120%), and above-average precipitation (>120%) relative to the 123-year record from Big Bear Dam, San Bernardino County, California (given in Fig. 17.2). Regardless of the total annual precipitation, 90% of the annual precipitation accumulates by April 1. Sixteen percent of the years had extreme drought, 26% had drought years, and 26% had above average precipitation (>120%).

frequently ponderosa pine historically has experienced moderate or extreme drought stress.

Moderate drought stress is defined physiologically as reduced cell turgor, which lowers stomatal conductance (reduced water loss from the leaf), and lowers cellular water potential, which in turn allows the tissue to hold more tenaciously to the water that is in the leaf (Levitt, 1980). In 1994, a year of 80% of the average precipitation (preceded by an above average precipitation year), ponderosa pine experienced moderate drought stress by mid-July, which was extended through the end of the growing season until the onset of autumn precipitation (Fig. 17.9; Grulke, 1999).

Extreme drought stress is also accompanied by reduced cell turgor, stomatal conductance, and cell water potential. However, extreme drought stress also exhibits increased cell solute concentrations sufficient to disrupt enzymatic function. Cell turgor is reduced sufficiently and, for a long enough duration, that elongation growth is limited. Needles produced in years of extreme drought stress are much shorter (e.g., 2002; Fig. 17.10). In 1996, a year of 60% of the average precipitation (preceded by an above average precipitation year), ponderosa pine experienced

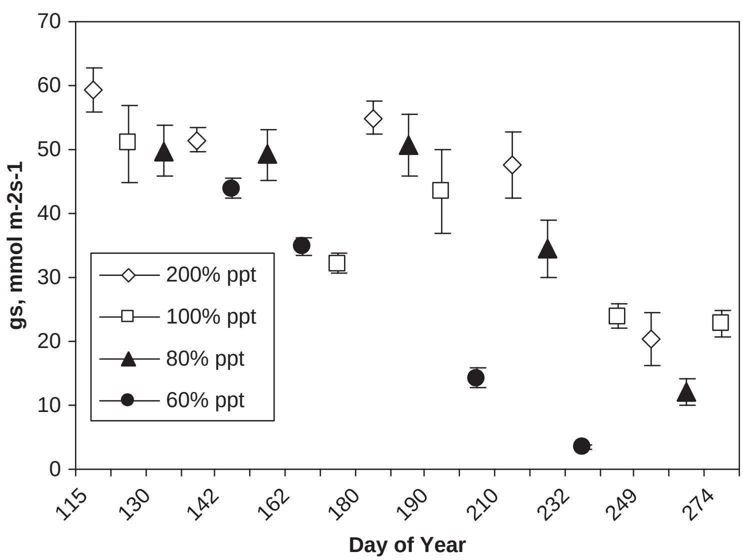

Figure 17.9. Seasonal change in stomatal conductance in years with 200% (1993), 100% (1995), 80% (1994), and 60% (1996) of the long-term precipitation record from Big Bear Dam, San Bernardino County, California. This site, eastern Barton Flats, was 10 km south-southeast of the dam.

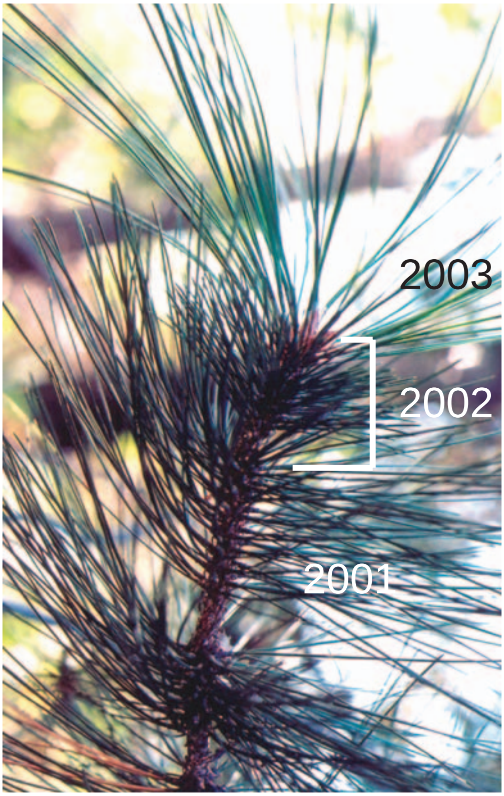

Figure 17.10. Illustration of reduced elongation growth in needles during extreme drought (2002) for ponderosa pine near Silverwood Lake, San Bernardino Mountains, California.

extreme drought stress from the end of June through the end of the growing season (Fig. 17.9), with reduced elongation growth.

Factors that strongly affect the level of physiological drought stress experienced include how precipitation is delivered in each storm, the level of antecedent moisture, and the depth of both the litter layer and mineral soil, by horizon above the bedrock. The San Bernardino Mountains were formed from a granitic dome, with the western half more weathered than the eastern half. However, similar to the Sierra Nevada, the litter layer and the soil depth (to bedrock) are highly variable. Mature pine can grow successfully from cracks in the bedrock, with only thin seams of soil in the cracks, because they have adequate access to moisture in the rock interstices (Hubbert et al., 2001). For example, an intense, single, summer precipitation event of 2 cm did not penetrate the deep litter layer at Camp

Paivika (Franco-Vizcaino et al., 2002). The same storm intensity at Barton Flats with little litter percolated 5 cm into the mineral horizon (Temple & Miller, 1998). At Camp Paivika, that precipitation event positively affected pine water status for a couple of hours, whereas at Barton Flats, pine water status was improved for several days (via reduced evapotranspiration; Temple & Miller, 1998). Until we understand how effective single precipitation events are in contributing to replenishing groundwater reserves, the level of physiological drought stress cannot be adequately modeled in these western ecosystems.

For the purposes of discussion, the following is a rough estimate of the frequency and degree of severity of physiological drought stress in forests of this region. Using the long-term precipitation record (Fig. 17.2), 15% of the years had low enough total annual precipitation to cause extreme drought stress in ponderosa pine, 30% of the years had low enough precipitation to result in moderate drought stress, and 26% of the years had above average precipitation ($>$ 120%). Using this rough index of the level of physiological stress, ponderosa pine experienced drought stress 45% of the years since 1883 when precipitation records were initiated (Fig. 17.2). Multiple years of drought, of course, would intensify the level of physiological stress experienced, but cannot be quantified in this example.

Because O_3 exposure and nitrogen deposition reduce root biomass, pines in the San Bernardino Mountains are already predisposed to drought stress independent of precipitation inputs. In general, low to moderate O_3 exposures ($<$60 ppb) reduce water loss from trees. O_3 reduces photosynthetic rates, less CO_2 is required, and stomatal apertures are reduced to conserve water. However, under moderate, high, or above concentrations, O_3 exposure modifies stomatal behavior in ways that increase drought stress. For example, sugar maple was exposed to O_3 concentrations of 70 ppb during daylight hours (Tjoelker et al., 1995). By mid-season of chronic exposure, there was a significant decrease in water-use efficiency: at the same level of carbon gain, seedlings growing in chronic O_3 exposure had twice the level of water use as control seedlings grown in charcoal-filtered air. In a field study of O_3-sensitive and -tolerant genotypes, sensitive Jeffrey pine had lower water loss under moist, favorable conditions and higher water loss under dry, unfavorable conditions (Patterson & Rundel, 1989). Under favorable conditions, sensitive Jeffrey pine had less water loss, but because the stomatal apertures were smaller, there was also less photosynthetic carbon gain for reparation activities. Under unfavorable conditions (most of the day in the Sierra Nevada), sensitive Jeffrey pine had higher water loss, which results in greater desiccation.

Although physiologists generally report plant response under ‘‘steady state’’ (stable) conditions, the light environment in the forest is dynamic. Understanding stomatal responses under rapidly changing environmental conditions with concurrent O_3 exposure may help explain why trees exposed to moderately high and higher concentrations of O_3 lose more water. In typical forest environments, foliage on a primary branch, on the southern aspect of an open-grown tree experiences ‘‘flecky’’ light two thirds of the time (Grulke, 2000). In experimental simulations of ‘‘sunflecks,’’ stomatal closure in response to abruptly reduced light level was slower in plants without nitrogen amendment: nitrogen amendment partially mitigated the desiccating effects of high O_3 exposure (in California black oak, *Quercus kelloggii*, at Camp Paivika; Grulke et al., 2005).

Moderate to high O_3 exposure can also maintain partially open stomata at night. In experimental O_3 exposures, this was first observed in Norway spruce (*Picea abies*; Weiser & Havranek, 1993) and in birch (*Betula pendula*; Matyssek et al., 1995). They reported nighttime water losses of 25% of that of full daytime rates of water loss. This was corroborated in ponderosa pine across the San Bernardino Mountain pollution gradient, with higher O_3, NO_2, and HNO_3^- exposure. In the latter case, nighttime water losses were 10% of that of full daytime rates of water loss (Grulke et al., 2004).

Because these studies were largely phenomenological, a new gas exchange system was designed and built to directly test the effects of known levels of O_3 concentrations on single leaves. Chronic, moderate O_3 exposure (70 ppb O_3 for 8 h day^{-1} for 1 month) significantly increased nighttime foliar water loss in California black oak and blue oak, *Quercus douglasii* (Grulke et al., 2006). Nighttime water losses were attributable directly to O_3 exposure and were 30% and 20%, respectively, that of daytime rates of foliar water loss in these species. Moderately high (or higher) O_3 exposure increases foliar water loss, and increases tree susceptibility to drought stress. This has been observed at the watershed level in the western Appalachians: on days of high O_3 exposure, less water flow was observed at the watershed level, presumably due to increased canopy transpiration (McLaughlin et al., 2007).

The mechanisms responsible for modified stomatal response (‘‘sluggish’’ resulting in increased foliar water loss) during O_3 exposure are not wholly understood. Ozone exposure mediates increases in apoplastic hydrogen peroxide H_2O_2, which alters membrane permeability, specifically to cation influx (Castillo & Heath, 1990; McAinsh et al., 2002; Pei et al., 2000; Torsethaugen et al., 1999). Increased guard cell cation concentration is associated with increased pH, decreased potassium (K^+)

and chloride (Cl^-), decreased guard cell turgor, and thus decreased stomatal aperture (e.g., reduced g_s or stomatal closure; Zhang et al., 2001). Also, if poor stomatal control in a moderately high O_3 environment resulted in a net increase in transpiration, abscissic acid (ABA) would further modify the H_2O_2-mediated, membrane hyperpolarization and cation influx (Pei et al., 2000). Guard cell zeaxanthin modulates CO_2-dependent changes in stomatal aperture (Zhu et al., 1998): its oxidation state and activity are directly modified by O_3 exposure. In Norway spruce, sluggish stomatal response to O_3 exposure was attributable to reduced cell wall lignification. Reduced cell wall lignification resulted in greater g_s, but also in slower stomatal movement because cellulose has a higher affinity for water than lignin (Maier-Maercker & Koch, 1992). These responses describe primary effects of O_3 exposure on the guard or subsidiary cells, or on the surrounding epidermal cells from physical collapse.

We believe that the mechanism of increased loss of water from the leaves in high O_3 environments occurs regularly at the stand level in the western San Bernardino Mountains. The historic (1938–2004) changes in stand cover and tree mortality rates are given for a subset of the plots (Fig. 17.11). The highest mortality rates were observed at the high pollution site, Camp Paivika, at 160 trees ha^{-1} detected after the 1999–2002 drought. Two sites with moderate air pollution (plot 9, Barton Flats, and plot 10, Snow Valley; Fig. 17.11) that had been thinned (9 in the mid-1960s) or succumbed to a wildfire (10, in 1970) had low tree cover, and low mortality. An additional site with moderately high pollution exposure, but lower tree cover due to logging in the mid-1960s (8, Camp Angelus), also had lower mortality rates. This is substantiated by higher mortality rates reported at three of the four sites with the highest pollution (Camp Paivika, Dogwood Campground (near Rim of the World-Switzer), and Camp Angelus; in Arbaugh et al., 1999) prior to the 1999–2002 drought. Combined, high predrought tree density was correlated (adjusted $r^2 = 0.56$) with postdrought tree mortality (Fig. 17.12). Because of high tree density, the light environment for most of the canopy is likely to be dynamic, not stable. Poor plant water control due to direct effects of O_3 exposure on guard cell control may have exacerbated drought stress and mortality at high O_3 exposure sites.

17.8. Susceptibility to successful bark beetle attack

Ultimately, plant health is determined by plant access to, and accumulation of, C, water, and nutrient resources. Environmental factors

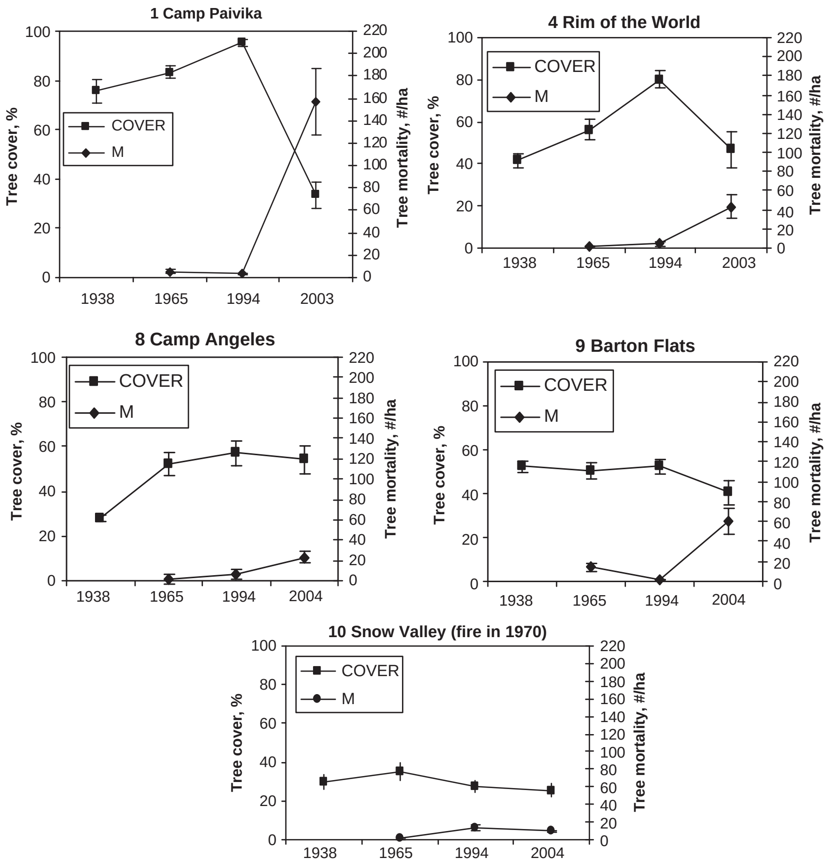

Figure 17.11. Development of tree canopy cover and associated tree mortality rate estimated from four to eight 1-ha plots at each of the five sites. Location of sites is given in Fig. 17.4. Across a pollution gradient in the San Bernardino Mountains (1: Camp Paivika is the most polluted site; 9: Barton Flats is the least polluted site in this sequence; 10: Snow Valley is an example of a site with moderate air pollution and wildfire in 1970).

such as drought that reduce stomatal aperture consequently reduce both C acquisition in the short term (daily, cumulative) and nutrient flow in the transpirational stream to the foliage over the long term (months). Nearly all species of bark beetles are opportunists that attack trees in a weakened state. Host colonization, and more specifically, host selection behavior in bark beetles is a complex process involving both long-range and proximal behavioral components (Fig. 17.13). With only a few exceptions, either the host tree is killed by the colonizing bark beetles, or the host resistance

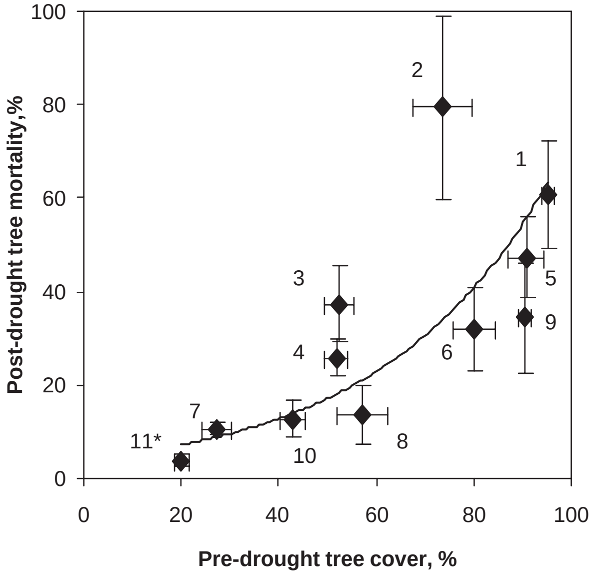

Figure 17.12. In the San Bernardino Mountains in southern California, predrought canopy cover (*x*-axis) in ponderosa pine-dominated mixed-conifer stands appears to influence the level of postdrought tree mortality (*y*-axis), largely due to successful bark beetle attack in these stands. Numbers correspond to plot numbers in Fig. 17.5. The upper four points are unmanaged stands. The lowest two points represent stands with prescribed burns (marked with a sun). Managed stands with thinning are indicated with arrows.

of the tree kills or otherwise repels the attacking adults. To kill a tree, large numbers of beetles must successfully colonize in a relatively short period of time (Paine et al., 1984, 1997). However, fewer beetles may be sufficient to kill a compromised tree (Paine et al., 1984). In a recent study in the San Bernardino Mountains, bark beetle activity and mortality of ponderosa and Jeffrey pine were positively related to O_3 injury and N deposition or experimentally amended N level (Eatough-Jones et al., 2004). Earlier studies also demonstrated that bark beetle damage was more severe, and host resistance decreased, in O_3-injured pines in the San Bernardino Mountains (Stark et al., 1968).

The primary bark beetles responsible for ponderosa pine mortality in the western San Bernardino Mountains are the western pine beetle, *Dendroctonus brevicomis* LeConte, and the mountain pine beetle, *D. ponderosae* Hopkins. Western pine beetle can produce up to four generations in a year in southern California due to the mild climate. As observed in the San Bernardino Mountains in 2003 through 2005

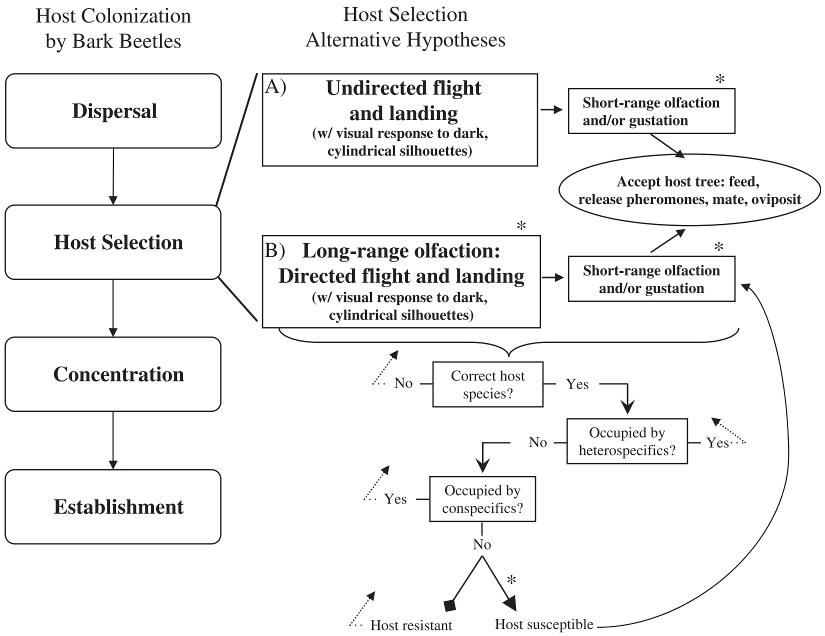

Figure 17.13. Host colonization by bark beetles is subdivided into four phases (dispersal, host selection, concentration (aggregation), and establishment) according to Wood (1982). Two major hypotheses to describe host selection are based on (A) undirected flight or (B) directed flight based on long-range olfactory signals (Borden, 1997; Byers, 2004; Campbell & Borden, 2006; Pureswaran & Borden, 2005; Wood, 1982). Both of these alternatives may also integrate vision with olfaction, as some species respond well in flight to dark, cylindrical silhouettes (Strom et al., 1999, 2001). Both hypotheses may also include short-range olfaction and gustatory (tasting) behavior (McNee et al., 2000, 2003) after landing on the stem of a host or nonhost. Prior to (long range) or after landing, a bark beetle may undergo a series of binary decisions to evaluate the suitability or susceptibility of a host (Borden, 1997). Host selection decision nodes likely to be affected by air pollution, drought, and wildfire are indicated by (∗). (This figure was developed with the assistance of A.D. Graves, University of Minnesota, Department of Entomology.)

(Fig. 17.14), beetle populations increase rapidly, and the spatial extent of groups of dead trees expands annually when there is an abundance of susceptible trees.

Bark beetles aggregate and feed on the phloem, cambium, and outer xylem (subcortical tissue) in the tree bole. Eggs are laid in the phloem, and the larvae excavate galleries in this tissue. For most species, the larvae and pupae occur only in the phloem. Western pine beetle is unusual in that larvae of the second of the four instars (stages) migrate to the outer bark to complete their development (Miller & Keen, 1960). Thus,

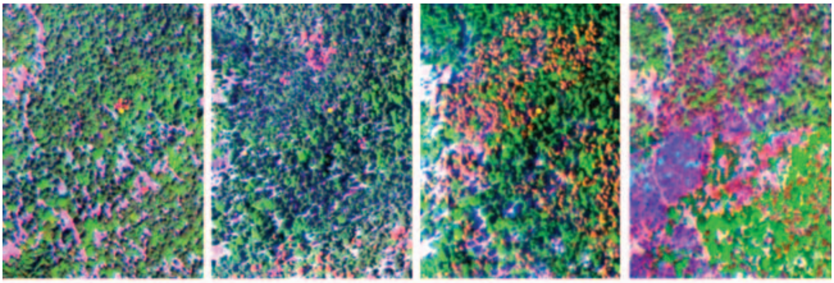

Figure 17.14. Remote imagery of Camp Paivika, San Bernardino National Forest, California. This forest stand is most affected by ozone and N deposition in North America. The sequence of remote imagery above was constructed from red, near-infrared, and thermal wavelengths at 5 km above the forest canopy. The yellow dot denotes the same location in each image. The forest stand is a mix of ponderosa pine, California black oak, white fir, incense cedar, and sugar pine. A dirt road and bare soil or dead herbaceous vegetation is indicated in fuchsia. On July, 20, 2001, the third year of a chronic drought, the first sign of bark beetle attack occurred on the site near the yellow dot (copper-colored trees). On May 27, 2003, after three years of chronic drought and an acute drought (2002), additional points of bark beetle infection were observed, including some possible drought-induced mortality (more scattered, individual dead ponderosa pine near the bottom of the image). On September 18, 2003, after the drought years plus the wet year (2003), tree mortality continued to accelerate, primarily ponderosa pine, white fir, and some sugar pine. On July 7, 2004, tree mortality was further increased (purple and fushia-colored areas) after the Old Fire swept through the area on October 12, 2003. At the stand level, the tree mortality for the first three dates, respectively, was 0%, 5%, and 42%. Observed mortality (estimated from proportion of pixels) declined to 32% in the July 7, 2004 image due to needle loss on standing dead trees.

pupation occurs either in the inner bark or in the outer bark, depending on the species of beetle. Adults emerge from the larval host tree and disperse to select new susceptible hosts (Fig. 17.13).

When attacked, healthy pines respond by exuding resin that either ‘‘pitches out’’ the adults, or blocks their progress. Resin production provides both a physical and chemical impedance to bark beetle attack. This response by pines is both constitutive and inducible after attempted colonization by the beetles (Franceschi et al., 2005; Langenheim, 2003; Nebeker et al., 1993). However, pines rely heavily on the preformed (i.e., constitutive) resin-based defense relative to other conifers (Nebeker et al., 1993). Oleoresin pressure, related to the turgor potential of cells lining the resin ducts, forces preformed resin to the site of injury or invasion. The cell turgor is derived from the transpirational stream; thus, if the tree is under drought stress, the cells lose turgor, the resin pressure is reduced, and the effectiveness of the preformed resistance is compromised (Vité, 1961).

In weak trees with reduced resin pressure, adult beetles are able to successfully colonize and produce specific pheromones that attract other colonizing adults (concentration phase, Fig. 17.13). In 2000 (an average precipitation year based on a 68-yr record), Jeffrey pine was under sufficient drought stress so that the outer 1–2 cm of xylem tissue was < 50% water content in August and September versus 95% earlier in the growing season, and the transpirational stream was nearly 0 in xeric microsites (in Sequoia National Park; Grulke et al., 2003a). Of 32 Jeffrey pine in xeric microsites, 4 had succumbed to bark beetle by 2006 versus 2 out of 32 Jeffrey pine in mesic microsites (Grulke, unpublished data; mortality due to bark beetle, John Wenz, pers. comm.).

Extreme drought and other stresses reduce the photosynthetic capacity of trees and the levels of carbohydrates used for growth, defense, and tissue repair. This can have significant impact on the ability of the tree to induce an effective response to invasion (Mattson & Haack, 1987; Paine & Stephen, 1987a,b), as plants have only a limited amount of resources to partition between growth and defense (Herms & Mattson, 1992). Environmental factors such as drought stress also alter within-plant allocation of carbohydrates (Kozlowski & Pallardy, 2002). As mentioned previously, the high pollution site (Camp Paivika) had elevated carbohydrate content in just the bole (stem) due to changes in within-plant allocation relative to sites with lower stress levels (Grulke et al., 2001). Such a change in subcortical tissue concentration of carbohydrates may be a "tipping point" for increases in bark beetle populations. Trees with elevated bole carbohydrate levels at Camp Paivika sustained the highest rates of tree mortality due to both drought and bark beetle in the San Bernardino Mountains (see Fig. 17.12, site 1). In the 1960s, a multidisciplinary team of scientists concluded that ponderosa pines in this area that had been exposed to atmospheric pollutants were predisposed to bark beetle infestation (Stark et al., 1968). Highly drought-stressed plants are also known to exhibit increased levels of free amino acids (such as proline; Ain-Lhout et al., 2001; Lei et al., 2006), which are thought to increase cellular solute concentration, and thus lower osmotic potential and increase the ability of the cell to retain water under drought stress (but see discussion in Hare et al., 1998). However, an increase in free amino acids in subcortical tissue may also improve nutritional value for bark beetles, but is as yet untested. Once mature bark beetles emerge from the galleries by tunneling through the outer bark, they begin searching for a host. Although they appear to be able to discriminate host from nonhost, while in flight it is unclear whether they can determine from a distance whether a host is susceptible or not (Fig. 17.13; Borden, 1997). Interestingly, conifers under moderate drought stress produce jasmonate, a plant hormone that stimulates resin production (for Norway spruce; Zeneli et al., 2006). There is no evidence that jasmonate itself elicits electrophysiological or behavioral responses from bark beetles. However, dense stands of pine, overgrown from excess N deposition and historic land management practices, may produce ample signal (terpene production), which could alter nonolfactory aspects of short-range host selection behavior (Fig. 17.13). During the extreme drought experienced in 2002, trees likely had insufficient turgor pressure in subcortical cells to exude resin. Thus, these trees may have been chemically competent, but physically incapable of exuding the resin as defense. Pollutant-exposed trees, already compromised and susceptible to drought stress, may be primed for successful bark beetle colonization.

17.9. Stand demographics across the San Bernardino Mountains

The type, timing, and magnitude of multiple stressors across the San Bernardino Mountains are presented in Table 17.2, which qualify the environmental conditions that led to bark beetle infestations. There were nine periods in the past 123 years that may have had sufficient tree drought stress to precipitate beetle epidemics. We can find evidence for five such events in the California Pest Reports that were first published annually in 1949. Prior to that, letters of the Forest Entomologist to the Regional Forester were used (written annually) to ascertain level of bark beetle infestation. Bark beetle was not considered significant (designated with a "+" in Table 17.2) unless more than four areas of 2000 ha or more were reported. Because the same areas were not inspected aerially and/or reported on each year, we report infestation qualitatively.

Since the forest in the San Bernardino Mountains had been thinned early in the late 19th century by commercial logging, we would not expect to observe an epidemic beetle infestation early in the 20th century, despite the drought stress experienced (Minnich et al., 1995) because tree density was low (Fig. 17.11). Human population in the Los Angeles Basin significantly increased after 1945, but air pollution levels were not quantified (or reconstructable) until 1963. From 1963 through 1980, peak 1-h O_3 concentrations averaged 250–425 ppb (Lee et al., 2003). From 1980 on, peak 1-h O_3 concentrations were still high (>250 ppb), but cumulative O_3 exposures over the growing season began to decline. Through strong regulatory controls, O_3 concentrations declined further

Table 17.2. List of drought years experienced regionally, bark beetle outbreaks, pollution levels, and stand density in the western San Bernardino Mountains. The years of moderate or extreme drought, the average percent of total average annual precipitation (based on the 120-yr record), the percent of total average annual precipitation in the year following drought, and whether a bark beetle epidemic occurred after the sequence of drought years is also presented

1st year of drought	Dates of aerial photos	% of 123-yr record[a]				3–4 year average	Bark Beetle[b]	Pollution SUM06[c]	Tree cover %[d]
		1	2	3	4				
	1860								(Logged)
1897		54	35	60		50			
1922		68	60	70		66			
1927		51	65	84	79	70			
	1938								76 ± 5
1947		78	88	84	64	79			
1958		71	73	46		63	++		
	1965							100	83 ± 3
1969		55	66	55		59	+++	170	
1973		61	63	79	42	61	++	140	
1986		47	37	48	48	45	++	160	
	1994							150	95 ± 1
1999		39	56	59	25	45	++++	110	
	2004								34 ± 5

[a]San Bernardino County Water Management District database, site 6032 Big Bear Dam, from 1983 to present.
[b]California Pest Reports, Annual, USDA Forest Service, San Francisco, California; 1949 to present for the San Bernardino Mountains area in general.
[c]Air pollution reconstructed for the Camp Paivika area, as an example from Lee et al. (2003).
[d]Changes in stand cover from Camp Paivika estimated from eight 1-ha plots drawn on aerial imagery (this chapter).

to tens of occurrences to only isolated occurrences of hourly concentrations exceeding 95 ppb from the mid-1990s to present. However, N continued to accumulate in these ecosystems, and drought stress was exacerbated by chronic O_3 exposure.

The effect of multiple stressors (pollutant deposition, stand densification, drought stress, effects of bark beetle infestations) on stand demography were evaluated across the San Bernardino Mountains at 11 sites (Fig. 17.5) using historic aerial photographs from 1938, 1965, 1994, and 2004 (archived at the SBNF Supervisor's Office, San Bernardino, California). These years were chosen with regard to prior multiple-year droughts and photographic quality. Stand demography (tree cover and density, recruitment, and mortality) was measured from four to eight 1-ha plots sampled sequentially from the aerial photographs taken in (Fig. 17.3). In the western San Bernardino Mountains (plot 1) and at other high pollutant exposure sites (plot 5, 6, 8) along the southern and western front of the range, tree density was especially high (as high as 160 trees ha^{-1}). Tree density increased the most from the mid-1960s to 1994 (Fig. 17.11). The highest mortality rates were observed between 1994 and 2004 at the sites with the highest initial density or tree cover (sites 1, 2, and 5, Fig. 17.12). At sites with the lowest canopy cover or tree density resulting from wildfire (1970 in Snow Valley, site 7, Figs. 17.5, 17.11, 17.12) or prescribed fire (1987 in Big Pine Flat, site 11, Fig. 17.5), mortality was <10 trees ha^{-1} (Fig. 17.12). Despite the high predrought tree density at Seeley Flats (site 2), we believe that mortality was lower than expected due to more consistent groundwater availability relative to other sites in the western San Bernardino Mountains. We cannot explain the high tree density development at Barton Flats (site 9), a moderate pollution site, but this is also reported by Miller et al. (1989) and Arbaugh et al. (1999) for plots located in the same area.

Although aerial photography illustrated decadal or multiple decadal changes in forest density and mortality rates, we were able to capture the specific effects of chronic drought (1999–2001), the acute drought (2002), the development of epidemic bark beetle infestation (2003–2004), and the incursion of the October 2003 Old Fire from the chaparral into the mixed-conifer forest (Fig. 17.14) at one of the sites (site 1, Camp Paivika, the high pollution site). A sequence of images was taken at 5 km above the forest canopy and constructed from the intensities of red, near-infrared, and thermal wavelengths.

After 3 years of chronic drought at this polluted site, clusters of tree mortality due to bark beetle attack were apparent in the July 20, 2001, imagery (red trees, Fig. 17.14). Based on imagery analysis, the mean stand tree mortality rate was 0% based on subsamples of four, 0.25 ha plots

(Fig. 17.14). After both chronic and acute drought, tree mortality due to both bark beetles and drought was 5% at the stand level (mostly ponderosa pine) based on the same imagery analysis (May 27, 2003). A field measure of mortality at this site yielded 9.5% mortality, also assessed in spring 2003 (based on a total of 62 yellow pine trees (ponderosa and Jeffrey pine combined); Eatough-Jones et al., 2004). In the spring following the wet winter, bark beetle populations reached epidemic proportions, and 42% of the trees had died (ponderosa pine, white fir, and sugar pine) by September 18, 2003 (proportion of imagery with "dead tree" signature of red, near-infrared, and thermal, Fig. 17.14). Estimates of mortality from true-color aerial photographs (42.7%) were very similar. Field assessments in the previous spring estimated that a total of 55.6% of the ponderosa pine had been affected by bark beetle activity (Eatough-Jones et al., 2004), suggesting that most of the tree mortality at the site was attributable to successful bark beetle colonization of ponderosa pine (assuming all ponderosa pine colonized in spring 2003 were destined to die by fall 2003). Discrepancies between field counts and imagery analysis are likely due to inability to count dead trees under large canopies (field count predicted higher mortality), the patchy distribution of beetle colonization (see Fig. 17.14), total sample size (aerial photos: 2920 trees in eight 1-ha plots; field count: 60 trees in three plots), and time lag between bark beetle colonization and tree death.

The stand was at high risk for an intense fire with high litter layers, high numbers of standing dead trees, and susceptible live trees exacerbated by drought stress. In autumn of that year, the Old Fire swept through the stand (imagery taken the following summer, July 10, 2004 Fig. 17.14). Interestingly, not all of the "red trees" (standing dead with needles retained) were consumed in a crown fire because the highly dense understory was not in contact with the lower branches of the $\sim$100-yr old trees. The effects of O_3 exposure, excess nitrogen deposition, and drought had promoted lower branch abscission so that the lowest branches were attached at 20 m or higher. Trees continue to be colonized by bark beetles and die at this site, but the rate of change is below statistical detection. We assume that the timing of most of the mortality observed between 1994 and 2004 follows that presented for site 1—that mortality occurred primarily between 2003 and 2004.

17.10. Conclusions

The role of air pollutants in increasing tree susceptibility to drought, successful bark beetle attack, disease, tree mortality, and thus to wildfire has been largely ignored by land managers. Elevated levels of photochemical oxidants and N deposition as described for the San Bernardino Mountains also occur over the western and southern regions of the Sierra Nevada. Ozone injury to pines and elevated nitrate export in streams have also been reported from these areas, suggesting that air pollution in these regions may be sufficient to predispose the most polluted forest stands in the Sierra Nevada to greater mortality and wildfire risk. In the San Bernardino Mountains air pollutants, specifically strong oxidants and nitrogen deposition, contribute to increased litter accumulation and increased tree susceptibility to drought stress. It is well known that drought-stressed trees are more susceptible to successful colonization by bark beetles. The combined chronic drought in 1999–2001 and acute drought in 2002 resulted in a bark beetle epidemic in the western San Bernardino Mountains. The evidence from our research shows that the severity of tree mortality in the western San Bernardino Mountains was significantly exacerbated by the higher air pollutant deposition in this region.

REFERENCES

Ain-Lhout, F., Zunzunegui, M., Diaz-Barradas, M.C., Tirado, R., Clavijo, A., and Garcia-Novo, R. 2001. Comparison of proline accumulation in two mediterranean shrubs subjected to natural and experimental water deficit. Plant Soil 230, 175–183.

Arbaugh, M.J., Peterson, D.L., and Miller, P.R. 1999. Air pollution effects on growth of ponderosa pine, Jeffrey pine, and bigcone Douglas-fir. In: Miller, P.R., and McBride, J.R., eds. Oxidant air pollution impacts in the montane forests of Southern California: A case study of the San Bernardino Mountains, Ecological Studies 134. Springer-Verlag, New York, pp. 179–207.

Asher, J.E., and Forrest, D.W. 1982. Lake arrowhead communities forest management plan's ''State of the Forest'' report. Lake Arrowhead Property Owners Association, Lake Arrowhead, CA.

Atkinson, R., and Arey, J. 2003. Gas-phase tropospheric chemistry of biogenic volatile organic compounds: A review. Atmos. Environ. 37, S197–S219.

Bauer, M.R., Hultman, N.E., Panek, J.A., and Goldstein, A.H. 2000. Ozone deposition to a ponderosa pine plantation in the Sierra Nevada Mountains (CA): A comparison of two different climatic years. J. Geophys. Res. 105, 123–136.

Berg, B. 2000. Litter decomposition and organic matter turnover in northern forest soils. For. Ecol. Manag. 133, 13–22.

Borden, J.H. 1997. Disruption of semiochemical-mediated aggregation in bark beetles. In: Cardé, R.T., and Minks, A.K., eds. Insect pheromone research: New directions. Chapman & Hall, New York, pp. 421–438.

Boyce, J.S. 1961. Forest pathology (Third ed.). McGraw-Hill, New York.

Breiner, J., Gimeno, B.S., and Fenn, M. 2007. Calculation of theoretical and empirical nutrient N critical loads in the mixed-conifer ecosystems of southern California. ScientificWorldJournal 7(S1), 198–205, doi: 10.1100/tsw.2007.65.

Byers, J.A. 2004. Chemical ecology of bark beetles in a complex olfactory landscape. In: Lieutier, F., Day, K.R., Battisti, A., Gregoire, J.-C., and Evans, H.F., eds. Bark and wood boring insects living in trees in Europe, a synthesis. Kluwer Academic Publishers, Dordrecht, The Netherlands, pp. 89–134.

Bytnerowicz, A., Arbaugh, M., Schilling, S., Fraczek, W., and Alexander, D. in press. Ozone distribution and phytotoxic potential in mixed conifer forests of the San Bernardino Mountains, southern California. Environ. Pollut.

Bytnerowicz, A., Tausz, M., Alonso, R., Jones, D., Johnson, R., and Grulke, N. 2002. Summer-time distribution of air pollutants in the Sequoia national park, California. Environ. Pollut. 118, 187–203.

Cahill, T.M., Seaman, V.Y., Charles, M.J., Holzinger, R., and Goldstein, A.H. 2006. Secondary organic aerosols formed from oxidation of biogenic volatile organic compounds in the Sierra Nevada Mountains of California. J. Geophys. Res. 111, D16312, doi: 10.1029/2006JD007178.

Campbell, S.A., and Borden, J.H. 2006. Close-range, in-flight integration of olfactory and visual information by a host-seeking bark beetle. Entomol. Exper. Applic. 120, 91–98.

Carreiro, M.M., Sinsabaugh, R.L., Repert, D.A., and Parkhurst, D.F. 2000. Microbial enzyme shifts explain litter decay responses to simulated nitrogen deposition. Ecology 81, 2359–2365.

Castillo, F., and Heath, R.L. 1990. Ca^{2+} transport in membrane vesicles from pinto bean leaves and its alteration after ozone exposure. Plant Physiol. 94, 788–795.

De Kok, L.J., and Tausz, M. 2001. The role of glutathione in plant reaction and adaptation to air pollutants. In: Grill, D., Tausz, M., and De Kok, L.J., eds. Significance of glutathione to plant adaptation to the environment. Kluwer Academic Publishers, Dordrecht, The Netherlands, pp. 185–205.

Dizengremel, P. 2001. Effects of ozone on the carbon metabolism of forest trees. Plant Physiol. Biochem. 39, 729–742.

Eatough-Jones, M., Paine, T.D., Fenn, M.E., and Poth, M.A. 2004. Influence of ozone and nitrogen deposition on bark beetle activity under drought conditions. Forest Ecol. Manag. 200, 67–76.

Fenn, M.E., and Dunn, P.H. 1989. Litter decomposition across an air-pollution gradient in the San Bernardino Mountains. Soil Sci. Soc. Am. J. 53, 1560–1567.

Fenn, M.E., Dunn, P.H., and Wilborn, R. 1990. Black stain root disease in ozone-stressed ponderosa pine. Plant Dis. 74, 426–430.

Fenn, M.E., and Poth, M.A. 1999. Temporal and spatial trends in streamwater nitrate concentrations in the San Bernardino Mountains, southern California. J. Environ. Qual. 28, 822–836.

Fenn, M.E., Poth, M.A., and Johnson, D.W. 1996. Evidence for nitrogen saturation in the San Bernardino Mountains in southern California. For. Ecol. Manag. 82, 211–230.

Fenn, M.E., and Poth, M.A. 2004. Monitoring nitrogen deposition in throughfall using ion exchange resin columns: A field test in the San Bernardino Mountains. J. Environ. Qual. 33, 2007–2014.

Fenn, M.E., Poth, M.A., Terry, J.D., and Blubaugh, T.J. 2005. Nitrogen mineralization and nitrification in a mixed-conifer forest in southern California: controlling factors, fluxes, and nitrogen fertilization response at a high and low nitrogen deposition site. Can. J. For. Res. 35, 1464–1486.

Fog, K. 1988. The effect of added nitrogen on the rate of decomposition of organic matter. Biol. Rev. 63, 433–462.

Franceschi, V.R., Krokene, P., Christiansen, E., and Krekling, T. 2005. Anatomical and chemical defenses of conifer bark against bark beetles and other pests. New Phytol. 167, 353–376.

Franco-Vizcaino, E., Escota-Rodriguez, M., Sousa-Ramirez, J., and Minnich, R.A. 2002. Water balance of the southern limit of the California mixed conifer forest and implications for extreme deficits watershed. Aridland Res. Manag. 16, 133–147.

Grulke, N.E. 1999. Physiological responses of ponderosa pine to gradients of environmental stressors. In: Miller, P.R., and McBride, J., eds. Oxidant air pollution impacts in the Montane Forests of southern California: A case study of the San Bernardino Mountains, Ecological Studies 134. Springer-Verlag, New York, pp. 126–163.

Grulke, N.E. 2000. An analysis of short-, medium-, and long-term O_3 exposure in influencing stomatal conductance of ponderosa pine. Proc., IUFRO Working Group 7.04, Air Pollution Effects, 28–31 May, Michigan Technical University: Houghton, MI.

Grulke, N.E. 2003. Physiological basis of ozone injury assessment in Sierra Nevadan conifers. In: Bytnerowicz, A., Arbaugh, M., and Alonso, R., eds. Assessment of ozone distribution and its effects on Sierra Nevada ecosystems. Dev.Environ. Sci. 2, 55–81. Elsevier Publishers, The Hague, The Netherlands, pp. 55–82.

Grulke, N.E., Andersen, C.P., Fenn, M.P., and Miller, P.R. 1998. Ozone exposure and N deposition reduces root biomass in ponderosa pine across the San Bernardino Mountains, California. Environ. Pollut. 103, 63–73.

Grulke, N.E., and Balduman, L. 1999. Deciduous conifers: High nitrogen deposition and ozone exposure effects on ponderosa pine. Water, Soil, Air Pollut. 116, 235–248.

Grulke, N.E., Andersen, C.P., and Hogsett, W.E. 2001. Seasonal changes in carbohydrate pools of ponderosa pine in stands under differing environmental stress. Tree Physiol. 21, 173–184.

Grulke, N.E., Preisler, H.K., Rose, C., Kirsch, J., and Balduman, L. 2002. O_3 uptake and drought stress effects on carbon acquisition of ponderosa pine in natural stands. New Phytol. 154, 621–631.

Grulke, N.E., Johnson, R., Esperanza, A., Jones, D., Nguyen, T., Posch, S., and Tausz, M. 2003a. Canopy transpiration of Jeffrey pine in mesic and xeric microsites: O_3 uptake and injury response. TREES 17, 292–298.

Grulke, N.E., Johnson, R., Jones, D., Monschein, S., Nikolova, P., and Tausz, M. 2003b. Variation in morphological and biochemical O_3 injury attributes of Jeffrey pine within canopies and between microsites. Tree Physiol. 23, 923–929.

Grulke, N.E., Alonso, R., Nguyen, T., Cascio, C., and Dobrowolski, W. 2004. Stomata open at night: Implications for pollutant uptake in ponderosa pine. Tree Physiol. 24, 1001–1010.

Grulke, N.E., Dobrowolski, W.L., Mingus, P., and Fenn, M.E. 2005. California black oak response to N-amendment at an N-saturated site. Environ. Pollut. 137, 536–545.

Grulke, N.E., Paoletti, E., and Heath, R.A. 2006. Direct measurements of foliar ozone uptake in crop and tree species. Environ. Pollut. 146, 640–647.

Hare, P.D., Cress, W.A., and Van Staden, J. 1998. Dissecting the roles of osmolyte accumulation during stress. Plant Cell Environ. 21, 535–553.

Hawksworth, F.G., and Shaw III, C.G. 1987. Damage and control of major diseases of ponderosa pine. In: Baumgartner, D.M., and Lotan, J.E., eds. Symposium proceedings, ponderosa pine: The species and its management, 29 September 29 to 1 October. Spokane, Washington, USA. Dept. Nat. Res. Sci., Coop. Ext., Washington State University, Pullman, WA, pp. 99–108.

Haynes, B.E., and Gower, S.T. 1995. Belowground carbon allocation in unfertilized and fertilized red pine plantations in northern Wisconsin. Tree Physiol. 15, 317–325.

Herms, D.A., and Mattson, W.J. 1992. The dilemma of plants: To grow or defend. Qtr. Rev. Biol. 67, 283–335.

Hubbert, K., Beyers, J.L., and Graham, R.C. 2001. Roles of weathered bedrock and soil in seasonal water relations of *Pinus jeffreyi* and *Arctostaphylos patula*. Can. J. For. Res. 31, 1947–1957.

James, R.L., Cobb, F.W. Jr., Miller, P.R., and Parmeter, J.R., Jr. 1980. Effects of oxidant air pollution on susceptibility of pine roots to *Fomes annosus*. Phytopath 70, 560–563.

Kimmins, J.P. 1997. Forest ecology: A foundation for sustainable management (Second ed.). Prentice Hall, Upper Saddle River, NJ, USA.

Knorr, M., Frey, S.D., and Curtis, P.S. 2005. Nitrogen additions and litter decomposition: A meta-analysis. Ecology 86, 3252–3257.

Kozlowski, T.T., and Pallardy, S.G. 2002. Acclimation and adaptive responses of woody plants to environmental stresses. Bot. Rev. 68, 270–334.

Kuyper, T.W. 1994. Fungal species diversity and forest ecosystem functioning in the Netherlands. In: Boyle, T.J.B., and Boyle, C.E.B., eds. Biodiversity, temperate ecosystems, and global change, NATO ASI series. Springer-Verlag, Berlin, Vol. I 20, pp. 99–122.

Langenheim, J.H. 2003. Plant resins—chemistry, evolution, ecology, and ethnobotany. The Timber Press, Portland, OR.

Lee, E.H., Tingey, D.T., Hogsett, W.E., and Laurence, J.A. 2003. History of tropospheric ozone for the San Bernardino Mountains of southern California, 1963–1999. Atmos. Environ. 37, 2705–2717.

Lei, Y., Yin, C., and Li, C. 2006. Differences in some morphological, physiological, and biochemical responses to drought stress in two contracting populations of *Populus przewalskii*. Physiol. Plant. 127, 182–191.

Levitt, J. 1980. Responses of plant to environmental stresses. Academic Press, London.

Maier-Maercker, U., and Koch, W. 1992. The effect of air pollution on the mechanism of stomatal control. Trees 7, 12–25.

Marks, G.C., Kassaby, F.Y., and Fagg, P.C. 1973. Die-back tolerance in eucalypt species in relation to fertilization and soil populations of *Phythophthora cinnamomi*. Aust. J. Bot. 21, 53–65.

Mattson, W.J., and Haack, R.A. 1987. The role of drought in outbreaks of plant-eating insects. BioSci 37, 110–118.

Matyssek, R., Gunthardt-Georg, M.S., Maurer, S., and Keller, T. 1995. Nighttime exposure to ozone reduces whole-plant production in Betual pendula. Tree Physiol. 15, 159–165.

Matyssek, R., and Sandermann, H. 2003. Impact of ozone on trees: An ecophysiological perspective, Progress in Botany 64. Springer-Verlag, Heidelberg, 349–404.

McAinsh, M.R., Evans, N.H., Montgomery, L.T., and North, K.A. 2002. Calcium signalling in stomatal responses to pollutants. New Phytol. 153, 441–447.

McLaughlin, S.B., Wullschleger, S.D., Sun, G., and Nosal, M. 2007. Interactive effects of ozone and climate on southern Appalachian forests in the USA: II. Effects on water use, soil moisture content, and streamflow. New Phytol. 174, 109–124.

McNee, W.R., Wood, D.L., and Storer, A.J. 2000. Pre-emergence feeding in bark beetles (Coleoptera: Scolytidae). Environ. Entomol. 29, 495–501.

McNee, W.R., Bonello, P., Storer, A.J., Wood, D.L., and Gordon, T.R. 2003. Feeding response of *Ips paraconfusus* to phloem and phloem metabolites of *Heterobasidion annosum*-inoculated ponderosa pine, *Pinus ponderosa*. J. Chem. Ecol. 29, 1183–1201.

Michalski, G., Meixner, T., Fenn, M., Hernandez, L., Sirulnik, A., Allen, E., and Thiemens, M. 2004. Tracing atmospheric nitrate deposition in a complex semiarid ecosystem using Δ^{17}O. Environ. Sci. Tech. 38, 2175–2181.

Miller, J.M., and Keen, F.P. 1960. Biology and control of the western pine beetle: A summary of the first fifty years of research. USDA Forest Service Misc. Publ. 800.

Miller, P.R., McBride, J.R., Schilling, S.L., and Gomez, A.P. 1989. Trend of ozone damage to conifer forests between 1974 and 1988 in the San Bernardino Mountains of southern California. In: Olson, R.K., and Lefohn, A.S., eds. Effects of air pollution on western forests. Trans., Air, Waste Manag. Assoc., June. Anaheim, CA. Air, Waste, Manag. Assoc.: Pittsburgh, PA, pp. 309–324.

Miller, P.R., Stolte, K.W., Duriscoe, D., and Pronos, J. 1996. Methods for monitoring air pollution: Effects on western conifers. USDA Forest Service PSW-GTR-155.

Minnich, R.A. 1988. The biogeography of fire in the San Bernardino Mountains of California: A historical survey, Geography 28. University of California Publication, Riverside, CA, 128 pp.

Minnich, R.A., Barbour, N.G., Burk, J.H., and Fernau, R.F. 1995. Sixty years of change in California conifer forest of the San Bernardino Mountains. Conserv. Biol. 9, 902–914.

Nebeker, T.E., Hodges, J.D., and Blanche, C.A. 1993. Host response to bark beetle and pathogen colonization. In: Schowalter, T.D., and Filip, G.M., eds. Beetle-pathogen interaction in Conifer Forests. Academic Press, London, pp. 157–173.

Nilsson, L.-O. 1995. Forest biogeochemistry interactions among greenhouse gases and N deposition. Water, Air, Soil Pollut. 85, 1557–1562.

Nohrstedt, H.-Ö., Arnebrant, K., Bååth, E., and Söderström, B. 1989. Changes in carbon content, respiration rate, ATP content, and microbial biomass in nitrogen-fertilized pine forest soils in Sweden. Can. J. For. Res. 19, 323–328.

Paine, T.D., Stephen, F.M., and Taha, H.A. 1984. Conceptual model of infestation probability based on bark beetle abundance and host tree susceptibility. Environ. Ent. 13, 619–624.

Paine, T.D., and Stephen, F.M. 1987a. Influence of tree stress and site quality on the induced defense system of loblolly pine. Can. J. For. Res. 17, 569–571.

Paine, T.D., and Stephen, F.M. 1987b. The relationship of tree height and crown class to the induced plant defenses of loblolly pine. Can. J. Bot. 65, 2090–2092.

Paine, T.D., Raffa, K.F., and Harrington, T.C. 1997. Interactions among scolytid bark beetles, their associated fungi and live host conifers. Ann. Rev. Entomol. 42, 179–206.

Panek, J.A., and Goldstein, A.H. 2001. Response of stomatal conductance to drought in ponderosa pine: Implications for carbon and ozone uptake. Tree Physiol. 21, 337–344.

Patterson, M.T., and Rundel, P.W. 1989. Seasonal physiological responses of ozone-stressed Jeffrey pine in Sequoia National Park, California. In: Olson, R.K., and Lefohn, A., eds. Effects of air pollution on western forests. Air Waste Manag. Assoc., Pittsburgh, PA, pp. 419–427.

Pei, A.-M., Murata, Y., Benning, G., Thomine, S., Klüsener, B., Allen, G.J., Grill, E., and Schroeder, J.I. 2000. Calcium channels activated by hydrogen peroxide mediate abscisic acid signalling in guard cells. Nature 406, 731–734.

Persson, T., Karlsson, P.S., Seyferth, U., Sjoberg, R.M., and Rudebeck, A. 2000. Carbon mineralisation in European forest soils. In: Schulze, E.-D., ed. Carbon and nitrogen cycling in European forest ecosystems, Ecological Studies 142. Springer-Verlag, Berlin, pp. 257–275.

Pronos, J., Merrill, L., and Dahlsten, D. 1999. Insects and pathogens in a pollution-stressed forest. In: Miller, P.R., and McBride, J.R., eds. Oxidant air pollution impacts in the Montane Forests of southern California: A case study of the San Bernardino Mountains, Ecological Studies 134. Springer-Verlag, New York, pp. 317–337.

Pureswaran, D.S., and Borden, J.H. 2005. Primary attraction and kairomonal host discrimination in three species of *Dendroctonus* (Coleoptera: Scolytidae). Agric. For. Entomol. 7, 219–230.

Reiter, I.M., Haberle, K.-J., Nunn, A.J., Heerdt, C., Reitmayer, H., Grote, R., and Matyssek, R. 2005. Competitive strategies in adult beech and spruce: Space-related foliar carbon investment versus carbon gain. Oecologia 146, 337–349.

Riggan, P.J., Lockwood, R.N., and Lopez, E.N. 1985. Deposition and processing of airborne nitrogen pollutants in Mediterranean-type ecosystems of southern California. Environ. Sci. Tech. 19, 781–789.

Snoeijers, S.S., Perez-Garcia, A., Joosten, M.H.A.J., and De Witt, J.G.M. 2000. The effect of nitrogen on disease development and gene expression in bacterial and fungal plant pathogens. Eur. J. Plant Path. 106, 493–506.

South Coast Air Quality Management District. 1997. The Southland's war on smog: 50 years of progress toward clean air. www.aqmd.gov/news1/Archives/History/marchcov.html

Sprugel, D.G., Hinckley, T.M., and Schaap, W. 1991. The theory and practice of branch autonomy. Ann. Rev. Ecol. Sys. 22, 309–334.

Stark, R.W., Miller, P.R., Cobb, F.W. Jr., Wood, D.L., Parameter, J.R. Jr., and Zavarin, E. 1968. Photochemical oxidant injury and bark beetle (Coleoptera: Scolytidae) infestation of ponderosa pine. Hilgardia 39, 121–152.

Strom, B.L., Roton, L.M., Goyer, R.A., and Meeker, J.R. 1999. Visual and semiochemical disruption of host finding in the southern pine beetle. Ecol. Appl. 9, 1028–1038.

Strom, B.L., Goyer, R.A., and Shea, P.J. 2001. Visual and olfactory disruption of orientation by the western pine beetle to attractant-baited traps. Entomol. Exp. Appl. 100, 63–67.

Swanston, C., Homann, P.S., Caldwell, B.A., Myrold, D.D., Ganio, L., and Sollins, P. 2004. Long-term effects of elevated nitrogen on forest soil organic matter stability. Biogeochem 70, 227–250.

Temple, P.J., and Miller, P.R. 1998. Seasonal influences on ozone uptake and foliar injury to ponderosa and Jeffrey pines at a southern California site. In: Bytnerowicz, A., Arbaugh, M.J., and Schilling, S.L., eds. Tech. coor., Proc., Internatl Symp. air pollution and climate change effects on forest ecosystems, 1996 February 5–9. Riverside, CA. General Technical Report, PSW-GTR-166. U.S. Dept. Agric., Forest Service, Pacific Southwest Research Station, Albany, CA, pp. 221–228.

Tingey, D.T., Hogsett, W.E., and Lee, E.H. 2004. Stricter ozone ambient air quality standard has beneficial effect on ponderosa pine in California. Environ. Manag. 34, 397–405.

Tjoelker, M.G., Volin, J.C., Oleksyn, J., and Reich, P.B. 1995. Interaction of ozone pollution and light effects on photosynthesis in a forest canopy experiment. Plant, Cell, Environ. 18, 895–905.

Torsethaugen, G., Pell, E.J., and Assmann, S.M. 1999. Ozone inhibits guard cell K^+ channels implicated in stomatal opening. Proc., Natl Acad. Sci. USA 96, 1357–13582.

Utkhede, R., and Smith, E. 1995. Effect of nitrogen form and application method on incidence and severity of *Phytophthora* crown and root rot of apple trees. Eur. J. Plant Path. 101, 283–289.

Vité, J.P. 1961. The influence of water supply on oleoresin exudation pressure and resistance to bark beetle attack in *Pinus ponderosa*. Contrib., Boyce Thompson Inst. 21, 37–66.

Vogt, C. 2003. Seasonal and permanent homeowners' past experiences and approval of fuels reduction. In: P. Jakes (comp.). Homeowners, communities, and wildfire: Science findings from the National Fire Plan. U.S. Dept. Agric., Forest Service, North Central Research Station, St. Paul, MN, pp. 63–73.

Vogt, C.A., and Cindrity, S.J. 2003. A changing landscape in the wildland-urban interface: Permanent and seasonal homeowners, recreation, and fuel management. In: Schuster, R., (comp). Proc., Northeastern Recreation Research Symposium; 13–16 April, 2002. Bolton Landing, NY. General Technical Report NE-302. U.S. Dept. Agric., Forest Service, Northeastern Research Station: Newtown Square, PA, pp. 208–214.

Weber, J.A., Clark, C.S., and Hogsett, W.E. 1993. Analysis of the relationships among O_3 uptake, conductance, and photosynthesis in needles of *Pinus ponderosa*. Tree Physiol. 13, 157–172.

Weiser, G., and Havranek, W.M. 1993. Ozone uptake in the sun and shade crown of spruce: Quantifying the physiological effects of ozone exposure. Trees 7, 227–232.

Westerling, A.L., Hidalgo, H.G., Cayan, D.R., and Swetnam, T.W. 2006. Warming and earlier spring increase western U.S. forest wildfire activity. Science 313, 940–943.

Wood, D.L. 1982. The role of pheromones, kairomones, and allomones in the host selection and colonization behavior of bark beetles. Ann. Rev. Entomol. 27, 411–446.

Zeneli, G., Krokene, P., Christiansen, E., Krekling, T., and Gershenzon, J. 2006. Methyl jasmonate treatment of mature Norway spruce (*Picea abies*) trees increases the accumulation of terpenoid resin components and protects against infection by *Ceratocystis polonica*, a bark beetle-associated fungus. Tree Physiol. 26, 977–988.

Zhang, X., Zhang, L., Dong, F., Gao, J., Galbraith, D.W., and Song, C.-P. 2001. Hydrogen peroxide is involved in abscisic acid-induced stomatal closure in *Vicia faba*. Plant Physiol. 126, 1438–1448.

Zhu, J., Talbott, L.D., Jin, X., and Zeiger, E. 1998. The stomatal response to CO_2 is linked to changes in guard cell zeaxanthin. Plant Cell Environ. 21, 813–820.

This page intentionally left blank

Developments in Environmental Science, Volume 8 405
A. Bytnerowicz, M. Arbaugh, A. Riebau and C. Andersen (Editors)

ISSN: 1474-8177/DOI:10.1016/S1474-8177(08)00018-1

Chapter 18

Fire Effects on Carbon and Nitrogen Cycling in Forests of The Sierra Nevada

Dale. W. Johnson, Mark. E. Fenn, Watkins W. Miller and Carolyn F. Hunsaker*

Abstract

Fire removes substantial quantities of nitrogen (N) by volatilization, and prescribed fire, over time, can remove as much as or more N than wildfire. This lost N can be quickly made up if fire is followed by N_2-fixing vegetation. Wildfire often has short-term deleterious effects on water quality because of N mobilization, but long-term fire suppression allows buildups of N-rich litter, a source of labile N to runoff waters. Prescribed fire usually has less impact on water quality than wildfire. Prescribed fire has been proposed as a management tool to mitigate N saturation (a result of chronic, excessive N deposition). However, a major limitation of this strategy is that while fire removes substantial quantities of N from the forest floor, it removes only a small fraction of the large N reservoir in the mineral soil and at the same time causes increases in soil ammonium over the short term. Periodic prescribed fire, reduced atmospheric N deposition and strategies to enhance plant and microbial N demand may all be required to reduce N-saturation symptoms in catchments exposed to long-term atmospheric N inputs.

18.1. Introduction

Fire is known to have major impacts on the carbon (C) and nitrogen (N) cycles of semi-arid forests, including those in the Sierra Nevada (Belillas & Feller, 1998; Carriera et al., 1996; DeBano & Conrad, 1978; Grier, 1975; Johnson et al., 1998, 2005; Neary et al., 1999; Newland & DeLuca,

*Corresponding author: E-mail: dwj@cabnr.unr.edu

2000; Raison et al., 1985; Trabaud, 1994). Fire has obvious and immediate effects on the carbon cycles of forest ecosystems: the process of burning itself involves converting organic C to carbon dioxide (CO_2), thereby causing a marked loss of ecosystem C capital. Because fire results in the emission of CO_2 and other greenhouse gases (Crutzen & Andreae, 1990), the recent trend toward more frequent and severe fires may contribute to a positive feedback in global warming. The contributions of fire to global CO_2 emissions are uncertain and highly variable, but may rival those of fossil fuel emissions (Mouillot & Field, 2005).

Because of its low volatilization temperature, most N is also volatilized from the materials that burn, in contrast to elements such as calcium (Ca) that are left behind in ash. Thus, fire always causes an immediate, short-term loss of ecosystem C and N capital. Fire effects on C and N cycles over the intermediate (1–3 year) and long-term (decadal to century) perspectives are far more complex than the simple removal of C and N by volatilization, however. Fire has significant and well-documented short-term effects on soil N availability and therefore water quality through soil heating effects and mid-term effects on N availability by causing changes in decomposition rates (Certini, 2005; Neary et al., 1999). Fire can have very substantial long-term effects on ecosystem C and N by causing changes in vegetation, often through the facilitation of occupancy of the burned site by N-fixing vegetation, which in turn can indirectly cause long-term increases in ecosystem C capital in N-limited ecosystems—as long as sufficient time elapses prior to the next fire (Choromanska & DeLuca, 2002; Gessel et al., 1973; Johnson & Curtis, 2001; Johnson et al., 2004, 2005).

The incidence of catastrophic wildfire in Sierra Nevada ecosystems has increased dramatically during the last few decades as a result of past fire suppression and consequent fuel buildups (Neary et al., 1999; Newland & DeLuca, 2000). Furthermore, recent analyses suggest that climate change may be causing increases in wildfire incidence and extent. Westerling et al. (2006) found that wildfire activity in the United States has increased markedly since the mid-1980s with greater frequency, longer wildfire seasons, and longer wildfire durations. These changes are associated with increased spring and summer temperatures and have taken place even in areas of the U.S. that have not strongly been affected by fuel buildups. In this chapter, we review the current state of knowledge about the effects of fire on C and N cycling in forests of the Sierra Nevada, including effects of fire on N volatilization, ammonification, nitrification, leaching, and how these compare with atmospheric N deposition in affecting long-term N budgets.

18.2. Fire effects on soil C and N and water quality

Even though there is usually a net loss of ecosystem C and N by volatilization during fire, soil C and N levels are often unaffected in all but the most severe wildfires (Certini, 2005; Neary et al., 1999). This is because soil temperatures often do not reach levels that would cause the combustion of soil organic matter aside from the very surface layers. Although in soil total C and N are usually not reduced by fire, soil NH_4^+ levels often increase following fire because of heat-induced decomposition of organic N in soil and possibly by inorganic N inputs from ash (Certini, 2005; Covington 1992; Covington & Sackett, 1984; Giardina et al., 2000; Grogan et al., 2000; Khanna & Raison, 1986; Monleon et al., 1997; Neary et al., 1999). At the same time, the reduction in biomass and leaf area (especially in wildfire), can cause increased water availability, providing good growing conditions for vegetation that is able to reoccupy the site (including undesirable invasive species). Because NH_4^+ is strongly absorbed to cation exchange sites, NH_4^+ leaching may not be substantial after fire, but the availability of substrate and good temperature and moisture conditions after fire can cause increases in nitrification and NO_3^- leaching. There are also indications that nitrification is favored by the presence of charcoal, perhaps because of the absorption of chemicals that inhibit nitrification (DeLuca et al., 2006).

The effects of fire on water quality are especially important in the Lake Tahoe Basin on the California–Nevada border (Murphy et al., 2006a; Stephens et al., 2005). Lake Tahoe is an ultra-oligotrophic freshwater lake renowned for its pristine conditions and extreme clarity. The 500-km^2 lake is surrounded by a forested watershed of approximately 800 km^2 (Boardman, 1959). The relatively small watershed to surface water area ratio has produced pristine water conditions resulting from historically low levels of nutrient input (Goldman, 1988). Since 1968 lake clarity (secchi depth) has diminished by an estimate of 0.37 m yr^{-1} from increased primary productivity due to accelerated N and phosphorus (P) inputs (Goldman, 1988). It is now believed that the N to P ratio of inputs into Lake Tahoe has shifted and currently reflects a P rather than N-limited system (Jassby et al., 1994). A substantial portion of the Lake Tahoe Basin has been recently categorized as a high-risk environment for catastrophic wildfire (Smith & Adams, 1991).

Stephens et al. (2005) found that prescribed fire in the Lake Tahoe Basin had no effect on soluble reactive phosphate and minimal effects on nitrate in streamwaters. Similarly, Murphy et al. (2006a) found no significant increases in soil solution concentrations or leaching of mineral N or P in a prescribed fire on andesitic soils near the Tahoe Basin. In contrast, we found substantial (approximately tenfold) increases in mineral N leaching for the first 2 years following a wildfire in the Tahoe Basin (Johnson et al., 2007; Murphy et al., 2006b). Soil solution concentrations of NH_4^+ increased from <3–180 μmol L^{-1}, and NO_3^- increased from <3 to >350 μmol L^{-1} during the first year after the fire (Murphy et al., 2006b). By year three after the fire, however, N leaching levels were back down to near control levels, and the total amount of additional N leaching (20 kg ha^{-1}) constituted only 4% of that lost to volatilization (500 kg ha^{-1}) in this fire. Ortho-P concentrations and leaching were slightly elevated following this fire, but by far the greatest increases were in soil solution SO_4^{2-} concentrations: from <20 to >8000 μmol L^{-1} (Murphy et al., 2006b). Other researchers have also found large increases in SO_4^{2-} concentrations in both soil solution and streamwater following fire in the Sierra Nevada (Chorover et al., 1994; Williams & Melack, 1997). This increase in SO_4^{2-} concentration is generally thought to be due to oxidation of organic S from soil organic matter, but may also be enhanced by increases in soil pH resulting in desorption SO_4^{2-} from soil anion exchange sites (Murphy et al., 2006b).

Postfire erosion can also cause substantial short-term decreases in water quality following wildfire, but much less information is available on that subject. Fire effects on soil hydrophobicity are well-documented, and this has a major effect on postfire erosion (Certini, 2005). Heating of the soil above 200°C causes the volatilization of some hydrophobic substances in soils, and they can then migrate downward in the soil profile, usually to depths of less than 10 cm (Certini, 2005). We found that a wildfire in the Lake Tahoe Basin caused the destruction of the hydrophobic layer that is normally present in surface soils of this region, causing a new layer of hydrophobicity to form at the 8–10 cm depth. A thunderstorm after the fire caused substantial erosion of the surface soil above the new hydrophobic layer (Carroll et al., 2007). We estimated that this caused <100 kg ha^{-1} of N loss via erosion, a value lower than that estimated to have been lost by volatilization (500 kg ha^{-1}). Baird et al. (1999) made estimates of postfire erosional N losses from a fire in eastern Washington that ranged from 14 to 22 kg ha^{-1}.

One hypothesis regarding wildfire and water quality that is not intuitively obvious was recently proposed by Miller et al. (2005) for forests of the Lake Tahoe Basin and vicinity. They found that subsurface runoff water that percolated through litter layers but did not enter mineral soils (due to either hydrophobicity or frozen soil) had very high concentrations of NO_3^-, NH_4^+, and ortho-P. The source of these nutrients was clearly the litter layer, which because of past fire suppression, had built up to well above normal levels. They speculated that in this way, fire suppression had actually indirectly contributed to the decline in water quality in Lake Tahoe. Thus, whereas fire is known to cause short-term pulses of increased NO_3^-, NH_4^+, and ortho-P in some cases, the results of Miller et al. (2005) suggest that fire exclusion rather than fire itself may cause long-term increases in these ions and contribute to declines in water quality over the long term. Further research is needed on an aerial, quantitative basis to determine the effects of this water.

18.3. Long-term effects of wildfire and postfire vegetation

Wildfire burns components of the ecosystem that have low C:N ratios (forest floor and foliage), leaving large woody tissues unburned in most cases (Auclair, 1985; Johnson et al., 1998). Thus, it would seem that wildfire causes disproportionately large losses of N compared to C. Lost N is often replaced and even exceeded by inputs from N fixers after fire, and the replenishment of lost N is key to the long-term replenishment of C in these N-limited ecosystems. There is likely to be a substantial delay in the replenishment of C pools compared to N, however, until high C:N ratio woody tissues (i.e., mature trees) reaccumulate.

The invasion of N-fixing vegetation on burned sites is a double-edged sword: while the benefits of replenishing N volatilized during fire are well known (Binkley et al., 1982; Johnson, 1995; Youngberg & Wollum, 1976; Zavitovski & Newton, 1968), the presence of this vegetation often presents a significant problem for tree reestablishment. Snowbush (*Ceanothus velutinus* Dougl.) is a pioneer species that invades after site disturbances such as fire in eastern Sierran forests. Snowbush is especially adapted to fire; heat treatment followed by cold stratification is required for seed germination (Zavitovski & Newton, 1968; Youngberg & Wollum, 1976). Snowbush seeds lying dormant in forest litter for many years are activated by fire and winter weather, resulting in prolific germination in wildfire, clearcut, and slash burned sites. Snowbush is shade intolerant and therefore disappears after overstory canopy closure. Snowbush presents serious competition for tree regeneration after fire; when it is not controlled by either herbicide or mechanical means, it may persist for many decades.

For a site in the eastern Sierra Nevada, we estimated the impacts of wildfire and postfire salvage logging on carbon (C) nutrient over a 16–20-year period (Johnson et al., 2005). We reconstructed prefire biomass and nutrient contents and compared them with values from the postfire ecosystem, which was dominated by snowbush (*C. velutinus* Dougl.) and manzanita (*Arcostaphylos patula* Greene). We estimated that the wildfire caused losses of at least 300 kg ha^{-1} of N and 15,500 kg ha^{-1} of C, assuming all foliage and O-horizon (litter layer) material was combusted (Fig. 18.1). Soil losses could not be reconstructed, but would cause this estimate to increase. Postfire salvage logging is estimated to have resulted in losses of an additional 130 kg ha^{-1} of N and 53,000 kg ha^{-1} of C. Comparisons of the prefire and current N budgets suggested that the lost N was rapidly replenished in O horizons and mineral soils due to N fixation by snowbush (*C. velutinus* Dougl.), the dominant shrub on the former fire site. Two decades after the fire, there were no significant differences in ecosystem P, potassium (K), or sulfur (S) contents and no consistent, significant differences in soil extractable P or S between the shrub and forested plots (Table 18.1). Exchangeable K, Ca, and magnesium (Mg) were consistently and significantly greater in shrub-dominated than in adjacent forested soils, however, and the differences were much larger than could be accounted for by estimated ash inputs (Fig. 18.1). In the case of Ca, even the combustion of all aboveground organic matter could not account for more than a fraction of the difference in exchangeable pools. We speculate that the apparent large increase in soil and ecosystem Ca content resulted from either the release of Ca from nonexchangeable forms in the soil or the rapid uptake and recycling of Ca by postfire vegetation. Carbon losses, most of which were due to salvage logging, will not be restored until a mature forest occupies the site again.

18.4. Nitrogen losses from prescribed fire in Sierran forests

Although wildfire typically causes a greater amount of N volatilization than prescribed fire in a given year, the cumulative effects of repeated prescribed fire can be very substantial and exceed wildfire losses in the long run. In a previous chapter, we used a simple spreadsheet model to illustrate this (Johnson et al., 1998). In the model, litterfall mass and N content are kept constant over a 100-year period, and litter is allowed to decay at a constant rate (*k*-value) taken from litterbag studies in the field (Stark, 1973). Figure 18.2 gives an example of calculated N losses with prescribed fire at 10- and 20-year intervals, assuming that half of the forest floor is consumed in each burn (top panel) and with a constant 10-year burn interval assuming 25%, 50%, and 75% consumption of the forest floor (bottom panel). Cumulative N losses are plotted in these burn scenarios range from 738 to 1434 kg ha^{-1} over a 100-year period, values which exceed those calculated if the cumulative forest floor mass was left unburned until complete combustion in a wildfire at 100 years

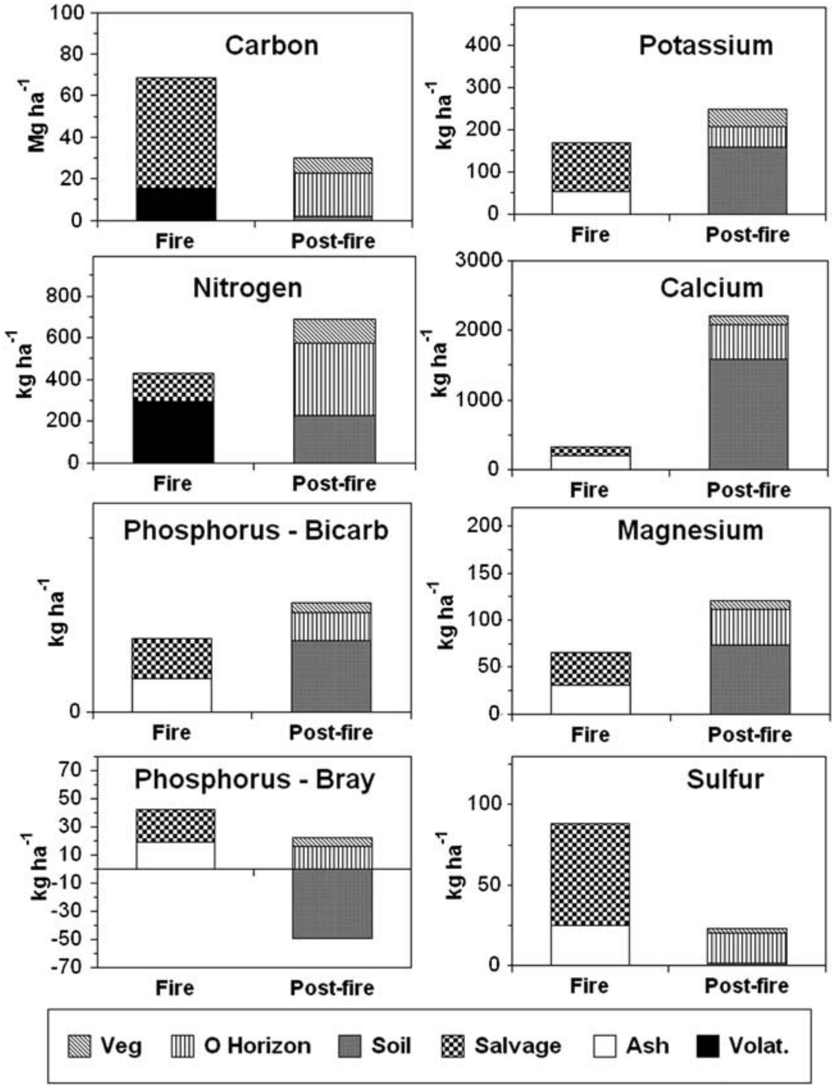

Figure 18.1. Estimated losses of carbon, nitrogen, phosphorus (showing bicarbonate- and Bray-extractable phosphorus in soils), potassium, calcium, magnesium, and sulfur by volatilization (Volat.) and conversion to ash during fire (assuming combustion of foliage and O horizons), removal by postfire salvage logging, and postfire increases in soils, O horizons, and vegetation (Veg) for the Little Valley fire site. Reprinted from Forest Ecology and Management, Johnson et al. (2005), with permission from Elsevier.

Table 18.1. Carbon and nutrient contents of shrub (burned by wildfire in 1981) and nearby forest ecosystems at Little Valley, Nevada (standard errors are shown; from Johnson et al., 2005)

Component	Carbon		Nitrogen		Phosphorus		Potassium		Calcium		Magnesium		Sulfur	
	($Mg\,ha^{-1}$)		($kg\,ha^{-1}$)											
Vegetation	9*** ±1	89 ±35	140** ±13	333 ±133	7** ±1	63 ±25	57** ±3	224 ±87	99** ±39	334 ±39	11** ±1	99** ±39	334 ±39	97 ±39
O horizon	26** ±3	15 ±1	434*** ±78	232 ±18	19* ±3	13 ±2	63* ±18	27 ±2	611** ±141	239 ±14	48*** ±5	611** ±141	239 ±14	24 ±3
Woody	10 ±9	4 ±3	16 ±15	7 ±4	3 ±2	1 ±1	12 ±11	5 ±3	14 ±13	6 ±4	4 ±4	14 ±13	6 ±4	2 ±1
Soil	58 ±8	53 ±8	3136 ±711	2529 ±699	157** ±12	106 ±7	514** ±70	301 ±32	2872*** ±399	825 ±119	172** ±37	2872*** ±399	825 ±119	71 ±23
Ecosystem	103* ±10	160 ±45	3726 ±618	3102 ±774	186 ±7	183 ±34	646 ±69	558 ±100	3573*** ±407	1168 ±115	323 ±27	3573*** ±407	1168 ±115	431 ±122

*,**, and *** refer to statistically significant differences, unpaired student's t-test.

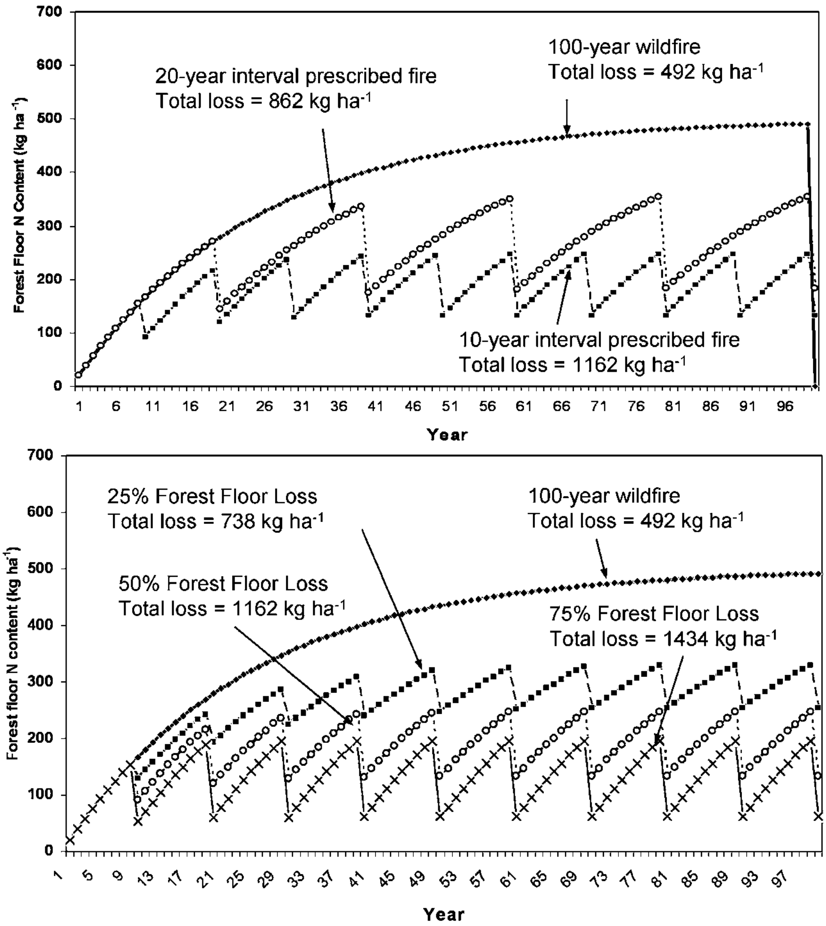

Figure 18.2. Simulated forest floor N content and cumulative N losses from the forest floor combustion using a spreadsheet model (Johnson et al., 1998). The top panel assumes that a 100-year wildfire consumes the entire forest floor, 50% of the forest floor is consumed at 10-year intervals with prescribed fire, and 75% of the forest floor is consumed at 10-year intervals with prescribed fire. The bottom panel assumes that a 100-year wildfire consumes the entire forest floor, prescribed fire at a 10-year interval consumes 50% of the forest floor, prescribed fire at a 10-year interval consumes 50% of the forest floor, and prescribed fire at a 10-year interval consumes 75% of the forest floor. Litterfall is assumed to be constant at 2000 kg ha^{-1} yr^{-1} containing 1% N (giving an N return of 20 kg ha^{-1} yr^{-1}), and decomposition constant (k) is set at 0.04 yr^{-1} (Stark 1973).

(492 kg ha^{-1}). Furthermore, prescribed fire at intervals of 10 years or less will prevent the reestablishment of N-fixing vegetation for sufficiently long intervals to allow for N fixation to commence in significant amounts. McNabb and Cromack (1983) indicate that fixation does not go ''into the black'' (i.e., fix more N than is taken up from the soil) until at least age 10 (primarily *C. velutinus* in the area that these fires burn in). Thus, the long-term effects of prescribed fire at short intervals can, in theory, cause very substantial amounts of N loss from the ecosystem and may actually result in growth declines, as has been observed in some studies in eastern Oregon (Monleon et al., 1997).

18.5. Fire effects on water quality in N-saturated catchments

Because fire causes considerable loss of N by volatilization (Neary et al., 1999), prescribed fire might be an appropriate tool for reducing the symptoms of N saturation in chaparral and forested watersheds in southern California where streamwater nitrate concentrations are the highest reported in North America for wildland watersheds. This strategy presumes that by reducing ecosystem N capital with the combustion of N stored in fuel, N-saturated watersheds could be returned to a state of conservative N cycling. Unfortunately, a study in chaparral catchments in the San Dimas Experimental Forest (SDEF) in the San Gabriel Mountains near Los Angeles, where N deposition inputs are approximately 35 kg ha^{-1} yr^{-1}, demonstrated that prescribed fire was not effective in improving water quality (Meixner et al., 2006).

Prescribed fire and simulated wildfire treatments, applied to N-saturated chaparral catchments in the SDEF in October 1984, provided an opportunity to test the effects of fire on streamwater nitrate export patterns. Paired catchments were either left untreated as controls, prescribe burned, or the *Ceanothus* chaparral was cut and later burned to simulate a wildfire burn. Dominant vegetation in these watersheds was a mix of *C. crassifolius* and *Adenostoma fasciculatum* chaparral. Over the subsequent winter and spring wet season, nitrate concentrations followed the predicted pattern of highest concentrations in the simulated wildfire treatment and lowest concentrations in the unburned control catchments. Volume-weighted nitrate concentrations in the wildfire burn were at or above the drinking water standard in a few instances (as high as 1120 μeq L^{-1}) and were 1.7 times higher than in the prescribed burn. Annual nitrate flux from the wildfire catchments was 7 times higher than the prescribed fire treatment and 40 times higher than the control (Riggan et al., 1994).

Long-term trends in nitrate runoff are the real test of whether prescribed fire is an effective treatment for mitigating N-saturation symptoms. Streamflow and nitrate concentrations were measured until 2002 (when the entire SDEF burned) in a subset of the catchments. For the first 7–10 years nitrate concentrations and annual flux were higher in the prescribe-burned catchments than in the unburned control, after which the order was reversed. However, nitrate concentrations remained high in both treatments for the duration of the study (varying from 40 to 200 μ eq L^{-1} in the burned catchments; Meixner et al., 2006). Considering the long lag time until nitrate concentrations were lower in the burned catchments and the persistently high nitrate concentrations in both treatments, it was concluded that prescribed fire is not an effective treatment for reversing N-saturation conditions. Only approximately 20% of the N in chaparral ecosystems is stored in the aboveground biomass plus litter (Gray & Schlesinger, 1981), with the remaining 80% found in soil storage pools, of which little is lost during or after fire (Wan et al., 2001). Presumably, the fire treatment was ineffective in improving water quality because the soil (Riggan et al., 1994) and continuing atmospheric N deposition supplied a continual source of excess nitrate.

The results from the N-saturated chaparral catchments in the SDEF beg the question of whether prescribed fire might be more effective in reversing N-saturation symptoms in forested areas of California, where N deposition inputs are elevated. To date, studies on the effects of fire on streamwater nitrate export from forests in California have only been done in areas of relatively low N deposition (Chorover et al., 1994; Murphy et al. 2006a, 2006b; Stephens et al., 2005; Williams & Melack, 1997). In these instances, burns had the effects observed in more mesic forests, with elevated nitrate concentrations for 2–3 years maximum after which concentrations returned to prefire levels. Forest N budgets also indicate that prescribed fire is not likely to remove enough N from N-saturated forested ecosystems, because typically 65–80% of the site N capital is stored belowground in California forests (Arbaugh et al., 1999; Busse & Riegel, 2005; Johnson et al., 2004).

In N-saturated forests in California, ozone is also a major stress factor, with particularly severe effects on ponderosa pine trees (Fenn et al., 2003b). In contrast to forests, ozone does not have major effects on chaparral ecosystems notwithstanding the high ozone exposures occurring in chaparral watersheds located downwind of urban centers (Stolte, 1982). Ponderosa pine is a major overstory species occurring throughout the mixed-conifer forests of California and in many forests of the western United States. Ponderosa pine is replaced by Jeffrey pine in more droughty or higher elevation sites. Ozone concentrations are often lower in Jeffrey pine sites; however, both species are sensitive to ozone injury. In polluted California forests, ozone and nitrogenous pollutants co-occur, and these pollutants have interacting effects on plant physiology and ecosystem C and N fluxes and pools (Fenn et al., 2003b). Nitrogen deposition increases aboveground growth of ponderosa pine. Ozone and increased N fertility both reduce C allocation belowground and fine root biomass (Grulke et al., 1998). Ozone causes premature foliar senescence and abscission. The results of the combined effects of ozone and elevated N deposition are increased C storage in the bole and woody aboveground biomass and accelerated foliar turnover and litter production (Arbaugh et al., 1999). This also results in increased accumulation of C and N in the forest floor. In these ozone-impacted and N-saturated mixed-conifer stands, aboveground N pools are much higher than in unimpacted stands (Arbaugh et al., 1999; Fenn et al., 2005). For example, at an N-saturated site in the San Bernardino Mountains about 30% of ecosystem N is stored in the thick forest floor, compared to about 11% at an N-limited site (Arbaugh et al., 1999; Fenn et al., 2005). The question remains whether periodic burning of this aboveground N pool would eventually reduce nitrate runoff from these catchments or if N stores in the mineral soil are a large enough source of N to sustain elevated nitrate runoff. In N-saturated Scots pine stands established on nutrient-poor sandy soils in southern Germany, 7 years of litter raking and harvesting reduced foliar N concentration (7–11%) and nitrate leaching (9%, 19%, and 71%) in the three study sites (Prietzel & Kaiser, 2005). Although nitrate leaching was high in these German forests (9.9, 16.2, and 43.0 kg ha^{-1} yr^{-1} in the three unraked control study sites), throughfall N deposition was low to moderate compared to most N-saturated forests, ranging from 16–18 kg ha^{-1} yr^{-1}. A number of researchers have noted that reducing N deposition is a key factor in reducing nitrate leaching (Gundersen et al., 2006; Rothe & Mellert, 2004). It seems likely that for N-saturated California forests where N deposition is elevated (25–70 kg ha^{-1} yr^{-1}) and where large pools of N have accumulated in soil, removal of N stores in the forest floor from periodic burns would likely need to be accompanied by decreases in N deposition in order to eventually reverse N-saturation symptoms.

Recent isotopic tracer data from the San Gabriel and San Bernardino Mountains in the Los Angeles Basin suggest that chaparral and forested systems in southern California are both highly prone to export nitrate from the watershed, and that a significant fraction of the leached nitrate is atmospheric nitrate without any prior biological assimilation (Michalski et al., 2004). During peak flow following storm events, approximately 40% of the exported N was direct throughput of atmospheric nitrate.

In the study by Michalski et al. (2004) all edaphic and aqueous samples had positive $\Delta^{17}O$ values, unambiguously showing that every sample of soil and water collected in the Transverse Ranges in southern California had some degree of unassimilated atmospheric nitrate. One of the factors thought to predispose these systems to nitrate loss under conditions of chronic N deposition is the temporal asynchrony between the period of peak N demand (spring and early summer) and peak runoff (mid-winter). Chronic nitrate export from these watersheds is also believed to be a function of actively nitrifying soils (Fenn et al., 1998). N inputs from atmospheric deposition provide a steady source of leachable nitrate and indirectly enrich organic N pools that function as substrate for mineralization and nitrification (Fenn et al., 2005). Gundersen et al. (2006) reported a threshold of N flux to the soil (50–60 kg N ha^{-1} yr^{-1}) from atmospheric deposition and litterfall above which nitrate leaching occurs in undisturbed mesic forests. Considering these factors, it seems that for prescribed fire to effectively reduce nitrate runoff, atmospheric N deposition fluxes would also have to be reduced, probably by as much as 60–80% in the most polluted areas. The threshold N deposition rate at which nitrate export begins to increase above the normal background levels in California montane systems is approximately 17 kg ha^{-1} yr^{-1} (Fenn et al., 2008), based on regression analysis of throughfall N deposition versus streamwater nitrate. This level of N deposition has been measured in much of the Transverse Ranges in southern California and in the southwestern Sierra Nevada (Fenn et al., 2003a, 2003b).

Having said all this, however, it remains true that fire causes large losses of N from ecosystems, and simple budget calculations would suggest that periodic fire (Busse & Riegel, 2005) should reduce excess N in the ecosystem and perhaps even lead to N deficiency unless N fixers or air pollution offset these losses. These net losses of N from fire may not suffice to offset the symptoms of N saturation, however, if postfire N inputs are substantial and sustained. Success in reducing nitrate concentration in runoff from chaparral and forested catchments in southern California will likely require the removal of N in fire and reduced N deposition. NO_x emissions from the South Coast Air Basin, which includes four counties near Los Angeles, have decreased by 44% from 1975 to 2005 (Cox et al., 2006), but trends in N deposition in the San Bernardino Mountains do not reflect these decreasing NO_x emissions trends (Andrzej Bytnerowicz, pers. comm.). This may be primarily because of large increases in population and vehicle traffic in the more easterly inland areas closer to the San Bernardino Mountains. Another factor seems to be increases in ammonia emissions within the Basin.

Ammonia emissions from motor vehicles are now known to be more significant than previously thought (Huai et al., 2005).

In summary, removal of N-containing biomass or necromass from N-saturated ecosystems is one strategy considered for reversing N-saturation symptoms in forests (Fenn et al., 1998; Gundersen et al., 2006; Prietzel & Kaiser, 2005), although a necessary and ultimate solution is to reduce N emissions to the atmosphere. Accumulation of organic N pools is particularly enhanced in mixed-conifer forests in southern California because of the co-occurrence of severe ozone effects, chronic N deposition, and long-term fire suppression. All of these factors enhance C and N accumulation aboveground. The accumulated litter layer also provides a mulch layer that likely reduces the establishment (Allen et al., 2007) and N uptake of understory vegetation and provides soil conditions that enhance nitrification. High nitrification rates, reduced N demand by understory vegetation, and reduced fine root production by trees as a result of ozone stress and high N fertility, are all factors that contribute to elevated nitrate leaching and gaseous nitrogen losses from the system (Fenn et al., 2003b). Because of the multiple effects of ozone, N deposition, and fire suppression in enhancing N saturation and N accumulation aboveground in some California forests, periodic prescribed fires may have a greater impact in reducing nitrate leaching in these catchments than in forests in other regions. However, the practicality of applying prescribed burns to the impacted areas in southern California is restrained by public concerns with the risks of using fire in the wildland-urban interface and because of air-quality issues associated with fire emissions in an already polluted environment.

18.6. Potential effects of fire on mesic forests

Although arid and semi-arid ecosystems burn more frequently and often more intensely, most forests of the world experience fires at one time or another. Temperate coniferous forests experience fire on a 50- to 200-year interval, temperate deciduous forests burn on intervals ranging from decades to centuries, and montane and boreal coniferous forests burn at intervals of centuries (Fisher & Binkley, 2000). Johnson et al. (2004) calculated the potential N losses with fire in a variety of mesic ecosystems given varying assumptions about fire return interval and degree of forest floor and vegetation combustion. They found that the potential C and N losses from a fire consuming the forest floor in these sites varied by an order of magnitude: from 6.8 to 70.8 $\mathrm{Mg\,C\,ha^{-1}}$ and from 240 to 2600 $\mathrm{kg\,N\,ha^{-1}}$, or from 6% to 30% of ecosystem C capital and from 4%

to 29% of ecosystem N capital. When expressed on an annualized basis, the potential loss of N with fire was calculated to be far greater than that due to leaching in all but two N-saturated ecosystems (red alder in Washington, USA, and Smokies red spruce site in North Carolina, USA). The number of years of atmospheric deposition that would be required to restore the N loss from such a hypothetical fire ranged from 30 to 1100 years with a mean of 193 and a median of 87. In most cases, the calculated N replenishment times were greater than stand age at the time of measurement. The number of years of leaching that would equal N losses in a hypothetical fire range from 47 in an N-fixing red alder stand with very high rates of leaching to 11,567 in the Sierra Nevada. If half the forest floor is assumed to be consumed in a fire, such as might occur with a typical prescribed fire (Caldwell et al., 2002; Murphy et al., 2006a), values would range from 27 to over 4738 years (mean = 1475, median = 646) to equal leaching. If only 10% of the forest floor burns, the values would range from 5 to 1157 years (mean = 148, median = 65). Given the normally very low rate of leaching in most temperate forests, it is quite clear that even a moderate ground fire every century or so will cause as much or more N loss on an annual basis than will leaching in all but N-saturated forests.

These budget calculations are very crude, but serve to illustrate the potential role of fire in C and N balances in more humid forest ecosystems, which burn infrequently. They show that potential N losses by fire, when expressed on an annual basis (estimated by dividing the N contents of ecosystem components presumed to burn by stand age), could be substantially greater than N leaching rates in many if not most cases. The calculations also show that atmospheric N deposition rates in all but the most polluted sites fall below these annualized estimates of fire N loss. In theory, infrequent fire could substantially deplete the N reserves of many of these systems and allow them to refill from atmospheric deposition and/or N fixation over time. In eastern Sierran ecosystems, with their typically low N deposition rates, it seems clear that even infrequent fire would deplete ecosystem N reserves without postfire N fixation.

Prescribed fire typically causes much less N loss than wildfire in that the forest floor and understory is usually only partly consumed and overstory vegetation is not much affected. However, burn intervals of 20 years or less can result in substantial N losses over time, with cumulative losses even exceeding N losses with wildfire over time periods of a century (Johnson et al., 1997).

Fire and other disturbances that remove N in large amounts over short periods may be one reason that most forest ecosystems show a net annual

N accumulation. Atmospheric deposition at even very low, pristine rates for thousands of years should have caused most ecosystems to come into steady state with respect to N in the absence of such disturbances.

REFERENCES

Allen, E.B., Temple, P.J., Bytnerowicz, A., Arbaugh, M.J., Sirulnik, A.G., and Rao, L.E. 2007. Patterns of understory diversity in mixed coniferous forests of southern California impacted by air pollution. TheScientificWorldJournal 7(S1), 247–263, doi:10.1100/tsw.2007.72.

Auclair, A.N.D. 1985. Postfire regeneration of plant and soil organic pools in a *Picea mariana–Cladonia stellaris* ecosystem. Can. J. For. Res. 15, 279–291.

Arbaugh, M.J., Johnson, D.W., and Pulliam, W.M. 1999. Simulated effects of N deposition, ozone injury and climate change on a forest stand in the San Bernardino Mountains. In: Miller, P.R., and McBride, J.R., eds. Oxidant air pollution impacts in the Montane Forests of southern California: A case study of the San Bernardino Mountains, Ecol. Studies 134. Springer-Verlag, New York, pp. 353–372.

Baird, M., Zabowski, D., and Everett, R.L. 1999. Wildfire effects on carbon and nitrogen in inland coniferous forests. Plant Soil 209, 233–243.

Belillas, C.M., and Feller, M.C. 1998. Relationships between fire severity and atmospheric and leaching nutrient losses in British Columbia's coastal western hemlock zone forests. Int. J. Wildland Fire 8, 87–101.

Binkley, D., K. Cromack, K., and Fredriksen, R.L. 1982. Nitrogen accretion and availability in some snowbrush ecosystems. Forest Sci. 28, 720–724.

Boardman, H.P. 1959. Some interesting and important facts about Lake Tahoe. Truckee Basin Water Committee and Nevada Cooperative Snow Surveys Committee of State Association of Soil Conservation Districts, Reno, NV.

Busse, M.D., and Riegel, G.M. 2005. Managing ponderosa pine forests in central Oregon: Who will speak for the soil? In: M.W. Ritchie, D.A. Maguire, and A. Youngblood (tech. coord.), Proceedings of the Symposium on Ponderosa Pine: Issues, Trends, and Management. 18–21 October. Klamath Falls, OR. Gen. Tech. Rep. PSW-GTR-198. Albany, CA. Pacific Southwest Research Station, Forest Service, U.S. Department of Agriculture, pp. 109–122.

Caldwell, T.G., Johnson, D.W., Miller, W.W., and Qualls, R.G. 2002. Forest floor carbon and nitrogen losses due to prescription fire. Soil Sci. Soc. Am. J. 66, 262–267.

Carriera, J.A., Arvevalo, J.R., and Neill, F.X. 1996. Soil degradation and nutrient availability in fire-prone Mediterranean shrublands of southeastern Spain. Arid Soil Res. Rehabil. 10, 53–64.

Carroll, E.M., Miller, W.W., Johnson, D.W., Saito, L.S., Qualls, R.G., and Walker, R.F. 2007. Spatial analysis of a high magnitude erosion event following a Sierran wildfire. J. Environ. Qual. 36, 1105–1111.

Certini, G. 2005. Effects of fire on properties of forest soils: A review. Oecologia 143, 1–10.

Choromanska, U., and DeLuca, T.H. 2002. Prescribed fire alters the impact of wildfire on soil biochemical properties in a ponderosa pine forest. Soil Sci. Soc. Am. J. 65, 232–238.

Chorover, J., Vitousek, P.M., Everson, D.A., Esperanze, A.M., and Turner, D. 1994. Solution chemistry profiles of mixed conifer forests before and after fire. Biogeochemistry 26, 115–144.

Covington, W.W. 1992. Spatial variation in soil mineral nitrogen following prescribed burning in ponderosa pine. For. Ecol. Manage. 54, 175–191.

Covington, W.W., and Sackett, S.S. 1984. The effect of a prescribed burn in southwestern ponderosa pine on organic matter and nutrients in woody debris and forest floor. Forest Sci. 30, 183–192.

Cox, P., Johnson, M., and Auyeung, J. 2006. The California Almanac of Emissions and Air Quality, 2006 edition. California Environmental Protection Agency, Air Resources Board. Sacramento, California.

Crutzen, P.J., and Andreae, M.O. 1990. Biomass burning in the tropics: Impact on atmospheric chemistry and biogeochemical cycles. Science 250, 1669–1678.

DeBano, L.F., and Conrad, C.E. 1978. The effect of fire on nutrients in a chaparral ecosystem. Ecology 59, 489–497.

DeLuca, T.H., McKenzie, M.D., Gundale, M.J., and Holben, W.E. 2006. Wildfire-produced charcoal directly influences nitrogen cycling in ponderosa pine forests. Soil Sci. Soc. Am. J. 70, 448–453.

Fenn, M.E., Poth, M.A., Aber, J.D., Baron, J.S., Bormann, B.T., Johnson, D.W., Lemly, A.D., McNulty, S.G., Ryan, D.F., and Stottlemyer, R. 1998. Nitrogen excess in North American ecosystems: Predisposing factors, ecosystem responses, and management strategies. Ecol. Appl. 8, 706–733.

Fenn, M.E., Haeuber, R., Tonnesen, G.S., Baron, J.S., Grossman-Clarke, S., Hope, D., Jaffe, D.A., Copeland, S., Geiser, L., Rueth, H.M., and Sickman, J.O. 2003a. Nitrogen emissions, deposition, and monitoring in the western United States. BioScience 53, 391–403.

Fenn, M.E., Poth, M.A., Bytnerowicz, A., Sickman, J.O., and Takemoto, B.K. 2003b. Effects of ozone, nitrogen deposition, and other stressors on montane ecosystems in the Sierra Nevada. In: Bytnerowicz, A., Arbaugh, M.J., and Alonso, R., eds. Developments in environmental science, volume 2: Ozone air pollution in the Sierra Nevada—distribution and effects on forests. Elsevier, Amsterdam, pp. 111–155.

Fenn, M.E., Poth, M.A., Terry, J.D., and Blubaugh, T.J. 2005. Nitrogen mineralization and nitrification in a mixed conifer forest in southern California: Controlling factors, fluxes, and nitrogen fertilization response at a high and low nitrogen deposition site. Can. J. For. Res. 35, 1464–1486.

Fenn, M.E., Jovan, S., Yuan, F., Geiser, L., Meixner, T., and Gimeno, B.S. 2008. Empirical and simulated critical loads for nitrogen deposition in California mixed conifer forests. Environ. Pollut, in Press.

Fisher, R.F., and Binkley, D. 2000. Ecology and Management of Forest Soils. Wiley, New York.

Gessel, S.P., Cole, D.W., and Steinbrenner, E.C. 1973. Nitrogen balances in forest ecosystems of the Pacific Northwest. Soil Biol. Biochem. 5, 19–34.

Giardina, C.P., Sanford, R.L., Dockersmith, I.C., and Jaramillo, V.J. 2000. The effects of slash burning on ecosystem nutrients during the land preparation phase of shifting cultivation. Plant Soil 220, 247–260.

Goldman, C.R. 1988. Primary productivity, nutrients, and transparency during the early onset of eutrophication in ultra-oligotrophic Lake Tahoe, California-Nevada. Limnol. Oceanogr. 33(6, part 1), 1321–1333.

Gray, J.T., and Schlesinger, W.H. 1981. Nutrient cycling in Mediterranean type ecosystems. In: Miller, P.C., ed. Resource use by Chaparral and Matorral: A comparison of vegetation function in two Mediterranean type ecosystems, Ecol. Stud 39. Springer-Verlag, New York, pp. 259–285.

Grier, C.L. 1975. Wildfire effects on nutrient distribution and leaching in a coniferous ecosystem. Can. J. For. Res. 5, 599–607.

Grogan, P., Burns, T.D., and Chapin, F.R. III. 2000. Fire effects on ecosystem nitrogen cycling in a Californian bishop pine forest. Oecologia 122, 537–544.

Grulke, N.E., Andersen, C.P., Fenn, M.E., and Miller, P.R. 1998. Ozone exposure and nitrogen deposition lowers root biomass of ponderosa pine in the San Bernardino Mountains, California. Environ. Pollut. 103, 63–73.

Gundersen, P., Schmidt, I.K., and Raulund-Rasmussen, K. 2006. Leaching of nitrate from temperate forests-effects of air pollution and forest management. Environ. Rev. 14, 1–57.

Huai, T., Durbin, T.D., Younglove, T., Scora, G., Barth, M., and Norbeck, J.M. 2005. Vehicle specific power approach to estimating on-road NH_3 emissions from light-duty vehicles. Environ. Sci. Technol. 39, 9595–9600.

Jassby, A.D., Reuter, J.E., Axler, R.P., Goldman, C.R., and Hackley, S.H. 1994. Atmospheric deposition of nitrogen and phosphorus in the annual nutrient load of Lake Tahoe (California-Nevada). Water Resour. Res. 30(7), 2207–2216.

Johnson, D.W. 1995. Soil properties beneath Ceanothus and pine stand in the eastern Sierra Nevada. Soil Sci. Soc. Am. J. 59, 918–924.

Johnson, D.W., Susfalk, R.B., and Dahlgren, R.A. 1997. Nutrient fluxes in forests of the eastern Sierra Nevada Mountains, USA. Global Biog. Cycl. 11, 673–681.

Johnson, D.W., Susfalk, R.B., Dahlgren, R.A., and Klopatek, J.M. 1998. Fire is more important than water for nitrogen fluxes in semi-arid forests. Environ. Sci. Policy 79–86.

Johnson, D.W., and Curtis, P.S. 2001. Effects of forest management on soil carbon and nitrogen storage: Meta Analysis. For. Ecol. Manage. 140, 227–238.

Johnson, D.W., Susfalk, R.B., Caldwell, T.G., Murphy, J.D., Miller, W.W., and Walker, R.F. 2004. Fire effects on carbon and nitrogen budgets in forests. Water, Air, Soil Pollut. Focus 4, 263–275.

Johnson, D.W., Murphy, J.D., Susfalk, R.B., Caldwell, T.G., Miller, W.W., Walker, R.F., and Powers, R.F. 2005. The effects of wildfire, salvage logging, and post-fire N fixation on the nutrient budgets of a Sierran forest. For. Ecol. Manag. 220, 155–165.

Johnson, D.W., Murphy, J.D., Walker, R.F., Miller, W.W., and Glass, D.W. 2007. Wildfire effects on forest carbon and nutrient budgets: Comparison of reconstructed versus measured values. Ecol. Eng. 31, 183–192.

Khanna, P.K., and Raison, R.J. 1986. Effect of fire intensity on solution chemistry of surface soil under a *Eucalyptus pauciflora* forest. Aust. J. Soil Res. 24, 423–434.

McNabb, D.H., and Cromack, K. Jr. 1983. Dinitrogen fixation by a mature *Ceanothus velutinus* Douglas Stand in the western Oregon Cascades. Can. J. Microbiol. 29, 1014–1021.

Meixner, T., Fenn, M.E., Wohlgemuth, P., Oxford, M., and Riggan, P. 2006. N saturation symptoms in chaparral catchments are not reversed by prescribed fire. Environ. Sci. Technol. 40, 2887–2894.

Michalski, G., Meixner, T., Fenn, M., Hernandez, L., Sirulnik, A., Allen, E., and Thiemens, M. 2004. Tracing atmospheric nitrate deposition in a complex semiarid ecosystem using $\Delta^{17}O$. Environ. Sci. Technol. 38, 2175–2181.

Miller, W.W., Johnson, D.W., Denton, C., Verburg, P.S.J., Dana, G.L., and Walker, R.F. 2005. Inconspicuous nutrient laden surface runoff from mature forest Sierran watersheds. Water, Air, Soil Pollut. 163, 3–17.

Monleon, F., Cromak, K. Jr., and Landsberg, J.D. 1997. Short- and long-term effects of prescribed underburning on nitrogen availability in ponderosa pine stands in central Oregon. Can. J. For. Res. 27, 369–378.

Mouillot, F., and Field, C.B. 2005. Fire history and the global carbon budget: a $1^\circ \times 1^\circ$ fire history reconstruction for the 20th century. Glob. Chang. Biol. 11, 398–420.

Murphy, J.D., Johnson, D.W., Miller, W.W., Walker, R.F., and Blank, R.R. 2006a. Prescribed fire effects on forest floor and soil nutrients in a Sierra Nevada ecosystem. Soil Sci. 171, 181–199.

Murphy, J.D., Johnson, D.W., Miller, W.W., Walker, R.F., Carroll, E.F., and Blank, R.R. 2006b. Wildfire effects on soil nutrients and leaching in a Tahoe Basin Watershed. J. Environ. Qual. 35, 479–489.

Neary, D.G., Klopatek, J.M., DeBano, L.F., and Ffolliot, P.F. 1999. Fire effects on belowground sustainability: A review and synthesis. For. Ecol. Manage. 122, 51–71.

Newland, J.A., and DeLuca, T.H. 2000. Influence of fire on native nitrogen-fixing plants and soil nitrogen status in ponderosa pine–Douglas-fir forests in western Montana. Can. J. For. Res. 30, 274–282.

Prietzel, J., and Kaiser, K.O. 2005. De-eutrophication of a nitrogen-saturated Scots pine forest by prescribed litter-raking. J. Plant Nutr. Soil Sci. 168, 461–471.

Raison, R.J., Khanna, P.K., and Woods, P.V. 1985. Mechanisms of element transfer to the atmosphere during vegetation fires. Can. J. For. Res. 15, 132–140.

Riggan, P.J., Lockwood, R.N., Jacks, P.M., Colver, C.G., Weirich, F., DeBano, L.F., and Brass, J.A. 1994. Effects of fire severity on nitrate mobilization in watersheds subject to chronic atmospheric deposition. Environ. Sci. Technol. 28, 369–375.

Rothe, A., and Mellert, K.H. 2004. Effects of forest management on nitrate concentrations in seepage water of forests in southern Bavaria, Germany. Water, Air, Soil Pollut. 156, 337–355.

Smith, E., and Adams, G. 1991. Incline Village/Crystal Bay defensible space handbook. SP-91-06. University of Nevada Cooperative Extension, Reno, NV.

Stark, N.M. 1973. Nutrient cycling in a Jeffrey Pine ecosystem. University of Montana, Missoula, MT.

Stephens, S.L., Meixner, T., Poth, M., McGurk, B., and Payne, D. 2005. Prescribed fire, soils, and stream chemistry in a watershed in the Lake Tahoe Basin, California. Int. J. Wildland Fire 13, 27–35.

Stolte, K.W. 1982. The effects of ozone on chaparral plants in the California South Coast Air Basin. M.Sc. Thesis. Dept. of Botany, University of California, Riverside. 108 pp.

Trabaud, L. 1994. The effect of fire on nutrient losses and cycling in a *Quercus coccifera* garrigue (southern France). Oecologia 99, 379–386.

Wan, S., Hui, D., and Luo, Y. 2001. Fire effects on nitrogen pools and dynamics in terrestrial ecosystems: A meta-analysis. Ecol. Applic. 11, 1349–1365.

Westerling, A.L., Hidalgo, H.G., Cayan, D.R., and Swetnam, T.W. 2006. Warming and earlier spring increases western U.S. forest wildfire activity. Science 313, 940–943.

Williams, M.R., and Melack, J.M. 1997. Effects of prescribed burning and drought on the solute chemistry of mixed-conifer forest streams of the Sierra Nevada, California. Biogeochem 39, 225–253.

Youngberg, C.T., and Wollum, A.G. 1976. Nitrogen accretion in developing *Ceanothus velutinus* stands. Soil Sci. Soc. Am. J. 40, 109–112.

Zavitovski, J., and Newton, M. 1968. Ecological importance of snowbrush *Ceanothus velutinus* in the Oregon Cascades. Ecology 49, 1113–1145.

This page intentionally left blank

Developments in Environmental Science, Volume 8 425
A. Bytnerowicz, M. Arbaugh, A. Riebau and C. Andersen (Editors)

ISSN: 1474-8177/DOI:10.1016/S1474-8177(08)00019-3

Chapter 19

Management Options for Mitigating Nitrogen (N) Losses from N-Saturated Mixed-Conifer Forests in California

Benjamin S. Gimeno, Fengming Yuan, Mark E. Fenn and Thomas Meixner*

Abstract

Mixed-conifer forests of southern California are exposed to nitrogen (N) deposition levels that impair carbon (C) and N cycling, enhance forest flammability, increase the risk of fire occurrence and air pollution emissions in fire, and increase nitrate runoff and soil N emissions both pre- and postfire. N-deposition abatement policies and prescribed fire treatments have been proposed to mitigate the interactive effects of fire suppression, N deposition, and wildfire occurrence. To test the most effective management options for N-enriched forests, a simulation study was done using a parameterization of the DAYCENT model for a mixed-conifer forest site currently experiencing 70 kg N ha^{-1} yr^{-1}. Five N deposition scenarios were defined, ranging from 5 to 70 kg N ha^{-1} yr^{-1}. Five abatement strategies ranging from 0% to 100% reductions in N deposition were considered for each N-deposition scenario. The influence of prescribed fire was tested for the selected N deposition and abatement scenarios, considering 15-, 30-, and 60-year intervals (PF15, PF30, and PF60, respectively), or no prescribed fires. When the most extreme N-deposition scenario was compared to the lowest, fuel loads were increased by 121%, resulting in 70% increases in wildfire emissions of particulate matter (PM_{10} and $PM_{2.5}$), methane (CH_4), carbon monoxide (CO), carbon dioxide (CO_2), and sulfur dioxide (SO_2). The estimated increase in wildfire nitrogen oxide (NO_x) emissions ranged from 56% to 210%. The larger values were derived when variations in fuel N content were taken into account. The combination of reduced N deposition and prescribed fire was most effective in reducing long-term N losses to the atmosphere and

*Corresponding author: E-mail: benjamin.gimeno@ciemat.es

in runoff. The PF15 treatment combined with 50–75% reduced N deposition were the best options for reducing N losses before and after fire. However, even prescribed fire at longer intervals and in combination with 25–50% reduced N deposition still resulted in large reductions in ecosystem losses of N. Implementation of such treatments would be considered a major achievement towards mitigating the symptoms of N saturation, even though in sites chronically exposed to 70 kg N ha^{-1} yr^{-1} a 100% reduction in N deposition may require many years to return N losses to baseline levels.

19.1. Introduction

Mixed-conifer forests in California are a multilayered community with a variable species composition extending across a range of moisture regimes. The dominant overstory species are ponderosa pine (*Pinus ponderosa*) or Jeffrey pine (*P. jeffreyi* Grev. and Balf.), and commonly associated species include California black oak (*Quercus kelloggi* Newb.), white fir (*Abies concolor* Gord. & Glend.), and incense cedar (*Calocedrus decurrens* [Torr.] Florin). Air pollution impacts on this ecosystem type are well documented, with tropospheric ozone and nitrogen (N) deposition as the most hazardous pollutants, impairing tree performance and ecosystem nutrient cycling (Fenn et al., 2003c; Miller & McBride, 1999).

The effects of N deposition on mixed-conifer forest sites in California have been studied across air pollution gradients consisting of twenty-seven sites ranging from 1000 to 2500 m a.s.l. and located in the Sierra Nevada Mountains, San Gabriel Mountains northeast of Los Angeles, and the San Bernardino Mountains east of Los Angeles (Fenn et al., 2008). Most of the sites are on weathered or decomposed granitic rock. The soils are generally sandy loam in texture, and percent base saturation ranges from 70% to 100%. Nitrogen deposition across the different sites ranges from 1.5 kg N ha^{-1} yr^{-1} to 71.5 kg N ha^{-1} yr^{-1} (Breiner et al., 2007), with sites receiving N loads that are among the highest in the world and showing symptoms of N saturation (Fenn et al., 2003a). Specific reviews on the effects of N deposition in this type of forest ecosystem have been provided for the sites located in the San Bernardino and San Gabriel Mountains (Fenn & Poth, 1999) as well as for Sierra Nevada sites (Fenn et al., 2003c). Increasing N loads have resulted in a series of well-documented effects, such as increased foliar N concentrations, increased tree growth rates of ponderosa pine, increased tree mortality as a result of stand densification, increased depth and N content of the forest floor, decreased C:N (carbon:nitrogen) ratios in litter and mineral soil, increased nitrification rates, increased emissions of soil gaseous compounds (nitric oxide [NO] and nitrous oxide [N_2O]), depletion of soil cation pools, increased soil acidification, and increased leaching of nitrate (NO_3^-) in soil solution and NO_3^- export in stream water. Nitrification is the key process driving these N-saturation responses. Soil conditions of high base cation saturation, moderate pH values, and the aerobic condition of these coarse-textured soils appear to be among the factors favoring active nitrification in the soils of California mixed-conifer forests. As a result, the N cycle is strongly nitrate dominated and higher in sites with elevated N deposition. Nitrogen cycling dominated by nitrate is typical of N-saturated sites (Fenn et al., 1998). Based on these findings Breiner et al. (2007) and Fenn et al. (2008) have recently established empirical dose-response relationships for N deposition inputs and N cycling processes with a high predictive power.

Recurrent fire is an integral component of mixed-conifer forests because the Mediterranean climate of winter rain and dry summers results in inefficient decomposition, rapid fuel buildup, and high fire hazard. Great changes in fire frequency have been documented when comparing presettlement conditions with current fire occurrence. Fire exclusion began in the late 1800s and early to mid-1900s in most parts of the Pacific regions (Houghton et al., 2000). Active fire suppression starting in the first quarter of the last century has altered fire regimes as well as ecosystem structure, resulting in increased fire intervals and fuel buildup and changes in species composition. For instance, Minnich et al. (1995) estimated that current conditions would lead to an estimated fire rotation period of 360 years, and reported that 60 years of suppression caused stem density increases of 100–200 stems/ha (dbh > 10 cm), with increases proportional to mean annual precipitation. Stand-thickening has been accompanied by an increasing density of standing dead trees. High mortality was due to an overabundance of trees competing for moisture and nutrients, with the shift in species dominance further heightened by differential responses to drought, bark beetle infestation, and air pollution. As a result, more intense and more extensive fires may occur than under a normal fire regime, converting the fire regime from a patchy mosaic continuum to a sustained cyclic stand-replacement fire regime (Minnich, 1999).

These wildfire events have large influences on the release of N. As Johnson et al. (2004) have pointed out, the potential loss of N with fire is far greater than due to leaching in most ecosystems, except for catchments experiencing high N-fixation rates or in N-saturated ecosystems. However, considering the whole C and N budget in the ecosystem, the effects of fire on soil C and N are very dependent on fire intensity and time since fire (Johnson & Curtis, 2001; Wan et al., 2001). Fire also influences water quality as postfire increases in mineral leaching rates have been observed that show ammonium (NH_4^+) loss predominant over NO_3^- export beginning immediately after fire and up to one year postfire, while NO_3^- export prevailed afterwards. Three years after fire, mineral N leaching was greatly reduced (Johnson et al., 2007). However, in N-saturated chaparral catchments near Los Angeles, California, NO_3^- dominated runoff in unburned catchments and postfire runoff NO_3^- was far greater than NH_4^+ in burned catchments (Riggan et al., 1994).

In addition to increased mineral leaching rates and subsequent impacts on stream water quality, increased C and N losses may also occur as a result of precipitation events occurring soon after the fire event by inducing runoff and erosion that would contribute to nutrient export from the forest floor and possibly also from the surface soil horizon (Johnson et al., 2008). Finally, fire-induced emissions of air pollutants may have a large impact on regional air quality (Cheng et al., 1998; Liu, 2004), enhancing regional haze (McMeeking et al., 2006), and adversely impacting human health, especially near densely populated areas (Clinton et al., 2006; Massie et al., 2006; Wu et al., 2006).

Atmospheric N deposition may enhance the direct and indirect impacts of fire (Fenn et al., 2003c). At the ecosystem level, N deposition has been found to change the chemical composition of different forest components, such as foliage, forest floor, and upper soil layers, resulting in an alteration of C and N cycles. N deposition also increases stand density and tree volume growth and increases foliar N content. These processes affect the chemical properties of fuel and increase fuel loading in the ecosystem, thus enhancing forest flammability and increasing the risk of fire occurrence with associated impacts on fire severity and intensity. Moreover, N deposition may also worsen the adverse consequences of fire, such as air pollution emissions (Yokelson et al., 2007) and nitrate runoff to stream water (Johnson et al., 2008; Riggan et al., 1994).

Prescribed fire is a forest management technique that lessens the damage from wildfire by removing a portion of the accumulating dead fuels and reducing the stature of the developing understory when burning conditions are not severe (Liu, 2004). Current U.S. policies for federal lands emphasize the use of prescribed fire, either alone or in combination with other techniques, to meet fuel reduction objectives (HFRA, 2003). Prescribed fire has been considered as a tool for alleviating the condition of N enrichment in forest and chaparral ecosystems (Fenn et al., 1998; Meixner et al., 2006).

Air pollution control would be the ultimate solution for alleviating the symptoms of N excess that occur under chronic N-deposition exposures.

The effectiveness of these measures would depend on the magnitude of N deposition and the number of years the forests have been exposed to elevated N-deposition rates, and thus the cumulative N-deposition loading. For instance, Fenn et al. (2008) indicated that a fivefold N-deposition reduction might be needed to prevent N losses at the San Bernardino Mountain site experiencing the highest deposition rate. It would be difficult to achieve this goal, at least in the short term, and therefore it is very likely that this site will continue to experience elevated N losses for the foreseeable future. Neither is prescribed fire alone expected to reverse N saturation symptoms (Johnson et al., 2008; Meixner et al., 2006). We propose that an appropriate combination of reduced N-deposition inputs, removal of a significant fraction of the accumulated N stores and reduced stand densification by prescribed fire, and stimulated postfire regrowth could be effective in mitigating the symptoms of N saturation.

19.2. Objectives

This chapter discusses different forest management and N-deposition scenarios that would result in long-term and short-term effects in ecosystem N cycling. A simulation study was carried out to test the following hypotheses:

- In the long-term, elevated N deposition leads to greater fuel loads and affects the N content of fuels. As a result, wildfire air pollution emissions will increase in forests experiencing high N-deposition rates.
- In the long-term, elevated N deposition enhances N losses from the ecosystem through increased gaseous emissions from soil and increased N runoff.
- In the short term, elevated N deposition enhances N losses to the atmosphere and stream water after prescribed fire events.
- These adverse effects could be mitigated through air pollution control policies and prescribed fire practices.

19.3. Materials and methods

19.3.1. Experimental design

In order to test these hypotheses, a simulation study was performed based on a California mixed-conifer forest site (Camp Paivika, CP) experiencing a high N deposition rate (71 kg N ha^{-1} yr^{-1}). The following N treatments were selected: N5, N15, N25, N40, and N70 corresponding to 5, 15, 25, 40, and 70 kg N $ha^{-1} yr^{-1}$, respectively. To estimate the benefits of different air pollution control policies, 0%, 25%, 50%, 75%, and 100% reductions in N deposition were considered for all the N deposition scenarios starting from 2006 and ending in the year 2210. Also, the influence of varying prescribed fire intervals on N cycling were tested for the selected N deposition scenarios, consisting of 15-, 30-, and 60-year intervals (PF15, PF30, and PF60, respectively), or no prescribed fires from 2006 to 2210. Wildfire occurred twice throughout the simulation, in the years 2100 and 2200.

The parameters chosen to evaluate the effect of the different treatments on N cycling were (1) fuel loads, N content in fuel loads, and air pollution emissions from wildfire; (2) nitrate export in stream water; and (3) nitrogenous trace gas emissions from soil. Long- and short-term ecosystem responses to N deposition and fire were assessed.

19.3.2. N Biogeochemical cycling simulation

DAYCENT version 4.5 was used in this study. The DAYCENT biogeochemistry model (Del Grosso et al., 2000; Parton et al., 1998; Parton et al., 2001) is the daily time step version of the CENTURY model (Parton et al., 1993). It simulates the biogeochemical processes of carbon, nitrogen, phosphorus, and sulfur associated with soil organic matter (SOM) in multiple ecosystem types. One feature of DAYCENT important to this study is the improvement of N cycling algorithms, including the simulation of N_2O, NO, and N_2 emissions resulting from nitrification and denitrification, and detailed soil N mineralization-immobilization processes associated with various organic matter pools (including microbial), which are distinguished by their decomposition rates. Required inputs to the model include daily maximum/minimum temperature and precipitation, site-specific soil properties and hydraulic characteristics, and current and historical land use.

Model runs were initialized and stabilized by repeatedly using site-specific weather data for 900 years (i.e., initially started from 1000 AD), background N deposition (1.0 kg N $ha^{-1} yr^{-1}$), and fire occurrence every 100 years. The model provides approximations of historical tree growth, litter C, SOM, and C:N ratios in the study area (Allen et al., 2007; Fenn et al., 2005; Grulke et al., 2001; Grulke & Balduman, 1999). Some parameters were modified in order to achieve reasonably well-fitted outputs with observations.

For model runs, N deposition was maintained at a background level of 1.0 kg N $ha^{-1} yr^{-1}$ from 1900 to 1930 and gradually increased linearly to the targeted values from 1931–1940. N deposition remained at the targeted values from 1941 to 2005 allowing annual random 10% variations in those values. The rationale and criteria followed to calibrate the model can be found elsewhere (Fenn et al., 2008). The various N deposition and prescribed fire scenarios were applied from 2006 to 2210, the year simulations ceased. Wildfire events occurred in the years 2100 and 2200.

To estimate the benefits of applying different air pollution control policies and forest management protocols in forests where the N-deposition levels have exceeded the empirical critical load for "N as a nutrient" effects (17 kg N ha^{-1} yr^{-1}; Fenn et al., 2008), only the N25 and N70 scenarios were considered. The parameters simulated for these evaluations were NO_3^- leaching and N emissions from soil.

19.3.3. Estimation of wildfire emissions

The First Order Fire Effects Model (FOFEM 5.0; Reinhardt, 2003) was selected to estimate air pollution emissions from wildfire events. The fuel loads corresponding to the different N deposition scenarios in the year 2099, 1 year before the first wildfire event occurred in the simulation, were estimated by DayCent and used as inputs for the FOFEM model. The selected inputs for FOFEM were Pacific West Region, SAF 243 Sierra Nevada Mixed-Conifer Forest cover type, and natural fuel type. The wildfire occurred in fall under very dry conditions. Duff was set at the default light value for this ecosystem type (20 t $acre^{-1}$), with a depth of 2.5 in. and 20% humidity. A centered log distribution was selected for woody fuels greater than 3 in. Relative humidity for woody fuel >3 in. in diameter, and 0.25–1 in. was 10% and 6%, respectively, as calculated by the model under the selected very dry conditions. These harsh conditions were chosen to simulate a likely scenario of wildfire occurrence in the area. Simulations were carried out considering three different wildfire severities: 100% crown burnt, 75% crown burnt, and 50% crown burnt. The other input variables remained constant for the three wildfire severity simulations.

The total fuel load and the percentage of fuel consumed for each fuel class were calculated by the model. The air pollution emissions from the different wildfire severities and two N-deposition scenarios (N25, N70) were also calculated by the model providing estimations of particulate matter (PM_{10} and $PM_{2.5}$), methane (CH_4), carbon monoxide (CO), carbon dioxide (CO_2), nitrogen oxides (NO_x), and sulfur dioxide (SO_2) emissions in lbs $acre^{-1}$. Since the FOFEM model does not allow for evaluations of the influence of N concentrations of the fuel material, the NO_x emission factors (EF) were recalculated using two procedures (Dennis et al., 2002; Lacaux et al., 1996) based on N concentrations in the different fuel materials. The two methods differ based on the algorithms for the calculation of NO_x EF as can be found in Eq. (19.1) (Dennis et al., 2002) and Eq. (19.2) (Lacaux et al., 1996).

$$\mathrm{EF\ NO_x(lb\ ton^{-1})} = -3 + 7.8\ (0.7 \times \%\mathrm{fuel\ N}) \qquad (19.1)$$

$$\mathrm{EF\ NO_x(g\ kg^{-1})} = 9.5 \times \mathrm{N}(\%) - 0.49 \qquad (19.2)$$

The default EF value of $1.14\,\mathrm{g\,kg^{-1}}$ was applied following Dennis et al. (2002) for those fuel types for which N concentration was not provided by the DayCent model (shrubs and herbaceous components) or for woody materials, because negative values were obtained when applying Eqs (19.1 or 19.2). This default EF value is close to the 1.17 value provided by Urbanski et al. (2008) as an average EF for temperate forests. The final value of NO_x emissions was obtained by multiplying the estimated EFs by the amount of fuel burned calculated from FOFEM.

19.4. Results

Long- and short-term interactive effects of N deposition, forest management practices, and reduced air pollution were found.

19.4.1. Long-term responses to N deposition and fire management

19.4.1.1. Fuel Loads and N Content in Fuel Load

Increasing N-deposition rates increased forest fuel loads. The largest difference in fuel loading in the year preceding wildfire occurrence (2099) was found between the N5 and N70 deposition levels, resulting in a 121% increase (Fig. 19.1). The long-term effects of N-deposition rates over 5 kg $\mathrm{N\,ha^{-1}\,yr^{-1}}$ were irreversible as N reduction was ineffective in reducing fuel loads to the N5 levels. This was the case even when 100% reductions in N deposition were considered (Fig. 19.1a). However, prescribed fire was very effective in reducing fuel loads to N5 levels, even under the N70 deposition scenario. PF15 and PF30 were more successful in this regard than PF60 (Fig. 19.1b).

Similarly, N content in fuel load also increased with increasing N deposition. The highest N concentration increases were found in litter (data not shown), which were slightly higher than for foliage. The critical value of $12\,\mathrm{g\,kg^{-1}}$ foliar N was reached for N-deposition rates $\geqslant 25$ kg $\mathrm{N\,ha^{-1}\,yr^{-1}}$ (Fig. 19.2a), in agreement with the empirical critical load value for this parameter proposed by Breiner et al. (2007), which was

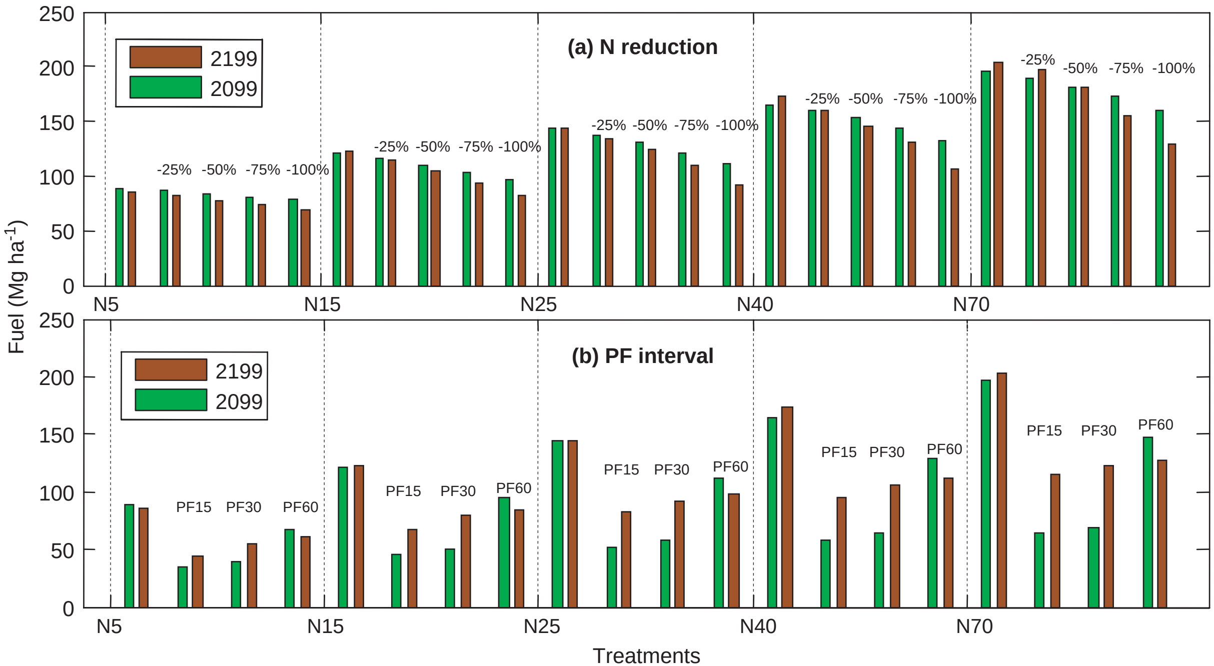

Figure 19.1. Fuel loads in the years right before wildfire occurrence under two simulation scenarios: (a) 0%, 25%, 75%, and 100% of N deposition abatement beginning in 2006, and (b) prescribed fire (PF) performed at 15-, 30-, and 60-year intervals. N5, N15, N 25, N40, and N70 correspond to N-deposition rates of 5, 15, 25, 40, and 70 kg N ha^{-1} yr^{-1}, respectively.

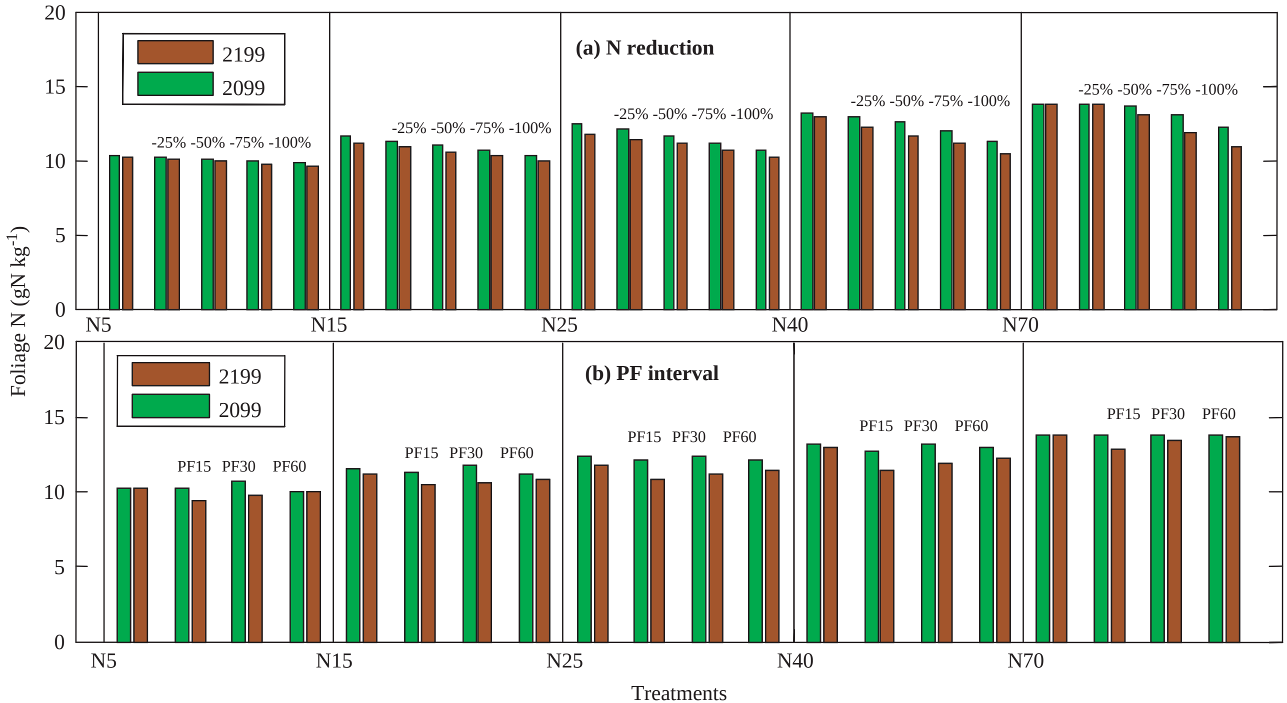

Figure 19.2. Foliage N concentration in the years right before wildfire occurrence under two simulation scenarios: (a) 0%, 25%, 75%, and 100% of N-deposition abatement beginning in 2006, and (b) prescribed fire (PF) performed at 15-, 30-, and 60-year intervals. N5, N15, N25, N40, and N70 correspond to N-deposition rates of 5, 15, 25, 40, and 70 kg N $ha^{-1}\,yr^{-1}$, respectively.

26 kg N ha^{-1} yr^{-1}. The percent of N-deposition reduction needed to return the system to foliage N concentrations below the critical value depended on the N-deposition scenario: 50% and 75% reductions for the N25 and N40 scenarios. Interestingly, the foliar N concentration did not return to levels below the critical value under the N70 scenario, even when 100% reductions in N-deposition rates were considered. Prescribed fire treatments were not effective in reducing foliar N when N-deposition rates were over 25 kg ha^{-1} yr^{-1} (Fig. 19.2b).

19.4.1.2. Wildfire Air Pollution Emissions

Fire severity influenced wildfire emissions of some pollutants (data not shown). For a given N-deposition scenario, fire severity, considered as percentage of crown burned, had no effect on the emissions of PM_{10}, $PM_{2.5}$, CH_4 or CO. However, when comparing 50% and 100% of the crown burned, emissions differed by 7–9% for CO_2, and 5–7% for SO_2. When the same comparison was performed to evaluate the effect of fire severity on NO_x emissions, large differences were found depending on the method used, ranging from 72–93% for FOFEM, 5% for Dennis et al. (2002) and 7–13% for the Lacaux et al. (1996) method.

As a result of the influence of N deposition on fuel loads, wildfire air pollution emissions also increased with N deposition. To evaluate the effect of N deposition on wildfire emissions, a wildfire that burned 75% of the canopy was simulated in the year 2100. No prior fire occurred after 1900 (to simulate fire exclusion policies), and N deposition was set at 5 and 70 kg ha^{-1} yr^{-1}. Emissions of PM_{10}, $PM_{2.5}$, CH_4, CO, CO_2, and SO_2 following the 2100 wildfire were about 70% higher in the N70 than the N5 treatment (Figs. 19.3a and b). Estimates of the increase in wildfire NO_x emissions between the N25 and N70 treatments when 75% of the crown was burned varied from 56% to 210% (Fig. 19.4) according to the three methods used. The increased NO_x emissions estimated by the FOFEM model were attributed to increased fuel build up in the N70 scenario. NO_x emissions increased by 56% in the N70 treatment compared to the N5 scenario according to FOFEM. However, these differences increased considerably (ranging from 166% to 210%) when comparing the N70 and N5 scenarios by the two methods that consider the influence of N-deposition rates on fuel N content (Fig. 19.4).

19.4.1.3. N Export in Stream Water

N deposition had a large effect on N export in stream water. N export was double the background levels by around 1980, 40 years after

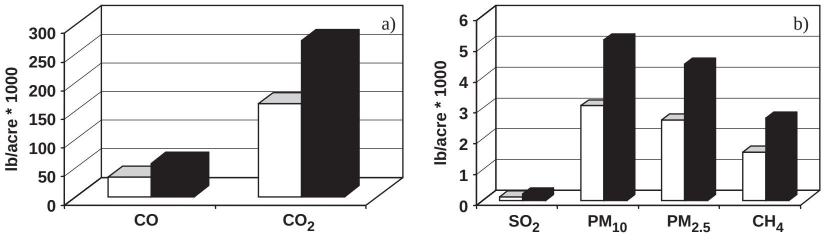

Figure 19.3. Estimation of CO, CO_2, SO_2, PM_{10}, $PM_{2.5}$, and CH_4 emissions from a wildfire (75% of the crown burned) occurring in the year 2100 and under N-deposition rates of 5 (white bars) and 70 (black bars) $kg\,ha^{-1}\,yr^{-1}$. The previous wildfire occurred prior to 1900.

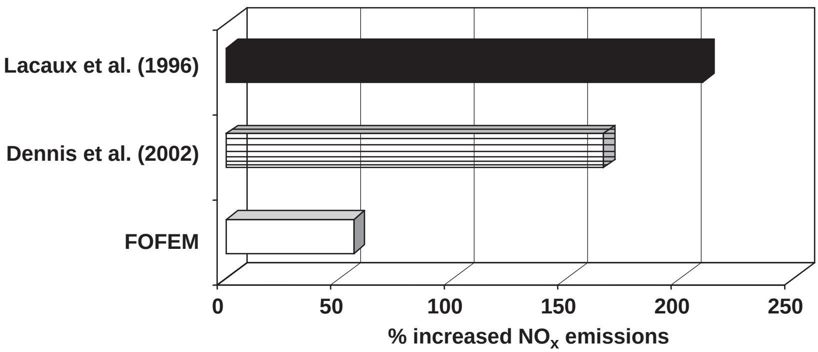

Figure 19.4. Percentage of increased NO_x emissions from a wildfire (75% of the crown burned) under N70 relative to N25 N-deposition scenarios as calculated by three different methods (Dennis et al., 2002; Lacaux et al., 1996, and FOFEM). The wildfire occurred in the year 2100, and the previous wildfire occurred prior to 1900.

N deposition increased to 25 $kg\,ha^{-1}\,yr^{-1}$ in the N25 scenario. Maximum N export reached up to five times background levels after 169 years of N deposition in 2109. The fastest return to background levels of NO_3^- (8 years) was achieved by reducing N deposition by 100% (Fig. 19.5a). Deposition reductions of 25 to 75% were proportionately less effective than the 100% reduction scenario (Fig. 19.5a). However, NO_3^- concentrations in the 75% reduction treatment were only slightly elevated over the 100% reduction.

Prescribed fire treatments alone did not reduce N runoff to basal levels. However, the combination of prescribed fire and N-deposition abatement was very effective in reaching stable N-export values in the background level

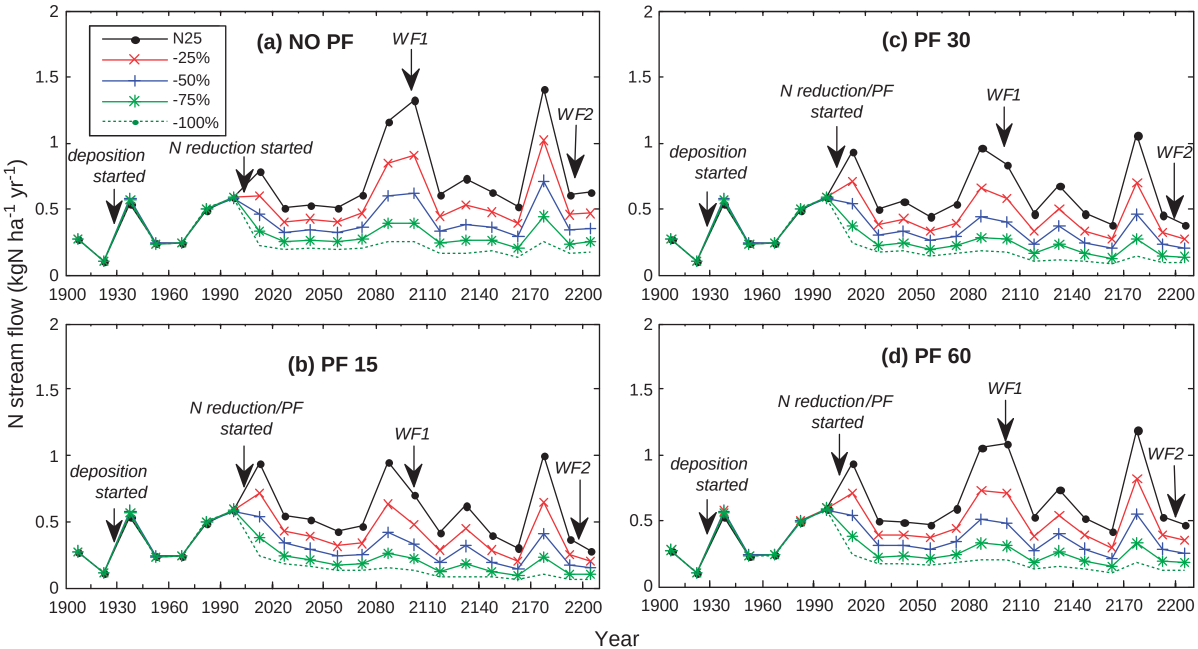

Figure 19.5. N leaching losses under the N-deposition scenario of 25 kg N ha^{-1} yr^{-1}, averaged every 15 years, impacted by different N-deposition reductions and three prescribed fire treatments (PF): (a) no prescribed fire, (b) 15-year interval prescribed fires, (c) 30-year interval prescribed fires, and (d) 60-year interval prescribed fires. Black line, no N-deposition reduction; red line, 25% N-deposition reduction; blue line, 50% N-deposition reduction; solid green line, 70% N-deposition reduction; and dark green dotted line, 100% N-deposition reduction. WF1 and WF2, occurrence of wildfire events.

range even after wildfire occurrence, particularly with a 75% N-deposition reduction and any prescribed fire interval treatment (Figs. 19.5b–d). Similarly, the combination of PF15 and 50% reductions ended in runoff values only slightly higher than background levels (Fig. 19.5b).

Because returning N losses to background levels may not be a realistic goal in the short term for heavily affected sites, an acceptable level of 0.5 kg N ha^{-1} yr^{-1} in stream water NO_3^- export was set based on previous research (Fenn et al., 2008). Under the N25 scenario, this threshold could be reached by using different strategies such as (1) 75% reduction in N deposition with or without prescribed fire, (2) 50% reduced N deposition and prescribed fire of any interval, and (3) 25% reduction in N deposition and prescribed fire, although with this level of deposition reduction there were three periods of N runoff slightly above the threshold (Fig 19.5). Under the N25 scenario, prescribed fire alone resulted in many periods when stream water NO_3^- export was below the 0.5 kg N ha^{-1} yr^{-1} NO_3^- runoff threshold, although N-deposition reductions $\geqslant$50% were needed to maintain N-runoff levels below the threshold (Fig. 19.5). In the absence of prescribed fire, N runoff exceeded the threshold intermittently in the 50% N-reduction treatment (Fig. 19.5).

Under the N70 scenario, N export was 7 times higher than background levels by 1980, 40 years after N deposition increased to 70 kg ha^{-1} yr^{-1}. Nitrogen export reached as much as 73 times higher than background levels after 169 years of N deposition in the N70 treatment (Fig. 19.6). Air pollution control polices or prescribed fire treatments alone were ineffective in reducing NO_3^- in runoff to background levels. Under the N70 scenario, the only way to completely return the system to basal levels, admittedly an unrealistic near-term goal, was to combine prescribed fire and reduced N deposition. A 100% N-deposition reduction and PF15 were needed to achieve this goal within 52 years. The PF30 treatment combined with 100% N-deposition reductions resulted in runoff levels slightly higher than background values.

The previously established acceptable N-export level (0.5 kg ha^{-1} yr^{-1}) was eventually approximated in the N70 scenario with 100% reductions in N deposition. When N deposition was reduced by 75–100% in combination with any prescribed fire treatment, N export also decreased to acceptable levels (Fig. 19.6). It should be appreciated that even a 50% reduction in N-deposition inputs, particularly when combined with any prescribed fire interval, also resulted in dramatic decreases in NO_3^- export both before and after wildfire (Fig. 19.6). If N deposition was decreased by at least 50% then a prescribed fire interval of 30 years was nearly as effective as the PF15 treatment (Fig. 19.6).

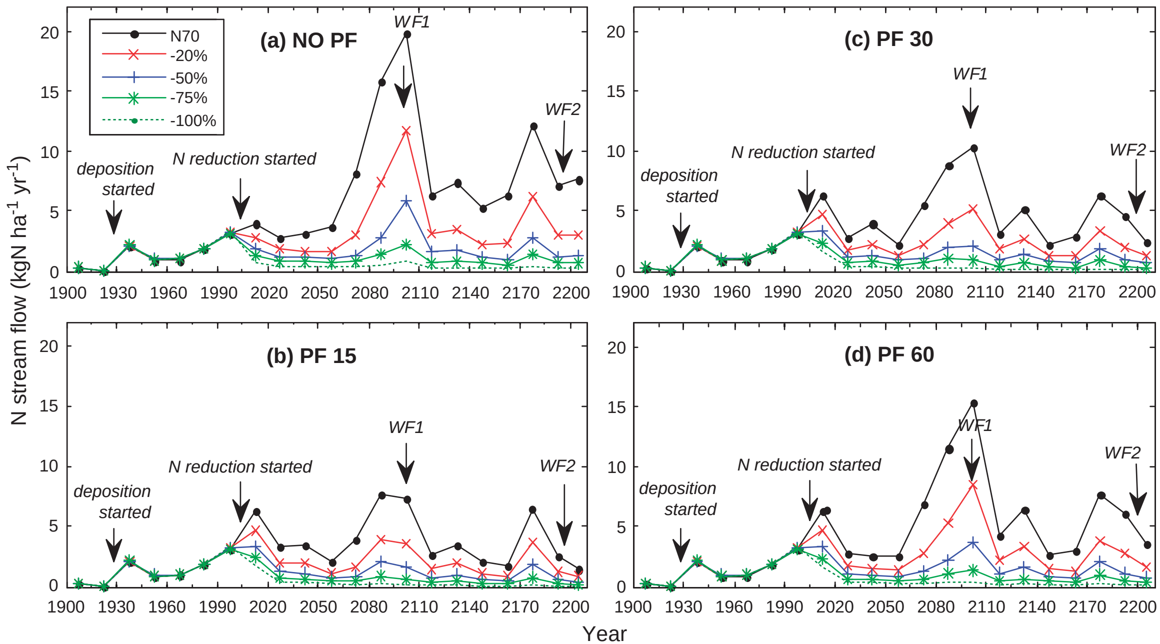

Figure 19.6. N leaching losses under the N-deposition scenario of 70 kg N ha^{-1} yr^{-1}, averaged every 15 years, impacted by different N-deposition reductions and three prescribed fire treatments (PF): (a) no prescribed fire, (b) 15-year interval prescribed fires, (c) 30-year interval prescribed fires, and (d) 60-year interval prescribed fires. Black line, no N-deposition reduction; red line, 25% N-deposition reduction; blue line, 50% N deposition reduction; solid green line, 70% N deposition reduction; and dark green dotted line, 100% N-deposition reduction. WF1 and WF2, occurrence of wildfire events.

19.4.1.4. Soil N Emissions

Increased N deposition enhanced soil N emissions, with N losses due to this process higher than N losses in stream water for a given N-deposition input. Prior to the year 2100 soil N emissions under the N25 and N70 scenarios reached values that were 27 and 144 times higher, respectively, than basal levels (Figs. 19.7–19.8). Soil emissions could be most efficiently reduced by combining air pollution abatement policies and prescribed fire treatments. Under the N25 scenario, background levels could only be achieved by combining 100% N-deposition reductions and PF15 for 82 years (Fig. 19.7). In the case of the N70 scenario, air pollution control and/or prescribed fire did not result in baseline soil emissions. An N-deposition reduction of 100% and a 15-year prescribed fire interval when maintained for 82 years resulted in soil N-emission levels four times greater than basal levels (Fig. 19.8).

Prescribed fire alone with a 15-year return interval reduced maximum gaseous N emissions by approximately 50% in both the N25 and N70 treatments (Figs. 19.7–19.8). In the N70 scenario, even with a 75% reduction in deposition after 22 years of N deposition control, annual N emissions from soil were 7–10 $kg^{-1} ha^{-1}$, and when PF15 was combined with the 75% reduced deposition, soil emissions were still elevated, ranging from 3–7 $kg\,ha^{-1}\,yr^{-1}$. By comparison, when the same period was considered in the N25 scenario, a 75% reduction in deposition combined with the PF15 treatment resulted in soil trace gas emissions ranging from values slightly over 2 $kg\,ha^{-1}\,yr^{-1}$ to less than 1 $kg\,ha^{-1}\,yr^{-1}$ (Figs. 19.7–19.8).

19.4.2. Short-term ecosystem responses to N deposition and fire management

Prescribed fire occurrence resulted in consistent patterns of N losses regardless of N deposition scenarios. Soil N emissions peaked 1 month after prescribed fire took place, while N export to stream water peaked 11, 23, and 35 months after prescribed fire (Figs. 19.9–19.12). However, the magnitude of these effects was influenced by N deposition. For instance, maximum nitrate leaching was 10 times higher for N70 than for N25 scenarios. Similarly, peak soil N emissions under the N70 scenario were double those of the N25 treatment following fire (Figs. 19.9–19.12), and also exhibited unusually high peak emissions during the second year postfire (Fig. 19.10). The PF15 treatment was very effective in reducing N export to stream water after prescribed fire, comparable to a 75% reduction in N deposition under the N25 scenario, and was more effective in the first year than a 100% reduction in N deposition under the N70 scenario (Figs. 19.10–19.11). In the N25 scenario the PF15 treatment or a

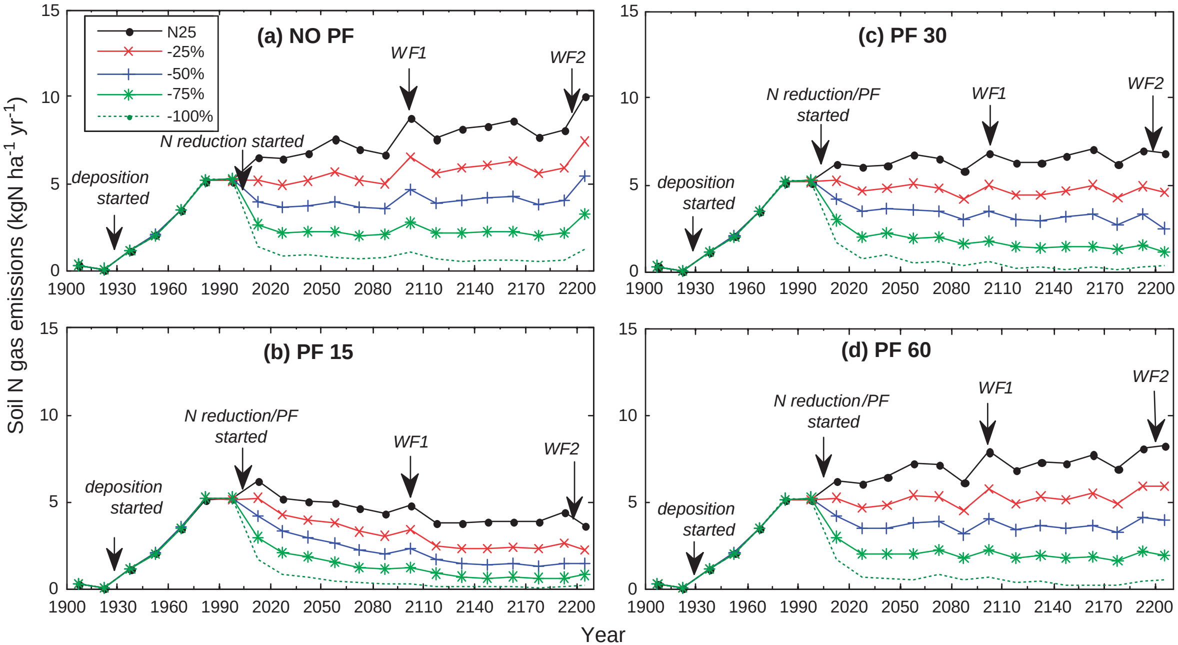

Figure 19.7. Soil N trace gas emissions under the N-deposition scenario of 25 kg N ha^{-1} yr^{-1}, averaged every 15 years, impacted by different N-deposition reductions and three prescribed fire treatments (PF): (a) no prescribed fire, (b) 15-year interval prescribed fires, (c) 30-year interval prescribed fires, and (d) 60-year interval prescribed fires. Black line, no N-deposition reduction; red line, 25% N-deposition reduction; blue line, 50% N-deposition reduction; solid green line, 70% N-deposition reduction; and dark green dotted line, 100% N-deposition reduction. WF1 and WF2, occurrence of wildfire events.

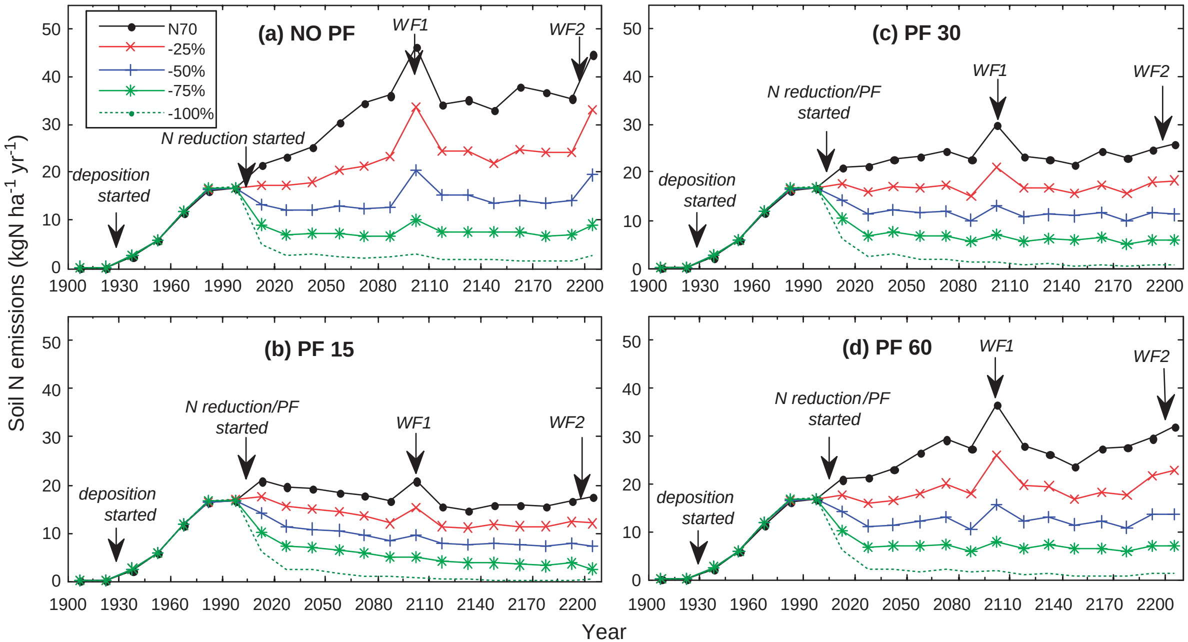

Figure 19.8. Soil N trace gas emissions under the N-deposition scenario of 70 kg N ha^{-1} yr^{-1}, averaged every 15 years, impacted by different N-deposition reductions and three prescribed fire treatments (PF): (a) no prescribed fire, (b) 15-year interval prescribed fires, (c) 30-year interval prescribed fires, and (d) 60-year interval prescribed fires. Black line, no N-deposition reduction; red line, 25% N-deposition reduction; blue line, 50% N-deposition reduction; solid green line, 70% N-deposition reduction; and dark green dotted line, 100% N-deposition reduction. WF1 and WF2, occurrence of wildfire events.

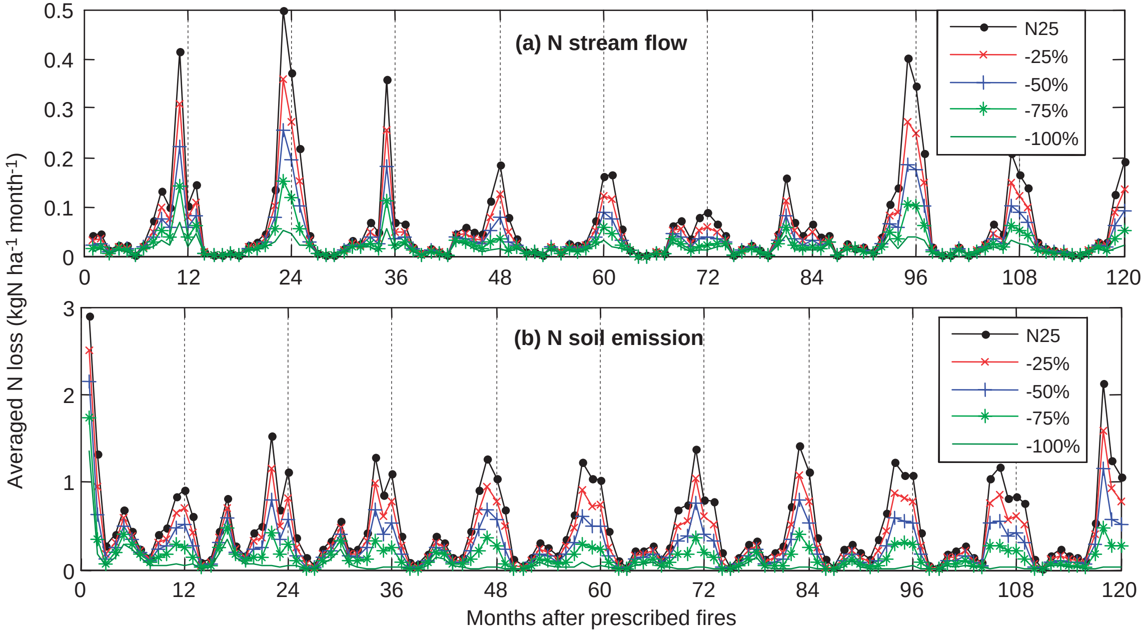

Figure 19.9. N in stream flow (a) and soil trace gas emissions (b) after prescribed fires (PF) under the N deposition scenario of 25 kg N ha^{-1} yr^{-1}, averaged for three PF treatments, impacted by different percentages of N-deposition reduction. Black line, no reduction; red line, 25% reduction; blue line, 50% reduction; light green line, 75% reduction; dark green line, 100% reduction.

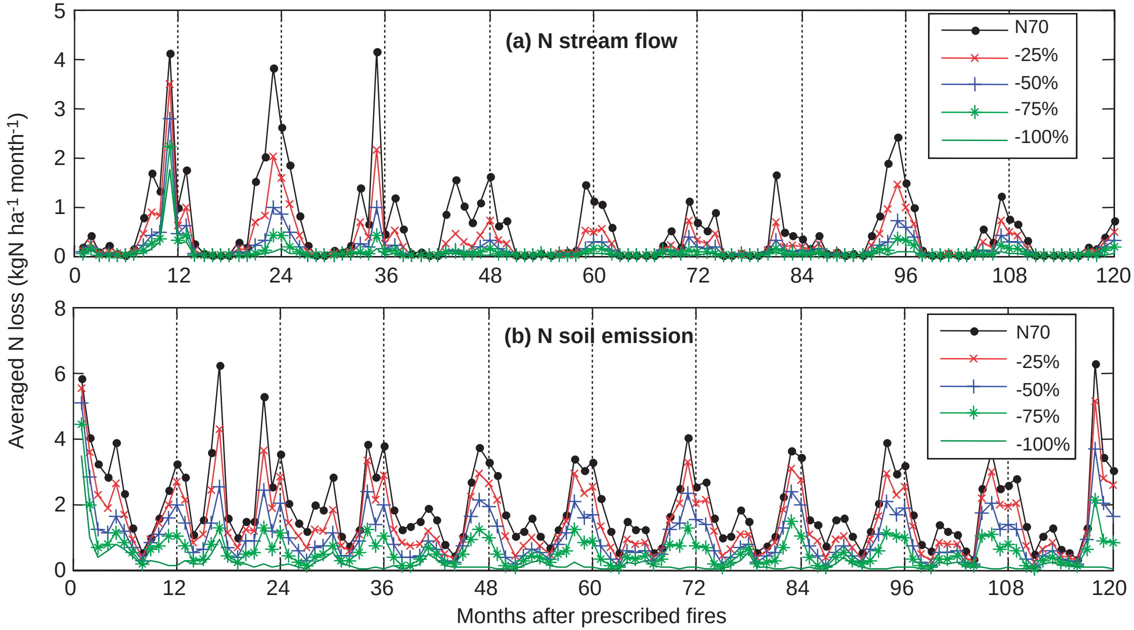

Figure 19.10. N in stream flow (a) and soil trace gas emissions (b) after prescribed fires (PF) under the N deposition scenario of 70 kg N ha^{-1} yr^{-1}, averaged for three PF treatments, impacted by different percentages of N-deposition reduction. Black line, no reduction; red line, 25% reduction; blue line, 50% reduction; light green line, 75% reduction; dark green line, 100% reduction.

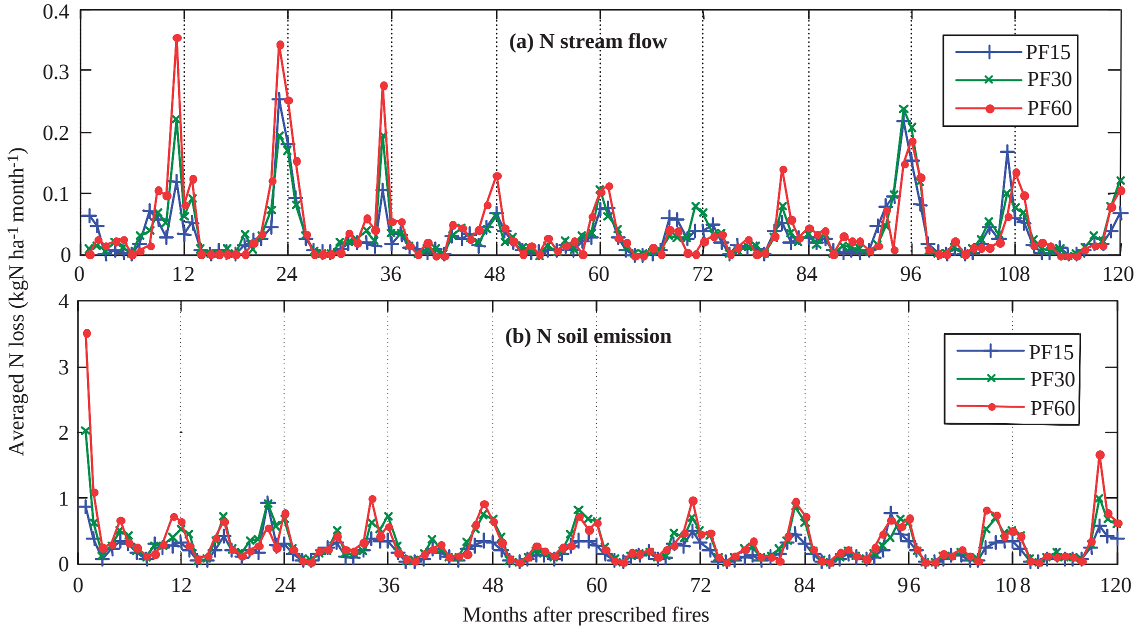

Figure 19.11. N in stream flow (a) and soil trace gas emissions (b) after prescribed fires (PF) under a deposition scenario of 25 kg N ha^{-1} yr^{-1} and considering three different PF intervals: 15 years (blue line), 30 years (green line), and 60 years (red line).

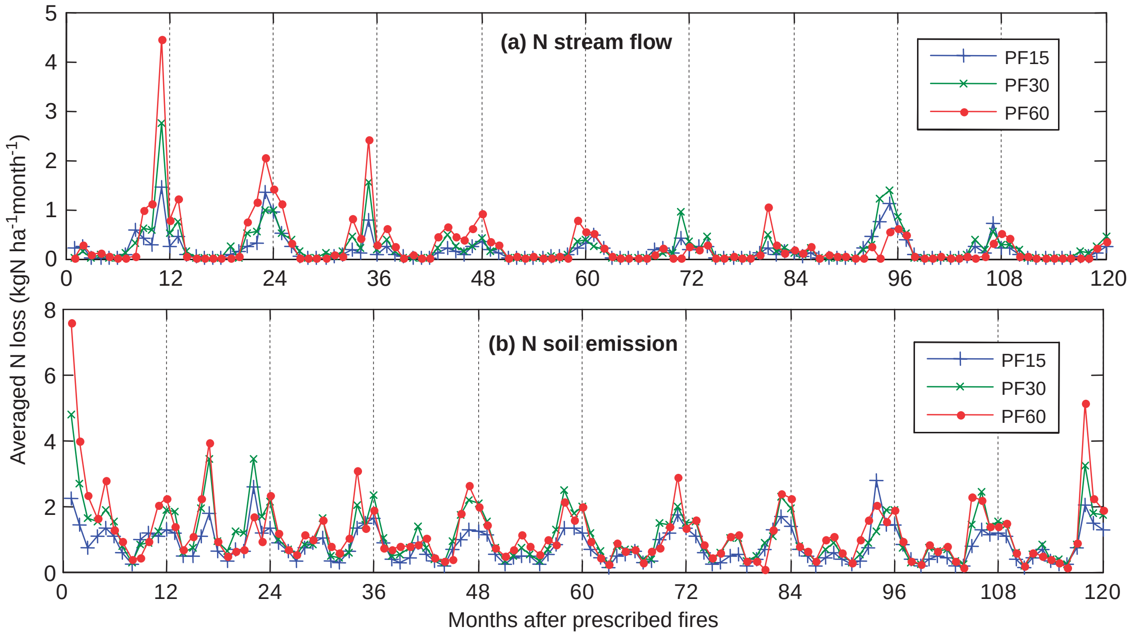

Figure 19.12. N in stream flow (a) and soil trace gas emissions (b) after prescribed fires (PF) under a deposition scenario of 70 kg N ha^{-1} yr^{-1} and considering three different PF intervals: 15 years (blue line), 30 years (green line), and 60 years (red line).

75% reduction in N deposition were the most effective treatments for mitigating short-term soil N losses following prescribed fire. In the N70 scenario only a 100% reduction in N deposition reduced peak soil emissions below $1\,kg\,ha^{-1}\,mo^{-1}$, but the PF15 or 75% N deposition reduction treatments reduced peak soil emissions to approximately $1.5–2.0\,kg\,ha^{-1}\,mo^{-1}$, compared to emissions of $4–6\,kg\,ha^{-1}\,mo^{-1}$ in the N70 treatment (Figs. 19.9–19.12).

19.5. Discussion

19.5.1. Simulation of ecosystem N losses

The simulations demonstrated that increased N deposition enhanced fuel-load buildup, soil nitrogen emissions, and N runoff to stream water, in agreement with previously reported field observations from California mixed-conifer forests (Fenn & Poth, 1999, 2001; Fenn et al., 2003c; Meixner & Fenn, 2004) and other ecosystems of the western United States (Fenn et al., 2003a). Simulated N emissions from soil were greater than N runoff regardless of the N deposition scenario. This result should be interpreted cautiously, considering that current parameterization of the DayCent model for CP appears to overestimate soil N emissions and underestimate stream water NO_3^- concentrations (Fenn et al., 2008; Fenn & Poth, 2001). Li et al. (2006) also reported that DayCent underestimated stream NO_3^- export in January in a small chaparral catchment in Sequoia National Park in central California. It should also be noted that DayCent does not simulate stream water NO_3^- concentrations per se; values are actually of soil seepage water NO_3^-. However, the soil emission patterns forecasted by the simulation properly matched previous field observations. Uncertainties apply to other aspects of the models used in this study as well. For instance, the co-exposure of this type of forest to N deposition and the elevated ozone concentrations occurring in southern California was not addressed in our simulations except to the extent that the model was parameterized with site-specific data from the San Bernardino Mountains, which would inherently include to some degree the effects of ozone in the field data used as input to DayCent. For example, the combined effects of ozone and N deposition are known to have major effects on C cycling and organic matter accumulation at CP (Fenn et al., 2003c).

These uncertainties in simulated N-cycling processes also feed into uncertainty in estimates of N-induced changes in fuel loads and therefore will influence the estimation of air pollutant emissions following wildfire.

A standardized protocol to estimate the influence of N concentrations in fuel on fire emissions would be very useful, as large differences in NO_x emissions were found when applying different methods (see below). Also, the influence of some global change components, such as increased atmospheric CO_2 concentrations and changes in temperature and precipitation regimes in the region, was not considered. Nevertheless, the rates of N deposition considered in our study ranging from 5 to 70 kg N ha^{-1} yr^{-1} properly covers the range of deposition inputs measured in southern California (Breiner et al., 2007; Fenn et al., 2008) and other areas of the western United States affected by N emissions (Fenn et al., 2003b).

19.5.2. Fire emissions and N deposition

The output of our simulation exercises highlight the existence of important N deposition and fire interactions, as increasing atmospheric N inputs resulted in larger air pollution wildfire emissions, including greater N emissions from soil 1 month after prescribed fire, and increased N runoff levels 11, 23, and 35 months after prescribed fire. These results also demonstrate the importance of including the effects of N deposition on fuel load and fuel chemistry in the models currently available for estimating fire impacts on ecosystems. Estimated NO_x emissions from wildfire events increased from 166% to 210% when comparing the lowest (N5) and highest (N70) N-deposition levels based on two methods that considered both fuel loads and fuel N concentration. These increases are three to four times higher than would be predicted by using models such as FOFEM, which only consider fuel loads and not N concentrations in fuels. The differences between these two types of models were largely due to the N content in the most flammable materials, such as foliage and litter. This finding is in agreement with the measurements recently carried out by Yokelson et al. (2007) in forest fires occurring in the surroundings of Mexico City, an area experiencing high N-deposition rates (Fenn et al., 1999; Fenn et al., 2002). Emissions of hydrogen cyanide (HCN) and NO_x in the forests near Mexico City were three to four times greater than the average values from U.S. pine forests (Yokelson et al., 2007). These authors associated the high N-emission levels with N enrichment of fuels components.

Our simulations suggest that the combined effect of increased fuel loads and increased N fuel content caused the increases in the emission of N compounds following wildfires. Approximately 70% increases in the emission of PM_{10}, $PM_{2.5}$, CH_4, CO, CO_2, and SO_2 emissions were found when comparing N70 and N5 treatments, with subsequent implications for air quality and also for human health. Our results also show that N deposition increases the risk of fire occurrence, not only as a result of an increased fuel amount but also because litter represents a major portion of this increase and litter accumulation enhances forest flammability, leading also to increased wildfire severity, and according to the results of our simulation, to increases in NO_x, CO_2, and SO_2 emissions. These N deposition-wildfire interactions are of particular concern as the area burned by wildfires in ponderosa pine forests of the southwestern US has been increasing over the past three decades (Grady & Hart, 2006). In October 2003 alone 235,267 ha were burned by wildfire in southern California (Clinton et al., 2006). Much of the burned area is exposed to high levels of N deposition, which undoubtedly affected the level of emissions from the 2003 fires and from more recent burns in the area, including at CP and the surrounding areas.

19.5.3. Management options

Air pollution abatement and forest management strategies could be used to reduce the long-term effects of increased N deposition on ecosystem N cycling; however, their effectiveness will vary as influenced by the magnitude of N deposition and the ecosystem process or parameter considered. To reduce the costs and the time frame of air pollution control policies needed to reach background or at least acceptable levels of N losses from forests, the N deposition reduction targets required to reverse chronic undesirable effects in ecosystem functioning should be defined.

Air pollution control policies alone showed a limited ability to recover ecosystem functioning when impaired by elevated N deposition. For instance, with N deposition rates $\geqslant 15\,\mathrm{kg\ N\,ha^{-1}\,yr^{-1}}$, air pollution control proved to be ineffective in returning fuel loads to the N5 levels, regardless of the time frame and the percentage of N deposition reduction that was applied. Nitrogen deposition reductions of 100%, a very unlikely and costly scenario, would be needed to reach background N runoff levels when forests are chronically exposed to $25\,\mathrm{kg\ N\,ha^{-1}\,yr^{-1}}$, although 75% N reduction resulted in acceptable levels of NO_3^- runoff. A 100% reduction of N deposition would be required to achieve marginally acceptable levels of NO_3^- runoff in forests that experience N deposition rates over $70\,\mathrm{kg\ N\,ha^{-1}\,yr^{-1}}$. A 100% reduction in N deposition caused a dramatic reduction in soil N emissions, but when combined with prescribed fire, emissions decreased further, eventually to levels observed with background N deposition.

Similarly, when the prescribed fire treatments were implemented singly, they were not effective in completely reversing the influence of N deposition in N ecosystem cycling, except for the reductions in fuel loads. The combination of prescribed fire and air pollution control proved to be a successful way to mitigate N-deposition effects on ecosystem N cycling and provided more options for reaching acceptable N runoff levels, although this became more difficult with extremely high N-deposition rates (e.g., $70\,kg\,ha^{-1}\,yr^{-1}$). Under the N25 scenario this goal could be achieved by combining PF15 and 50% reduction in N deposition or with a 75% reduction in N deposition even without prescribed fire. A more intense deposition reduction resulted in a shorter time period to reach to an acceptable N-runoff level. As this simulation study and field manipulation experiments (Gundersen et al., 1998) have demonstrated, in high deposition areas even large reductions in N deposition do not readily lead to significant reductions in the N content of key fuel components, such as litter and foliage. This is probably the result of a chronic excess of N availability, resulting in the luxurious consumption of this normally-limiting nutrient. Thus, it may be that only forest thinning, prescribed fire, and reduced N deposition can return these mixed-conifer forests to a less fire-prone and N-rich condition.

However, the use of prescribed fire to reduce fuel loads has been shown to have adverse impacts on key forest components and processes, such as soil properties (Moghaddas & Stephens, 2007), N runoff (Wan et al., 2001), increased mortality of older pine trees (Kolb et al., 2007), and wildlife (Tiedemann et al., 2000). In addition, the adverse effects of prescribed fire on air quality is a major public health issue, although this can be mitigated by conducting this forest management practice under the most favorable smoke dispersal conditions (Knapp et al., 2005). However, the release of CO_2 and other greenhouse gases is unavoidable (Carter & Foster, 2004). Moreover, there is experimental evidence showing that significant N losses from ecosystems occur as a result of prescribed fire treatments in areas experiencing high N-deposition loads (Johnson et al., 2008; Meixner et al., 2006; Riggan et al., 1994). Our study showed that this would be the case under the present N-deposition scenario at CP, especially when 30- or 60-year prescribed fire intervals are involved. However, soil N emissions or N runoff were almost four times lower and three times lower, respectively, when 15-year intervals were compared with the PF60 treatment. Therefore our results suggest that PF15 could be the best option to be combined with air pollution abatement policies to mitigate N-deposition impacts, although such frequent use of prescribed fire will be difficult to implement in these highly populated forests. Further research should be carried out to evaluate the potential use of alternative forest management techniques, such as thinning, possibly in tandem with less frequent prescribed fire, to be used singly or in combination with reduced N deposition to mitigate the long- and short-term adverse impacts of N deposition and fire events.

Under the N70 scenario unrealistic, costly and long-lasting 100% reductions would be needed to return ecosystem N losses to background levels. However, the 75% reduction in N deposition combined with prescribed fire may be the best scenario for reducing N losses, but even this is not realized in the short term. A 50% reduction in N deposition combined with prescribed fire does lead to large reductions in N export and would be considered as major progress towards mitigating the symptoms of N saturation. In forests, exposed to 20–30 kg N ha^{-1} yr^{-1}, a more common scenario in southern California than the extreme (70 kg N ha^{-1} yr^{-1}), we conclude that a 50% reduction in N deposition in combination with prescribed fire will be effective in returning the ecosystem to a more conservative state of N cycling.

19.6. Conclusions

The results of this simulation exercise highlight important interactions between N deposition and fire management practices. Forest fire suppression and increased N deposition in southern California contribute to increasing fuel loads and to an increase in fuel N content. Model simulations suggest that this will affect wildfire severity and result in increases in air pollution emissions from fires, increases in peak N emissions from soil right after fire, and increases in peak N export to stream water during the first three years postfire.

Both forest management and air pollution control policies could be used to mitigate these effects. Prescribed fire was effective in reducing fuel loads and mitigating short-term N export after fire events, while the combination of N-deposition reduction and prescribed fire was most effective in reducing long-term N losses to the atmosphere and in runoff. Implementation of 15-year prescribed fire intervals in these combinations would be the best option to avoid high N-ecosystem losses following fire, although in highly populated forests, such as in the San Bernardino Mountains, such short fire intervals are unlikely to be implemented. In any case, it would be extremely difficult to return N losses to near baseline levels when forests experience N deposition of 70 kg N ha^{-1} yr^{-1}, as even 100% reductions in N deposition for more than 80 years would not completely achieve this goal for some key N ecosystem cycling processes.

Therefore, early applications of air pollution control measures in combination with fuels reduction options such as prescribed fire treatments are recommended.

ACKNOWLEDGMENTS

Benjamin S. Gimeno was funded by the State Secretary for Universities and Research of the Spanish Ministry of Education and Science and a Centro de Investigaciones Energéticas Medioambientales y Tecnológicas (CIEMAT)-Spanish Ministry of Environment contract on Critical Loads and Levels. This research was funded in part by a National Science Foundation grant (NSF DEB 04-21530).

REFERENCES

Allen, E.B., Temple, P.J., Bytnerowicz, A., Arbaugh, M.J., Sirulnik, A.G., and Rao, L.E. 2007. Patterns of understory diversity in mixed coniferous forests of southern California impacted by air polution. ScientificWorldJournal 7(S1), 247–263, doi:10.1100/tsw.2007.72.

Breiner, J., Gimeno, B.S., and Fenn, M. 2007. Calculation of theoretical and empirical nutrient N critical loads in the mixed-conifer ecosystems of southern California. ScientificWorldJournal 7(S1), 198–205, doi:10.1100/tsw.2007.65.

Carter, M.C., and Foster, C.D. 2004. Prescribed burning and productivity in southern pine forests: A review. For. Ecol. Manag. 191, 93–109.

Cheng, L., McDonald, K.M., Angle, R.P., and Sandhu, H.S. 1998. Forest fire enhanced photochemical air pollution: A case study. Atmos. Environ. 32, 673–681.

Clinton, N.E., Gong, P., and Scott, K. 2006. Quantification of pollutants emitted from very large wildland fires in Southern California, USA. Forest fire enhanced photochemical air pollution. A case study. Atmos. Environ. 40, 3686–3695.

Del Grosso, S.J., Parton, W.J., Mosier, A.R., Ojima, D.S., Kulmala, A.E., and Phongpan, S. 2000. General model for N_2O and N_2 gas emmisions from soils due to denitrification. Global Biogeochem. Cycles 14, 1045–1060.

Dennis, A., Fraser, M., Anderson, S., and Allen, D. 2002. Air pollutant emissions associated with forest, grassland, and agricultural burning in Texas. Atmos. Environ. 36, 3779–3792.

Fenn, M.E., and Poth, M.A. 1999. Temporal and spatial trends in streamwater nitrate concentrations in the San Bernardino Mountains, southern California. J. Environ. Qual. 33, 2007–2014.

Fenn, M.E., and Poth, M.A. 2001. A case study of nitrogen saturation in western U.S. forests. In: Galloway, J., Cowling, E., Erisman, J.W., Wisniewski, J., and Jordan, C., eds. Optimizing nitrogen management in food and energy production and environmental protection: Proceedings of the 2nd international nitrogen conference, 14–18 October 2001, Potomac, Maryland, USA. A.A. Balkema Publishers, Lisse, The Netherlands, and TheScientific World. www.thescientificworld.com. DOI 10.1100/tsw.2001.280, 433-439.

Fenn, M.E., Poth, M.A., Aber, J.D., Baron, J.S., Bormann, B.T., Johnson, D.W., Lemly, A.D., McNulty, S.G., Ryan, D.F., and Stottlemyer, R. 1998. Nitrogen excess in North American ecosystems: Predisposing factors, ecosystem responses, and management strategies. Ecol. Applic. 8, 706–733.

Fenn, M.E., de Bauer, L.I., Quevedo-Norlasco, A., and Rodríguez-Frausto, C. 1999. Nitrogen and sulfur deposition and forest nutrient status in the Valley of Mexico. Water Air Soil Poll. 113, 155–174.

Fenn, M.E., de Bauer, L.I., Séller, K., Quevedo, A., Rodríguez, C., and Hernández-Tejeda, T. 2002. Summary of air pollution impacts on forests in the Mexico City air basin. In: Fenn, M.E., de Bauer, L.I., Hernández-Tejeda, T., eds. Urban air pollution and forests. Resources at risk in the Mexico City Air Basin. Ecological Studies 156. Elsevier, New York, 298–319.

Fenn, M.E., Baron, J.S., Allen, E.B., Rueth, H.M., Nydick, K.R., Geiser, L., Bowman, W.D., Sickman, J.O., Meixner, T., Johnson, D.W., and Neitlich, P. 2003a. Ecological effects of nitrogen deposition in the western United States. BioScience 53, 404–420.

Fenn, M.E., Haeuber, R., Tonnesen, G.S., Baron, J.S., Grossman-Clarke, S., Hope, D., Jaffe, D.A., Copeland, S., Geiser, L., Rueth, H.M., and Sickman, J.O. 2003b. Nitrogen emissions, deposition, and monitoring in the western United States. BioScience 53, 391–403.

Fenn, M., Poth, M.A., Bytnerowicz, A., Sickman, J.O., Takemoto, B.K. 2003c. Effects of ozone, nitrogen deposition and other stressors on montane ecosystems in the Sierra Nevada. In: Bytnerowicz, A., Arbaugh, M.J., and Alonso, R., eds. Ozone air pollution in the Sierra Nevada: Distribution and effects on forests. Developments in Environmental Science 2. 2003c, Elsevier, Amsterdam, 111–155.

Fenn, M.E., Poth, M.A., Terry, J.D., and Blubaugh, T.J. 2005. Nitrogen mineralization and nitrification in a mixed-conifer forest in southern California: Controlling factors, fluxes, and nitrogen fertilization response at a high and low nitrogen deposition site. Can. J. For. Res. 35, 1464–1486.

Fenn, M.E., Jovan, S., Yuan, F., Geiser, L., Meixner, T., and Gimeno, B.S. 2008. Empirical and simulated sritical loads for nitrogen deposition in California mixed-conifer forests. Environ. Pollut. (in press).

Grady, K.C., and Hart, S.C. 2006. Influences of thinning, prescribed burning, and wildfire on soil processes and properties in southwestern ponderosa pine forests: A retrospective study. For. Ecol. Manag. 234, 123–135.

Grulke, N.E., and Balduman, L. 1999. Deciduous conifers: High N deposition and O_3 exposure effects on growth and biomass allocation in ponderosa pine. Water Air Soil Poll. 116, 235–248.

Grulke, N.E., Andersen, C.P., and Hogsett, W.E. 2001. Seasonal changes in above- and belowground carbohydrate concentrations of ponderosa pine along a pollution gradient. Tree Physiol. 21, 173–181.

Gundersen, P., Emmett, B.A., Kjønaas, O.J., Koopmans, C.J., and Tietema, A. 1998. Impact of nitrogen deposition on nitrogen cycling in forests: A synthesis of NITREX data. For. Ecol. Manag. 101, 37–55.

HFRA (Healthy Forest Restoration Act). 2003. Public Law No. 108-148, Statutes at Large 117, 1887.

Houghton, R.A., Hackler, J.L., and Lawrence, K.T. 2000. Changes in terrestrial carbon storage in the United States. 2: The role of fire and fire management. Glob. Ecol. Biogeogr. 9, 145–170.

Johnson, D.W., and Curtis, P.S. 2001. Effects of forest management on soil C and N storage: Meta analysis. For. Ecol. Manag. 140, 227–238.

Johnson, D.W., Susfalk, R.B., Caldwell, T.G., Murphy, J.D., Miller, W.W., and Walker, R.F. 2004. Fire effects on carbon and nitrogen budgets in forests. Water Air Soil Poll. 4, 263–275.

Johnson, D.W., Murphy, J.D., Walker, R., Glass, D.W., and Miller, W.M. 2007. Wildfire effects on forest carbon and nutrient budgets. Ecol. Eng. 31, 183–192.

Johnson, D.W., Fenn, M.E., and Hunsaker, C. 2008. Fire effects on carbon and nitrogen cycling in forests of the Sierra Nevada Mountains. In: Bytnerowicz, A., Arbaugh, M., Andersen, C., and Riebau, A., eds. Wildland Fires and Air Pollution. Developments in Environmental Science. Elsevier Publishers, The Hague, Netherlands, 411–429.

Knapp, E.E., Keeley, J.E., Ballenger, E.A., and Brennan, T.J. 2005. Fuel reduction and coarse woody debris dynamics with early season and late season prescribed fire in a Sierra Nevada mixed conifer forest. For. Ecol. Manag. 208, 383–397.

Kolb, T.E., Agee, J.K., Fulé, P.Z., McDowell, N.G., Pearson, K., Sala, A., and Waring, R.H. 2007. Perpetuating old ponderosa pine. For. Ecol. Manag. 249, 141–157.

Lacaux, P., Delmas, R., Jambert, C., and Kuhlbusch, T.A.J. 1996. NOx emissions from African savanna fires. J. Geophys. Res. 101, 23,585–23,595.

Li, X., Meixner, T., Sickman, J.O., Miller, A.E., Schimel, J.P., and Melack, J.M. 2006. Decadal-scale dynamics of water, carbon and nitrogen in a California chaparral ecosystem: DAYCENT modeling results. Biogeochem 77, 217–245.

Liu, Y. 2004. Variability of wildland fire emissions across the contiguous United States. Atmos. Environ. 38, 3489–3499.

Massie, S.T., Gille, J.C., Edwards, D.P., and Nandi, S. 2006. Satellite observations of aerosol and CO over Mexico City. Atmos. Environ. 40, 6019–6031.

McMeeking, G.R., Kreidenweis, S.M., Lunden, M., Carrillo, J., Carrico, C.M., Lee, T., Herckes, P., Engling, G., Day, D.E., Hand, J., Brown, N., Malm, W.C., and Collet, J.L. Jr. 2006. Smoke-impacted regional haze in California during the summer of 2002. Agr. For. Meteorol. 137, 25–42.

Meixner, T., and Fenn, M. 2004. Biogeochemical budgets in a Mediterranean catchment with high rates of atmospheric N deposition—importance of scale and temporal asynchrony. Biogeochemistry 70, 331–356.

Meixner, T., Fenn, M.E., Wohlgemuth, P., Oxford, M., and Rigan, P. 2006. N saturation symptoms in chaparral catchments are not reversed by prescribed fire. Environ. Sci. Technol. 49, 2887–2894.

Miller, P.R., and McBride, J.R. 1999. Oxidant air pollution impacts in the Montane Forests of Southern California. A case study of the San Bernardino Mountains. Ecological Studies 134. Springer-Verlag, New York.

Minnich, R.A. 1999. Vegetation, fire regimes, and forest distribution. In: Miller, P.R., and McBride, J.R., eds. Oxidant air pollution impacts in the montane forests of southern California. A case study of the San Bernardino mountains. Ecological Studies 134. Springer-Verlag, New York, 44–78.

Minnich, R.A., Barbour, M.G., Burk, J.H., and Fernoe, R. 1995. Sixty years of change in conifer forest of the San Bernardino Mountains, California. Conserv. Biol. 9, 902–914.

Moghaddas, E.E.Y., and Stephens, S.L. 2007. Thinning, burning, and thin-burn fuel treatment effects on soil properties in a Sierra Nevada mixed-conifer forest. For. Ecol. Manag. 250, 156–166.

Parton, W.J., Scurlock, J.M.O., Ojima, D.S., Gilmanov, T.G., Scholes, R.J., Schimel, D.S., Kirchner, T., Menaut, J.-C., Seastedt, T., Garcia-Moya, E., Apinan-Kamnalrut, , and Kinyamario, J.I. 1993. Observations and modeling of biomass, soil organic matter dynamics for the grassland biome worldwide. Global Biogeochem. Cycles 7, 785–809.

Parton, W.J., Hartman, M., Ojima, D., and Schimel, D. 1998. DAYCENT and its land surface submodel: Description and testing. Glob. Planet. Change 19, 35–48.

Parton, W.J., Holland, E.A., Del Grosso, S.J., Hartman, M.D., Martin, R.E., Mosier, A.R., Ojima, D.S., and Schimel, D.S. 2001. Generalized model for NO_x and N_2O emissions from soils. J. Geophys. Res.-Atmos. 106, 17403–17419.

Reinhardt, E. 2003. Using FOFEM 5.0 to Estimate Tree Mortality, Fuel Consumption, Smoke Production, and Soil Heating from Wildland Fire. USDA Forest Service, Missoula Fire Sciences Lab, Missoula, MT. http://fire.org/fofem/download/FOFEM5 Using.pdf;vi.2003.

Riggan, P.J., Lockwood, R.N., Jacks, P.M., Colver, C.G., Weirich, F., DeBano, L.F., and Brass, J.A. 1994. Effects of fire severity on nitrate mobilization in watersheds subject to chronic atmospheric deposition. Environ. Sci. Technol. 28, 369–375.

Tiedemann, A.R., Klemmedson, J.O., and Bull, E.L. 2000. Solution of forest health problems with prescribed fire: Are forest productivity and wildlife at risk? For. Ecol. Manag. 127, 1–18.

Urbanski, S.P., Hao, W.M, and Baker, S. 2008. Chemical composition of wildland fire emissions. In: Bytnerowicz, A., Arbaugh, M., Andersen, C., and Riebau, A., eds. Wildland fires and air pollution. Developments in environmental science. Elsevier Publishers, The Hague, Netherlands, 79–107.

Wan, S., Hui, D., and Luo, Y. 2001. Fire effects on nitrogen pools and dynamics in terrestrial ecosytems: A meta-analysis. Ecol. Appl. 11, 1349–1365.

Wu, J., Winer, A.M., and Delfino, R.J. 2006. Exposure assessment of particulate matter air pollution before, during, and after the 2003 Southern California wildfires. Atmos. Environ. 40, 3333–3348.

Yokelson, R.J., Urbanski, S.P., Atlas, E.L., Toohey, D.W., Alvarado, E.C., Crounse, J.D., Wenberg, P.O., Fisher, M.E., Wold, C.E., Campos, T.L., Adachi, K., Buseck, P.R., and Hao, W.M. 2007. Emissions from forest fires near Mexico City. Atmos. Chem. Phys. 7, 5569–5584.

This page intentionally left blank

Developments in Environmental Science, Volume 8
A. Bytnerowicz, M. Arbaugh, A. Riebau and C. Andersen (Editors)

ISSN: 1474-8177/DOI:10.1016/S1474-8177(08)00020-X

Chapter 20

Interactive Effects of Climate and Wildland Fires on Forests and other Ecosystems—Section III Synthesis

*Nancy E. Grulke**

The chapters in Section III of this book provide an overview of how components of climate change, including air pollution, are likely to interact with fire in modifying key ecosystem processes, whether those processes were demographic, successional, or elemental cycling. These chapters primarily discuss increased temperature, reduced available soil moisture, and pollutant deposition or exposure as the key climate change attributes. Most of the chapters suggest that changes in frequency and intensity of disturbance regimes, such as wildfire and insect infestation, will likely be the instigators of ecosystem change.

McKenzie et al. (this volume) provide a broader biogeographic context for the subsequent chapters, which all focus on response of the mixed-conifer forest or chaparral in the Sierra Nevada, the Transverse Range in southern California, or the Peninsular Range of southern California and northern Baja California. Minnich and Franco-Vizcaíno (this volume) contrast how management policies in California and Mexico have altered fire size, interval, frequency, and its intensity in the landscape, thus causing vegetation susceptibility to fire in California or resilience to fire in Mexico. In a case study for the mixed-conifer zone in the Transverse Range of southern California, Grulke et al. (this volume) describe the role of air pollution—ozone (O_3) and nitrogen (N) deposition—as a causative stressor in increasing forest susceptibility to wildfire. Johnson, Fenn, Miller, and Hunsaker (this volume) describe partitioned losses of carbon (C) and N as atmospheric emissions and catchment runoff and net accretion of calcium after fire in the mixed-conifer forest. They describe the facilitation by N-fixing fire successional species in incorporating N back into an N-limited ecosystem. In the last chapter, Gimeno et al. (this

*Corresponding author: E-mail: ngrulke@fs.fed.us

volume) simulate the effect of different frequencies of prescribed fire management in combination with reduced N deposition on mitigating long-term effects of excess N deposition in this ecosystem. All chapters present conceptual models or use simulation models to illustrate likely interactions between components of climate change and fire on forest structure and function.

McKenzie et al. (this volume) propose conceptual models for ecosystem response to climate change and wildfire in four regions: southwestern pinyon pine-juniper woodlands, Sierra Nevada mixed-conifer forests, Rocky Mountain lodgepole pine, and the interior boreal forests of Alaska. By all climatic projections, these four regions are very likely to have a more negative water balance than under current conditions. Warmer climate, soil moisture stress, plant drought stress, bark beetle epidemics, and wildfire comprise a disturbance complex that is predicted to have region-specific effects and different trajectories for the affected ecosystems. The authors suggest that the synergy amongst disturbances will invoke new fire regimes, new species complexes, and broad-scale changes.

Except for interior Alaskan forests underlain by permafrost, all other forest types discussed in this chapter had similar sequences of disturbances; namely, global warming is likely to increase drought- and insect-induced tree mortality, result in excessive fuel accumulation, and will in turn increase forest susceptibility to extensive, intense fires. The authors present four models in which the first for pinyon pine-juniper woodlands could be considered the base model of climate-mediated ecosystem response. For interior continental lodgepole pine forests, the base model is modified by an initial stand-replacing fire regime, which is typical of this species' ecology. For Sierra Nevada mixed-conifer forests, tropospheric O_3 exposure is an additional synergistic stressor with drought, bark beetles, and defoliators contributing to tree mortality. The authors suggest that severe extended droughts could directly induce intense fires in the mixed-conifer forests, without the precursor of bark beetle, as presented in the base model. In all three lower latitude forest types, the change in fire frequency and severity will likely precipitate changes in species composition, including exotics. Although higher temperatures and drought alone could alter species composition in the mixed-conifer and interior lodgepole pine forests, these climatic factors did not directly alter species composition in pinyon pine-juniper woodlands: the ecosystem is relatively simple floristically, and already highly water-limited.

The sequence of disturbance vectors in Alaskan interior forests on permafrost-free soils was similar to that of continental coniferous forests.

However, the increased temperature directly affected beetle fecundity in Alaska, rather than a drought-mediated increase in tree susceptibility to beetle infestation, as predicted for lower latitude forests. For interior forests underlain by permafrost soils, global warming mediated permafrost degradation. In low topographic areas, permafrost degradation would likely lead to a type conversion from deciduous forests to wetlands, fens, and bogs. In upland interior forests underlain by permafrost, the loss of permafrost would likely increase drought stress and forest susceptibility to wildfires, and increase deciduousness in the resulting forest. Overall, the authors suggest that the interaction between climate, vegetation, and resulting fire creates a ‘‘disturbance synergy’’ that drives ecosystem change via new fire regimes on a decadal basis and habitat change over a multi-century time period.

Minnich and Franco-Vizcaíno (this volume) contrast the resulting vegetation patterns in forest and chaparral under highly suppressed (southern California) and largely unmanaged (Mexico) fires. Based on historical accounts (>100 years ago), wildfire was known to burn at low levels over months in the chaparral surrounding Los Angeles. Under current conditions in Mexico, such fires are common and of low intensity. Because of their frequency, fuel accumulation is generally not excessive, and burning may be discontinuous within a stand, resulting in patchiness in the resulting age structure and remaining fuels. In southern California, fire suppression began in the early 20th century, and fuels have inexorably accumulated since. Since then, when fire occurred (and occurs), fires are intense and extensive, and burn out only when insufficient fuels support them (e.g., previously burned areas), or they are extinguished. Fires occurring in early summer or small fires (<0.4 ha) are relatively easily suppressed. Fires occurring in late summer under Santa Ana conditions (dry, hot, offshore winds) burn through areas of high fuel accumulation, cannot be suppressed, burn intensely, and are carried through or across previously burned areas that under different conditions would not likely burn. These conditions result in much larger areas that are intensely burned.

The authors detail the role of differences in fire weather conditions between southern California and northern Baja California. On the one hand, offshore, hot, dry Santa Ana winds propagate fire across large areas in southern California. In northern Baja California, onshore moist winds in early summer and more moist monsoonal storms in late summer are less effective in promoting large fires. Despite these climatic differences, one could argue that a finer vegetation mosaic might have been in place or could develop in southern California if fuel loading were lower (e.g., under current conditions could be mechanically removed or via a low-intensity prescribed fire), and less intense early summer fires were allowed to burn (the very ones we can successfully control)—if not freely, then more extensively. However, reducing fire suppression within the context of current land use is untenable due to the large number of mountain communities and private landowners adjacent or within at-risk forests and chaparral in southern California without a fire-defensible space. Perhaps the best way to defend communities is with consolidated land use, and a well-defined, reduced fuels, defensible zone bordering the wildlands.

Minnich and Franco-Vizcaíno (this volume) present a conceptual model to help explain fire-generated and maintained mosaics of multi-age stands. Their model shows that as carbohydrate (or carbon, energy, or biomass) builds up on a site, plant available water declines as more leaf area is translated to higher transpirational losses. When there is little vegetative regrowth immediately after the fire, and the ratio of available water to plant biomass on the site is high, the probability of fire is low. Similarly, as the carrying capacity for biomass on the land base increases, the plant available water declines. With ignition, fires are carried when the energy of accumulated biomass exceeds the heat capacity of plant water content (Rothermel, 1972). This best explains the fire patterns in old stands of chaparral as they are generally completely consumed in fires. Old-growth forests may persist if the fires were early enough in the growing season, sufficient site water was available, and thus ratio of water available to stand biomass were high.

The same conceptual model can be applied to forest susceptibility to flammability within a given growing season or across different slope aspects in the landscape. In the case of aging chaparral with maximized biomass, less water is available per unit biomass, which hastens the onset and duration of drought stress, and consequently, susceptibility to flammability within a growing season. Interestingly, this difference in the ''window of susceptibility to flammability'' for different aged and types of vegetation is the mechanism by which a multi-aged mosaic is established and perpetuated. With sufficient fire suppression, even multi-aged mosaics develop sufficient biomass for extensive fires when it does occur, leading to intense fires, which disrupt the very vegetation structure that provides some measure of resistance to such fires. The initial point of ignition is stochastic, but flammability is a function of the rate of ignition from all sources, patch size, and vegetation fuel threshold (a function of biomass accumulation since the last fire). That ''self-organized patch emplacement'' develops across the landscape is not surprising, considering the underlying relationship between biomass accumulation and plant available water, which are very much influenced by elevation, topographic position, aspect, and both short- and long-term changes in climate.

Grulke et al. (this volume) present a conceptual model of a single location of pine-dominated mixed-conifer forest in the western San Bernardino Mountains (eastern Transverse Range) experiencing the highest pollution deposition in North America. They show that the combination of historical changes (human settlement, timber utilization to recreation, human attitudes towards fire safety), increase in stand density, pollution deposition (high O_3 exposure and N deposition), episodic drought stress, bark beetle epidemics, tree mortality, and anomalously high litter accretion results in forest susceptibility to wildfire. The authors show that although we have inherited a ''tinderbox'' from historical fire suppression policies (see Minnich and Franco-Vizcaíno, this volume), the main thesis of the chapter is that air pollution is more than an additional stressor; it is causative to increased forest susceptibility to wildfire. The primary evidence includes the following: (1) air pollution (both O_3 exposure and N deposition) increases older needle and lower branch loss, increasing litter accumulation; (2) air pollution decreases long-term litter decomposition of litter by altering litter chemistry, further promoting litter accumulation; (3) air pollution decreases root mass, increasing individual tree susceptibility to drought; (4) high O_3 exposure increases, not decreases, canopy transpiration, further increasing individual tree susceptibility to drought; (5) pollution-induced changes in within-tree allocation of resources are such that bole carbohydrate is increased, and bole protein may be increased due to drought stress, increasing tissue quality for bark beetles; (6) drought is common in Mediterranean climates, and ponderosa pine experiences moderate or severe drought about half of the time based on a 125-year regional precipitation record; (7) bark beetle epidemics are known to occur after multi-year droughts (increased tree susceptibility to successful bark beetle attack), followed by a year of above average precipitation (increased numbers of generations of beetles); and (8) tree mortality under both drought and bark beetle attack is high. Air pollution modifies many ecosystem components in ways that increase susceptibility to wildfire.

The case study was illustrated using a temporal sequence of aerial imagery beginning with the point of bark beetle infection after three years of chronic drought, followed by the expansion of bark beetles with chronic and one year of acute drought, and then full beetle outbreak in a wet year (promoting survival), following the chronic and acute drought. It is no surprise that wildfire is then easily transmitted through a forest with high standing dead biomass (40% mortality). Air pollution increases standing live and dead biomass and reduces plant available water within a stand. Both phenomenological and experimental evidence is presented to support air pollution as cause, rather than a contributing stressor. Using aerial photographs from the pre-drought to post-drought periods for sites across the San Bernardino Mountains with a range of pollutant deposition and stand densities, a relationship between pre-drought canopy cover or tree density and post-drought tree mortality was demonstrated. Stands in the eastern San Bernardino Mountains, despite less water availability, had lower initial stand density and lower mortality rates. In the central and western San Bernardino Mountains, stands had higher initial stand density and much greater mortality rates. The relationship offers a quantitative risk assessment: stand cover $<45\%$ yielded the lowest mortality rates ($<20\%$) with the concurrent stressors of air pollution, drought stress, and bark beetle infestation.

Similar to the first two chapters of Section III (McKenzie et al., this volume; Minnich and Franco-Vizcaíno, this volume), Johnson et al. (this volume) present a series of studies on the effect of fire on different vegetation types (forest and chaparral, mesic and xeric forests). They describe nutrient losses during fire due to emissions, mineralization, and leaching, as well as post-fire nutrient accretions of ecosystem carbon, N, and calcium over immediate, medium, and long-term time periods. A simple, effective accounting model was used to illustrate net ecosystem changes in these partitions with wildfire versus prescribed fire at two return rates in mixed-conifer forest. In mixed-conifer forests, soil carbon pools may not recover until the vegetation returns to the original pre-fire state. In contrast, ecosystem N losses by fire can be recouped within two decades by N-fixing, successional species. A watershed-scale experiment was presented that elucidated how different initial ecosystem partitioning in chaparral alters carbon and N loss after prescribed fire and wildfire. In chaparral catchments, prescribed burning could not mitigate excess atmospheric N loading and did not significantly modify high nitrate leaching from the ecosystem. In mesic forests, N losses from fire far exceed N leaching and result in a net loss of ecosystem N except for the few forests that are known to be N-saturated.

Johnson et al. (this volume) compare an unburned site and a site that had been burned 20 years prior to the study in the eastern Sierra Nevada mixed-conifer forest. Immediately after fire, there was an increase in mineral N leaching, which declined to near control levels within three years. The total loss of nitrate due to leaching was a fraction of that lost to volatilization during the fire. Soil solution concentrations of NH_4^+ and NO_3^- increased 100-fold during the first year after fire, but declined significantly after the second year. Although aboveground carbon and N is largely lost in wildfires, belowground carbon pools are often unaffected by the fire itself, but have low-level, long-term losses from decomposition of roots and residual soil organic material. Carbon pools were not expected to recover until the vegetation itself returned to pre-fire conditions. In this ecosystem, the short-term pulse of fire-mediated release and mobilization of plant available N is followed by prolonged N accretion over decades by secondary successional, N-fixing plants after fire that largely recoup N lost to volatilization (during combustion) and short-term leaching (several years). Results of a simple accounting model demonstrated greater total N losses from prescribed fires at 10- and 20-year intervals over 100 years than for all-consumptive wildfires occurring once in 100 years. Of interest is the shift of the hydrophobic layer after severe fires, from near-surface to 8–10 cm in the mineral soil horizon. This had significant limitations on percolation of nitrate-rich leachate to deeper soil horizons, and increased the volume of soil susceptible to erosion. The depth to the hydrophobic layer may also have an effect on seedling survival after fire, because conifers that were able to penetrate this layer were more likely to survive to 15 years (Grulke, unpublished data).

The authors describe no net differences in ecosystem phosphorus, potassium, or sulfur between burned and unburned areas, but potassium and calcium were significantly greater in burned areas. Exchangeable potassium, calcium, and magnesium were greater in shrub-dominated (burned) than the forest site. Calcium levels were unaccounted for by pre-fire stand content. The authors posit that either post-fire vegetation readily takes up and redeposits these elements or they were released from extreme heating of soil minerals *in situ*. An increase in plant available calcium would increase soil pH and base saturation, mitigating acidification of N-saturated conifer forests, but may have little affect in chaparral or forests with low N deposition. The largest ion increases in soil solution was SO_4^{2-}, probably resulting from oxidation of soil organic material, but also possibly from soil pH increases previously mentioned.

The clarity of Lake Tahoe has declined since the late 1960s, due in large part to stream water N inputs such that phosphorus is considered limiting. Interestingly, accumulated N deposition in litter layers, unburned from fire suppression policies and not percolating through mineral horizons due to shallow hydrophobic soil layers, may have contributed to increased N pulses into Lake Tahoe. Thus, wildfires and fire suppression in the Lake Tahoe Basin, are expected to continue to threaten water quality.

In southern California, pollution has been transported into the foothills and mountains over the past 50 years, resulting in excessive N content of litter and soils. In the reviewed study by Johnson et al., soil and stream water chemistry were monitored in chaparral-dominated watersheds with experimental manipulations conducted to test whether prescribed fire could mitigate N accumulation in chaparral soils. Because 80% of the chaparral ecosystem N is stored belowground, prescribed fire did not mitigate high soil N nor stream water nitrate effluxes over time. The authors suggested that prescribed fire alone could not reduce excess N in the chaparral unless atmospheric inputs were also decreased. They hypothesized that prescribed fire in N-saturated mixed-conifer forests may be more effective because more of ecosystem N is aboveground and combusted during fires. This hypothesis was tested independently in the chapter by Gimeno et al. using a simulation model.

Gimeno et al. (this volume) performed simulations to test the effectiveness of prescribed burns in mixed-conifer forests on reducing stream water nitrate and soil N emissions within the context of low to high N loading using a biogeochemical model (DAYCENT; Parton et al., 1998). Different N loads (5–70 $\text{kg ha}^{-1}\,\text{yr}^{-1}$) were applied to drive different ecosystem allocation of carbon and N, especially to fuel loading and its N content, and allowed to equilibrate over 100 years. Then 0–100% reductions in atmospheric N deposition were imposed for the following 200 years of simulations, with or without concurrent prescribed fires at three intervals (15, 30, and 60 years), assuming that two 100-year wildfires would occur regardless of prescribed fire. The simulation produced N losses in stream water and as trace gas emissions from soil, total fuel load, N content in fuel load, and air pollution emissions (linking the biogeochemical model to the First Order Fire Effects Model [FOFEM]), which simulates pollution emissions from wildfire events. Stream water nitrate is an excellent indicator of ecosystem N saturation (Fenn et al., 2003), with critical loads already identified for this ecosystem. Simulations were validated using field data of stream water nitrate in catchments of different N loading.

The simulated N deposition increased fuel mass by 120% between the lowest (5 $\text{kg ha}^{-1}\,\text{yr}^{-1}$) and the highest (70 $\text{ha}^{-1}\,\text{yr}^{-1}$) deposition rate. The effect of the highest N deposition was mitigated to the lowest N deposition level by applying prescribed fire at either 15- or 30-year intervals. Nitrogen content in litter increased with simulated N deposition, but allocation of N to foliage did not increase past the N deposition rate of 25 $\text{kg ha}^{-1}\,\text{yr}^{-1}$, nor were prescribed fire treatments effective in reducing foliar N levels at N deposition rates of the same value.

In Gimeno et al. (this volume) simulations, wildfire emissions increased with N deposition, because of its effect on total litter produced.

Atmospheric emissions from wildfires were 470% greater for the highest versus the lowest N deposition loading scenario, although NO_x emissions were as much as 210% higher at the highest N deposition level. Simulated N deposition had a significant effect on stream water nitrate export when N deposition was 25 kg ha^{-1} yr^{-1} or greater. If N deposition were reduced by 100%, nitrate export returned to background levels in eight years, after approximately 50 years with 50% reduced N deposition and prescribed fire. Prescribed fire alone did not reduce stream water nitrate to background levels, possibly because prescribed fire itself increases total ecosystem nitrate losses, especially in the short term, and because fire does not remove the large organic N stores in soil that provide a large pool of N to be mineralized and nitrified (see Johnson et al., this volume). However, the combined application of prescribed fire (at 15-year return rates), and a 75% reduction in N deposition, permitted ecosystem nitrate exposure to reach near background levels. Reducing N deposition by 50% in combination with prescribed fire also caused major decreases in stream water N export, although not to background levels. Prescribed fire and stricter air quality regulations also reduced nitrate export after sporadic wildfire.

Using the biogeochemical model, soil N emissions increased with increased N deposition, which was greater than that N lost to stream water. Because Johnson et al. (this volume) estimations ''set'' soil emissions and tracked soil nitrate outputs, the results are not comparable. In Gimeno et al. simulations, soil N emissions were high at equilibrium, and could not be controlled with prescribed fire (15-year return) in the 25 kg N ha^{-1} yr^{-1} atmospheric N deposition scenario unless deposition were eliminated. Under these conditions, background levels of soil N emissions were reached in about 80 years.

In their simulations, significant reductions (50–100%) in anthropogenic N deposition were required in combination with short rotation prescribed fire (15–30 years) to return nitrate leaching or soil N emissions to near baseline levels, or at least to levels below those associated with critical N loading. Although complete reductions in N deposition are unlikely to occur in order to improve water quality and restore forest health, the simulations presented in Gimeno et al. highlight the potential for prescribed fire in mitigating ecosystem N losses after wildfire. Their simulations elucidate the important interrelationships among N deposition, fuel loading and litter N content, nitrate losses to stream water, and soil N emissions. Even a 25–50% reduction in N deposition in combination with prescribed fire of any interval resulted in major progress towards reducing chronic N losses from mixed-conifer forests.

Prescribed fire has rarely been permitted in inhabited wildlands, due to the narrow band of time annually when such fires can be set safely and air pollution effects on human health. However, because it is clear that much of the N loading is found in forest floor litter, mechanical removal of litter could mitigate both total nitrate losses and soil N emissions when a wildfire does occur. Mechanical removal combined with a reduction in understory biomass, implemented in a noncontiguous mosaic, may help slow and redirect wildfire in forests. In chaparral ecosystems, reestablishment of mosaics of different aged stands as fire breaks, whether by mechanical or prescribed burns, would do much to mitigate fire risk to the many homes and structures in close proximity to wildlands, although this is unlikely to mitigate N saturation unless N deposition is also greatly reduced.

The chapters in Section III of this book provide insight into potential interactive perturbation of climate change (drought, air pollution) and fire in western North American forest ecosystems. There are several reasons why these perturbations are important. A recent increase in fire frequency and intensity is of academic interest because of the effects such emissions may have as a direct, positive feedback to global warming. At the regional scale, a change in climate and fire regimes will disrupt ecosystem structure and processes and reduce the capacity of current ecosystems to resist other, lesser perturbations (invasive species, insect epidemics), but different forest structure and processes will emerge. Anticipating that ecosystems are likely to change, as well as the magnitude and location of change, will help us plan for it. Conceptual models of how ecosystems might change are the first step towards planning for change.

Perturbations to forest health reduce the quantity and quality of ecosystem processes. That fire suppression reduces forest health through increased stand density is not a new phenomenon, but that fire suppression disrupts maintenance of a mosaic of stand age classes in the landscape, the characteristic that could reduce the risk of extensive and intensive wildfire spread, adjusts our perception of the ‘‘cost’’ of fire suppression. Likewise, that air pollution could impair forest health is not a new idea, but that high air pollution *instigates* increased canopy transpiration, exacerbates tree drought stress, and increases tree susceptibility to insect attack and success adjusts our perception of the ‘‘cost’’ of air quality regulation. In addition, we know that fire causes short-term reductions in air and water quality, but that frequent prescribed fire, at return rates known to improve attributes of forest health, increases the total nitrate lost from the ecosystem relative to a single, large wildfire every 100 years questions our perceptions of the benefits of prescription. Last, because the current high levels of atmospheric N inputs into the landscapes surrounding large urban areas cannot be mitigated by prescribed fire alone, better air quality regulations must be implemented along with societal changes in energy use. However, not all mitigation strategies have been investigated. Implied in these assessments is that mechanical removal and disposal (or green use) of excess biomass, especially the N-enriched litter in forests affected by high air pollution, is untenable at the landscape level. Other mitigative strategies need to be incorporated into biogeochemical models to assess their relative effects on air and water quality, and on subsequent risk for the occurrence of catastrophic wildfire. Although biogeochemical and economic models have been linked to understand global responses to climate change, there is a pressing need to link these models to help solve regional dilemmas as well.

REFERENCES

Fenn, M.E., Baron, J.S., Allen, E.B., Rueth, H.M., Nydick, K.R., Geiser, L., Bowman, W.D., Sickman, J.O., Meixner, T., Johnson, D.W., and Neitlich, P. 2003. Ecological effects of nitrogen deposition in the western United States. BioScience 53, 404–420.

Gimeno, B.S., Yuan, F., Fenn, M.E., and Meixner, T. this volume. Management options for mitigating N losses from N-saturated mixed conifer forests in California.

Grulke, N.E. Unpublished data. Giant sequoia seedling recruitment and survival, 1989–2004.

Grulke, N.E., Minnich, R.A., Paine, T.D., Seybold, S.J., Chavez, D., Fenn, M.E., Riggan, P.J., and Dunn, A. this volume. Air pollution increases forest susceptibility to wildfires: A case study in the San Bernardino Mountains in southern California.

Johnson, D.W., Fenn, M.E., Miller, W., and Hunsaker, C. this volume. Fire effects on carbon and nitrogen cycling in forests of the Sierra Nevada Mountains.

McKenzie, D., Peterson, D., and Littell, J. this volume. Global warming and stress complexes in forests of western North America.

Minnich, R.A., and Franco-Vizcaíno, E. this volume. A probabilistic view of chaparral and forest fire regimes in southern California and northern Baja California.

Parton, W.J., Hartman, J., Ojima, D., and Schimel, D. 1998. DAYCENT and its land surface submodel: Description and testing. Glob. Planet. Change 19, 35–48.

Rothermel, R.C. 1972. A mathematical model for predicting fire spread in wildland fuels. USDA Forest Service Research Paper INT0115. Intermountain Forest and Range Experiment Station, Ogden, UT.

This page intentionally left blank

Section IV: Management Issues

This page intentionally left blank

Developments in Environmental Science, Volume 8 471
A. Bytnerowicz, M. Arbaugh, A. Riebau and C. Andersen (Editors)

ISSN: 1474-8177/DOI:10.1016/S1474-8177(08)00021-1

Chapter 21

Fire Danger and Fire Behavior Modeling Systems in Australia, Europe, and North America

Francis M. Fujioka, A. Malcolm Gill, Domingos X. Viegas and B. Mike Wotton*

Abstract

Wildland fire occurrence and behavior are complex phenomena involving essentially fuel (vegetation), topography, and weather. Fire managers around the world use a variety of systems to track and predict fire danger and fire behavior, at spatial scales that span from local to global extents, and temporal scales ranging from minutes to seasons. The fire management application determines the makeup of the planning tool, which usually incorporates one or more computer models. Advanced computing technology has spawned a new generation of fire planning tools to predict fire occurrence and fire behavior. We reviewed fire danger and fire behavior modeling systems from Australia, Europe, and North America, including operational tools that have been in use for decades, and newer models that profoundly enhance the spatial and temporal resolution of the resultant predictions. Linkages between these models and air quality models could very likely improve the mapping and prediction of air pollution due to wildland fires.

21.1. Introduction

Wildland fire challenges management, wherever it occurs. The dimensions of the fire problem largely reflect the characteristics of the fire environment: the vegetation (fuel), topography, and weather/climate for any given place and time period. Significant differences in any of these factors may occur when comparing the fire environment from one place

*Corresponding author: E-mail: ffujioka@fs.fed.us

to another. The complexities of wildland fire management spawned a specialized fire science that has produced a variety of systems globally to assess fire danger even before a fire starts and to predict fire behavior once it occurs. This chapter describes the products of fire danger and fire behavior research in Australia, Europe, and North America.

21.1.1. History of fire research: A U.S. perspective

From its inception in 1905, the USDA Forest Service acquired the responsibility of protecting the nation's forests and the public from the damaging effects of wildfire. By fire historian Stephen Pyne's account, fire research was nonexistent at the beginning of the 20th century. Thus, Forest Service professionals schooled in forestry science generated and applied the knowledge needed to meet the agency's fire protection mandate (Pyne, 1982). In the early years of fire research, the dominant theme was the economics of fire protection, which would provide the basis for a fire management policy. Show and Kotok (1929) described the need for a fire danger index in 1929 as a means of determining the difference in fire control required in major vegetation cover types. They had earlier underscored the importance of weather on fire activity by statistically relating relative humidity and wind to fire size and number of fires (Show & Kotok, 1925). But it was Gisborne who set the stage for a methodical diagnosis of the weather impact on fire danger.

Gisborne (1928) identified three factors that constitute fire danger:

1. The present number of fires burning, or the probability that fires will be started.
2. The present rate of spread (ROS) of fire, or the probability that fires will spread.
3. The loss occurring from existing fires, or the probability that fires will result in loss.

Through the research and leadership that Gisborne provided from Priest River, Idaho, the fire danger meter emerged in 1930, a precursor of the modern fire danger rating system. The meter assigned a fire danger level on the basis of ignition factors, visibility (visibility reductions increase fire danger because they visually obscure new fires from detection), fuel moisture, and wind speed (Hardy & Hardy, 2007). Pyne (1982) described the fire danger meter as "a philosopher's stone for forest administrators … a quantitative measurement by which to compare fire seasons and to contrast fire problems among different regions." Much of fire research subsequently would focus on refinements to the fire danger meter and the development of similar meters for the nation's other forests.

Despite the administrative successes that its fire research program achieved for the Forest Service, a subdued minority in the agency lamented the lack of fundamental knowledge of fire behavior, which could only be gained by approaching it as a research problem in physics, chemistry, meteorology, and biology. Wallace Fons, a mechanical engineer with the California Experiment Station, along with John Curry, paved the way for fundamental fire physics research starting in the late 1930s. In 1946, Fons published a mathematical model to predict rate of fire spread (Fons, 1946), which would inspire the development of the Rothermel (1972) fire spread model more than two decades later and provide the basis for the modern U.S. National Fire Danger Rating System and the Fire Area Simulator (FARSITE) fire behavior prediction system.

Inasmuch as wildland fire is not uniquely a U.S. problem, research and development activities in fire danger rating and fire behavior prediction are not limited to the United States. The next section is a description of fire danger rating and fire behavior prediction systems from Australia, North America, and Europe. While rating fire danger and predicting fire behavior are very similar functions, they occupy different domains on a spatial/temporal scale. Fire danger rating assessments cover large areas, typically on the order of 10^3 ha (10^4 acres), over a period of days. They quantify the potential fire activity under a given scenario of fuels, weather, and topography. On the other hand, the coverage of fire behavior forecasts is typically an order of magnitude or more smaller in area, and for present purposes, not more than 48 h.

21.2. Operational fire occurrence and behavior systems in Australia

In Australia, there is an unbroken tradition of studying fire behavior in the field in order to develop empirical models for predicting the behavior of unplanned (wild) or prescribed fires. Fire behavior models are designed, in the first instance, to predict the ROS of fires burning with the wind.

Using the fire weather component of fire models, fire danger—defined as the "chance[s] of a fire starting, its ROS, intensity and difficulty of suppression" (McArthur, 1967)—can be determined and public warnings issued. When used in this way, models are applied to regional areas on a daily basis throughout the fire season whether there is a fire or not.

For fires prescribed for various purposes, burning safely and effectively is the motivation for the development of fire behavior guidelines. In Australia, prescribed burning is the deliberate application of fire to a defined area in order to obtain an explicit result under safe working conditions. Prescribed fires may be ignited during a relatively narrow window of weather conditions to reduce fuels and thereby potential fire intensity, to increase the chance of fire control to enable better protection of life and property, or to achieve desired ecological outcomes.

21.2.1. A geographical sketch

Australia is approximately 7.7 million km^2 in area divided into states and territories. It straddles the Tropic of Capricorn, where much of it lies within the tropics. Eucalypt forests and woodlands spread across the north in a wide belt that continues down the east coast; across the south are further discontinuous occurrences including those in the island state of Tasmania. A vast arid zone, vegetated with hummock grasslands and *Acacia* shrublands, occupies a large part of the center and central west of the continent. A modest mountain range, by world standards, parallels the east coast. Climates include wet tropical in the northeast, wet-dry monsoonal across the north, arid tropical and arid temperate in the arid zone, moist-temperate in the southeast, Mediterranean in the southwest and part of the south, and subalpine-alpine embedded in moist-temperate parts of the southeast.

Major cities are found in the temperate zone in coastal locations. Pastoralism is common in the north and center, while cropping and farming are common in the southeast and southwest. Conservation lands occupy about 10% of the continent (B. Cummings, personal communication).

The vast majority of the country is fire-prone. Most of the area burnt each year is in the northern tropical savanna (Russell-Smith et al., 2002).

21.2.2. Fire danger rating

Fire danger rating across the country is determined largely or entirely on the basis of McArthur's models for grasslands (McArthur, 1966) and eucalypt forests (McArthur, 1967). Ratings consist of categories of the Forest Fire Danger Index (FFDI), a 100-point scale consisting of the following inputs: screen air temperature (T), screen relative humidity (RH), and wind speed in the open at 10 m height (V), plus a Drought Index—a measure of moisture in a hypothetical soil profile holding a maximum 200 mm water (initially based on the work of Keetch & Byram, 1968 in the United States)—and a Drought Factor—a variable with values from 1 to 10 determined by the amount of recent rainfall and days since the last rainfall event. For the Grassland Fire Danger Index (GFDI) inputs are grassland curing (proportion of dead grass), relative humidity, air temperature, fuel weight (in later versions), and wind speed as for the FFDI. The equations for these systems are to be found in Noble et al. (1980).

On the basis of the forecast fire danger, fire warnings are issued to the public by the Bureau of Meteorology, a federal government organization. On the basis of fire weather warnings, land management agencies, usually state- or territory-based, may then issue Total Fire Bans—no lighting of fires in the open. Local land managers, public and private, are expected to heed the warnings and assess their local fuels and terrain in order to decide what their response should be in terms of preparedness for fire occurrence and firefighting.

21.2.3. Fire behavior models and guides

Fire behavior research in Australia arose from the need to predict the behavior of unplanned fires during firefighting operations or to preemptively modify fuels using prescribed fires. Observations of unplanned fires were made and experiments conducted so that quantitative guidelines could be created to assist fire practitioners (McCaw et al., 2003). Fire behavior models and field guides predicted the ROS of the perimeter where it is most directly affected by the wind—the ‘‘head’’ of the fire. Results were often reported in ways related to their practical use rather than as rigorous scientific models in scientific journals. Beck (1995), in presenting a set of equations for the fire behavior guidelines known as the *Forest Fire Behavior Tables for Western Australia* (Sneeuwjagt & Peet, 1985) remarked that, ‘‘Despite its operational success, the incompleteness of published data behind the WA [Western Australian] fire behavior prediction system detracts from its scientific credibility.’’

Fire behavior guides from the Commonwealth Scientific Industrial and Research Organization. (CSIRO) (1997), include influential variables such as slope and grazing history (related to height of treated pasture), not used in the original research (Cheney et al., 1993), to allow them to be more generally applicable. McArthur’s (1966) GFDI was linked directly with the predicted ROS of the head fire, but for forests (McArthur, 1967), ROS of the head fire was considered to be proportional to FFDI multiplied by the fuel load of litter less than 6 mm in diameter found on the forest floor (Noble et al., 1980).

McArthur's forest fire work in eastern Australia was expanded geographically to south-western Australia in a collaboration with Peet, who developed a set of tables suited to local conditions (McCaw et al., 2003). Various modifications to these pioneering efforts in Australia have taken place for various reasons, including conversion to metric units, and can be seen in the five versions of the *Forest Fire Danger Meter* (Noble et al., 1980) and a series of revised editions of the *Forest Fire Behavior Tables for Western Australia* (McCaw et al., 2003; Sneeuwjagt & Peet, 1985).

Predicting spot fire development close to or distant from a fire front remains a problem. McArthur's (1967) model for distance of spotting was based on ROS and fuel load (Noble et al., 1980) and includes the effects of different bark type on different species of eucalypt trees. The comprehensive experiments of forest fire behavior in south-western Australia over the last decade (*Project Vesta*; McCaw et al., 2003) are expected to soon provide better understanding of the effects of fuel in different parts of the fuel array, not just the litter layer, on rates of spread and spotting behavior (Gould et al., 2004).

As with forest fire-behavior models there have been five versions of the McArthur Grassland Meter (Noble et al., 1980), mostly manifested as circular slide rules. While McArthur's (1966) model was for annual and perennial pastures of unspecified composition, Condon (1979) saw the need to identify the behaviors of fires burning in stands of particular grass species in more-open semi-arid western New South Wales (NSW) grasslands; modifications were made on the basis of experiences of bushfire-brigade captains in the widespread fires in western NSW in 1974–1975. In the revised model, grass height was added as well as the effects of the main fuel species. The *Western Australian Bush Fires Board* also modified the meter using grass height, density, and texture in an undated meter.

While the McArthur (1966) model and its successors were for grasslands with continuous cover, the vast arid lands of Australia contain grasslands formed by discrete clumps of hummock grasses. A spread model for the latter type was first developed by Griffin and Allan (1984), while the latest hummock grassland model has been developed by Burrows et al. (2006); this breaks new ground for Australian models in first predicting the likelihood of spread, then predicting the ROS, assuming spread is possible.

A consensus shrub-fire model using data from Australia and New Zealand uses wind speed and vegetation height as its only variables

(Catchpole et al., 1999). While the predictions of ROS were "rather more variable than is desirable for an operational tool," the model fitted available data "reasonably well" (Catchpole et al., 1999).

21.3. Operational fire danger/behavior systems in Canada

The Canadian Forest Fire Danger Rating System (CFFDRS; Stocks et al., 1989) is used across Canada each day of the fire season for a range of fire management decisions from prevention planning to fire occurrence prediction and evaluating fire behavior potential. The system has also been adopted by or adapted to a number of countries around the world (e.g., New Zealand, Mexico, Indonesia, Malaysia, and Portugal). The CFFDRS contains two major subsystems: the Canadian Forest Fire Weather Index (FWI) System and the Canadian Forest Fire Behavior Prediction (FBP) System. The FWI System (Van Wagner, 1987) provides a means of evaluating the severity of fire weather conditions in a common standardized forest type, including numerical ratings of fuel moisture in important fuel layers and several relative indices of fire behavior. The FBP System (Forestry Canada Fire Danger Group, 1992) relies on outputs from the FWI System and other site-specific information (such as topography and time of year) and provides quantitative assessments of fire behavior in a number of major fuel types across Canada.

The CFFDRS also contains two other components that have not been formally developed or implemented nationally; these are the Accessory Fuel Moisture (AFM) System and the Fire Occurrence Prediction (FOP) System. The AFM System contains additional fuel moisture models to add temporal resolution to existing models or to model moisture in specific fuel layers (e.g., Lawson et al., 1996a; Van Wagner, 1987; Wotton et al., 2005); it also converts moisture code values to stand-specific moisture (e.g., Lawson & Dalrymple, 1996b; Wotton & Beverly, 2005). The FOP System is an important component of the CFFDRS, as it represents the fire risk component of fire danger rating assessment. However, it is not implemented throughout Canada. Several regional fire occurrence prediction models developed by numerous researchers are available in Canada, but fire managers typically rely on their experience in processing fuel moisture codes (from the FWI System) and ignition risks from lightning or potential human activity to determine expected fire occurrence.

The models within the CFFDRS are based on a common approach or philosophy. Basic physical reasoning and understanding of the physical processes governing fire spread or fuel moisture exchange are used to develop models, which are then calibrated with field-based observations (from both experimental and wildfire observations). This approach ensures that the model outputs capture the true physical range of the phenomena being modeled, which has to a large extent been responsible for the successful adoption of the system across Canada and in other countries. Implementation can be problematic when adapting the system beyond its original design (Taylor & Alexander, 2006).

21.3.1. The FWI System

The current fire danger system in Canada has its roots in an extensive program of meteorological observations and field sampling of moisture and ignition sustainability research that began in the early part of the 20th century. From experimental sites across the country, fire hazard and fire danger tables were developed for numerous regions in Canada. In the late 1960s, the need for common indices led to the development of a universal system, which was released nationally in 1970 (Muraro, 1968; Van Wagner, 1974).

21.3.1.1. Inputs

The FWI System relates weather information to fuel moisture and fire danger indices for a standard forest type (mature jack pine, *Pinus banksiana* Lamb.) or lodgepole pine (*Pinus contorta*). The system relies on daily measurements (taken at 1200 local standard time (LST)) of air temperature and relative humidity (measured at 1.4 m above the ground in a radiation shielded screen), 10 m open wind speed, and 24-hour accumulated precipitation, as well as the estimated fuel moistures in three fuel layers from the previous day.

21.3.1.2. Outputs

The system has three codes to track moisture in different levels of the forest floor and three fire behavior indices that are relative ratings of fire behavior potential. All of the moisture codes in the FWI System are based on an exponential model of moisture exchange. The moisture content values are converted to a code value so that increasing dryness of the fuel increases the value of the code itself. The user therefore readily associates a high code value with high fire danger.

Moisture in the surface litter layer of the standard pine stand is tracked by the Fine Fuel Moisture Code (FFMC). This surface litter layer is considered a 1.2 cm thick layer of pine litter, sitting atop a thick, generally wet, organic layer, with a fuel load of $0.25\,kg\,m^{-2}$. The response time of this layer varies with ambient weather but is about half a day when air temperature is 25 °C, RH is 30%, and wind speed is 10 km h^{-1}. Moisture in the upper portions of the organic layer—a layer approximately 7 cm deep with a biomass load of 5 kg m^{-2}—is modeled by the Duff Moisture Code (DMC). The response time of this layer varies with temperature and RH, and is about 10 days in mid-summer, when temperature and RH average 25 °C and 30%, respectively. Moisture in the deep organic layer is modeled by the Drought Code (DC), which is similar to other drought models such as the Keetch-Byram Drought Index (Keetch & Byram, 1968) and the Palmer Drought Index (Palmer, 1988). The DC accounts for the long-term effect of drying on fuels and has a response time of approximately 50 days in mid-summer.

Although these moisture codes nominally represent moisture content in the standard jack/lodgepole pine stand, they can also track changes in the moisture content of other stand types (Wotton & Beverly, 2005). Figure 21.1 shows the relationship between the calculated FFMC and actual litter moisture sampled in several stands of pine and several stands of aspen as part of the Canadian Forest Service's small-scale test fire program (Paul, 1969; Simard, 1970). While the absolute relationship between FFMC and actual litter moisture is different for pine and aspen litter, changes in moisture content in both stands can be tracked by changes in the FFMC.

Potential fuel consumption on the landscape is characterized by the Build-up Index (BUI), which in its simplest form, is a harmonic mean of the DMC and DC. Relative ROS is indicated by the Initial Spread Index (ISI), a nonlinear function of FFMC and wind speed. BUI and ISI are combined following Byram's concept of fireline intensity (Byram, 1959) to form the FWI, which represents the relative intensity of a potential fire on the landscape. It is important to remember that these three fire behavior indices are relative indicators that have been scaled based on observed fire behavior to provide a meaningful range of output values. The FBP System converts these relative indices to stand-specific, physically recognizable, and interpretable predictions of fire behavior.

21.3.2. FBP System

The FBP System produces predictions of fire behavior in 16 major fuel types in Canada (including both conifer and deciduous types) and accounts for influences of factors such as topography and foliar moisture content. In its secondary outputs the system employs a simple elliptical model of fire growth to estimate flank and backfire rates of spread and fire shape. A model of acceleration predicts fire spread from either a single point or an ignition line. The models that makeup the FBP System

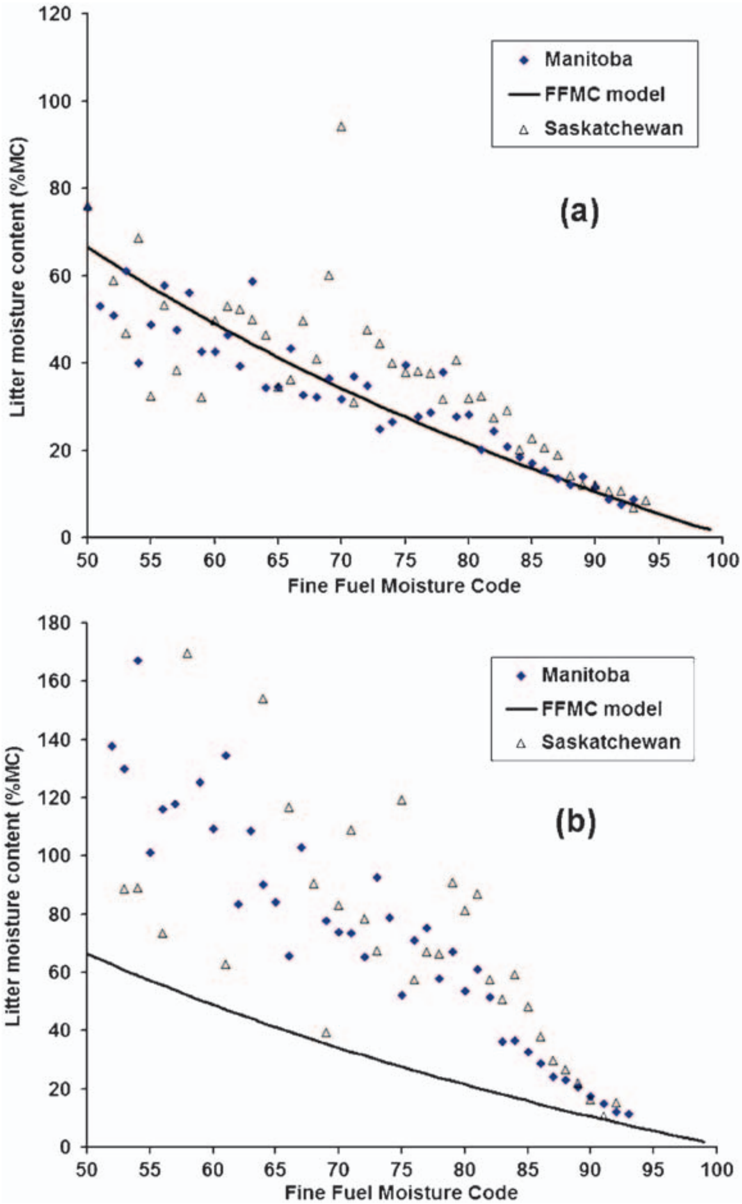

Figure 21.1. Fuel moisture and fine fuel moisture code (FFMC) relationship for (a) pine stands and (b) aspen stands in Canada.

are based on years of experimental burning under a range of weather conditions and forest types. These experiments attempted to capture the range of fire danger conditions encountered operationally; however, performing experiments under extreme conditions can be difficult, though not impossible (Stocks et al., 2004). Experimental fire data are also supplemented with well-documented wildfire observations.

21.3.2.1. Inputs

Predictions from the FBP System require information about the fuel type in which the fire is spreading (e.g., grass, slash, insect-killed mixedwood), the location of the fire (latitude and longitude), topographical information (slope and aspect), and time of year. The System also uses the codes and indices from the FWI System (specifically the FFMC, ISI, BUI) as well as wind speed and direction. When combined with slope and aspect, the wind data account for the slope/wind interaction using vector analysis. The FBP System does not currently allow the user to input fuel load for a stand specifically; it specifies a standard load for each of the FBP fuel types (with the exception of the grass fuel type).

21.3.2.2. Outputs

The three primary outputs of the FBP System are analogous to the three relative fire behavior indices of the FWI System. The system predicts surface fuel consumption (SFC) in a range of stand types using the BUI. SFC includes consumption of forest floor organic material, litter, and down and dead woody material. Crown fuel consumption (CFC) is estimated from a standard crown loading for each fuel type and an estimate of the crown fraction burned. Empirical relationships between head fire ROS and the ISI have been developed for each of the FBP fuel types. Figure 21.2 shows an example of the relationships between SFC and BUI and ROS and ISI for the mature jack/lodgepole pine model of the FBP System. Fireline intensity is calculated in the FBP System from the total fuel consumed (SFC and CFC) and ROS, using Byram's classic equation (Byram, 1959).

21.3.2.3. Applications

The CFFDRS is used operationally across Canada throughout the fire season for a lengthy list of fire management activities, such as prevention planning, setting alert levels, fire suppression planning, and evaluating fireline safety. Predicting fire occurrence is another important application in which fire managers couple experience with an understanding of the

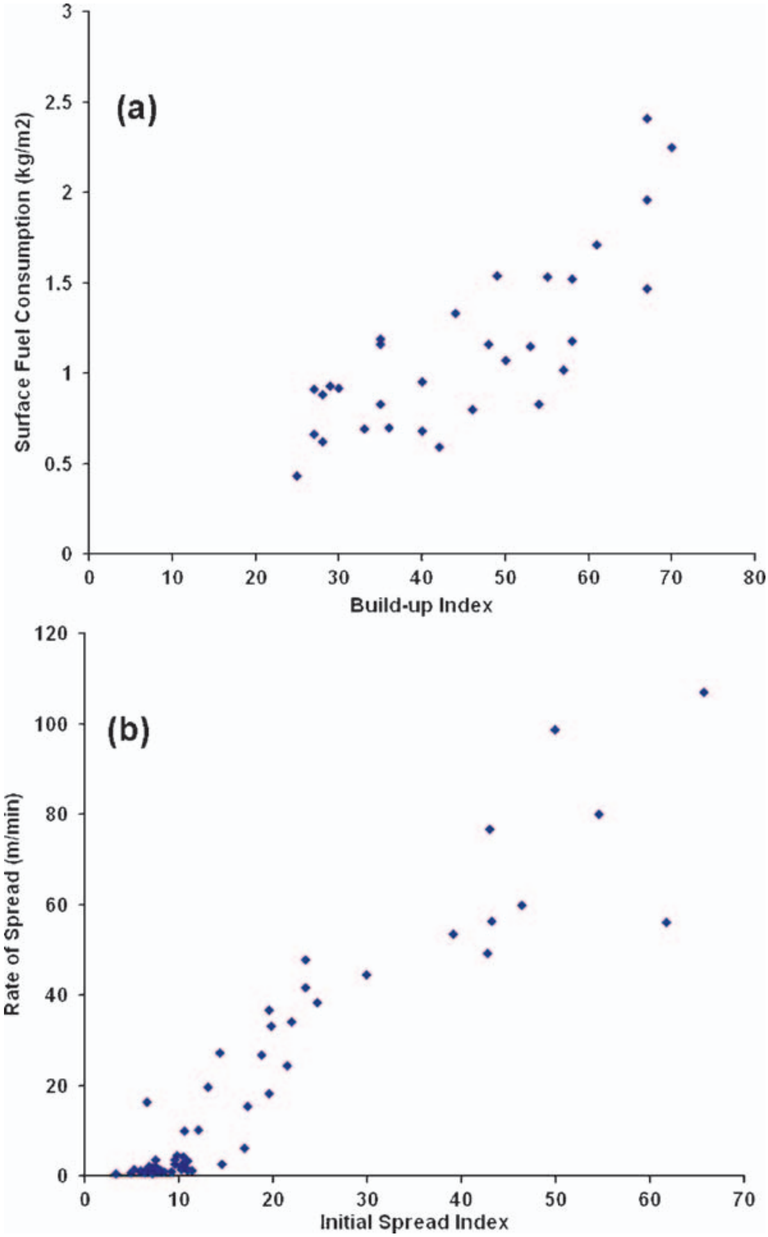

Figure 21.2. Example of the fire behavior prediction (FBP) System relationships for (a) surface fuel consumption versus build-up index and (b) rate of spread versus initial spread index for the mature jack pine fuel type (known in the FBP system as C-3) in Canada.

FWI System fuel moisture codes, to predict daily expected fire activity. Human- and lightning-caused fires are distinctly different and hence separate predictions are made for these ignition types. The FFMC has been found to be a good indicator of the receptivity of surface fuels to ignition and is used to determine expected human-caused fire occurrence. Figure 21.3a shows the relationship between human-caused fire occurrence and FFMC for two regions of the province of Ontario.

Of course, expected human activity in the forest must also be considered in any prediction. Numerous models that characterize the relationships between fuel moisture and human-caused fire occurrence have been developed for specific regions of Canada (e.g., Martell et al., 1989; Poulin-Costello, 1993; Wotton et al., 2003). Moisture in the upper organic layer is important for determining the probability of ignition from lightning strikes; lightning discharges tend to run down tree boles and ignite the surface fuels or organic material near the base of the tree. The DMC has become the standard indicator in Canada of landscape receptivity to ignition by lightning. Figure 21.3b shows the probability of lightning fire ignition as a function of DMC for historical fires and lightning from the forested area of Alberta. Detailed models of lightning fire occurrence have been developed for specific regions and include dependencies on the DMC and other factors (Anderson, 2002; Kourtz & Todd, 1992; Wotton & Martell, 2005).

It is important to remember that, while the FFMC and DMC seem to be robust relative indicators of fire occurrence, these relationships will vary from region to region. To provide quantitative predictions the users must understand the character of the relationship between these fuel moisture codes and fire occurrence in their fire management district.

In Canada fire growth across the landscape is modeled using the Prometheus fire growth model (Tymstra, 2002). Prometheus is very similar to the FARSITE system (Finney, 1998), relying on the elliptical wavelet fire propagation formulation (Anderson et al., 1982; Richards, 1990, 1995). In Prometheus, however, the FBP System forms the core fire behavior engine that drives fire growth. This model, which continues to be enhanced, is beginning to be used for fire growth scenario evaluation on large project fires in Canada.

21.4. Fire danger rating and fire behavior prediction in the USA

21.4.1. Fire danger rating

The current version of the U.S. National Fire Danger Rating System (Fig. 21.4; Schlobohm & Brain, 2002) expresses fire danger through four

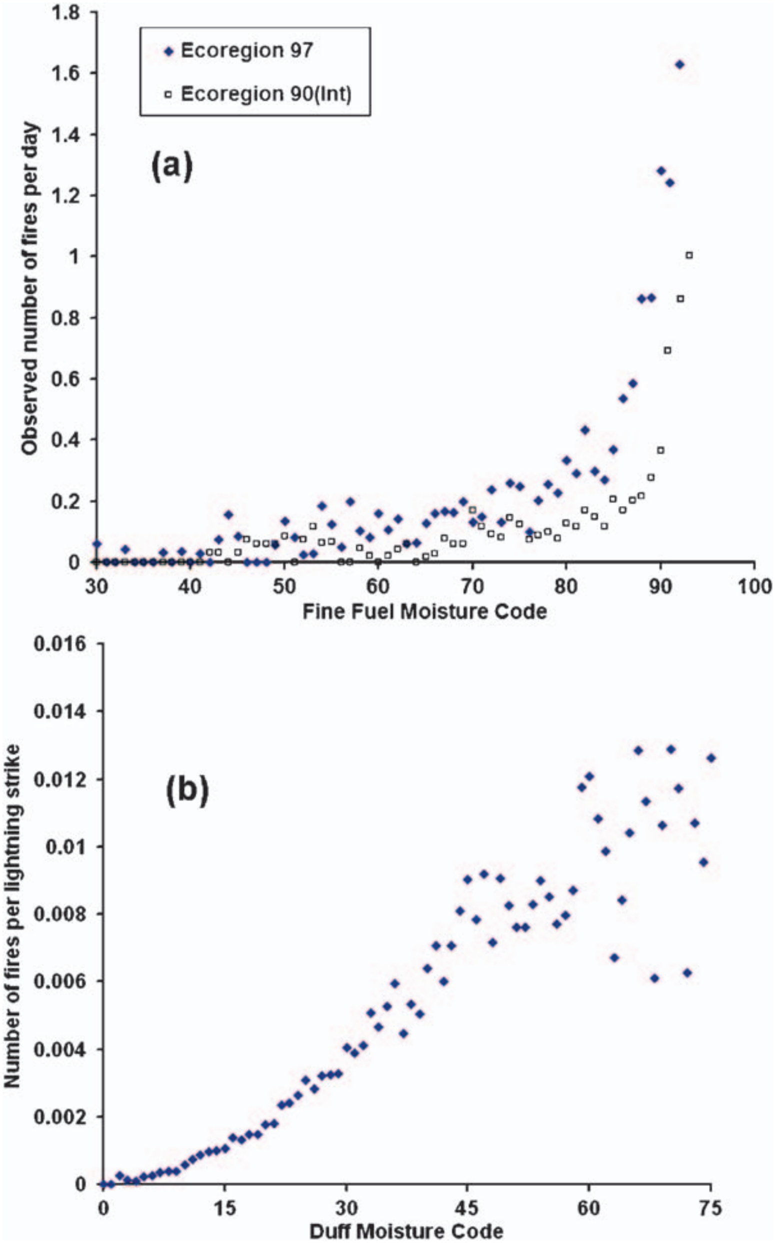

Figure 21.3. Examples of fire occurrence and moisture code relationships for (a) human-caused fires (1976–2004) for two ecoregions in Ontario and (b) lightning-caused fires in the forested area of Alberta (1984–2004).

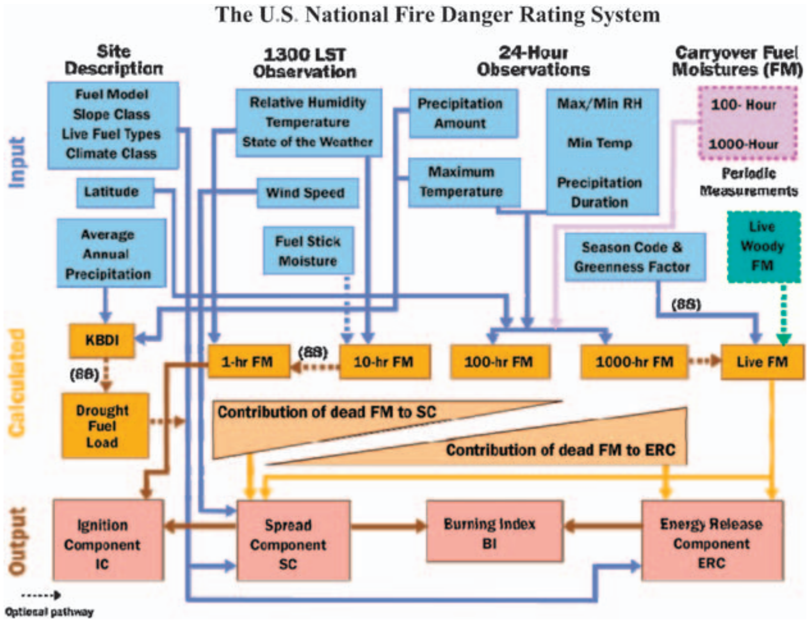

Figure 21.4. Structural diagram of the U.S. National Fire Danger Rating System (NFDRS).

indices, of which two—the ignition component (IC) and the spread component (SC)—match Gisborne's (1928) elements of fire danger. The IC is a number ranging from 0 to 100 that may be interpreted as the probability that a firebrand will start a fire with growth potential. Schroeder used empirical studies of ignitions in slash pine litter by Blackmarr (1972) to develop the original ignition probability algorithm of the 1972 system (Bradshaw et al., 1984). The dependency of IC on SC (Fig. 21.4) is a modification of the 1972 NFDRS IC that the 1978 NFDRS introduced, to limit the ignition probability to fires that achieve a reportable size.

The SC is the ROS from the Rothermel model, expressed as feet per minute (Rothermel, 1972). It is very sensitive to wind speed and the surface area-to-volume ratio of a fuel particle. Because fine fuels have large surface area-to-volume ratios, they yield relatively high values of SC compared to larger fuels. Topographic slope also influences SC. The slope factor in Rothermel's equation is a continuous variable, but is limited to five classes in the 1978 NFDRS.

The energy release component (ERC) represents the energy flux from the flaming front of the head fire. It is directly proportional to the heat release rate per unit area of the flaming front—the reaction intensity—and inversely proportional to the surface area-to-volume ratio. Hence, larger fuels have more influence on ERC than smaller fuels, in contrast to the SC. The sensitivity of the ERC to fuel moisture content of both dead and live fuels makes it the most useful of the four NFDRS indices in Fig. 21.4 for monitoring short-term drought effects on vegetation. The 1988 revision to the NFDRS integrated the Keetch-Byram Drought Index (KBDI; Keetch & Byram, 1968) as an intermediate variable that controlled dead fuel loading due to drought. Other 1988 changes modified the calculation of live fuel moisture and the 1-hour dead fuel moisture, as shown in Fig. 21.4 by the ‘‘(88)’’ annotation (Burgan, 1988).

The SC and ERC combine to give the Burning Index (BI), a number conceptually equal to 10 times the flame length. It is based on a relationship Byram (1959) derived between flame length on the one hand and spread rate and residence time of the flaming front on the other. The BI therefore has implications for the magnitude of the fire-control problem under the specified conditions, and of fire effects on vegetation. Note the similarity of the BI to the FWI in the CFFDRS.

The inputs to the NFDRS (Fig. 21.4) may be classified as weather and nonweather data, the latter comprising fuel and topographic characteristics that are assumed to be fixed over time. The weather variables, of course, change dynamically over time, but note that the NFDRS uses two types of weather data. One is an instantaneous description of weather (1300 LST observation), while the other is composed of summary statistics of weather over a 24-hour period: maxima and minima, and totals. In fact, the NFDRS integrates the weather variables over a period longer than 24 hours in the boxes represented by the Carryover Fuel Moistures and the KBDI.

The SC, ERC, and flame length describe fire behavior characteristics, but the NFDRS is not considered a fire behavior prediction system. The NFDRS provides a large area assessment of worst case conditions for a quasi-steady-state surface fire. On the other hand, FARSITE has been designed by Finney (1998) as a fire behavior prediction system.

21.4.2. Fire behavior prediction

Whereas the NFDRS output is a series of indices that characterize fire danger, FARSITE is a system capable of generating a sequence of fire perimeters representing the growth of a fire under given fuel, weather, and terrain conditions. Both systems employ the Rothermel fire spread model, which predicts the head fire ROS. FARSITE simulates fire growth in two dimensions with spread algorithms that augment the one-dimensional

Rothermel model. Finney implemented Richards' (1990) algorithm employing Huygens' principle of wave propagation (Anderson et al., 1982), which assumes that fire spreads locally in the shape of an ellipse. By computing the localized fire growth at multiple points of the given fire perimeter, FARSITE generates the growth increment from the curve that envelops the local ellipses tangentially. Fuels and terrain data at 30 m intervals satisfy the need for local fire environment, nonweather data.

FARSITE uses the same weather variables that the NFDRS requires, a necessity imposed by the Rothermel model. Unlike the NFDRS, however, FARSITE is not limited to describing the worst case fire scenario. It has to map the dynamic changes in fire behavior, particularly as the weather changes over the area of interest, temporally and spatially. When he introduced FARSITE, Finney (1998) utilized algorithms that calculated diurnal temperature and humidity variations from given maxima and minima of those variables (Beck & Trevitt, 1989; Rothermel et al., 1986), apparently to minimize the weather input requirements. Subsequently, weather models provided significantly higher spatial and temporal resolution, not to mention a comprehensive physics-based approach to generate the weather data that FARSITE needs. Finney modified FARSITE to take advantage of gridded weather data, when such data are available.

Fujioka (2002) evaluated the accuracy of FARSITE fire growth predictions with and without gridded weather inputs for a southern California fire that burned in 1996. Figure 21.5 is a FARSITE output showing the fuels (colored polygons), terrain, afternoon wind vectors, and predicted fire perimeters from this case study. A high-resolution weather model calculated hourly weather variables at a 2 km grid interval over the area. The study, which focused on the early, essentially free-burning stage of the fire, revealed complex simulation error patterns, which included both overprediction and underprediction. It exemplified the severe test that fire specialists face in predicting fire behavior in complex fire environments. Although it would be highly desirable to have weather data on the same 30 m grid interval as the fuels and terrain data, the lack of a suitable weather model and operational capability make it an unlikely prospect for the foreseeable future.

21.5. Operational fire systems in Europe

Forest fires in Europe as in many other parts of the world are the result of a complex interaction between natural processes and human-related activities, such that it is difficult to determine the relative

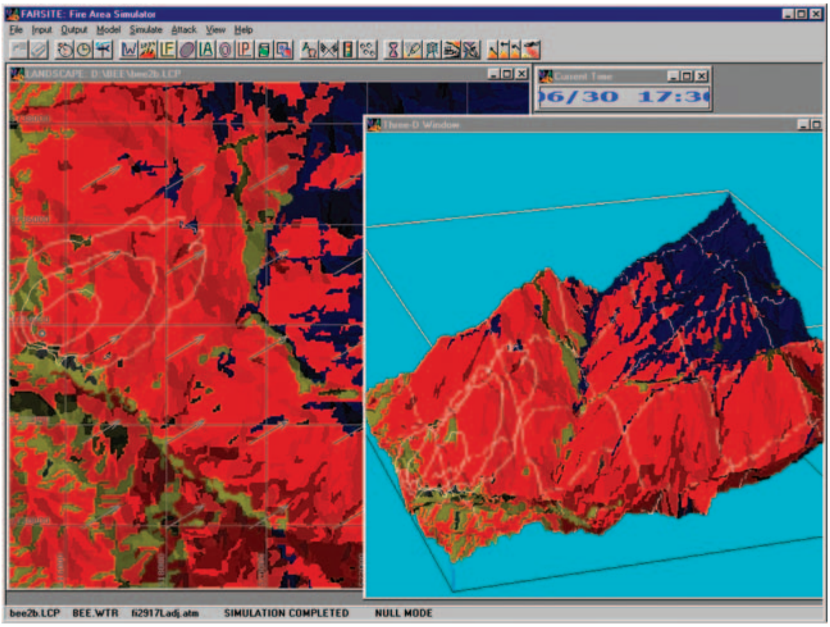

Figure 21.5. FARSITE simulation of the bee fire in the San Bernardino national forest, California, summer 1996.

importance of each. Despite the fact that forest fires are mainly caused by human activity, it is generally recognized that natural phenomena, namely meteorological conditions, play a very important role in the entire process. It is therefore very understandable that the analysis of meteorological factors and their influence on fire activity has always been a basic requirement in fire science and management.

In Western Europe forest fires have a greater incidence in its southern extent, namely in Portugal, Spain, France, Italy, Greece, and the other countries of the Mediterranean basin. Fires occur mainly during summer, but in some regions there are also winter fires. The countries of central and northern Europe have fire problems as well, but on a much smaller scale. Russia and the other countries of the former Soviet Union, with their vast territories, experience very large fires. In Europe there were several methods to assess fire danger associated with meteorology. Some of these methods were developed for a particular set of conditions, for example a particular region or a fire season, but others attempted a broader scope.

21.5.1. Historical overview

In Portugal a very simple method developed by Ångström in Sweden was used between 1970 and 1986. This method is based on a very simple ratio between air temperature and relative humidity. The daily value of the Ångström index was evaluated at mid-day and threshold values were established to determine three fire danger classes then in use. The index was noncumulative in the sense that it did not take into account the pronounced effect of a sequence of days with high values of Ångström index and no precipitation. In 1987 a method based on the Nesterov index was applied (Instituto Nacional de Meteorologia e Geofisica, 1988). This method had a cumulative component and used daily values of precipitation and wind velocity in addition to temperature and relative humidity. The modified Nesterov index performed quite well and was well accepted by operational institutions.

In Italy, Bovio et al., 1984, developed an original method, the IREPI, that estimated evapo-transpiration and was applied mainly in the Alpine Region of Italy to winter fires (from January to April). In France there were several methods applied by fire experts, and it was common practice to evaluate more than one index in each region and base operational decisions on trends deemed significant by the decision makers. The more common methods were developed by Meteo France (Drouet and Sol, 1990). In Spain, a method based on the McArthur system of Australia, described earlier in this chapter, was applied (Instituto Nacional para la Conservacion de la Naturaleza, 1988). This was a noncumulative index that used daily values of air temperature and relative humidity as well.

21.5.2. Comparative study

The variety of methods in use in southern Europe made overall assessment of the fire danger situation in each country or region very difficult. For this reason, the European Union (EU) sponsored a study comparing fire danger rating practices in 1992, which is briefly summarized here (for further details see Viegas et al., 1999).

The four methods that were used in Portugal, Spain, France, and Italy, as well as the methods of the CFFDRS (Van Wagner, 1987) were selected for the study. The U.S. National Fire Danger Rating System (Bradshaw et al., 1984) was also considered, but it was not retained because it included other factors besides meteorological ones that made implementation difficult. The regions, time periods, and relevant fire statistics of the study are given in Table 21.1.

Different parameters were considered to statistically test the relative efficiency of the various fire danger rating methods. In practically all cases

Table 21.1. Study areas and period of analysis considered in the comparative study of fire danger rating practices in southern Europe

Region of study	Fire season	Period of study	Area (km^2)	Number of fires		Burned area (ha)	
				Total	Daily av.	Total	Daily av.
Alps Haute Provence, France	Jan./Apr.	1981–1990	6925	191	0.18	1920	1.77
Bouches du Rhone	Jan./Apr.	1981–1990	5087	675	1.47	3434	50.94
Var, France	Jul./Sep.	1986–1990	5973	954	2.07	48,939	106.39
Eastern Pyrenées, France/Spain	Jul./Sep.	1986–1990	4116	292	0.63	7098	15.43
Veneto, Italy	Jan./Apr.	1988–1990	18,368	515	1.43	5244	14.53
Savona, Italy	Jan./Apr.	1987–1989	1544	284	0.79	2329	6.45
	Jun./Sep.	1987–1989		282	0.77	2017	5.51
Central Portugal	Jun./Sep.	1988–1992	17,216	29,080	23	159,373	261.3

it was found that the FWI performance was better than those of other methods, even for winter fires. As a consequence of this study a recommendation was made to the European Commission in 1997 to adopt the CFFDRS as a standard method to assess fire danger in EU countries. This proposal was immediately adopted by Portugal and France. Subsequently, the Joint Research Center of the EU developed a common Web-based service disseminating daily values of the CFFDRS components computed on a grid of 10 km $\times$ 10 km.

Similar studies have been carried out in other regions using other methods, with the result that the FWI performed better than the other methods almost always. As a consequence the CFFDRS has become a common language not only among scientists but also between practitioners dealing with fire danger assessment. Recent studies on the impact of climate change on forest fire activity also use the Canadian system as a standard tool to quantify the relative changes on fire activity predicted in the various future climate scenarios.

21.5.3. Calibration of FWI in Portugal

The application of the CFFDRS in each region requires a calibration because the measurements of each weather station do not represent the meteorological conditions in absolute terms in the region. Viegas et al. (2004) applied the Canadian system by performing a calibration of the FWI to estimate the threshold values for five fire danger classes in each of the 18 districts of the Portuguese territory, and by using meteorological and statistical data on fire occurrence between 1988 and 1996 (Table 21.2).

A good correlation between burned area in Portugal and the average value of the DC during the summer months was found after a nonlinear

Table 21.2. Threshold values of FWI defining fire danger classes for six districts of Portugal

District	Fire danger class				
	Low	Moderate	High	Very high	Extreme
V. do Castelo	<10	15	30	45	>45
Bragança	<23	30	45	55	>55
Guarda	<8	15	25	50	>50
Coimbra	<15	22	30	45	>45
Évora	<40	50	65	75	>75
Faro	<30	40	60	75	>75

transformation of the data (Fig. 21.6). Similarly, it was found that the live fuel moisture content of shrub vegetation during the summer is well correlated with a nonlinear transformation of the DC (Fig. 21.7).

The FFMC is a good estimator of the moisture content of dead leaves of pine and eucalyptus trees that are a very important part of fuel litter in Portugal (Fig. 21.8). The ISI is in principle correlated with the ROS of fire in a given fuel bed. Experimental results obtained in Central Portugal for *Erica* type shrubs confirm this assertion after applying a nonlinear transformation (Fig. 21.9).

21.6. Summary

Fire science, now about a century old, has contributed substantially to wildland fire management. Nevertheless, many knowledge gaps remain. Although there are many challenges in predicting unplanned fires, predicting the behavior of prescribed fires creates new challenges because the pattern of ignition becomes an added variable. Prescribed burning takes place under relatively mild conditions, and the degree of precision sought for this activity may be higher than in the case of unplanned fires (McArthur, 1962). The prescription is often designed to achieve a certain fuel reduction, such as over a certain proportion of ground at an intensity that allows fire control with available resources (e.g., Marsden-Smedley, 1993). Prescribed fire behavior guides have been developed for many situations including different vegetation types, standing timber crops of various types, and logging debris.

As wildland fire management is a global problem, its solution suggests the need for a global enterprise. Similarities between the operational systems in Australia, Europe, and North America reflect the benefit of shared knowledge and experience. The Canadian FWI has become a

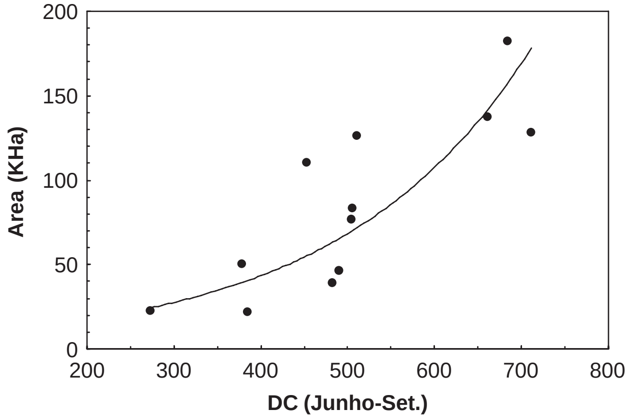

Figure 21.6. Total burned area as a function of the average value of the drought code (DC) in Portugal in the period 1987–2000.

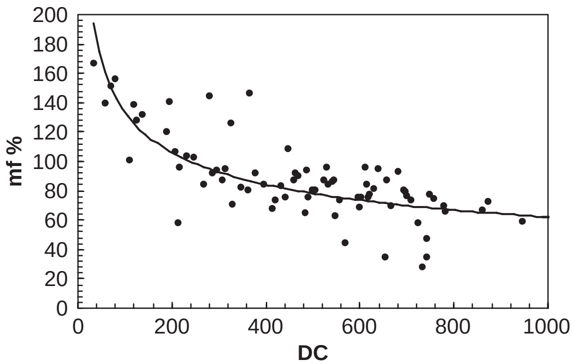

Figure 21.7. Live fuel moisture content of shrubs (*Calluna vulgaris*) as a function of drought code (DC) in Portugal during summer.

standard tool to estimate fire danger conditions correlated to meteorology in Europe. Provided that it is calibrated using local data, it can be applied to a large range of conditions, and its components can be used to assess various relevant properties of fire danger, namely the fuel moisture content and the overall severity of a fire season. Currently, new methods are being developed combining FWI with other sources of data, such as those derived from satellite sensors.

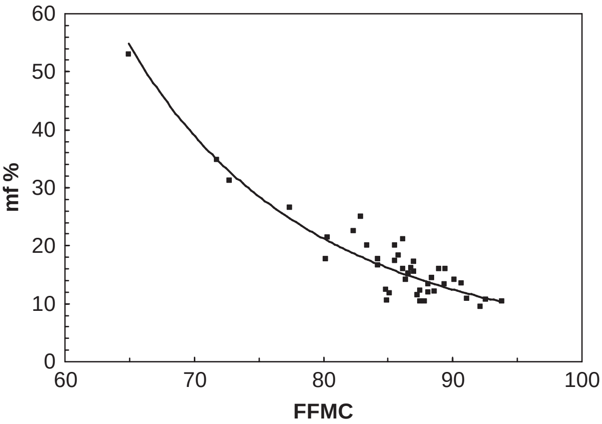

Figure 21.8. Dead fuel moisture content of tree leaves (*Eucalyptus globulus*) as a function of fine fuel moisture code (FFMC).

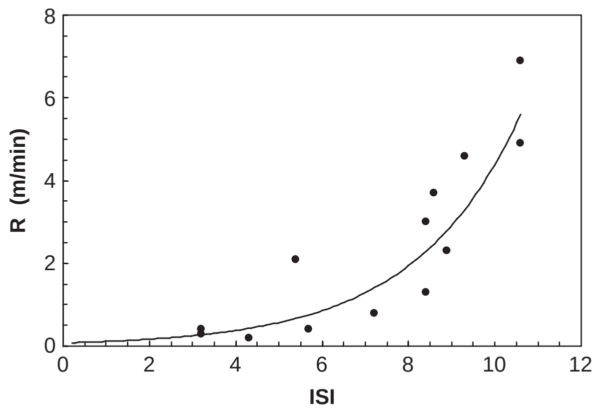

Figure 21.9. Rate of spread of a fire in shrub vegetation (*Erica arborea*) as a function of initial spread index (ISI).

Mounting concerns about wildland fire impacts on air quality and global climate also require further research. In this area, the linkage between fire behavior modeling and air quality modeling is yet to be explored. This research would result in a more dynamic and therefore more realistic description of the temporal and spatial variability of fire emissions and their effects on ecosystems and people.

ACKNOWLEDGEMENTS

The authors thank Geoffrey J. Cary of CSIRO and Graham Mills of the Australian Bureau of Meteorology for their assistance in the preparation of this manuscript. In Portugal, the co-workers of D. Viegas were generous with their assistance in this project. Colin Hardy of the USDA Forest Service and his father, Charles E. Hardy (retired USDA Forest Service fire scientist and Project Leader), provided valuable information about the historical development of the fire danger meter in the United States.

REFERENCES

Anderson, K.R. 2002. A model to predict lightning-caused fire occurrences. Int. J. Wildland Fire 11, 163–172.

Anderson, D.H., Catchpole, E.A., De Mestre, N.J., and Parkes, T. 1982. Modelling the spread of grass fires. J. Austral. Math. Soc. (Ser. B) 23, 451–466.

Beck, J.A. 1995. Equations for the forest fires behavior tables for Western Australia. CALMScience 1, 325–348.

Beck, J.A., and Trevitt, A.C.F. 1989. Forecasting diurnal variations in meteorological parameters for predicting fire behavior. Can. J. For. Res. 19, 791–797.

Blackmarr, W.H. 1972. Moisture content influences ignitability of slash pine litter. Research Note, SE-173. USDA Forest Service, Southeastern Forest and Range Experiment Station. 7 pp.

Bovio, G., Quaglino, A., and Nosenzo, A. 1984. Individuazione di un indice di previsione per il Pericolo di Incendi Boschivi. Monti e Boschi, Anno XXXV(4), 39–44.

Bradshaw, L.S., Deeming, J.E., Burgan, R.E., and Cohen, J.D. 1984. The 1978 National Fire-Danger Rating System: Technical Documentation. General Technical Report, INT-169. USDA Forest Service, Intermountain Forest and Range Experiment Station. Ogden, Utah. 44 pp.

Burgan, R.E. 1988. 1988 Revisions to the National Fire-Danger Rating System. Research Paper, SE-273. USDA Forest Service. Southeastern Forest and Range Experiment Station. 39 pp.

Burrows, N.D., Ward, B., Robinson, A.D., and Behn, G. 2006. Fuel dynamics and fire behavior in spinifex grasslands of the western Desert. In: Tran, C., ed. Life in a fire-prone environment: Translating science into practice, Proceedings of the Bushfire 2006 conference, Brisbane, June 6–9, 2006. Compact Disk, Item 202.

Byram, G.M. 1959. Combustion of forest fuels. Forest fire control and use (2nd ed.). McGraw-Hill, New York, 61–89.

Catchpole, W.R., Bradstock, R.A., Choate, J., Fogarty, L.G., Gellie, N., McCarthy, G.J., McCaw, W.L., Marsden-Smedley, J.B., and Pearce, G. 1999. Cooperative development of prediction equations for fire behavior in heathlands and shrub lands. In: Bushfire 99 Proceedings, Australian Bushfire conference, Albury, Australia, 7–9 July, 1999. Charles Sturt University, Albury, 77–83.

Cheney, N.P., Gould, J.S., and Catchpole, W.R. 1993. The influence of fuel, weather and fire shape variables on fire spread in grasslands. Int. J. Wildland Fire 3, 31–44.

Condon, R.W. 1979. The modified grasslands fire danger meter for arid zone rangelands. The Australian Grasslands Society Conference, Adelaide, May.

Commonwealth Scientific and Industrial Research Organisation (CSIRO). 1997. CSIRO Grassland Fire Spread Meter. Commonwealth Scientific and Industrial Research Organization, Forestry and Forest Products. Canberra, Australia.

Drouet J.C., and Sol, B., 1990. Mise au point d'un Indice numérique de risque météorologique d'incendie. Revue Génerale de Securité 92.

Finney, M.A. 1998. FARSITE: Fire Area Simulator—model development and evaluation. Research Paper, RMRS-RP-4. USDA Forest Service, Rocky Mountain Research Station. 47 pp.

Fons, W. 1946. Analysis of fire spread in light forest fuels. J. Agric. Res. 72, 93–121.

Forestry Canada Fire Danger Group. 1992. Development and structure of the Canadian forest fire behavior prediction system. Report ST-X-3. Forestry Canada, Science and Sustainable Development Directorate. Ottawa, Ontario, 64 pp.

Fujioka, F.M. 2002. A new method for the analysis of fire spread modeling errors. Int. J. Wildland Fire 11, 193–203.

Gisborne, H.T. 1928. Measuring forest-fire danger in northern Idaho. Miscellaneous Publication No. 29, USDA. Washington, DC, 64 pp.

Gould, J.S., McCaw, W.L., and Cheney, N.P., 2004. Project Vesta-findings, extension and validation for south eastern Australian eucalypt forests. In: Bushfire 2004: Earth, wind and fire – fusing the elements conference, Adelaide, May. Compact Disc.

Griffin, G.F., and Allan, G.E. 1984. Fire behavior. In: Saxon, E., ed. Anticipating the inevitable: A patch-burn strategy for fire management at Uluru (Ayers Rock – Mt Olga) National Park. Commonwealth Scientific and Industrial Research Organization, Melbourne, Australia, pp. 55–68.

Hardy, C.C., and Hardy, C.E. 2007. Fire danger rating in the United States of America: An evolution since 1916. Int. J. Wildland Fire 16, 217–231.

Instituto Nacional para la Conservacion de la Naturaleza. 1988. Experimentation de un nuevo sistema para determinacion del peligro de incendios forestales derivado de los combustibles: Instrucciones de calculo. Madrid, Spain.

Instituto Nacional de Meteorologia e Geofisica. 1988. Nota explicativa sobre o Índice de Risco Meteorológico de Incêndios Rurais. Divisão de Meteorologia Agrícola, Lisbon, Portugal.

Keetch, J.J., and Byram, G.M. 1968. A drought index for forest fire control. Research Paper, SE-38. USDA Forest Service, Southeastern Forest and Range Experiment Station. 32 pp.

Kourtz, P.H., and Todd, J.B. 1992. Predicting the daily occurrence of lightning-caused forest fires. Information Report, PI-X-112. Petawawa National Forestry Institute. Chalk River, Ontario, Canada. 18 pp.

Lawson, B.D., Armitage, O.B., and Hoskins, W.D. 1996a. Diurnal variation in the Fine Fuel Moisture Code: Tables and computer source code. Canada–British Columbia Partnership Agreement on Forest Resource Development: FRDA II. FRDA Report 245. Canadian Forest Service, Pacific Forestry Center. Victoria, British Columbia.

Lawson, B.D., and Dalrymple, G.N. 1996b. Ground-truthing the Drought Code: Field verification of over-winter recharge of forest floor moisture. Canada-British Columbia Partnership agreement on Forest Resource Development: FRDA II. Report 268. Canadian Forest Service, Victoria, British Columbia. 21 pp.

Marsden-Smedley, J. 1993. Fuel characteristics and fire behavior in Tasmanian Buttongrass Moorlands. Parks and Wildlife Service, Tasmania.

Martell, D.L., Bevilacqua, E., and Stocks, B.J. 1989. Modelling seasonal variation in daily people-caused forest fire occurrence. Can. J. For. Res. 19, 1555–1563.

McArthur, A.G. 1962. Control burning in eucalypt forests. Leaflet 80. Forestry and Timber Bureau. Commonwealth of Australia.

McArthur, A.G. 1966. Weather and grassland fire behavior. Leaflet 100. Forestry and Timber Bureau. Commonwealth of Australia.

McArthur, A.G. 1967. Fire behavior in eucalypt forests. Leaflet 107. Forestry and Timber Bureau. Commonwealth of Australia.

McCaw, L., Cheney, P., and Sneeuwjagt, R. 2003. Development of a scientific understanding of fire behavior and use in south-west Western Australia. In: Abbott, I., and Burrows, N., eds. Fire in ecosystems of south-west Western Australia. Backhuys Publishers, Leiden, pp. 171–187.

Muraro, S.J. 1968. A modular approach to a revised national fire danger rating system. In: Contributions to the development of a national fire danger rating system. Information Report, BC-X-37. Canadian Forest Service, Pacific Forestry Center.

Noble, I.R., Bary, G.A.V., and Gill, A.M. 1980. McArthur's fire-danger meters expressed as equations. Austral. J. Ecol. 5, 201–203.

Palmer, W.C. 1988. The Palmer Drought Index: When and how it was developed. Wkly. Wea. Crop Bull. 75, 5.

Paul, P.M. 1969. Field practices in forest fire danger rating. Information Report, FF-X-20. Canadian Forest Service, Forest Fire Research Institute. 27 pp.

Poulin-Costello, M. 1993. People-caused forest fire prediction using Poisson and logistic regression. Master of Science Thesis. Department of Mathematics and Statistics, University of Victoria, Victoria, British Columbia, Canada, 116 pp.

Pyne, S.J. 1982. Fire in America: A cultural history of wildland and rural fire. Princeton University Press, Princeton, New Jersey, 462–514

Richards, G.D. 1990. An elliptical growth model of forest fire fronts and its numerical solution. Int. J. Num. Meth. Eng. 30, 1163–1179.

Richards, G.D. 1995. A general mathematical framework for modelling two-dimensional wildland fire spread. Int. J. Wildland Fire 5, 63–72.

Rothermel, R.C. 1972. A mathematical model for predicting fire spread in wildland fuels. Research Paper, INT-115. USDA Forest Service, Intermountain Forest and Range Experiment Station. 40 pp.

Rothermel, R.C., Wilson, R.A., Morris, G.A., and Sackett, S.S. 1986. Modeling moisture content of fine dead fuels: input to the BEHAVE fire prediction system. Research Paper, INT-359. USDA Forest Service, Intermountain Forest and Range Experiment Station. 61 pp.

Russell-Smith, J., Craig, R., Gill, A.M., Smith, R., and Williams, J.E., eds. 2002. Australian fire regimes: Contemporary patterns (April 1998–March 2000) and changes since European settlement. Australia: state of the environment. Second Technical Paper Series No. 2. (Biodiversity). Department of Environment and Heritage, Canberra.

Schlobohm, P., and Brain, J. 2002. Gaining an Understanding of the National Fire Danger Rating System. National Wildfire Coordinating Group, PMS-932, Boise, Idaho. 82 pp.

Show, S.B., and Kotok, E.I. 1925. Weather conditions and forest fires in California. Department Circular 354. USDA, Washington, DC. 24 pp.

Show, S.B., and Kotok, E.I. 1929. Cover type and fire control in the national forests of northern California. Department Bulletin No. 1495. USDA, Washington, DC. 36 pp.

Simard, A.J. 1970. Reference manual and summary of test fire, fuel moisture and weather observations made by forest fire researchers between 1931 and 1961. Information Report, FF-X-19. Canadian Forest Service, Forest Fire Research Institute. 39 pp.

Sneeuwjagt, R.J., and Peet, G.B. 1985. Forest fire behavior tables for western Australia. Western Australian Department of Conservation and Land Management, Perth.

Stocks, B.J., Lawson, B.D., Alexander, M.E., Van Wagner, C.E., McAlpine, R.S., Lynham, T.J., and Dube, D.E. 1989. The Canadian forest fire danger rating system: An overview. Forest. Chron. 65, 450–457.

Stocks, B.J., Alexander, M.E., Wotton, B.M., Stefner, C.N., Flannigan, M.D., Taylor, S.W., Lavoie, N., Mason, J.A., Hartley, G.R., Maffey, M.E., Dalrymple, G.N., Blake, T.W., Cruz, M.G., and Lanoville, R.A. 2004. Crown fire behavior in a northern jack pine-black spruce forest. Can. J. For. Res. 34, 1548–1560.

Taylor, S.W., and Alexander, M.E. 2006. Science, technology and human factors in fire danger rating: The Canadian experience. Int. J. Wildland Fire 15, 121–135.

Tymstra, C. 2002. Prometheus: The Canadian wildland fire growth model. Initial Attack (Spring) 8–9.

Van Wagner, C.E. 1974. The structure of the Canadian Forest Fire Weather Index System. Publication 1333. Canadian Forest Service, Petawawa Forest Experiment Station, Chalk River, Ontario. 44 pp.

Van Wagner, C.E. 1987. The development and structure of the Canadian forest fire weather index system. FTR-35. Canadian Forest Service, Petawawa National Forestry Institute, Chalk River, Ontario.

Viegas, D.X., Bovio, G., Ferreira, A., Nosenzo, A., and Sol, B. 1999. Comparative study of various methods of fire danger evaluation in Southern Europe. Int. J. Wildland Fire 9, 235–246.

Viegas, D.X., Reis, R.M., Cruz, M.G., and Viegas, M.T. 2004. Calibração do Sistema Canadiano de perigo de incêndio para aplicação em Portugal (in Portuguese). Silva Lusit. 12, 77–93.

Wotton, B.M., and Beverly, J.L. 2005. Stand specific litter moisture content calibrations for the Canadian Fine Fuel Moisture Code. In: Proceedings, sixth symposium on fire and forest meteorology/19th Interior West Fire Council meeting, Canmore, Alberta, October 25–27, 2005. American Meteorological Society, Boston, MA.

Wotton, B.M., and Martell, D.M. 2005. A lightning fire occurrence model for Ontario. Can. J. For. Res. 35, 1389–1401.

Wotton, B.M., Martell, D.M., and Logan, K.A. 2003. Climate change and people-caused forest fire occurrence in Ontario. Clim. Change 60, 275–295.

Wotton, B.M., Stocks, B.J., and Martell, D.M. 2005. An index for tracking sheltered forest floor moisture within the Canadian forest fire weather index system. Int. J. Wildland Fire 13, 169–182.

This page intentionally left blank

Developments in Environmental Science, Volume 8 499
A. Bytnerowicz, M. Arbaugh, A. Riebau and C. Andersen (Editors)

ISSN: 1474-8177/DOI:10.1016/S1474-8177(08)00022-3

Chapter 22

Regional Real-Time Smoke Prediction Systems

*Susan M. O'Neill**, *Narasimhan (Sim) K. Larkin, Jeanne Hoadley, Graham Mills, Joseph K. Vaughan, Roland R. Draxler, Glenn Rolph, Mark Ruminski and Sue A. Ferguson*

Abstract

Several real-time smoke prediction systems have been developed worldwide to help land managers, farmers, and air quality regulators balance land management needs against smoke impacts. Profiled here are four systems that are currently operational for regional domains for North America and Australia, providing forecasts to a well-developed user community. The systems link fire activity data, fuels information, and consumption and emissions models, with weather forecasts and dispersion models to produce a prediction of smoke concentrations from prescribed fires, wildfires, or agricultural fires across a region. The USDA Forest Service's BlueSky system is operational for regional domains across the United States and obtains prescribed burn information and wildfire information from databases compiled by various agencies along with satellite fire detections. The U.S. National Oceanic and Atmospheric Administration (NOAA) smoke prediction system is initialized with satellite fire detections and is operational across North America. Washington State University's ClearSky agricultural smoke prediction system is operational in the states of Idaho and Washington, and burn location information is input via a secure Web site by regulators in those states. The Australian Bureau of Meteorology smoke prediction system is operational for regional domains across Australia for wildfires and prescribed burning. Operational uses of these systems are emphasized as well as the approaches to evaluate their performance given the uncertainties associated with each system's subcomponents. These real-time smoke prediction systems

*Corresponding author: E-mail: susan.oneill@por.usda.gov

are providing a point of interagency understanding between land managers and air regulators from which to negotiate the conflicting needs of ecological fire use while minimizing air quality health impacts.

22.1. Introduction

Smoke from fire is a local, regional, national, and often international issue. Large wildfires cause air quality impacts that are detectable on continental scales and beyond. Because fire is a natural and often integral part of many ecosystems, it is necessary for continued ecosystem health and maintenance. In the United States, prescribed fire use is increasing in order to counteract a history of fire suppression that has left many forests susceptible to catastrophic wildfires. Meanwhile wheat stubble burning and grass seed burning are typical practices in many farming communities. Many of these burning activities occur at rural/urban interfaces and can impact sensitive populations such as children, asthmatics, and the elderly. In order to maximize the ability of land managers and farmers to utilize planned burning activities for ecological and crop productivity, while at the same time avoiding adverse air quality impacts, tools for predicting the impacts of burning are necessary to balance conflicting goals (Sandberg et al., 1999) and effectively manage smoke.

In many parts of the world fire is seasonally a large component of the atmospheric chemistry and atmospheric burden of pollutants, contributing significantly to ozone formation, $PM_{2.5}$ emission and formation, and emissions of other trace gases into the atmosphere. Therefore, global air quality prediction systems have begun incorporating fire emissions. Examples include Goddard Earth Observing System global chemical transport model (GEOS-Chem; Bey et al., 2001), Fire Locating and Modeling of Burning Emissions (FLAMBE; Reid et al., 2001), and the Navy Aerosol Analysis and Prediction System (NAAPS, http://www.nrlmry.navy.mil/aerosol/), which are run in real-time or near real-time.

Unlike these global systems, most regional air quality prediction systems do not yet routinely include fire emission estimates in their emission inventories and output products. However, four air quality dispersion systems not only include fire emission data but also provide smoke predictions from fire. These systems all have well-defined user bases and produce real-time predictions available via the Web, by integrating with burn information systems (both land-based and satellite-based). The USDA Forest Service's (USFS) BlueSky system serves the smoke management community and operates regionally across the United States, using both prescribed and wildfire burn information. The U.S. National Oceanic and Atmospheric Administration (NOAA) smoke prediction system is designed to support the air quality community needs and operates nationally using satellite fire detections. Washington State University's ClearSky prediction system focuses on agricultural burning in the U.S. Pacific Northwest and contains user input burn information. The Australian Bureau of Meteorology smoke prediction system is operational for regional domains across Australia covering both wildfires and prescribed burning.

Smoke forecasts link together, either explicitly or implicitly, a number of steps including the amount of fuel available, the fuel consumed, the speciated emissions and when they are released, how high the plume rises, and the resulting smoke transport. Each of these steps can be modeled explicitly or simplified with bulk formula calculations that combine steps. Thus, smoke forecasts rely on a number of models and assumptions that make smoke predictions inherently uncertain. Before these regional real-time smoke prediction systems existed, the burden was on the land manager to gather the various inputs and run them with smoke prediction programs installed on their personal computer (PC), as discussed in Breyfogle and Ferguson (1996). Only single fires or a set of fires known by the user could be processed with these PC-based systems. The Department of Forestry in Florida, USA, developed the first online tool that integrates meteorological forecasts, GIS data, and smoke dispersion models to give a smoke prediction based on user-entered burn information (http://flame.fl-dof.com/wildfire/). With the advent of regional real-time smoke prediction systems that integrate the necessary data, despite the uncertainties associated with each smoke prediction, the systems profiled here are providing a point of interagency understanding between land managers and air regulators from which to negotiate the conflicting needs of ecological fire use while minimizing air quality health impacts.

This chapter compares and contrasts the four systems, their methodology, and user needs for each, in order to examine the common components and differences inherent in each approach to smoke forecasting. We first examine the components that make up a smoke prediction system in Section 22.2, before detailing the specifics of the four systems in Section 22.3. System evaluation issues are discussed in Section 22.4 and operational uses, both current and potential, are discussed in Section 22.5. Finally, we discuss the future of real-time smoke prediction systems in Section 22.6.

22.2. Components of a smoke prediction system

In order to model smoke from fire, a smoke prediction system links together a series of logical steps, as shown in the schematic in Fig. 22.1. Dispersion models require knowledge of fire emissions distributed over time, which in turn rely on knowledge of the amount of fuel consumed. This process begins with the primary inputs: fire activity data such as fire size and location, and atmospheric model data describing the full three-dimensional state of the atmosphere as it evolves over time. It ends with smoke concentrations, typically in terms of particulate matter (PM) with an aerodynamic diameter less than or equal to 2.5 μm ($PM_{2.5}$), estimates of plume extents, and trajectories showing where a neutrally buoyant parcel of air will travel over the course of the next several hours. Some real-time smoke prediction systems also include information about other trace gases and aerosols emitted from fires, such as carbon dioxide (CO_2), carbon monoxide (CO), methane (CH_4), hydrocarbons (HC), oxides of nitrogen (NO_X), ammonia (NH_3), and particulate matter with aerodynamic diameter less than 10 μm (PM_{10}).

By linking together the latest information in fire tracking, meteorological forecasts, fuels, consumption/emissions, dispersion, and trajectories, smoke prediction systems integrate the current state of knowledge in all of these areas. Each modeling step is discussed in detail below.

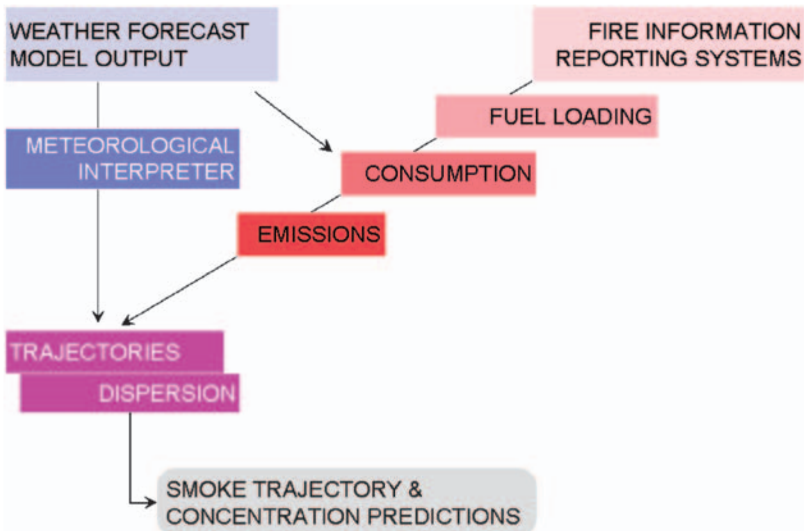

Figure 22.1. Modeling and data components of smoke prediction systems.

22.2.1. Meteorological data inputs

The availability and quality of the meteorological predictions are a key factor controlling the accuracy of the smoke predictions. Meteorological inputs are supplied by real-time weather prediction models such as the Pennsylvania State University/National Center for Atmospheric Research 5th generation Mesoscale Meteorological (MM5) model (Grell et al., 1994), the Weather Research and Forecasting (WRF) model (Skamarock et al., 2005), the North America Model (NAM, Janjic, 2003, formerly known as the Eta model, Mesinger et al., 1988), the Global Forecast System (GFS, Kalnay et al., 1990), or the Australian Limited Area Prediction System (LAPS; Puri et al., 1998). The accuracy of the meteorological forecasts, particularly the wind speed and direction and planetary boundary layer height, directly control the resulting accuracy of the smoke prediction.

22.2.2. Fire activity data inputs

To create a smoke prediction, fire information—minimally location and some measure of area burned—is needed. This can be obtained from ground-based reporting systems or remotely sensed from satellites. The information available varies widely, particularly from ground-based systems, which are usually driven by regulatory requirements. Some systems only record a wide range of potential dates for a permitted burn and not actual ignitions; some report only total fire size even for multi-day burns such as wildfires; some have significant (multi-day) lags before information becomes available. In each case care must be taken to appropriately use the recorded information. Consistency in the reported data (e.g., types of burns reported) is also problematic as databases maintained by regulatory agencies vary from region to region.

Detecting fires by satellite can provide a complete and relatively homogenous picture of where fires are currently occurring. A variety of satellite products are available, with perhaps the most popular platforms being the polar satellites (NASA's MODerate Resolution Imaging Spectroradiometer-MODIS, and NOAA-15/17/18) due to their higher spatial resolution (1 km). Depending on the product used, reports can be obtained within 15 min to 3 h of detection, and coverage can be continuous from geostationary satellites (e.g., the Geostational Operational Environmental Satellite (GOES)), or daily swathes from polar orbiting satellites (e.g., MODIS). Combined reports are also available. In all cases, however, satellite detections suffer from coverage issues, as clouds and thick smoke obscure fire detection. Polar orbiting satellites also have issues of variable swath timing for a given location, thus potentially missing (not detecting) short duration fires such as prescribed fires, agricultural burns and other small fires. However, the satellite sensor can detect fires as small as 0.5 ha under optimal conditions.

22.2.3. Fuel loadings

Quantification of the fuels that are burning is necessary in order to estimate emissions. Fuel-loading information can be provided as part of the fire activity data, obtained from regional maps of fuel load estimations, or set at some best estimate for a region or burn type. In the United States there are two national maps of fuel loadings, both on 1-km grids: the National Fire Danger Rating System (NFDRS; Cohen & Deeming, 1985) and the Fuel Characteristic Classification System (FCCS; McKenzie et al., 2007). In the future, mapped fuel loadings that extend beyond national borders will be necessary to provide consistent fuel-loading estimates for systems operating at an international and global scale.

22.2.4. Fire growth

To create a smoke prediction, fire growth must also be estimated over the future period of interest. In the case of prescribed fire and agricultural burns, this growth is known and can be utilized. For wildfires, growth must be calculated. Most real-time smoke prediction systems assume simple growth equations such as persistence (fire growth tomorrow = fire growth today).

22.2.5. Consumption and emissions

After determining the fire growth, fuel consumption and emissions can be modeled. Fuel consumption and emissions are a function of the efficiency of combustion, which is a function of the fire lighting technique, fuel moisture, and atmospheric conditions. Consumption models estimate the quantity of fuel consumed by a fire, utilizing meteorological and fuel moisture conditions. Emissions models then apply emission factors to the consumed material for various gases and aerosols, including CO, CO_2, CH_4, HC, NO_X, NH_3, $PM_{2.5}$, and PM_{10}. Consumption and emissions models are sometimes combined, such as in the commonly used Emissions Production Model (EPM)/CONSUME model (Sandberg & Peterson, 1984). Most consumption and emissions models (such as EPM/CONSUME) rely on emission factors based on empirical data measured from burns conducted under a variety of atmospheric conditions and fuel types (Andreae & Merlet, 2001; Battye & Battye, 2002). The Fire Emissions Production System (FEPS; Anderson et al., 2004) uses combustion efficiency to calculate fuel consumption and emissions, and efforts are underway to incorporate FEPS into real-time smoke prediction systems. For uniform fuels (such as wheat stubble and seed crop residue) fire emissions can be estimated from the fire spread rate and fuel loading.

22.2.6. Dispersion and trajectory models

Smoke transport can be simulated using either Lagrangian trajectory or dispersion models, or Eulerian air quality modeling systems. Trajectory models provide information on the location of the plume, while dispersion models also provide plume concentration values. Typically smoke prediction systems focus on Lagrangian particle or puff models, while air quality modeling systems that extend beyond fire smoke utilize more complex Eulerian chemistry models. Two U.S. air quality dispersion models currently used in real-time smoke predictions systems are the Hybrid Single-Particle Lagrangian Integrated Trajectory Model (HYSPLIT; Draxler & Hess, 1997, 1998) and the CALifornia Lagrangian PUFF (CALPUFF) model (Scire et al., 2000).

HYSPLIT was developed and is maintained by NOAA's Air Resources Laboratory (ARL) and is designed to support a wide range of simulations related to the transport, dispersion, and deposition of pollutants, including ash from volcanic eruptions, smoke from wildfires, and emissions of anthropogenic pollutants. HYSPLIT can compute both trajectories and particulate concentration fields from a pollutant source. The HYSPLIT computation is composed of three components: particle transport by the mean wind, a turbulent transport component, and the computation of air concentration. Recent revisions to the model to support the smoke forecasting include a plume rise component and links with fire emission models. At a minimum, HYSPLIT requires three-dimensional fields of the vector wind components and temperature.

CALPUFF was developed by Sigma Research Corporation (now part of Earth Tech, Inc.) and is a U.S. Environmental Protection Agency (EPA) recommended guideline model for regulatory applications estimating air quality impacts (40 Code of Federal Regulations (CFR) 51 Appendix W). CALPUFF is a Gaussian puff dispersion model that simulates nonsteady point, volume, line, and area source emissions, and the resulting downwind concentrations by assuming that plume dispersion occurs in a Gaussian pattern. For buoyant area sources (such as fires), CALPUFF estimates plume rise, accounting for differences between the plume and ambient air temperatures and providing for mixing between the two as the plume advects downwind. Puffs are released at flame height, which is calculated from Cetegen et al. (1982) using the heat-released estimates from EPM. CALPUFF requires three-dimensional fields of the vector wind components and temperature, and two-dimensional fields describing atmospheric stability and mixing height.

Table 22.1 summarizes the source of fire activity, fuel-loading information, and the consumption, emission, meteorological, and air quality data/models used in each of the real-time smoke prediction systems.

22.3. Real-time smoke prediction systems

Several real-time smoke prediction systems are currently operational around the globe, providing predictions of smoke concentrations from fire to a clientele of land managers, farmers, and air quality regulators. Profiled below are four systems currently operational for regions of North America and Australia that provide forecasts to well-developed user communities.

22.3.1. BlueSky: Predicting smoke from prescribed and wildland fires regionally across the United States

The concept of the BlueSky smoke modeling framework was developed in the U.S. Pacific Northwest by a group of land managers, fire researchers, and air quality regulators seeking to link existing information about fire, fuels, meteorology, and air quality into a system that could aid in smoke management. BlueSky's original goal was to help burners understand where the smoke from a burn will go before it is ignited; however, BlueSky's use has expanded to include wildfire incident command teams and air quality regulators (O'Neill et al., 2005).

BlueSky is a modular framework of fire activity, fuels information, consumption, emissions, meteorological, and air quality modeling systems that produces daily predictions of $PM_{2.5}$ concentrations across the region. The USFS Atmosphere and Fire Interaction Research and Engineering (AirFIRE) Team (http://www.fs.fed.us/bluesky) leads the development efforts of the system. By defining standard interfaces, BlueSky is able to implement a variety of model choices at each modeling

Table 22.1. Source of fire activity, fuel loading, and the consumption, emission, meteorological and air quality data/models used in each of the real-time smoke prediction systems

	Fire activity	Fuel loading	Consumption model	Emissions model	Meteorological model	Dispersion model
BlueSky	Ground-based, satellite	FCCS	CONSUME	EPM	MM5/WRF	CALPUFF, HYSPLIT
ClearSky	Ground-based	kg/ha[a]	100%	g/kg[a]	MM5/WRF	CALPUFF
NOAA	Satellite	NFDRS	CONSUME	EPM	NAM-WRF/GFS	HYSPLIT
Australia	Ground-based, satellite	None	None	Single fixed emission rate	Australian meso-LAPS	HYSPLIT

[a]Estimates provided for wheat stubble and Kentucky bluegrass residue burning.

step (the most common choices are listed in Table 22.1). Additionally, since the framework can be started and stopped at any interface, BlueSky can be used to process emissions for other smoke prediction efforts, such as inputs to Eulerian air quality models or hind-casts of smoke impact episodes.

Currently, daily BlueSky predictions of surface $PM_{2.5}$ concentrations are available across the U.S. through a collection of regional modeling efforts run by the USFS Fire Consortia for the Advanced Modeling of Meteorology and Smoke (FCAMMS; http://www.fs.fed.us/fcamms; Fig. 22.2a). Additionally, BlueSky-processed wildfire emissions are used in other smoke prediction systems including the ClearSky and NOAA systems discussed below. In the U.S. Pacific Northwest, wildfire emissions are processed through BlueSky into a format for input into the Community Multi-scale Air Quality (CMAQ; Byun & Schere, 2006) modeling system as described in Pouliot et al. (2005) and used in the AIRPACT-3 (Vaughan et al., 2004, http://www.airpact-3.wsu.edu) air quality forecast system operational for the northwestern United States. This was the first inclusion of daily fire information in a real-time Eulerian air quality modeling system to predict downwind chemical concentrations from fires.

BlueSky has been developed to be flexible in how it obtains and utilizes fire activity data, partially because of the wide variety of reporting systems implemented regionally in the U.S. At a minimum, BlueSky requires fire location and daily fire growth, which can be problematic for wildfires in which typically only fire size and initial ignition point are reported. If additional fire activity data, such as fuel loadings, fuel moisture, and fire type, are included in the input, this information is carried through the framework and used preferentially. If this information is not available, default values or models are used.

For regional forecasts by the FCAMMS, BlueSky is connected to a variety of ground-based fire-reporting systems and automatically downloads data from these systems. BlueSky uses a variety of generic download methods, including a Web form interface to allow outside users to enter information on their fire, as well as a simple Web or ftp download. Nationally, BlueSky is connected to the U.S. national wildfire and wildland fire use reporting system, via the Incident Command System (ICS)-209 reports. The daily ICS-209 reports contain information, such as current area burned and ignition location for wildfires typically greater than 100 acres in size. Regionally, for the U.S. Pacific Northwest,

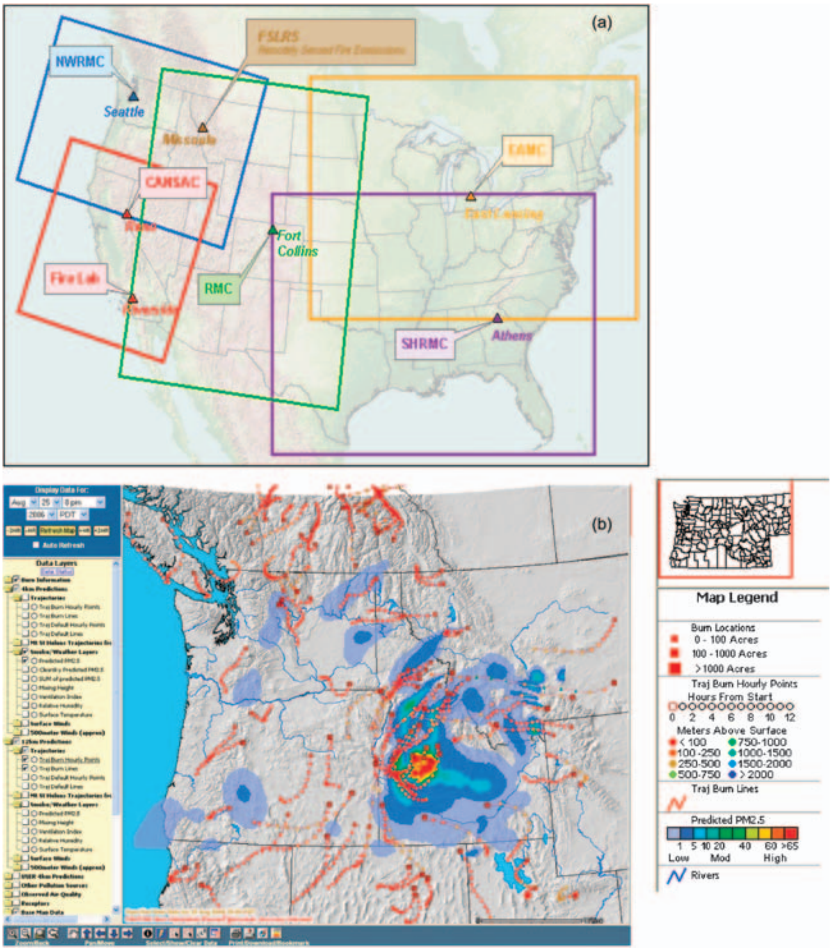

Figure 22.2. Location of regional BlueSky predictions across the U.S. implemented by the USDA Forest Service Fire Consortia for the Advanced Modeling of Meteorology and Smoke (FCAMMS; http://www.fs.fed.us/fcamms) (a). BlueSkyRAINS output for August 25, 2006, at 8 P.M. $PM_{2.5}$ concentrations (colored contours in units of $\mu g/m^3$) and trajectories (initiated at red squares) predicted from wildfires across the northwestern U.S. and western Canada are overlaid on gray-shaded topography. Trajectory dots are color-coded with height (see map legend, b). Acronyms: Northwest Regional Modeling Consortium (NWRMC), California and Nevada Smoke and Air Committee (CANSAC), Rocky Mountain Consortium (RMC), Southern High Resolution Modeling Consortium (SHRMC), Eastern Area Modeling Consortium (EAMC). Forest Service Lab-Remote Sensing (FSLRS).

BlueSky is connected to many ground-based prescribed fire-reporting systems including:

- The Fuel Analysis, Smoke Tracking, and Report Access Computer System (FASTRACS; http://www.fs.fed.us/r6/fire/fastracs), which includes federal prescribed fire data in the states of Oregon and Washington.
- The Montana/Idaho airshed group prescribed burn reporting system, which includes private, state, and federal prescribed fire data in the states of Montana and Idaho.
- The Washington State Department of Natural Resources system, which includes private, state, and federal prescribed fire data in Washington State.
- The Oregon Department of Forestry burn reporting system, which includes private and state prescribed fire data in Oregon State.
- The British Columbia wildfire reporting system.
- The ClearSky agricultural burn prediction system, which includes private and tribal agricultural fire data in the states of Washington and Idaho.

Also, BlueSky is now connected to a system that reconciles these ground reports with satellite fire detects from the NOAA Hazard Mapping System. This system will become the default for FCAMMS BlueSky predictions across the United States in summer 2008.

With all prescribed burning operations there is a difference between what is planned for a particular day and what is actually accomplished. BlueSky also obtains burn accomplishment reports from the above systems where available to initialize each forecast with carry-over smoke from the previous day's burn.

Meteorological data, used to drive the emission estimates and dispersion and trajectory models can be obtained from several sources, including the MM5 and/or the WRF mesoscale meteorological models. The meteorology defines the domain of the BlueSky simulation, another feature that allows BlueSky's quick and easy adaptation to domains nationally and internationally. BlueSky is typically run on 4-km and 12-km grids; however 1-km and 36-km gridded domains have also been applied over North Carolina and the western United States, respectively (http://www.fs.fed.us/bluesky).

Many different models are available for each calculation step in BlueSky; here we describe only the most common configuration. If fuel-loading information is not provided by the user or the burn reporting system, then the U.S. 1-km FCCS mapping is used by default. Consumption and emissions are calculated by the EPM model, which is integrated with the CONSUME model. For prescribed fires, EPM provides an emission profile allocating emissions over time, while for wildfires, the diurnal emissions profile developed by the Western Regional Air Partnership (WRAP; http://www.wrapair.org) is applied. $PM_{2.5}$ concentrations are estimated using the buoyant area source input method of CALPUFF. The HYSPLIT model is used to calculate trajectories from each fire. Currently, trajectories are released at a height of 10 m and travel for 12 h so that a land manager can view not only where smoke from a particular burn may travel through the day but where the smoke goes into the evening when it can become trapped in mountain valleys. Efforts are underway to incorporate plume rise estimates into the trajectory release height.

Graphics of BlueSky output are produced in two forms: (1) static and animated images and (2) the RAINS (Rapid Access Information System), Geographical Information System (GIS)-based Web interface, developed by the EPA in the U.S. Pacific Northwest. Figure 22.2b shows an example of the BlueSkyRAINS (http://www.fcamms.org) display of $PM_{2.5}$ concentrations and trajectories from wildfires across the northwestern United States and western Canada. RAINS allows the user to customize the display by zooming in and out—selecting various data layers, such as smoke concentrations and trajectories, meteorological forecasts, sensitive receptors, roads and terrain—and obtaining quantitative results from a variety of database queries. Features of RAINS include the ability to query the underlying data to obtain fuel-loading information and total emissions of $PM_{2.5}$, CO_2, CO, CH_4, NO_X, HC, SO_2, and PM_{10}, and access data from air quality monitoring networks.

22.3.2. ClearSky: Predicting smoke from agricultural fires in the northwestern United States

In the arid intermountain region of the northwestern United States, which includes the eastern part of Washington State, parts of the Idaho Panhandle, and parts of eastern Oregon, smoke from agricultural burning, a typical practice in this region, has become a subject of litigation, legislation, and governmental and scientific interest. In January 2001, the Idaho Division of Environmental Quality proposed creation of a smoke modeling tool for decision support in the Idaho smoke management program administered by Idaho's Department of Agriculture. This led to the development of Washington State University's ClearSky smoke prediction system (http://www.clearsky.wsu.edu).

Agricultural burning in this area is primarily of two kinds: wheat stubble and residue after harvest of Kentucky bluegrass (KBG), a

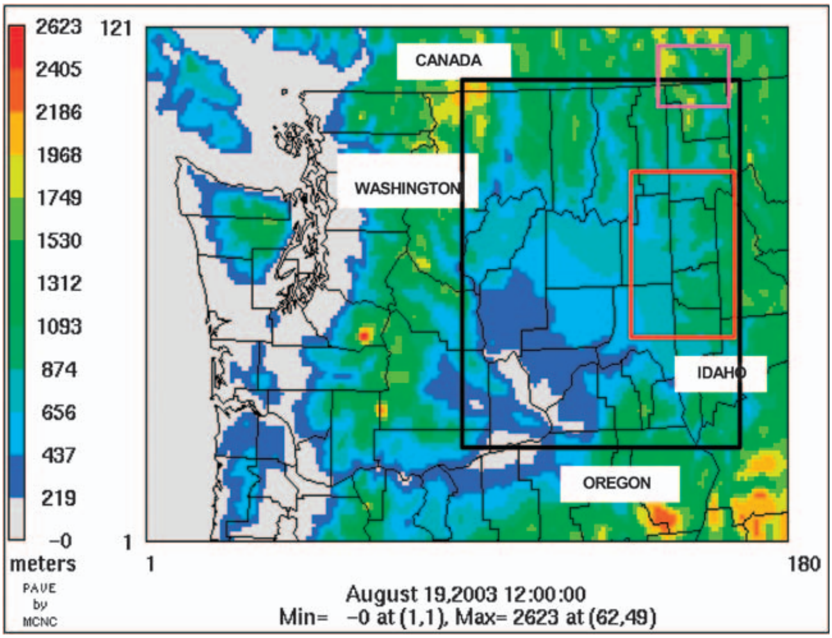

Figure 22.3. ClearSky domain elevations. The red rectangle indicates the original application for the Rathdrum Prairie and Coeur d'Alene tribal reservation. The black rectangle indicates the expansion to Eastern Washington and the Nez Perce Tribal reservation in Idaho. The pink rectangle indicated the application for boundary county, Idaho.

profitable seed crop. ClearSky was initially formulated for treatment of smoke for burning on the KBG fields of the Rathdrum Prairie near Coeur d'Alene (CDA), Idaho, and also for burning on the nearby Coeur d'Alene tribal reservation (Fig. 22.3, red rectangle). The ClearSky system became operational in the summer of 2001 for the Rathdrum Prairie and CDA areas, and was significantly expanded in 2002 to include eastern Washington and the Nez Perce Tribal (NPT) reservation (Fig. 22.3, black rectangle).

Operationally, ClearSky uses the 4-km real-time MM5 numerical meteorological domain prediction from the University of Washington (Mass et al., 2003), and emission scenarios defined by users, to drive a CALPUFF simulation producing hourly surface level $PM_{2.5}$ concentrations. Fundamental to the concept of ClearSky is the user generating a hypothetical burn scenario for their jurisdiction and reviewing the ClearSky results for that burn scenario before making decisions to ignite a burn. Field burning scenarios are defined via a Web-application the day before, and the simulation runs overnight after the meteorological forecast becomes available. Typically, about 10 scenario forecasts are run nightly, including a set of default scenarios. Comprehensive databases of fields from which the users create scenarios have been created specific to the Coeur d'Alene Tribe, Rathdrum Prairie, Nez Perce Tribe, and Washington State Department of Ecology operational regions. Animations of gif images are produced for viewing the $PM_{2.5}$ concentration fields on the Web and are used by the local state and tribal agencies in their burn decision-making process.

In converting acreage and crop type into emissions parameters, information such as areal burn rates (ha/h), fuel loadings (kg/ha), and emission factors (g/kg) must be specified. Areal burn rates and fuel loadings are estimated based on agency expertise and are included in the database of agricultural fields. Emissions factors are based on values from wheat stubble and KBG from studies conducted by Air Sciences, Inc. (2003, 2004).

The initial ClearSky treatment of emissions assumed that the plume from a field of burning stubble should be handled through CALPUFF's buoyant area-emissions capability. Observation of field burning suggested that addition of a line source might better capture the intense buoyancy associated with the flaming front in a field fire. Particulate production is most strongly associated with combustion stages that are not flaming, primarily post-flaming smoldering (Ward, 2001). Field observations show that the buoyancy from the flame front generates horizontal flows of replacement air, which entrain much of the smoke produced by nearby non-flaming combustion that carries the smoke into the flame front. Therefore, a buoyant line source is used to simulate the flaming front, in addition to an area source.

Another research effort to improve the ClearSky predictions and provide a measure of uncertainty explored using an ensemble of 17, 12-km MM5 meteorological simulations to generate an ensemble of CALPUFF $PM_{2.5}$ predictions, thereby providing probabilistic guidance (Heitkamp, 2006). ClearSky ensembles were analyzed for 2 days with heavy field burning in 2004, using accomplished burn data (Jain et al., 2007). Ensemble average hourly $PM_{2.5}$ results were compared with hourly monitoring results to calculate normalized mean error in $PM_{2.5}$ for each day. The 12-km ensemble system average results were encouraging, showing slightly better error statistics than the original 4-km ClearSky system.

22.3.3. The NOAA-HYSPLIT smoke forecast system: Predicting smoke from satellite sensed fires across North America

NOAA's interest in fires and smoke started in the spring of 1998 during the massive transport of smoke from fires in Central America across

Texas, the southeast United States and as far north as the Mid-Atlantic States. In response, an operational fire and smoke program at NOAA's National Environmental Satellite and Data Information Service (NESDIS) was developed primarily to support National Weather Service (NWS) needs in that region. As part of that program the Hazard Mapping System (HMS) was developed in 2001 (Ruminski et al., 2006) as an interactive tool to identify fires and smoke produced over North America in an operational environment. The NOAA-HYSPLIT "Interim Smoke Forecast Tool" was then implemented until the fire emissions could be implemented in the operational air quality modeling (Otte et al., 2005).

The HMS fire detection system uses two geostationary and five polar orbiting environmental satellites with automated fire detection algorithms employed for each sensor. The polar satellites (NASA's MODIS and NOAA-15/17/18) are the preferred platforms for determining fire size due to their higher spatial resolution (1 km). Each algorithm utilizes multispectral imagery and applies a form of temperature threshold to evaluate each hotspot. The HMS analysis domain includes all of North America but is adjusted seasonally to include each specific region's prime burning activity season (i.e., Central America in spring, Alaska in summer).

Human analysts use visual satellite imagery and apply quality control procedures for the automated fire detections to eliminate hot spots that are deemed to be false and to add hot spots that the algorithms have not detected. The addition and deletion of fire locations are based on analyst experience in satellite image interpretation, consistency of a fire signal across image times and platforms, and confirmation via the presence of smoke emissions. (These data are available daily at: http://www.firedetect.noaa.gov.)

The NOAA real-time smoke prediction system (http://www.arl.noaa.gov/smoke/forecast.html) uses the HYSPLIT dispersion model coupled with the NAM-WRF meteorological data, which is run on a 12-km grid at intervals of 1-hr over the continental United States; and the 3-h 1-degree grid-spacing GFS data fields for any fire locations that may be outside of the NAM domain. Therefore, the smoke prediction system can include fires in Alaska, Canada, and south through Central America, approximately 7–75 degrees north latitude. Fires identified as producing smoke in the satellite imagery by the HMS analysts are utilized. These fires are a subset of all fire hot spots. The number of input points representing a fire is considered to be proportional to an approximation of the areal extent of the fire. Dispersion calculations are run once a day using the 0600 UTC forecast cycle. Hourly average output maps of $PM_{2.5}$ concentrations are produced using the HMS fire locations for the previous day. Because of the concern over the effects of fine particulates, the model simulation is focused on $PM_{2.5}$ concentrations, although any species available in the emission inventory could be modeled. The dispersion simulation consists of a 24-h analysis simulation run for the previous day, and a 48-h forecast simulation, which assumes that yesterday's fires will continue to burn today and tomorrow unless fire duration information is available for a particular fire. The smoke particle positions at the end of each analysis period are used to initialize the next day's analysis simulation.

$PM_{2.5}$ emissions and heat released are estimated from the emissions processing portion of the BlueSky system based on fire size and location. The system consists of the EPM model integrated with the CONSUME model and the NFDRS fuel loadings. The fire area is computed from the sum of the number of fire locations provided by the HMS analysis within an emission aggregation grid currently set to a 20-km resolution. In the smoke prediction computation, particles are released at the final plume rise height from the center of each emission grid cell that contains one or more fire locations. The heat release rate from EPM/CONSUME, in conjunction with the forecast meteorology, is used to compute a final plume rise (Briggs, 1969).

Two $PM_{2.5}$ concentration grids are defined for each simulation, each having a grid spacing of 15 km. One grid creates hourly averaged $PM_{2.5}$ concentrations from the ground to 5 km (Fig. 22.4) for comparison with satellite smoke plume observations. The second grid defines the layer in the lowest 100 m as hourly average $PM_{2.5}$ concentrations for air quality applications.

The official NWS hourly graphical output for each forecast hour over the continental United States is posted daily as part of the Air Quality Forecast Guidance from the NWS National Digital Guidance Database (http://www.weather.gov/aq). An archive of data for 30 days as well as the current forecast maps for various geographic regions or the national domain are available from NOAA's Air Resources Laboratory's web page (http://www.arl.noaa.gov/smoke/forecast.html).

Although the NOAA-HYSPLIT smoke prediction system features the incorporation of real-time satellite fire detection data, these data are a source of uncertainty. The number of fires undetected by the automated algorithms and added by analysts can represent over 50% the annual total. Some of this is due to the navigational discrepancies between the satellites and variation even from image to image for the same satellite platform. Thus, a single fire may be represented by multiple automated hot spots clustered around the actual fire location. Another major issue is predicting which fires will be continuous through the forecast period.

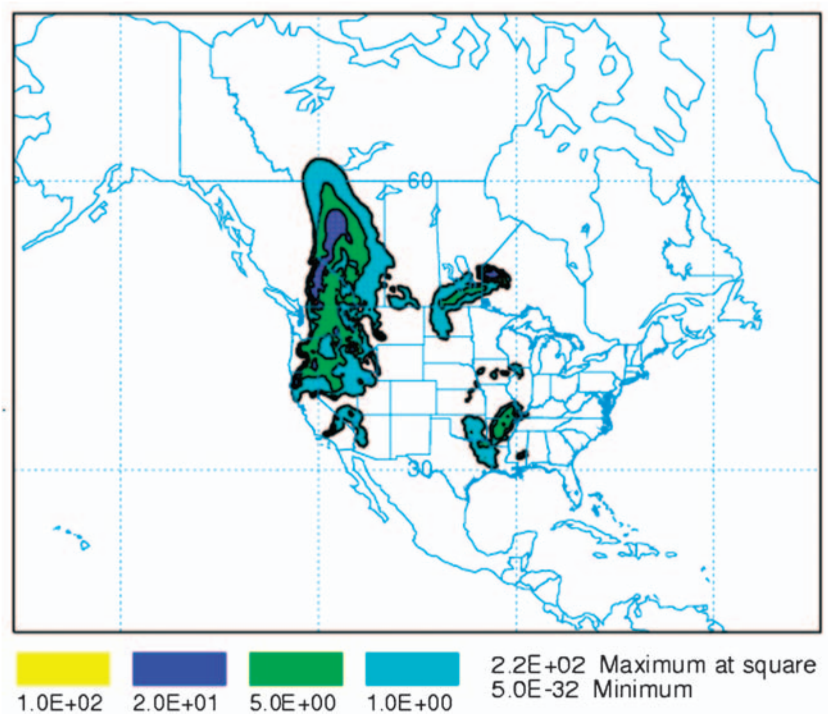

Figure 22.4. One-hour average (6 am–7 am 9/9/2006) 0–5000 m column integrated $PM_{2.5}$ concentration calculated by the NOAA-HYSPLIT smoke prediction system at the end of the 24-hour analysis period used for the initialization of the 48-hour forecast.

Some fires, such as large wildfires, are both easily detected and likely to continue to burn. However, this is not the case for most of the agricultural and prescribed burns and many of the small wildfires. The fire area is currently determined by the number of detections in a grid cell—this can also be problematic for the smaller fires.

The HMS smoke plume analysis is used to evaluate the NOAA-HYSPLIT smoke prediction. As part of the HMS, areas of smoke are outlined by an analyst using animated visible channel imagery. Visible band imagery is used to detect the HMS smoke plumes, but clouds can hinder detection during the day, and detection is not possible at night. In November 2006, a quantitative estimate of the smoke concentration associated with the HMS plume analysis was implemented. The estimation is based on output from the GOES Aerosol and Smoke Product (GASP; Knapp, 2002) and visual inspection of the plume. While

GASP utilizes reduced 4-km visible band imagery, the analyst views the full 1-km resolution available from GOES. Three categories of smoke concentration are specified by the analyst: 5 (light), 16 (medium), and 27 (thick) $\mu g/m^3$. This single value is the midpoint of a range of values that are being represented: 0.1–10.5 $\mu g/m^3$ (light), 10.5–21.5 $\mu g/m^3$ (medium), and greater than 21.5 $\mu g/m^3$ (thick).

22.3.4. Predicting smoke from wildfires in Australia

The Australian Smoke Management System (Wain & Mills, 2006) was developed to assist land managers in planning prescribed burns while mitigating impacts of smoke from these fires. The climatological window for prescribed burning in southern Australia occurs in the Australian spring and autumn, avoiding summer drought and winter rains. Unfortunately, optimum conditions for prescribed burning coincide with typically anti-cyclonic weather patterns, providing less then ideal dispersion conditions. Dispersion forecasts are also issued based on hot spots identified from MODIS satellite imagery to provide information on smoke from wildfires.

Components of the system are the meteorological fields from the Numerical Weather Prediction (NWP) systems operated by the Australian Bureau of Meteorology (the Bureau) and transport and dispersion calculations from the HYSPLIT model. Specifically, the smoke prediction system relies on several higher resolution domains (0.05 degree) over the populated areas of the country as shown in Fig. 22.5. Concentration grids are output at four vertical levels: 10, 150, 500, and 1500 m. For the initial system implementation a source concentration of 1 arbitrary unit has been specified, with the forecast concentrations being relative to this value. This was done because of large uncertainties in the fuel-loading information and lack of an emissions model. The outermost contour interval for the concentration forecasts was selected to coincide with the edges of the visible smoke plume based on field studies where both aircraft and ground observations of the smoke plumes from prescribed burns were made. The plume rise was initially set arbitrarily at 1500 m, the approximate height of the typical subsidence inversion during ideal autumn prescribed burning conditions. It has been found that using the depth of the mixed layer, as diagnosed by the NWP model and input to the dispersion model, to specify the plume height greatly improves the predictions (Wain, 2006). This assumes that the fire is a low-intensity burn as typified by many prescribed burns, rather than a high-intensity burn where the plume may penetrate the inversion (as in large wildfires).

Product delivery has been designed in close collaboration with land managers in order to complement their decision-making processes.

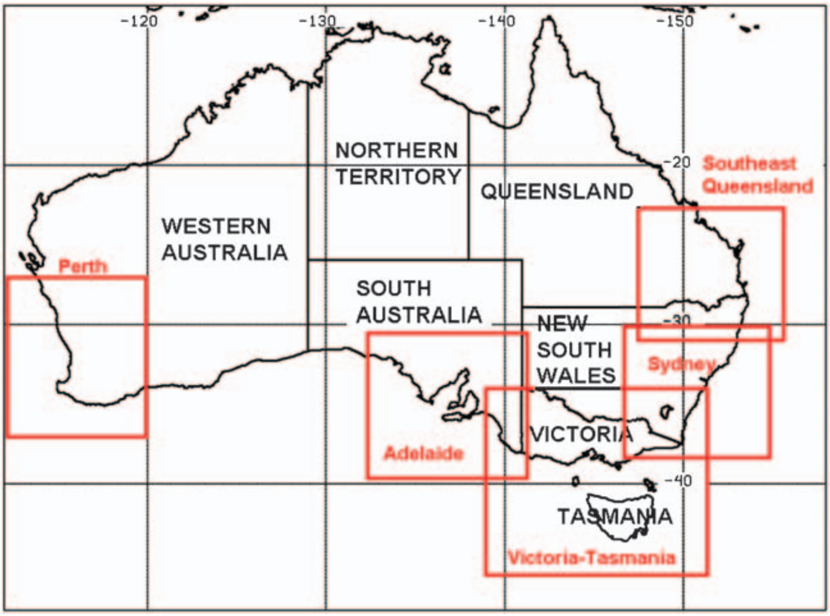

Figure 22.5. The Australian mesoscale domain. Smoke predictions are issued for the higher resolution 0.05° grid-spacing regions in red. State boundaries are in bold black, state names in bold black capitals, and the locally used descriptors for the high-resolution model domains are labeled in red.

The guidance is delivered via a password-protected Web site, with individual pages for each state. Within each state the land management agencies have nominated a number of locations representative of their major forestry operations for the coming season, which forms a set of fixed source points used throughout each prescribed burning season. The number of these fixed source points per state ranges from 6 (Tasmania) to 16 (Northern Territory). Dispersion forecasts are prepared based on each of these potential fire locations, with ignition times each day spanning the times during which fires would normally be lit. These times have been chosen by each state to suit their operational practices, with the earliest ignition time being 1000 local time and the latest 1600 local time, and with emission intervals of either 2 or 3 h.

Within each state, the dispersion prediction shows only three or four source points on a single display panel, to reduce the possibility of overlapping plumes making interpretation difficult—the guidance is intended to show where smoke from a single potential fire may impact, not the combined forecast concentrations from a number of actual fires.

A separate set of dispersion forecasts are issued for the country, based on hot spots identified in MODIS satellite imagery by Geosciences Australia using their Sentinel system (http://sentinel2.ga.gov.au/acres/sentinel/index.shtml). These are used to assist community understanding of the source of smoke from wildfires.

In Australia, the smoke prediction system is run twice a day based on the 0000 UTC and 1200 UTC meteorology. The 0000 UTC run completes early in the afternoon to provide guidance for broad decision making for the next day's burning program. Then, the 1200 UTC run executes overnight, and results are available in the early morning for finalizing whether to ignite a burn at sites provisionally selected the previous afternoon. The system also allows the land management agency to interactively change a standard burn location to one of particular interest before the 1200 UTC dispersion predictions are initiated.

A typical page from the guidance products is shown for Victoria in Fig. 22.6. The dispersion panel shows the average concentration between the surface and 1500 m from 1700 to 1800 EST, following a noon ignition. Roads, rivers, and townships are shown to assist planning. The presentation can be animated or stepped manually ("Manual Controls"), and the user can select an earlier or a later forecast base time (top left), an ignition time (upper left), or other station groups (middle left). There is a range of supplementary information that can be accessed through this page to assist the decision maker. In the lower left (the gray buttons), the user can select "Trajectories" (Fig. 22.6). Under this option a larger number of forward trajectories, representing the mid-line of the dispersion plumes, can be displayed, or alternatively, backward trajectories from "high impact" sites can be displayed. This latter form of guidance may indicate areas where fires should NOT be ignited if these sensitive locations are not to be impacted by smoke. In the upper portion of the panel there is provision for a forecaster to add interpretive comments to the guidance, and this facility is usually invoked only if a wind shift is mistimed by the model. This ensures consistency between these products and other fire weather meteorological forecasts. In the upper right of the panel forecast vertical wind, temperature, and humidity profiles at each of the source locations can be selected, and these include the predicted height of the mixed layer and the ventilation index at 3-h intervals.

22.4. Evaluation of real-time smoke prediction systems

Evaluation of smoke prediction systems is a complex task, and methodologies and techniques are continuing to evolve. Analysis of

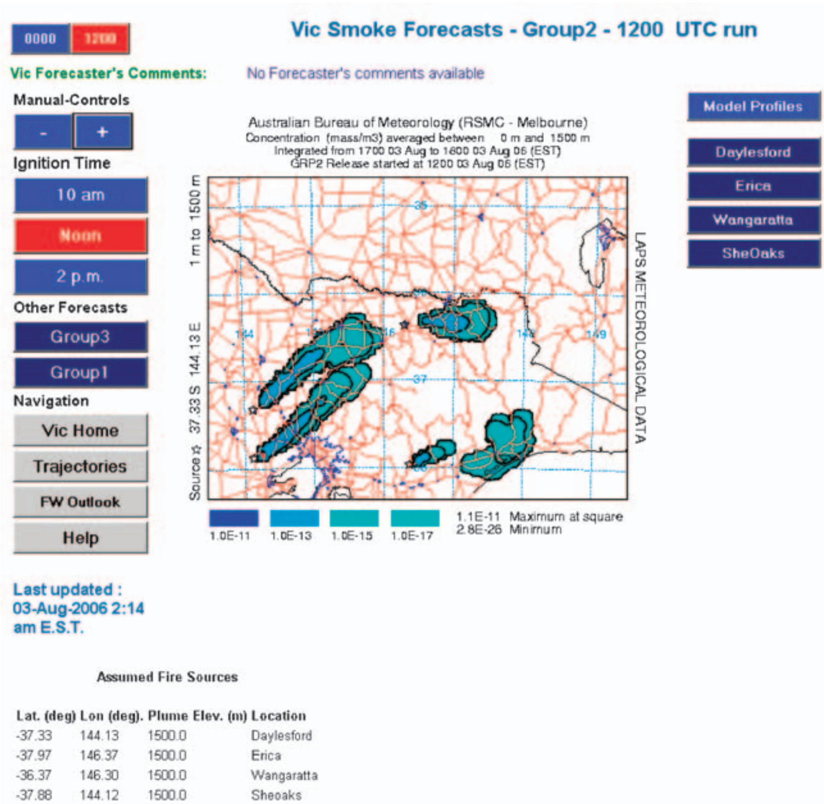

Figure 22.6. Predicted smoke concentrations (relative to a unit emission rate) averaged between the surface and 1500 m for August 3, 2006, from 1700 to 1800 EST for the Victoria, Australia, domain.

surface smoke concentrations are a primary concern because pollutants at the surface impact human and ecosystem health. However, limited ground-based measurements make it difficult to thoroughly evaluate model output, and model-to-point comparisons are complicated in complex terrain and confounded by the presence of other pollution sources. Satellite measures provide greater coverage, but are inherently limited to integrated measures of the entire atmospheric column. Additionally, apportioning the sources of error to the component models (fire activity, fuel loading, consumption, emissions, plume rise, dispersion, and transport) requires multiple case studies. This section details some of the techniques and results from a variety of evaluation efforts that have been performed.

Satellite imagery has proved very useful in monitoring smoke from the larger prescribed burns and wildfires, as long as the atmosphere is clear and the underlying surface and the smoke plume have different radiative properties. The best results using satellites are frequently obtained when the smoke plume is transported over the ocean, although there is still considerable uncertainty between the minimum concentration that a ground-based observer can discern and the smoke plume as seen in the imagery. A number of case studies of smoke dispersion from prescribed and wildfires are presented in Wain and Mills (2006).

Typically, two types of satellite data can be used in evaluation: Aerosol Optical Depth (AOD) measurements that represent a quantitative measure of integrated aerosol loading over the entire air column, and smoke plume extents. Because they integrate the entire air column, AOD observations require assumptions to allow allocation to specific heights in the atmosphere or require a vertically integrated result from the smoke prediction system for comparison, and this has limited its utility to date.

The NOAA-HYSPLIT real-time smoke prediction system uses the HMS smoke plume extents for evaluation. Figure 22.7 shows NOAA-HYSPLIT output alongside the HMS satellite smoke graphic and illustrates the basic evaluation metric—the "Figure of Merit in Space" (FMS), a fraction representing the ratio of the intersection to the union of

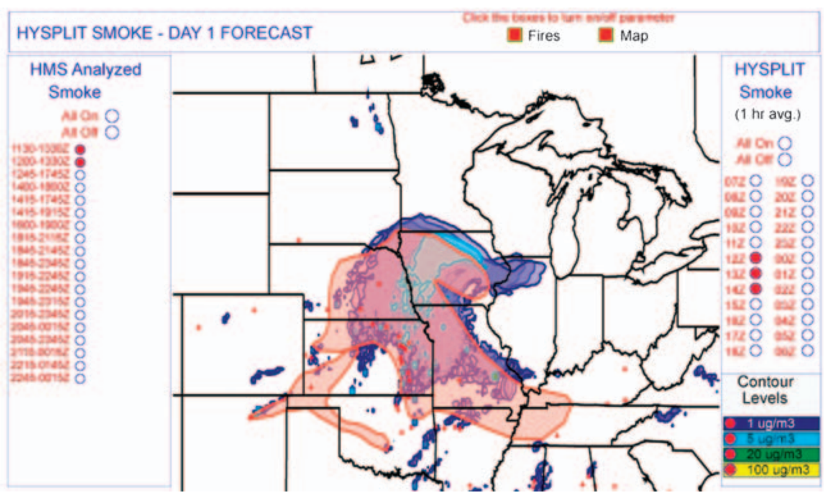

Figure 22.7. The 24-hour prediction for April 13, 2006, by the NOAA-HYSPLIT smoke prediction system available through the online archive, showing the model predictions at various concentration levels (blue and cyan) overlayed with the HMS observed smoke plume (red).

the analyzed and calculated smoke plume areas (higher is better). Because of uncertainties in fire detections and the possibility that some of the detected smoke is not due to the fire locations represented in the model, only smoke plumes with a non-zero overlap are included in the statistics. Furthermore, the FMS is computed for several concentration values (1, 5, 20, and 100 $\mu g/m^3$) because of uncertainties in the emissions and the threshold concentrations representing the visible edge of the HMS-analyzed smoke plume. Because it is not possible to assign a fixed threshold concentration to the HMS plume, the best verification contour may vary from day to day. Typical FMS values range from 10% to 20% for the 1 and 5 $\mu g/m^3$ contours. For instance, the FMS of the calculation shown in Fig. 22.7 is 15% when averaging all plumes with equal weights and 30% if the FMS is computed using an area weighting. A limitation of the FMS approach is that the statistic tends to show poorer performance than what might be suggested by a qualitative examination of the graphical smoke plume products. This is due to the fact that all nonoverlap plume regions result in an FMS of zero. Even for cases where there is complete overlap, if the measured or calculated plume is much larger than the other, the FMS will be reduced in magnitude. The NOAA-HYSPLIT real-time smoke prediction system regularly calculates both daily and 30-day running averages for real-time evaluation, allowing forecasters to judge the applicability of the current forecast based upon how well the fire locations and model predicted smoke compared with the actual smoke detection. Objective automated evaluation procedures are under investigation that use predicted grid point concentrations compared with satellite-derived aerosol optical depth values.

While satellite data can provide insight into overall performance, ground-based observations are also needed for predictive skill evaluation. In-situ monitoring networks of PM and trace gases can provide useful long-term evaluation data and are being used in several evaluation studies for the BlueSky, ClearSky, and Australian systems. Although such studies provide insight into overall predictive skill, they have several issues. Air Quality monitors are typically located at population centers, whereas agricultural and prescribed burning may only occur when concerned agency personnel judge that the approved burning will not significantly elevate $PM_{2.5}$ in those population centers (i.e., at the monitors). Thus, successful use of real-time smoke prediction systems should result in PM monitors showing no significant elevations in concentrations attributable to burning. Additionally, because these monitors are typically spaced hundreds of kilometers apart, many fires do not impact a monitor, and even when they do, the accuracy of the shape of the predicted plume cannot be judged. Thus, dedicated field campaigns are needed to obtain sufficient data downwind of active fires to characterize and evaluate system performance. Hess et al. (2006) discuss the use of in-situ monitors for evaluation of predictions from Australian wildfires.

Recent work (Liu et al., 2006) has shown that integration of basic fire behavior is necessary to simulate the larger wildfires. Many large wildfires are not a single convective column, but rather are multiple fire cores that are grouped together into a wildfire complex. Emissions from single convective column fires (single core) are released higher in the atmosphere relative to similar size fires that exhibit multiple convective columns (multiple core). Evaluation of the Rex Creek wildfire that occurred in 2001 in Washington State showed that simulating the wildfire as multiple smaller cores dramatically improved the results when comparing BlueSky model predictions with observations (Fig. 22.8). This fire behavior had

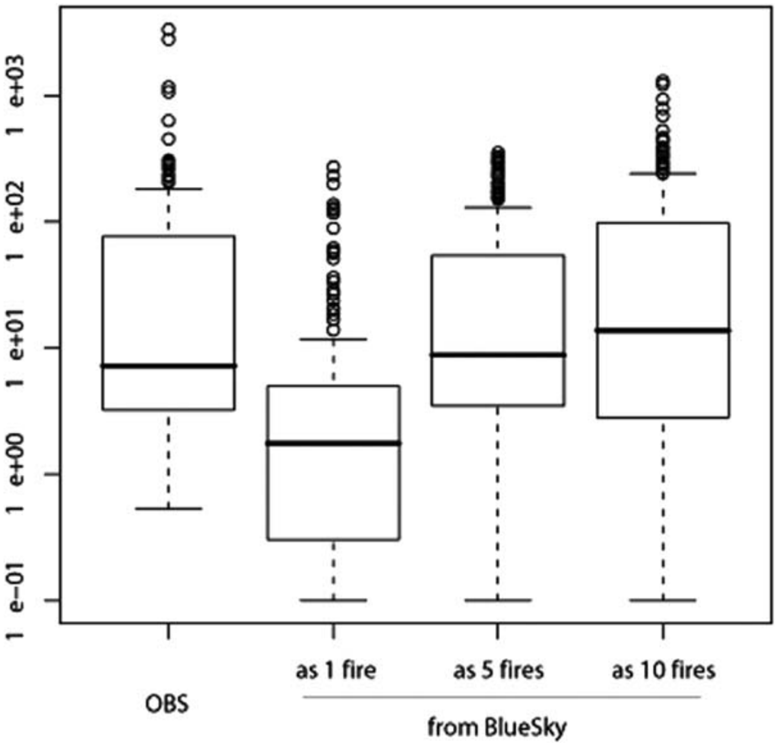

Figure 22.8. $PM_{2.5}$ concentrations near Twisp, Washington, for the Rex Creek fire for the period of August 19–26, 2001. Box-whisker plots show observed concentrations (OBS) and BlueSky concentrations for the one-fire, five-fire, and ten-fire cases. Values below 0.1 are set to 0.1 for plotting purposes.

greater impact on improving the prediction than various fuel models and consumption/emission algorithms (Larkin et al., 2008) and can be included in the forecasts without significant operational performance impact.

Evaluation of plume rise in ClearSky was undertaken in 2004, when plume rise measurements were made for four wheat stubble burns in Washington and five Kentucky bluegrass residue burns in Idaho (Heitkamp, 2006). Final plume height was measured by aircraft altimeter. ClearSky simulations were conducted for the nine field burns using plume rise parameterizations from Jain et al. (2007), based upon review of field burning studies conducted collaboratively by Air Sciences, Inc. (ASI), the USFS Missoula Fire Sciences Laboratory and Washington State University (Air Sciences, Inc., 2003, 2004). Figure 22.9 shows how for seven of the nine experiments, the ClearSky plume height results compared well to the observed plume heights.

22.5. Operational applications of a real-time smoke prediction system

Real-time smoke predictions have only become available in the last several years. While these systems were developed to address specific needs in forestry and agricultural burning, it is becoming clear that they possess utility far beyond their original purposes.

22.5.1. Prescribed fire and agricultural burning

Perhaps the clearest utility of real-time smoke predictions is in the decision process surrounding whether to ignite prescribed and agricultural fires. The goal is to provide the burner with information as to whether smoke from their fire, if ignited, will have impacts on sensitive receptors downwind or yield excessive concentrations. Past history has shown that these types of fires can have significant smoke impacts resulting in negative effects on health, public relations, and the acceptance of burning as a land management tool. The hope is that real-time smoke predictions can reduce such impacts and mitigate their negative consequences.

The Dutchler prescribed burn, which occurred approximately 20 miles (32 km) northwest of Salmon, Idaho, in September 2004, is an example of where a smoke prediction system could have been used to help mitigate smoke impacts. The plan was to burn over a period of 2 days, with 1000 acres burned on day one, and another 1200 acres on day two. However, smoke accumulated overnight in Salmon (population 3100), resulting in

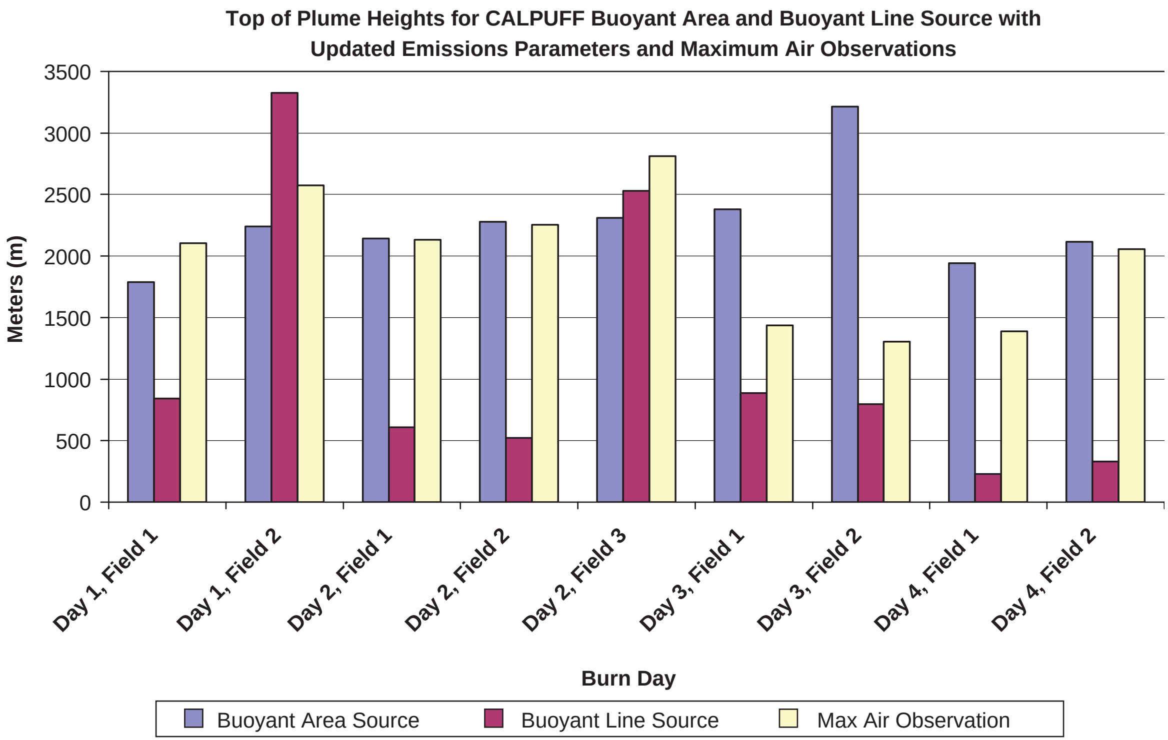

Figure 22.9. ClearSky plume rise results as calculated by CALPUFF, using updated plume rise parameters, and aircraft observed plume heights.

health complaints and multiple calls to city and county officials, prompting the mayor and county commissioner to contact land managers in charge of the burn. As a result, the second day's burn was cancelled, and considerable effort was necessary to repair relations with local officials and the public. Examination of BlueSky results, and in particular the trajectories from the burn and the ventilation index, yielded insights into what occurred. This is a region of very complex topography, and the burn was located in another valley away from the population center. The ventilation index was good for the afternoon period in the vicinity of the burn, but was marginal over Salmon. Afternoon trajectories showed smoke from the burn moving directly over the town. While mixing heights during the afternoon were high enough to not cause smoke problems, by 1700 local time the mixing height lowered and winds became calm, setting up conditions to trap smoke in the valleys as the burn continued to smolder into the evening. Analysis of BlueSky indicates that limiting the size of the burn or postponing to a period with more favorable ventilation conditions could have mitigated the impacts on the town and allowed the second day burn to occur. This case example illustrates that forecasting tools such as BlueSky that combine trajectories, $PM_{2.5}$ concentration fields, and meteorological data can be used to refine burn decisions, allowing land managers to accomplish their fuels reduction and ecosystem management goals while mitigating the impacts of smoke on sensitive receptors downwind.

The ClearSky agricultural smoke prediction was created in response to litigation regarding field burning in the northwestern U.S. Health and environmental activists brought suit against government and land owners, contending that smoke harms people both directly and indirectly. The State of Washington took the approach of banning the burning of the KBG stubble and operating a permit system for burning of wheat stubble. Idaho made the legislative finding that burning of KBG stubble is an economic necessity for KBG growers and thus administers a program overseeing such burning. Similarly, the Nez Perce Tribe administers its own smoke management program for field burning. ClearSky is consulted by these agencies as a key tool in their daily burn decision process.

22.5.2. Wildfires

Wildfires and wildland fire managed for resource benefits are naturally occurring or unplanned fires. Although firefighters have limited options for reducing smoke from wildfires, smoke prediction systems can be useful in managing fire operations, alerting the public to potential health risks and informing a public concerned about scenic vistas, recreation, road closures, and air operation impacts. Additionally, in the United States, the need to reintroduce fire into fire-adapted ecosystems after years of fire suppression along with limited fire fighting resources and concerns for fire fighter safety, has led to the concept of appropriate management response (AMR) when managing a wildfire. Under AMR, wildfires are managed by a suite of response options from full suppression to allowing it to burn for resource benefits. Smoke impacts to communities are an important consideration when managing a wildfire project and are monitored throughout the life of the project. Smoke prediction systems aid in this monitoring effort, as exemplified by a wildfire project in 2003 in the California Sierra Nevada. In this case, smoke management specialists were concerned about smoke from the fire entering the Sacramento Valley. By using BlueSky, they were able to ascertain that it was smoke from another fire further north that was impacting the valley, that smoke from their fire was going east over an unpopulated region of Nevada, and therefore mitigation strategies were not needed that particular day on the wildfire project.

Tactical decisions can also be based on smoke predictions. Burnout operations, which are deliberately ignited fires designed to prevent wildfire spread by reducing fuels and providing a fire break at a predetermined location, can be timed to have minimal smoke impacts. This was the case with the Square Lake fire near Leavenworth, Washington, in 2003, where a large-scale burnout (thousands of acres) was delayed because the prevailing winds would have carried the smoke into this tourist town during a holiday. Other tactical decisions include where to focus fire suppression efforts, what degree of effort should be employed, and timing of aircraft operations dependent on visibility.

22.5.3. Regulatory applications of smoke predictions

One application of smoke predictions is to track the source of smoke that may have caused (or could potentially cause) a negative impact. Some systems, such as the Australian system, allow calculation of backward trajectories to show likely source areas for smoke. In Australia, these backward trajectories are used to indicate which fires should not be ignited. Other systems require analysis and interpretation to determine which burns or fires may have contributed to a smoke event. In many cases it is the regulatory agencies that make the decision to allow or disallow burning on any given day. Of particular interest to regulatory agencies is the ability of smoke prediction systems to provide information about cumulative impacts caused by multiple burns. This provides an opportunity to open a dialogue among the various land management agencies about sharing the airshed and minimizing smoke impacts to communities.

22.5.4. Challenges

Development of these applications requires overcoming two important challenges: the collection of input data and the ability to produce a prediction that is timely enough to be useful. We discussed above the challenges associated with ground-based and satellite-based fire activity inputs, such as interagency data consistency issues in the ground-based systems and detection issues with the satellite-based systems. These challenges are being overcome as the two types of fire activity sources are merging to complement each other for the purposes of smoke forecasting.

One important application of smoke prediction systems is to make a go/no-go or tactical decision about a burn based on the potential for smoke impacts to a community or sensitive receptor. Such decisions are generally made early in the morning and require that all model processing be complete and output available to the decision maker by 6–8 A.M. In some cases decisions must be made the day before burning is scheduled, requiring a lead time of 48 h for the real-time smoke prediction system to gather the inputs and provide predictions suitable for decision support.

22.6. The future of real-time smoke prediction systems

The merging of existing fire science and air quality research into these real-time smoke prediction systems is proving useful to the agricultural, land, fire, smoke, and air quality management communities who regard these systems as providing useful guidance based upon the latest available science. Despite the wide application of these systems to prescribed fires, agricultural fires, and wildland fires, significant opportunities for future development remain. Two ways in which the usefulness of real-time smoke predictions can be improved is through advances in how the information is presented and by providing more accurate forecasts.

Users play an important role in how the results from the real-time smoke prediction systems are presented because smoke predictions must be tailored to a region. Some of these differences can be seen in the approaches of the four systems profiled here. BlueSky offers surface $PM_{2.5}$ concentrations as simple animations, and a variety of other meteorological, landuse, $PM_{2.5}$, and trajectory output products are available through the more complex RAINS GIS interface. The ClearSky and Australian systems were developed in close collaboration with a user community who regarded scenario-based output products as providing the best guidance. Therefore, these systems provide smoke concentration data based on where burns are most likely to be ignited and are not designed to capture exact $PM_{2.5}$ concentrations from fire across the region. The NOAA-HYSPLIT and BlueSky systems demonstrate that real-time smoke prediction systems can serve not only the fire community concerned with tactical decisions about fire but also the air quality community concerned about downwind impacts of smoke and all pollutant sources. The NOAA-HYSPLIT smoke prediction system at its inception was designed to be an interim tool until daily fire emissions could be made available to the NOAA national air quality prediction system (Otte et al., 2005), and daily wildfire emissions from BlueSky are being incorporated into the U.S. Pacific Northwest's AIRPACT-3 air quality prediction system (http://www.airpact-3.wsu.edu). BlueSky predictions are also being incorporated into the U.S. EPA's AirNow (http://www.airnow.gov) air quality prediction and monitoring portal. These output products and linkages are continually being updated to reflect the growing and changing needs of the user communities.

The usefulness of smoke predictions can also be improved by improving their accuracy, which involves improving the accuracy of the individual components and integrated field campaigns to obtain evaluation data. Smoke prediction systems are collections of models representing different pieces of information needed to generate the prediction—weather models, fire activity, fuel loading, consumption models, emissions models, plume rise algorithms, and dispersion/trajectory/transport models. Uncertainties are associated with each of the component models, making resulting errors challenging to analyze and diagnose. Yet determination of the uncertainties associated with a given prediction and dissemination of that information to the user community is necessary for these systems to be useful as decision-support tools. Therefore, understanding these uncertainties and how they relate to forecast skill needs to be a top priority of future development.

Evaluation of these systems has shown the importance of incorporating knowledge about fire behavior into the forecasts. Researchers at the USFS Missoula Forest Fire Laboratory (http://www.firelab.org/rsl/beowulf.htm) are working on incorporating the fire area simulator (FARSITE; Finney, 1998) model into a smoke prediction system utilizing the WRF model coupled with chemistry (WRF-Chem; Grell et al., 2005). Fire behavior also affects plume rise which determines the vertical allocation of the fire emissions in the atmosphere, thereby critically affecting overall surface concentrations (Larkin et al., 2008; Liu et al., 2006). Further research and development of methods of incorporating fire behavior into these real-time smoke prediction systems is necessary.

Accurate meteorological forecasts are critical because they determine direction and speed of the pollutant transport. Advances in meteorological forecasts—including ensembling techniques, improved planetary boundary layer schemes and land-surface models, and greater resolution—will improve the quality of the smoke prediction. The ClearSky results have shown that ensembling techniques can directly benefit smoke forecasts and allow for the calculation of the ensemble spread, a measure of forecast uncertainty.

Large fires can create their own fire weather by changing local wind patterns and temperature, and furthermore, emissions from fires can alter the radiative properties of the atmosphere. Clark et al. (2004) describe a fire-atmosphere model that couples fire dynamics with meteorology, where local winds are used to predict fire spread, and then the heat and moisture fluxes from the fire are fed back to the meteorology, allowing the fire to influence the local winds. Linn and Cunningham (2005) and Mell et al. (2007) have developed computational fluid dynamic models that explicitly simulate fuel/flame interactions and plume/atmosphere interactions. In addition, researchers at the Missoula Forest Fire Laboratory (http://www.firelab.org/rsl/beowulf.htm) are working with the WRF-Chem model (Grell et al., 2005) to fully couple the chemical solver within the meteorological model in order to account for atmospheric chemistry effects on the radiation budget and aerosol interactions with cloud formation. While implementation of many of these developments into real-time smoke predictions systems is further in the future, such work resolving fire/atmosphere feedback loops advances fundamental fire science and will eventually be beneficial operationally as computing resources improve.

Additionally, improvements to both ground-based fire tracking systems and satellite fire detection algorithms are necessary. Satellite detection of fire can provide a large-scale consistent data record; however, improvement is needed in the detection algorithms to more accurately detect small fires, remove confounding factors such as clouds, and accurately obtain an area estimate of fire size. Similarly, ground-based fire-reporting systems need improvement to augment and correlate with satellite data, provide the necessary inputs to the smoke prediction systems, and provide consistency across regions, systems, and agencies.

The quantity and type of emissions from fire are a function of the fuel combustion, which is largely driven by the method of ignition, the vegetation type, weather conditions, and fuel moisture. Most emission models, however, do not rely on combustion physics but rather empirical emission factors derived from field studies and therefore cannot represent all burn scenarios and conditions. Improving emissions models to take into account combustion physics, such as being empirically estimated by FEPS (Anderson et al., 2004) and explicitly modeled (Linn & Cunningham, 2005; Mell et al., 2007), is necessary.

Advances in smoke prediction systems will progress faster when more observational data are available to evaluate the systems and component models. Integrated field campaigns that measure trace gases and aerosols from the fire both near-field and far-field, fuel loadings and consumption, and fire spread, are necessary. Furthermore, ground-based measurements are not enough; a three-dimensional analysis of the plume as it advects and undergoes chemical transformation is necessary. Satellite data can also be used to evaluate smoke prediction models, as demonstrated by work done with the NOAA-HYSPLIT system. Research into correlating the column integrated aerosol optical depth satellite measurement with results from the smoke prediction systems is also needed.

The beauty and benefit of the systems profiled here is that each system has taken a different approach to meeting the needs of their users. Fundamentally, however, they all rely on similar fire science and air quality models. Thus, improvements to individual systems have benefits for all. Because of the interdisciplinary nature and scale of the challenges in creating timely, accurate, and usable smoke forecasts, significant advances will be more easily achieved through continued close collaboration regarding specialized field work, understanding of component interdependencies and uncertainties, and creation of new modeling and analysis schemes for plume rise and other critical issues. In this way smoke prediction is becoming a community-modeling enterprise.

ACKNOWLEDGMENTS

We acknowledge the four reviewers for reviews that greatly enhanced the quality of this manuscript. We would also like to thank and dedicate this chapter to Dr. Sue A. Ferguson whose vision and energy helped revolutionize fire/atmosphere research and create the community that supports it.

REFERENCES

Air Sciences Inc. 2003. Final Report: Cereal grain crop open field burning emissions study, Project 152-02. www.ecy.wa.gov/programs/air/pdfs/FinalWHeat_081303.pdf

Air Sciences Inc. 2004. Quantifying post-harvest emissions from bluegrass seed production field burning. www.ecy.wa.gov/programs/air/pdfs/Bluegrass_final_report.pdf

Anderson, G.K., Sandberg, D.V., and Norheim, R.A. 2004. Fire emission production simulator (FEPS) user's guide version 1.0. http://www.fs.fed.us/pnw/fera/feps

Andreae, M.O., and Merlet, P. 2001. Emission of trace gases and aerosols from biomass burning. Global Biogeochem. Cy. 15(4), 955–966.

Battye, W., and Battye, R. 2002. Development of emissions inventory methods for wildland fire. US Environmental Protection Agency. www.epa.gov/ttn/chief/ap42/ch13/related/firerept.pdf

Bey, I., Jacov, D.J., Yantosca, R.M., Logan, J.A., Field, B., Fiore, A.M., Li, Q., Liu, H., Mickley, L.J., and Schultz, M. 2001. Global modeling of tropospheric chemistry with assimilated meteorology: Model description and evaluation. J. Geophys. Res. 106, 23073–23096.

Breyfogle, S., and Ferguson, S.A. 1996. User assessment of smoke-dispersion models for wildland biomass burning. USDA Forest Service, Pacific Northwest Research Station, General Technical Report, PNW-GTR-379, December 1996.

Briggs, G.A. 1969. Plume rise, US Atomic Energy Commission. TID-25075, NTIS, Springfield, VA, 81 pp.

Byun, D.W., and Schere, K.L. 2006. Review of the governing equations, computational algorithms, and other components of the Models-3 community multiscale air quality (CMAQ) modeling system. Appl. Mech. Rev. 59, 51–77.

Cetegen, B.M., Zukoski, E.E., and Kubota, T. 1982. Entrainment and flame geometry of fire plumes, Report NBS-GCR-82-402, Center for fire research, national Bureau of Standards, Gaithersburg, MD.

Clark, T.L., Coen, J., and Latham, D. 2004. Description of a coupled atmosphere-fire model. Int. J. Wildland Fire 13(1), 49–63.

Cohen, J.D., and Deeming, J.E. 1985. The National Fire-Danger Rating System: Basic Equations. PSW GTR PSW 82 16p.

Draxler, R.R., and Hess, G.D. 1997. Description of the HYSPLIT_4 modeling system. NOAA Tech. Memo. ERL ARL-224, 24p. [NTIS PB98-116593].

Draxler, R.R., and Hess, G.D. 1998. An overview of the HYSPLIT_4 modeling system for trajectories, dispersion, and deposition. Aust. Meteorol. Mag. 47, 295–308.

Finney, M.A. 1998. FARSITE: Fire area simulator—Model development and evaluation. USDA Forest Service, Rocky Mountain Research Station, Research Paper RMRS-RP-4 Revised.

Grell, G.A., Dudhia, J., and Stauffer, D.R. 1994. A description of the fifth-generation Penn State/NCAR Mesoscale Model (MM5). NCAR Technical Note, NCAR/TN-398+STR. Mesoscale and Microscale Meteorology Division, National Center for Atmospheric Research, Boulder, CO.

Grell, G.A., Peckham, S.E., Schmitz, R., McKeen, S.A., Frost, G., Skamarock, W.C., and Eder, B. 2005. Fully coupled online chemistry within the WRF model. Atmos. Environ. 39, 6957–6975.

Heitkamp, K. 2006. Evaluation of the ClearSky smoke dispersion ensemble forecast system for agricultural field burning in Eastern Washington and Northern Idaho, M.S. Thesis, Department of Civil and Environmental Engineering, Washington State University, Pullman, WA. 115 pp.

Hess, G.D., Tory, K., Lee, S., Wain, A.G., and Cope, M. 2006. Modeling the King Island bushfire smoke. Aust. Meteorol. Mag. 55(2), 93–103.

Jain, R., Vaughan, J., Heitkamp, K., Ramos, C., Claiborn, C., Schreuder, M., Schaaf, M., and Lamb, B. 2007. Atmos. Environ. 41(32), 6745–6761, Oct 2007.

Janjic, Z.I. 2003. A nonhydrostatic model based on a new approach. Meteorol. Atmos. Phys. 82, 271–285.

Kalnay, E., Kanamitsu, M., and Baker, W.E. 1990. Global numerical weather prediction at the national meteorological center. Bull. Amer. Meteorol. Soc. 71, 1410–1428.

Knapp, K.R. 2002. Aerosol optical depth retrieval from GOES-8: Uncertainty study and retrieval validation over South America. J. Geophys. Res. 107(D7), doi:10.1029/2001JD00505.

Larkin, N.K., O'Neill, S.M., Solomon, R., Krull, C., Raffuse, S., Rorig, M., Peterson, J., and Ferguson, S.A. 2008. The BlueSky smoke modeling framework. Accepted to Int. J. Wildland Fire.

Linn, R., and Cunningham, P. 2005. Numerical simulations of grass fires using a coupled atmosphere-fire model: Basic fire behavior and dependence on wind speed. J. Geophys. Res. 110, D13107, doi:10.1029/2004JD005597.

Liu, Y., Achtemeier, G., and Goodrick, S. 2006. Modeling air quality effects of prescribed burn in Georgia with CMAQ-Daysmoke. Proceedings of the workshop on agricultural air quality, ESA, p. 129.

Mass, C.F., Albright, M., Ovens, D., Steed, R., Grimit, E., Eckel, T., Lamb, B., Vaughan, J., Westrick, K., Storck, P., Coleman, B., Hill, C., Maykut, N., Gilroy, M., Ferguson, S., Yetter, J., Sierchio, J.M., Bowman, C., Stender, D., Wilson, R., and Brown, W. 2003. Regional environmental prediction over the Pacific Northwest. Bull. Amer. Meteorol. Soc. 83(10), 1–2.

McKenzie, D., Raymond, C.L., Kellogg, L.-K.B., Norheim, R.A., Andreu, A.G., Bayard, A.C., Kopper, K.E., and Elman, E. 2007. Mapping fuels at multiple scales: Landscape application of the fuel characteristic classification system. Can. J. For. Res. 37(12), 2421–2437.

Mell, W., Jenkins, M.A., Gould, J., and Cheney, P. 2007. A physics based approach to modeling grassland fires. Int. J. Wildland Fire 16(1), 1–22.

Mesinger, F., Janjic, Z.I., Nickovic, S., Gavrilov, D., and Deaven, D.G. 1988. The step-mountain coordinate: Model description and performance for cases of Alpine lee cyclogenesis and for a case of Appalachian redevelopment. Mon. Wea. Rev. 116, 1493–1518.

O'Neill, S.M., Hoadley, J.L., Ferguson, S.A., Solomon, R., Peterson, J., Larkin, N.K., Peterson, R., Wilson, R., and Matheny, D. 2005. Applications of the BlueSkyRAINS smoke prediction system, EM. Air and Waste Management Association, September, 20–23.

Otte, T.L., G. Pouliot, G., Pleim, J.E., Young, J.O., Schere, K.L., Wong, D.C., Lee, P.C.S., Tsidulko, M., McQueen, J.T., Davidson, P., Mathur, R., Chuang, H.-Y., DiMego, G., and Seaman, N.L. 2005. Linking the Eta model with the community multiscale air quality (CMAQ) modeling system to build a national air quality forecasting system. Wea. Forecast. 20, 367–384.

Pouliot, G., Pierce, T., Benjey, W., O'Neill, S.M., and Ferguson, S.A. 2005. Wildfire emission modeling: Integrating BlueSky and SMOKE. In: 14th international emission inventory conference, 4/11-14/2005, Las Vegas, NV.

Puri, K., Dietachmayer, G.D., Mills, G.A., Davidson, N.E., Bowen, R.A., and Logan, L.W. 1998. The new BMRC limited area prediction system (LAPS). Aust. Meteor. Mag. 47, 203–223.

Reid, J.S., Prins, E.M., Westphal, D.L., Christopher, S., Schmidt, C., Richardson, K.A., Theirsen, M., Reid, E.A., and Eck, T. 2001. Flambe: The fire locating and modeling of burning emissions project. Presented at the Fall meeting of the American Geophysical Union, San Francisco, CA.

Ruminski, M., Kondragunta, S., Draxler, R., and Zeng, J. 2006. Recent changes to the hazard mapping system. In: 15th international emission inventory conference—"Reinventing inventories-new ideas in New Orleans", EPA on-line proceedings. http://www.epa.gov/ttn/chief/conferences.html

Sandberg, D.V., and Peterson, J. 1984. A source-strength model for prescribed fires in coniferous logging slash. In: Proceedings, 21st annual meeting of the Air Pollution Control Association, Pacific Northwest International Section. Air Pollution Control Association, Pittsburgh, PA.

Sandberg, D.V, Hardy, C.C., Ottmar, R.D., Snell, J.D.K., Acheson, A.L., Peterson, J.L., Seamon, P., Lahm, P., and Wade, D. 1999. National strategic plan: modeling and data systems for wildland fire and air quality. USDA Forest Service, Pacific Northwest Research Station, General Technical Report PNW-GTR-450, February.

Scire, J.S., Strimaitis, D.G., and Yamartino, R.J. 2000. A user's guide for the CALPUFF Dispersion Model (version 5). Earth Tech Inc., Concord, MA.

Skamarock, W.C., Klemp, J.B., Dudhia, J., Gill, D.O., Barker, D.M., Wang, W., and Powers, J.G. 2005. A description of the advanced research WRF Version 2. NCAR Technical Note (NCAR/TN-468+STR).

Vaughan, J., Lamb, B., Wilson, R., Bowman, C., Kaminsky, C., Otterson, S., Boyer, M., Mass, C., Albright, M., Koenig, J., Collingwood, A., Gilroy, M., and Maykut, N. 2004. A numerical daily air-quality forecast system for the Pacific Northwest. Bull. Amer. Meteorol. Soc. 85, 549–561.

Wain, A.G. 2006. Smoke plume behavior—variable source heights. Australasian Fire Authorities Council/Bushfire Cooperative Research Centre Annual Conference 2006, Melbourne Australia. www.bushfirecrc.com/publications/melb_2006_posters_progb.html

Wain, A.G., and Mills, G.A. 2006. The Australian smoke management forecast system. BMRC Research Report No. 117. Bureau of Meteorology Research Centre, Box 1289K Melbourne, Australia. 54pp. www.bom.gov.au/bmrc/pubs/researchreports/RR117.pdf

Ward, D. 2001. Chapter 3: Combustion chemistry and smoke. In: Johnson, E.A., and Miyanishi, K., eds. Forest Fires, Behavior and Ecological Effects. Academic Press, New York, pp. 55–77.

Developments in Environmental Science, Volume 8 535
A. Bytnerowicz, M. Arbaugh, A. Riebau and C. Andersen (Editors)

ISSN: 1474-8177/DOI:10.1016/S1474-8177(08)00023-5

Chapter 23

Managing Smoke from Wildfires and Prescribed Burning in Southern Australia

Alan Wain, Graham Mills, Lachlan McCaw and Timothy Brown*

Abstract

In Australia the responsibility for management of forests and other public lands rests largely with state governments, and multiple government agencies may be involved in fire management. Whether resulting from wildfire, fuel reduction, or silvicultural operations, biomass burning often stimulates community concerns about hazards from fine particulates and chemical compounds contained in smoke. Management practices and community perceptions of smoke from biomass burning differ from region to region according to social and environmental factors. Recognition of the need for a response to concerns has led to the development of a smoke management research program within the Bushfire Cooperative Research Centre, in conjunction with fire and land management agencies and the Australian Bureau of Meteorology (the Bureau). This program aims to assist land management planning by predicting where smoke from scheduled burns would be transported, thus providing the opportunity to avoid burning in situations where there is potential for adverse community impact. The primary tool provided is a dispersion model forecast using input from the Bureau's operational mesoscale numerical weather prediction (NWP) models. Decision tools are applied in a similar manner for prescribed burning and wildfires and have been used by agencies to provide community advice and to avoid smoke hazards during aircraft operations. We investigated strategies used by land management agencies to minimize community impact of smoke from prescribed burns, and studied the way in which the dispersion model forecasts are integrated into their decision support systems. Included

*Corresponding author: E-mail: A.Wain@bom.gov.au

are details of HYbrid Single Particle Lagrangian Integrated Trajectory's (HYSPLIT) configuration, several examples of its use in prescribed and wildfire events, and the research direction being pursued to improve both the quality of the dispersion forecasts and to enhance the use of these forecasts in agency planning.

23.1. Introduction

We describe the development and implementation of smoke dispersion forecasting in southern Australia representing areas of the continent below latitude 30°S including the southern third of Western Australia, most of South Australia and New South Wales (NSW), and all of Victoria and Tasmania (Fig. 23.1). We focus on this region because it includes six of the nation's capital cites, the majority of Australia's population, and much of the transport and industrial infrastructure on which the nation depends. The socio-economic setting of southern Australia, in combination with the generally fire-prone nature of the landscape, results in a situation where management of smoke from fires in native vegetation is an important and topical issue for land managers, the

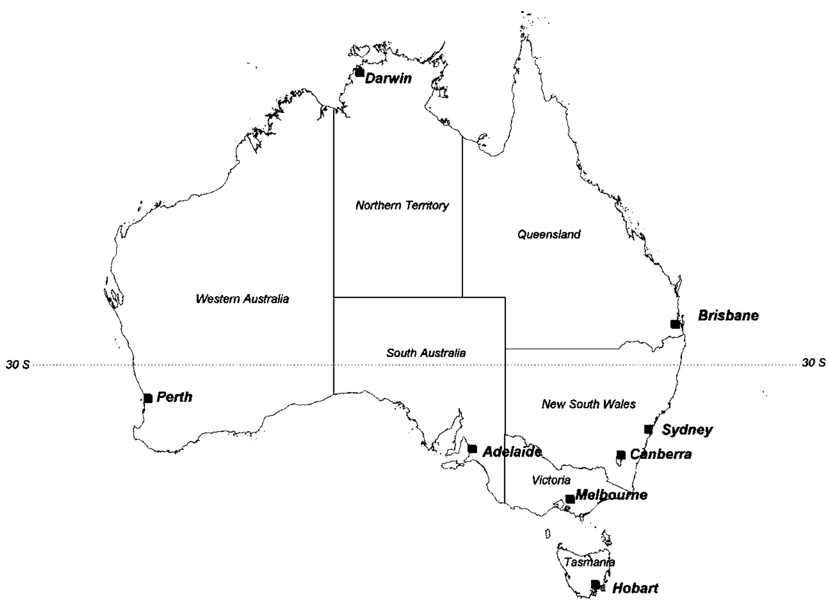

Figure 23.1. Map of Australia showing state boundaries and capitals.

community, and governments. Notwithstanding this, fires in the vast rangelands and tropical savannas of northern Australia contribute the majority of Australia's fire-related emissions of greenhouse gases, particulates, and volatile organic compounds (Australian Greenhouse Office, 2006; Meyer et al., 2004).

Large areas of southern Australia are managed for agricultural land uses including dryland cereal cropping, grazing, and irrigated horticulture. Agricultural landscapes are typically flat to gently undulating with small remnants of the original woodland vegetation dispersed amongst broadacre paddocks of introduced crops and annual grasses. Pastoralism for sheep and cattle production is also widespread in semi-arid areas with annual rainfall below 350 mm. Tall forests, comprised predominantly of eucalypts, occur in association with the Great Dividing Range that rises to elevations above 2000 m and extends northeast from Melbourne, through the Australian Capital Territory and into northern New South Wales, where it forms a distinct escarpment separating elevated tablelands from coastal lowlands. Much of Tasmania is mountainous and heavily forested, with eucalypt forests giving way to temperate rainforest in high rainfall areas on the western half of the island. Eucalypt forests also occur in the southwest corner of Western Australia extending southwards from Perth to Albany in areas where annual rainfall exceeds 600 mm.

The climate of southern Australia is dominated by the subtropical band of high pressure that migrates north and south across the southern half of the continent with the change of seasons. During the winter months, cold fronts embedded within moist westerly and southerly winds on the southern side of the subtropical ridge bring rainfall to areas up to several hundred kilometers inland. Annual rainfall declines and becomes more variable with increasing distance from the coast, although occasional heavy summer rainfall may result from decaying tropical cyclones. Southerly areas experience a summer/autumn fire season with fire danger highest from December to March, whereas much of eastern NSW experiences peak fire danger during spring (Luke & McArthur, 1978). Fire regimes in forested landscapes of southern Australia have recently been reviewed by Gill and Catling (2002).

State government agencies are responsible for managing a high proportion of the forest and other remaining native vegetation in southern Australia (National Forest Inventory, 2003). Multiple-use forestry is practiced on state forests, with national parks and other categories of land reserved for nature conservation and recreation. Land management agencies operate within a framework of state legislation governing fire protection and emergency response in rural landscapes and are responsible for integrating fire with land uses and for responding to unplanned fire events (wildfires).

Prescribed fire is used for a range of purposes, including regenerating forests after timber harvesting, managing wildlife habitat, and limiting the accumulation of flammable litter and understorey fuels in order to reduce the intensity and suppression difficulty of unplanned fires. Forest regeneration burning is generally confined to harvested areas and adjacent buffer strips that may be on a scale of tens, and sometimes hundreds, of hectares. Burning is often conducted under dry conditions at the end of the summer in order to maximize consumption of large woody debris and creation of ashbeds favorable for eucalypt seedling establishment. Ignition techniques and burning conditions conducive to strong convective activity may be used to generate intense fires (Tolhurst & Cheney, 1999).

In contrast, prescribed fires implemented to reduce fuel loads in forests and other vegetation types are typically of low to moderate intensity ($< 3000\,\mathrm{kW\,m^{-1}}$; Cheney, 1980) and are lit under stable atmospheric conditions. The scale of prescribed fires used to reduce fuel loads varies from limited burning around high value built assets and urban interface zones to landscape scale application of strategic burning programs. Prescribed fire can be applied to thousands of hectares in a single day using aerial incendiaries under suitable conditions of weather, terrain, and forest type. Aerial ignition was introduced in the late 1960s following a period of intensive research and development into fire behavior prediction and aerial ignition technology (McCaw et al., 2003; Packham & Peet, 1967). The extent of prescribed burning conducted for fuel and habitat management purposes varies considerably from year to year according to seasonal conditions. Typically, 150,000–200,000 ha per annum are burnt in southwest Western Australia, predominantly during the spring months (October to December). In the southeastern states including Tasmania prescribed burning tends to be undertaken during autumn (March to May) with an aggregate area of 100,000–150,000 ha per annum across Victoria, NSW, and Tasmania. Until recently, the use of prescribed burning in land management has been very limited in South Australia. Increasingly, burning prescriptions are seeking to create mosaics of burnt and unburnt vegetation within a designated management area to better accommodate biodiversity conservation objectives (Burrows, 2004). This may require ignition to be conducted in a dispersed pattern over a large area and staged over a period of days or weeks to optimize burning conditions for fuel types that dry at different rates.

Australia's population is concentrated in large coastal cities, and the proportion of the population living in traditional rural communities continues to decline. At the same time, major cities are experiencing rapid growth of peri-urban communities at the interface with agricultural lands and native vegetation under public or private ownership (Cottrell, 2005). This trend has important implications for fire management, including an increasing risk to peri-urban communities from wildfires and changing community expectations in relation to environmental factors including air quality and visibility. Rural communities dependent on agriculture or forestry tend to be more tolerant of occasional inconvenience from smoke than do peri-urban communities sustained by manufacturing and service industries. Smoke haze events from prescribed burning that affect major urban centers can also provide a catalyst for broader debate within the community about the perceived impacts of prescribed fire on the environment and its effectiveness in reducing the scale and severity of wildfires (Esplin et al., 2003). Away from the urban interface, other rural land users including viticulturalists and tourism operators may have an expectation that smoke from prescribed burning will not unduly impact their activities at critical periods of the year. Currently, there is no attempt to regulate or manage smoke dispersal from burning on agricultural lands or private forests even though it may contribute substantially to the volume of smoke in the atmosphere in some years, particularly during late autumn when stubble is burnt prior to sowing of cereal crops.

The importance of managing smoke from prescribed burning was realized at the outset of the aerial burning program in Australian forests, with initial research seeking to characterize the composition of bushfire smoke, its dispersal, and its ultimate fate in the environment (Vines et al., 1971). Further studies quantified the amounts of nitrogen dioxide (NO_2) and sulfur dioxide (SO_2) in smoke and the extent of ozone formation on the top of the smoke plume (Evans et al., 1976), the latter being of potential concern because of its role in photochemical smog (Evans et al., 1974; Rye, 1995). Recognizing the need to avoid smoke accumulation over airports and major population centers, some agencies developed decision models based on basic weather factors (current and future wind direction, inversion strength), scale of proposed burning, and distance from the proposed burn to the impact area (Sneeuwjagt & Smith, 1995). Preliminary research by the Australian Bureau of Meteorology (the Bureau) also demonstrated that useful forecasts of smoke transport could be achieved by combining mesoscale numerical weather predictions (NWPs) with a transport model (Mills et al., 1996). This led to an initial agreement in 2000 between the Australasian Fire Authorities Council and the Bureau for a project to develop a system to aid decision making for smoke management from prescribed burning. This chapter describes the subsequent research conducted by the Bushfire Cooperative Research

Centre to integrate dispersion model forecasts into fire management support systems.

23.2. Forecasting smoke dispersion

The smoke dispersion forecasting system developed for southern Australia consists of a 12-hour dispersion forecast based upon meteorology from a mesoscale NWP model delivered via the World Wide Web (WWW). Smoke forecasts began as a trial program in three states during 2001 and were expanded to a national coverage in 2004.

23.2.1. Meteorology

The meteorological information required for the smoke dispersion forecasts is obtained from NWP model fields. The Bureau operates a hierarchical suite of limited area NWP systems over Australia, with latitude/longitude grid resolutions ranging from 0.375° to 0.05°. These are all variations of the Limited Area Prediction Scheme (LAPS) system described by Puri et al. (1998). Until March 2006, smoke dispersion forecasts for all Australian states utilized the 0.125° grid version of meso-LAPS, this being the highest resolution configuration covering the entire continent. Having 29 levels, with some 10 levels below 1500 m above the surface, 48-hour forecasts are calculated twice daily at 0000 and 1200 UTC. The full atmospheric state is output every 3 h of the model integration. In March 2006 the staged implementation of the 0.05° grid version began. This model version is available for limited areas of Australia on independent grids generally co-incident with capital cities. Its initial conditions are derived from the 0.375° LAPS, and the operational version currently has 29 vertical levels, with the horizontal grid spacing of 0.05° equating to a distance of approximately 5 km. Areas not covered by the 0.05° meso-LAPS will continue to use data from the 0.125° version.

23.2.2. Transport-dispersion model

The transport and dispersion model used is version 4 of the HYbrid Single Particle Lagrangian Integrated Trajectory (HYSPLIT) modeling system (Draxler & Hess, 1997). This model is a hybrid Lagrangian/Eulerian transport and dispersion model, with the advection and diffusion calculations performed in a Lagrangian framework, and the concentrations calculated on an Eulerian grid. Diffusion is modeled in a combined particle/puff formulation to take advantage of the increased accuracy in the vertical diffusion calculation of the particle formulation, and of the efficiency of the puff formulation in the horizontal diffusion.

The HYSPLIT model is highly configurable. For operational smoke forecasts the concentration grid is specified with a horizontal spacing of 0.05° and four levels at 10, 150, 500, and 1500 m. While near-surface concentrations are most important for determining possible adverse community impact, it was found that the most useful product for verification, particularly when comparing forecasts with remote sensing data, was given by the average concentration through the four vertical levels of the concentration grid. To provide quantitative forecast guidance it is necessary to specify a source plume for the prescribed burn, both in terms of a source concentration and of an initial plume rise. It quickly became apparent that the current degree of uncertainty in the amount of fuel to be burnt and its moisture content made the calculation of plume rise from any individual planned burn unrealistic. In addition, emissions models for these burns were not available, meaning that source particulate concentrations could not be specified. Accordingly, for the first version of the system, an arbitrary source concentration of one dimensionless unit was specified. Forecast concentrations are relative to that arbitrary value. Contour intervals for concentration plots were then selected such that the outermost contour roughly coincided with the "edges" of the visible smoke plume based on some early field observations provided by participating agencies, and the forecast relative concentration plots are interpreted in this way by the agencies. The plumes are specified to be 1500 m in height, chosen because this approximates the typical height of the subsidence inversion that is a common feature during the ideal prescribed burning conditions of clear-sky conditions with light winds. Case studies (Wain & Mills, 2006) indicate some more problematic forecasts could be improved if the height of the smoke plume is set to the depth of the diurnally varying mixed layer from the meso-LAPS model. An amended version of HYSPLIT, which contains this formulation, has been tested and implemented in selected states. However, the latest revision of the software, HYSPLIT 4.8, contains provision for plume rise calculations that utilize the buoyancy terms of Briggs' equations and the total heat output of a fire. While testing of this new feature is in progress, the lack of fuel data noted earlier may limit its usefulness to research applications.

23.2.3. Timing

Each state has determined a number of locations representative of forest management areas where prescribed burns are planned. Dispersion forecasts are prepared based on each of these potential fire locations, with three ignition times each day spanning the times during which fires would normally be lit. These times have been chosen by each state to suit their operational practices, with the earliest ignition time being 1000 local time (0000 UTC), and the latest 1600 local time (0600 UTC) with either 2 or 3 h between each time. Forecasts are grouped regionally, but with only two or three source points on each display panel in order to minimize the possibility of overlapping plumes reducing the clarity of the guidance. The number of source points per state ranges from 8 to 12. In the early afternoon, forecasts based on the 1000 local time NWP model run are prepared for ignition times "tomorrow." This guidance is intended for use in broad decision making regarding the next day's burning program. As the forecast is already some 24 h in the future at the initiation of the modeled smoke plume, and with the expectation of a later forecast generally being more accurate than an earlier one, a later set of runs based on the 2200 local time NWP model forecast, is prepared overnight. These are available at the commencement of final planning in the early morning, and are intended to be used for final "yes or no" decisions at particular sites. A feature of the system is that an agency can interactively change the coordinates of a source point to a particular location of interest before the 1200 UTC NWP forecast is run. Thus, if a planned burn of particular interest lies between two of the standard ("fixed") points and it is considered that these points may not be representative of the desired point, then the source position can be amended via the submission of a Web-based form.

23.2.4. Operational products

The smoke dispersion forecasts are provided as a set of graphical products delivered via the WWW from a secure section of the Bureau's Web server to which only user agencies have access.

The basic forecast product (Fig. 23.2) shows multiple smoke plumes that are contoured according to their relative concentration levels and each contour is shaded to aid in discrimination. The contours overlay a reasonably detailed map background containing the locations of major roads, coastline, and built-up areas. The initial display is currently in the form of an animated gif file. Manual controls are provided to allow users to step through the forecast. Navigation buttons provide access to alternate start times and locations, other information pages, and forecast atmospheric profiles that are generated for each starting point.

The latter are aerological diagrams of the skewT-logP form (tephigrams) (Fig. 23.3). These are provided for each source location at 3-hour intervals through the forecast period. Derived from the meso-LAPS

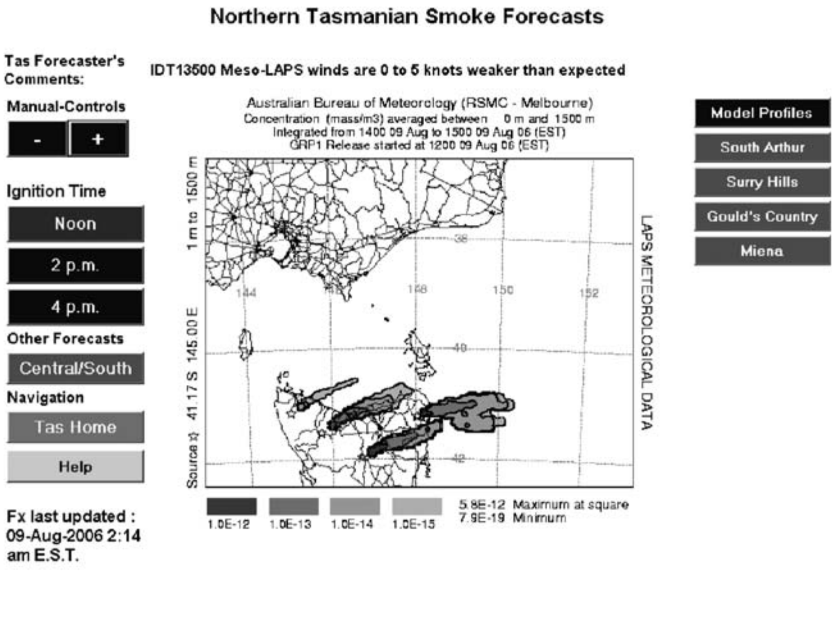

Lat. (deg)	Lon (deg).	Plume Elev. (m)	Location
-41.17	145.00	1500.0	South Arthur
-41.52	145.72	1500.0	Surrey Hills
-41.23	148.05	1500.0	Goulds Country
-41.98	146.70	1500.0	Miena

Figure 23.2. Operational smoke forecasts for Northern Tasmania.

model, the forecast vertical profiles shown in these diagrams provide users with forecasts of additional fire weather information, such as stability, inversion height, and vertical profiles of wind speed and direction and temperature. A ventilation index is also calculated and printed in the top right of the diagram. Derived from a similar U.S. index (Ferguson, 2001), this provides users with an indication of the expected ability of the atmosphere to disperse any smoke (or other pollutant) at the time of the forecast.

Forward trajectories track the projected route followed by a hypothetical parcel of air. Since the inception of the smoke forecasting system, Victoria has utilized forward trajectory forecasts from 18 locations across the state. The path followed by a forward trajectory is equivalent to the centerline of a plume dispersion forecast calculated from the same point. Trajectories require much shorter computation times, an attractive feature when considering many source points.

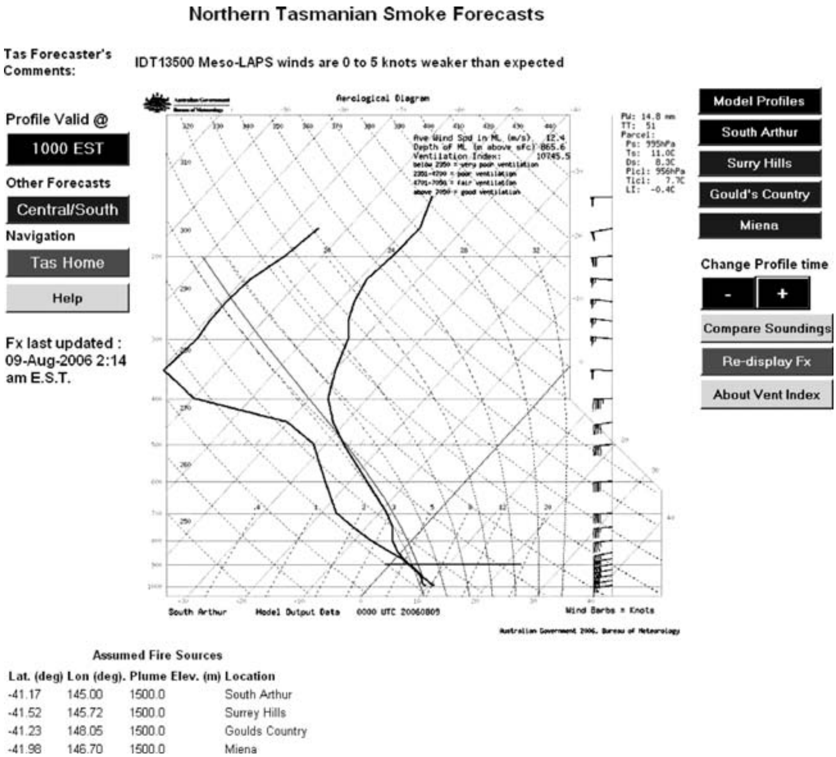

Figure 23.3. Aerological diagram of smoke forecasts for Northern Tasmania derived from model data.

While not part of the basic smoke dispersion forecasting system, backward trajectories have been widely used in air pollution studies to identify potential pollutant source regions, and as such are a very useful aid to decision making. During the Melbourne Commonwealth Games forecast back trajectories were calculated for several vertical levels at 3-hourly intervals from all major games locations (Fig. 23.4). This assisted in planning for prescribed burns by identifying where the air reaching the games venues was coming from over the forecast period.

Perhaps the most important aid to informed decision making is suitable training. A recent survey of land managers highlighted the need for general meteorological and smoke-specific training within their organizations. An html-based modular instruction guide has been designed to provide users information on basic meteorology, stability, and the models used to create the forecasts. In the final section all this information is used

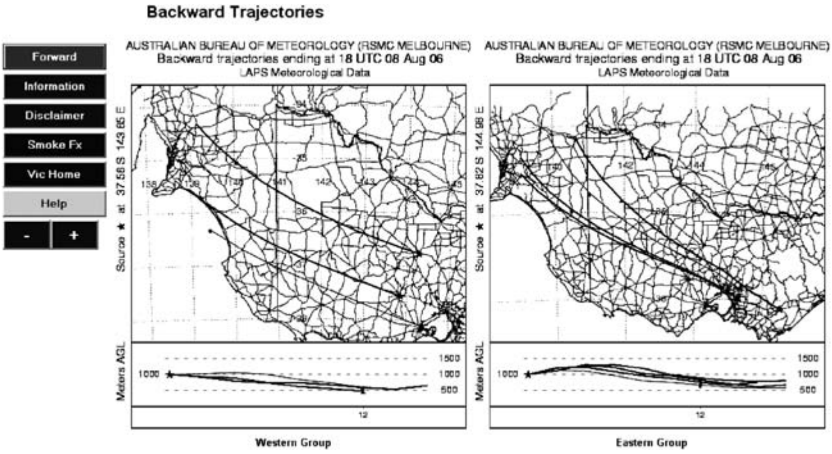

Figure 23.4. Backward trajectories from Commonwealth Games venues in Victoria.

to demonstrate to the user how the various products should be used and interpreted. The wider dissemination of this guide via the Web together with more formal training sessions is planned.

Another forecast aid end-users have identified as invaluable is the comment by operational weather forecasters regarding the validity of the underlying meso-LAPS model data. Initially these were very brief descriptions, such as "Meso-LAPS winds are 5–10 knots stronger than expected." However the inclusion of more detailed comments including details of inversion heights and wind shifts has made them a very useful aid to users in assessing the likely accuracy of smoke forecasts.

23.2.5. Wildfires

Land managers can do little to control smoke from wildfires. Nonetheless, smoke dispersion forecasts can assist them with providing information to the community about the likely presence of smoke in their vicinity. This information can be important to vulnerable groups within the community such as asthmatics, particularly in situations where smoke plumes contain toxic compounds released by the combustion of industrial or agricultural chemicals (Wain & Mills, 2006). Forewarning of reduced visibility on major roads can also minimize disruption to transport networks and commuters. Interruptions to transport networks caused by smoke from wildfires are by no means restricted to the present day; Foley (1947) reported a notable haze event in Western Australia in

February 1924 when dense smoke from bushfires in coastal shrubland around Perth disrupted shipping movements over several days and caused a ship to run aground in Fremantle Harbor.

While improvements in dispersion forecasting have been impressive, smoke from prescribed fires may still accumulate over population centers in situations where a burn has been commenced and must be completed prior to the expected onset of severe fire weather conditions. This is most likely to occur with burns containing several vegetation types with different rates of fuel drying, as is the case in the southern karri (*Eucalyptus diversicolor*) forests of Western Australia and the foothill forests of southeastern Australia where the meteorological aspects exert a strong effect on fuel drying.

Knowing where the smoke is going to be is of great interest to the general aviation industry and to fire aviation controllers whose fire support aircraft operate under visual flight rules and need good visibility for take-off and landing. This was highlighted during the Alpine Fires in Eastern Victoria during January to February 2003 when large areas were blanketed by thick smoke for extended periods. Normal smoke forecast points were relocated to correspond with the going fires. Also, at this time hotspot data from the MODerate resolution Imaging Spectroradiometer (MODIS) instrument became readily available and daily smoke forecasts were made from all hotspots.

Most recently an automated system was implemented for the Commonwealth Games that queried the Department of Sustainability and Environment's (DSE) database for active fires at frequent intervals and ran smoke forecasts from the fire locations every 3 h (Fig. 23.5).

23.3. Future directions

Smoke management in southern Australia has progressed from its beginnings of a basic forecast of the path traveled by a smoke plume to the current system that includes

- Model aerological diagrams
- Forward and backward trajectories
- Forecasts from MODIS hotspots
- Ventilation Index

Impetus for further development is coming from increasing community concerns for public health and "global warming," two factors likely to

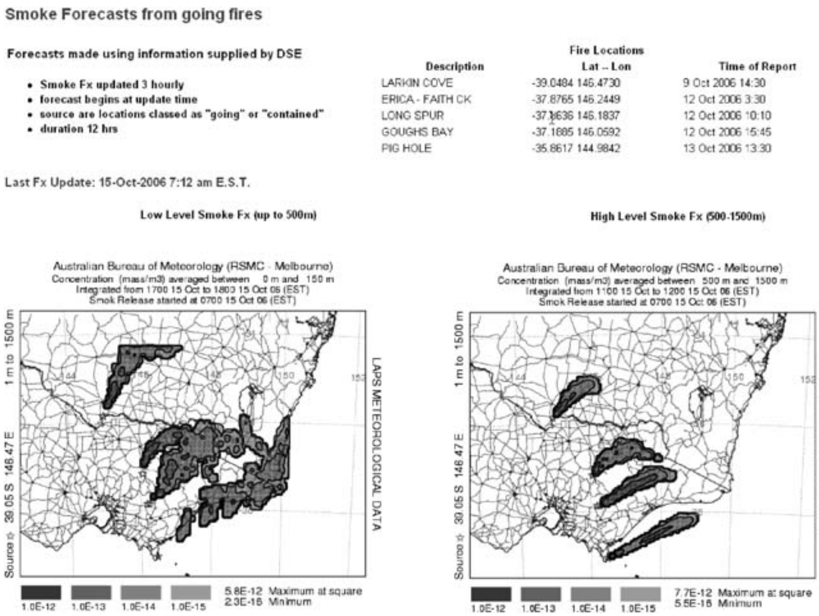

Figure 23.5. Smoke forecasts from wildfires in Victoria.

impinge upon future prescribed burning operations. Already there is increasing pressure from regulators to meet tougher emission standards for respirable particles. Current Australian regulations lag behind the U.S. standards. However, we foresee this changing in the near future, thus increasing the requirement for more sophisticated smoke management tools.

To assist in the determination of future directions, a survey of users was initiated in June 2006 (Wain et al., 2008). Sixteen staff in five agencies were interviewed and questioned about their experiences with the current smoke forecasts and their vision for future requirements. Areas of focus included usefulness, requirements, standards, other needs, and barriers to use. While generally satisfied with the usability of the current system, respondents indicated a desire for:

- More accurate quantitative forecasts
- Better visualization including 3-dimensional views
- Longer forecast outlook
- Integration with other available meteorological data
- Inclusion of pre-existing smoke.

The survey also addressed the future use of probabilistic ensemble forecasts, if and when they were available, which had received a positive user response. The exact type of ensemble to be used is unclear. Draxler (2003) utilized a perturbed source location to generate an ensemble of 27 dispersion members using a single meteorological dataset. Straume (2001) used meteorological data from both individual ensemble members and ensemble forecast cluster means as input for a dispersion model. In addition to perturbations to the meteorological fields, there is considerable merit in using variations in plume rise (varying fire intensities) or varying emission factors in future systems to provide greater ensemble spread in the concentration forecasts.

Improved meteorology and transport models should assist in achieving the end-user's desires for a more accurate forecast. The smoke forecasts in several states are already using a finer resolution NWP model than previously available. Future needs will necessitate finer scales to capture topographic/local-scale influences. An experimental version of meso-LAPS with 51 vertical levels is currently being assessed. Most of the additional levels are within the region of most interest to users of the smoke dispersion forecasts: the atmospheric boundary layer. The Bureau is also testing a rapid update version of meso-LAPS with new model runs available at 6-hourly intervals rather than the current 12 h. The increased temporal resolution should reduce errors later in the forecast period.

The current version of HYSPLIT is 9 years old with essentially only minor revisions made to the source code since the last major rewrite in 1997. It is a transport and dispersion model not an air quality model and as such does not perform sophisticated chemistry calculations required for deterministic concentrations. One initial aim of the project was to conduct a gradual move from HYSPLIT to a full atmospheric chemistry model, the Australian Air Quality Forecasting System (AAQFS; Cope et al., 2004). The current smoke dispersion forecast system does not provide quantitative results, while AAQFS does not include emissions from prescribed burns in its pollutant inventory. This is largely because of the lack of a suitable emissions model to provide "realistic" estimates of the pollutants produced during the combustion of Australian biomass. Such a model will require up-to-date vegetation mapping and some form of growth and litter accumulation model to calculate fuel loads. At present significant uncertainty exists in the available estimates for emissions such that quantitative forecasts are not attempted. The development of such vegetation mapping, growth, and emissions models will enable smoke forecasting in Australia to progress to a level where useful quantitative forecasts can be provided not only to the land managers but also to the general public.

REFERENCES

Australian Greenhouse Office. 2006. National Greenhouse Gas Inventory 2004. Australian Government Department of the Environment and Heritage.

Burrows, N.D. 2004. Implementing fire mosaics to prevent large wildfires and enhance ecosystem health. In: Program and Abstracts, 11th Annual Australasian Fire Authorities Council and Inaugural Bushfire Cooperative Research Centre Conference, 7–9 October 2004, Perth, Western Australia.

Cheney, N.P. 1980. Fire behaviour. In: Gill, A.M., Groves, R.H., and Noble, I.R., eds. Fire and the Australian biota. Australian Academy of Science, Canberra.

Cope, M.E., Hess, G.D., Lee, S., Tory, K.J., Azzi, M., Carras, J., Lilley, W., Manins, P.C., Nelson, P., Ng, L., Puri, K., Wong, N., Walsh, S., and Young, M. 2004. The Australian air quality forecasting system. Part I. Project description and early outcomes. J. Appl. Meteor. 43, 649–662.

Cottrell, A. 2005. Communities and bushfire hazard in Australia: More questions than answers. Environ. Hazards 6, 109–114.

Draxler, R.R. 2003. Evaluation of an ensemble dispersion calculation. J. Appl. Meteor. 42, 308–317.

Draxler, R.R., and Hess, G.D. 1997. Description of the HYSPLIT_4 Modeling System. NOAA Tech. Mem. ERL ARL-224, NOAA, Air Resources Laboratory, Silver Spring, Maryland, 24 pp.

Esplin, B., Gill, A.M., and Enright, N. 2003. Report of the Inquiry into the 2002–2003 Victorian Bushfires. Government of Victoria, Department of Premier and Cabinet.

Evans, L.F., King, N.K., Packham, D.R., and Stephens, E.T. 1974. Ozone measurements in smoke from forest fires. Environ. Sci. Tech. 8, 75–76.

Evans, L.F., King, N.K., MacArthur, D.A., Packham, D.R., and Stephens, E.T. 1976. Further studies on the nature of bushfire smoke. Commonwealth Scientific and Industrial Research Organisation, Division of Applied Organic Chemistry Technical Paper No. 2.

Ferguson, S.A. 2001. Dispersion prediction systems. In: Hardy, C.C., Ottmar, R.D., Peterson, J.L., Core, J.E., and Seamon, P., eds. Smoke management guide for prescribed and wildland fire 2001 edition. National Wildfire Co-ordinating Group Boise, Idaho, pp. 161–176.

Foley, J.C. 1947. A study of the meteorological conditions associated with bush and grass fires and fire protection strategy in Australia. Bureau of Meteorology, Melbourne.

Gill, A.M., and Catling, P.C. 2002. Fire regimes and biodiversity of forested landscapes of southern Australia. In: Bradstock, R.A., Williams, J.E., and Gill, A.M., eds. Flammable Australia: The fire regimes and biodiversity of a continent. Cambridge University Press, Cambridge, pp. 351–372.

Luke, R.H., and McArthur, A.G. 1978. Bushfires in Australia. Australian Government Publishing Service, Canberra.

McCaw, L., Cheney, P., and Sneeuwjagt, R. 2003. Development of a scientific understanding of fire behaviour and use in south-west Western Australia. In: Abbott, I., and Burrows, N., eds. Fire in ecosystems of south-west Western Australia: Impacts and management. Backhuys Publishers, Leiden, The Netherlands, pp. 171–187.

Meyer, C., Beer, T., Muller, J., Gillett, R., Weeks, I., Powell, J., Tolhurst, K., McCaw, L., Cook, G., Marney, D., and Symons, C. 2004. Dioxin emissions from bushfires in Australia. National Dioxins Program Technical Report No.1. Australian Government Department of the Environment and Heritage.

Mills, G.A., Hanstrum, B., Puri, K., and Hess, D. 1996. Linking mesoscale numerical weather prediction model forecasts and a dispersion model to forecast bushfire smoke transport over southwestern Australia. In: Proceedings of the 13th Fire and Forest meteorology Conference, Lorne, Australia 1996. International Association of Wildland Fire.

National Forest Inventory. 2003. Australia's State of the Forests Report 2003. Australian Government Department of Agriculture, Fisheries and Forestry, Bureau of Rural Sciences, Canberra.

Packham, D.R., and Peet, G.B. 1967. Developments in controlled burning from aircraft. Commonwealth Scientific and Industrial Research Organisation, Chemical Research Laboratories, Melbourne.

Puri, K., Dietachmeyer, G.D., Mills, G.A., Davidson, N.E., Bowen, R.A., and Logan, L.W. 1998. The new BMRC limited area prediction system. LAPS. Aust. Met. Mag. 47, 203–223.

Rye, P. 1995. Contribution by bushfire smoke to photochemical smog. CALMScience (Suppl. 4), 129–134.

Sneeuwjagt, R.J., and Smith, R. 1995. Smoke management in Western Australia's southwest forests. CALMScience (Suppl. 4), 135–144.

Straume, A.G. 2001. A more extensive investigation of the use of ensemble forecasts for dispersion model evaluation. J. Appl. Meteor. 40, 425–445.

Tolhurst, K.G., and Cheney, N.P. 1999. Synopsis of the knowledge used in prescribed burning in Victoria. Department of Natural Resources and Environment, Melbourne.

Vines, R.G, Gibson, L., Hatch, A.B., King, N.K., MacArthur, D.A., Packham, D.R., and Taylor, R.J. 1971. On the nature, properties and behaviour of bush-fire smoke. Commonwealth Scientific and Industrial Research Organisation, Division of Applied Chemistry Technical Paper No. 1.

Wain, A.G., and Mills, G.A. 2006. The Australian smoke management forecast system. BMRC Research Report No. 117, Bureau of Meteorology Research Centre, 64 pp. www.bom.gov.au/bmrc/pubs/researchreports/RR117.pdf

Wain, A.G., Brown, T., and Mills, G.A. 2008. Utilisation of Australian smoke forecasts. BMRC Research Letter No. 8, 14–21. http://www.bom.gov.au/bmrc/pubs/researchletter/reslett_08.pdf

Developments in Environmental Science, Volume 8 551
A. Bytnerowicz, M. Arbaugh, A. Riebau and C. Andersen (Editors)

ISSN: 1474-8177/DOI:10.1016/S1474-8177(08)00024-7

Chapter 24

A Statistical Model for Forecasting Hourly Ozone Levels During Fire Season

Haiganoush K. Preisler, Shiyuan (Sharon) Zhong, Annie Esperanza, Leland Tarnay and Julide Kahyaoglu-Koracin*

Abstract

Concerns about smoke from large high-intensity and managed low-intensity fires have been increasing during the past decade. Because smoke from large high-intensity fires are known to contain and generate secondary fine particles ($PM_{2.5}$) and ozone precursors, the effect of fires on air quality in the southern Sierra Nevada is a serious management issue. Various process-based models have been developed for forecasting PM and ozone levels in the presence and absence of fires. Although these models provide deterministic predictions, few of them give measures of uncertainties associated with these predictions. Estimates of uncertainties are essential for model evaluation and forecasting with known precision levels. In this chapter we present a statistical procedure for forecasting next-day ozone levels at given sites. The statistical model takes into account some of the known sources of ozone fluctuations, including changes in temperature, humidity, wind speed, wind direction and, during fire season, effects of smoke from fires. Other sources of variation not directly accounted for in the model—e.g., variability in daily amount of ozone produced by sources other than fire—are included in the uncertainty measure as random effect variables. The advantage of a model that is capable of estimating mean effects and uncertainties simultaneously is that evaluation of model performance is immediate and predictions are available with specific precision levels. The ability of the model in making accurate forecasting with specified precisions is demonstrated by applying it to real data set of observed ambient ozone and weather values at two sites in the Sierra Nevada for the

*Corresponding author: E-mail: hpreisler@fs.fed.us

period from 1 January to 31 July 2006. Forecasted $PM_{2.5}$ values from the BlueSky Smoke Dispersion Model are tested as a proxy for the amount of pollution precursors reaching a given site from specific fires. The forecasts from the statistical model may be useful as a tool for air quality managers to time-prescribed fire treatment.

24.1. Introduction

Concerns about smoke from large high-intensity and managed low-intensity fires have been increasing during the past decade. There is a growing awareness that smoke from some fires may cause exposure to hazardous air pollutants. Studies using satellite images and long-range atmospheric transport models have shown that smoke from large high-intensity fires can be transported across continents or even oceans, producing air quality impacts that can be detected on a continental scale or beyond. Managed low-intensity burns, although usually smaller and less intense, nevertheless may also have an impact on local and regional air quality.

Emissions from managed low-intensity and large high-intensity fires are of special concerns for landscape and air quality managers in the Sierra Nevada. Fire is a natural part of the landscape of the Sierra Nevada. Fire history studies show pre-European fires were widespread and both low-intensity and high-severity fires were frequent (Caprio & Lineback, 2000). Fire suppression beginning in the late 19th century has dramatically changed the historical fire regime, altering the ecological structure and function of Sierra forests. Current fuel conditions show substantial accumulation of live and dead fuels, and require that federal land and air quality managers develop strategies to reduce fire danger and maintain ecosystem integrity. As such, one of the strategies is to use managed low-intensity burns for air quality, safety and resource benefits.

Smoke generated by managed low-intensity burns can have a substantial impact on the air quality in the Sierra Nevada, especially on local scales. Particulate matter contained in fire smoke is one of the greatest concerns due to its impacts on public health and visibility (Billington et al., 2000). At larger scales, burning of forests can also generate substantial concentrations of O_3 downwind of the fire through reaction of nitrogen oxides (NO_x), volatile organic compounds (VOC) and sunlight (Finlayson-Pitts & Pitts, 1993; U.S. EPA, 2001), although only very large fires have been shown to contribute substantially to higher ozone levels at regional scales.

The Sierra Nevada is home for several National Parks and Wilderness Areas that have been, under the Clean Air Act, designated as Class-I airsheds and must maintain the highest standard for air quality. The Sierra Nevada and its National Parks are susceptible to poor air quality because of its close proximity to the San Joaquin Valley, CA that contains four of the top six most polluted cities in the United States. Pollutants emitted from sources in the San Joaquin Valley can be transported to the National Parks in the Sierra Nevada by terrain-induced regional and local circulations. In 2003 alone, Sequoia and Kings Canyon National Park recorded 72 days when the observed ozone level exceeded the federal 8-h ozone standard (NPS, 2003). Smoke from wildland and prescribed fires in the Sierra Nevada may lead to the exceedances of ozone and particulate air quality standards in the National Parks in the mountains, but also contribute to the already serious air pollution problem in the San Joaquin Valley through atmospheric transport. The Sierra Nevada federal land managers are, therefore, constantly challenged by the conflict between the use of managed low-intensity burns to reduce fire danger and maintain ecosystem integrity and the protection of air quality in the Class-I airsheds in the Sierra Nevada where the background ozone concentration is already high.

Land managers require a tool that may aid their decisions in planning burn operations in ways that create more efficient burn opportunities while minimizing their air quality impact. It has been suggested that a process-based atmospheric dispersion models may be a useful tool in this regard. However, although these models may provide deterministic predictions of amounts of pollutant being dispersed from particular sources (including fires) hardly any of them give measures of uncertainties associated with these predictions. Without measures of uncertainties, it is almost impossible to evaluate model performance. This chapter describes how a statistical model may be developed, using historical ozone and meteorological data from given sites together with output from an atmospheric dispersal model, to obtain estimates of next-day hourly ozone levels with estimates of uncertainties. The statistical methods are an extension of those used in Preisler et al. (2005). As an example of the procedures, the statistical model is used to produces next-day ozone estimates at two sites in the Sierra Nevada. The model uses meteorological variables at each site together with predicted fire-produced $PM_{2.5}$ (particulate matter with diameter less than or equal to 2.5 μm) values from the BlueSky Smoke Dispersion Modeling System (Larkin et al., 2008). The BlueSky $PM_{2.5}$ values are used as a proxy for potential contributions of smoke from fires in the region. Since atmospheric dispersion models such as BlueSky already utilize real-time meteorological variables to make predictions of PM concentrations, the question may be raised as to why meteorological variables are used again in the statistical model. One reason for including meteorological variables is to assess the output of the dynamic dispersal model. If the dynamic model is capturing the full effects of meteorological variables then these variables would ideally drop out of the statistical model (i.e., found not significant). The latter is particularly relevant when we are forecasting PM levels at a site using the PM values from a dynamic model as one of the predictors. When the goal is to forecast ozone levels, however, the weather variables at the site are likely to be the most important predictors of background diurnal ozone values. Since weather stations are commonly found at many sensitive locations in the Sierra Nevada and BlueSky real-time forecasts are also available for the region, the statistical model developed here for two sites in the region may be adapted and applied to other sensitive locations in the Sierra Nevada. The models are not limited to BlueSky. Forecasts from other dynamic transport models may be used in a similar fashion in order to appraise their ability to forecast next-day ozone or PM levels during fire season.

24.2. Methods

24.2.1. Data

Meteorological data were obtained from two weather stations in Sequoia National Park. The Lower Kaweah station is located at 1902 m above mean sea level (MSL) and Ash Mountain station is at 535 m MSL. The meteorological data included hourly values of temperature, relative humidity, wind speed, wind direction and solar radiation. Ozone concentrations (ppb) were also recorded at these stations (Fig. 24.1). Ozone concentrations were measured with a Thermo Environmental Model 49 UV absorption instrument operated by the National Park Service. The ozone monitor was calibrated at the beginning of the season and checked against a calibrator on a weekly basis. Air temperature and relative humidity were measured with a Vaisala temperature and humidity sensor mounted at approximately 2 m in a self-ventilated, louvered shelter. Wind speed and direction were monitored with a MetOne anemometer mounted on a 10-m tower.

Forecasted $PM_{2.5}$ values at the two locations were obtained from BlueSky output for the same period. BlueSky is a smoke dispersion modeling forecasting system that combines burn information with models of consumption, emissions, meteorology, and dispersion to yield a

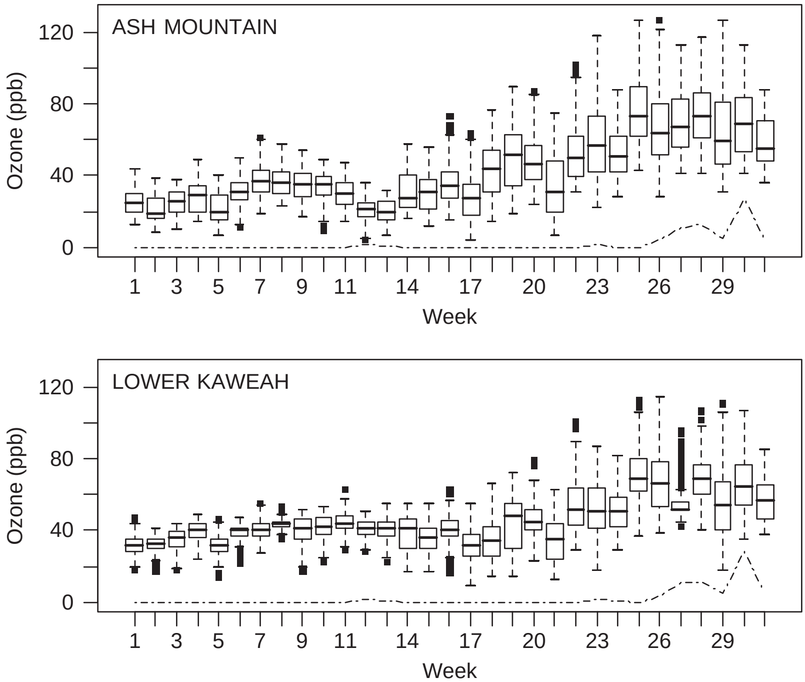

Figure 24.1. Boxplots of hourly ozone values at two sites in Sequoia National Park for the first 31 weeks (1 January to 31 July) in 2006. The dashed curves at the bottom of each panel are the weekly total $PM_{2.5}$ values from BlueSky simulations for that site.

prediction of trajectories and surface concentrations of particulate matter (both $PM_{2.5}$ and PM_{10}) from managed low-intensity fires, wildfires, and agricultural burn activities (Larkin et al., 2008). Currently BlueSky smoke predictions from wildfires are available daily for many locations in the United States. In California, BlueSky has been implemented by the California and Nevada Smoke and Air Committee (CANSAC, http://www.cefa.dri.edu/COFF/coffframe.php) (Brown et al., 2003) into its operational weather forecast system. The system employs the Fifth Generation Penn State University/National Center for Atmospheric Research (NCAR) Mesoscale Model (MM5, http://www.mmm.ucar.edu/mm5/) (Grell et al., 1994) in an operational mode. The initial and boundary condition inputs for the MM5 model are prepared using 6-hourly 40-km ETA forecasts and observations obtained from the NCAR's Unidata data stream. The BlueSky $PM_{2.5}$ forecasts for each day include smoke emissions from all fires reported by various agencies and individuals for the previous day. Simulations for each day start at 5 am local time. All fires from the previous day are assumed to have started at the starting time of the simulations.

We used the predicted $PM_{2.5}$ values from BlueSky forecast to characterize the amount of PM produced by smoke from both large high-intensity and managed low-intensity fires in the region. Outputs from other transport models, with the capability to produce spatially and temporally explicit values in real time, may also be used.

24.2.2. Statistical model

A statistical model is developed that links the observed ozone concentrations with the observed meteorological conditions and BlueSky-predicted $PM_{2.5}$ values at two sites in the Sequoia National Park. The goal here is to forecast next-day ozone concentrations at a given site. While meteorological conditions at the site are likely to be good predictors of background ozone concentrations they will not pick potential fluctuations due to a particular source of pollution such as fires. For that we use predicted $PM_{2.5}$ values from BlueSky output. Observed PM values at the site may be better predictors; however many sites, including the two in this study, do not have observed PM values. Even at sites that have PM observations, it is very difficult to separate the PM concentration produced by fire emissions from the contributions by other PM sources. The BlueSky-predicted PM values at a given location and a given time is a result of smoke plumes as they are transported and dispersed from the locations of all fires in a region.

Standard multiple regression models are not appropriate for the analysis of ozone data for a variety of reasons. First, the distribution of hourly ozone values is not well approximated by a Gaussian or other symmetric distribution (Fig. 24.2a). Second, the assumption of independent observations is not valid because hourly ozone values are serially correlated. Lastly, the relationships between ozone levels and the various predictors are nonlinear. For example, the relationship between hourly ozone and wind direction in the Sequoia National Park region is likely to be cyclical with ozone values being higher when wind directions are from the southwest potentially transport ozone precursors from the heavily polluted San Joaquin Valley.

In our study we used a multiple regression model with cube root of ozone as the dependent variable and with an autoregressive error term to account for the serial correlation. The cube transform of ozone values were more closely approximated by the Gaussian distribution

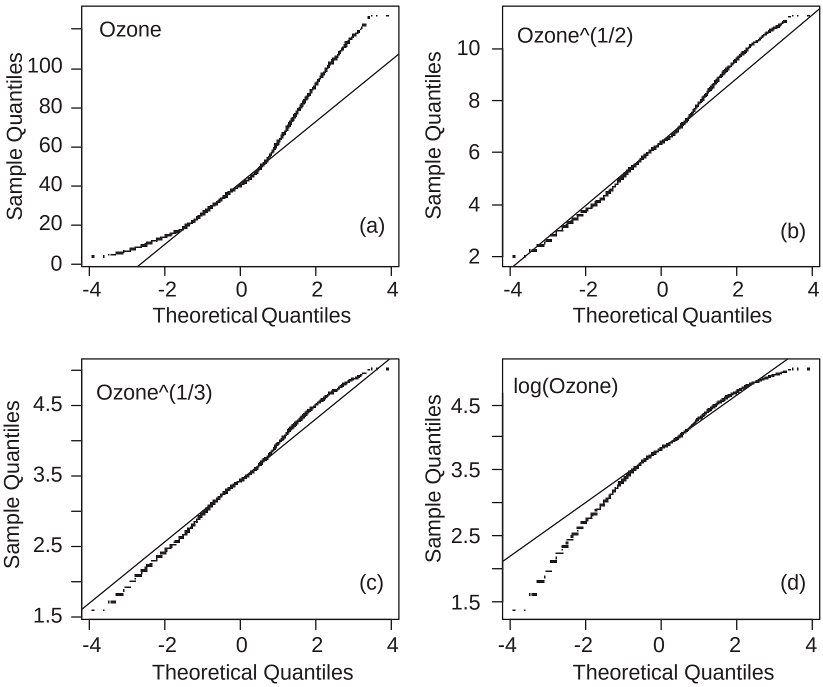

Figure 24.2. Normal probability plots for hourly ozone values (top left panel) and for three transformations. The cube root transformation of the observed ozone values (bottom left) appeared to be more closely approximated by the Gaussian distribution when compared to the square root (top right) or the logarithmic transformations (bottom right).

(Fig. 24.2c). The statement for the statistical model is

$$Y_t = \mu(\mathbf{X}_{t-24}) + \beta Y_{t-24} + \varepsilon_t$$

where Y_t is the cube root of the ozone value at t^{th} hour of the day; μ an additive function of the columns in **X**; $\mathbf{X}_{t-24}$ is a matrix of bases spline transforms of the predictor variable (e.g., weather and BlueSky variables) for the previous day; $\boldsymbol{Y}_{t-24}$ the cube root of the ozone value for the previous day; β a coefficient to be estimated and where $\varepsilon_t = \rho\varepsilon_{t-1}$ is the autoregressive error term. In ordinary regression it is often customary to use some parametric transformation of the predictors (e.g., polynomial or logarithmic function of X) to describe non-linear relationships between the predictors and the predictant. The regression equation described above uses non-parametric transforms of the predictors (e.g., splines), thus allowing the data to suggest the nonlinearities. The latter is achieved

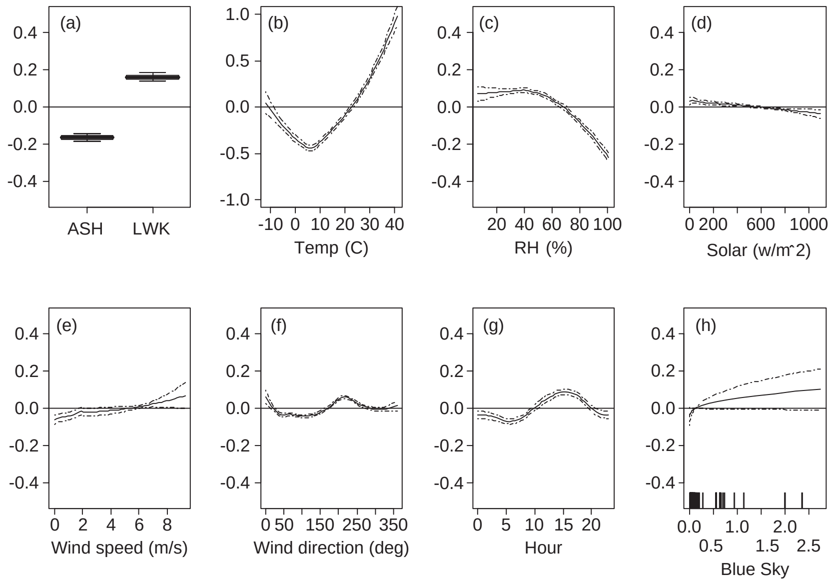

Figure 24.3. Estimated relationships (and 95% point-wise approximate confidence bounds) between predictors and hourly ozone levels. The effects are standardized to have mean zero. If the horizontal line at zero is completely within the confidence bounds then that predictor does not have a significant effect on diurnal ozone concentration. The BlueSky variable is the 80th percentile of the previous day's hourly $PM_{2.5}$ values produced by BlueSky. The hatch marks at the bottom of panel h are the distribution of the observed BlueSky variable.

by fitting polynomial regressions locally after dividing the range of the predictor variables into subsets at specified knots (Hastie et al., 2001). The plots in Fig. 24.3 are an example of fitted non-parametric relationships for the present data. Note that while in ordinary parametric regression the slopes and intercepts of the linear relationships for each predictor are estimated from the data, in non-parametric regression the whole non-linear curves are estimated from the data for all predictors simultaneously.

The above model allowed us to assess the ability of the previous day predictor variables in predicting next-day ozone levels. One may use a similar method to assess the skill of forecasted weather data on ozone levels.

The predictor variables used in the model were temperature, relative humidity, solar radiation, wind speed and wind direction as measured at the two sites. Other two predictors used were hour-of-day in addition to a predictor based on the hourly BlueSky-predicted $PM_{2.5}$ values for that location and time. The $PM_{2.5}$ predictor we used was the 80th percentile of the simulated hourly $PM_{2.5}$ values for the previous 24 h. It was anticipated that the meteorological variables in the model will account for most of the variability in ozone values due to local weather conditions at the time and the BlueSky variable will account for weather conditions at the regional scale that affect the transport of particulate matter and other possible ozone precursors from fires in the region in the previous day. The hour-in-day variable was included as a surrogate for unobserved factors (other than the measured local weather conditions and $PM_{2.5}$ values) that may be affecting ozone levels and that have a 24-hour daily cycle. All estimations were done with the R statistical package (R Development Core Team, 2006).

One outcome of interest to land and air quality managers is whether the ozone level at a particular sensitive site will exceed some critical value (e.g., 90 ppb). We used the forecasted hourly ozone values and their estimated standard errors to appraise the following decision rule:

If $\max_{24\text{ h}}(\hat{Y} + 2\hat{se}) \geq \sqrt[3]{90}$ prescribed burn not recommended on this day, where $\hat{Y}$ and $\hat{se}$ are the forecasted cube root of ozone and its corresponding estimated standard error. Using the above rule, prescribed burns are not recommended on days where the chance of ozone levels exceeding the critical 90 ppb value is greater than a small value ($\sim$2.5%).

We used data from 1 January to 30 July 2006 (the only time period that we had archived BlueSky forecasts) to build the model. We used the period 1 May to 30 July as a test period to calculate the error rate in our decision rule. Ozone concentrations for each day in the test period were forecasted from a model estimated using data from all the days except the day being forecasted.

24.3. Results

On average ozone values at the Ash Mountain site were significantly lower than the corresponding values at the Lower Kaweah site (Fig. 24.3a). All five local weather variables included in the model had significant effects on hourly ozone levels. The partial effect plots (Fig. 24.3b–f) are the estimated non-parametric functions describing the relationships between the predictors and the dependent variable (cube root of ozone). The significant relationship between ozone and hour-of-day (Fig. 24.3g) appears to indicate that there are other sources of variation with a 24-hour cycle that were not accounted for by the five meteorological variables in the model. The hour-of-day variable in the model may be viewed as a surrogate for these missing predictors. Finally, there is some evidence of increases in ozone levels with increasing values of the BlueSky-predicted $PM_{2.5}$ values (Fig. 24.3h). The effect of the BlueSky's $PM_{2.5}$ variable was significant (p-value = 0.0418), however, the standard errors around the estimated curve were large, due to the small sample sizes. The BlueSky-predicted $PM_{2.5}$ levels during the study period were very low. It remains to be seen if the relationship between the BlueSky predictor and ozone concentrations remains the same when a longer period is studied with a wider range of BlueSky values, namely, during a period with more fire activities including some intense fires.

The statistical model appeared to have considerable skill in forecasting ozone levels for the next 24 h using the local weather and ozone levels in the previous day (Figs. 24.4 and 24.5). The decision rule used to forecast whether ozone values will exceed a critical level seems to work well. The forecast missed only one day where the actual/observed ozone level was in excess of the critical level of 90 ppb while the forecasted maximum level (+2SE's) was lower than that. (Fig. 24.6). However, there were many days when the forecast was greater than 90 ppb while the actual observed value was below 90 ppb. One can decrease the number of false positives by making a decision rule based on a lower confidence bound. However, in doing so, the chance that the forecast will miss days with ozone in excess of 90 ppb will increase.

24.4. Discussions

Process-based models for forecasting PM levels during fire season may be a useful tool for land managers if their performance was evaluated and their accuracy of PM forecasts for a particular area or sensitive locations are documented. In order to evaluate model performance it is necessary to quantify the uncertainties of the model predictions. The statistical model developed here is an attempt to demonstrate how uncertainties may be quantified and precisions of forecasts estimated given observational data at a specific site. In this chapter we first demonstrated how one may quantify uncertainties using observational data by applying the statistical model to two meteorological stations in the Sierra Nevada. We then used the estimated statistical model to forecast next-day ozone values during the start of 2006 fire season using BlueSky forecasted $PM_{2.5}$ values as a surrogate for the level of fire activity on a given day. The model can be used as an aid to land managers in making a 'go' or 'no-go' decision with respect to managed low-intensity fires in the Sierra Nevada. To make a

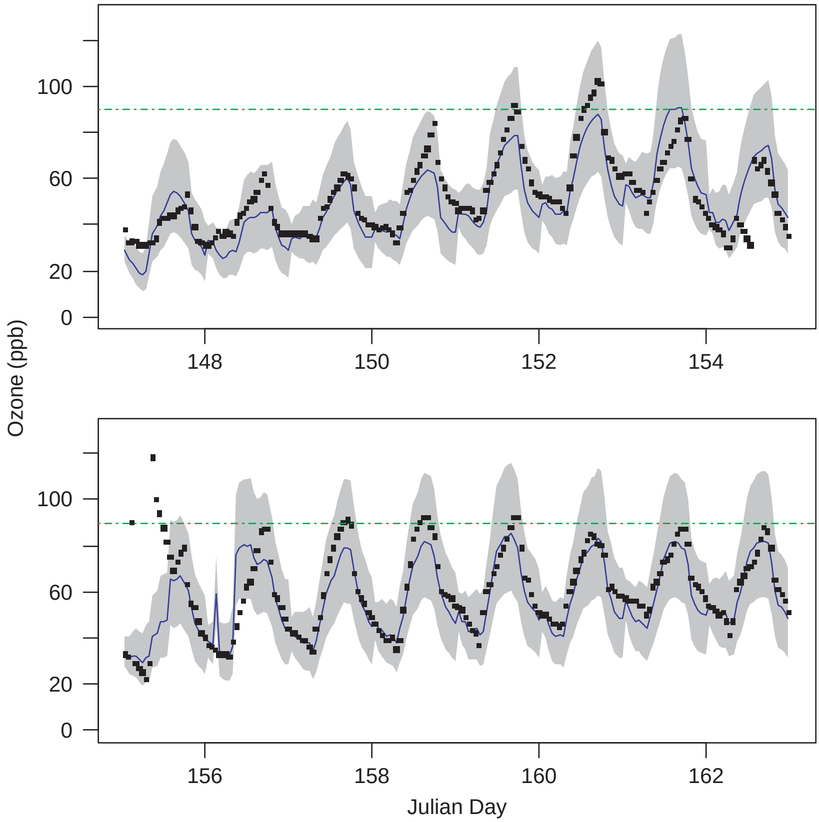

Figure 24.4. Observed (dots) and forecasted (blue curves) hourly ozone values at the Ash Mountain site for a period of 16 days (27 May to 11 June 2006). The gray regions indicate the forecasted point-wise approximate 90% bounds. The green dashed line is at 90 ppb.

forecast for given locations in the Sierra Nevada using the statistical model suggested in this study, the following steps need to be taken:

1. Install meteorological stations at sites near smoke sensitive areas in the Sierra Nevada (i.e., schools and hospitals). These meteorological stations need to have web-based accessibility to retrieve real-time hourly weather information. Co-location of ozone and $PM_{2.5}$ monitors would make these sites ideal for forecasting efforts and would complement efforts to accurately monitor air quality in this region.
2. Collect hourly weather and ozone data from these sites for at least one year. If the site also has the capability to collect $PM_{2.5}$ data, then the

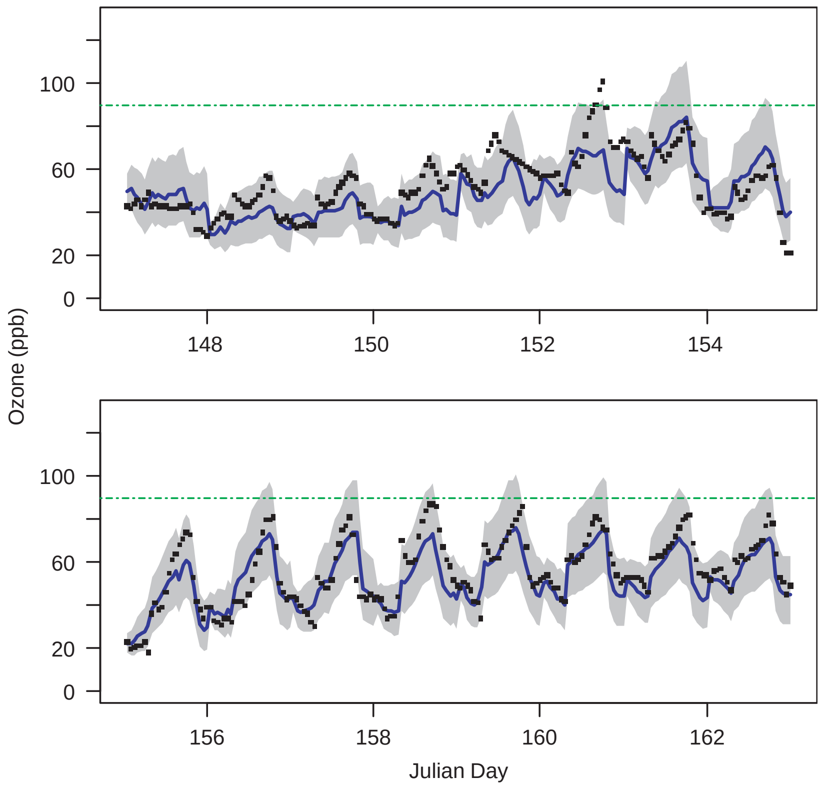

Figure 24.5. Observed (dots) and forecasted (blue curves) hourly ozone values at the Lower Kaweah site for a period of 16 days (27 May to 11 June 2006). The gray regions indicate the forecasted point-wise 90% bounds. The green dashed line is at 90 ppb.

data can be used directly in the statistical model to replace the BlueSky-predicted $PM_{2.5}$ values. Otherwise, BlueSky-predicted $PM_{2.5}$ values will also be needed for the same time period. The observed ozone and meteorological variables and the $PM_{2.5}$ values will then be used to evaluate the statistical model and determine the coefficients that best describe statistically the conditions for the specific location. Historical data at existing monitoring sites may also be used to train the statistical model.

3. During fire seasons, download previous-day data from the meteorological sites by 5:00 am present day.
4. Obtain BlueSky-predicted $PM_{2.5}$ values for that day, also by 5:00 am.
5. Produce forecasted hourly ozone values (and approximate confidence bounds) for the next 24 h starting at 5:00 am.

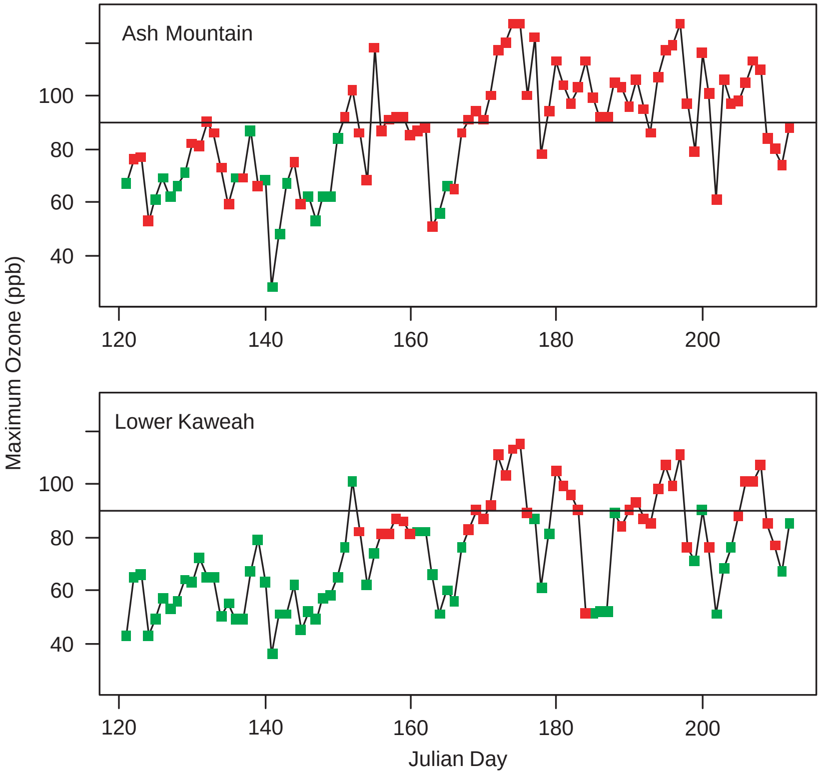

Figure 24.6. Observed 24-hour maximum ozone values at Ash Mountain and Lower Kaweah for the period 1 May to 30 July 2006. Red indicates days when the forecasted upper 95th percentile exceeded 90 ppb. Green indicates days when the forecasted upper 95th percentile was less than 90 ppb.

6. Produce a map indicating all the sites in the study area with red or green sites depending on whether the site is forecasted to exceed the critical level (e.g., 90 ppb hourly average) or not. The latter based on some criteria such as the one described above.
7. Repeat the process the next day.

The current statistical model may be improved by replacing the observed previous day weather conditions with the forecasted values from mesoscale weather forecast models for the current day. As mentioned earlier, mesoscale weather forecasts using the MM5 model, together with forecasts of PM concentrations due to large high-intensity and managed low-intensity fires using the BlueSky Smoke Dispersion Modeling System, are made available operationally by CANSAC for the State of California and Nevada at 4-km horizontal grid spacing.

One potential problem, however, with these mesoscale model forecasts is that for a given location in the Sierra Nevada Mountain Range that is subject to strong influence of local topography, relative large errors may occur in forecast of surface meteorology, especially wind speed and direction. At these locations, the statistical model based on actual on-site observations from previous day, as described in this study, may do a better job in predicting the likelihood of ozone exceedance for the next day at the site.

During this past fire season in 2006, more observational data have been collected at other locations in Sequoia and Yosemite National Parks and Sequoia National Forest in the Sierra Nevada. These data will be used to test the robustness of the statistical model for making ozone forecasting for different weather conditions and topographic settings.

ACKNOWLEDGMENT

We thank the reviewers for their constructive comments and Dr. Andrzej Bytnerowicz for the editorial work essential to the success of this book. We thank the National Park Service Air Resources Division for the hourly ozone and meteorological data from the Lower Kaweah and Ash Mountain stations. The research is funded by a grant from the USDA Forest Service under the Joint Fire Science Plan.

REFERENCES

Billington, J., Ommering, L., Haden, C., Linse, E., Ramalingam, R., and Black, K. 2000. Proposed Amendments of California's Agricultural Burning Guidelines. Staff Report. CALEPA, Air Resources Board, Planning and Technical Support Division, Sacramento, CA.

Brown, T.J., Fujioka, F., and Fontana, C. 2003. The California and Nevada smoke and air committee—an interagency partnership to meet decision-making needs. Proceedings American Meteorological Society Fifth Symposium on Fire and Forest Meteorology, 6 pp.

Caprio, A.C., and Lineback, P. 2000. Pre-twentieth century fire history of Sequoia and Kings Canyon National Parks: A review and evaluation of our knowledge. In Proceedings of the Conference on Fire in California Ecosystems: Integrating Science, Prevention, and Management. 17–20 November 1997, San Diego, CA.

Finlayson-Pitts, B., and Pitts, J. 1993. Atmospheric chemistry of tropospheric ozone formation: Scientific and regulatory implications. Air Waste 43, 1091–1100.

Grell, G.A., Dudhia, J., and Stauffer, D.R. 1994. A Description of the Fifth-Generation Penn State/NCAR Mesoscale Model (MM5). NCAR Technical Note TN-398, June 1994, 138 pp.

Hastie, T., Tibshirani, R., and Friedman, J. 2001. The elements of statistical learning: Data mining, inference, and prediction. Springer-Verlag, New York.

Larkin, N.K., O'Neill, S.M., Solomon, R., Krull, C., Raffuse, S., Rorig, M., Peterson, J., and Ferguson, S.A. 2008. The bluesky smoke modeling framework. Atmos. Environ. (Accepted).

Preisler, H.K., Grulke, N.E., Bytnerowicz, A., and Esperanza, A. 2005. Analyzing effects of forest fires on diurnal patterns of ozone concentrations. Phyton (Austria) 45(Special Issue), 33–39.

R Development Core Team. 2006. R: A language and environment for statistical computing. R Foundation for Statistical Computing, Vienna, Austria. ISBN 3-900051-07-0. http://www.R-project.org.

U.S. EPA. 2001. Air quality criteria for particulate matter: Second external review draft. EPA 600/P-99/002aB, bB. http://www.epa.gov/nceawww1/pm_vol1.htm

This page intentionally left blank

Developments in Environmental Science, Volume 8
A. Bytnerowicz, M. Arbaugh, A. Riebau and C. Andersen (Editors)

ISSN: 1474-8177/DOI:10.1016/S1474-8177(08)00025-9

Chapter 25

Managing Air Pollution Impacted Forests of California

Michael J. Arbaugh, Trent Procter and Annie Esperanza*

Abstract

Fuel treatments (prescribed fire and mechanical removal) on public lands in California are critical for reducing fuel accumulation and wildfire frequency and severity and protecting private property located in the wildland–urban interface. Treatments are especially needed in forests impacted by air pollution and subject to climate change. High ambient ozone (O_3) concentration and elevated nitrogen (N) deposition weakens and predisposes trees to bark beetle attacks, increases foliar senescence and fuel build-up, and increases water stress during drought periods. Climate variability is expected to increase beyond historic ranges of variation, resulting in more severe droughts. Combinations of future climate variability and air pollution are likely to increase risk of episodic tree mortality, long-term ecosystem changes, and frequency and severity of wildland fires. Fuel treatments, however, are difficult to implement in these forests. Smoke from prescribed fires can adversely affect local and regional air quality leading to conflicts with local and regional air regulatory agencies. Over the past several years federal land air quality and fire managers have responded to these conflicting needs by expanding beyond the boundaries of their historical job responsibilities. For example, they are now actively forging cooperative relationships with local, state, and federal air regulators. The result has been fewer conflicts about smoke in populated or protected areas, with managers achieving an adequate level of prescribed fire treatments. Smoke monitoring by air managers has played a key role in this success. Social and regulatory acceptance of fire as a management tool in air polluted forests will depend on land managers developing a better understanding of air pollution and smoke interactions and interactions between air pollution, drought,

*Corresponding author: E-mail: mjarbaugh@charter.net

and insects. Acceptance of fire as a management tool also requires better large-scale monitoring efforts (field collected and remotely sensed), development of models for predicting spatial and temporal distribution of air pollution and smoke resulting from forest fires, and incorporation of air pollution and climate effects into forest mensuration models used to predict stand development.

25.1. Introduction

Managing the impacts of air pollution on public lands in California is a complex ecological, political, and regulatory task. The federal Clean Air Act (CAA, 1990) mandates that the National Park Service (NPS) and the USDA Forest Service (FS) protect air quality-related values in Class I Areas. Class I areas are defined as National Parks over 6000 acres and Wilderness Areas over 5000 acres that were in existence on August 7, 1977. All other clean air regions are designated Class II areas, which allow moderate pollution increases. New wilderness areas added since that time have not been designated as additional Class I areas, but additions to existing mandatory areas added after 1977 are also Class I Areas. Class I Areas are provided with special protection from new and modified major stationary sources emissions. Historically, program emphasis of both agencies has been to review and comment on the applications and proposed permits related to the primary and secondary emissions from stationary sources and their accumulated impacts to Class I areas.

The CAA requires the permitting authority consult with federal land managers (FLM) when considering applications from major stationary sources near Class I areas. This requirement provided impetus to the NPS and FS to establish management and then research programs that have developed leadership roles in research, monitoring, and management strategies to address the effects of air pollution on forest ecosystems in the United States.

Original program emphasis of both agencies was to understand and mitigate the effects of criteria pollutants (defined by the Environmental Protection Agency (EPA) as indicators of air quality that have established maximum concentrations above which adverse effects on human health may occur) on air quality-related values in parks and forests of the United States. Over time additional threats have required FLM to expand their roles and responsibilities. The roles of air resource managers in California have expanded, as smoke from prescribed and wildland fire have become issues of increasing concern to air quality regulatory agencies seeking to regulate particulate, toxic, and ozone precursor emissions. The complexity of air management is further increased by the need to consider prescribed fire effects on regional haze and California's Assembly Bill 32 that established regulations limiting greenhouse gas (GHG) emissions. Changes in climate variability also present challenges to management, especially in areas where changes in weather patterns may result in abnormally high mortality of trees.

25.2. Regulatory complexity of federal land air resource management

The respective air quality management programs of the NPS and FS developed as a response to the 1977 amendments to the CAA. The CAA gives the NPS and FS an affirmative responsibility to protect air quality-related values in designated Class I Areas. In addition to the CAA, several other laws specify air, air quality, or the atmosphere as a resource to protect and manage. They include:

- The Federal Land Policy and Management Act (FLPMA, 1976) that specifies clean air as an important forest resource to be protected.
- The Organic Act (NPS 1916) that created the NPS to preserve and protect natural and cultural resources and allow visitors to experience National Parks now and in future.
- The Forest and Rangeland Renewable Resources Planning Act (FRRRPA, 1974) that directs the Secretary of Agriculture to protect and, where appropriate, improve soil, water, and air resources.
- The Wilderness Act (1964) requires natural conditions to be sustained in wilderness areas.

The air quality regulatory structure and agencies responsible for compliance with these laws include the California EPA, Air Resources Board (ARB), regional air quality regulatory agencies, and county-level air pollution control districts (Fig. 25.1).

25.2.1. Environmental Protection Agency

Federal agencies implement regulations of national air quality standards, oversee state and local actions and implement programs for toxic air pollutants, heavy-duty trucks, locomotives, ships, aircraft, off-road diesel equipment, and some types of industrial equipment. The role of federal, state, and local governments builds on the CAA and amendments of 1977 and 1990. Some of the components, regulations, and policies related to

Figure 25.1. Local air quality regulatory jurisdictions in California.

the CAA that may directly or indirectly affect land management in California include the following:

- National Ambient Air Quality Standards (NAAQS)—These are standards for pollutants considered harmful to public health and the environment. The EPA has set NAAQS for six principal pollutants, which are called “criteria pollutants” (Table 25.1).
- Prevention of Significant Deterioration and Class I Areas—Class I Areas include National Parks, Wilderness Areas, and some U.S. Fish and Wildlife Refuges that were in existence at the passage of the 1977 CAA amendments. They are provided special protection from new and

Table 25.1. National and California Ambient Air Quality Standards set by the EPA for seven principal pollutants

Pollutant	U.S. standard value	California standard value
Carbon monoxide (CO)		
8-hour average	9 ppm ($10\,mg\,m^{-3}$)	9 ppm ($10\,mg\,m^{-3}$)
1-hour average	35 ppm ($40\,mg\,m^{-3}$)	20 ppm ($25\,mg\,m^{-3}$)
Nitrogen dioxide (NO_2)		
Annual arithmetic mean	0.053 ppm ($100\,\mu g\,m^{-3}$)	0.030 ppm ($57\,\mu g\,m^{-3}$)
1-hour average	None	0.018 ppm ($34\,\mu g\,m^{-3}$)
Ozone (O_3)		
1-hour average	0.12 ppm ($235\,\mu g\,m^{-3}$)	0.09 ppm ($176\,\mu g\,m^{-3}$)
8-hour average	0.08 ppm ($157\,\mu g\,m^{-3}$)	0.07 ppm ($137\,\mu g\,m^{-3}$)
Lead (Pb)		
Quarterly average	$1.5\,\mu g\,m^{-3}$	None
30-day average	None	$1.5\,\mu g\,m^{-3}$
Particulate matter (PM_{10})		
Annual arithmetic mean	None	$20\,\mu g\,m^{-3}$
24-hour average	$150\,\mu g\,m^{-3}$	$50\,\mu g\,m^{-3}$
Particulate matter ($PM_{2.5}$)		
Annual arithmetic mean	$15\,\mu g\,m^{-3}$	$12\,\mu g\,m^{-3}$
24-hour average	$35\,\mu g\,m^{-3}$	Federal Standard Used
Sulfur dioxide ($S0_2$)		
24-hour average	0.14 ppm	0.04 ppm
1-hour average	None	0.25 ppm

modified major stationary sources. The Prevention of Significant Deterioration is the permitting rule and concept for federal attainment areas (areas that meet federal standards). Only a small increment of additional pollution is allowed in these "clean air areas." Federal land managers are mandated an affirmative responsibility to protect air quality-related values that can be impacted by air pollution, including visibility. Other values include flora, fauna, soils, water, cultural resources, and geologic features. Sensitive receptors such as species or populations known to have documented sensitivity have been established. Sensitive indicators are measurable elements of injury or change. An example of this concept for ozone might include the following elements: vegetation as an air quality-related value, ponderosa pine as the sensitive receptor, and chlorotic mottle as the sensitive indicator. Although this concept was originally developed to fulfill the mandates of Class I protection, it is used frequently now throughout Class II National Forests and Parks as well.

- Regional Haze Rule—These regulations require states to review how pollution emissions from within the state affect visibility at "Class I" areas across a broad region. The rule also requires states to make ''reasonable progress'' in improving visibility conditions in Class I areas and to prevent future impairment of visibility. The states are required by the rule to develop a plan which brings Class I areas from current conditions to ''natural background'' conditions by 2064. Natural background visibility exists when no human-caused pollution is present. This program, while aimed at Class I areas, will improve regional visibility and air quality throughout the country.

- Conformity Rule—This applies in federal nonattainment areas and prohibits the federal government from taking actions that cause or contribute to any new violation or delays the timely attainment of a standard. A project or activity ''conforms'' if its air pollution emissions are included in an approved State Implementation Plan (SIP).
- EPA Interim Policy on Wildland and Prescribed Fire—This EPA interim policy integrates two public policy goals: to allow fire to function, as nearly as possible, in its natural role of maintaining healthy wildland ecosystems; and to protect public health and welfare by employing best management practices to mitigate the impacts of air pollutants on air quality and visibility.
- Exceptional Events Rule—Exceptional events are unusual or naturally occurring events that can affect air quality and may impair an air regulatory agency's ability to attain the National Ambient Air Quality Standards. Qualifying events are not reasonably controllable with regulatory techniques. This rule establishes the procedures and criteria that will be used to identify and evaluate data to establish an exceptional events determination.

25.2.2. California air resources board

State governments are responsible for developing SIPs that describe how each state will achieve the requirements of the CAA. In California the SIP is a collection of plans and regulations used to clean up polluted areas. The EPA maintains oversight authority, must approve each SIP, and can take over enforcement action if reasonable progress is not made. The California ARB has set more stringent state air quality standards than many of those established by the U.S. EPA, oversees state and local actions, and implements local programs for toxic air pollutants, heavy-duty trucks, locomotives, ships, aircraft, off-road diesel equipment, and some types of industrial equipment. ARB supports over 200 air-monitoring stations and maintains the statewide emissions inventory. ARB also oversees the regulatory activity of 35 local and regional air districts.

In addition, Assembly Bill (AB) 32, the California Global Warming Solutions Act, was passed in September 2006. AB 32 requires that the ARB adopt regulations for reporting and verification of statewide GHG emissions. AB 32 also requires that ARB adopt a statewide GHG emissions limit equivalent to the statewide GHG limit set in 1990, which should be achieved by the year 2020.

25.2.3. Regional and county air quality regulatory agencies

There are 35 local air quality regulatory agencies in California. The agencies develop plans and implement control measures in their areas of jurisdiction. These plans collectively contribute to California's SIP. These controls primarily affect stationary sources but do include sources of dust and smoke. Air pollution control districts are classified as attainment (meeting the standard) or nonattainment (not meeting the standard) for each criteria pollutant including ozone.

25.3. Emerging regulatory issues

FLMs of forested ecosystems will always need to address the role of fire. General types of fire include wildfires, wildland fire use, and prescribed fire. Wildfires usually fall into a full suppression category, whereas wildland fire use and prescribed fire warrant management attention at different levels.

25.3.1. Prescribed and wildland fire use

Prescribed fires are ignited by management to achieve resource objectives, most often a combination of ecosystem restoration or habitat maintenance objectives, and reduction of high hazard fuel loadings. These objectives are not mutually exclusive and usually all prescribed fire operations contain a combination of them.

Wildfire use is the management of unplanned wildland fires, such as lightning-ignited fires, to accomplish specific resource management objectives. Lighting-caused wildland fires will receive appropriate management responses that give consideration to values, hazards, and risks. They are a preferred means for achieving resource management objectives in designated zones where restoration and ecological values dominate considerations.

There is a perceived conflict between clean air goals and wildland fire use and/or prescribed fire goals. The main concern is smoke and its related air quality and visibility impacts. For FLMs in the southern Sierra Nevada, the problem is more complex. FS and NPS lands in the southern Sierra Nevada are located within the San Joaquin Valley Air Pollution Control District. This air district is classified as serious and severe nonattainment for particulate matter (PM) and ozone, respectively. Best Available Control Measures (BACM) are implemented in the air basin by requiring federal fire programs within the basin to comply with a series of emission control measures that are some of the most stringent in the nation.

As wildland areas are treated and maintained with prescribed fire, fire use projects, and mechanical treatments, the potential amount of smoke emissions can be reduced. Smoke emissions released during unwanted wildfires usually produce more serious air quality impacts, potential harm to life and property, and an unnatural alternation to protected ecosystems than do controlled management fires.

25.3.2. Regional haze rule

The 1977 amendments to the CAA provided a national visibility goal of ‘‘the prevention of any future, and the remedying of any existing, impairment of visibility in mandatory Class I federal areas in which impairment results from manmade air pollution.’’ The 1977 amendments required the EPA to issue regulations that would ensure ‘‘reasonable progress’’ towards meeting the national visibility goal. Congress placed additional emphasis on regional haze in the 1990 amendments to the CAA, requiring the EPA to establish the Grand Canyon Visibility Transport Commission to address visibility in 16 Class I areas on the Colorado Plateau. Regional haze is generally considered visibility impairment from a multitude of sources and activities over a broad geographic region. Haze usually consists of fine particles and precursors broadly categorized as sulfates, nitrates, organic carbon, elemental carbon, and dust. The final Regional Haze Rule was passed in July 1999. The regulations require states to develop coordinated strategies and programs to make ‘‘reasonable progress’’ towards the national visibility goal. Each state was required to submit a SIP by December 17, 2007. Preparation of the SIP should have included consultation with FLMs. However, most states have not met this deadline. The goal of the planning effort is to reduce human-caused emissions nationwide to improve visibility in 156 federal Class I wilderness areas and National Parks. Twenty-nine Class I areas are in California. Natural conditions are to be achieved by 2064 with an interim assessment in 2018. California will be required to submit coordinated SIPs for PM2.5 and ozone on the same planning schedule as regional haze, providing an opportunity for FLMs to collaborate on control strategies for those pollutants as well. Although the Regional Haze Rule emphasizes control strategies on industrial and mobile sources, it does require consideration of smoke management techniques for agricultural and forestry management practices in the development of a SIP. It also requires determination of natural background for regional haze prior to setting reduction goals. Natural background must take into consideration the fire histories of the respective ecosystems. Wildland fire and agricultural smoke will be important due to its significance in organic carbon inventories but will be a challenge to project into future inventories because timing and location is uncertain.

25.3.3. Climate change effects on air and forest resources

Managing air resources surrounding forest lands will become more difficult in the future. Most climate change projections (California Climate Action Team, 2006) indicate higher annual average daily temperatures and increased numbers of days conducive to air pollution formation. Future scenarios predict that California will have an increased number of very hot days and fewer cold days. Climate change may increase the number of days conducive to pollution formation by as much as 75–85% in high ozone areas such as Los Angeles and the San Joaquin Valley. Background ozone is projected to increase 4–25% by 2100 (Kleeman & Cayan, 2006). The increase in hot days is projected to increase large wildfire risk by 35% and cost by 30% over the next 50 years (Westerling & Bryant, 2006). Moderate to high ambient ozone reduces net carbon uptake, and high ozone and N deposition alter carbon sequestration, its distribution, and its residence time in the ecosystem (Grulke et al., 2008). Air pollution and climate change are also reducing winter precipitation and increasing the severity of summer drought stress. Cumulative effects of changing climate is forecasted to exacerbate insect and disease affects on forests by weakening tree defenses and expanding historical ranges of pathogens. Tree mortality from insects and pathogens or directly from physiological stress is expected to increase due to longer and more intense drought periods. Changing climate is also expected to impact natural fire regimes. Recent projections indicate that large wildfires may increase almost 35% by mid-century, 55% by the end of the century under medium-high CO_2 emissions scenarios (Climate Action Report, 2006).

25.4. Changing roles, strategies, and organizations

Management techniques can be categorized into direct and indirect opportunities. Direct opportunities include utilizing the legislated mandates and regulatory mechanisms to evaluate impacts and provide recommendations on permit issuance and mitigations to air regulatory agencies. These are actions that are coordinated with air regulatory agencies to directly reduce emissions from contributing sources. Indirect management opportunities include resource manipulation to slow or reduce effects, such as thinning, prescribed fire, soil treatment, water treatment, and visitor health warnings. These indirect measures are generally applied to monitoring and modeling studies that attempt to understand the complex of stressors impacting forest ecosystems and human health and require long-term commitment of resources (Bytnerowicz et al., 1999).

25.4.1. Regulatory coordination

Two of the most significant environmental and public safety issues in California are air pollution and catastrophic wildfire as a result of unnatural fuel loadings. Dedicated professionals and scientists often champion strategies to prevent both issues, and early attempts at coordination often strained working relationships of the public agencies charged to manage these issues. Recently, communication and relationships have improved through a number of forums leading to a better understanding of both issues. These forums have become institutionalized and are leading to more informed solutions and balanced progress. Improved communication has led to collaboration on policy shifts and partnerships in the development of technical tools for improving smoke management.

Three levels of working groups have evolved in California and have become very effective in resolving issues related to wildland fire:

- Interstate—The Western Regional Air Partnership (WRAP) is an organization of western states, tribes, and federal agencies to coordinate visibility improvement in all western Class I areas by providing technical and policy tools.
- Statewide—The California Interagency Air and Smoke Council (IASC) serves as a forum for sharing information and developing technical tools and processes for improved smoke management. Scientists and managers from EPA, ARB, local/regional air regulatory agencies, and land management agencies attend this quarterly forum. The Air

and Land Managers (ALM) group meets quarterly and consists of executive level staff from ARB and the land management agencies. This group typically addresses policy and unresolved issues raised by IASC.

- Air Basin—Most local air regulatory agencies and land management agency units in California have developed smoke management working groups in common air basins. These groups coordinate the operational procedures of permit issuance, fire and dispersion meteorology, smoke modeling, daily burn allocations, smoke monitoring, public safety, and public health. During periods of prescribed fire, fire use, or wildfire these elements are discussed and decisions made in daily conference calls.

25.4.2. Monitoring

An important component of agency air resource management is to conduct or coordinate a variety of monitoring activities in rural and remote areas. Monitoring allows land management agencies to better understand current conditions and trends. Trends in ambient air quality and the relationship with biological and physical resource condition can be valuable information for policy makers and regulators. Air pollution monitoring is an important activity that supports national programs such as the Interagency Monitoring of Protected Visual Environments (IMPROVE) and the Clean Air Status and Trends Network (CASTNET) and provides air quality data for remote areas lacking continuous air monitors. One important tool for monitoring air pollution in remote areas is the use of passive samplers for monitoring O_3 and other gaseous air pollutant concentrations (Koutrakis et al., 1993). Ozone sampling utilizes cellulose filters coated with nitrite (NO_2^-) that is oxidized by ambient ozone to nitrate (NO_3^-). The rate of NO_3^- formation (amount of NO_3^- formed on a filter over time of exposure) serves as a measure of O_3 concentration. Concentrations of O_3 measured with passive samplers are compared at selected sites with real-time O_3 measurements with the UV absorption Thermo Environmental Model 49 or portable UV absorption 2B Technologies monitors (Bognar & Birks, 1998). The empirically derived coefficients are used for calculating O_3 concentrations from other passive sampler sites. By using this approach, regional monitoring networks that consist of 50–100 sites can be maintained for several growing seasons. Passive samplers provide 2-week averages (or other chosen periods of time) of O_3 or other gaseous air pollutants. Information on real-time concentrations of O_3 can be obtained from existing O_3

monitors (CASTNET, National Acid Deposition Program (NADP), and ARB networks, and portable 2B Technologies monitors). These monitoring efforts allow O_3 distribution surfaces to be estimated using geostatistical estimation.

Various PM monitors are distributed at several National Forests and Parks in California. These monitors consist of BAM 1020, EBAM and E-Samplers (Met One Instruments, Inc.). The BAM 1020 and EBAM instruments work on the principle of beta attenuation. The BAM 1020 is a federal reference instrument that requires ambient temperature control. The EBAM is not a federal reference instrument, but serves as a portable air monitor without a requirement for ambient temperature control. The BAM 1020 is equipped with wind speed/wind direction, air temperature, relative humidity, barometric pressure, solar radiation, and precipitation. The EBAM can be equipped with the same meteorological parameters except for solar radiation and precipitation. The E-Sampler is a portable instrument based on the principle of near-forward light scattering and incorporates a gravimetric filter device that can be used to improve the accuracy of the concentrations. E-Samplers compare reasonably well with the Federal Reference Method (Procter et al., 2003).

PM monitors can be used at fixed locations year around, such as the BAM 1020 instruments located in Kernville, Springville, and Pinehurst (Sequoia National Forest), but the majority of monitors are used just during periods of wildland and prescribed fires. Mobile monitors are distributed over regions at National Forests and Parks that conduct frequent prescribed fires or are prone to severe wildland fires. These instruments are typically operated only during fire seasons or as support for regional monitoring or modeling studies. Networks of PM monitors allow air regulatory agencies and land management agencies to collaborate on burn decisions and improve smoke management strategies that are more effective at protecting public health.

Monitoring forest health and injury have also been important components of air resources management. Beginning in the early 1970s, ozone injury monitoring sites were established in California National Forests and Parks. Some sites were maintained jointly with FS and NPS by research institutes, such as the San Bernardino Mountain sites and some have been maintained by FS Pacific Southwest Region's Air Quality Management unit or the NPS Air Management program. As funding allowed, sites have been evaluated for ozone, insect, and drought damage but few comprehensive evaluations have been conducted since the early 1990s. As a result there is little information on recent regional changes in ozone injury severity or the regional relationships between ozone injury and tree mortality.

25.4.3. Modeling

Air quality models use mathematical techniques to simulate chemical and physical processes that influence air pollution as it disperses and chemically reacts in the atmosphere. Air quality models are a valuable tool to land managers attempting to understand the significance of a proposed source, the effectiveness of proposed control strategies, potential issues related to multiple sources, and the concentration or loading of pollutants ultimately delivered to resources on federal land. In addition, models that can estimate biological damage or impact to physical features, such as visibility, help land managers provide more informed input to regulatory permit decisions. Dispersion models, that estimate the concentration of pollutants downwind, are often used in the analysis of proposed major stationary sources to estimate the concentration or deposition of pollutants transported to Class I areas. This is often the most important data an FLM has to work with in making a recommendation on the issuance of permits to construct stationary sources. Dispersion models are also used in land management agency actions and decisions that may produce regulated emissions. Smoke from wildland fire may be the most common of these activities, but other examples include recreation activities, oil and gas development, and construction activities. These modeling activities provide valuable information to FLMs regarding potential regulatory violations that may directly affect a decision. Additional modeling issues include:

- Increasing the understanding of fire behavior and smoke dispersion.
- Expanding knowledge of the physics of fire–atmosphere interactions on all scales.
- Developing products and transferring new technologies related to national and regional fire-weather and air quality dynamics.
- Enhancing the ability to predict climate change effects on forests.
- Improving the accuracy of carbon accounting.
- Modeling to understand complex emissions trade-off scenarios between wildfire and prescribed fire.

25.4.4. Research partnerships

Air management is no longer just the province of the air resource specialists and regulators. Information and expertise needs have exponentially increased, often beyond either the knowledge of individuals or groups of managers. Air managers increasingly depend on researchers for information, advice, and direction on complex multidisciplinary issues. In the past cooperation has been conducted on a project level, but new and complex issues will require much more routine partnership between managers and researchers. Some research involvement will be limited to overlapping areas of interest, but some will also require joint work-plan development and joint positions.

A variety of research is needed to support air management activities. Understanding the effects of single and multiple pollutants on forest ecosystems is critical to understanding future forest composition changes. Similarly, development and application of air-monitoring equipment and computer models of plume dispersal and transport are also important. The following air pollution research questions represent a partial but not comprehensive list of research needs related to air pollution issues in California:

- What are the mass transport patterns, spatial and temporal distributions, and deposition rates of ecologically significant pollutants to Californias mountains?
- What are the effects of ozone, long-term deposition, and the interactions among nitrogen compounds, sulfur compounds, ozone, drought, and pests on the composition, structure, and function of mountain ecosystems?
- Are models used to examine emissions production and transport adequately representing conditions in California forests?
- What are the transport processes that control air pollutant and smoke concentrations and delivery in the Sierra Nevada?
- How will climate change affect future patterns of air pollution and from downwind sources? Can we project, with effects from climate change, whether these thresholds have meaning in the future? For instance, have thresholds already changed measurably from 1980?
- Are the current critical loads, thresholds, and sensitive receptors sufficient for the protection of wilderness and ecosystem values?
- What are the effects of atmospheric pollutants, smoke, and drought on terrestrial wildlife, insect species, soil invertebrates, and soil microfauna?
- What is the role of global and trans-Pacific transported pollutants in air pollution impacts on U.S. forests?
- Would progress in California emissions reductions be compromised by increased future global transport of air pollutants?
- Has existing research knowledge been effectively implemented in management plans?

25.5. Summary

Forest ecosystems are impacted by a complex of abiotic stressors, including air pollution, smoke, and climate change effects. Moderate to high ambient ozone reduces net carbon uptake, and high ozone and N deposition alter carbon sequestration, its distribution, and its residence time in the ecosystem. Air pollution and climate change are also reducing winter precipitation and increasing the severity of summer drought stress, leading to increased insect and pathogen outbreaks.

Present regulatory requirements for protection of Class I areas and proposed regulations for regional haze and climate change goals for Class I and Class II areas will increase the complexity and difficulty of prescribed fire application in these forests. Despite these challenges it is important to maintain prescribed fire as a management tool to reduce the likelihood of large fire smoke and air pollution events. To maintain prescribed fire as a tool requires increased air pollution monitoring and computer modeling tools. Better understanding, measurement and prediction of smoke plume dispersal and transport will be needed to enable fire managers to minimize the impacts of prescribed fire, wildland fire use, and wildland fire smoke on the heath and welfare of firefighters and nearby communities.

The complexity of multiple forest stressors and increased number and diversity of federal and state regulations are changing the roles and responsibilities of air managers. In addition to understanding the distribution and impacts of urban air pollution transported into wilderness areas, managers are concerned about smoke, regional haze, and climate change impacts. Coordination and facilitation efforts between land managers, air regulators, and researchers will become increasingly important aspects of federal land management. Flexibility and enhanced working relationships within and across agencies will be crucial to implementing a successful fuel management program in air pollution impacted forest areas in the future. Strong interagency partnerships between air regulators, fire managers, and researchers will be critical for successful continuation of prescribed or wildland fire use fires as viable fuel treatment strategies in polluted areas.

REFERENCES

Bognar, J.A., and Birks, J.W. 1998. Miniaturized ultraviolet ozone sensor for atmospheric measurements. Anal. Chem. 68, 3059–3062.

Bytnerowicz, A., Fenn, M.E., Miller, P.R., and Arbaugh, M.J. 1999. Wet and dry pollutant deposition to the mixed conifer forest. In: Miller, P., and McBride, J., eds. Oxidant Air Pollution Impacts in the Montane Forests of Southern California: The San Bernardino Mountain Case Study. Springer-Verlag, New York, pp. 235–269.

CAA (Federal Clean Air Act). 1990. United States Code, Title 42, Chapter 85. http://www.epa.gov/air/oaq_caa.html/index.html.

California Climate Action Team. 2006. Report to Governor Schwarzenegger and the Legislature, California Environmental Protection Agency, March 2006. http://www.climatechange.ca.gov/climate_action_team/reports/index.html

FLPMA (Federal Land Policy and Management Act). 1976. United States Code, Title 43, Chapter 35. http://www.blm.gov/flpma/FLPMA.pdf

FRRRPA (Forest and Rangeland Renewable Resources Planning Act). 1974. United States Code, Title 16, Chapter 36. http://www.fs.fed.us/emc/nfma/includes/range74.pdf

Grulke, N.E., Minnich, R.A., Paine, T.D., Seybold, S.J., Chavez, D., Fenn, M.E., Riggan, P.J., and Dunn, A. 2008. Air pollution increases forest susceptibility to wildfires: A case study in the San Bernardino Mountains in Southern California. In: Bytnerowicz, A., Arbaugh, M.J., Riebau, A., and Andersen, C., eds. Wild Land Fires and Air Pollution, Developments in Environmental Science 8, Elsevier, Amsterdam.

Kleeman, M., Cayan, D. 2006. Impact of climate change on meteorology and regional air quality in California. Interim Report to ARB. January 2006.

Koutrakis, P., Wolfson, J.M., Bunyaviroch, A., Froelich, S.E., Hirano, K., and Mulik, J.D. 1993. Measurement of ambient ozone using a nitrite-saturated filter. Anal. Chem. 65, 210–214.

Met One Instruments, Inc. http://www.metone.com

Organic Act. 1916. United States Code Title 16, Sections 1 2 3, and 4. August 25, 1916. http://www.nps.gov/legacy/organic-act.htm

Procter, T., Ahuja, S., and McCorison, M. 2003. Managing air pollution affected forests in the Sierra Nevada. In: Bytnerowicz, A., Arbaugh, M., Alonso, R., eds. Ozone Air Pollution in the Sierra Nevada: Distribution and Effects on Forests. Developments in Environmental Science, Elsevier, Amsterdam, Vol. 2, pp. 359–370.

Westerling, A., Bryant, B., 2006. Climate change and wildfire in and around California: Fire modeling and loss modeling. http://www.climatechange.ca.gov/

Wilderness Act. 1964. United States Code, Title 16 Conversation, Chapter 23, National Wilderness Preservation System; 16 U.S.C.A. §§ 1131–1136. http://www.fws.gov/laws/lawsdigest/WILDRNS.HTML

Section V:
Concluding Section

This page intentionally left blank

Developments in Environmental Science, Volume 8 585
A. Bytnerowicz, M. Arbaugh, A. Riebau and C. Andersen (Editors)

ISSN: 1474-8177/DOI:10.1016/S1474-8177(08)00026-0

Chapter 26

Integrating Research on Wildland Fires and Air Quality: Needs and Recommendations

Andrzej Bytnerowicz, Michael J. Arbaugh, Christian Andersen and Allen R. Riebau*

Abstract

A summary is presented that integrates general information on the causes and effects of wildland fires and emissions with various ecological impacts of forest fires and air pollution in forests and other ecosystems. We also synthesize information on the regional effects of wildland fires on ambient air quality in Europe, North America, Australia, and Asia, and how this may impact visibility and human health and security. In addition, advances in remote sensing (RS), modeling, and management of wildland fires and the resulting air pollution are summarized. We also provide information for researchers and managers on the most important needs and recommendations about the interactions of wildland fires and air pollution that have been discussed in this book.

26.1. Introduction

This book has presented a wide range of chapters focusing on the effects and interactions of wildland fires and air pollution and the implications of these factors for land and air resources managers. Information in the book is particularly important given the current research on carbon sequestration and carbon trading in terrestrial ecosystems in a changing climate. Regulators and land managers are increasingly interested in the effects of fire on residence time of carbon in forests and future management practices that could be used to improve long-term carbon

*Corresponding author: E-mail: abytnerowicz@fs.fed.us

storage on both public and private land. The use of prescribed fire as a management tool needs to be reevaluated on the basis of carbon budget, its effectiveness to control fuel buildup, risks of starting catastrophic fires, or compromised air quality. Our book provides a comprehensive reference for researchers and land and air resources managers dealing with these complex issues of the interactions of wildland fire and air pollution.

Information presented in this book has been divided into four sections: I, General information and emissions; II, Ambient air quality, visibility, and human health—regional perspectives; III, Ecological impacts of forest fires and air pollution; and IV, Advances in remote sensing (RS), modeling, and management. This chapter provides an integrative synthesis of the book and presents the most important needs and recommendations for researchers and managers.

26.2. Integration of processes: causes and effects of wildland fires

26.2.1. Causes of wildland fires

Wildland fires are complex combustion processes involving various types of fuels and fire behaviors changing over time and space (Goldammer et al., this volume). Availability of fuel and fuel properties (Ottmar et al., this volume), as well as climatic and weather conditions, have a profound influence on wildland fire ignition potential, fire behavior, and fire severity (Benson et al., this volume). Air pollution, specifically elevated concentrations of ambient ozone (O_3) and nitrogen (N) deposition resulting from N pollutant emissions, predispose forests to adverse effects from drought, attacks of bark beetles, or other pests and diseases (Fig. 26.1). Indeed, impacts of air pollution may be increased with adverse climate change, escalating forest threat. Air-pollution-affected forests are characterized by increased presence of weakened or dead trees and a thick litter layer (easily available and highly combustible fuel) making them highly susceptible to catastrophic fires (Fenn et al., 1998; Grulke et al., this volume; Takemoto et al., 2001). Forest management and fire prevention management practices (Arbaugh et al., this volume), especially long-term prevention of all forest fires (such as that practiced for almost a century in the United States), have pronounced effects on probability of fire occurrence and fire severity (Minnich & Franco-Vizcaino, this volume). All of these complex processes can become more severe due to global warming (McKenzie et al., this volume) and a high incidence of arson

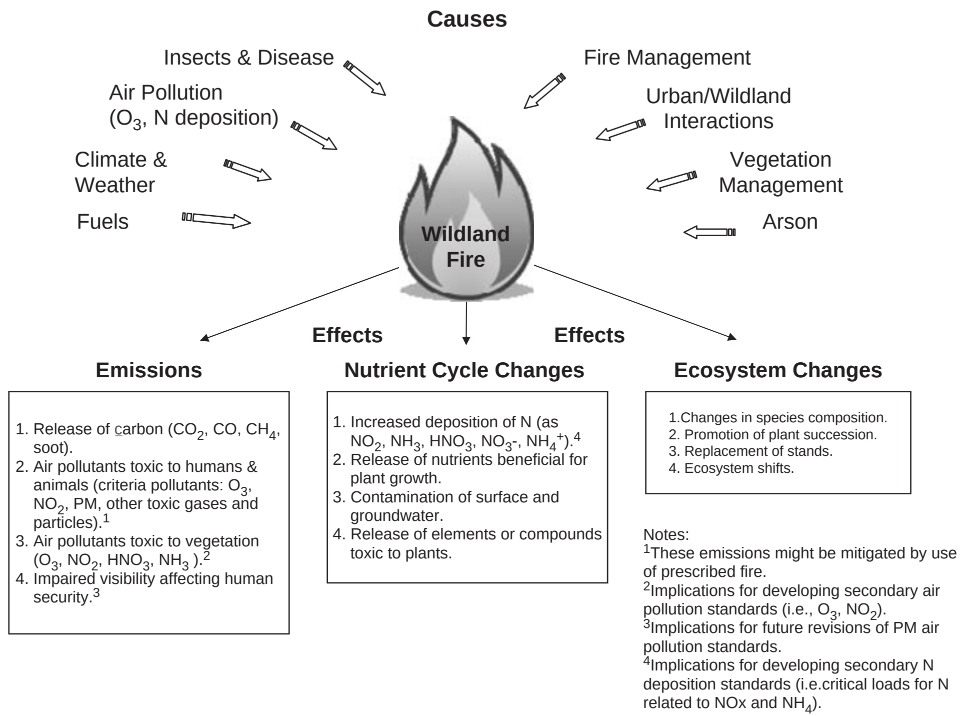

Figure 26.1. Integration of knowledge presented in Section I "General information and emissions" and Section III "Ecological impacts of forest fires and air pollution."

(Goldammer et al., this volume). Finally, large uncontrollable fires can result from climate pulses over large regions that have resulted in fire danger beyond any previously recorded level (Chubarova et al., this volume).

26.2.2. Effects of wildland fires

26.2.2.1. Emissions

Understanding potential fire emissions requires knowledge of fire sources that include size of the area burned, burn period, characteristics and condition of the fuels, amount of fuel consumed, and emission factors for specific pollutants (Ottmar et al., this volume). Smoke from fire is composed of hundreds of chemicals in gaseous, liquid, and solid forms that undergo complex chemical reactions and transformations. As a result, substantial concentrations of elemental carbon, volatile organic compounds (VOCs), carbon monoxide (CO), carbon dioxide (CO_2), nitrogen oxides (NO_x), O_3, and particulate matter (PM) may be found downwind of fires, sometimes thousand miles from the source (Goldammer et al., this volume; Urbanski et al., this volume). Some of these compounds are classified as criteria pollutants (pollutants with established air quality standards), and these include NO_x, O_3, and PM, which affect human health, reduce visibility, and impact human security (Fig. 26.1; Goldammer et al., this volume). Numerous field studies and modeling efforts indicate that changing climate is likely to increase the extent and frequency of wildfires, highlighting the importance of accurately quantifying the regional and global effects of wildfire on carbon stocks and release of atmospheric carbon compounds (Conard & Solomon, this volume).

Visibility impairment is caused mostly by aerosols (both solid and liquid), and wildland fire smoke is one of the major sources of those at the global scale. Between 25% and 60% of the organic carbon (OC) measured in ambient air is a result of smoke from wildfire. In relation to estimated natural background values, this suggests that the vast majority of the natural background of OC aerosol in the western United States results from fire, while in the eastern United States nearly 50% of it may be due to fire. A significant portion of the remaining OC in the eastern United States is likely attributable to secondary aerosol formation from vegetation emissions of reactive hydrocarbons. Visibility in the United States is also affected by fine particles transported long distances from Asia and Africa (Fox & Riebau, this volume).

26.2.2.2. Changes in Nutrient Cycling

There is a distinctive difference between the effects of wildland and prescribed fires on N status of forests. Wildfire removes substantial quantities of N by volatilization, and prescribed fire, over time, can remove as much or more N than wildfire. However, this lost N can be quickly replaced if fire is followed by N_2-fixing vegetation. Wildfire often has short-term deleterious effects on water quality because of increased N mobilization, and long-term fire suppression allows buildup of N-rich litter, a source of labile N to runoff waters (Fig. 26.1). Prescribed fire usually has less impact on water quality than wildfire (Johnson et al., this volume).

In southern California, forest fire suppression and increased N deposition contribute to increasing fuel loads and to an alteration of N fuel content. Model simulations suggest that this will affect wildfire severity and result in increases in air pollution emissions from fires, increased soil N emissions right after fire, and elevated N export to stream water (Gimeno et al., this volume).

26.2.2.3. Changes in Ecosystems

Emissions from wildland fires may result in elevated concentrations of ambient O_3 and N pollutants (Goldammer et al., this volume; Urbanski et al., this volume). Grulke et al. (this volume) found that changes in forests impacted by air pollution may be creating increased fire hazards in forests near urban areas, which have already been predisposed to occurrences of high severity (catastrophic) fires by effective fire suppression used as the prevailing management strategy in the United States in the 20th century (USDA Forest Service, 2001). Catastrophic forest fires in southern California in 2003 clearly demonstrated the consequences of such changes due to air pollution (Keeley et al., 2004). These fires can cause long-term changes in species composition during various successional stages, or can even lead to a complete replacement of forests by other ecosystems, such as chaparral or steppe (Fig. 26.1; Minnich & Franco-Vizcaino, this volume). Grulke (this volume) provides a comprehensive synthesis of the effects of altered nutrient cycling and ecosystem processes caused by wildfires, air pollution, and changing climate.

26.3. Regional issues related to fires and emissions

Effects of forest fire emissions on air pollution in Europe are described in three complimentary chapters in this book that focus on the entire

European Union (Barbosa et al., this volume), southern Europe (Miranda et al., this volume), and central and eastern Europe (Szczygiel et al., this volume). About two-thirds of the fires occurred in southern Europe (France, Greece, Italy, Portugal, and Spain) where about half million hectares of forest land burn every year, representing around 86% of the total burned area in the European Union (Barbosa et al., this volume). In southern Europe, forest fires emit large quantities of pollutants every summer that result in severe air pollution episodes. These are caused mostly by emissions from forest fires but also by emissions from aircrafts used to fight the fires (Miranda et al., this volume). In central and eastern Europe, diversified and relative young forest stands and humid climate result in much lower (moderate) fire risk than in southern Europe. In that part of Europe between 1991 and 2001 about 387,680 fires burned 757,000 ha, which is just slightly more than the average area of forest burnt in southern Europe annually (Szczygiel et al., this volume).

Examples of the effects of wildland fire emissions on human health and safety are described in this book for two well-known recent events in Russia and in Ukraine. In summer 2002, the prolonged period of high temperatures and drought in central Russia resulted in large, long-lasting fires of peat bogs and forest that caused massive smoke emissions. Smoke was transported into Moscow for a period of almost 2 months, severely reducing visibility and exposing people to the unhealthy levels of air pollutants. The fire smoke cloud was characterized by high aerosol optical thickness and high concentrations of the optically active gas species such as elevated levels of O_3 (Chubarova et al., this volume). The Chernobyl nuclear power plant explosion in Ukraine in 1986 was one of the worst environmental disasters of recent times. The fallout and accumulation of radionuclides in the soil and vegetation have had long-term impacts on the surrounding area. It is feared that radionuclides released during potentially large, catastrophic vegetation fires (especially from the Chernobyl Exclusion Zone) could spread to continental Europe, Scandinavia, and Russia. The potential for large fire occurrence was assessed based on composition of radionuclides in soil, vegetation, and in PM emitted by fires. The highest atmospheric radionuclide ^{137}Cs levels occurred in early spring and late fall, corresponding to the most intense periods of burning in the Exclusion Zone. Satellite images showed that a smoke plume from the Exclusion Zone in May 2003 dispersed several hundred kilometers southeast, reaching the major metropolitan area of Kiev (Hao et al., this volume).

These incidents, along with the late 1990s and early 2000s exposures of southeast Asian and Indonesian populations to wildland and agricultural fire emissions (Goldammer et al., this volume), are some of the best known examples of the recent effects of wildland fire smoke on human populations. Similar events are expected to happen even more frequently, given the effects of changing climate (higher temperatures and increased drought) interacting with other stresses, such as the phytotoxic effects of air pollution. The probability of the occurrence of these events is very high in Asia, especially in rapidly developing China (Qu et al., this volume). In Australia wildland fires (bushfires) range from the annual savanna fires in the north to the sporadic but extensive forest fires in the south. In addition, prescribed burning is frequently being used as a means of reducing fuel loads, for maintenance of plant and animal biodiversity, and in forestry management practices. However, here little is known about production or composition of smoke from biomass burning and the effects of fire emissions on the human population. It has been recognized that emissions from bushfires or fuel-reduction burns need to be monitored and assessed. A large proportion of the vegetation of Australia is composed of forests dominated by native species of *Eucalyptus* and *Acacia*, while large expanses of plantations are dominated by single species of *Eucalyptus,* which are well-known emitters of VOCs. Consequently, Australia's environment is unique in terms of fuel type and emissions produced from these fuels in the generally low background levels of ambient air pollutants and very different fire regimes and fuel types in most of the country (Bell & Adams, this volume).

26.4. Remote sensing, modeling, and management issues

26.4.1. Remote sensing

Application of RS (both satellites and aircraft platforms) helps with monitoring fire occurrence, fire physical characteristics, and emissions (smoke) intensity and transport patterns (Goldammer et al., this volume). Among various systems used, the FireMapper system (Riggan & Tissell, this volume) provides new abilities to study wildlfire behavior and helps to incorporate improved fire intelligence in daily firefighting operations. The remotely acquired fire-behavior data sets form an important base that can be used for validating and improving fire-behavior simulation models.

In recent years China has begun using RS as a tool for monitoring regional fire hazards, and to a lesser extent, air quality emissions. Satellite instruments such as the Advanced Very High-Resolution Radiometer (AVHRR) and the Moderate Resolution Imaging Spectroradiometer

(MODIS) have been used in Chinese field experiments and in routine monitoring of wildfires and air quality. In addition, the Landsat measurements have been used for land cover mapping to determine fuel type and loading to estimate fire emissions. All of these measurements can be useful for forest management and air quality management in China, given that forest fires could significantly increase under a warming global climate (Qu et al., this volume).

Hao et al. (this volume) recommend that a satellite receiving station to detect fires in real-time in the Chernobyl area, Ukraine, be installed. In addition, smoke dispersion and air quality forecasting model to predict the radioactivity levels downwind from catastrophic fires should be developed to reduce the risk of catastrophic exposures of inhabitants of the neighboring rural and metropolitan areas.

26.4.2. Models

Fire managers around the world use a variety of systems to track and predict fire danger and fire behavior at spatial scales that span from the local-to-global levels and at temporal scales ranging from minutes to seasons. Fire management software applications that usually incorporate one or more computer models can determine the types of planning tools used. Advanced computing technology has spawned a new generation of fire planning tools to predict fire occurrence and fire behavior. Linkages between different fire danger and behavior modeling systems and air quality models could greatly improve mapping and prediction of air pollution due to wildland fires (Fujioka et al., this volume).

Several real-time smoke prediction systems have been developed worldwide to help land managers, farmers, and air quality regulators balance land management needs against smoke impacts. Four systems that are currently operational for regional domains in North America and Australia link fire activity data, fuels information, and consumption and emissions models with weather forecasts and dispersion models to produce a prediction of smoke concentrations from prescribed fires, wildfires, or agricultural fires across a region. These real-time smoke prediction systems are providing a point of interagency understanding between land managers and air regulators from which negotiations of the conflicting needs of ecological fire use while minimizing air quality health impacts can start (O'Neill et al., this volume; Wain et al., this volume).

Various process-based models have been developed for forecasting PM and O_3 levels in the presence and absence of fires. Although these models provide deterministic predictions, few of them give measures of uncertainties associated with these predictions, which are essential for model evaluation and forecasting with known precision levels. A statistical procedure for accurate forecasting of next-day ozone levels by applying it to a real data set of the observed ambient ozone and weather values has been developed. Forecasted $PM_{2.5}$ values from the BlueSky Smoke Dispersion Model were tested as a proxy for the amount of O_3 precursors reaching a given site from specific fires. The forecasts from the statistical model may be useful as a tool for air quality managers to time-prescribed fire treatments (Preisler et al., this volume).

26.4.3. Management

The interaction between smoke and air pollution creates a basic conflict between public health and fuels treatments. Fuels treatments (prescribed fire and mechanical removal) proposed for forest and other wildlands are intended to reduce fuel accumulations and wildfire frequency and severity, as well as to protect property located in the wildland–urban interface (USDA Forest Service, 2001). However, prescribed fires produce toxic gases and aerosols that have instantaneous and long-term effects on air quality (Fang et al., 1999). If fuels treatments are not conducted, however, then wildfires may become more severe and frequent, resulting in elevated public health and safety effects. A better understanding of air pollution and smoke interactions is needed in order to protect the public health and allow for socially and ecologically acceptable use of fire as a management tool. This could be accomplished by innovative wide-scale monitoring efforts (field and remotely sensed) and development of models predicting spatial and temporal distribution of air pollution and smoke resulting from forest fires and other sources. These problems impact the general public, land managers, and policy makers, especially if urban areas or wildland-urban interfaces are affected. The U.S. Environmental Protection Agency (EPA) in cooperation with federal land managers, states, and tribes issued the Interim Air Quality Policy on Wildland and Prescribed Fire (EPA, 1998) to protect public health and welfare by mitigating the impacts of air pollutant emissions from wildland fires on air quality.

In California, fuels treatments on public lands are critical for reducing fuel accumulation and wildfire frequency and severity and for protecting private property located in the wildland–urban interface. Treatments are especially needed in forests impacted by air pollution and subject to climate change. Combinations of future climate variability and air pollution are likely to increase the risk of episodic tree mortality, long-term ecosystem changes, and increased frequency and severity of wildland fires. Fuel treatments, however, are difficult to implement in these forests.

Smoke from prescribed fires can adversely affect local and regional air quality, leading to conflicts with local and regional air-regulatory agencies. Federal air quality and fire managers have responded to these conflicting needs, actively forging cooperative relationships between fire managers and local, state, and federal air regulators. The result has been fewer conflicts about smoke in populated or protected areas while striving to achieve an adequate level of prescribed fire treatments. Social and regulatory acceptance of fire as a management tool in air-polluted forests will depend on land managers developing a better understanding of air pollution and smoke interactions and interactions between air pollution, drought, and insects. Acceptance of fire as a management tool also requires better large-scale monitoring efforts and development of models for predicting spatial and temporal distribution of air pollution and smoke from forest fires. Air pollution and climate effects have to be incorporated into forest mensuration models used to better predict forest stand development (Arbaugh et al., this volume).

Prescribed fire has also been proposed as a management tool to mitigate N saturation (a result of chronic, excessive N deposition). However, a major limitation of this strategy is that while fire removes substantial quantities of N from the forest floor, it removes only a small fraction of the large N reservoir in the mineral soil and at the same time causes increases in soil ammonium over the short term. Periodic prescribed fire to reduce fuel loads and atmospheric N deposition (through control of N air pollution) and strategies to enhance plant and microbial N demand may all be required to reduce N saturation symptoms in catchments exposed to long-term atmospheric N inputs (Gimeno et al., this volume; Johnson et al., this volume). Past and future vegetation and fire management activities also play a role in ecosystem potential to store carbon. The nature and magnitude of these impacts vary greatly among regions and ecosystems (Conard & Solomon, this volume).

To monitor and minimize the transboundary effects of air pollution resulting from vegetation fires, international policies based on science are needed to avoid excessive fire application and to establish effective fire and smoke management practices and protocols of cooperation at the international level (Goldammer et al., this volume).

26.5. Research and management needs and recommendations

This book has provided a wide range of research studies, monitoring tools, and management practices that focus on the interactions of fire and air pollution. Based on this knowledge and information, we present the following future research needs and recommendations.

26.5.1. Fuels

- More detailed characteristics of complex fuels are required for the development of more precise fire-behavior models. Specifically, improved knowledge of moisture content and its effects on ignition and combustion efficiency, spatial and qualitative complexity of fuels, vertical and horizontal description of fuel beds, and combustion characteristics of rotten fuel and organic layers are needed.
- Better methods for mapping real fuel characteristics at the broad scales relevant for regional air quality modeling, and for understanding how small-scale variation can be captured in broad-scale data are required.

26.5.2. Climate/weather

- Improved weather forecasting of changing climate/atmospheric circulations at the local-to-regional scales are recommended, as well as more precise seasonal forecasts to better predict fire behavior.
- Better understanding of atmosphere/biosphere interactions that may result from the increase of greenhouse gases in the atmosphere is needed.
- Full physics-based models of fire behavior that incorporate interactions with the atmosphere need to be developed.
- To improve fire danger and fire-behavior modeling, very fine scale (48- to 96-hour) wind simulations in complex terrain at the scale of tens of meters that are linked to mesoscale weather are needed.
- Because current resolution of regional climate models is too low ($\sim$50 km), more accurate empirical and statistical downscaling tools need to be developed for assessing the impact of climate change on fire behavior and fire emissions.

26.5.3. Fire detection

- Continued improvement in fire detection capabilities, especially in regard to size estimates and actual fuel consumed, are necessary. Specifically, high-resolution fire imagery is needed in real-time to monitor and map fire activity and smoke dispersion.
- Remote Sensing of fire occurrences should assess fire dynamics and be integrated with information on fire intensity (which can be derived

from the fire-radiative energy). This approach would help in a better assessment of fire effects and smoke emissions.

- Mapping burn scars and fire intensity using a variety of satellite data is needed for inventory of the effects of fires on forest and other ecosystems.

26.5.4. Prediction of fire behavior

- Better linkage of fire behavior models with atmospheric dispersion and air quality models is needed. Improved coupled fire-atmosphere models should help to predict the effects of fire on atmospheric processes.
- Physics-based models of fire behavior that function on small to large scales and include more accurate dynamics of fire behavior (such as extreme fire behaviors—both spot and crown fires) are needed. These models would provide levels of uncertainty that are essential for fire prediction in operational fire management (see Section 26.5.2).
- In-situ observations at the fire-atmosphere interface are recommended to validate fire behavior models.
- Improved forecasts for lightning events at the short and medium range are necessary.
- More sophisticated models are needed to understand the coupling between the atmosphere and vegetation under increased atmospheric carbon dioxide scenarios.

26.5.5. Emissions chemistry and in-plume chemistry

- Improved characterization of emissions of air pollutants and greenhouse gases during fire events is needed to increase accuracy of international emissions estimates. Consequently, more and better field studies on fuel consumption and emissions in various natural fuel beds should be conducted.
- Emissions from peat and bog fires, which are extremely important for greenhouse gas inventories and understanding extreme smoke events in the northern hemisphere, must be better understood and characterized.
- Treatment of fire emissions (including H_2O) in the models simulating atmospheric chemistry and formation of secondary aerosols should be improved.
- Chemical synthesis of forest fire smoke as the synergistic or the additive result of different types of fuels burnt and materials contained in the smoke haze must be investigated (especially when the forest fire front expands into the urban-rural interface).

- Field studies designed to measure smoke concentrations in three dimensions (not just at the surface) should be conducted. Use of an unmanned aerial vehicle (UAV) with $PM_{2.5}$ (and other trace gas species) monitors or canister samples for chemical analysis should be considered.
- Detailed identification and chemical analysis of functional groups of VOCs is needed to develop markers (gaseous or aerosol tracers) that could be used to distinguish smoke from prescribed versus wildland fires.
- To improve air quality models, the treatment of smoke plumes as they move and encounter pollutants from other sources need to be tested and improved. This is crucial for understanding secondary aerosol formation or ozone generation.
- Effects of chronic N deposition and N accumulation in ecosystem on fire emissions chemistry should be better understood.
- Measurements of plume heights, dynamics, movement, and aerosol properties are needed in order to validate smoke dispersion models.
- The unique fuel types and emissions in Australian environments (low levels of air pollution in much of the country in contrast to fire regimes and fuel types from north to south) could be used as a testing ground for future emission studies.

26.5.6. Ambient air quality

- Real-time monitoring of ambient air quality during forest fires, using improved field analytical methods is recommended to assess potential impacts to public health.
- Regional air quality models need to include realistic wildland fire emissions. Therefore, fire prediction models must be used in conjunction with smoke prediction models, especially to quantify the spatial and temporal dynamics of fire emissions.
- Fire behavior models should be coupled with meteorological and chemical models for improved pollution transport models. Transport patterns, spatial and temporal distributions of pollution plumes, and complexity of mountain terrain and effects of changing climate should be better characterized in such models, which could lead to improved accuracy and precision of predictions.
- Air quality forecasting models predicting pollutant levels downwind from large fires and catastrophic mega-fires should be developed. These models should be verified during large-scale field measurement campaigns.

- Long-range transport of pollutants (trans-Pacific, trans-Atlantic, and cross-continental) that may affect background levels of pollutants toxic to humans and vegetation should be evaluated.

26.5.7. Carbon release and greenhouse effects

- Information on the extent and severity of fire, the feedbacks between fire and climate, and the effects of changing fire regimes on all aspects of the carbon cycle is recommended before we can fully predict the magnitude, or perhaps even the direction, of the effect of changing fire regimes on global carbon balance, greenhouse gas emission, and atmospheric chemistry. To accomplish this, much better information about the amount of burned biomass, especially during wildfires, is needed, as well as a better understanding of industrial and urban sources of carbon release.
- Valid, accurate, and precise emissions inventories have to be developed and maintained by countries for all fire types, especially in those regions where fire is significant. This is especially true as the next generation of carbon accounting is developed.
- The relationship between changing fire and agricultural regimes should be better understood and included in the greenhouse gas mitigation strategies.

26.5.8. Ecological impacts on forests

- The effects of ozone and nitrogen atmospheric deposition must be better understood, as well as the interactions among various pollutants, drought, and pests on the composition, structure, and function of forests and other ecosystems. This research should include the effects of these pollutants on biodiversity, including changes in vegetation, wildlife, insects, soil invertebrates, and soil microorganisms.
- Critical loads of atmospheric deposition, thresholds of toxic effects of air pollutants, and sensitive receptors that can be easily identified must be determined for the protection of wilderness and ecosystem values from the effects of wildfire emissions and other types of air pollution exposures.
- Long-term effects of fire on nutrient budgets (especially carbon, nitrogen, and phosphorus), in forest ecosystems should be determined.
- Models aimed at better understanding of the effects of air pollution and climate change on forests at the landscape scale (that incorporate topography, land use, etc.) are needed.

26.5.9. Health effects of smoke

- The quantification of hazardous compounds in smoke from biomass burning should be used in risk analysis of health and safety of firefighters and the general public during wildfire and prescribed burning activities. This would allow for a better-informed decision-making process.
- Representative key indicators (target forest-fire smoke compounds) for monitoring of air quality during wildland firefighting operations should be defined.
- Effectiveness of personal protective equipment for firefighters and the exposed population should be tested.
- Long-term effects of smoke exposure on the health of firefighters should be understood. In order to accomplish this goal, some novel approaches (e.g., chemical analysis of expired air) should be used.
- Exposure limits to hazardous compounds during forest fire and evacuation criteria for sensitive groups of population should be determined.

26.5.10. Management issues

- Because smoke affects air quality and therefore must be measured so that air quality can be improved, a better link between forest fire and air quality communities is needed.
- Data generated by meteorological and smoke prediction systems should be meaningfully and usefully delivered to the user communities (land managers, air quality regulators). Continued collaboration is required between the tool developers and the users if benefits of scientific advancements are to be realized. Effective use of information management concepts should be applied to improve usefulness of data and to safeguard it.
- Effective collaboration between air resources and land managers is needed to evaluate opportunities to increase the utility of prescribed fire to treat accumulated fuels in wildlands. Increased air monitoring efforts and development of probabilistic dispersion models to better manage smoke and minimize public health impacts are recommended. The existing knowledge on the use of prescribed fire and its effects on air quality should be effectively implemented in future management plans.
- Effective technology development addressing new problems, challenges, and program elements is needed. It should include development of new technologies for fire and air quality monitoring, information

management, and modeling. Strong linkages between specialists in various fields (fire sciences, climatology, atmospheric sciences, forestry, ecology, and others) are recommended.

- Successful air resource management based on close coordination with other land managers, air resource specialists, researchers, air-regulatory agencies, and public and private organizations with environmental interests is strongly encouraged.
- Tradeoffs between short-term smoke management and the potential for greater future impacts from restricting prescribed fires and by suppressing fires must be better understood.
- Comparison of land management options used in the northern hemisphere (e.g., Europe, United States, and Canada) with those used in the southern hemisphere (e.g., Australia and New Zealand) is needed given the wide variability of wildfires and the effects of air pollution in these different environments and ecosystems.
- Effects of large fires and mega-fires on air quality and the implications for public health have to be better understood. Occurrence of such fires is increasing in both the northern and southern hemispheres, perhaps as a result of record-breaking fire weather extremes exacerbated by increased climate variability. Profound advances in fire and air quality science are needed for characterizing these fire classes and should be considered imperative.

ACKNOWLEDGMENTS

We thank all contributors who provided suggestions for the needs and recommendations presented in this chapter. This summary was supported by Joint Fire Science Program, the U.S. Forest Service Pacific Southwest Research Station and a National Science Foundation grant (NSF DEB 04-21530). This document has been revised in accordance with U.S. Environmental Protection Agency Policy and approved for publication. Mention of trade names or commerical products does not constitute endorsement or recommendation of use.

REFERENCES

Arbaugh, M. J., Procter, T., and Esperanza, A. this volume. Managing air pollution impacted forests of California.

Barbosa, P., Camia, A., Kucera, J., Liberta, G., Palumbo, I., San-Miguel, J., and Schmuck, G. this volume. Assessment of forest fires impact and emissions in the European Union based on the European Forest Fire Information System.

Bell, T., and Adams, M. this volume. Smoke from wildfires and prescribed burning in Australia: Health and environmental issues.

Benson, R.P., Roads, J.O., and Weise, D.R. this volume. Climatic and weather factors affecting fire occurrence and behavior.

Chubarova, N.Y., Prilepsky, N.G., Rublev, A.N., and Riebau, A.R. this volume. A mega-fire event in central Russia: Fire weather, radiative and optical properties of the atmosphere, and consequences for subboreal forest plants.

Conard, S.G., and Solomon, A.M. this volume. Effects of wildland fire on regional and global carbon stocks in a changing environment.

EPA. 1998. Interim Air Quality Policy on Wildland and Prescribed Fires, Office of Air Quality Planning and Standards, Research Triangle Park, N.C., USA, 40 pp.

Fang, M., Zheng, M., Wang, F., To, K., Jaafar, A., and Tong, S. 1999. The solvent-extractable organic compounds in the Indonesia biomass burning aerosols-characterization studies. Atmos. Environ. 33, 783–795.

Fenn, M.E., Poth, M.A., Aber, J.D., Baron, J.S., Bormann, B.T., Johnson, D.W., Lemly, A.D., McNulty, S.G., Ryan, D.F., and Stottlemeyer, R. 1998. Nitrogen excess in North American ecosystems: Predisposing factors, ecosystem responses, and management strategies. Ecol. Appl. 8, 706–733.

Fox, D., and Riebau, A.R. this volume. Effects of forest fires on visibility and air quality.

Fujioka, F.M., Malcolm Gill, A., Viegas, D.X., and Wotton, B.M., this volume. Fire danger and fire behaviour modeling systems in Australia, Europe, and North America.

Gimeno B.S., Yuan F., Fenn M.E., and Meixner T. this volume. Management options for mitigating nitrogen (N) losses from N-saturated mixed-conifer forests in California.

Goldammer, J.G., Andreae, M.O., and Statheropoulos, M. this volume. Impacts of vegetation fire emissions on the environment, human health and security—a global perspective.

Grulke, N. this volume. Interactive effects of climate and wildland fires on forests and other ecosystems—Section III synthesis.

Grulke, N.E., Minnich, R.A., Paine, T., Dunn, A., and Chavez, D. this volume. Air pollution increases forest susceptibility to wildfires in southern California.

Hao, W.M., Bondarenko, O.O., Zibtsev, S., and Hutton, D. this volume. Vegetation fires, smoke emissions, and dispersion of radionuclides in the Chernobyl exclusion zone.

Johnson, D.W., Fenn, M.E., Miller, W.W., and Hunsaker, C.F. this volume. Fire effects on carbon and nitrogen cycling in forests of the Sierra Nevada.

Keeley, J.E., Fotheringham, C.J., and Moritz, M. 2004. Lessons from the October 2003 wildfires in southern California. J. For. 26–31.

McKenzie, D., Peterson, D.L., and Littell, J. this volume. Global warming and stress complexes in forests of western North America.

Minnich, R.A., and Franco-Vizcaino, E. this volume. A probabilistic view of chaparral and forest fire regimes in southern California and northern Baja California.

Miranda, A.I., Marchi, E., Millan, M., and Ferretti, M. this volume. Forest fires and air quality issues in southern Europe.

O'Neill, S.M., Larkin, N.K., Hoadley, J., Mills, G., Vaughan, J.K., Draxler, R., Rolph, G., Ruminski, M., and Ferguson, S.A. this volume. Regional real-time smoke prediction systems.

Ottmar, R., Miranda, A.I., and Sandberg, D.V. this volume. Characterizing sources of emissions from wildland fires.

Preisler, H.K., Zhong, S., Esperanza, A., Tarnay, L., and Kahyaoglu-Koracin, J. this volume. A statistical model for forecasting hourly ozone levels during fire season with specified precision.

Qu, J.J., Hao, X., Liu, Y., Riebau, A.R., Yi, H., and Qin, X. this volume. Remote sensing applications of wildland fire and air quality in China.

Riggan, P.J., and Tissell, R.G. this volume. Airborne remote sensing of wildland fires.

Szczygiel, R., Ubysz, B., and Zawila-Niedzwiecki, T. this volume. Spatial and temporal trends in distribution of forest fires in Central and Eastern Europe.

Takemoto, B.K., Bytnerowicz, A., and Fenn, M.E. 2001. Current and future effects of ozone and atmospheric nitrogen deposition on California mixed conifer forests. For. Ecol. Manage. 144, 159–173.

Urbanski, S.P., Hao, W.M., and Baker, S. this volume. Chemical composition of wildland fire emissions.

USDA Forest Service. 2001. Record of decision: Sierra Nevada forest plan amendment environmental impact statement. http://www.r5.fs.fed.us/sncf/eis/rod/rod.pdf.

Wain, A., Mills, G., McCaw, L., and Brown, T. this volume. Managing smoke from wildfires and prescribed burning in southern Australia.

Author Index

Abbadie, L. 8
Aber, J.D. 18, 418, 427–428, 586
Abushenko, N. 114
Acheson, J.A.K. 62
Acheson, J.D.K. 500
Achtemeier, G.L. 52, 523, 530
Adachi, K. 428, 448
Adamowicz, W.L. 27
Adams, G.C. 360, 407
Adams, M.A. 307, 591
Adams, R.P. 306
Aden, H. 295
Aditama, T.Y. 297
Agee, J.K. 116–117, 450
Agsorn, S. 297
Aiga, I. 302
Ain-Lhout, F. 392
Akimoto, K. 94
Albini, F.A. 49–51, 80, 87
Albright, M. 508, 512
Alessio, G.A. 307
Alexander, M.A. 333
Alexander, M.E. 49, 51, 477–478, 481
Alexander, W. 373
Alfred, J. 114
Allan, G.E. 476
Alleaume, S. 85
Allen, C.D. 323, 331, 333, 431–432, 435–436
Allen, E.B. 374, 416–417, 426, 430, 447, 464
Allen, G.J. 376, 386–387
Allgower, B. 66
Alonso, R. 373, 375, 386
Al-Saadi, J. 177, 180
Altyntsev, D. 114
Alvarado, E.C. 65, 72, 428, 448
Alvarez, A. 66
Ames, R.B. 185
Amiro, B.D. 27, 41, 121
Amorim, J.H. 10–11, 62, 70, 72, 210, 221, 292
Amundson, R.G. 325
Andersen, C.P. 303, 373–374, 379, 392, 416, 430
Anderson, D.H. 483
Anderson, E.R. 115
Anderson, G.K. 67, 178, 505, 531
Anderson, H.E. 65, 80
Anderson, J.J. 323
Anderson, K.R. 483, 487
Anderson, P.D. 298
Anderson, S. 431–432, 435–436
Andersson, M. 122
Andrade, M.N. 64
Andreae, M.O. 4, 8, 13, 61–63, 66, 70, 85, 88, 92, 94, 113, 210, 164–165, 291, 293–294, 301–302, 406, 505, 586
Andreu, A.G. 504
Andreu, D.V. 66
Andreu, R.A. 66
Andrews, P.L. 42, 46–48, 50, 52, 65, 116, 118, 283, 297
Angle, R.P. 428
Annegarn, H.J. 85
Antonovskiy, M. 53
Apinan-Kamnalrut, 430
Apituley, A. 217
Apps, M.J. 114–115, 117
Arbaugh, M.J. 325, 373, 379–380, 387, 395, 415–416, 430, 576, 594
Arbelbide, S.J. 72
Archer, J. 307
Arellano, A.F. 80, 111–113, 121, 126, 207
Arey, J. 93, 373
Armitage, O.B. 41, 477
Arnebrant, K. 379
Arnold, S. 94
Arnolds, E. 304
Arnott, W.P. 82, 84, 87, 268
Artaxo, P. 12, 16, 45, 85, 91
Arvevalo, J.R. 405

Ashbaugh, L.L. 185
Asher, J.E. 368
Asner, G.P. 322, 331
Assmann, S.M. 386
Atkinson, R. 93, 95, 373
Atlas, E.L. 88, 91, 94, 428, 448
Auclair, A.N.D. 409
Avery, M. 94
Axler, R.P. 407
Azzi, M. 548

Babbit, R.E. 84, 87–88, 91, 107
Babbitt, R.A. 82–83, 91–92
Babbitt, R.E. 62, 70, 82–84, 87, 91, 268
Bachelet, D. 127, 329
Back, P.V. 115
Backor, M. 125
Baer, B.L. 83
Baeza, M.J. 118
Baird, M. 408
Bais, H.P. 306
Baisan, C.H. 125, 127
Baker, D. 111
Baker, S.P. 84, 87–88, 91, 103, 107, 117, 120–122
Baker, W.E. 503
Baker, W.L. 360
Baker, W.M. 88, 91
Bala, G. 127
Balduman, L. 377, 380, 430
Balice, R.G. 323
Balkanski, Y. 93
Ballenger, E.A. 450
Balzter, H. 126
Banta, R.M. 51
Barbosa, J. 72, 214
Barbosa, P.M. 111, 200–201, 590
Barbour, M.G. 343, 352, 354, 427
Barbour, N.G. 393
Barker, D.O. 503
Barlow, B.A. 290
Barna, Schichtel, M.G. 191
Barnes, I. 93
Baron, J.S. 333, 417–418, 426–428, 447–448, 464, 586
Barro, S.C. 345
Barry, D.A. 19, 42
Barth, M. 418
Bartram, B.W. 51
Bary, G.A.V. 475–476
Bates, T.S. 94
Battaglia, F. 51
Battye, R. 62–63, 70, 178, 505
Battye, W.B. 62–63, 70, 178, 505
Baudet, J. 8
Bauer, G. 125
Bauer, M.R. 375
Baughcum, S. 216
Baulch, D.L. 95
Baum, H.R. 51
Baumann, K. 91
Bayard, A.C. 504
Bayard, A.G. 66
Bazzaz, F.A. 18
Beck, J.A. 475, 487
Beck, J.P. 217
Becker, A. 17
Beer, R. 85
Beer, T. 41, 49, 295, 537
Behn, A.D. 476
Beirle, S. 52, 114
Bekele, F. 40
Belillas, C.M. 405
Bell, J.N.B. 305
Bell, T.L. 307, 591
Belnap, J. 323
Belote, A. 80, 112, 121
Belote, C. 180
Belward, A. 53
Benito, J.G. 126
Benjamin, M.T. 306
Benkoussas, B. 81
Benning, G. 376, 386–387
Benson, R.P. 586
Bentz, B.J. 327
Berg, B. 379
Berg, E.E. 329
Berger, W.H. 356
Bergeron, Y. 39, 127
Beringer, J. 294, 329
Berlowitz, D. 224
Bertman, S.B. 94
Bertschi, I.T. 52, 62, 82–85, 88, 91–92, 107
Betancourt, J.L. 39, 125, 320, 323, 360
Beverly, J.L. 477, 479
Bevilacqua, E. 483
Bevilacqua, R. 114
Bey, I. 500
Beyers, J.L. 384
Bezlova, A. 278

Bigler, C. 320
Billington, J. 552
bin Abas, M.R. 293
Binkley, D. 409, 418
Binnie, J. 305
Birdsey, R.A. 115
Birdsey, S. 322, 331
Birks, J.W. 577
Bjorndal, K.A. 356
Black, R. 552
Black, V.J. 303
Blackmarr, W.H. 485
Blackmon, M.L. 40
Blair, J.M. 122, 297
Blake, D.R. 12, 16, 80, 85, 88, 91, 93–95, 107, 292
Blake, T.W. 117–118, 120, 122, 481
Blakeslee, R.J. 47
Blanc, P.D. 297
Blanche, C.A. 391
Blank, R.R. 407–408, 415, 419
Blubaugh, T.J. 378, 416–417, 430
Boardman, H.P. 407
Boccippio, D.J. 47
Boden, T.A. 111
Boeck, W.L. 47
Boehm, H.-D.V. 111–112, 121, 126
Boersma, K.F. 85
Bognar, J.A. 577
Bogorodskaya, A. 121
Bohn, B. 228
Bohn, U. 201
Boissard, C.C. 91, 305–306
Bolch, L. 306
Bolin, B. 110, 126
Bonan, G. 127
Bond, T.C. 85
Bond, W.J. 306
Bondarenko, O.O. 590, 592
Bonello, P. 390
Bonsal, B. 40, 320
Bonsang, B. 8, 91
Booze, T.F. 9, 297
Borden, J.H. 390, 393
Borken, W. 122
Bormann, B.T. 418, 427–428, 586
Borrego, A.G. 62, 210, 223, 227–228
Borrego, C. 10–11, 62, 70, 72, 210–211, 214–215, 219–221, 292
Borrego, P. 228
Botelho, H. 86–87
Both, R. 302, 304
Botsford, L.W. 356
Boucher, T.V. 329
Boulter, S.L. 304
Bourgeau–Chavez, N.H.F. 83
Bourgeois, G. 307
Bourque, B.J. 356
Bousquet, P. 111
Bovio, G. 489
Bowen, R.A. 503, 540
Bowman, C. 508, 512
Bowman, D.M.J.S. 290, 297
Bowman, K. 85
Bowman, W.D. 426, 447, 464
Boyce, J.S. 381
Boyer, M. 508
Brace, S. 325
Bradbury, R.H. 356
Bradshaw, L.S. 283, 485, 489
Bradstock, R.A. 477
Brain, J. 483
Brancaleoni, E. 296, 305
Brandt-Rauf, P.W. 297
Brass, J.A. 8, 118, 140, 142–145, 147, 151–153, 155, 360, 414–415, 428, 450
Brasseur, G.P. 13, 111, 113, 268
Brauer, M. 13, 295, 297, 305
Breiner, J. 373–374, 380, 426–427, 432, 448
Brennan, T.J. 450
Breshears, D.D. 323, 331
Breyfogle, S. 71, 501
Breysse, P.A. 295
Breysse, P.N. 13, 80
Bridgman, H.A. 40
Briffa, K.R. 324
Briggs, G.A. 515
Brocard, D. 293
Brooks, F.E. 360
Brotak, E.A. 42, 45
Browell, E. 94
Brown, A.R. 305
Brown, J.K. 73, 83, 87–88, 115, 118
Brown, L. 592
Brown, M. 125–126
Brown, T. 547
Brown, N.A.C. 304, 428
Brown, P.J. 305
Brown, S. 110, 114
Brown, T.J. 39, 127–128, 187, 349, 555

Brown, W. 512
Bruhwiler, L.P. 111–112, 121
Brumme, R. 122
Brunke, E.-G. 111
Brustet, J.M. 8, 210
Bryant, B. 575
Bååth, E. 379
Buchshtaber, V. 53
Buck, C.C. 46
Buckley, T.G. 13
Buckley, T.J. 80
Buechler, D.E. 47
Builtjes, M. 228
Bukenhofer, G.A. 117
Bull, E.L. 450
Bunkers, M.J. 40
Bunnell, W.J. 116–117, 129
Bunyaviroch, A. 577
Burgan, R.E. 65, 177, 201, 207, 283, 345, 486
Burgan, S. 47
Burk, J.H. 343, 352, 354, 393, 427
Burke, R.A. 123
Burns, M.F. 117, 120, 178
Burns, T.D. 407
Burnside, R.E. 329
Burrows, N.D. 476, 538
Burrows, W.H. 115
Burtscher, H. 295
Buseck, P.R. 428, 448
Busse, M.D. 415, 417
Butler, B.W. 51
Byers, J.A. 390
Byles, J.J. 297
Byram, G.M. 51, 475, 479, 481, 486
Byrne, R. 356
Bytnerowicz, A. 298–301, 325, 373, 415–418, 430, 553, 576, 586
Byun, D.W. 508

Caballero, D. 211
Cachier, H. 8
Cahill, T.M. 373
Cahoon, D.R. 91–93, 111–112, 180
Caldeira, K. 127
Caldwell, B.A. 379
Caldwell, T.G. 405–406, 409, 412, 415, 418–419, 427
Callander, B.A. 18
Calogine, D. 66
Camia, A. 590
Camia, P. 201
Campbell, J.L. 124
Campbell, S.A. 390
Campos, T.L. 8, 88, 91, 118, 140, 142–145, 147, 151–153, 428, 448
Canagaratna, M.R. 94
Cape, J.N. 298, 301, 303, 305–306
Caporn, S.J.M. 304
Caprio, A.C. 552
Cardoso Pereira, J.M. 111
Carey, C. 333
Carlson, T.N. 45
Carmichael, G.R. 62, 80, 210, 294
Carmona-Moreno, C. 53, 293
Carouge, C. 111
Carras, J.N. 91, 548
Carreiro, M.M. 379
Carrico, C.M. 428
Carriera, J.A. 405
Carrillo, J. 428
Carroll, A. 326
Carroll, E.F. 408, 415
Carroll, E.M. 408
Carter, J.O. 115
Carter, M.C. 450
Caruana, A. 8–10, 21
Carvalho, A.C. 62
Carvalho, P. 72, 214
Carvalho, V. 228
Cascio, C. 375, 386
Cass, G. 9
Castilla, C. 210
Castillo, F. 386
Castro, R. 349
Catchpole, E.A. 48, 483
Catchpole, W.R. 48, 475, 477
Catling, P.C. 537
Cavaleiro, J.A.S. 307
Cayan, D.R. 38–39, 125, 129, 320, 349, 360, 366, 406, 575
Caylor, K.K. 85
Cecchetti, G. 304
Cecinado, A. 296, 305
Certini, G. 406–408
Cesti, G. 27
Cetegen, B.M. 506
Chacon, N. 128
Chakrabarty, R.K. 268

Chambers, S.D. 127
Chang, S. 179
Chao, Y. 360
Chapin, F.R. 407
Chapin III, F.S. 127, 329
Chapman, W.L. 329
Charles, M.J. 373
Chase, C.H. 65, 283
Chase, E. 297
Chatfield, R. 45
Chavez, A. 586, 589
Chavez, S.J. 457, 461
Chazette, P. 217
Chen, L.-W.A. 82, 84, 87, 297
Chend, J.M. 121
Cheney, N.P. 45, 65, 294, 475–476, 530–531, 538
Cheng, L. 428
Chepfer, H. 217
Chin, M. 114, 187
Chiu, N. 283
Choromanska, U. 406
Chorover, J. 408, 415
Chou, Y.H. 340, 342–344, 346, 348, 360–361
Chow, J.C. 9, 82, 84, 87
Christensen, N.L. 64, 114, 117
Christian, H.J. 47
Christian, T.J. 12, 16, 80, 85, 88, 91, 94, 107
Christiansen, E. 391, 393
Christopher, D.L. 500
Christopher, S.A. 18
Chuang, H.-Y. 514, 529
Chubarova, N.A. 252, 258
Chubarova, N.Y. 588, 590
Churkina, T.V. 117, 120, 122
Chuvieco, E. 293
Ciais, P. 111, 293
Ciccioli, P. 296, 305
Cihlar, J. 111
Cindrity, S.J. 371
Claiborn, C. 513, 524
Clark, C.S. 376
Clark, T.L. 530
Clavijo, A. 392
Clements, M. 91
Clinton, N.E. 428, 449
Cobb, F.W. 381, 389, 392
Cobb, N.S. 323
Cochrane, M.A. 111, 120
Coen, J.L. 51, 530
Cofer, W.R. 91–93, 111–112
Cohen, C. 66
Cohen, J.D. 50, 177, 504
Cohen, R.E. 485, 489
Colarco, P.R. 80
Cole, D.W. 406
Coleman, B. 512
Collatz, G.J. 80, 111–113, 121, 126, 207
Collet, J.L. 428
Collingwood, A. 508
Collins, C.D. 305
Colls, J. 26
Colman, J.J. 51
Colman, R. 40
Colver, C.G. 155, 414–415, 428, 450
Conard, P.W. 39
Conard, S.G. 91, 111–112, 117–118, 120–122, 345, 588, 594
Conard, S.L. 122
Condon, R.W. 476
Conedera, M. 50, 122
Conrad, C.E. 405
Conrad, R. 111
Consalvi, J.-L. 51, 81
Content, J. 305
Conti, M.E. 304
Cook, E.R. 39
Cook, G.D. 91
Cook, L. 537
Cooke, R. 356
Cope, M.E. 523, 548
Copeland, S. 417, 448
Corbett, S.J. 295
Core, B. 83, 87
Core, J.L. 62–64, 67, 70, 73, 118, 215, 292–293, 296, 305
Cornejo, J.J. 305
Cottrell, A. 539
Countryman, C.M. 50
Coutinho, H. 221
Coutinho, M. 62, 215
Couvert, P. 217
Covington, W.W. 407
Cox, P. 417
Cox, R.A. 95
Craig, R. 474
Cress, W.A. 392
Crews, C. 305
Crock, J. 19

Crocker, M.C. 360
Cromack, K. 407, 409, 414
Crookston, N.L. 65
Crounse, J.D. 428, 448
Crowley, J.N. 95
Crutzen, P.J. 61–63, 66, 70, 80, 82, 84, 87, 107, 110–113, 164–165, 210, 291, 294, 301–302, 306, 406
Cruz, M.G. 51, 481, 490
Csiszar, I. 86, 153
Cuiñas, A. 66
Cummings, D.L. 83, 86, 91, 93
Cunningham, P. 530–531
Cupp, R.E. 51
Curtis, P.S. 379, 406, 428
Cushman, S.C. 321
Cushon, G.H. 65–66, 177
Czapiewski, K.von. 8–9
Czimczik, C.I. 117, 128

Da Silva, U.L. 126
Dahlgren, R.A. 405, 409–410, 413, 419
Dahlsten, D. 381
Dalrymple, G.N. 49, 477, 481
Damoah, R. 52, 114
D'Amours, R. 17
Dana, G.L. 408–409
Danaher, T. 115
Danielsen, E.F. 45
Darrall, N.M. 301
Daterman, G.E. 329
David, J. 323
Davidenko, E.P. 21, 112
Davidson, N.E. 503, 540
Davidson, P. 514, 529
Davies, M.A. 70, 91
Davies, S.J. 19
Davis, K.P. 45
Davis, L.G. 349
Davis, S.D. 360
Davison, A.W. 301, 303, 305
Dawson, T.P. 321
Dawud, Y. 27
Day, D.E. 428
Díaz-Delgado, R. 353
de Bauer, L.I. 448
de Dominicus, V. 304
De Geer, L.-E. 17
de Gouw, J.A. 94–95, 306
De Kok, L.J. 376
De Luís, M. 118
De Mestre, N.J. 48, 483
de Volder, A.D. 329
De Witt, J.G.M. 381
Deaven, D.G. 503
Debano, L.F. 66, 155, 405–407, 414–415, 428, 450
DeBell, L.J. 80
Deeming, J.E. 65, 177, 485, 489, 504
deGaetano, A.T. 40
Deitchman, S.D. 8–11, 26
Del Grosso, S.J. 430
Delfino, R.J. 428
Delire, C. 127
Delmas, R. 8, 91, 293, 431–432, 435–436
Delmond, B. 307
DeLuca, T.H. 406–407
Dennis, A. 431–432, 435–436
Dentener, F.J. 93
Denton, C. 408–409
Derwent, R.G. 293
Deser, C. 40
Desjardins, R.L. 121
Dettinger, M.D. 39
Deuz, J. 217
Dezzeo, N. 128
Dial, R. 329
Dias, B. 83, 91
Diaz, H.F. 39
Diaz-Barradas, M.C. 392
Dibb, J.E. 80
Dietachmayer, G.D. 503, 540
Diette, G.B. 13, 80
Dijkstra, P. 303
DiMego, G. 514, 529
Dimitrakopoulos, A.P. 306
Dixon, R.K. 110, 114, 121
Dixon, K.W. 304
Dizengremel, P. 378–379
Dlugokencky, E.J. 111
Dobrowolski, W.L. 375, 386
Dockersmith, I.C. 407
Dockery, D.W. 295
Dokas, I. 22
Dokken, D. 216
Dong, F. 376, 387
Donkin, M. 305
Donnegan, J. 320
Dost, F.N. 62, 295–296
Dowdy, P.R. 85

Dozier, J. 143
Drake, B.G. 303
Drapek, R. 127, 329
Draper, J. 216
Draxler, J.K. 592
Draxler, R.R. 221, 505, 540, 548
Driscoll, K.T. 47
Drouet J.C. 489
Dube, D.E. 477
DuBois, D. 216
Dubovik, O. 253–254, 258
Duclos, P. 297
Dudhia, J. 503, 555
Duffy, P.A. 329
Dunlap, M.R. 94
Dunn, P.H. 379, 381
Dunn, P.J. 457, 461
Dunn, T. 586, 589
Dupuy, J.L. 81
Durbin, T.D. 418
Dusha-Gudym, S.I. 10–11, 16
Dutchak, K. 217

Earnest, G. 297
Eaton, D.L. 23
Eatough-Jones, M. 389, 396
Eck, E.A. 500
Eck, T.F. 82, 88, 92, 94, 254
Eckel, T. 512
Eder, B. 530
Edgerton, E.S. 91
Edwards, A.C. 86, 292
Edwards, D.P. 428
Eggleston, P.A. 13, 80
Ehle, D. 360
Eisner, M.D. 297
Eldering, A. 85
Eldred, R.A. 185
Eleuterio, D.P. 82, 88, 92, 94
Ellis, S. 290
Elman, A.G. 66
Elman, E. 504
Elman, K.E. 66, 504
Emile-Geay, J. 39
Emmanuel, S.C. 297
Emmett, B.A. 450
Emmons, J.-F. 18
Engelmark, O. 127
Engle, D.M. 117
Engling, G. 428
Epstein, H.E. 329
Erickson, D. 127, 306
Erlandson, J. 356
Ervens, B. 93
Escarré, A. 118
Escoto-Rodríguez, M. 358, 382, 385
Esperanza, A.M. 392, 408, 415, 553
Esplin, B. 539
Estes, J.A. 356
Estiarte, M. 307
Etman, C. 324
Euskirchen, E.S. 329
Evans, L.F. 539
Evans, N.H. 376, 386
Everett, R.L. 408
Everson, D.A. 408, 415
Ewers, F.W. 360
Ezhov, L.G. 21

Facchini, M.C. 93
Fagg, P.C. 381
Fagre, D. 333
Falk, D.A. 331
Fall, R. 306
Fallon, L.F. 297
Fan, S.M. 18
Fang, M. 593
Fangmeier, A. 302, 304
Farrington-Smith, J.G. 302
Fastie, C.L. 329
Fearnside, P.M. 86, 93
Fehsenfeld, F.C. 94
Feichter, J. 80
Feller, M.C. 405
Fellner, R. 304
Fenn, D. 457, 461
Fenn, M.E. 298, 303, 373–374, 378–381, 386, 389, 396, 414, 416–418, 426–430, 447–448, 450, 457, 462, 464–465, 576, 586, 589, 594
Fenn, M.P. 373–374, 379
Ferek, R.J. 91, 94
Ferguson, J. 524, 530, 553, 555
Ferguson, M. 592
Ferguson, S.A. 71, 501, 512, 543
Ferguson, S.M. 62, 181, 508
Fernandes, N. 66
Fernandes, P. 66, 86–87
Fernandez-Pello, A.C. 51
Fernau, R.F. 343, 393

Fernoe, R. 427
Ferrare, R. 94
Ferreira, A.D. 48, 221, 489
Ferreira, J. 10–11, 62, 70, 72, 210, 292
Ferrell, G.T. 320, 324–325
Ferretti, M. 217, 590
Ferrin, D.M. 360
Ffolliot, P.F. 405–407, 414
Fiebig, M. 94
Fiedler, S. 122
Field, B.D. 95, 500
Field, C.B. 406
Field, J.C. 322, 331
Figueroa, L. 95
Figueroa-González, J. 349
Filliatre, C. 307
Fine, P.M. 80, 295
Finlayson-Pitts, B. 552
Finney, M.A. 50, 67, 86–87, 483, 486–487, 530
Fiore, A.M. 500
Fischer, E.V. 80
Fischer, W.C. 73
Fisher, B. 85
Fisher, M.E. 428, 448
Fisher, R.F. 418
Fishman, J. 114
Fitzjarrald, D.R. 18
Flanner, M.G. 127
Flannigan, M.D. 19, 39–42, 44, 47, 127–128, 481
Flassak, T. 224
Flocke, F.M. 94
Flocke, S. 255
Floyd, M.L. 323
Fog, K. 366, 378–379
Fogarty, J. 477
Foley, J.C. 545
Folliott, P.F. 66
Fons, W. 473
Fontan, J. 210
Foote, J. 329
Forrest, D.W. 368
Forster, C. 52, 114
Forthofer, J.M. 51
Fosberg, M.A. 127–128
Foster, C.D. 450
Fotheringham, C.J. 346, 348, 356, 589
Fowler, C.T. 27
Fowler, D. 305
Fox, D.G. 185, 279, 588
Fox, J. 179
Fraczek, W. 373
Fragoso, J.M.V. 322
Frame, C.K. 66
Franceschi, V.R. 391
Francesetti, P. 66
Franco-Vizcaíno, E. 342, 358, 382, 385, 457, 459–462, 586, 589
Frankenfeld, M. 302, 304
Franklin, J. 321, 343, 346
Franklin, S.E. 360
Fraser, M. 431–432, 435–436
Fraser, P.J. 91
Fraser, R.H. 111
Fraszewski, D. 240–241
Frattoni, M. 296, 305
Fredriksen, R.L. 409
Freeborn, P.H. 83
Freitas, S.R. 45
French, N.H.F. 63, 92–93, 111–112, 121
Frey, S.D. 379
Friedli, H.R. 19, 81, 88, 91
Friedman, J. 558
Froelich, S.E. 577
Frolking, S.E. 80
Fromm, M.D. 52, 92, 114
Frost, G. 530
Fujioka, F.M. 47–48, 50, 487, 555, 592
Fujita, E. 9
Fulé, P.Z. 450
Fuzzi, S. 93

Gaegauf, C.H. 295
Galbraith, D.W. 376, 387
Ganio, L. 379
Gao, J. 376, 387
Gao, S. 85, 88, 91, 107, 292
Garcia-Alegre, M. 53
Garcia-Moya, E. 430
Garcia-Nieto, P.J. 292
Garcia-Novo, R. 392
Garner, J.H.B. 301–303
Garro, M.A. 268
Gautheir, S. 39
Gavrilov, D. 503
Gayev, Y.A. 49
Gedalof, Z.M. 320–323, 332
Geiser, F. 417
Geiser, L. 417, 426, 447–448, 464

Gellie, L.G. 477
George, C.T. 126
Gerard, F.F. 126
Geron, C. 80, 112, 121, 306
Gershenzon, J. 393
Gershunov, A. 39
Gessel, S.P. 406
Ghil, M. 360
Giardina, C.P. 407
Gibson, L. 292
Giglio, L. 80, 86, 111–113, 121, 126, 153, 207
Gilbert, M.E. 302
Gill, A.M. 47, 64, 475–476, 537, 539
Gill, J. 503
Gille, J.C. 428
Gille, L.K. 18
Gillett, J. 537
Gilmanov, T.G. 430
Gilroy, M. 508, 512
Gimeno, B.S. 373–374, 380, 426–427, 432, 448, 458, 464, 589, 594
Gimeno, T. 417
Giovanni, L. 88, 91
Girardin, M.P. 39
Gisborne, H.T. 472, 485
Glass, D.W. 408, 428
Glick, J.D. 40
Glukhovskiy, A.S. 268
Godzik, B. 261
Goforth, B.R. 343, 356
Goldammer, J.G. 4, 6, 9, 19, 21, 29, 91–93, 117, 240–241, 293, 586
Goldan, P.D. 94, 306
Goldberg, R. 41, 129
Goldman, C.R. 407
Goldstein, A.H. 373, 375, 377
Goloub, P. 217
Gomez, S.L. 380, 395
Gong, P. 428, 449
Goode, J.G. 62, 70, 82–84, 91–92
Goode, S. 345
Goodman, S.J. 47
Goovaerts, F.P. 63, 92–93, 111
Gordon, T.R. 390
Gotway-Crawford, C. 297
Gould, J.S. 475–476, 530–531
Goulden, M.L. 127
Govindasamy, L.B. 127
Gower, S.T. 379
Goyer, R.A. 390
Grady, K.C. 449
Graedel, T. 306
Graf, H.-F. 92
Graham, H.E. 50
Graham, J.M. 329
Graham, N.E. 39
Graham, R.C. 384
Graham, W.C. 83, 87
Granier, C. 13, 111, 113
Grant, C.D. 86
Grant, L.D. 11, 295
Grantz, D.A. 301–303
Graumlich, L.J. 324
Gray, D. 306
Gray, J.T. 415
Greenberg, J.P. 81, 91, 307
Gregoire, J.M. 80, 111
Grell, G.A. 45, 503, 530, 555
Grenfell, I.C. 86–87
Grier, C.L. 405
Griffin, G.F. 476
Griffith, D.W.T. 12, 16, 61, 70, 82, 84–85, 91–92
Grigoriev, S. 125
Grill, E. 376, 386–387
Grimit, E. 512
Grishin, A.M. 50
Grogan, P. 407
Grossman-Clarke, S. 417, 448
Grote, R. 377
Grulke, N.E. 299, 301, 303, 325, 373–377, 379–380, 383, 386, 392, 416, 430, 457, 461, 463, 553, 586, 589
Gruzin A.D. 50
Guenther, A.B. 12, 16, 81, 85, 91, 95, 306–307
Guisan, A. 321
Gulledge, J. 123
Gundale, M.J. 407
Gundersen, P. 416–418, 450
Gunson, M. 85
Gunthardt-Georg, M.S. 386
Gupta, V.K. 322–323, 331

Haack, R.A. 392
Haberle, K.-J. 377
Hackler, J.L. 427
Hackley, S.H. 407
Hadley, K.S. 320

Haeuber, R. 417, 448
Haines, D.A. 40, 42–43, 50
Hall, B.L. 127–128, 187, 349
Hall, J.M. 47
Hampson, R.F. 95
Hand, J.L. 175, 428
Hann, C.C. 116–117, 129
Hansel, A. 61, 95
Hanson, D. 81
Hanson, J.N. 117, 120, 178
Hanstrum, B. 539
Hao, G.A. 121–122
Hao, X. 591–592
Hao, R.A. 88, 91
Hao, W.M. 12, 16, 52, 62, 70, 80, 82–88, 91–92, 103, 107, 113, 117, 120, 122, 268, 291, 428, 448, 588–590, 592
Harden, J.W. 19, 127
Hardes, G. 125
Hardy, C.C. 62, 64, 70, 73, 86–87, 91, 120, 291–292, 302, 472
Hardy, C.E. 472
Hare, P.D. 392
Harley, D. 307
Harley, P.C. 81, 306
Harnik, N. 126
Harrington, J.B. 42, 47
Harrington, T.C. 389
Hart, S.C. 122, 449
Hartford, R.A. 283
Hartley, A. 53
Hartley, G.R. 127–128, 481
Hartman, J. 464
Hartman, M.D. 430
Hastie, T. 558
Hatano, R. 121
Hatch, A.B. 539
Hatfield, C.A. 323
Hatton, T.J. 48
Hauglustaine, D.A. 111
Hauglustaine, J.C. 18
Havranek, W.M. 386
Hawksworth, F.G. 381
Haylock, M. 40
Haynes, B.E. 379
He, C. 307
Heald, C.L. 94
Heath, J. 301
Heath, L.S. 115
Heath, R.A. 386
Heath, R.L. 386
Heck, W.W. 299–300
Heerdt, C. 377
Heffter, J.L. 187
Hegg, D.A. 8, 82, 91, 93, 164, 292
Heidt, L.E. 91, 110–111
Heil, A. 9, 19, 293
Heimer, S. 297
Heinselman, M.L. 117
Heitkamp, K 513, 524
Helas, G. 8, 91
Held, I. 126
Helmig, L. 307
Helms, J.A. 298
Hely, C. 85
Hendon, H.H. 40
Henihan, H.S. 356
Henry, B.K. 115
Henry, J.D. 329
Henry, M.C. 39
Herckes, P. 428
Herman, J.R. 13
Hermann, S.M. 86–87
Herms, D.A. 392
Hernandez, L. 374, 416–417
Hernando, A. 66
Hernando, C. 66
Hersey, S. 80
Herweijer, C. 39
Herzog, M. 92
Hess, G.D. 38, 505, 523, 540, 548
Hess, K. 539
Hess, P.G. 127
Hessl, A.E. 320, 322
Hewitt, C.N. 305–307
Hewson, J.H. 111–112, 121
Heyerdahl, E.K. 125–126
Hicke, J.A. 322, 327, 331
Hidalgo, H.G. 38, 125, 129, 287, 320, 360, 366, 406
Higgins, R. 8, 118, 140, 142–145, 147, 151–153
Higurashi, A. 13
Hill, C. 512
Hinckley, T.M. 377
Hinkle, C.R. 91, 303
Hinzman, L.D. 329
Hirano, K. 577
Hirano, T. 302
Hirsch, K.G. 42

Hirsch, K.J. 65
Hoadley, J.L. 506
Hobbs, P.V. 8, 82, 85, 88, 91–94, 107, 164, 292
Hodges, J.D. 391
Hodzic, A. 217, 228
Hoelzemann, J.J. 13, 111, 113
Hoffa, E.A. 120
Hoffmann, M.B. 115, 331
Hofstetter, S. 50
Hogsett, W.E. 373–374, 376, 379–380, 392–394, 430
Hogue, C. 19
Holben, B.N. 83, 91, 254
Holben, W.E. 407
Holl, B.S. 122
Holland, E.A. 430
Holloway, E.T. 51
Holloway, J.S. 94
Holopainen, J.K. 305–306
Holper, P.J. 295
Holsten, E.H. 327, 329
Holzinger, R. 61, 80, 306, 373
Homann, P.S. 379
Honrath, R.E. 80
Hope, D. 417, 448
Hoppel, K. 114
Horel, J.D. 40
Hornstein, J. 114
Horowitz, L.W. 80, 85
Horth, J. 93
Houghton, J.T. 18
Houghton, R.A. 110, 114, 427
Houpis, J.L.J. 298
Howarth, R.W. 18
Hoyningen-Huene, W. 10
Hraber, P.T. 323
Hu, H. 349
Huai, T. 418
Huang, H.-P. 126
Hubbert, K. 384
Hudman, R.C. 94
Huebert, B.J. 94
Hueglin, C. 295
Hughes, T.P. 356
Hui, D. 415, 428, 450
Hultman, N.E. 375
Hungate, B.A. 303
Hunsaker, W.W. 457, 462, 465, 589, 594
Hunt, J.C.R. 49
Huntrieser, H. 94
Hurst, D.F. 91
Husan, D.C. 324
Hutchison, K. 18
Hutton, S. 590, 592
Hyer, E.J. 111–112, 121
Hymus, G. 303

Ichoku, S.P. 83
Idema, C. 297
Isaev, A.P. 121
Ito, A. 80, 93, 111, 113
Ivanov, A.V. 117, 120, 122
Ivanov, V.A. 117, 120, 122
Ivanova, G.A. 112, 117–118, 120, 122

Jaafar, A. 593
Jacks, P.M. 155, 345, 414–415, 428, 450
Jackson, J.B.C. 356
Jacob, D.J. 18, 94–95, 114, 187, 500
Jaffe, D.A. 52, 417, 448
Jain, R. 513, 524
Jalaludin, B. 297
Jambert, C. 91, 431–432, 435–436
James, P. 52, 114
James, R.L. 381
Janjic, Z.I. 503
Jaramillo, V.J. 86, 93, 407
Jassby, A.D. 407
Jayak, A. 111–112, 121, 126
Jean, M. 17
Jenkins, M.A. 530–531
Jenkins, R. 322, 331
Jensen, M. 122
Jerdau, M. 306
Jia, G. 329
Jin, J.-Z. 118, 127–128
Jin, X. 387
Jin, Y. 111, 127
Johnson, A.R. 323
Johnson, M. 417
Johnson, B.J. 80
Johnson, D.W. 301–303, 374, 405–410, 412–413, 415–416, 418–419, 426–428, 447, 457, 462, 464–465, 586, 589, 594
Johnson, E.A. 320
Johnson, R. 7–8, 373, 376, 392
Johnston, F.H. 297
Johnstone, J.F. 329
Jones, P.D. 324, 373, 376, 392

Joosten, M.H.A.J. 381
Jordan, A. 61
Jorgensen, M.T. 329
Jourdain, L. 85
Jovan, S. 417
Jungkunst, H.F. 122
Jupp, T.E. 126
Justice, C.O. 85–86, 88, 91, 111, 153, 293

Kadygrib, A.M. 268, 268
Kafatos, M. 284–285
Kahyaoglu-Koracin, L. 593
Kaiser, K.O. 416, 418
Kajii, Y. 114
Kalnay, E. 503
Kaminsky, C. 508
Kanakidou, M. 93–94
Kanamitsu, M. 503
Kanatharana, P. 297
Kanowski, P. 290
Karl, T. 12, 16, 81, 85, 91
Karlsson, P.S. 379
Karma, S. 7, 9–12, 22, 25
Kashian, D.M. 123–124
Kashparov, V.A. 268, 268
Kashyap, A.K. 123
Kasibhatla, P.K. 111, 113
Kasibhatla, P.S. 80, 111–113, 121, 126, 207
Kasischke, E.S. 42, 63, 83, 92–93, 111–112, 114, 117, 121, 126
Kassaby, F.Y. 381
Kastens, J.H. 323
Kato, S. 114
Katz, P.P. 297
Kauffmann, J.B. 83–84, 86–87, 91, 93, 107
Kaufman, Y.J. 83, 91, 254
Kavanagh, A.M. 297
Kawakami, S. 292
Kaye, J.P. 122
Kazan, V. 293
Keane, R.E. 65, 69–70, 88, 117, 120
Keeley, J.E. 305, 346, 348, 356, 450, 589
Keen, F.P. 390
Keene, W.C. 94
Keetch, J.J. 475, 479, 486
Keifer, M. 324–325
Keitt, T.H. 323
Keller, T. 386
Kelley, J. 324–325
Kellogg, L.-K.B. 504
Kelly, J. 9, 26
Kemmett, S. 329
Kern, J. 297
Kerr, J.A. 95
Kerstiens, G. 301
Kesselmeier, J. 305–306
Kessler, C. 224
Key, C.H. 120
Key, J.R. 329
Keyser, D. 45
Khan, M.R. 303
Khan, M.W. 303
Khandekar, M. 40
Khanna, P.K. 294, 406–407
Khedim, A. 91
Khodzer, T.V. 114
Khomutinin, Yu.V. 268, 268
Kidwell, S. 356
Kim, J.E. 10
Kim, Y.J. 10
Kimmins, J.P. 379
King, A.B. 292
King, M.D. 85, 253–254
King, N.K. 539
Kinnersley, R.P. 302
Kinyamario, J.I. 430
Kirby, M.X. 356
Kirchner, T. 430
Kirchstetter, T.W. 85, 88, 91, 107, 292
Kirsch, J. 377
Kitching, R.L. 304
Kittaka, B. 177, 180
Kittel, T. 127, 329
Kitzberger, T.P. 125–126, 320
Kiyota, M. 302
Kjøller, A. 122
Kjønaas, O.J. 450
Klaassen, C.D. 23
Klaver, R.W. 177
Kleeman, M.J. 9, 575
Klein, E. 329
Kleiss, B. 80
Kleissl, J. 13, 80
Klemmedson, J.O. 450
Klemp, J.B. 503
Klingeli, J.T. 331
Klinger, L. 306–307
Klopatek, J.M. 405–407, 409–410, 413–414
Klüsener, B. 376, 386–387
Knapp, A.K. 122

Knapp, E.E. 450
Knapp, K.R. 516
Knorr, M. 379
Koch, D. 85
Koch, J.M. 86
Koch, W. 387
Koenig, J.Q. 295, 297, 508
Koetz, C. 66
Koike, M. 292
Kolb, T.E. 450
Koller, A.M. 91
Kondo, Y. 292
Kondragunta, S. 514
Koopmans, C.J. 450
Kopper, A.C. 66
Kopper, K.E. 66, 504
Koppmann, R. 8–9, 82, 88, 91–92, 94
Korontzi, S. 85, 88
Koshak, W.J. 47
Kotok, E.I. 472
Kottke, I. 304
Kotz, B. 66
Kourtz, P.H. 483
Koutrakis, P. 291, 577
Koutsias, B. 66
Koutzenogij, K.P. 117, 120, 122
Kovaleva, N. 117, 120, 122
Kovtun, M.V. 268, 268
Kozlowski, T.T. 299–302, 392
Krankina, O.N. 114, 121
Krasnec, J.P. 110–111
Kreidenweis, S.M. 428
Krekling, T. 391, 393
Kärenlampi, T. 305–306
Krokene, P. 391, 393
Kropfli, R.A. 51
Kruger, F.J. 50
Krull, R. 524, 530, 553, 555
Krupa, S.V. 299
Krzyzanowski, M. 217
Kucera, J. 201
Kucsera, T.L. 80
Kuhlbusch, T.A.J. 70, 82, 84, 87, 91, 107, 431–432, 435–436
Kulakowski, D. 320
Kulan, A. 273
Kulawik, S.S. 85
Kulmala, A.E. 430
Kunzel, S. 295
Kurz, W.A. 114–115, 117
Kushnir, Y. 39, 126
Kuster, W.C. 94, 306
Kutiel, H. 50
Kutiel, P. 50
Kuyper, T.W. 379
Kyriakou, S. 8

Lacaux, J.P. 8, 91, 293, 431–432, 435–436
Lagana, A. 304
Lahm, P. 62, 500
Lamb, B. 508, 512–513, 524
Lambert, G. 91
Lambin, E.F. 128
Landsberg, J.D. 407, 414
Lang, P.M. 111
Lange, C.B. 356
Langenfelds, R.L. 111
Langenheim, J.H. 391
Lanoville, R.A. 481
Lanshin, V.P. 268, 268
Lapina, K. 80
Lapszin, I.I. 304
Larini, M. 51
Larkin, N.K. 592
Larkin, J. 506
Larkin, N.K. 177, 524, 530, 553, 555
Larko, D.E. 80
Larson, T.V. 295, 297
Latham, D.J. 42, 44, 47, 84, 87, 107, 283, 530
Lathiere, J. 111
Lau, N.-C. 126
Laumonier, Y. 292
Laurence, J.A. 373–374, 380, 393–394
Laursen, K.K. 82, 91, 93, 164
Laven, R.D. 42, 46–48, 50, 52, 116, 118
Lavenu, F. 210
Lavoie, N. 481
Lavorel, S. 128
Law, B.E. 124
Law, K.S. 94
Lawrence, K.T. 127–128, 427
Lawson, B.D. 477
Le Cloarec, M.F. 91
Le Maitre, D.C. 50
Lebel, P.J. 91
Lee, E.H. 373–374, 380, 393–394
Lee, J.A. 304
Lee, K.H. 10
Lee, P.C.S. 514, 529

Lee, S. 91, 523, 548
Lee, T. 428
Leeder, S.R. 297
Leenhouts, B. 116, 201
Leetmaa, A. 126
Lefebvre, P. 126
Legg, C.A. 292
Lei, Y. 392
Leith, I.D. 305
LeMaitre, D.C. 305
Lemly, A.D. 418, 427–428, 586
Lendzian, K.J. 301
Lenihan, J. 127, 329
Lerdau, M.T. 306
LeVan–Green, S.L. 81–83
Levchuk, S.E. 268, 268
Levine, J.S. 63, 66, 91, 207
Levitt, J. 383
Lewis, G.M. 115
Lewis, P.E. 111
Lewis, P.R. 295
Li, C. 126, 392
Li, Q. 85, 95, 500
Li, X. 447
Li, Z.Q. 111, 114
Liang, J. 216
Liao, H. 94
Liberta, J. 590
Liebmann, B. 40
Likens, G.E. 18
Lilley, W. 548
Lim, L. 297
Limin, S. 111–112, 121, 126
Lin, C.-D. 306
Lincoln, E.N. 82, 84, 87, 268
Lindberg, N. 66
Lindinger, D.H. 61
Lineback, P. 552
Linn, R. 51, 530–531
Linse, C. 552
Liodakis, S. 8
Liousse, C. 80, 91, 94
Lipsett, M. 297
Lischke, H. 322
Lister, Griggs, D. 216
Littell, J.S. 320, 322–323, 331
Litton, C.M. 124
Liu, A.R. 284–285
Liu, H. 127, 500
Liu, J. 121
Liu, M.-H. 52, 86, 113
Liu, W.T. 349
Liu, Y. 428, 523, 530
Liu, Z. 41
Lloret, F. 353
Lloyd, A.H. 329
Llusià, J. 306–307
Lobell, D.B. 127
Lobert, J.M. 70, 82–84, 87, 107, 291–292, 351
Lockwood, R.N. 8, 118, 140, 142–145, 147, 151–153, 155, 345, 374, 414–415, 428, 450
Logan, J.A. 126, 320, 323, 326–327, 331, 500
Logan, K.A. 41, 483
Logan, L.W. 503, 540
Lohmann, U. 80
Loneragan, W.A. 86
Long, D.G. 120
Long, K. 66
Longo, K.M. 45
Lopes, M. 211
Lopez, E.N. 374
Loppi, S. 304
Loraud, J.C. 51, 81
Los, C. 322, 331
Loureiro, P. 66
Lu, J. 126
Luderer, G. 92
Lueker, T.J. 80
Luhker, B. 125
Luke, R.H. 537
Lunden, M. 428
Lundin, S.M. 268, 268
Lunsford, J.D. 83
Luo, Y. 415, 428, 450
Lövblad, G. 217
Lynch, A.H. 329
Lynch, A.M. 320
Lynham, T.J. 127–128, 477
Lyons, E. 127
Lyons, J.H. 82, 91, 93, 164
Lyons, T. 307

Ma, C.Y. 305
MacArthur, N.K. 292, 539
MacGorman, D.R. 42
Mach, D.M. 47
Machida, T. 292
Mack, M.C. 127

Mackie, A.E. 307
Mackie, N. 305
MacPherson, J.I. 121
Madronich, S. 228, 255
Maffey, M.E. 481
Magi, B. 292
Mahalingam, S. 48, 50–51
Maier-Maercker, U. 387
Main, W.H. 40
Maingi, J.K. 39
Mak, E.H.T. 306
Malcolm Gill, Viegas, A. 592
Maleknia, S.D. 307
Malilay, J. 27, 295
Malingreau, J.-P. 53, 153
Malm, W.C. 174–175, 185, 428
Maloshtan, I.M. 268, 268
Manins, P.C. 295, 548
Mann, D.H. 329
Manning, A.J. 293
Manning, W.J. 261, 299
Mannino, D. 297
Mansfield, T.A. 301
Mantua, N. 320
Marchewka, M. 94
Marchi, E. 590
Marinone, S.G. 349
Marks, G.C. 381
Marland, G. 111
Marney, G. 537
Marsden-Smedley, J.B. 48, 491
Marsden-Smedley, W.L. 477
Martell, D.L. 40, 320, 483
Martell, D.M. 477, 483
Martin, J.E. 51
Martin, R.E. 430
Martin, R.V. 114, 187
Martinez, B. 200
Martins, H. 223, 227–228
Martins, J.V. 94, 221
Marxer, P. 122
Marzano, H. 66
Masarie, K.A. 111
Mason, J.A. 127–128, 481
Mason, S.A. 94
Mass, C.F. 508, 512
Massie, S.T. 228, 428
Masters, R.E. 117
Matheny, R. 506
Mathur, R. 514, 529
Matson, M. 143
Matson, P.A. 18
Matsuoka, S.M. 329
Mattis, I. 52, 114
Mattson, W.J. 392
Matyssek, R. 376–377, 386
Maufette, Y. 345
Maurer, S. 386
Mauzerall, D.L. 80, 85
Maykut, N. 508, 512
McAinsh, M.R. 376, 386
McAlpine, R.S. 477
McArthur, A.G. 50, 473–476, 491, 537
McBride, J.R. 380, 395
McCallum, I. 114, 126
McCammon, B. 48
McCarthy, N. 477
McCaw, G.J. 477
McCaw, K. 537
McCaw, L. 475–476, 538
McCaw, W.L. 48, 476
McDonald, J.D. 9
McDonald, K.M. 428
McDowell, N.G. 450
McFadden, J.P. 329
McFarland, D. 216
McGrattan, K.B. 51
McGuire, A.D. 329
McGurk, B. 407, 415
McHugh, C.W. 86–87
McKay, W.A. 306
McKee, I.F. 321
McKeen, S.A. 530
McKelvey, K.S. 324
McKenney, D.W. 127–128
McKenzie, A. 180
McKenzie, D. 66, 80, 112, 121, 177, 320–323, 332–333, 457–458, 462, 504, 586
McKenzie, L.M. 70, 291
McKenzie, M.D. 407
McKeon, G.M. 115
McKinsey, D.E. 343, 346
McKnight, T.L. 38
McLaughlin, S.B. 386
McMeeking, G.R. 428
McMillan, W.W. 80
McNabb, D.H. 414
McNee, W.R. 390
McNulty, S.G. 418, 427–428, 586
McQueen, J.T. 514, 529

McRae, D.J. 111–112, 117–118, 120, 122
McRae, W.M. 121–122
McWilliams, J.C. 360
Mead, B.R. 329
Mearns, L. 127–128
Meeker, J.R. 390
Meinardi, S. 80, 91, 93, 292
Meixner, L. 417
Meixner, M.E. 458, 464, 589, 594
Meixner, T. 374, 407, 414–417, 426, 428–429, 447, 450, 464
Melack, J.M. 408, 415, 447
Mell, W. 530–531
Mellert, K.H. 416
Menakis, J.P. 116–117, 129
Menaut, J.C. 8, 430
Menke, N. 115
Mennicken, S. 307
Mensing, S.A. 356
Menut, L. 217, 228
Menzel, W.P. 153
Merlet, P. 85, 88, 291, 293–294, 505
Merlot, P. 70
Merrill, L. 381
Mesinger, F. 503
Methven, J. 94
Meyer, C.W. 323, 537
Meyer, P. 297
Michaelson, J. 343, 346, 356
Michalski, G. 374, 416–417
Michel, C. 80
Michelsen, A. 122
Mickley, L.J. 500
Middlebrook, A.M. 94
Midgley, G.F. 322
Midgley, J.J. 306
Miller, A.E. 447
Miller, B.R. 80
Miller, J.B. 111
Miller, J.M. 390
Miller, J.R. 40
Miller, P.R. 303, 325, 373–374, 377, 379–382, 385, 387, 389, 392, 395, 416, 576
Miller, W.L. 123
Miller, W.M. 428
Miller, W.W. 405–409, 412, 415, 418–419, 427
Mills, G.A. 51, 503, 517, 521, 539–541, 545
Mills, J. 592
Mills, G. 592
Milne, B.T. 322–323, 331
Milovich, J. 127
Minaeva, T. 20
Mingus, P. 386
Minko, N.P. 114
Minnich, R.A. 340, 342–344, 346–349, 351–354, 356, 358, 360–361, 367, 382, 385, 393, 427, 457, 459–462, 586, 589
Minobe, S. 360
Minski, M.J. 302
Miranda, A.C. 8, 18, 72, 140, 142–145, 147, 151–153
Miranda, A.I. 9–11, 62, 70–72, 210–211, 214–215, 223–225, 227–228, 292, 586, 588, 590
Miranda, H.S. 8, 118, 140, 142–145, 147, 151–153
Mirin, A. 127
Mobley, H.E. 21
Moghaddas, E.E.Y. 450
Molina, M. 66
Molina, R. 66
Momen, B. 298
Monleon, F. 407, 414
Monschein, S. 376
Monson, R.K. 306
Monteiro, A. 211, 228
Monteiro, L. 221
Montgomery, L.T. 376, 386
Moortgat, G.K. 93
Moosmüller, H. 82, 84, 87, 268
Morais, M. 346, 348, 356
Moravec, J. 50
Morgan, P. 120, 331
Morisette, J.T. 153
Moritz, M.A. 356, 589
Morris, G.A. 80
Morsdorf, D. 66
Morvan, D. 51, 81
Mosier, A.R. 430
Mote, P. 320–323, 332
Mott, J.A. 297
Mouillot, F. 406
Moussiopoulos, N. 224
Moutinho, P. 126
Mudelsee, M. 39
Muhle, J. 80

Mulik, J.D. 577
Munger, J.W. 80
Munoz, F.G. 305
Muraleedharan, T.R. 8–10, 21
Muraro, S.J. 478
Murata, Y. 376, 386–387
Muriel, S. 13
Murphy, J.D. 405–409, 412, 415, 418–419, 427–428
Murray, F. 307
Musselman, R. 261
Mustajbegovic, J. 297
Myers, O.B. 323
Myhre, C.E.L. 93
Myrold, D.D. 379

Nada, T. 297
Naeher, L.P. 91
Naik, N. 39, 126
Naik, V. 80, 85
Nakajima, T. 13
Nance, J.D. 82, 91–93
Nandi, S. 428
Nathan, R. 322
Naveh, Z. 46
Neary, D.G. 66, 405–407, 414
Nebeker, T.E. 391
Neff, J.C. 127
Neill, F.X. 405
Neilson, R.P. 127, 322, 329
Neitlich, P. 426, 447, 464
Nel, E.M. 320
Nelson, P. 548
Nelson, R.M. 47–48, 50–51
Nenes, A. 93
Nepstad, D. 126
Neuhäusl, R. 201
Neuman, J.A. 94
Newland, J.A. 406
Newman, M. 40
Newton, M. 409
Ng, L. 548
Nguyen, T. 375, 386, 392
Nichol, J. 292
Nickovic, S. 503
Nielsen, C.J. 93
Nielson, J.E. 80
Nikolova, P. 376
Nilsson, L.-O. 379
Nilsson S. 20, 114–115, 126
Nishi, N. 292
Noble, I.R. 475–476
Noble, J.C. 50
Nohrstedt, H.-Ö. 379
Norbeck, J.M. 418
Nordgren, C.A. 83
Norheim, L.-K.B. 66
Norheim, R.A. 177, 504
North, K.A. 376, 386
Northway, M. 306
Nosal, M. 386
Nosenzo, A. 489
Notaro, M. 41
Novakov, T. 85, 88, 91, 107
Novelli, P.C. 111–112, 121
Nowak, D. 9
Nunn, A.J. 377
Nydick, K.R. 426, 447, 464

O'Brian, K. 333
Ocampo-Torres, F. 349
Oechel, W.C. 345
Oertel, D. 118
Ogawa, T. 292
Ojima, D.S. 327, 430, 464
Olbu, G.J. 84, 87–88, 91, 103 107
O'Leary, J.F. 343, 346
Oleksyn, J. 385
Oliver, J.E. 40
Olivier, L.D. 51
Olsen, S.C. 126
Olson, C.S. 65
Oltmans, S.J. 80
Ommering, L. 552
Ondov, J. 13, 80
O'Neill, K.P. 83, 121
O'Neill, S.M. 80, 112, 121, 177, 179, 524, 530, 553, 555, 592
O'Neill, W. 62, 181, 508
O'Neill, X. 180
Onuchin, A. 126
Oppenheimer, M. 80, 85
Orlando, J.J. 268
Ormrod, D.P. 303
Oros, D.R. 293
Osterkamp, T.E. 329
Osterman, G. 85
O'Toole, B. 297
Otte, T.L. 514, 529
Otterson, S. 508

Ottmar, R.D. 9, 11, 24, 26, 62–67, 70, 72–73, 83, 87, 117–118, 120, 177–178, 210, 215, 292–293, 296–297, 305, 500, 586, 588
Ouzounov, B. 283
Ovens, D. 512
Overpeck, J.T. 41, 129
Owen, R.C. 80
Owen, S.M. 305–306
Owens, M.K. 306
Oxford, M. 414–415, 428–429, 450

Pace, J. 177, 180
Packham, D.A. 292, 294, 539
Packham, D.R. 292, 538–539
Page, S.E. 111–112, 121, 126
Paine, T.D. 389, 392, 396
Paisarn-Uchapong, O. 297
Palacios-Orueta, A. 293
Pallardy, S.G. 392
Palmer, W.C. 479
Palumbo, G. 590
Pandis, S.N. 93
Pandolfi, J.M. 356
Panek, J.A. 375, 377
Paoletti, E. 386
Papa, F. 111
Papio, C. 306
Pappa, A. 8
Parameter, J.R. 389, 392
Parfenova, E.I. 127
Park, R.J. 94, 114, 187
Parkes, T. 483
Parkhurst, D.F. 379
Parlange, M.B. 13, 80
Parmeter, J.R. 304, 381
Parra, A. 293
Parsons, S.J. 324
Parton, W.J. 430, 464
Patterson, M.T. 385
Paul, J.T. 52
Paul, P.M. 479
Pawson, S. 80
Payne, D. 407, 415
Payne, N. 19
Pearce, J.B. 477
Pearson, K. 450
Pearson, R.G. 321
Peckham, S.E. 530
Peet, G.B. 475–476, 538
Pei, A.-M. 376, 386–387
Pell, E.J. 386
Pelletier, R.T. 27
Peltier, R.E. 94
Penner, J.E. 80, 93, 111, 113, 216
Penuelas, J. 306
Percy, K. 217
Pereira, J.A.R. 8, 140, 142–145, 147, 151–153
Pereira, M. 221
Pereira, Ribeiro, M. 219–220
Perez-Garcia, A. 381
Perlińska, A. 240
Persson, T. 379
Peterson, A.L. 62, 500
Peterson, C.H. 356
Peterson, D.L. 320–323, 325, 332–333, 379–380, 387, 395, 457–458, 462, 586
Peterson, D.W. 321–323
Peterson, J.L. 29, 62–64, 69, 71, 73, 83, 87, 178, 504
Peterson, J.S. 321
Peterson, M. 524, 530, 553, 555
Peterson, N.K. 506
Peterson, R. 506
Petkau, J. 297
Petzold, A. 94
Peñuelas, J. 307
Peylin, P. 111
Pfister, G. 80, 127
Phillips, T.J. 127
Phonboon, K. 297
Phongpan, S. 430
Phuleria, H.C. 80, 295
Pierce, T. 62, 181, 306, 508
Pinciarelli, L. 296, 305
Ping, C.-L. 329
Pinto, J.P. 11, 91, 295
Pitchford, M.L. 185
Pitelka, L.F. 322
Pitts, J. 552
Pivovarov, V. 53
Plante, M. 216
Platnick, S. 85
Pleim, J.E. 514, 529
Podaire, A. 210
Pollack, D. 283
Pollard, D. 127
Polle, A. 299
Pollock, W.H. 91, 110–111

Pons, X. 353
Pope, C.A. 295
Porterie, B. 51, 81
Portwood, K.A. 360
Posch, S. 392
Post, M.J. 51
Poth, M.A. 373–374, 378, 389, 396, 407, 415–418, 426–428, 430, 447, 586
Potter, B.E. 43, 50–51
Poulin-Costello, M. 483
Pouliot, G. 62, 181, 508, 514, 529
Powell, I. 537
Powell, J.A. 126, 320, 323, 326–327, 331
Power, S. 40
Powers, R.F. 405–406, 409, 412
Powers, W. 503
Poyarkov, V. 10, 16
Prather, K.A. 80
Preisler, H.K. 377, 553, 593
Price, D.N. 305
Price, K.P. 323, 329
Price, O.F. 86
Prichard, S.J. 64, 66, 69, 73
Prietzel, J. 416, 418
Prigent, C. 111
Prilepsky, N.G. 588, 590
Prins, E.M. 45, 153, 500
Privette, J.L. 85
Procter, T. 594
Pronos, D. 377
Pronos, J. 381
Protsak, V.P. 268, 268
Prüter, J. 240
Pszennym, A.A.P. 94
Pétron, G. 18
Pulliam, W.M. 415–416
Pureswaran, D.S. 390
Puri, K. 503, 540, 548
Putaud, J.P. 93
Pyne, S.J. 42, 46–48, 50, 52, 116, 118, 472

Qin, H. 591–592
Qu, J.J. 283–285, 591–592
Quaglino, A. 489
Qualls, R.G. 408, 419
Quayle, B. 80, 112, 121, 180
Quevedo-Norlasco, A. 448
Quigley, J.L. 329
Quigley, T.M. 72
Quiring, S.J. 9, 297

Racine, C.H. 329
Radke, L.F. 8, 19, 62, 82–85, 88, 91–93, 103, 164, 293
Radojevic, M. 8–10, 21, 291
Raffa, K.F. 389
Raffuse, C. 524, 530, 553, 555
Raghubanshi, A.S. 123
Raison, R.J. 294, 406–407
Raison, R.L. 304
Raizenne, M. 295
Ramalingam, E. 552
Ramaswamy, V. 80, 85
Ramonet, M. 111, 293
Ramos, C. 513, 524
Randerson, J.T. 80, 111–113, 121, 126–127, 207
Rao, L.E. 430
Raposo-Pereira, J.A. 118
Rasmussen, E.M. 40
Rasmussen, R.A. 8, 83, 91
Raufer, R. 278–279
Raulund-Rasmussen, K. 416–418
Raventós, J. 118
Ray, D. 126
Raymond, C.L. 66, 504
Read, D.J. 304
Read, J. 304
Real, E. 94
Reardon, J. 82, 92
Rebertus, A.J. 320
Recuero, F.S. 45
Redd, S.C. 297
Reddy, V.S. 123
Regniere, J. 126, 320
Reh, C.M. 8–11, 26
Rehm, R.G. 51
Reich, P.B. 325, 385
Reid, J.S. 8–9, 82, 88, 91–92, 94, 500
Reid, M.S. 320, 500
Reifsnyder, W.E. 42, 45
Reiling, K. 301, 303
Reinbold, C.R. 187
Reinhardt, D.V. 70
Reinhardt, E.D. 65, 69–70, 73, 83, 87–88, 117, 120, 210
Reinhardt, T.E. 9, 11, 24, 26, 62, 297
Reis, R.M. 490
Reisner, J. 51
Reiter, I.M. 377
Reitmayer, H. 377

Repert, D.A. 379
Restrepo, C. 322–323, 331
Reuter, J.E. 407
Reynolds, R.W. 40
Rühling, A. 304
Ribeiro, F. 66
Ribeiro, M. 221
Riccardi, C.L. 64, 66
Rich, P.M. 323
Richards, G.D. 70, 483, 487
Richards, G.N. 291
Richardson, C. 500
Richter, D.D. 121
Riddle, L.G. 349
Riebau, A.R. 279, 284–285, 588, 590–592
Riegel, G.M. 415, 417
Rieley, J.O. 111–112, 121, 126
Riggan, M.E. 457, 461
Riggan, P.J. 8, 82, 91, 93, 118, 140, 142–145, 147, 151–153, 155, 164, 345, 360, 374, 414–415, 428–429, 450, 591
Rigolot, L.M. 66
Rigolot, M. 66
Rind, D. 41, 129
Rinsland, C.P. 85
Ripley, B.S. 302
Ritters, M. 212
Rittmaster, R. 27
Roads, J. 47
Roads, J.O. 586
Roberts, G. 86
Roberts, J.M. 94
Robertson, G.P. 123
Robinson, L.J. 325
Robinson, M.F. 301
Robock, A. 292
Roche, I.M. 304
Rodríguez-Frausto, C. 448
Rodriguez, M.A. 191
Roiger, A. 94
Rollins, M.G. 66, 120
Rolph, R. 592
Romme, W.H. 117, 123–124, 323
Rorig, S. 524, 530, 553, 555
Rose, C. 377
Ross, D.W. 329
Rossi, M.J. 95
Rothe, A. 416
Rothermel, R.C. 80, 210, 224, 345, 460, 473, 485, 487
Roton, L.M. 390
Rottenberger, S. 306
Rowell, R.M. 81–83
Rowland, C.S. 126
Rowland, F.S. 80, 93, 292
Roy, D.P. 111
Rublev, A. 258
Rudebeck, A. 379
Rudolph, J. 91
Rueth, H.M. 417, 426, 447–448, 464
Ruminski, G. 592
Rundel, P.W. 345, 385
Rupp, T.S. 329
Russell, A.G. 91
Russell, L.M. 94
Russell–Smith, J. 86, 292, 474
Rust, W.D. 42
Ryall, D. 293
Ryan, D.F. 418, 427–428, 586
Ryan, K.C. 115, 118
Ryan, M. 123–124
Ryan, W.M. 83
Rye, P. 539

Sachse, G. 94
Sackett, G.A. 487
Sackett, S.S. 407
Sadilek, M. 292
Sagebiel, J. 9
Saharjo, B.H. 80
Sahm, P. 224
Saito, L.S. 408
Sala, A. 450
Salisbury, H.E. 286
Samsonov, Y.N. 117, 120, 122
Samuels, M.L. 323
Sandberg, D.V. 62–67, 69–70, 73, 118, 177–178, 215, 293, 296, 305, 500, 504–505, 531
Sandermann, H. 376
Sanderson, L.M. 297
Sandhu, H.S. 428
Sandoval-Soto, L. 306
Sandström, T. 9
Sanford, R.L. 407
Sanhueza, E. 95
San-Miguel, I. 590
San-Miguel-Ayanz, A. 201
San-Miguel-Ayanz, J. 200–201
Sannikov, S.N. 117

Santana, M. 95
Santos, M. 72
Santos, P. 10–11, 62, 70, 72, 210, 292
Sapakota, A. 80
Sapkota, A. 13
Sarody, N. 51, 81
Sato, H.S. 64
Savage, M. 331
Sawamoto, T. 121
Schaaf, M.D. 65, 513, 524
Schaap, A. 228
Schaap, W. 377
Schachter, E.N. 297
Schade, G. 61
Scharfe, G. 61
Scharffe, D.H. 70, 82, 84, 87, 107
Schaub, D. 122
Schauer, J.J. 91
Schellhaas, R. 320
Schemm, J.E. 40
Schere, K.L. 508, 514, 529
Schichtel, B.A. 185
Schichtel, W.C. 185
Schimel, D.S. 111, 430, 464
Schimel, J.P. 123, 329, 447
Schindler, D.W. 18
Schlager, H. 94
Schlesinger, P. 126
Schlesinger, W.H. 18, 415
Schlobohm, P. 483
Schmidt, I.K. 416–418
Schmidt, K.M. 116–117, 129
Schmidt, M. 111
Schmidt, S. 500
Schmitz, R. 530
Schmuck, G. 200
Schmuck, J. 590
Schmullius, C. 126
Schoennagel, T. 117
Scholes, B. 306
Scholes, M.C. 128
Scholes, R.J. 85, 293, 430
Schollnberger, H. 295
Schreuder, M. 513, 524
Schroeder, J.I. 376, 386–387
Schroeder, M.J. 46
Schulke, T. 331
Schultz, M.G. 13, 111, 113, 500
Schulze, E.-D. 117, 125, 128
Schulze, M.D. 120
Schumann, U. 216
Schuur, E.A.G. 127
Schwarzkopf, M.D. 80, 85
Schweingruber, F.H. 320, 324
Scire, J.S. 505
Scora, G. 418
Scott, B.R. 295
Scott, J.H. 65, 345
Scott, K. 428, 449
Scott, R.K. 297
Scurlock, J.M.O. 430
Söderström, B. 379
Seager, R. 39, 126
Seaman, N.L. 514, 529
Seaman, V.Y. 373
Seamon, J.E. 62, 64, 70, 73, 292
Seamon, J.L. 62, 500
Seastedt, T. 430
Seaward, M.R.D. 304
Sebacher, D.I. 91
Sebastian, L.A. 201
Seiler, W. 110–113, 294
Seinfeld, J.H. 93–94
Serafino, G. 283
Serreze, M.C. 329
Servranckx, R. 17, 52, 92, 114
Sestak, M. 179
Setzer, A.W. 83, 91, 153
Seuwen, R. 82, 84, 87, 107
Seybold, T.D. 457, 461
Seyenaeve, G. 25–27
Seyferth, U. 379
Shabbar, A. 40, 320
Shapiro, M.A. 45
Sharpe, A.D. 305
Shauer, J.J. 9
Shaw, G. 302
Shaw III, C.G. 302, 381
Shea, P.J. 390
Shea, R.W. 84, 87, 91, 107
Sheesley, R.J. 91
Shettle, E. 114
Shirai, T. 292
Shostakovich, V.B. 6
Show, S.B. 472
Shugart, D.R. 39
Shugart, H.H. 85, 111–112, 180
Shvidenko, A.Z. 114–115, 126
Sickman, J.O. 415–418, 426, 447–448, 464
Siegert, F. 111–112, 121, 126

Sierchio, J.M. 512
Sillman, S. 93
Silva Dias, M.A.F. 45
Silva Dias, P.L. 45
Silvestre, A.J.D. 307
Sim, M. 295
Simard, A.J. 40, 479
Simmonds, P.G. 293
Simon, M. 111, 113
Simoneit, B.R.T. 293
Simoneit, B.T. 9
Simpson, I.J. 80, 85, 88, 91, 93, 107
Singh, H.B. 95
Singh, J.S. 123
Singh, S. 123
Sinha, P. 85, 88, 91, 107
Sinsabaugh, R.L. 379
Sioutas, C. 80, 291, 295
Sirulnik, A.G. 374, 416–417, 430
Siry, M. 125
Sjoberg, R.M. 379
Skamarock, W.C. 503, 530
Skewes, M. 305
Skinner, C.N. 324
Skinner, W.R. 40–41, 320
Slaughter, J.C. 297
Slutsker, I. 254
Smirnov, A. 252, 254
Smith, A.M. 474
Smith, E.M. 297, 381, 407
Smith, G.C. 8–10
Smith, J.E. 115
Smith, J.K. 115, 118
Smith, M.A. 86, 297
Smith, M.C. 50
Smith, R. 539
Smithwick, E.A.H. 88
Sneeuwjagt, R.J. 475–476, 538–539
Snell, R.D. 62
Snoeijers, S.S. 381
Soja, A.J. 39, 111–112, 180
Sol, B. 489
Sollins, P. 379
Solomon, A.M. 110, 114, 322, 588, 594
Solomon, S.A. 506
Solorzano, L. 126
Song, C.-P. 376, 387
Song, W. 304
Sosa-Ramírez, J. 343, 352, 354, 358, 382, 385
Sousa, J. 72
Sparks, J.C. 117
Sparks, S.R. 345
Spengler, J.D. 295
Sperry, J.S. 360
Spichtinger, N. 52, 114
Sprugel, D.G. 377
Séro-Guillaume, E. 66
Stacey, P.B. 331
Stackhouse, H.H. 39
Stackhouse, P.W. 111–112, 180
Stark, N.M. 410, 413
Stark, R.W. 389, 392
Statheropoulos, M. 7–12, 22, 25–26
Staudt, M. 305
Steed, R. 512
Steeghs, M. 306
Steele, L.P. 111
Steele, M.D. 86, 93
Stefanidou-Loutsidou, M. 24–25
Stefner, C.N. 481
Steinbrecher, R. 306
Steinbrenner, E.C. 406
Stender, D. 512
Steneck, R.S. 356
Stephanou, E.G. 93
Stephen, F.M. 389, 392
Stephens, D.R. 539
Stephens, E.T. 539
Stephens, S.L. 39, 348, 407, 415, 450
Stephenson, N.L. 323–325, 333
Steubing, L. 302, 304
Stewart, A.J. 305
Stewart, D. 94
Stewart, M.F. 47
Stiling, P. 303
Stine, S. 324
Stocks, B.J. 40–41, 50, 91–93, 111–112, 114, 117, 121, 123, 127–128, 320, 477, 481, 483
Stohl, A. 52, 80, 94, 114
Stolte, K.W. 377, 415
Storck, P. 512
Storer, A.J. 390
Stottlemyer, R. 418, 427–428, 586
Straume, A.G. 548
Street, R.A. 307
Streets, D.G. 85, 114
Strimaitis, D.G. 505
Strom, B.L. 390
Stroud, V.R. 88, 91

Stunder, B. 221
Sturm, M. 329
Su, Y. 80
Suckling, K.F. 331
Sudo, K. 94
Sudol, M. 306
Sukhinin, A.I. 39, 111–112, 117–118, 120–122, 126, 180
Sukumar, R. 110, 126
Sullivan, A.P. 45, 65, 94
Sun, G. 386
Sun, L. 48, 50
Sun, O.J. 124
Suppiah, P.N. 295
Susfalk, R.B. 405–406, 409–410, 412–413, 415, 418–419, 427
Susott, R.A. 62, 70, 82–84, 87–88, 91–92, 107, 120, 268
Sutkus, D. 216
Suttles, J.T. 85
Suwanwaree, P. 123
Swanston, C. 379
Swap, R.J. 85
Swetnam, D.R. 287
Swetnam, T.W. 38–39, 120, 125–127, 129, 320, 324, 331, 360, 366, 406
Sweuwen, R. 70
Swietlicki, E. 93
Symons, D. 537
Symons, J.M. 13, 80
Szczygieł, R. 203, 240, 590
Szykman, C. 177, 180

Taha, H.A. 389
Tait, L.J. 115
Takahashi, K. 121
Takegawa, N. 292
Takemoto, B.K. 298, 415–418, 586
Takeuchi, N. 13
Talbot, R.W. 80
Talbott, L.D. 387
Tallamraju, R. 306
Tang, Y. 304
Tanre, D. 254
Tansey, K. 80
Tape, K.D. 329
Tapper, N. 294
Tarantini, T. 297
Tardif, J.C. 39
Tarnay, A. 593
Tarr, M.A. 123
Tarrasón, L. 217
Tausz, M. 373, 376, 392
Taylor, C.A. 306
Taylor, D.R. 292, 539
Taylor, G. 221
Taylor, J.L.S. 303, 306
Taylor, S.W. 49, 478, 481
Tchebakova, N.M. 127
Teesdale, J.C. 91
Tegner, M.J. 356
Temple, P.J. 382, 385, 430
Terrill, R. 349
Terry, J.D. 378, 416–417, 430
Textor, C. 92
Theirsen, K.A. 500
Thiemens, M. 374, 416–417
Thomas, P.H. 50
Thomine, S. 376, 386–387
Thompson, A.M. 80
Thompson, C.D.C. 329
Thompson, K. 322
Thompson, S.L. 127
Thornton, P.E. 321–322
Tibshirani, R. 558
Tiedemann, A.R. 450
Tietema, A. 450
Tieu, S. 304
Tilman, D.G. 18
Ting, M. 39, 126
Tingey, D.T. 373–374, 380, 393–394
Tinker, D.B. 123–124
Tinner, W. 50
Tirado, R. 392
Tissell, R.G. 8, 118, 140, 142–145, 147, 151–153, 591
Tjoelker, M.G. 385
To, K. 593
Todd, J.B. 40, 483
Tolhurst, J. 537
Tolhurst, K.G. 538
Tomasella, J. 126
Tompsett, A.A. 305
Tong, R.O. 285
Tong, S. 297, 593
Tonnesen, G.S. 417, 448
Toohey, D.W. 428, 448
Torsethaugen, G. 386
Tory, K.J. 523, 548
Trabaud, L. 64, 306, 406

Trainer, M. 13, 114
Trembach, V. 258
Trenberth, K.E. 40
Trentmann, J. 92, 94
Treseder, K.K. 127
Trevitt, A.C.F. 487
Trexler, M.C. 110, 114
Trijonis, J.C. 174
Troe, J. 95
Trotsenko, A. 258
Tsai, N.Y. 114
Tschiersch, J. 268, 268
Tsidulko, M. 514, 529
Tsigaridis, K. 93–94
Tucker, J.T. 322, 331
Turetsky, M.R. 19
Turner, D. 408, 415
Turner, M.G. 123–124
Turquety, S. 80, 94
Tyler, G. 304
Tyler, S.C. 111
Tymstra, C. 41, 483
Tyndall, G.S. 268
Tzamtzis, N. 8

Ubysz, B. 203, 240, 590
Uhrenholdt, B. 304
Uliumdzhieva, N. 252
Uman, M.A. 44
Unam, L. 19
Ungar, K. 17
Unger, N. 85
Unsworth, M.H. 298, 301, 303
Urbanski, S.P. 428, 448, 588–589
Utkhede, R. 381

Val Martín, M. 80
Valente, J. 10–11, 62, 70, 72, 210, 292
Valente, M. 72, 214
Valette, O. 66
Van Bree, L. 9
van der Werf, G.R. 80, 85, 111–113, 121, 126, 207
Van Dingenen, R. 93
van Mantgem, P.J. 324–325
van Staden, J. 303–304, 392
Van Wagner, C.E. 477–478, 489
Van Wilgen, B.W. 50
van Wagtendonk, D.J. 324
Varela, M.C. 6
Varney, S.K. 18
Vaughan, G. 592
Vaughan, J. 508, 512–513, 524
Vautard, R. 211, 217
Vavrus, S. 41
Veblen, T.T. 117, 125–126, 320
Vecchi, G. 126
Vedal, S. 297
Velez, J. 39, 126
Verburg, P.S.J. 408–409
Verrall, K. 297
Vickos, J. 210
Viegas, C. 62, 210
Viegas, D.X. 48, 51, 210, 489–490
Viegas, M.T. 490
Viegas, M.T.S.P. 48
Viereck, L. 329
Vierling, M. 307
Vigilante, T. 304
Vignati, E. 93
Vigy, E. 66
Vihnanek, R.E. 64–65
Villalba, R. 320
Vines, R.G. 292, 539
Viney, N.R. 48
Viskari, E.-L. 305–306
Vité, J.P. 392
Vitale, K. 297
Vitousek, P.M. 18, 408, 415
Vivanco, J.M. 306
Vogt, C.A. 371–372
Vogt, P. 201
Volin, J.C. 385
Volney, W.J.A. 117
Vricic-Keglevic, M. 297
Vygodskaya, N.N. 125

Wade, D.D. 83–84, 91
Wade, P. 62, 500
Wagner, T. 52, 114
Wain, A.G. 517, 521, 523, 541, 545, 592
Wakimoto, R.H. 51, 120
Walker, D.A. 329
Walker, J. 268
Walker, R.F. 405–409, 412, 415, 418–419, 427–428
Wallace, J.M. 40
Wallenda, T. 304
Walsh, J.E. 329

Walsh, R. 295
Walsh, S. 548
Walter, B.P. 111
Walters, J.C. 329
Wan, S. 415, 428, 450
Wandinger, U. 52, 114
Wang, D.M. 503
Wang, F. 593
Wang, H. 39
Wang, J. 18
Wang, L. 13, 80
Wang, X. 40
Wangler, M.J. 346
Ward, B. 476
Ward, D.E. 9–10, 29, 61–62, 70–71, 80, 82–85, 87–88, 91–93, 103, 107, 120, 164, 210, 291–293, 296, 302, 513
Ward, T.J. 8–10
Waring, R.H. 450
Warnatz, J. 83, 291–292, 351
Warneck, P. 82, 84, 87, 107
Warneke, C. 61, 94–95
Warner, J. 80
Warner, R.R. 356
Warnesk, P. 70
Watson, J.G. 82, 84, 87
Waugh, A. 8–10, 21
Weatherspoon, J.W. 324
Webb, A. 216
Weber, J.A. 376
Weber, M. 122
Weber, R.J. 94
Weber, U. 320
Webster, P. 361
Weeks, R. 537
Weinzierl, B. 94
Weirich, F.H. 155, 414–415, 428, 450
Weise, D.R. 48, 50–51
Weiser, G. 386
Weiss, R.E. 82, 91, 93, 164
Weiss, R.F. 80
Welker, J.M. 329
Welling, M. 91
Wells, M.L. 343, 346
Welp, L.R. 127
Wenberg, P.O. 428, 448
Werner, R.A. 327, 329
Westerling, A.L. 38–39, 125, 127–129, 287, 320, 349, 360, 366, 406, 575
Westrick, K. 512
Wheatley, R.E. 307
Whelan, R.J. 297
Whisenant, S.G. 306
White, J. 111
White, M. 174
White, R. 297
Whiteman, C.D. 45
Wickett, M. 127
Wiedinmyer, C.E. 80, 112, 121, 180, 228
Wilborn, R. 381
Wild, O. 94
Wildermuth, P. 307
Williams, A. 41
Williams, D.J. 42, 91
Williams, E. 42, 44, 47
Williams, J. 177, 180
Williams, M.R. 408, 415
Williams, R. 474
Wills, T.J. 304
Wilson, J. 93
Wilson, A.A.G. 65
Wilson, R.A. 50, 295, 487, 506, 508, 512
Wilson, S.A. 298
Winer, A.M. 306, 428
Winstead, E.L. 91–93
Winterhalter, R. 93
Winterkamp, J. 51
Winterrath, T. 92, 94
Wirth, C. 117, 125, 128
Wisniewski, J. 110, 114
Wisthaler, A. 95
Witte, J.C. 80
Wofsy, P.S. 18
Wohlgemuth, P. 414–415, 428–429, 450
Wohlgemuth, T. 50
Wold, C.E. 82, 84, 87, 268, 428, 448
Wolfson, J.M. 577
Wolkowskaja, I.L. 304
Wollum, A.G. 409
Wong, D.C. 514, 529
Wong, N. 548
Woo, J.H. 80
Wood, D.L. 389–390, 392
Woods, P.V. 406
Woodward, F.I. 321
Wooster, M.J. 83, 86, 118

Worden, H.M. 85
Worden, J.R. 85
Worsnop, D.R. 94
Wotawa, G. 13, 17, 114
Wotton, B.M. 40, 44, 49, 127–128, 477, 479, 481, 483
Wotton, D.X. 47, 592
Wowchuk, D.R. 320
Wu, J. 428
Wullschleger, S.D. 386
Wuthrich, C. 122
Wynne, K.K. 80, 112, 121
Wynne S. 180

Xinwen, Z. 285

Yajima, T. 121
Yamartino, R.J. 505
Yang, Q. 127–128
Yantosca, R.M. 500
Yedinak, I.C. 50
Yelin, E.H. 297
Yetter, J. 512
Yi, A.R. 591–592
Yin, C. 392
Yokelson, R.J. 12, 16, 61–62, 70, 80, 82–85, 88, 91–92, 94, 107, 428, 448
Yoschenko, V.I. 268, 268
Young, J.O. 514, 529
Young, M. 548
Youngberg, C.T. 409
Younglove, T. 418
Yuan, F. 458, 464, 589, 594
Yuan, C. 285

Zabowski, D. 408
Zagory, D. 304
Zavarin, E. 389, 392
Zavitovski, J. 409
Zedler, P.H. 306
Zeiger, E. 387
Zender, C.S. 127
Zeneli, G. 393
Zeng, R. 514
Zenker, T. 91
Zepp, R.G. 123
Zeugin, F. 50
Zhang, D. 180
Zhang, H. 279
Zhang, L. 376, 387
Zhang, X. 80, 112, 121, 376, 387
Zheng, M. 593
Zhong, S. 593
Zhou, X. 48, 50–51
Zhu, J. 387
Zhu, Y. 80, 295
Zhuang, Y.H. 278–279
Zhukov, B. 118
Ziegler, W. 125
Zielinska, B. 9
Zimet, T. 51
Zimmerman, P.R. 91, 306–307
Zimmermann, L. 50
Zimmermann, N.E. 321
Zitzer, S. 307
Zukoski, E.E. 506
Zunzunegui, M. 392
Zuskin, E. 297
Zvarich, S.I. 268, 268
Zweifel, R. 50

Subject Index

Acacia 290, 307
Accessory Fuel Moisture (AFM) System 477
acetaldehyde 9, 81
acetic acid 9, 81, 82, 305
achievable future conditions 333
acrolein 9, 296
adenostoma 414
Advanced Very High-Resolution Radiometer (AVHRR) 277, 591
  satellite 273
aerial ignition 538
aerial photographs 348
aerological data 225
aerosols 79, 172, 248
Aerosol Optical Thickness (AOT) 257
Africa 85
agricultural burning 501, 511, 524
agriculture 86, 212
air polluted forests 567
air pollution 366, 373, 393, 567, 569, 571, 573, 575, 577, 579, 581, 585
  emissions 425, 428
  episodes 209
  monitoring 577
air quality 171, 209, 277, 539, 585
  forecasting models 597
  Framework Directive 220
  management strategies 211
  modelling system 209–210
  models 471, 579
  simulation models 180
  standards 260, 569
  related values 568–569
aircraft emissions 215
AIRFIRE 224
AirNow 529
AIRPACT-3 508, 529
Alaska 19, 86, 319
alkanes 93
alkenes 93
alkylbenzenes 9
Amazonia 210
ambient air quality 597
ambient ozone (O_3) 325, 567
ammonia (NH_3) 8, 61, 213, 373
ammonification, nitrification 406
ammonium (NH_4^+) 408, 428
Annosus root disease 381
annual average exposure 295
anthropogenic ignition rate 347
anthropogenic nitrogen 80
antioxidant 376
area burned 61
aromatic hydrocarbons 9, 93
arson 6, 241, 586
Asia 585, 591
asphyxiants 24
ASTER 12
asthma 297
atmosphere 129
atmospheric
  carbon 130
  deposition 417, 419–420
  dispersion models 553
  emissions 197
  lifetimes 94
  N deposition 594
  particulate matter 268
Australia 85, 210, 290, 471, 499, 501, 506–507, 517, 519, 527, 536, 585, 591
Australian Fire Danger Rating System 65
Austria 233
autoregressive error 556

background ozone 575
bacteria 307

Baja California 339
bark beetle 320, 366, 388, 392, 395–396, 567, 586
beetle epidemics 393
Belarus 233
belowground biomass 83
benzaldehyde 9
benzene 9, 294, 296
benzo (a) pyrene 9
benzofuran 9
benzoic acid, methyl ester 9
bioclimatic "envelope" 321
biogenic emissions 307
bioindicator plant species sensitive to ozone 261
bioindicators 304
biomass burning 9, 291, 293, 295–299, 302–303, 305, 307, 535
biomass emissions 110–111
black carbon 9
Black Dragon Fire 286
black stain root disease 381
BlueSky 499–500, 506–508, 510–511, 515, 522–523, 526–529, 553
BlueSkyRAINS 511
boreal forest 88
Brazil 6, 85, 210
burn intervals 419
burn severity 130
burned area 110, 130, 197, 198
burned biomass 197, 238
Burning Index (BI), 486
burning period 62

calcium (Ca) 410
California 339, 425, 567, 569, 571–573, 575, 577, 579, 581, 593
California Interagency Air and Smoke Council (IASC) 576
CALPUFF 505–507, 511–513
  $PM_{2.5}$ 513
Canada 86, 477
Canadian Fire Danger Rating System 65
Canadian Forest Fire Behavior Prediction (FBP) System 477
Canadian Forest Fire Weather Index (FWI) System 477
Canadian Yukon 19
carbohydrate 379, 392
carbon (C) 405–411, 413, 415, 416–419, 421, 423, 585
  accounting 579
  acquisition 377
  and N budget 427
  balance 128–129
  budget 586
  dynamics 115
  gain 385
  mass balance method 84
  release 598
  sequestration 114, 585
  stocks 109, 114, 130
  storage 110, 124, 130
  trading 585
carbon (C) and nitrogen (N) cycling 425
carbon dioxide (CO_2) 8, 61, 92, 210, 239, 425, 588
carbon monoxide (CO) 7, 18, 61, 80, 92, 210, 212, 214, 239, 291–294, 296, 425, 588
carboxylic acids 9
carcinogen 24
catastrophic forest fires 589
catastrophic wildfire 576
causes of wildland fires 586
Ceanothus chaparral 414
Central and Eastern Europe 233, 590
Central Asia 86
Central Russia 247, 249, 251, 253, 255, 257, 259, 261, 263
cesium (Ce) 11, 84
CFFDRS 486
changes in species composition 427
changing climate 585, 591
  effects on wildfire 130
chaparral 339, 415
char oxidation 81
charcoal 407
chemical composition of the emissions 8, 80
Chernobyl 10, 13, 265, 590
China 277, 591
chloro-methane 9
Class I areas 568
Class II areas 568
Clean Air Act 568
Clean Air Status and Trends Network (CASTNET) 577
ClearSky 499, 501, 507–508, 510–513, 522, 524, 526, 528, 530

climate 38
change 128, 277, 280, 287, 567, 586
variability 3, 567
zones 38
climate-fire-carbon interactions 129
climate/weather 595
combustion of vegetation 291
combustion process 81
combustion products 241
coniferous forest 88, 234, 339, 418
Consume 3.0 model 69
consumption 129
contributions of smoke from fires 553
controlled burning 290
criteria pollutants 570
cross-analysis of air quality 210
crown fire 49, 87
crotonaldehyde 9
Czech Republic 233

DAYCENT model 425
decision support systems 535
decomposition 379
defensible space 371
degradation in atmospheric quality 362
deposition 210
dibenzo-furans 10
dibenzo-p-dioxines 10
Direcc-ão Geral das Florestas 229
dispersion model 64, 535, 579
dispersion of radionuclides 265, 267, 269, 271, 273, 275
distillation 81
distribution of air pollution 568
distribution of fires 339
distribution of ozone 556
disturbance 419–420
drought 39, 126, 247, 287, 319, 366, 586
factor 475
index 474
stress 365, 376, 381, 383, 385, 392–393
Drought Code (DC), 479
dynamic transport models 554

EC_{50} 23
ecological impacts 598
ecosystem carbon fluxes 124
ecosystem disturbance 366
ecosystems 287
effects of fire on carbon fluxes 115
effects of forest fires 171, 173, 175, 177, 179, 181, 183, 185, 187, 189, 191, 193, 195, 197
El Niño 125–126
cycle 360
El Niño Southern Oscillation (ENSO) 40
elemental carbon 9, 588
EMISPREAD 72
emission(s) 61, 111, 126, 209, 233, 294, 588
data 83
factors 62, 84
inventory 71, 172
source strength 64
chemistry 596
from aircrafts 209
from wildland fires 589
energy 376
release component (ERC) 485
transformation industries 212
limited 322
Environmental Protection Agency (EPA) 568
EPM 504, 506–507, 510–511, 515
equilibrium moisture content 48
erosion 408
esters 9
Estonia 233
ethyl-benzene 9
ethylene 305
EU fire database 199
eucalypt forests 537
eucalyptus 290, 306, 307
Europe 86, 471, 589
European Commission 209, 230
European Forest Fire Information System (EFFIS) 197
European Union (EU) 197, 210, 489, 590
evapotranspiration 358
exceedances of permissible ozone levels 218
extreme fire events 211
extreme weather 247, 339

FARSITE 67, 483, 486
FASTRACS 510
fate of wildland fire emissions 81
fauna 297–298
FCAMMS 508
BlueSky 510
FCCS 504, 507, 510
feedbacks between fire and climate 130

FFMC 491
fine and coarse particulate matter 80
Fine Fuel Moisture Code (FFMC) 478
fine root biomass 416, 418
fire 126, 319, 419
  and patch dynamics 342
  as a management tool 594
  behavior 62, 80, 471, 579, 586, 592
  characteristics 209
  control 472
  detection 287, 595
  dynamics 117
  effects on carbon 118
  environment 471
  exclusion 324, 427
  frequency 427
  hazard 368, 371
  impacts 197, 199, 201, 203, 205, 207
  intervals 343, 427
  occurrence 277, 586, 592
  plume dynamics 80
  prevention management 586
  regime 115, 128, 342
  risks 266
  severity 320, 586
  spread rates 348
  weather 342, 346
  weather window 342
Fire Area Simulator (FARSITE) 473
fire danger 283, 471, 473, 475, 477, 479, 481, 483, 485, 487, 489, 491, 493, 495, 497
  index 472
  level 472
  dynamics 118
fire emissions 111, 120, 129–130, 277
  Production Simulator 67
fire management 3, 281
  policies 361
Fire Occurrence Prediction (FOP) system 477
fire suppression 279, 283, 339, 366, 406, 409, 425, 589
  planning 481
  policy 342
fire-safe activities 368
fire-scar dendrochronology 360
firefighter health and safety 297
firefighting 215
  operations 210
fireline safety 481
FireMapper system 591
firestorms 356
First Order Fire Effects Model (FOFEM 5.0) 65, 431
Flaming 7, 64, 82, 292
  combustion 48, 81, 291–292
  phase 9
flammability of plants 306, 340
flanking fire 50
foliar N concentrations 426
foliar N content 428
foliar senescence 567
forecasting smoke-radionuclide dispersion 274
forest(s) 247, 279, 405–410, 413–419, 585
  densification 366
  density 368, 395
  fire behavior data 210
  fires 197, 209, 233, 235, 237, 239, 241, 243, 245
  flammability 425
  health 374
  herbaceous plant development 247
  management 586
  mensuration models 568
  susceptibility to wildfires 365
Forest Fire Danger Index (FFDI), 474
Forest Fire Danger Rating System (CFFDRS) 477
Forest Fire Regimes 339
forestry 537
formaldehyde (HCHO) 9, 82, 253, 296
formic acid 82, 296, 305
France 488, 590
free-running fire 340
frequency of fires 339, 342
Frisia 5
fuel 9, 129
  accumulation rates 342
  build-up 427, 567
  Characteristic Classification System 66
  characteristics 62, 80
  chemistry 80
  combustion 79
  combustion process 80
  consumption 62, 118
  load 197
  Load Models 65
  loads in forests 538

moisture 47, 284, 472
N content 425
properties 342
property 284
reduction 290, 295
treatments 567, 593
type 277
fuel models and modeling systems 65, 471, 473, 475, 477, 479, 481, 483, 485, 487, 489, 491, 493, 495, 497
fuelbed 81
fundamental niche 321
fungi 304, 306
furans 9
furfural 9

gas-to-particle conversion 94
gases (gaseous compounds) 210
gaseous emissions 293
Gaussian distribution 557
genotypes 332
geographic zones 79, 85
Germany 233
global fire emissions 126
global phenomena 210
global warming 41, 319, 321, 323, 325, 327, 329, 331, 333, 335, 337, 586
GOES 503, 516–517
Gradient modeling 321
Grassland Fire Danger Index (GFDI) 475
Greater Hinggan Forest 286
Greece 211, 488, 590
greenhouse effects 598
greenhouse gases (GHG) 79–80, 214
greenness 283
ground fire 49

halocarbons 88
haze 290, 292–293, 307
heading fire 49
health 28
effects of smoke 599
hazard 260
of firefighters 599
heat release rate 62
herbaceous fuels 92
herbaceous vegetation 92
high temperatures 247
high-intensity fires 339
historic evidence 3
history of land-use 4
HMS 514–516, 521–522
human fatalities 211
human health 3, 290, 293–296, 428
human population 366, 393
human-induced changes 368
Hungary 233
hydrocarbons 215
hydrogen sulfide (H_2S) 8
hydrophobicity 408
HYSPLIT model 221, 505, 507, 511, 514, 517, 536

ICS-209 508
ignition factors 472
illegal forestry activities 6
impact assessments 12
IMPROVE network 172
in-plume chemistry 596
incense cedar (*Calocedrus decurrens*) 426
India 86
indicators 304
Indonesia 22, 210
indoor biomass smoke 295
Initial Spread Index (ISI), 479
insects 319
intensity of wildfires 87
interactions between air pollution, drought, and insects 568
interactions between climate, fire regimes, and carbon 128
interactions of wildland fires and air pollution 585
interactive effects 425
Interagency Monitoring of Protected Visual Environments (IMPROVE) 577
invasive species 320
irritants 24
isoprene 305–307
isotopic tracer 416
Italy 211, 488, 590

jack pine (*Pinus banksiana*) 478
Jeffrey pine (*Pinus jeffreyi*) 415
Joint Research Centre (JRC) 198

Kazakhstan 16
Keetch-Byram Drought Index 479, 486
Kiev 590

Lake Tahoe Basin 407–409
land cover 277
land management 210, 535
land surface temperature 284
land-use fires 5
LANDFIRE 65
Landsat 277
large diameter fuels 83
Latvia 233
LC_{50} 23
leaching 406–408, 419
leaching of nitrate 427
leaf turnover 379
lightning 43
  detection rate 347
lignin 379
lignocelluosic biomass 81
Limited Area Prediction Scheme (LAPS) 540
Lithuania 233
litter 396, 418
litterfall 377
local and regional air quality 567
lodgepole pine (*Pinus contorta*) 327, 478
logging 393
long-range transport of pollutants 270, 598
long-term carbon storage 586
long-term dynamics of fuel accumulation 339
long-term ecosystem changes 567
Los Angeles 426
low-intensity smoldering fires 248
lung function 297
lung volume 296

Madden Julian Oscillation 40
magnesium (Mg) 410
Malaysia 21
management issues and strategies 568, 585, 599
managing smoke from prescribed burning 539
MCE 84
mechanical removal 567
Mediterranean basin 488
Mediterranean France 211
Mediterranean climate 340
Mega-Fire(s) 247, 249, 251, 253, 255, 257, 259, 261, 263
mercury (Hg) 19
MERIS 12
mesoscale numerical weather prediction 535
meteorological conditions 217
meteorological data 554
meteorology 80
methane (CH_4) 9, 18, 61, 80, 210, 239, 425
methanol 81
methyl acetate 81
microorganisms 303, 306
mineral leaching 428
mistletoe 381
mitigating nitrogen losses 425
mixed-conifer forests 343, 416, 418, 425
mixed-severity fire regimes 117
modal weather states 342
Moderate Resolution Imaging Spectroradiometer (MODIS) 12, 273, 274, 277, 503, 514, 517, 519, 546, 592
MODIS satellite image of fire locations 273
moisture content 92
monitoring networks 209
monoterpene 305–307
monoterpenoids 306
MOPITT 18
mortality 397
  rates 395
Moscow 20, 247, 590
mountain pine beetle 326, 389
multiple regression 556
mutagen 25

N-fixing vegetation 409, 414
N-saturated 416, 418
  chaparral 414–415
  forests 415–416
N-saturation 415–416, 418
  responses 427
N_2O (nitrous oxide) 210, 570
National Ambient Air Quality Standards (NAAQS) 570
National Parks (NPS), 553, 568
natural global atmosphere 4
natural hazards 277
negative water balances 323
NESDIS 514
Nesterov's flammability indices 249
New South Wales (NSW) 476
New Zealand 476
NFDRS 504, 507, 515

nitrate (NO_3^-) 407, 414–417
leaching 416–418
runoff 425, 428
nitric oxide (NO) 407–409, 417, 427
nitrification 407, 417–418, 427
nitrogen (N) 405–411, 413–421, 423
content 426
cycle 427
deposition 373, 416–417, 419, 425–426, 567, 586
deposition scenarios 425
fixation 419
leaching 408, 419
pollutant emissions 586
saturation 414, 426, 594
volatilization 406
nitrogen dioxide (NO_2) 19, 253
nitrogen oxides (NO_x) 61, 80, 210, 212, 278, 291–294, 296, 425, 588
nitrous oxide (N_2O) 210, 427
NMHC 210, 212
NMVOC 80
NOAA 273, 499, 501, 503, 505, 507–508, 510, 513–515
NOAA AVHRR 12
NOAA POES 17
NOAA-HYSPLIT 513–514, 521–522, 529, 531
NOAA-HYSPLIT smoke prediction 515–516, 529
non-hydrostatic meteorological model (MEMO) 224
nonmethane hydrocarbons 61, 210
nonmethane volatile organic carbon 80
normal probability plots 557
Normalized Difference Vegetation Index (NDVI) 283
North America 87, 210, 471, 585, 592
North American ecosystems 85
nuclear accidents 274
numerical modeling 224
nursery stock 332
nutrient budgets 598
nutrient cycling 426, 589

Occupational Exposure Limits (OELs) 26
ocean circulation patterns 125–126
Old Fire 395
old-growth 339
onshore winds 340
open flames 92
organic carbon (OC) 588
oxidative stress 376
oxygen-to-fuel ratio 7
oxygenated compounds 93
ozone (O_3) 19, 217, 293, 296, 302, 303–304, 415–416, 418, 586
formation 80, 94
damage 261
precursors 219, 559
tropospheric 210, 217, 426

Pacific Decadal Oscillation 40
PAHs 291, 293, 295
Palmer Drought Index 479
particles 80
particulate emissions 278
particulate matter (PM, PM_{10}, $PM_{2.5}$) 9, 10, 61, 79, 80, 171, 210, 292, 295, 425, 500, 502, 504, 506, 508, 511–515, 522, 526, 528–529, 588
monitors 578
particulates 210, 291, 295, 297, 302, 305
passive samplers 577
patch mosaic dynamics 342
peat and bog fires 596
peat bog fires 248
peat bogs 247
peatland fires 19
peatlands 3
Peninsular Range 342
permafrost 319
personal protective equipment (PPE) 28, 599
pests and diseases 586
phenology changes 261, 262
Philippines 210
phosphorus (P) 407, 410, 411
Photo Series 65
photochemically reactive compounds 79–80
pinyon-juniper 319
plant flammability 306
plant injury 248, 261
plant mortality 262
plant phenology 248
plant responses 298
plant successions 339
plant vigor 325
plume rise 541

plume-dominated fire 51
plutonium (Pu) 16
Poland 233
polyaromatic hydrocarbons 9
polynomial regressions 558
ponderosa pine (*Pinus ponderosa*) 367, 415–416, 426
Portugal 6, 211, 488
postfire carbon dynamics 122, 123
postfire soil respiration 121–122
precipitation 346
precisions of forecasts 560
prediction of air pollution 471
prediction of fire behavior 596
prescribed burning 296–297, 474, 535
prescribed fire 69, 405, 414–415, 418–419, 428, 538, 567, 569, 573, 586, 589
primary pollutants 80
private property 593
probability of fire spread 349
PROMETHEUS 66
property damage 211
public health 210
public lands 567–568, 593
pyrolysis 7, 81

radiative forcing 258
radioactive emissions 3, 10
radioactivity 268
  in soil and vegetation 267
radionuclides 3, 13, 267
Recommended Exposure Limits (RELs) 26
recreational use 368
reducing fuel accumulation 567
refugia 333
regional air quality 428
  models 597
regional haze 571, 574
  regulation 171
relative humidity 44
remote sensing 197, 277, 279, 281, 283, 285, 287, 585
research needs (wildfire/carbon interactions) 131
resin production 391, 393
respiratory illness 297
road transport 212
roots 303, 306
  biomass 379, 385
Rothermel fire progression model 224
Russia 86, 210, 488, 590
Russian Federation 20

San Bernardino Mountains 366, 416–417
San Dimas Experimental Forest 414
San Gabriel Mountains 351, 414, 426
San Joaquin Valley Air Pollution Control District 574
Santa Ana winds 340, 356
satellite imagery 348
scattering albedo 247
sclerophyllous vegetation 290, 298
secondary air pollutants 79, 80
security 3
sediment and ice core studies 4
seed germination 304
semi-volatile organic compounds 8
severity of fire 120, 128
sheep grazing 324
shifting cultivation 6
Short-term Exposure Limits (STELs) 26
Sierra Nevada Mountains 319, 419, 426, 560, 574
Sierra San Pedro Mártir 352
simulations 555
Singapore 21
slash-and-burn agriculture 6
Slovakia 233
small fires 342
smoke
  aerosol 4
  cloud 247
  dispersion 13, 224, 579
  forecasting 540
  emissions 4, 61, 265, 267, 269, 271, 273, 275, 339
  exposure 599
  haze 539
  management 3, 501, 506, 511, 517, 526–527, 535
  monitoring 567
  plumes 217, 270
  prediction 499, 500–508, 514–515, 517, 519, 521–522, 524, 526–531
  transport 6, 539
smoldering 7, 64, 82, 291–292
smoldering combustion 123, 291, 292
soil(s) 299, 301–304, 306
  acidification 427

bacteria 304, 306
hydrophobicity 408
microbes 304
microbial community 306
microorganisms 303
N emissions 425
organic matter 407
processes 121
respiration 122, 129
solution 408
solution SO_4^{2-} 408
solar radiation 218, 247–248
source strength 61
South America 86
Southeast Asia 6, 19, 86
southern California 339, 353, 589
southern Europe 209, 211, 213, 215, 217, 219, 221, 223, 225, 227, 229, 231, 590
Southwest 319
Spain 211, 488, 590
SPOT 12
spruce bark beetle 329
stand demography 395
stand densification 426
stand development 568
stand-replacement fires 123, 343
stand-replacing fires 116
state and federal air regulators 567
statistical model 553, 556
stomata 299, 301–303, 386
streamwater 408
nitrate 414–415
stress complexes 319, 321, 323, 325, 327, 329, 331, 333, 335, 337
strontium (Sr) 13
subboreal forest 247
sulfur (S) 8, 410
deposition 80
sulfur dioxide (SO_2) 8, 61, 253, 278, 291, 296, 303–304, 425
sulfur oxides (SO_X) 212
surface albedo 127
surface fire 49, 117
surface temperature 283
susceptibility of forests to wildfire 365

teleconnection 39
temperate continental forests 234
temperate forest 88
temperate mountain forests 234
temperate oceanic forest 234
temperate rangelands 88
temperate zone wildfires 87
temperature 42, 346
inversions 52
terpenes 81, 306
terrestrial ecosystems 585
Threshold Limit Values (TLVs) 26
threshold of combustion 342
threshold of flammability 343
thunderstorm activity 347
timber utilization 366
toluene 9
total aerosols 253
total suspended particles (TSP) 278
toxicity 22
trace gases 79
trajectory technique 221
Transbaikal Region 17
transboundary transport 29
transformation of fire emissions 80
transport 80, 210
Transverse ranges 342, 417
tree density 387
tree growth 426
tree mortality 387, 395, 426, 567
tropical forest 88
tropical savanna 86, 88
tropospheric chemistry 79

U.S. National Fire Danger Rating System 473, 483
Ukraine 233, 590
uncertainties 560
understory vegetation 418
urban air pollution 278
urban areas 589

vegetation
burning 291
fires 265, 292–295, 298–299, 303, 305
fuel threshold 347
growth 342
mosaics 339
recovery 129
smoke 298
types 88
visibility 21, 171, 290, 292, 472, 571
visibility impairment 588

volatile organic compounds (VOCs) 8, 81, 290, 291–296, 305–307, 588, 591
emissions from plants 306
volatilization 407–408

warmer climate 319
water
loss 366, 385–386
quality 407
stress 567
vapor 215
use efficiency 385
weather 42, 287
and climate 125
and fuel conditions 339
conditions 219
stations 554
western conifer forests 88
Western North America 319
western pine beetle 389
Western Regional Air Partnership (WRAP) 576
western United States 88
wet and dry deposition 93
white pine blister rust 325
wilderness areas 568
wildfire(s) 129, 366, 405–410, 413–414, 419, 535
frequency 567
hazard 6
occurrence 425
risk 397
severity 589
wildland fire(s) 61, 109, 139, 247, 277, 567, 585
emissions 79, 88
ignition potential 586
management 472
occurrence and behavior 471
Wildland Fire Assessment System (WFAS) 283
wildland-urban interface 418, 567, 593
woodsmoke 295–296
World Health Organization (WHO) 278

xylene 9